ENERGY

CONSERVATION

ORNL/Sub/80-0082/3
Dist. Category UC-95d

BI-RADIANT OVEN
A
LOW-ENERGY OVEN SYSTEM

VOLUME III—APPLICATION AND TRANSFER OF THE TECHNOLOGY

TASK REPORTS

PURDUE UNIVERSITY
West Lafayette, IN 47907

Work Performed for
OAK RIDGE NATIONAL LABORATORY
Operated by
UNION CARBIDE CORPORATION
for the

U. S. DEPARTMENT OF ENERGY

Office of Buildings and Community Systems

Printed in the United States of America. Available from
National Technical Information Service
U.S. Department of Commerce
5285 Port Royal Road, Springfield, Virginia 22161
NTIS price codes—Printed Copy: A21 Microfiche A01

This report was prepared as an account of work sponsored by an agency of the United States Government. Neither the United States Government nor any agency thereof, nor any of their employees, makes any warranty, express or implied, or assumes any legal liability or responsibility for the accuracy, completeness, or usefulness of any information, apparatus, product, or process disclosed, or represents that its use would not infringe privately owned rights. Reference herein to any specific commercial product, process, or service by trade name, trademark, manufacturer, or otherwise, does not necessarily constitute or imply its endorsement, recommendation, or favoring by the United States Government or any agency thereof. The views and opinions of authors expressed herein do not necessarily state or reflect those of the United States Government or any agency thereof.

ORNL/Sub/80-0082/3
Dist. Category UC-95d

BI-RADIANT OVEN

A

LOW-ENERGY OVEN SYSTEM

VOLUME III — APPLICATION AND TRANSFER OF THE TECHNOLOGY

TASK REPORTS

HEAT TRANSFER LABORATORY
SCHOOL OF MECHANICAL ENGINEERING
PURDUE UNIVERSITY
W. Lafayette, Indiana 47907

Date Published: March 1982

Prepared under Subcontract 86X-0082C for the

OAK RIDGE NATIONAL LABORATORY
Oak Ridge, Tennessee 37830

Operated by

UNION CARBIDE CORPORATION
for the
U.S. DEPARTMENT OF ENERGY
Contract No. W-7405-eng-26

FOREWORD

This is a report of work performed by Purdue University covering Phase 2 of the technology transfer of a bi-radiant oven. The work was sponsored by the Consumer Products Division of the Department of Energy through the Oak Ridge National Laboratory.

This Volume III contains the final reports of the three major tasks performed in Phase 2.

- In Part 1, several heating element configurations for uniform radiant flux over the entire food surface were evaluated through computer simulation. The best configuration of those considered was a diamond-shaped element.

- For Part 2, a control system was developed which provided proper power levels to the upper and lower heating elements. Also, the thermal performance of the oven system was determined through experimental testing in the laboratory.

- Part 3 deals with the categorization of foods into groups with common baking rates so that proper controls could be developed. In addition, characteristics of baking utensils were studied to determine effects on radiation within the oven system.

Volume II contains a final summary report of the information in Volume III.

BI-RADIANT OVEN

A LOW-ENERGY OVEN SYSTEM

Part 1 — Enclosure Analysis for Determining Cavity Efficiency

BI-RADIANT OVEN

A

LOW ENERGY OVEN SYSTEM

VOLUME III — APPLICATION AND TRANSFER OF THE TECHNOLOGY

PART 1 - ENCLOSURE ANALYSIS FOR DETERMINING CAVITY EFFICIENCY

Gordon G. Scheitlin
Dr. D. P. DeWitt

HEAT TRANSFER LABORATORY
SCHOOL OF MECHANICAL ENGINEERING
PURDUE UNIVERSITY
W. Lafayette, Indiana 47907

June 15, 1981

Prepared under Subcontract 86X-0082C for the

OAK RIDGE NATIONAL LABORATORY
Oak Ridge, Tennessee 37830

Operated by

UNION CARBIDE CORPORATION
for the
U.S. DEPARTMENT OF ENERGY
Contract No. W-7405-eng-26

TABLE OF CONTENTS

Page

LIST OF TABLES 1-v

LIST OF FIGURES 1-vii

NOMENCLATURE 1-ix

ABSTRACT 1-xi

1. INTRODUCTION 1-1

1.1 Background Literature 1-2
1.2 Objectives 1-4

2. ANALYTICAL PREDICTIONS OF HEAT FLUX CHARACTERISTICS 1-7

2.1 Model I: Irradiance Distribution 1-7
2.1.1 Heating Element Analysis, Bi-Radiant Oven III 1-10
2.1.2 Heating Element Selection, Bi-Radiant Oven IV 1-15
2.2 Model II: Enclosure Analysis 1-21
2.2.1 Radiant Exchange Analysis 1-21
2.2.2 Transient Thermal Analysis 1-23

3. EXPERIMENTAL HEAT FLUX CHARACTERISTICS 1-26

3.1 Description and Principles of the Heat Flux Gage 1-26
3.2 Time Dependent Heat Flux Measurements 1-30
3.3 Steady-State Heat Flux Measurements: Irradiance Distribution 1-35

4. COMPARISON OF ANALYTICAL AND EXPERIMENTAL RESULTS 1-39

4.1 Irradiance Distribution 1-39
4.2 Oven Temperatures 1-43

Page

5. PARAMETRIC STUDY OF OVEN PERFORMANCE..... 1-51

5.1 Effects of Insulation Thermal Conductivity..... 1-51
5.2 Effects of Cavity Wall Emissivity..... 1-53
5.3 Effects of Heating Element Diameter..... 1-53
5.4 Effects of Heating Element Input Power..... 1-56

6. SUMMARY AND CONCLUSIONS..... 1-59

LIST OF REFERENCES..... 1-67

APPENDICES

Appendix A: Model I: Irradiance Distribution..... 1-71

Appendix B: Model II: Transient Thermal Analysis..... 1-85

Appendix C: Heat Flux Measurements..... 1-99

Appendix D: Emissivity Measurements for Various Oven Materials 1-113

Appendix E: Program Listings..... 1-117

Appendix F: Nodal Placement and Sample Calculations..... 1-187

LIST OF TABLES

Table | Page

2.1 Description and Features of Experimental Bi-Radiant Ovens..... 1-11

2.2 Percentage of Total Irradiance Increase above the Minimum Irradiance Represented by each Iso-Irradiance Line..... 1-14

Appendix Table

A-1 Input Variables for Program COIL..... 1-73

A-2 Definition of Fortran Variables Used for Determining Cosβ at the Heating Element..... 1-82

B-1 Input Variables for Program OVENRAD..... 1-87

B-2 AGTAP Input for the Radiation Exchange Analysis..... 1-92

B-3 AGTAP Input for the Transient Thermal Analysis..... 1-92

B-4 Primary Input for Program AGTAP..... 1-95

C-1 Gage Response to Incident Heat Flux..... 1-108

C-2 Comparison of the Heat Flux Gages with Manufacturer's Specification..... 1-108

C-3 Intercomparison of Gage Responsivities..... 1-108

D-1 Normal Total Emissivity Values for Various Oven Materials..... 1-116

F-1 Nodal Element Definitions 1-189

F-2 Nodal System Initial Temperatures-Program AGTAP Input..... 1-198

F-3 Nodal System Thermal Capacitances-Program AGTAP Input 1-199

F-4 Nodal System Conductance Terms-Program AGTAP Input..... 1-200

F-5 Nodal System Radiative Links-Program AGTAP Input..... 1-204

F-6 Temperature Dependent Thermal Properties-Program AGTAP Input.. 1-205

LIST OF FIGURES

Figure		Page
2.1	Front View of the Oven Cavity Depicting the Direct and Single Reflection of Radiation Emitted from the Heating Elements to the Product Utensil.	1- 9
2.2	Analytical Mapping of Irradiance in Bi-Radiant Oven III. .	1-13
2.3	Analytical Mapping of Irradiance in Bi-Radiant Oven III. .	1-16
2.4	Analytical Mapping of Irradiance	1-18
2.5	Analytical Mapping of Irradiance	1-19
2.6	Analytical Mapping of Irradiance	1-20
3.1	Photograph of the Water-Cooled Heat Flux Gage.	1-27
3.2	Schematic of the Water-Cooled Heat Flux Gage	1-28
3.3	Irradiation and Convective Heat Flux in a Conventional Oven	1-31
3.4	Irradiation and Convective Heat Flux in a Bi-Radiant Oven.	1-33
3.5	Experimental Mapping of Irradiance in Bi-Radiant Oven III.	1-36
3.6	Experimental Mapping of Irradiance in Bi-Radiant Oven IV-A	1-37
4.1	Comparison of Predicted (a) and Measured (b) Irradiance Distribution Maps for Bi-Radiant Oven III.	1-40
4.2	Comparison of Predicted (a) and Measured (b) Irradiance Distribution Maps for Bi-Radiant Oven IV-A	1-42
4.3	Comparison of Predicted and Measured Element Temperatures.	1-44
4.4	Comparison of Predicted and Measured DOE Test Block Temperatures	1-45
4.5	Comparison of Predicted and Measured Average Cavity Wall and Door Temperatures	1-46

Page

4.6 Comparison of Predicted and Measured Cavity Air Temperature... 1- 47

5.1 The Effect of Insulation Thermal Conductivity on Oven Efficiency..... 1- 52

5.2 The Effect of Cavity Wall Emissivity on Oven Efficiency..... 1- 54

5.3 The Effect of Heating Element Diameter on Oven Efficiency..... 1- 57

5.4 The Effect of Heating Element Input Power on Oven Efficiency.. 1- 58

Appendix
Figure

A-1 Division of the Product Utensil and Heating Element into Differential Areas..... 1- 74

A-2 Oven Coordinate System showing Coordinates for Differential Areas on the Heating Element and at the Baking Plane..... 1- 78

A-3 Determination of β_c, the Angle Between the Normal to the Heating Element Differential Area and the Line Connecting the Two Differential Areas..... 1- 80

A-4 Thermal Radiation Emitted from the Lower Heating Element, Reflecting off the Lower Oven Wall, and Intercepting a Baking Plane Differential Area..... 1- 83

C-1 Cross-Sectional View of the Sensing Element Depicting the Heat Flow Through the Sensing Element and the Net Heat Flux to the Sensing Element..... 1-100

C-2 Placement of the Gage in Front of a Blackbody Furnace for Calibration..... 1-105

F-1 Photograph of the Experimental Apparatus, Bi-Radiant Oven IV-B 1-188

F-2 Expanded Schematic of the Outer Covers and Support Structure..... 1-190

F-3 Location of Inner Cavity Wall Nodal Elements..... 1-191

F-4 Location of Insulation Nodal Elements..... 1-192

F-5 Location of Exterior Oven Cover Nodal Elements..... 1-193

NOMENCLATURE

Symbol	
A	area, m^2
α	absorptivity
β	angle between the normal to a surface and the line connecting it to another surface
D	diameter of the furnace opening, cm
e	heat flux sensor output, mV
ε	emissivity
$E_b(T)$	blackbody emissive power at temperature T, W/m^2
F	view factor for radiant exchange
G	irradiance, W/m^2
h	convection coefficient, W/m^2-K
k	thermal conductivity, W/m-K
L	distance separating the furnace opening and the heat flux sensor, cm
l	distance separating the centers of two surfaces involved in radiant exchange, m
q''	net heat flux to sensing element, W/m^2
q''_c	convective heat flux, W/m^2
R	responsivity, $mV/(W/m^2)$
r_o	outer radius of the heat flux sensor, cm
S	sensitivity, $(W/m^2)/mV$
σ	Stefan-Boltzman constant, W/m^2-K^4

Symbol

t	thickness of the sensing element, cm
T	temperature, K
T_∞	ambient temperature,
T_1	temperature at r=0 on the heat flux sensing element, K
T_2	temperature at $r=r_o$ on the heat flux sensing element, K
ω	uncertainty value in experimental measurement procedures

Subscripts

b	black sensor surface
c	heating element (coil)
f	blackbody furnace
g	heat flux gage
bp	baking plane
r	reflective sensor surface
a	ambient air

ABSTRACT

In a Bi-Radiant Oven, absorption of irradiation from the heating elements -- both directly and through reflections at the cavity walls -- at the product is enhanced by the use of highly absorptive utensils and highly reflective cavity walls. Because of the close coupling between the product and heating elements, it is essential that the heating elements provide a uniform radiant flux over the entire product surface. To predict this flux field as a function of the heating element configuration, computer program COIL was developed. This program provides a mapping of the irradiance distribution at the product and determines the ratio of the maximum-to-minimum irradiance levels. Comparing the mappings from several different elements, the best configuration was found to be a modified, diamond-shaped element.

A special water-cooled heat flux gage was developed for providing absolute magnitudes of the radiant and convective heat flux at its surface. Since these modes of heat transfer play important roles in supplying heat flux to the product, the gage is a useful tool in determining the time dependent heat flux characteristics within an oven. Under conditions of steady-state operation, the heat flux gage is also used to

experimentally map the irradiance distribution at a plane within the oven cavity.

Further analytical modeling is accomplished through the generation of computer codes OVENRAD and AGTAP which predict the thermal response for the entire oven. From these programs, oven temperatures are predicted for a specific oven design under conditions of constant power input to the heating elements. Comparing analytical predictions with laboratory measurements made under identical conditions showed that the predicted oven efficiency was in error by only 0.5%. Achieving good results from the comparison of predicted and measured oven temperatures provided a basis for using the analytical model for testing the effects of basic oven design parameters on oven thermal efficiency.

From the parametric study on oven efficiency, two oven parameters are seen to have major effects. The first parameter is the cavity wall emissivity which markedly increases oven efficiency for values less than 0.10. Decreasing the cavity wall emissivity from 0.31 to 0.10 resulted in an increase in oven efficiency from 17.9% to 24.9%. The second important parameter is the heating element diameter which causes oven efficiency to rise sharply as the element approaches a filament-type heater. The effect of decreasing the element diameter from 0.66 cm to 0.3 cm is to increase the oven efficiency from 17.9% to 35.3%

1. INTRODUCTION

In a domestic electric oven, energy is dissipated from the upper and lower heating elements by both radiation and convection. The processes by which this energy is transferred to a product depend on the design and construction of the oven cavity and on the thermal properties of the material used. In a conventional oven, with high emissivity (absorptivity) walls and a low emissivity utensil, as the heating element cycles (maintaining the mean temperature as set by the thermostat), radiant energy dissipated from the element is absorbed at the walls but reflected from the utensil. The purpose of the walls is to reradiate energy to the product, as well as convect heat to the oven air, thereby providing a high temperature ambiance for convection to the product.

In a Bi-Radiant Oven system, on the other hand, cavity walls have a low emissivity and product utensils have a high emissivity. The heating element is operated continuously, instead of cycling, and radiant energy dissipated from the element is reflected from the walls and absorbed at the utensil. Therefore, radiant power dissipated from the heating element is transferred more directly to the product.

The purpose of this study is to perform the thermal analysis of domestic electric ovens, thereby providing quantitative methods of characterizing oven performance. The analysis will apply to both

conventional and Bi-Radiant Ovens. However, special emphases is placed on aspects peculiar to the Bi-Radiant Oven system.[1]

1.1 Background Literature

A literature search was conducted for studies concerning the radiative and convective heat exchange within oven enclosures and the heat loss through oven walls. Pertinent literature included a study conducted at Corning Glass Works in 1931 [1] and, more recently, reports published under the sponsorship of the Department of Energy (DOE)[2,3,4].

The Corning [1] study established the amounts of energy delivered to a product by convective and radiative modes of heat transfer. Separation of these two modes was accomplished by comparing the water boiling rates of a low emissivity tinware pan and a high emissivity glass pan. The results showed that baking in glassware caused an improvement in energy efficiency due to an increased absorption of radiative energy. A limitation of this study is its inability to discern the instantaneous or local heat flux characteristics. Also, the analysis makes no attempt to characterize the performance of the oven itself, centering instead only on the effects of pan emissivity on energy efficiency.

The reports sponsored by DOE provided background information concerning energy efficiency standards for home appliances, including electric ovens. The recommended method for determining oven efficiency [3] is to measure the total heating element input power required to increase

1 Five versions of the Bi-Radiant Oven have been built since 1974 and their construction details are summerized in Table 2.1.

the temperature of a black anodized aluminum block (referred to as the DOE test block) by 130°C. The efficiency factor (EF), hereafter referred to simply as oven efficiency, is defined as the ratio of the energy stored in the block to the total energy input to the heating elements.

As a basis for setting minimum efficiency standards, Science Applications Incorporated (SAI) developed an analytical model for predicting oven performance[2]. The model, consisting of an electrical-thermal analog of the oven system, is used to compare oven efficiencies when several oven design parameters are altered. Each major oven component is represented as a node in the model, a thermal capacitance is calculated for each node, and the resistive network consisting of conductive, convective, and radiative elements is laid out between nodes. The distribution of nodes in the oven is as follows: 1 node per heating element, 2 nodes for the DOE test block, 1 node for the upper cavity air, 1 node for the lower cavity air, 1 node per interior cavity wall, 1 node for the ambient room air, and 3 nodes between each interior wall node and the ambient air node. Input assumptions for interior wall and test block heat transfer coefficients and oven vent flow rates were varied such that computed values of energy consumption and block temperature matched laboratory test data.

The design parameters tested by the analytical model were the power to the heating elements, oven vent flow rate, door glass area, heating element surface area, insulation thermal conductance, and overall oven thermal mass. Of these, the power to the heating element and the door glass area affect the efficiency by less than 5%, while the effects of

insulation conductance and overall thermal mass are shown to be the most important design parameters effecting efficiency.

The SAI analytical model provides a general description of the oven as an enclosure. However, their nodal network does not consider two very important design features which greatly affect oven performance. Specifically, these are the heating element diameter and cavity wall emissivity. Note that these two aspects are of special importance in a Bi-Radiant Oven. Additional drawbacks to the model are the somewhat arbitrary method of handling the convective processes within the oven cavity and the limited nodal arrangement (especially the single node per cavity wall) which defines the oven system.

1.2 Objectives

Having reviewed the available literature, a need is recognized for an improved understanding of the heat transfer processes which occur within an oven. The purpose of the present study is to provide more detailed analytical and experimental methods for determining heat transfer characteristics within an oven enclosure. The objectives are:

1. To develop heat transfer models and computer codes for predicting radiant heat transfer within an oven enclosure.

2. To develop a methodology for experimentally characterizing heat flux levels within an oven enclosure.

3. To provide a capability for predicting oven performance (efficiency) and to compare predictions with experimental oven results.

The first objective involves the analytical assessment of the radiant heat exchange within an oven enclosure. A model was developed for predicting the distribution of irradiance over a utensil surface as a function of the heating element configuration. This model was essential for the evolution of a second model which performs a diffuse oven enclosure analysis predicting the heat flux levels and temperatures within the oven.

To satisfy the second objective, a special heat flux gage was developed. This gage consists of a water-cooled baseplate with two, circular-foil heat flux sensors press fitted into its surface. The output from the sensors is used to discern the convective and radiative components of the total heat flux incident at the gage surface. The gage is an important tool in characterizing the oven and in validating the analytical models which predict heat flux levels within the oven cavity.

The final objective states a desire to improve oven performance through the use of the analytical models and the heat flux gage. The goal is to realize improvements in the thermal efficiency of an oven without the necessity of constructing and testing each energy saving design which is of interest.

For the purpose of fulfilling these objectives, a dual approach has been used: analytical modeling paralleled with experimental measurements. For the most part, radiation is handled using analytical models, while parameterization of the convective exchange is handled experimentally. In this manner, a complete analysis of oven performance and

operation is provided. In this report, analytical results will be presented first, then experimental, followed by the verification of analytical predictions through intercomparison with experimental measurements. Finally, a parametric study of the effects of oven design parameters on oven efficiency is presented.

2. ANALYTICAL PREDICTIONS OF HEAT FLUX CHARACTERISTICS

Analytical modeling of the radiant exchange within an oven cavity is used to predict the irradiance distribution over a baking plane as a function of the heating element configuration. The major parameters considered in the irradiance distribution model, referred to as Model I, are the heating element configuration, cavity size, and product geometry.

The enclosure analysis model, referred to as Model II, incorporates the logic of its predecessor (Model I) into a diffuse enclosure analysis. Model II is limited only by the stipulation of diffuse surfaces; walls, product, and heating elements. In use, Model II predicts the thermal response of the oven cavity, including temperatures of the cavity air, heating elements, cavity walls, and product, as a function of the heating element input power.

2.1 Model I: Irradiance Distribution

In a Bi-Radiant Oven it is very important for a heating element to provide a uniform field of radiant flux over the surface of a product and utensil, due to their high absorptivities. If an element were to present a non-uniform flux, it would result in an inconsistent product doneness. Note that while intuition alone might permit the construction of an acceptable element shape for providing a uniform flux field, if

numerous element configurations are to be evaluated, a quantitative intercomparison between proposed shapes is needed. It is the purpose of Model I, then, to provide a systematic, consistent means for assessing the performance of individual heating element configurations.

As the basis for comparison, Model I predicts the irradiance distribution on the baking plane for a specified heating element configuration. The model assumes the conditions of isothermal, circular cross sectional heating elements with diffuse-gray radiating surfaces and that any reflection of radiation at the cavity walls is perfectly specular. Also, only direct emission from the heating elements and single reflections of this emission at the cavity walls are considered in determining the irradiation at the baking plane. Referring to Figure 2.1, input to the model consists of element configuration and location; size, shape and location of the product utensil; cavity size; and baking plane elevation. Heating element configurations are specified as a series of straight line segments and any effects of shadowing by the product/utensil are considered. Further information on Model I is presented in Appendix A. The program listing (Program COIL) is provided in Appendix E.

Note that considering only the direct and single, specular reflection paths of radiation emitted from the heating elements imposes a special restriction on the analysis since irradiation at the product will also be due to multiple cavity wall reflections as well as cavity wall emission. These effects, however, are considered as secondary. Accounting for them would tend to even out the irradiance distribution, and at the same time seriously complicate the model. Neglecting them

ORNL-DWG. 81-23715

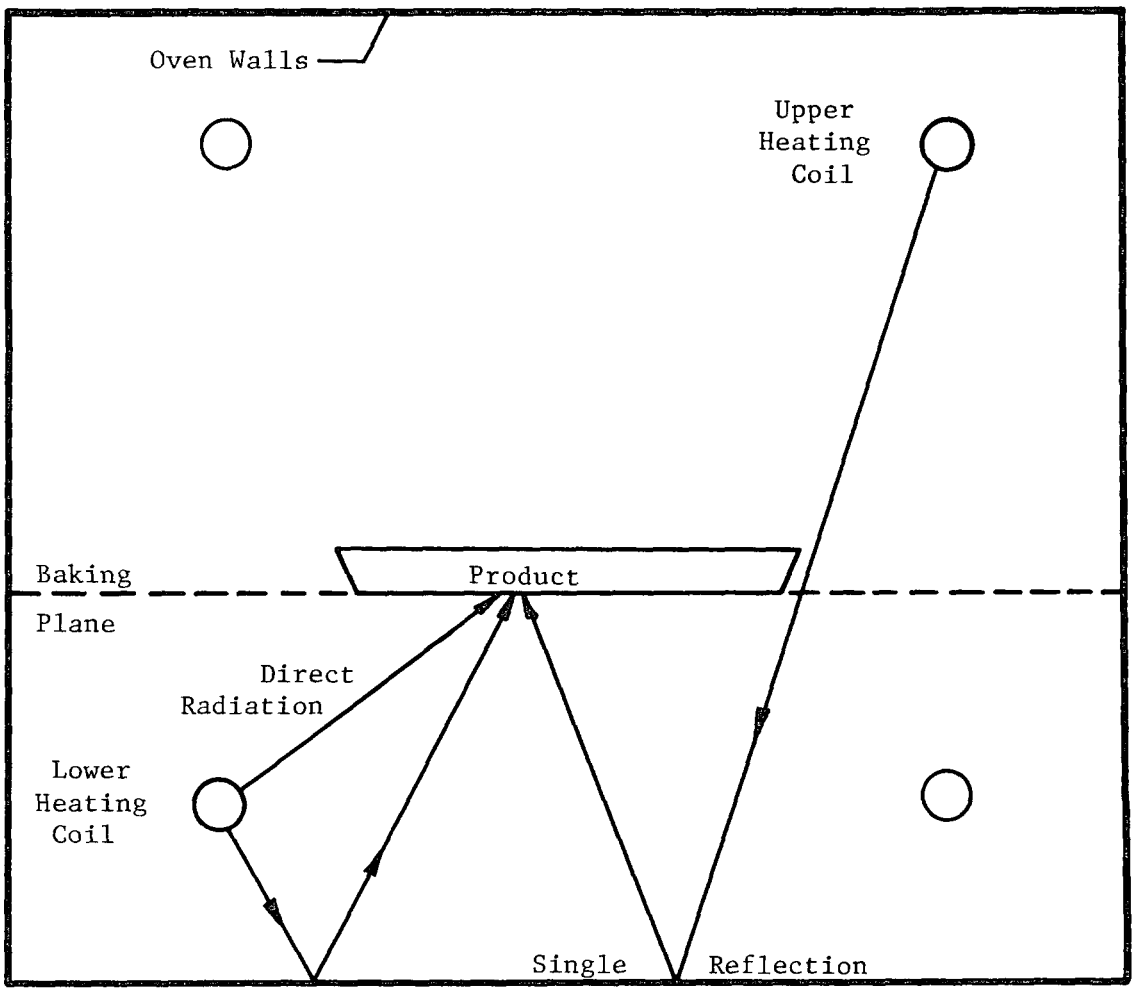

Figure 2 Front View of the Oven Cavity Depicting the Direct and Single Reflection of Radiation Emitted from the Heating Elements to the Product Utensil

increases the ability of the model to indicate faults in an element design through the calculation of a much higher ratio of the maximum to minimum irradiance levels than otherwise would be obtained. Along with this, the ability to predict the irradiation level which would be experienced in an actual oven is reduced. The use of Model I, then, provides the means to calculate the following parameters:

1. The view factor from either heating element to an arbitrarily small area on the baking plane, and

2. The ratio of the irradiance at any location on the baking plane to a reference value, thus generating a dimensionless irradiance distribution which is used to illustrate the performance of the heating element.

Output from Model I consists of view factors or irradiance values from either heating element to discrete points on the baking plane, each point being the center of an arbitrarily small differential area as discussed in Appendix A. The view factor calculated in Model I is defined as the fraction of diffuse radiant energy emitted from the heating element which strikes the differential baking plane area either directly or after a single specular reflection at one of the cavity walls. Finally, inputing Model I results into a contour plotting routine, plots are obtained indicating lines of constant irradiance (iso-irradiance lines) over the x,y span of the baking plane.

2.1.1 Heating Element Analysis, Bi-Radiant Oven III

Table 2.1 describes the construction of three of the five prototype Bi-Radiant Ovens which have been built to date. From this table,

TABLE 2.1. Description and Features of Experimental Bi-Radiant Ovens

Model*	Description	Cavity Size DxWxH (cmxcmxcm)	Heating Element
III	Converted Sears Kenmore Oven Model 911.9257611 with hand polished walls of emissivity 0.11	43x56x41	Figure 2.2
IV-A	Prototype oven with replacable cavity walls; 10.8 cm thick insulation with thermal conductivity 0.046 W/m-K; heating element diameter of 0.66 cm; aluminum sheet metal cavity walls, specular, with emissivity of 0.03; no venting; equipped with product weighing system.	43x58x43	Figure 2.6
IV-B	Same construction features as above, but with diffuse cavity walls of emissivity 0.31.	43x58x43	Figure 2.6

* Bi-Radiant Ovens I and II were the initial ovens in which the Bi-Radiant oven concept was demonstrated. These ovens were not suitable for obtaining laboratory measurements, but were intended only for demonstrating qualitative results.

consider Bi-Radiant Oven III, and its heating element configuration as shown in Figure 2.2(a). The elements for this oven are positioned 38 mm (1.5 in) from the upper or lower cavity wall and the baking plane is located 89 mm (3.2 in) from the lower wall.

For the conditions of no product and equal power to the upper and lower heating elements, Model I provides the dimensionless irradiance distribution on the baking plane as shown in Figure 2.2(b). The eleven curves on this plot, labeled A through K, represent lines of constant irradiance, G (W/m^2), with the maximum irradiance value, G_{max}, near K (95% level) and the minimum, G_{min}, near A (5% level). Table 2.2 lists the percent of the total irradiance increase above G_{min} associated with each iso-irradiance line. The ratio of the maximum to minimum irradiance, G_{max}/G_{min}, is 5.74 for this element shape and cavity size. This relatively high ratio is an indication of the non-uniformity of the irradiance over the baking plane.

In the irradiance distribution plot of Figure 2.2(b), widely space iso-irradiance lines indicate slow gradual changes in irradiance levels. Regions of closely spaced iso-irradiance lines indicate sharper or steeper changes in irradiance. It follows from this plot that the heating element of Bi-Radiant Oven III provides a highly uniform irradiance distribution in the central region of the baking plane, making this area desirable for baking. Nearer the walls, however, the rapid decline in the irradiance level could cause a product located in this region to be unevenly cooked. Such an effect was qualitatively observed when white cakes were baked in this region.

ORNL-DWG. 81-23716

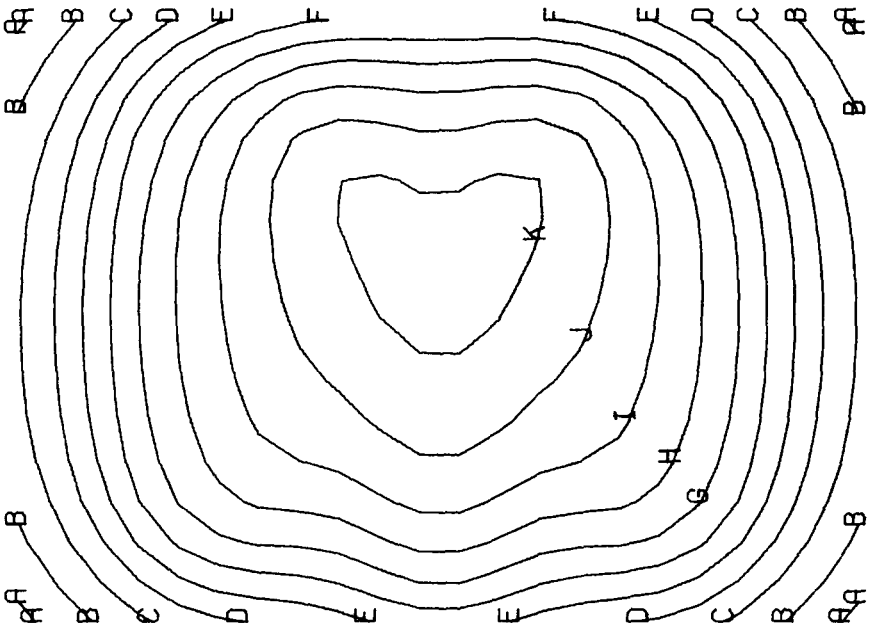

(b)

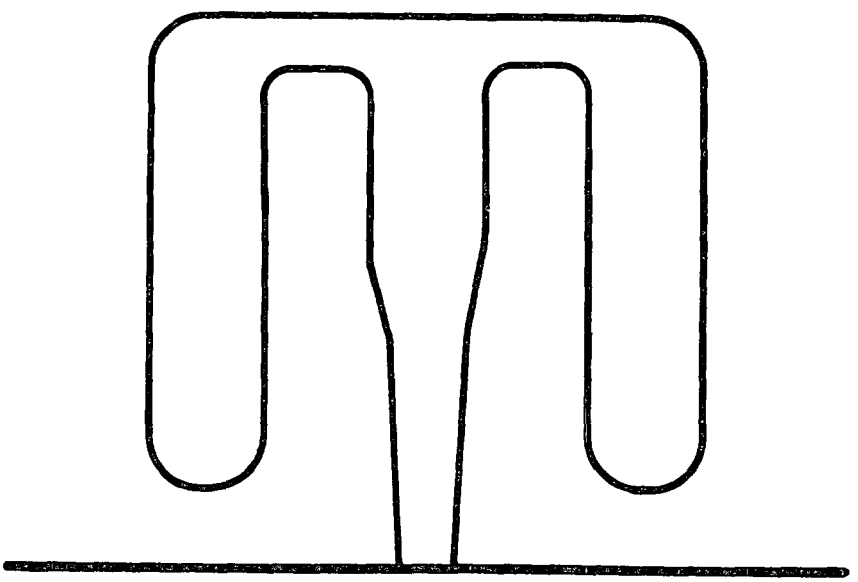

(a)

Figure 2.2 Analytical Mapping of Irradiance in Bi-Radiant Oven III

(a) Element Configuration, Total Length = 248 cm.
(b) Irradiance Distribution with no Product, $G_{max}/G_{min} = 5.74$

TABLE 2.2. Percentage of Total Irradiance Increase above the Minimum Irradiance Represented by Each Iso-Irradiance Line.

LINE	% OF TOTAL INCREASE*
A	5.0
B	10.0
C	20.0
D	30.0
E	40.0
F	50.0
G	60.0
H	70.0
I	80.0
J	90.0
K	95.0

* The irradiance difference between G_{max} and G_{min} is considered to be 100%. It follows that line A, for example, represents the iso-irradiance level that is 5% above G_{min}.

The presence of a product on the baking plane will of course change the irradiance distribution. Consider a cake pan utensil (230 mm diam. x 38 mm high) on the same baking plane as described above for Figure 2.2, but positioned relative to the heating elements as shown in Figure 2.3(a). The distribution over the utensil surface is shown in Figure 2.3(b), where curves A through K represent irradiance increments between the minimum and maximum values as indicated in Table 2.2. Note that the maximum to minimum irradiance ratio, G_{max}/G_{min}, is only 1.18. Compared to the irradiance ratio of 5.74 for the entire baking plane, as was indicated in Figure 2.2(b), this smaller ratio reinforces the previous implication of a highly uniform irradiance distribution over a utensil in this region.

2.1.2 Heating Element Selection, Bi-Radiant Oven IV

In the design of a new prototype Bi-Radiant Oven, designated as Bi-Radiant Oven IV, special emphasis was placed on the selection of a heating element configuration. The irradiance distribution plot of Figure 2.2(b) suggests two features for optimizing element performance. First, it is desirable to have a small G_{max}/G_{min} ratio, indicating a small change in irradiance levels over the baking plane. Second, a large region of widely spaced iso-irradiance lines is desirable since this would indicate a large region of uniform irradiance conducive for baking. Also, it is favorable to minimize the total heating element length, thus decreasing its thermal mass and thereby reducing its stored energy.

Three of the more promising configurations devised for Bi-Radiant Oven IV (as described in Table 2.1) are presented in Figures 2.4(a),

ORNL-DWG. 81-23717

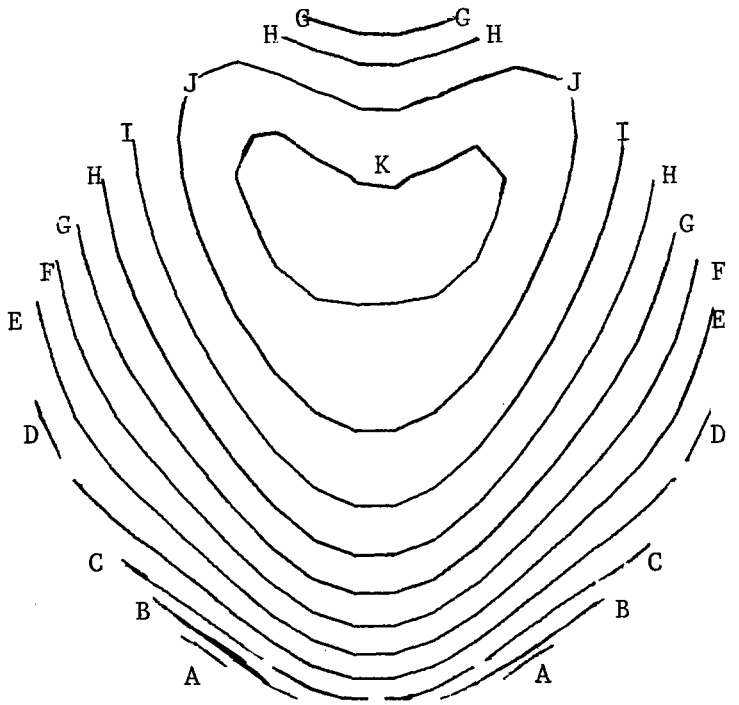

(b)

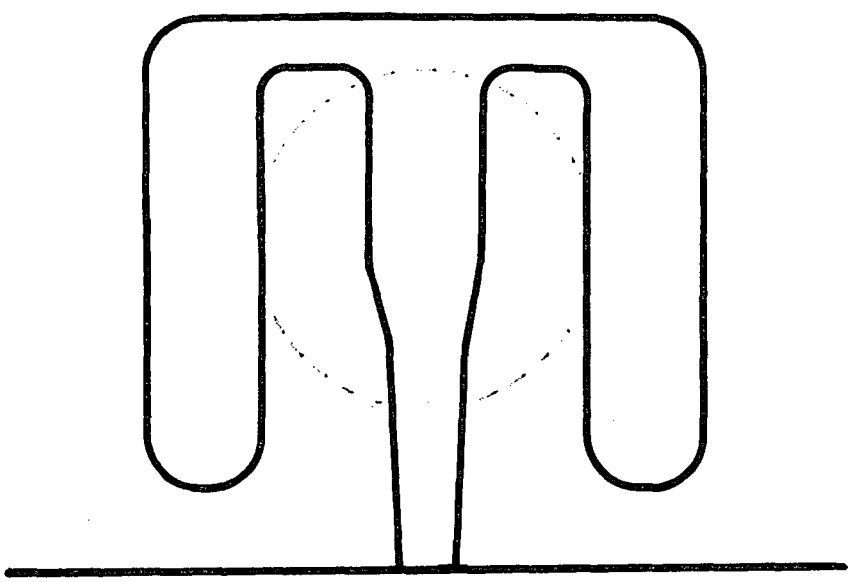

(a)

Figure 2.3 Analytical Mapping of Irradiance in Bi-Radiant Oven III

(a) Outline of Pan above Lower Heating Element
(b) Irradiance Distribution Over the Pan, $G_{max}/G_{min} = 1.18$

2.5(a), and 2.6(a), and their associated irradiance distribution plots are shown in Figures 2.4(b), 2.5(b), and 2.6(b), respectively. The conditions for the ensuing comparisons are a baking plane location 114 mm (4.5 in) from the lower wall, and a heating element plane located 38 mm (1.5 in) from the lower wall. For these comparisons, wall reflectivity is considered to be unity.

The three-loop element of Figure 2.4(a) is a common shape seen in many conventional ovens. The diamond-shaped element of Figure 2.5(a) is a design proposed by virtue of its shorter length and comparably low irradiance ratio. Attempts at improving the irradiance distribution of the diamond-shaped element resulted in the modified-diamond shaped element shown in Figure 2.6(a). Applying the optimization parameters listed above, it is readily seen that both the diamond and modified-diamond shaped elements provide a better irradiance distribution for a product, a lower overall irradiance ratio, and a lesser thermal mass by virtue of their shorter lengths.

Through a close examination of the irradiance distribution plots for the diamond and modified-diamond elements, it is seen that the latter element provides a slight improvement over the former element, while also having a slightly shorter overall length. Offsetting this advantage is the slightly larger irradiance ratio of the modified-diamond shaped element. It was decided that the modified-diamond element of Figure 2.6(a) should be used in Bi-Radiant Oven IV due to its probable ease of construction (the sharp bend in the Diamond shaped element was seen as a possible point of difficulty.)

ORNL-DWG. 81-23718

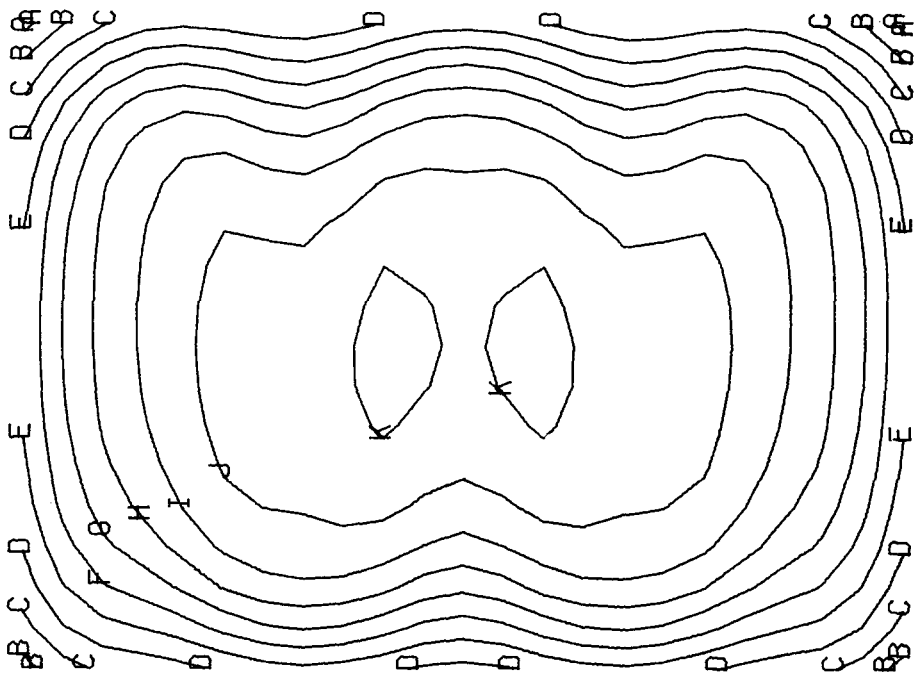

(b)

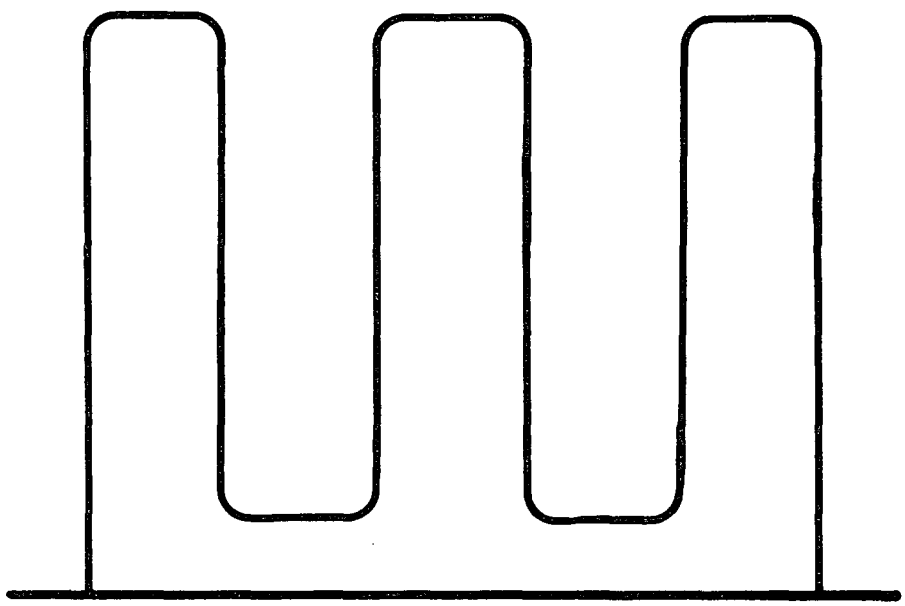

(a)

Figure 2.4 Analytical Mapping of Irradiance

(a) Three-Loop Element, Total Length = 256 cm.
(b) Irradiance Distribution, $G_{max}/G_{min} = 3.33$

ORNL-DWG. 81-23719

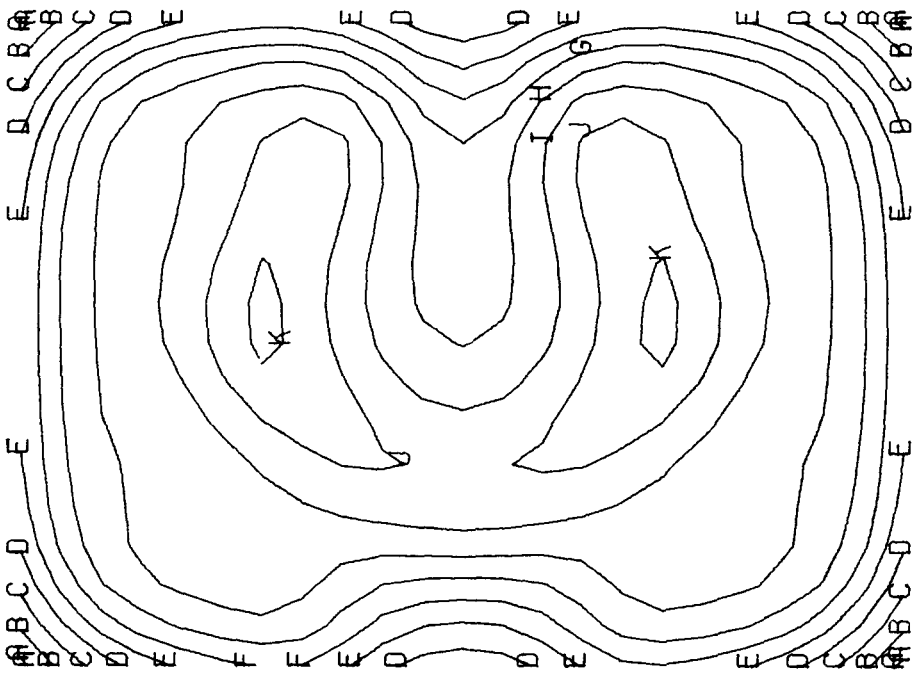

(b)

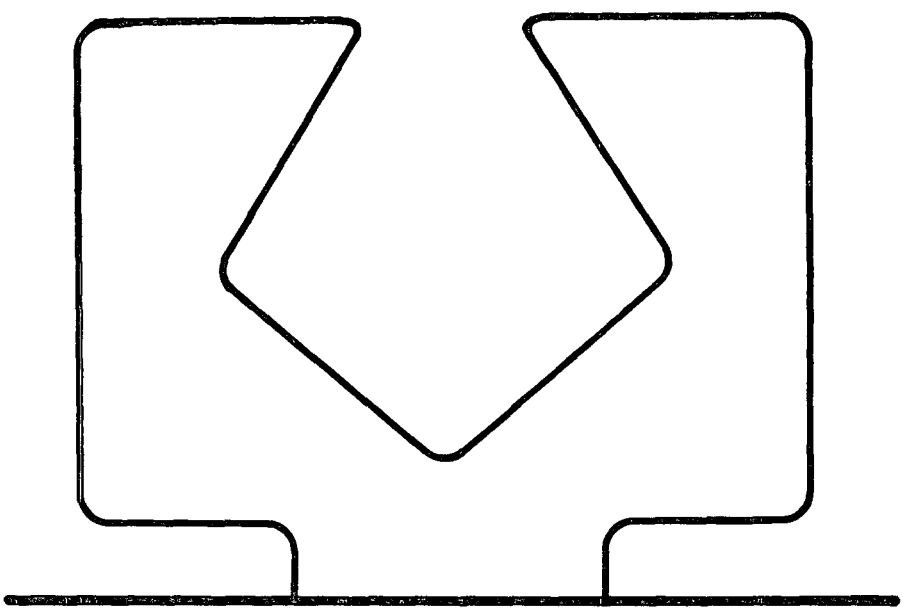

(a)

Figure 2.5 Analytical Mapping of Irradiance

(a) Diamond Shaped-Element, Total Length = 222 cm.
(b) Irradiance Distribution, $G_{max}/G_{min} = 3.11$

ORNL-DWG. 81-23720

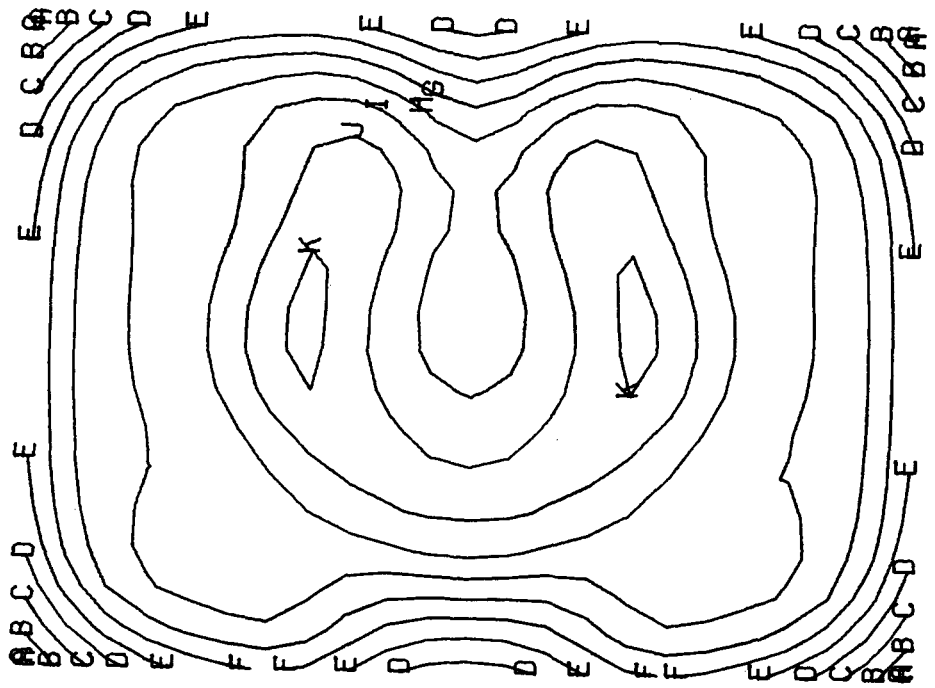

(b)

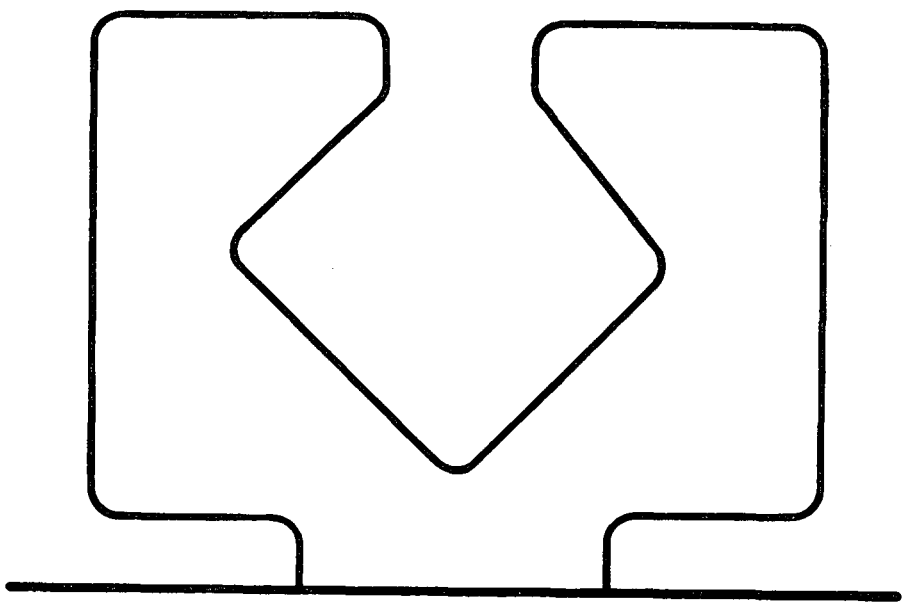

(a)

Figure 2.6 Analytical Mapping of Irradiance

(a) Modified Diamond Shaped Element, Total Length=222 cm.
(b) Irradiance Distribution, $G_{max}/G_{min} = 3.16$

Note that while Model I does not perform a complete analysis of the radiant exchange within an oven cavity, it does handle an important part of it. The ability to predict the irradiance distribution on the baking plane as a function of the heating element configuration increases the current understanding of the radiative coupling between the product and heating element. Improving the performance of the oven through the determination of a pseudo-optimum element configuration is a practical application of the understanding gained from Model I.

2.2 Model II: Enclosure Analysis

Thermal analysis of oven operation is divided into two parts, a radiant exchange analysis and a transient thermal analysis. Written as two separate programs, the output from the radiant exchange analysis program, OVENRAD, is held in semi-permanent storage to be used as input for the transient thermal analysis program, AGTAP. (Abbreviated General Thermal Analysis Program.[1]) For the sake of consistency, and for later comparisons with laboratory data, the analytical modeling considers oven response when the DOE test block is used as the thermal load.

2.2.1 Radiant Exchange Analysis

The radiant exchange analysis considers the interior of the oven cavity as a combination of diffuse-gray surfaces and determines the radiant heat exchange between individual surfaces using the radiosity method[5]. The simplifying assumption of diffuse-gray surfaces substantially reduces the calculations involved in determining the total radiant exchange factors necessary for the radiosity method. Since the oven

1 Program AGTAP was made available through the program office of the Technology and Consumer Products Branch, DOE, Washington.

is actually an enclosure, it is envisioned that the differences of specular versus diffuse reflections at the cavity walls will have little effect on the outcome from the analytical analysis. Also, since the spectral distributions of the absorbed and emitted radiation are similar, and there are no large variations in spectral emissivity for any of the oven materials over the wavelength region involved, the gray surface assumption is reasonable. In the radiosity method, the interior cavity, comprised of the heating elements, product, and oven walls, is subdivided into isothermal regions (surfaces). The view factors between all these surfaces are calculated and expressed in matrix form, and are a function of only the geometry, location, and number of surfaces which are used to represent the oven interior. Once a particular cavity is subdivided into individual surfaces, and the view factor matrix generated, this matrix remains unchanged throughout the remainder of the analysis. Therefore, in the transient analysis of an oven cavity, where surface temperatures and heat fluxes are being recalculated at small discrete time intervals, the view factor matrix need not be re-evaluated.

The calculation of the view factor matrix is accomplished in Program OVENRAD. Much of the logic and programming methods used in OVENRAD stem directly from Model I, the Irradiance Distribution Model (Program COIL). The details of Program OVENRAD are explained in Appendix B, a program listing is provided in Appendix E.

Output from OVENRAD, besides being printed for user scrutiny, is placed in semi-permanent storage to be used as input for the transient thermal analysis program. The stored information consists of the upper

and lower heating element diameters, the number of surfaces which represent the oven interior, the surface area of each of these surfaces, and the view factor matrix.

2.2.2 Transient Thermal Analysis

The transient thermal analysis predicts temperatures at the numerous nodal points which define the oven. These nodal points may be arbitrarily defined, however, the optimum nodal network has each node as the center of an isothermal region (volume).

This analysis is subdivided into two parts. First is the radiation heat exchange between the interior oven cavity surfaces (nodal points) as a result of the given power inputs to the upper and lower heating elements. Second is the conduction and convection exchange between all nodal points and the determination of the resulting nodal temperatures through an energy balance.

Estimation of the convective heat transfer occurring in the oven cavity is accomplished through the use of standard correlations [6,7] and the heat flux gage for the walls and product. The Rebrov equation [8], for the convective heat transfer coefficient about a horizontal cylinder is applied at the heating elements. The convective heat transfer coefficients at the cavity walls and product (test block) are assumed to be constant throughout the course of oven operation. At the heating elements, the convective heat transfer coefficient is recalculated at each time increment. More information concerning the establishment of the convective phenomena within the oven cavity is found in Appendix B.

The radiation heat exchange analysis is a separate subroutine which is called at the start of each time step during the transient analysis. This subroutine determines the magnitude of the radiant heat flux levels at each nodal surface involved in radiant exchange with the heating elements. Once these flux levels have been calculated, control is returned to the main program, AGTAP.

Program AGTAP determines the temperature at each nodal point as a function of the thermal capacitance of the node and the thermal resistance network adjoining nodes. At each time increment, a lumped thermal capacitance method [6] is used to predict the new nodal temperatures. The nodal network used to define the oven consists of a total of 162 nodes. There is 1 nodal point for each heating element, 1 nodal point for the DOE test block, 1 nodal point each for the upper and lower halves of the cavity air, 4 nodal points for each of the six inner cavity walls, and 1 nodal point representing the ambient surroundings. The remaining 132 nodes are divided among the insulation, exterior cover, and oven door. With this arrangement, it is possible to approximate the temperature gradient over the surface of each cavity wall and to account for the differences in bulk air temperature between the upper and lower portions of the oven cavity.

Handling of temperature dependent properties for some nodal elements (such as the insulation, test block, cavity air, rack, and air temperature probes) is accomplished through the use of the tabular input allowed by AGTAP. This input scheme involves specifying independent and dependent variables in tabular form for AGTAP. A linear interpolation within these tables is conducted by the program to obtain values for the

dependent variables whenever they are specified.

The input[2] to the transient thermal analysis program is simplified such that the effects of single parameters on oven efficiency can be examined. Wall emissivity, insulation thermal conductivity, heating element input power, and heating element diameter are some of the parameters which can easily be varied within the program input. More information on the transient thermal analysis program, including the radiation heat exchange calculations, is presented in Appendix B. A listing of the thermal analysis program, AGTAP, is provided in Appendix E.

Output from the analytical enclosure analysis, provided at specific time increments, consists of the temperatures for all nodal elements defining the oven. The oven efficiency is calculated and printed when the temperature of the node representing the DOE test block reaches 130°C above the ambient. From the program output, plots are generated depicting the heating element temperature, DOE test block temperature, cavity walls and door temperatures, and average cavity air temperature versus time. In order to eliminate repetition, presentation of these results is delayed until Section 4.

[2] The nodal placement and sample calculations for determining input to Program AGTAP are presented in Appendix F.

3. EXPERIMENTAL HEAT FLUX MEASUREMENTS

In order to experimentally characterize the heating environment within an oven, a heat flux gage was developed to provide local measurements of the irradiance, G (W/m^2), and the convection heat flux, q''_c (W/m^2). Use of the gage involves two types of measurements: time dependent heat flux measurements to determine the dynamics of heat flux levels at a single point within the oven cavity and steady-state heat flux measurements to obtain the irradiance distribution over an entire baking plane. Details concerning the gage operation and calibration are given in Appendix C.

3.1 Description and Principles of the Heat Flux Gage

The heat flux gage is shown in the photograph of Figure 3.1. The body of the unit is a nickel-coated, water-cooled, copper plate which serves as the mounting base for the flux sensors, identified as the black and reflective discs on the upper surface of the plate. The water and sensor output leads are wrapped in metallic shielding to minimize adverse thermal effects of the oven cavity. The water-cooling arrangement shown in Figure 3.2 serves to maintain the unit at a constant temperature during its use.

ORNL-Photo 8877-81

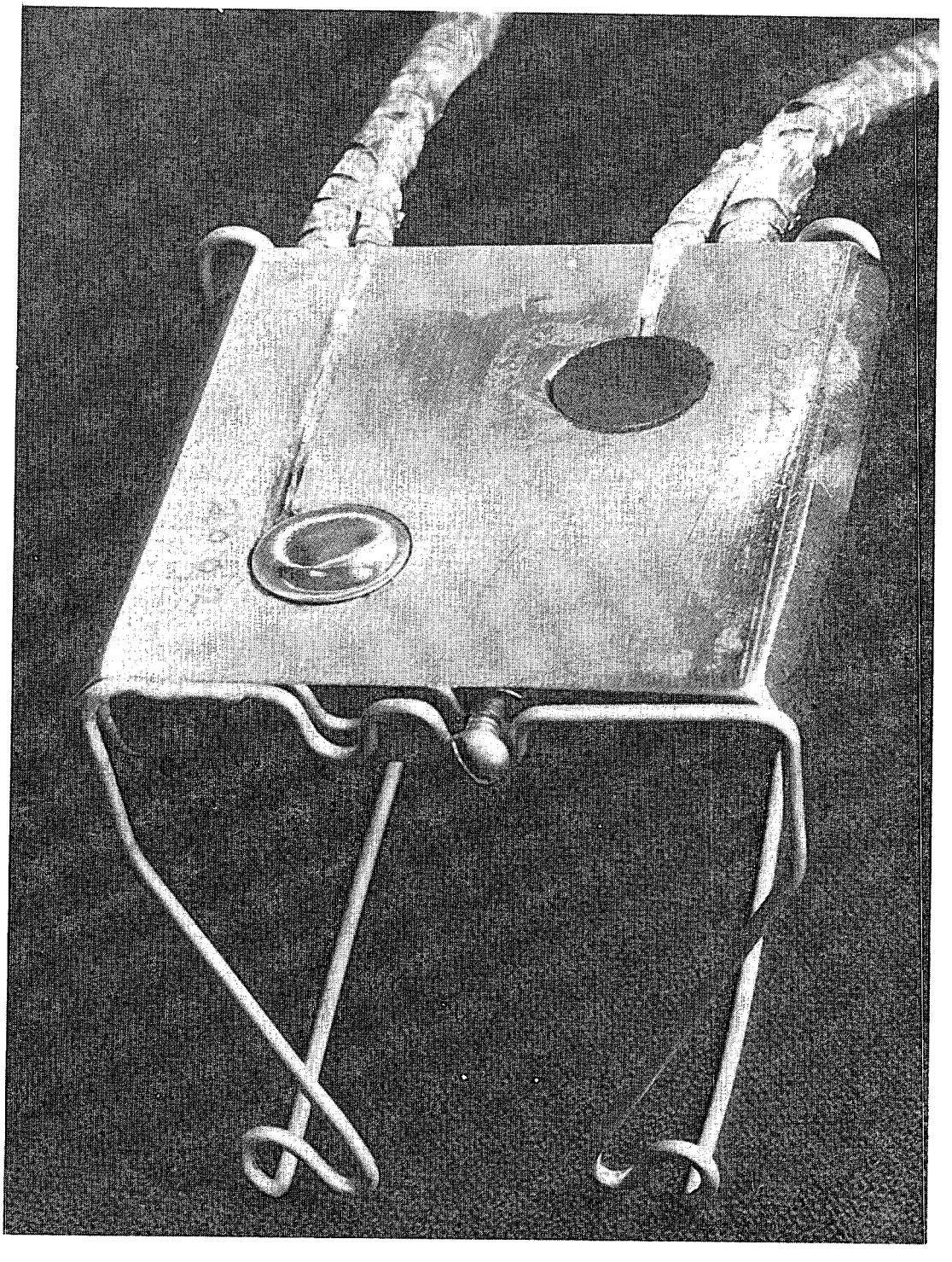

Figure 3.1 Photograph of the Water-Cooled Heat Flux Gage

ORNL-DWG. 81-23721

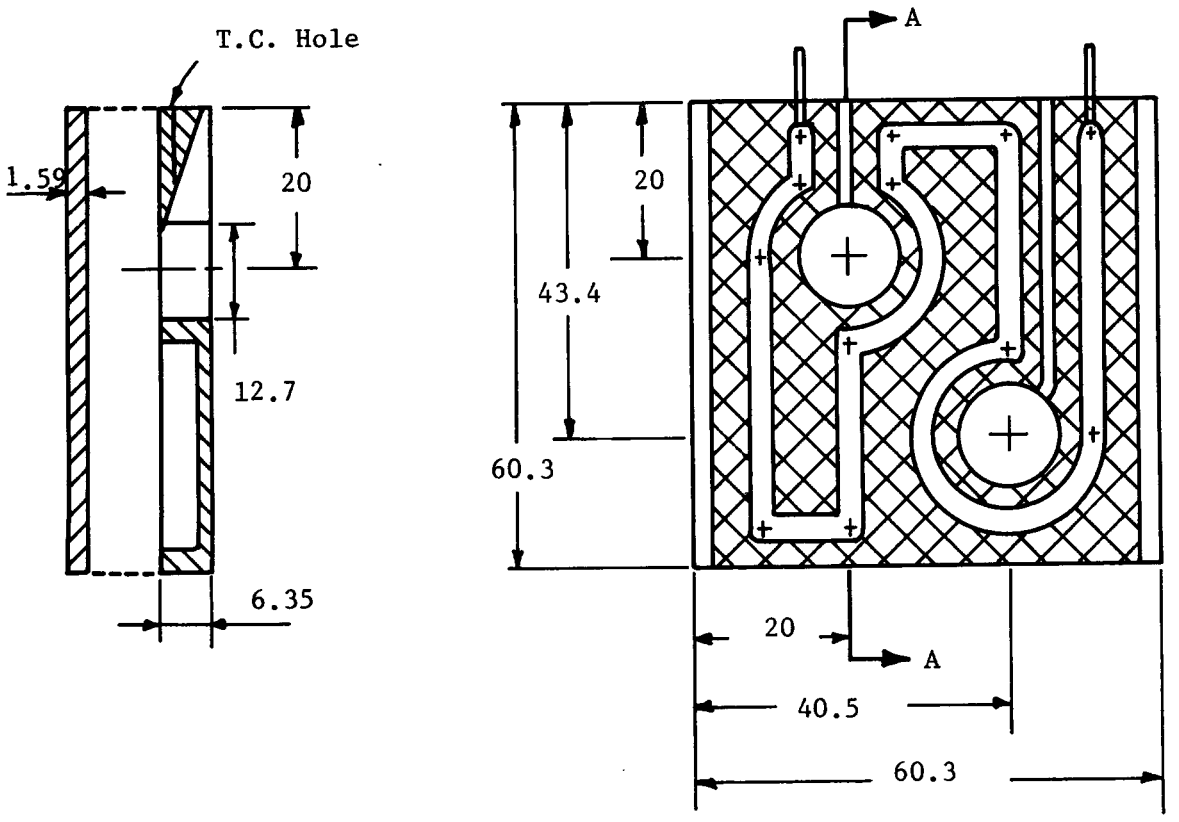

Figure 3.2 Schematic of the Water-Cooled Heat Flux Gage (all dimensions in millimeters).

The gage sensors are Gardon-type[2] flux sensors which provide a signal output proportional to the net heat flux on their surface. For the gage, two types of surfaces are employed. With the black surface, the dominant heat transfer process to the gage is absorption of irradiation from the oven energy sources. With the reflective surface, absorption of irradiation is substantially reduced and the net heat flux to the gage is mostly due to the convection process between the sensor surface and the oven ambient air. For the separate sensors, it was shown in Appendix C that the signal output, e (mV), for the black (b) and reflective (r) surfaces, can be expressed as

$$e_b = R_b\left[\left[\alpha_b G - \varepsilon_b \sigma T_g^4\right] + h(T_\infty - T_g)\right] \tag{3.1}$$

$$e_r = R_r\left[\left[\alpha_r G - \varepsilon_r \sigma T_g^4\right] + h(T_\infty - T_g)\right] \tag{3.2}$$

where R, $(mV/(W/m^2))$, is the responsivity of the sensor, and the terms in the brackets represent the net absorbed heat flux at the gage surface. The first two terms include the radiative processes of absorbed irradiation and gage emission. The third term within the brackets represents the convection process, where T_∞ is the ambient air temperature and T_g is the temperature of the gage surface.

Observations of oven air temperature in the vicinity of the gage provide a representative value for T_∞ as a function of baking time. The temperature of the sensor surface, T_g, is taken to be that of the water-cooled plate (as discussed in Appendix C) and is monitored during the course of operation of the gage. From these observations, and from

2 The heat flux sensors were supplied by Thermogage Inc., Frostburg, Maryland.

knowledge of the gage characteristics (ε, α, R)[3], the measurement equations, Equations 3.1 and 3.2, can be solved simultaneously to obtain values for the irradiation, G, and the convective heat flux, q''_c.

3.2 Time Dependent Heat Flux Measurements

For time dependent heat flux measurements, simultaneous recordings of the sensor output signals e_b and e_r are taken at various time intervals. Gage capabilities are demonstrated by taking these measurements in a conventional, domestic electric oven, where the process of cycling the heating element input power produces a repetitive upward and downward swing in the irradiance level. With a conventional[4] oven operating at 175°C (350°F), the heat flux gage assembly, facing upward, was placed at midheight in the center of the oven cavity. Equations 3.1 and 3.2 are applied to the gage sensor output and the resulting irradiance and convective heat flux values are shown in Figure 3.3. Note how the heat flux level cycles, due to the cycling of the heating element input power, and that the mean convective heat flux level is approximately 20% of the mean irradiance level.

In contrast to the cyclic heating process in the conventional oven, the Bi-Radiant Oven provides, under constant power input, a more constant flux level. To illustrate this, a series of experimental measurements were performed in Bi-Radiant Oven IV-B[5] (see Table 2.1 for a description of this oven). The heat flux gage assembly, facing upward,

---

3 See Appendix D for emissivity measurements of the gage surface.

4 Whirlpool Model RFE 3360 electric oven.

5 See Martin [9] for a description of the data aquisition system used for experimental observations in the Bi-Radiant Oven.

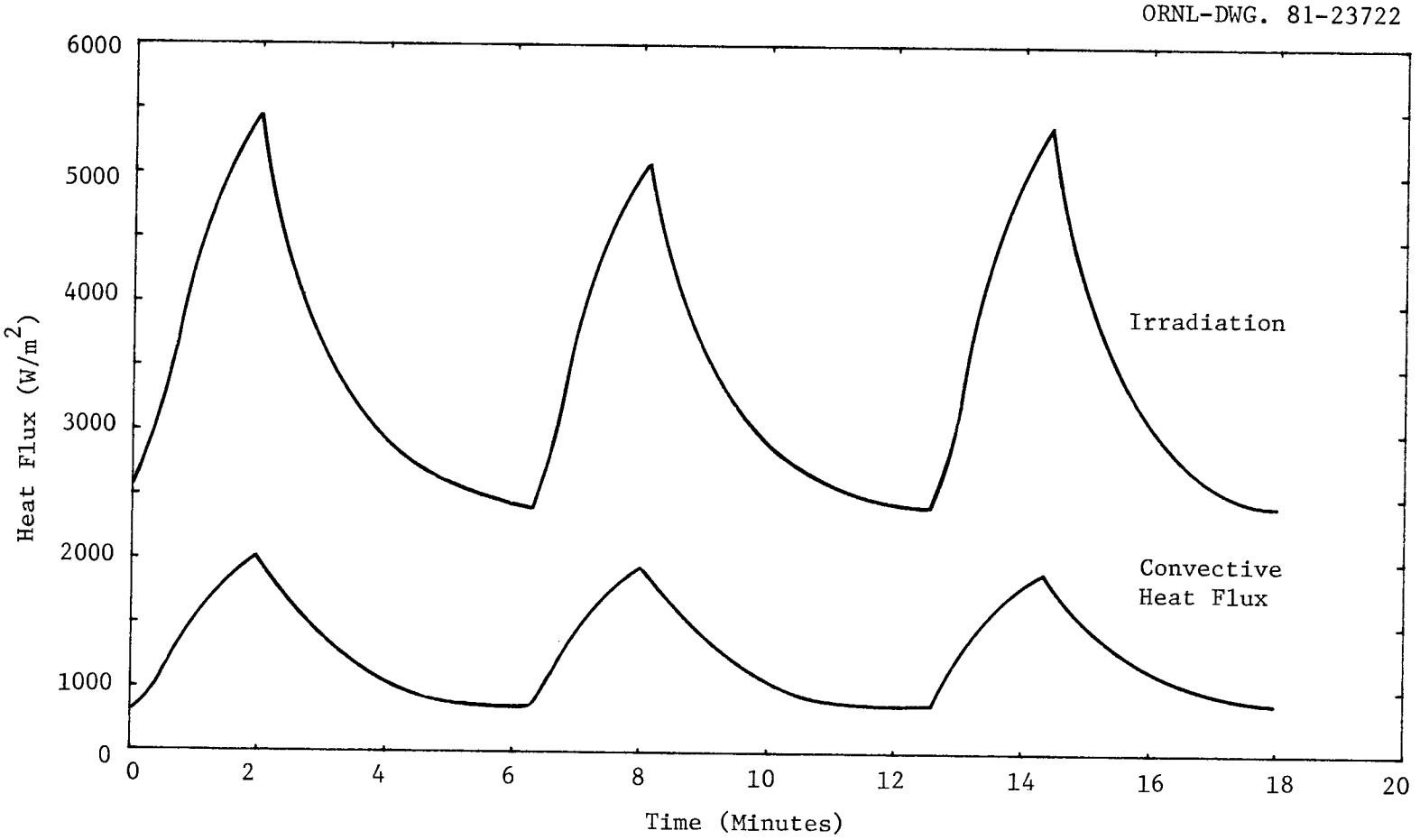

Figure 3.3 Irradiation and Convective Heat Flux in a Conventional Oven (Run 11.7.79, 1800 hrs).

was mounted on its wire stand, attached to the oven rack, and placed at midheight in the center of the oven cavity. Both heating elements were switched on (top element: 1040 W; bottom element: 64 W) and sensor signal observations taken. It should be noted that this setting approximates the 175°C (350°F) setting of the conventional oven.

The results for the above experiment, after power has been supplied to the elements, are presented in Figure 3.4. The low initial heat flux levels, as indicated in this figure, are to be expected since there is no preheat period during normal use of the Bi-Radiant Oven. Note the relatively low convective heat flux level as compared to the irradiation level. Since the convection coefficient, h (W/m^2-C), is expected to remain fairly constant, the increasing convective heat flux is a result of the increasing temperature difference between the gage and cavity air.

The irradiation curve of Figure 3.4 displays the heating element and oven wall dynamics. The rapid increase in irradiation heat flux after oven turn-on is due to the rapid increase in heating element emission, as element temperatures rise. The later slow, steady increase in irradiation heat flux represents the increasing emission from the oven walls as their temperatures rise.

Since the view factor from the gage to the walls is much larger than the view factor from the gage to the element, the walls are capable of providing a large portion of the radiative heat flux at the gage surface (even though their temperatures are much less than the element temperatures). In fact, Martin [9] has shown that it is possible for wall

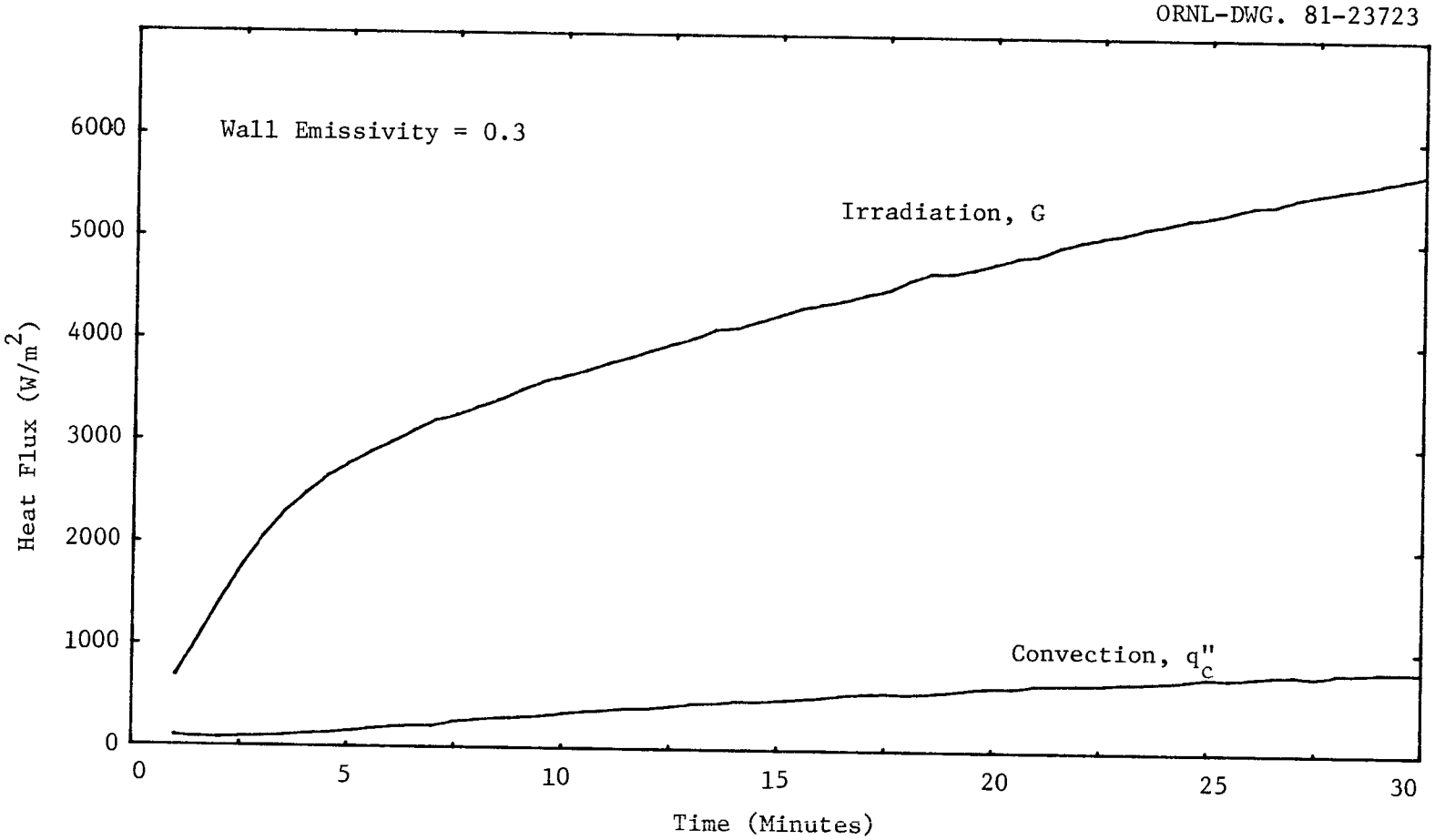

Figure 3.4 Irradiation and Convective Heat Flux in a Bi-Radiant Oven

emission to become the largest source of heat flux at the gage or product. This is especially true for high emissivity cavity walls, since their temperatures rise faster than those of low emissivity walls, due to their greater absorptance of incident radiant flux.

From Figures 3.3 and 3.4, note that the total measured mean heat flux levels are approximately the same for both the conventional and Bi-Radiant ovens. The means by which these levels are maintained, however, give an indication of the differing operational aspects between the ovens. In a conventional oven, high emissivity (high absorptivity) walls and a low emissivity (high reflectivity) product utensil are used. These aspects are necessary in order to protect the product from the detrimental periods of peak irradiance. In a Bi-Radiant oven, the walls have low emissivities and the product utensil has a high emissivity. The intent here is to provide a greater absorptance of the incident irradiance, and, by supplying continuous, low level power to the heating elements, to maintain the incident irradiance at a desirable level.

It is important to indicate that the convective heat flux and the convective heat transfer coefficient obtained from the gage are useful for comparison purposes, but are not specifically applicable to other objects within the oven cavity. For instance, the convective coefficient and the convective heat flux to a pan would be different than those to the heat flux gage. These differences are due to their different surface geometries which affect the thermal boundary layer

development. Different boundary layers produce different local heat transfer coefficients, thus altering the overall convective heat transfer[9].

3.3 Steady-State Heat Flux Measurements: Irradiance Distribution

Experimental, steady-state irradiance mappings were conducted in two different Bi-Radiant Ovens: III and IV (as described in Table 2.1). In Bi-Radiant Oven III, the heat flux gage was positioned on a baking plane located 11.43 cm below the upper heating element, and input power of 300 W was supplied to this element only. The heating elements are located 3.81 cm from the upper and lower cavity walls. In Bi-Radiant Oven IV-B, the baking plane was located 11.42 cm below the upper heating element and again input power (430 W) was to this element only. Also, the elements are again located 3.81 cm from the upper and lower cavity walls.

For either oven, the experimental method for obtaining steady-state heat flux measurements is the same. The oven is switched on, with the specified input power being supplied to the upper element only, until steady-state operation is achieved (about 10 hours). The heat flux gage is then placed, facing upward, at 42 discrete locations over half the baking plane, and heat flux measurements taken. Employing symmetry, and making use of a contour plotting routine, the irradiance distribution is obtained for the entire baking plane. Figures 3.5 and 3.6 display the heating element configurations and the constant irradiance (iso-irradiance) lines for the baking planes of Bi-Radiant Ovens III and IV, respectively.

ORNL-DWG. 81-23724

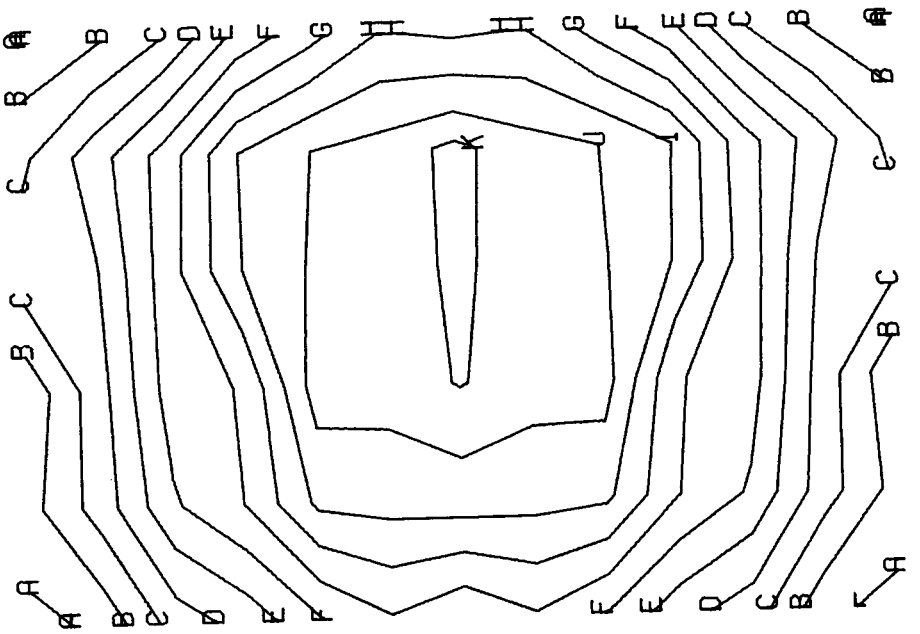

(b)

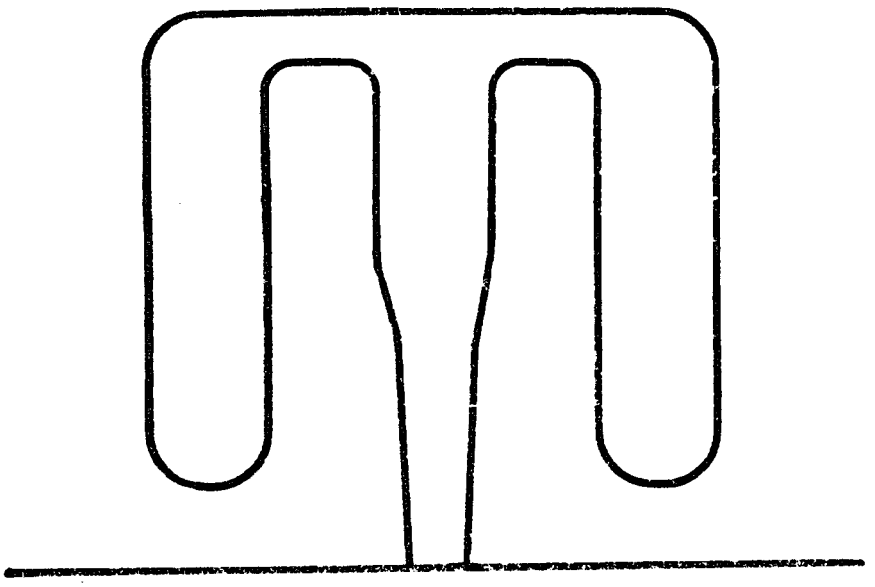

(a)

Figure 3.5 Experimental Mapping of Irradiance in Bi-Radiant Oven III

(a) Heating Element Configuration
(b) Iso-Irradiance Lines, $G_{max}/G_{min} = 1.17$

ORNL-DWG. 81-23725

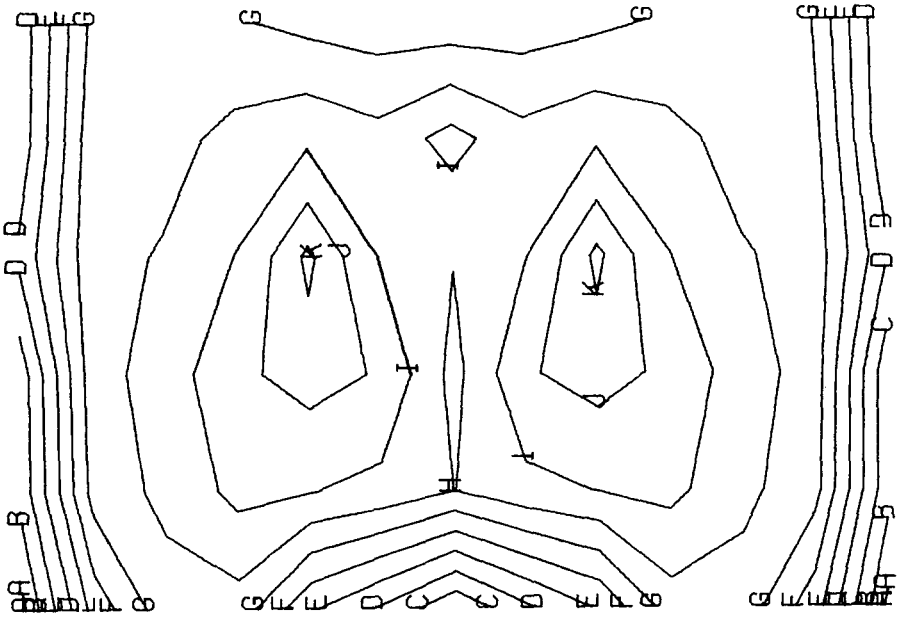

(b)

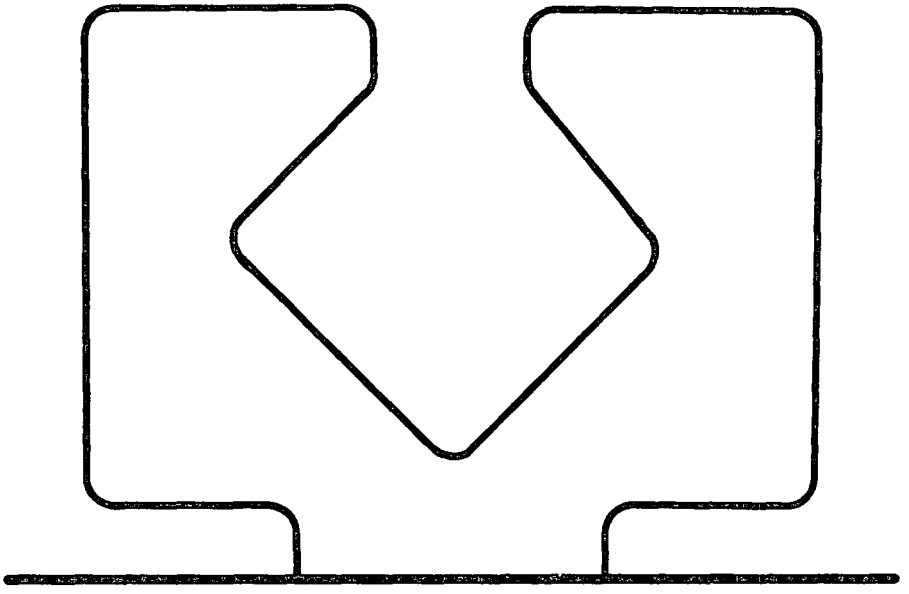

(a)

Figure 3.6 Experimental Mapping of Irradiance in Bi-Radiant Oven IV-A

(a) Heating Element Configuration

(b) Iso-Irradiance Lines, $G_{max}/G_{min} = 1.06$

Comparing the irradiance maps of Figures 3.5(b) and 3.6(b), a larger region of fairly uniform irradiance is evidenced in the latter. This is indicated by the widely spaced iso-irradiance lines covering most of the baking plane of Figure 3.6(b). Note also that the irradiance ratio, G_{max}/G_{min}, from Figure 3.6(b) is only 1.06 as compared to 1.17 for Figure 3.5(b). The lower irradiance ratio signifies an improvement in the overall uniformity of irradiance levels at the baking plane. Thus, the heating element configuration of Figure 3.6(a) provides an irradiance field at the baking plane which is more conducive to the baking of a product. Even the rapid decline in irradiance levels, indicated in Figure 3.6(b) by closely spaced lines near the cavity walls, does not indicate serious problems due to the low overall irradiance change which this decline represents (as suggested by the extremely low irradiance ratio.)

4. COMPARISON OF ANALYTICAL AND EXPERIMENTAL RESULTS

In the previous two sections, methods for characterizing oven thermal processes were presented and discussed. Section 2 discussed the optimization of heating element performance through a comparison of analytically generated irradiance distribution plots. Also outlined, was the analytical modeling of oven thermal response (when loaded using the DOE test block).

The experimental measurement techniques, as outlined in Section 3, provided the means for obtaining laboratory heat flux data during oven operation. Additional laboratory measurements involving oven temperatures during efficiency tests (where the thermal load consists of the DOE test block) were performed by Martin[9] It is the purpose of the present section to compare the results from analytical predictions for heating element and oven performance with measured laboratory test data.

4.1 Irradiance Distribution

The analytical prediction of the irradiance distribution produced by the heating element configuration of Bi-Radiant Oven III is shown in Figure 2.2(b). The experimental mapping of the irradiance distribution associated with this same element is shown in Figure 3.6(b). Bringing these two figures together for comparison indicates a very close agreement between predictions and measurements, as seen in Figures 4.1(a) and 4.1(b). Both plots of Figure 4.1 depict a central region of relatively

ORNL-DWG. 81-23726

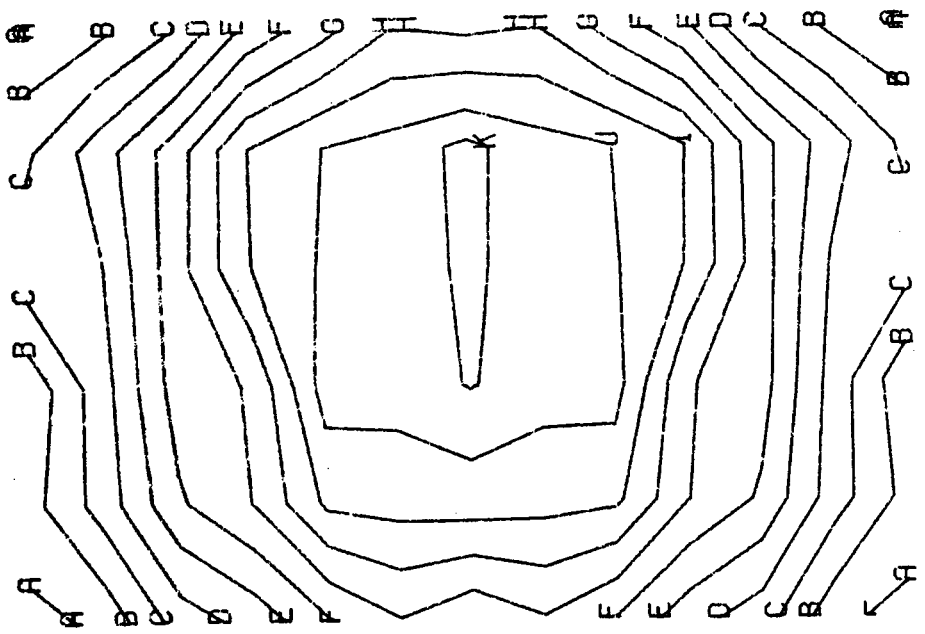

(b)

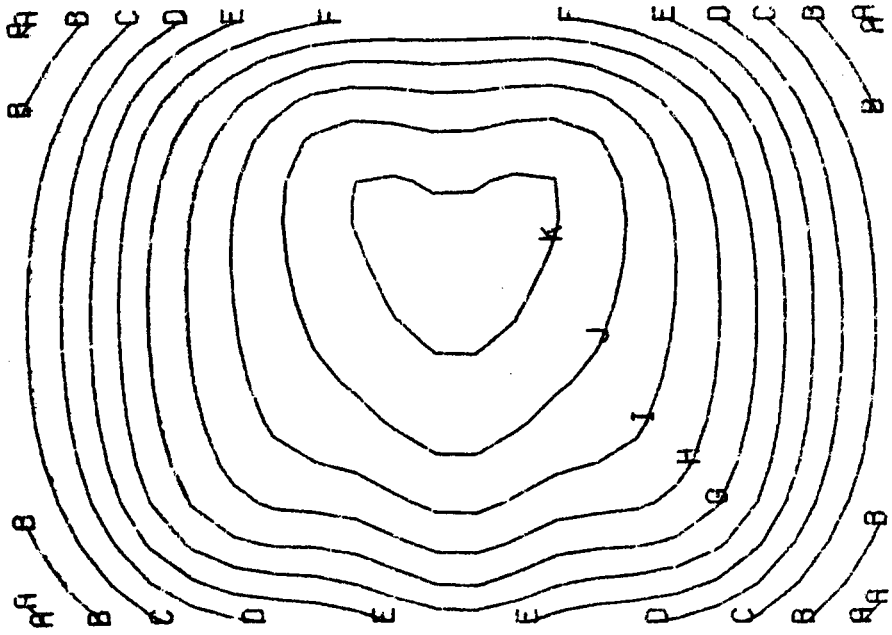

(a)

Figure 4.1 Comparison of Predicted (a) and Measured (b) Irradiance Distribution Maps for Bi-Radiant Oven III

uniform irradiance which is surrounded by steadily decreasing levels near the walls. Note that the predicted change in irradiance, $(G_{max}/G_{min})_{pred}$, is 5.74. This is a factor of 5 higher than the measured change, $(G_{max}/G_{min})_{meas}$, of 1.17. The discrepancy is seen as resulting from a combination of factors. Since experimental mapping is performed after the oven has reached steady-state operation, as discussed in Section 3.3, wall temperatures are nearly the same as the element temperatures. With the higher than normal wall temperatures, the contribution of irradiance at the baking plane resulting from emission from the cavity walls is much larger than normally expected. For simplicity, and since this is not the case during normal oven operating conditions, the analytical model totally neglected the irradiance contribution from the cavity walls. Thus, the effect of wall emission is seen as the largest factor contributing to the extremely low measured irradiance ratio as compared to the predicted value. Not accounting for multiple reflection paths of radiant energy emitted from the heating element and striking the baking plane is considered a much smaller factor contributing to the discrepancy between measured and predicted irradiance ratios.

For the modified-diamond element of Figure 2.6(a), the predicted and experimentally measured irradiance plots of Figures 2.5(b) and 3.7(b), respectively, are displayed in Figures 4.2(a) and 4.2(b). Comparing these two plots again depicts a good agreement. The fairly large region of relatively uniform irradiance and the rapid irradiance decline very near the cavity walls are indicated in both plots. Also, the predicted change in the irradiance is again greater than the measured change for the same reasons as explained above.

ORNL-DWG. 81-23727

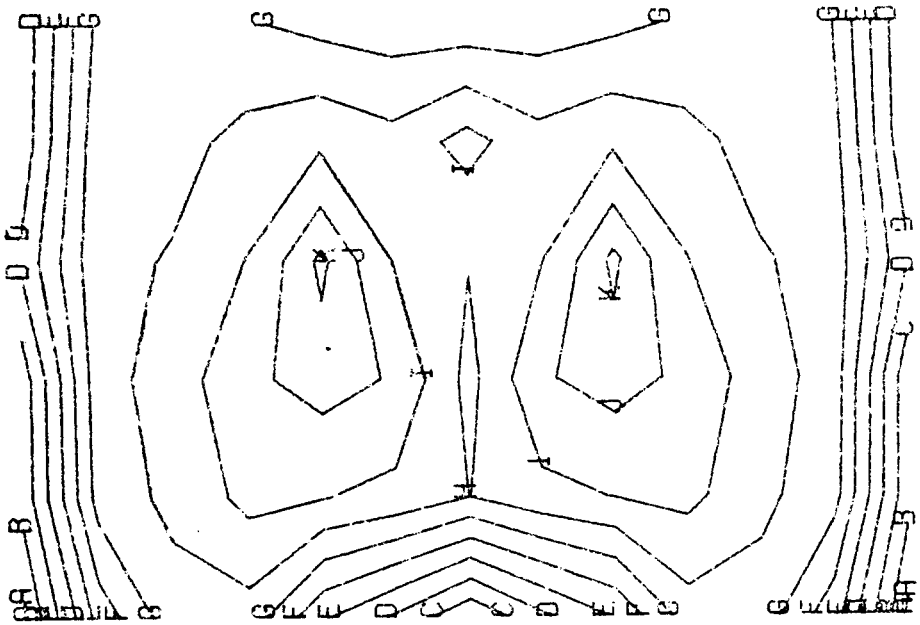

(b)

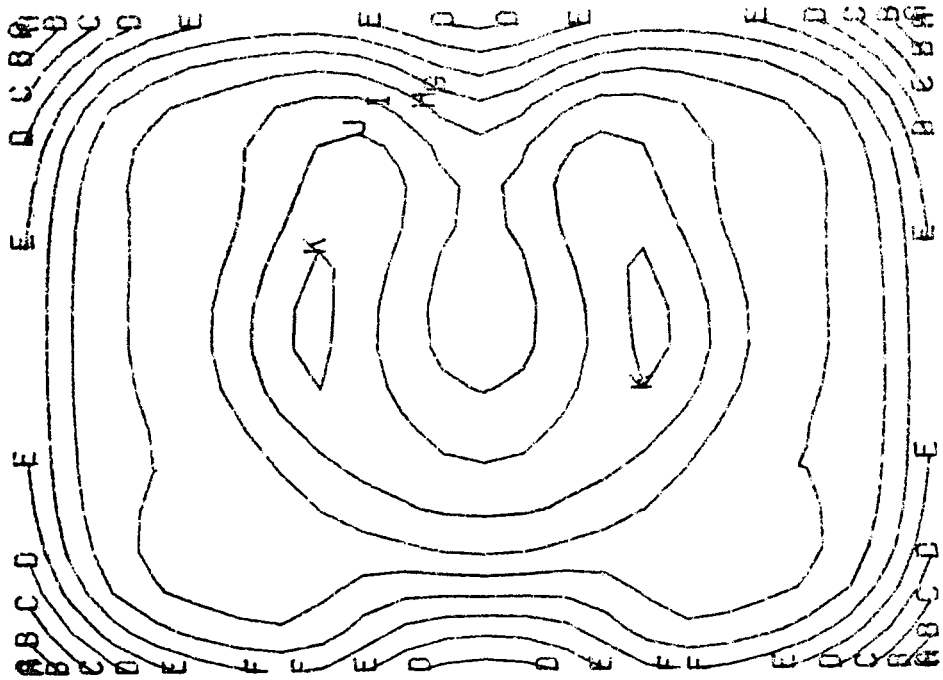

(a)

Figure 4.2 Comparison of Predicted (a) and Measured (b) Irradiance Distribution Maps for Bi-Radiant Oven IV-A

More importantly, note the analytically predicted irradiance plot of Figure 4.2(a) and the experimentally measured plot of Figure 4.2(b) show a larger region of uniform irradiance conducive for baking, and a lesser overall irradiance change than is indicated by their counterparts in Figure 4.1(a) and 4.1(b). This gives confidence in the capabilities of Analytical Model I to predict the influence of heating element configuration on performance.

4.2 Oven Temperatures

Comparisons of predicted and measured oven temperatures will be presented for Bi-Radiant Oven IV-B, as described in Table 2.1. The test was conducted with a constant input power (482 W) to both the upper and lower heating elements and with the DOE test block centrally located within the oven cavity. The analytical method for predicting element temperatures, block temperature, cavity wall temperatures, and cavity air temperature was introduced in Section 2.3. Laboratory measurements of these same characteristics were obtained by Martin [9]. The comparison plots of the analytical predictions versus the experimental measurements are given in Figures 4.3 through 4.6. Analytical predictions in the figures are indicated by smooth curves while the experimental measurements are represented by + marks.

Figure 4.3 shows the comparison of the predicted and measured heating element temperatures, indicating the rapid initial increase in element temperatures with oven turn on, followed by a slower, more gradual temperature rise as the rest of the oven becomes increasingly warmer. In this figure, the predicted element temperature differs from the actual element temperature by at most only 30°C. Since the convective

ORNL-DWG. 81-23728

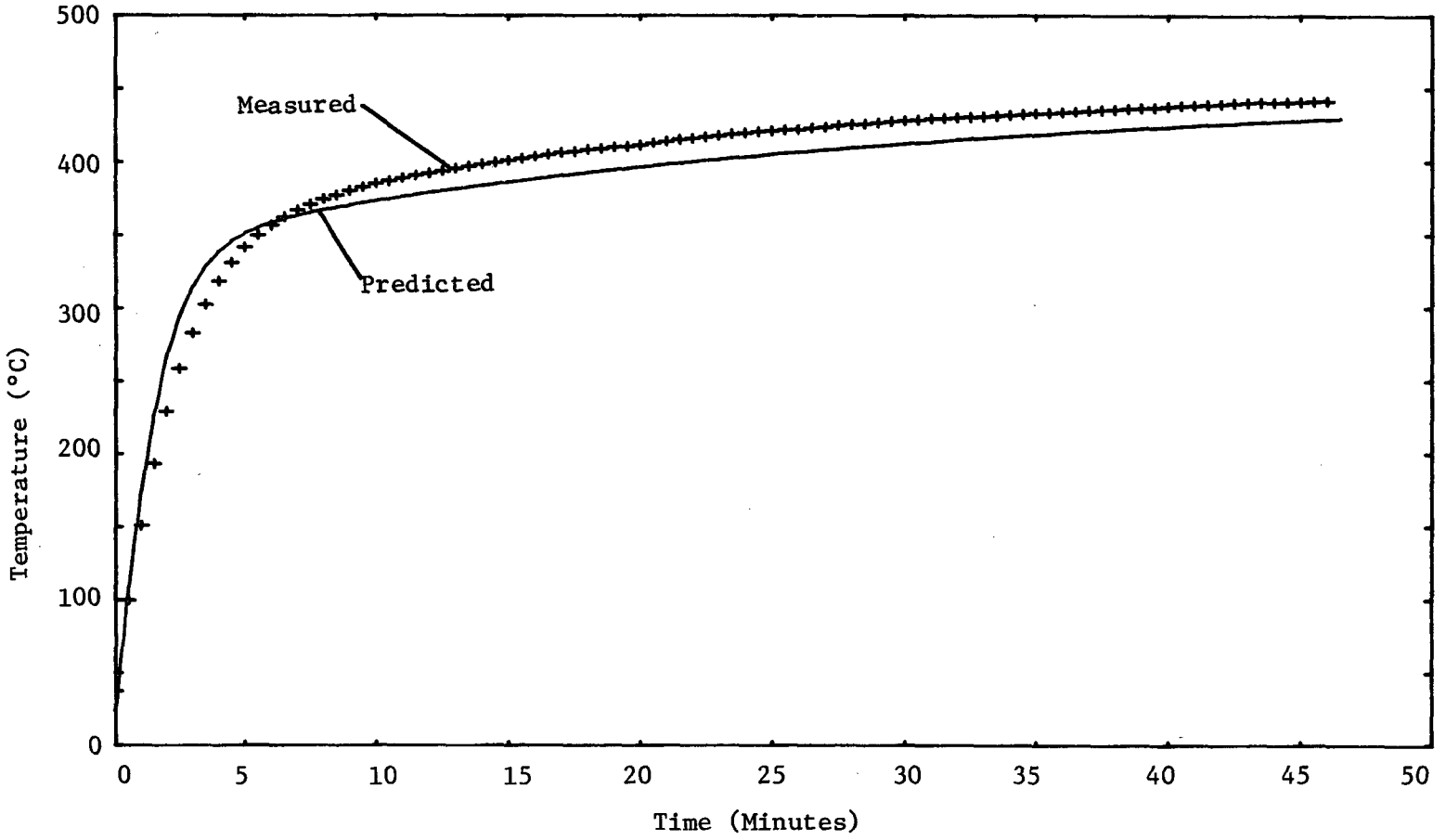

Figure 4.3 Comparison of Predicted and Measured Element Temperatures

ORNL-DWG. 81-23729

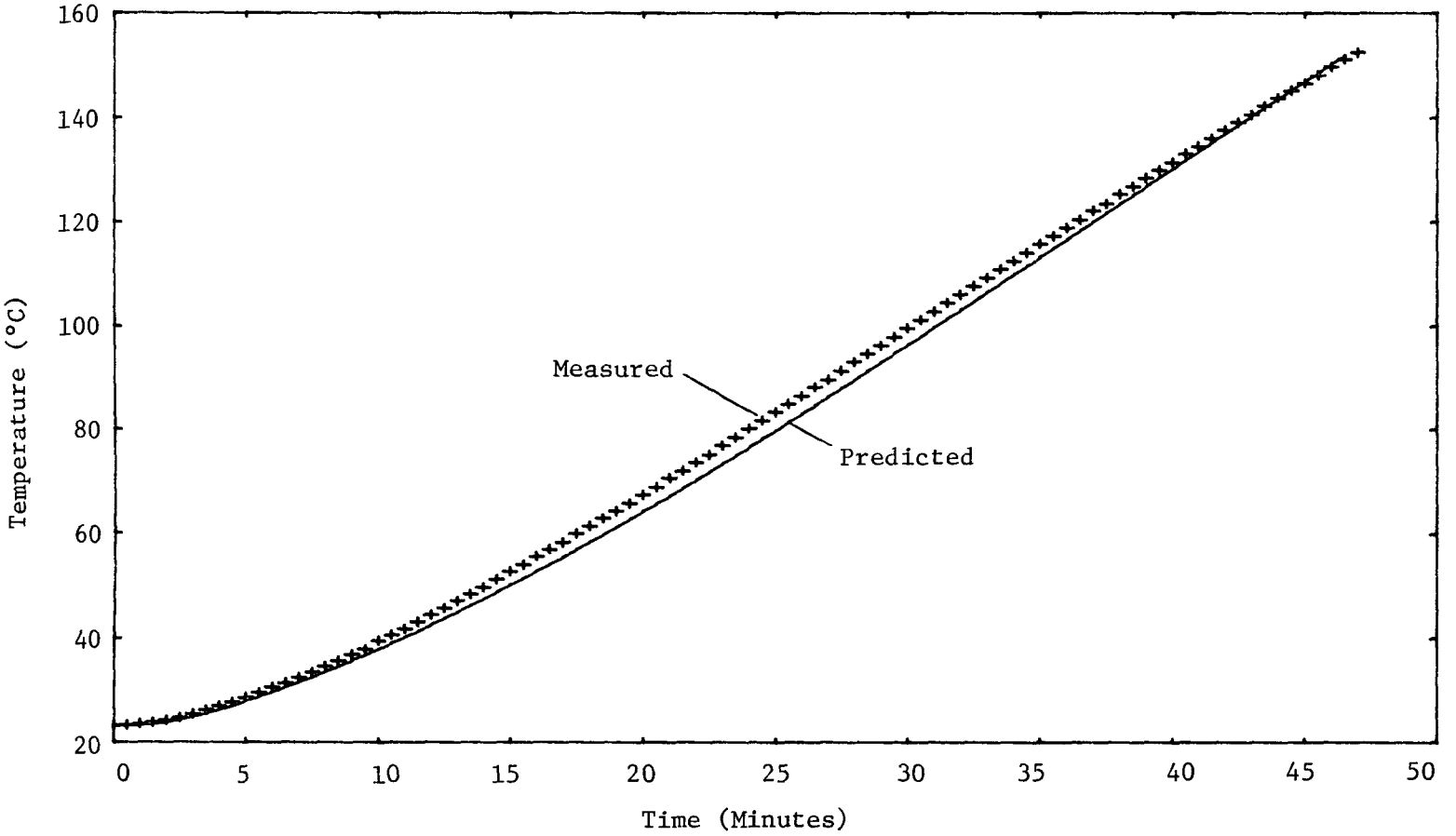

Figure 4.4 Comparison of Predicted and Measured DOE Test Block Temperature

ORNL-DWG. 81-23730

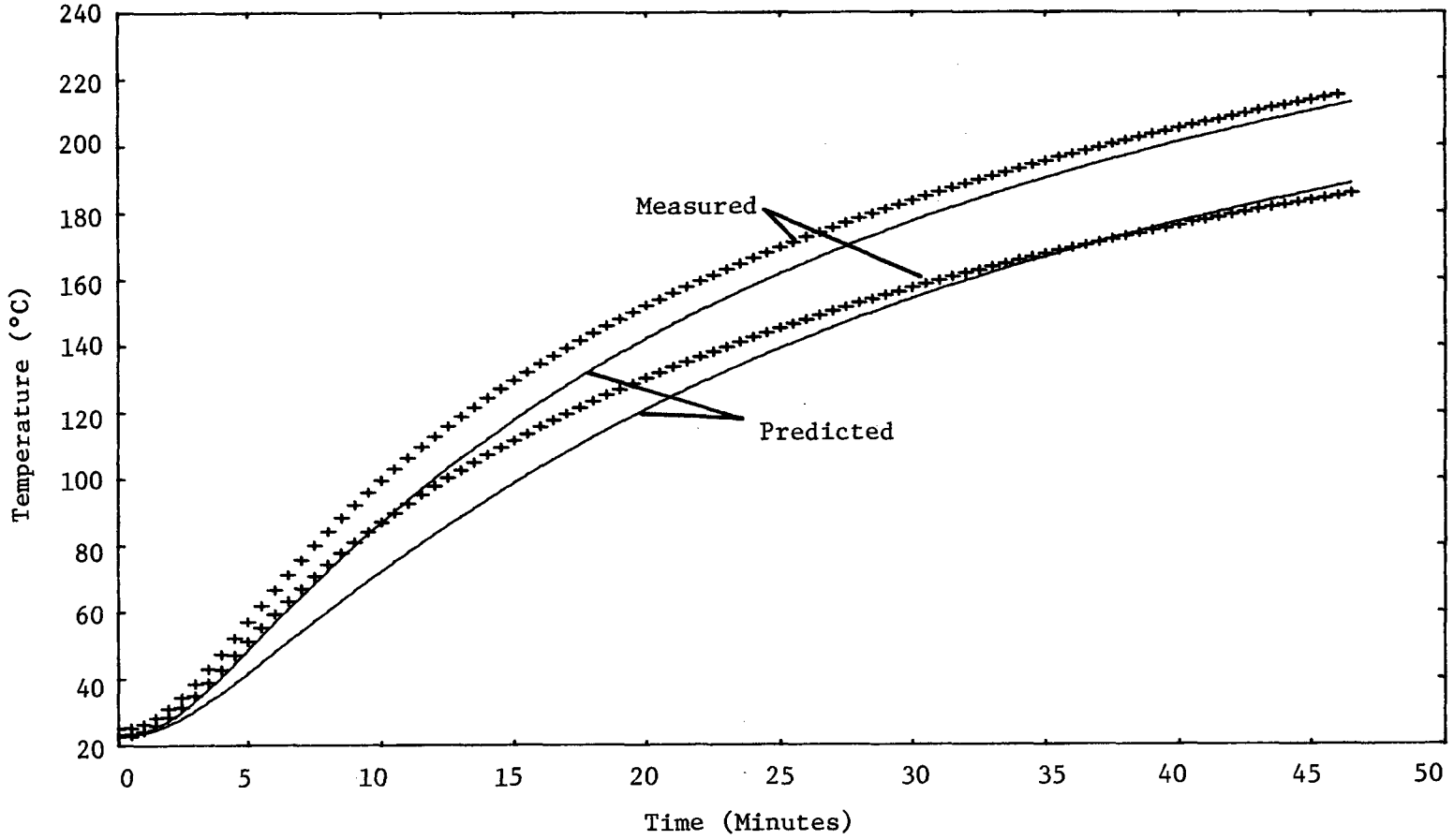

Figure 4.5 Comparison of Predicted and Measured Average Cavity Wall and Door Temperatures

ORNL-DWG. 81-23731

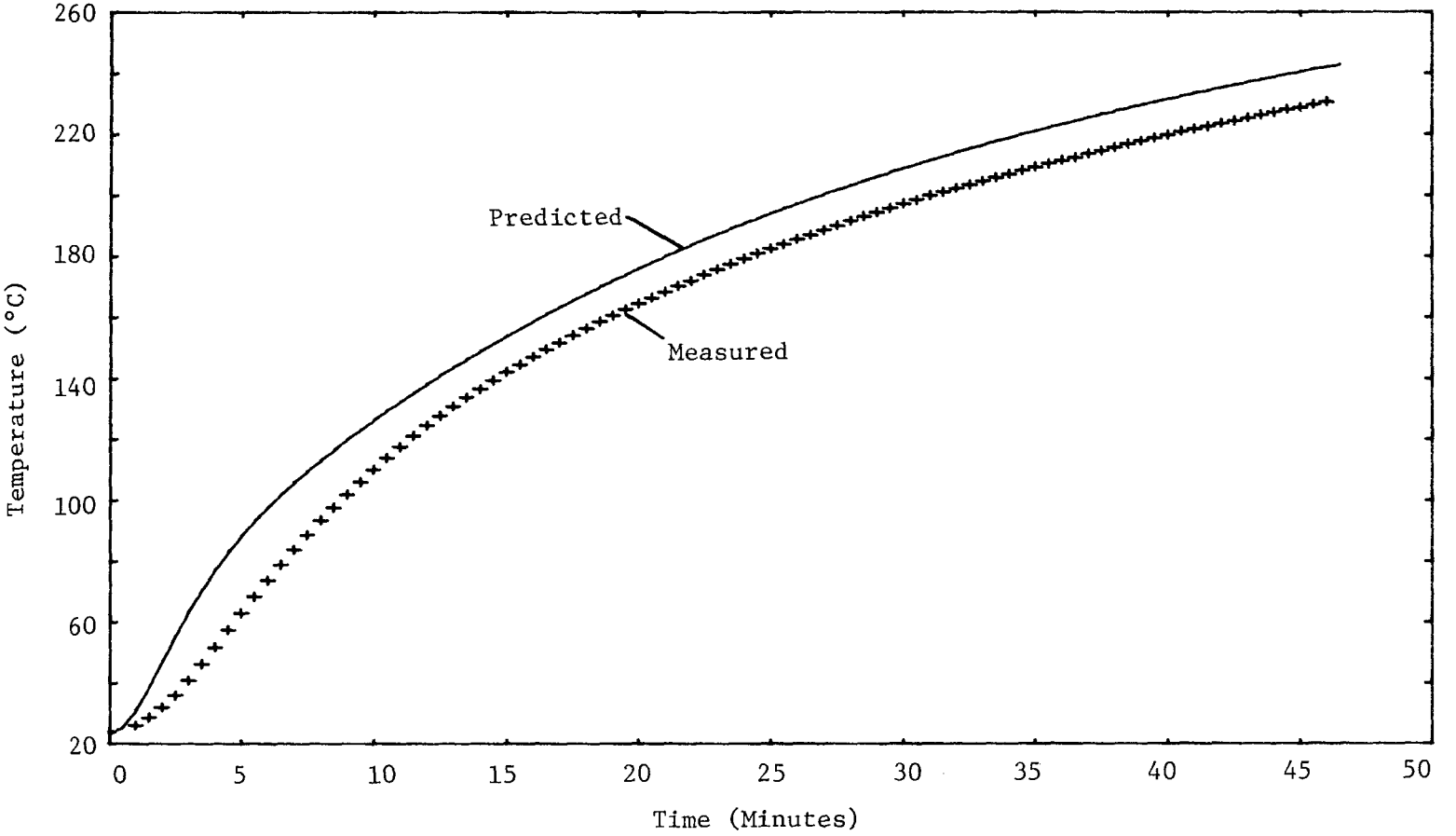

Figure 4.6 Comparison of Predicted and Measured Cavity Air Temperature

and radiative processes at the element are so complex, to be able to analytically predict the thermal response of the heating element with this type of accuracy is a strong feature of the model.

Comparison of the DOE test block temperatures is presented in Figure 4.4. Calculation of the oven efficiency is performed when the temperature of the block reaches 130°C above its initial temperature. For the conditions of this test, the predicted oven efficiency was 17.92 and the measured efficiency was 17.83, an error of only 0.5%. This high accuracy is to be expected since very good agreement is shown to exist for the predicted and actual temperatures of the block. (A maximum error of only about 4°C is indicated over the entire 47 minute time span of the test.)

Indications of how the average predicted wall temperatures and the cavity door temperature compare to the actual measured values are shown in Figure 4.5. In this figure, two curves are displayed for both the analytical predictions and the experimental measurements. The upper curve represents the average interior wall temperature not including the oven door and the lower curve represents the door temperature. Both the predicted and measured door temperatures are seen to be less than the the predicted and measured average wall temperatures, respectively. Lower door temperatures are a direct result of the greater conduction losses which are present at the door. Note the predicted temperatures rise slower than the measured temperatures and then tend to become too hot. This type of trend could be due to an error in predicting the actual thermal mass of the nodal wall elements. In the analytical model, the thermal mass of the support frame and corner braces were

lumped together with the thermal mass of the walls, providing a thermal capacitance which is initially too high, explaining the slower initial temperature response. As the wall temperatures increase, the thermal capacitance of the walls would also increase (since the thermal capacitance of aluminum increases with higher temperatures), tending to lessen the slope of the predicted temperature response curve with time, and tending to lower the temperatures which the walls (and door) would eventually achieve. Accounting for these two aspects would tend to shift the predicted temperature curves to match more nearly the measured temperature curves.

Finally, Figure 4.6 compares the predicted and measured average cavity air temperature. Experimental measurements of cavity air temperature were accomplished using 8 thermocouples which were placed in the oven cavity and shielded from radiation errors using nickel coated probes[9]. Analytical predictions of the cavity air temperature were obtained by lumping the air temperature probes, rack, and cavity air into two nodal elements; one for the upper portion and one for the lower portion of the oven cavity. Even with this general analytical treatment, note that the predicted air temperature is consistently higher than the measured value by only about 15°C. Due to the many aspects which would be involved in a more accurate prediction of the cavity air temperature; circulation, stratification, and individual attention to the rack and air temperature probes; the predicted air temperature is seen as a very good approximation to the measured value.

Overall, the ability of the analytical model to predict the thermal response of the oven is rated as highly accurate. It is important to

realize that the predictions presented here were obtained using the most accurate means available for determining the oven properties and the convective and radiative phenomena. Once oven properties were selected, convective coefficients predicted, and emissivities measured, there was no tweaking of these parameters to obtain the close match between the predicted and measured thermal response which was presented here.

5. PARAMETRIC STUDY OF OVEN PERFORMANCE

Up to this point, the transient thermal analysis programs have only been applied to the existing prototype Bi-Radiant Oven. Comparing the results of predicted oven thermal response with laboratory measurements conducted in this prototype has validated the accuracy of the analytical modeling. It is reasonable to expect, then, that the model will correctly indicate oven efficiency changes with specific oven design parameters.

For comparison purposes, consider as the baseline case, Bi-Radiant Oven IV-B, as described in Table 2.1. Testing involves varying a single baseline parameter and examining the resulting effects on oven efficiency. The parameters which are tested consist of the insulation thermal conductivity, cavity wall emissivity, heating element diameter, and heating element input power.

5.1 Effects of Insulation Thermal Conductivity

The effect of decreasing the thermal conductivity of the cavity insulation is to decrease the loss of energy through the cavity walls. While at first this might seem to be a good method for increasing oven efficiency, examining Figure 5.1, it is seen that over a range of insulation thermal conductance from 200% to 25% that of the baseline value, the oven efficiency only changes from 16.9 up to 18.9%. The small

ORNL-DWG. 81-23732

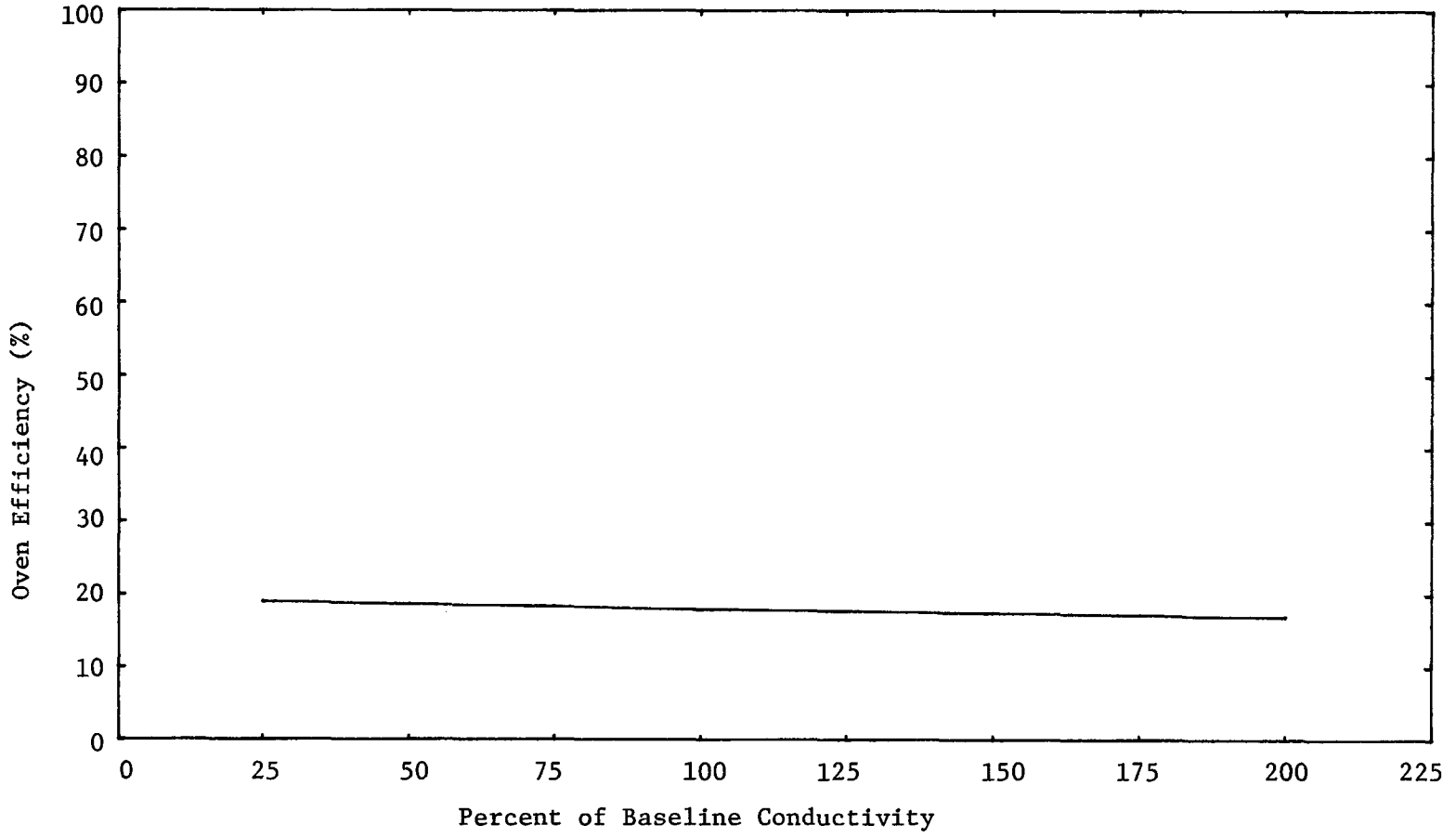

Figure 5.1 The Effect of Insulation Thermal Conductivity on Oven Efficiency

variation in oven efficiency with respect to cavity insulation change is due to the magnitude of other loss mechanisms besides conduction through the insulation. Other significant conduction losses at the walls include those through the oven door cover, oven support frame, and flange mounts.[6]

5.2 Effects of Cavity Wall Emissivity

Radiant coupling between the cavity walls and heating element is a strong function of cavity wall emissivity. Lowering the wall emissivity decreases the absorption and increases the number of reflections of irradiation at the cavity walls. These processes improve the chances for radiation emitted from the heating elements to be intercepted by the product. The net effect, as shown in Figure 5.2, is an increase in oven efficiency with decreasing cavity wall emissivity. For wall emissivities less than about 0.10, altering the wall emissivity has quite a dramatic effect on oven efficiency. This is to be expected since as the wall emissivity approaches zero, so does wall absorption of irradiance, implying that all radiation emitted from the heating elements would be continually reflected at the cavity walls until finally absorbed by the product (test block).

Also indicated in Figure 5.2 are two distinct data points obtained from laboratory measurements. The point at a cavity wall emissivity of

[6] The oven door cover was assigned nodal points, making it possible to model the conduction losses associated with its connection to the interior wall. The oven support frame and flange mounts, however, were not assigned individual nodes, having their masses lumped together with either the interior or exterior oven walls. However, since these pieces inherently connected the interior and exterior oven walls, their contribution to conduction losses were estimated through a consideration of their thermal conductivity, cross sectional area, and length.

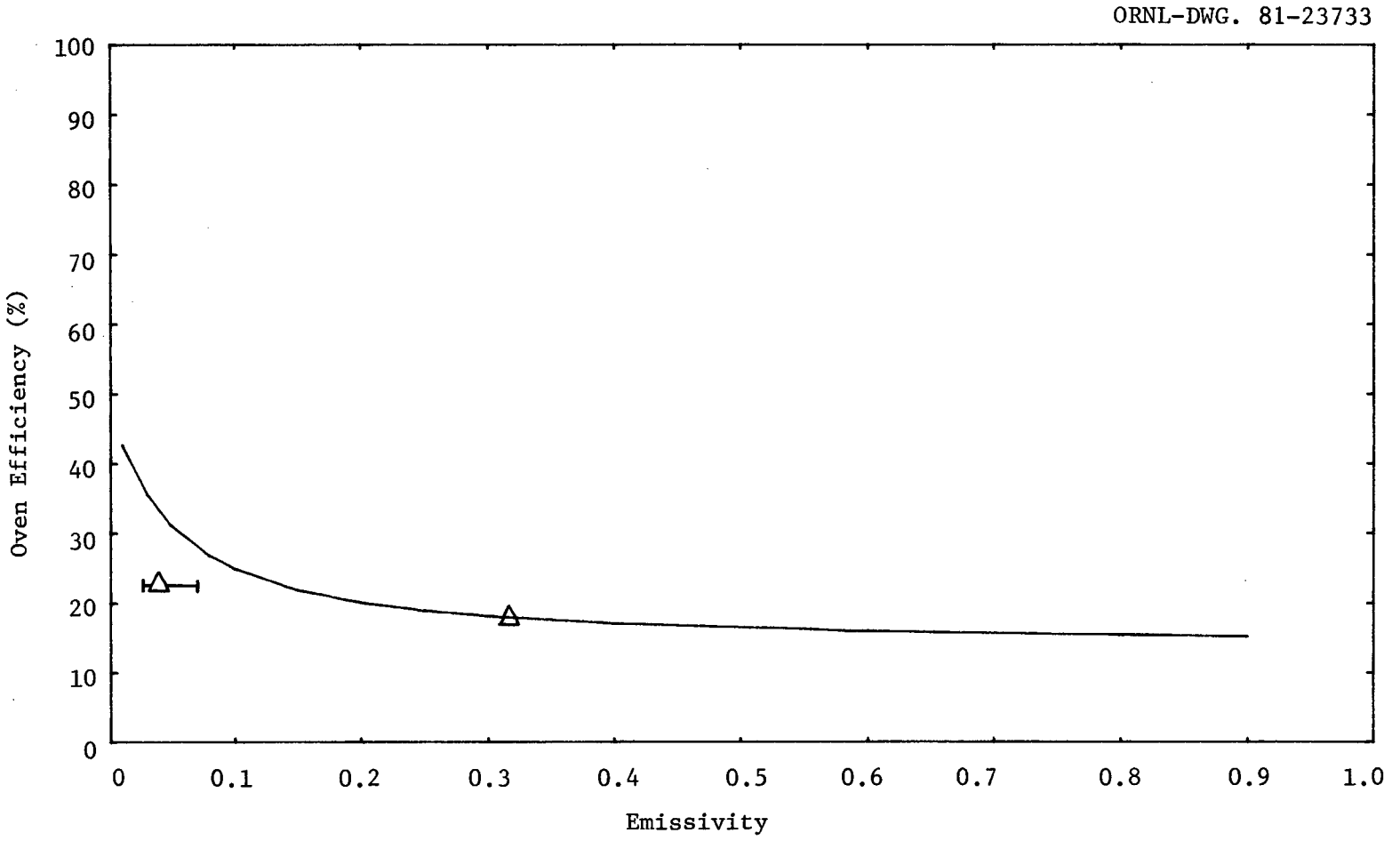

Figure 5.2 The Effect of Cavity Wall Emissivity on Oven Efficiency

0.31 corresponds to the base case condition of Bi-Radiant Oven IV-B, and is seen to lie almost exactly on the analytical curve. The data point at a measured emissivity of less than 0.10 results from laboratory tests conducted in Bi-Radiant Oven IV-A. (From Table 2.1, this oven is the same as IV-B except for having specular walls of very low emissivity.) This data point seems in poor agreement with the analytical predictions. However, there are two major factors which explain this discrepancy. The first factor is the uncertainty of the emissivity value itself. Measurements were taken on a clean sample, and the resulting emissivity was found to be 0.03, with a possible error placing the value up to 0.07. (See Appendix D.) The second factor is that the oven walls had been subjected to numerous thermal cycles and contamination which would tend to increase their emissivity. Under these conditions, it would not be unreasonable to expect the emissivity of the actual cavity walls to be closer to a value of 0.10. If this were the case, the measurements and predictions would be in close agreement. Therefore, it is the value of the wall emissivity, and not the degree of specular versus diffuse reflections which explains the discrepancy between measurements and predictions.

5.3 Effects of Heating Element Diameter

At constant power input to a heating element, decreasing the element diameter will cause an increase in the element temperature, due to the reduction of element thermal mass. Since emission from the heating element is dependent on T^4, increasing the element temperature will cause the percent of the input power dissipated by radiation to increase. It follows that the percent of the total input power

dissipated through convection must decrease.

The effect of decreasing the element diameter or increasing the percentage heat rate dissipated by radiation is to increase the oven efficiency, as shown in Figure 5.3. This is expected in a Bi-Radiant Oven due to the lower emissivity walls which tend to reflect the increasing amounts of radiation, creating an even stronger coupling between the heating elements and product. As the element approaches a filament-type heater, the efficiency rises sharply, and will eventually level out and intersect the axis at a point less than 100%, depending on the cavity wall emissivity.

5.4 Effects of Heating Element Input Power

The effect of altering the heating element input power on oven efficiency is displayed in Figure 5.4. Note the negligible change in oven efficiency as a function of the percent of baseline input power. The only definite effect is that with very low input power levels the oven efficiency drops steadily off. In fact, at 25% of the baseline input power, the test block does not reach the 130°C temperature rise prescribed for the efficiency calculation.

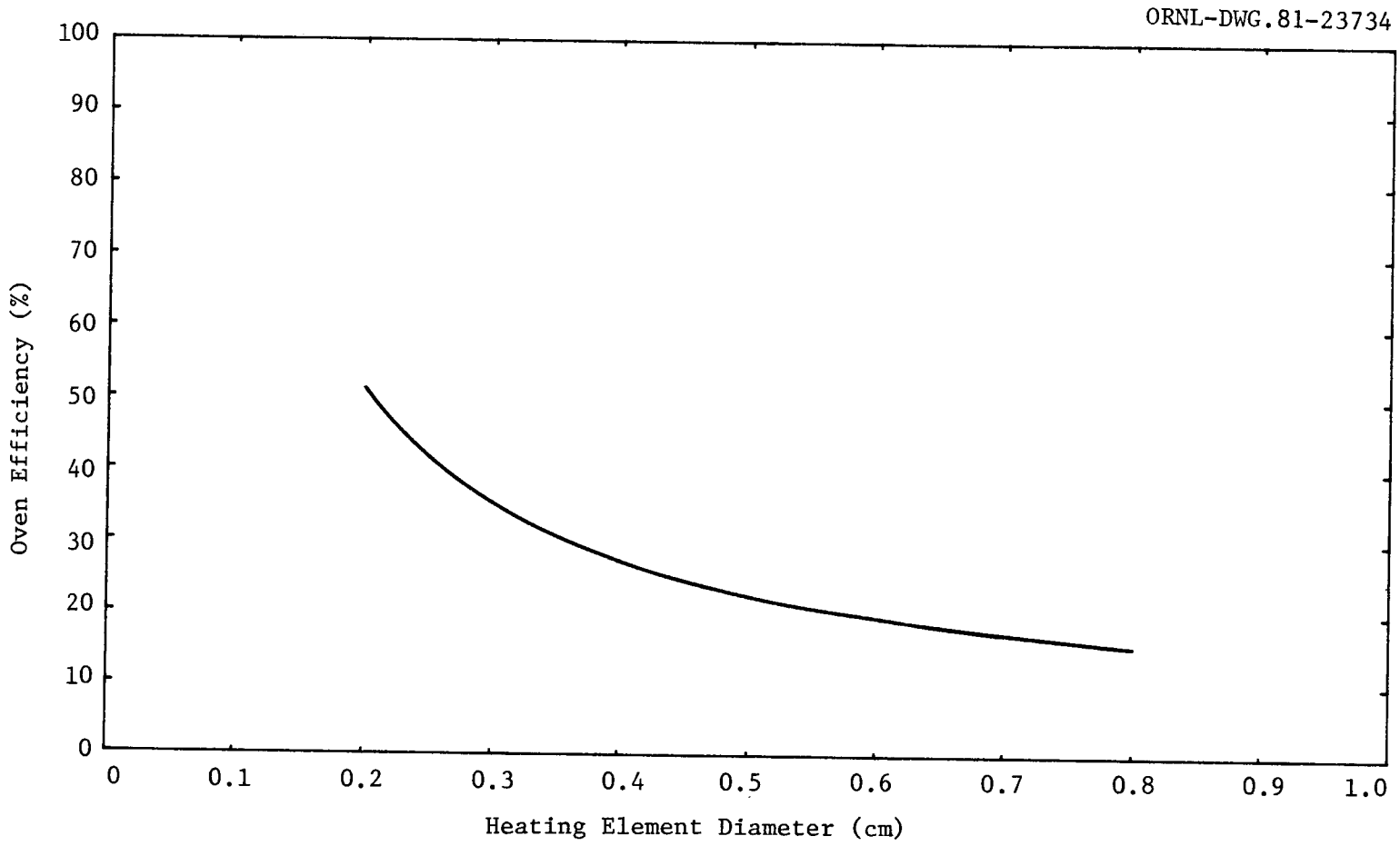

Figure 5.3 The Effect of Heating Element Diameter on Oven Efficiency

ORNL-DWG. 81-23735

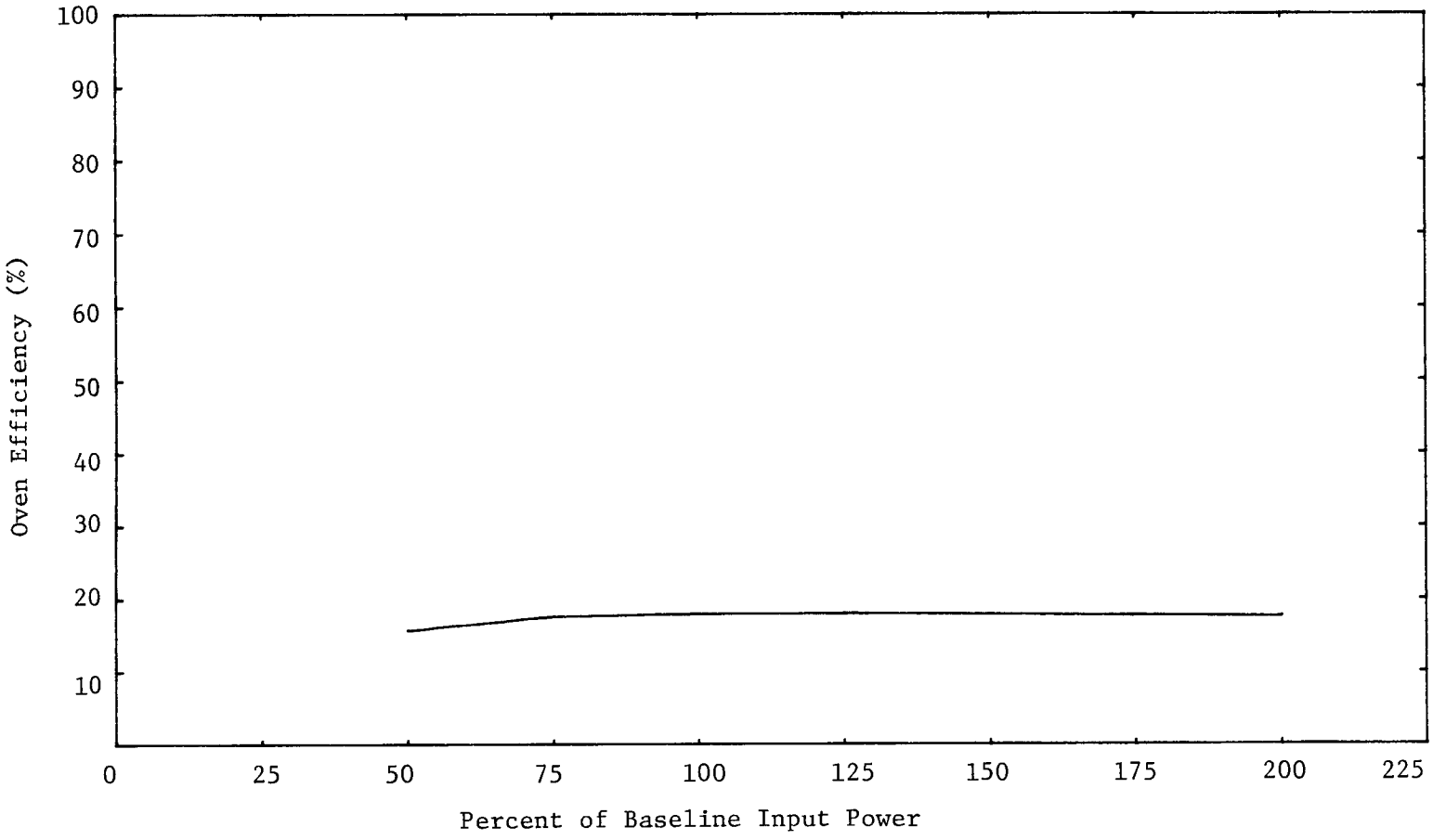

Figure 5.4 The Effect of Heating Element Input Power on Oven Efficiency

6. SUMMARY AND CONCLUSIONS

In order to model the radiant coupling between a product and heating element within a Bi-Radiant Oven, the computer program COIL was generated. This program was employed in the analysis of the design of element configuration where the main optimization parameter would be the overall uniformity of irradiance at the baking plane. By comparing the performance of several different heating element shapes, the best configuration was found to be the modified-diamond shape for which the predicted irradiance ratio, G_{max}/G_{min}, was shown to be 3.16.

The development and use of the heat flux gage provided the means for measuring absolute magnitudes of radiant and convective heat flux. This is a new tool which should prove useful for characterizing any system in which the processes of radiation and convection play simultaneous roles of comparable magnitude in the transfer of heat from a surface. For the purpose of this study, the heat flux gage provided means for comparing the performance of the heating elements (through the generation of irradiance distribution maps) and for the comparison of the different operational aspects between a conventional and Bi-Radiant Oven. It was shown that a conventional oven provides a mean heat flux level to a product through a cyclic process which is driven by the cyclic operation of the heating elements. In comparison, a Bi-Radiant Oven was shown to supply a more constant, controlled flux level at the product

due to the constant power input to its heating elements. Both ovens supplied approximately the same amount of heat flux to a product, but in a conventional oven the convective component is approximately 20% of the total, while in a Bi-Radiant Oven the convective component is less than 10% of the total.

When comparing the irradiance distribution ratios generated analytically by Program COIL and measured experimentally using the heat flux gage, it was found that, due to the experimental procedure necessary to obtain steady-state heat flux measurements, the experimentally measured ratio was less than the analytically predicted value by nearly a factor of 5. This effect is due to the large portion of irradiance over the baking plane resulting from wall emission, thus tending to even out the irradiance distribution. However, a comparison of irradiance distribution maps from analytical and experimental data showed that regions of uniform irradiance and regions of large irradiance change were similarly indicated on both maps. Therefore, Program COIL is useful in evaluating new heating element configurations.

In order to describe the performance of the oven, a detailed analysis was conducted employing computer programs OVENRAD and AGTAP. Considered in Program OVENRAD are the geometrical aspects of the interior oven cavity, for the purpose of the calculating the view factor matrix necessary for the thermal radiation exchange analysis. Output from this program is an important part of the input to Program AGTAP.

Program AGTAP modeled the transient thermal response of the entire oven structure, predicting component temperatures (wall, element, air,

DOE test block, etc.) and oven efficiency. The modeling included defining the oven structure as a collection of nodal elements linked together through thermal resistance paths of radiation, convection, and conduction. Comparing the predicted oven thermal efficiency to the measured value for Bi-radiant Oven IV-B resulted in an error of only 0.5%. For Bi-Radiant Oven IV-A the comparison was not as good. The reason for the discrepancy in this case was suggested as being the inaccuracy in determining the actual cavity wall emissivity. The model then became a useful tool for comparing the effects of several oven design parameters on oven thermal efficiency.

The parametric study considered the baseline oven to be Bi-Radiant Oven IV-B, having an insulation thermal conductivity of 0.046 W/m-K at 300 K, a diffuse cavity wall of emissivity 0.31, a heating element diameter of 0.66 cm, and an input power of 964 W. Varying these parameters indicated that the effects of insulation thermal conductivity and heating element input power on oven efficiency were negligible in comparison to the effects of cavity wall emissivity and heating element diameter. For instance, doubling the thermal resistance of the insulation resulted in an increase in oven efficiency from 17.9% up to only 18.6%. However, lowering the cavity wall emissivity from 0.31 to 0.10 increased the oven efficiency from 17.9% to 24.9%. For the heating element, under baseline wall emissivity and input power conditions, decreasing the diameter from the baseline value of 0.66 cm to 0.3 cm caused an increase in the oven efficiency from 17.9% to 35.3%. Thus, the cavity wall emissivity and heating element diameter are the two oven design parameters shown to have the most significant effects on oven performance.

When examining the effect of cavity wall emissivity on oven efficiency, the degree of specular versus diffuse wall reflections was indicated as having little bearing on the outcome of the results. More important than the analysis of the specular effects of the cavity walls is the accurate measurement of the cavity wall emissivity. This is to be expected since the oven acts as an enclosure with the resistance to heat loss through the oven walls being more dependent on the reflectance of irradiation, and less dependent on the directional aspects of the incident or reflected radiant flux.

The effect of the heating element diameter on oven efficiency is not due to any changes in the cavity resistance to heat loss, but is rather due to the increasing percent of radiant flux from the heating element with decreasing heating element diameter. Since the cavity walls reflect a great portion of the radiant flux incident on their surface, increasing the percentage of radiant versus convective dissipation from the heating element serves to more strongly couple the heating element with the product.

It may be desirable to extend this work by comparing the effects of combining some of the individual oven design parameters which were shown to improve oven efficiency. If necessary, the computer programs which perform the analysis may be altered to suit any special conditions which may arise. Changes in the convective analysis or the analysis of temperature dependent properties could be easily obtained within the subroutines which perform these tasks. However, if improved accuracy is desired, it would be necessary to increase the number of nodes which are used to represent the oven structure. This does not pose any problems

for Program OVENRAD, since the number of surfaces is a simple input parameter to this analysis. In Program AGTAP, however, it would be necessary to start with node 1 and redefine all the conduction, convection, and radiation (where applicable) links for the entire oven system. This is a very tedious process; note that there are 541 conduction links which had to be defined for the present model. It is possible, however, to add additional nodes to the present analysis without any great difficulty. The added nodes must only have their thermal resistance links defined and if they take the place of existing nodes, the existing resistance links must be removed.

With the model, the significance of two features not seriously considered previous to this study were discovered. These are the dominant effects of cavity wall emissivity and heating element diameter on the oven thermal efficiency. Thus, it is expected that in future designs of energy efficient ovens, these two parameters will be given special attention. It is also hoped that, for future oven design strategies, the analytical modeling presented here will be used to evaluate ideas before they are implemented and tested in prototype ovens.

LIST OF REFERENCES

LIST OF REFERENCES

[1] Phillips, C.J, and Mary J. Nordberry, "Ovenware and Fuel Economy," Journal of Home Economics, pp.37-41, 1934.

[2] Erickson, Robert C., "Energy Efficiency Program for Kitchen Ranges and Ovens," Science Applications Inc., La Jolla California, report to the Department of Energy under contract number CR-04-60727-00, Nov. 1977.

[3] Federal Energy Administration, "Energy Conservation Program for Appliances," Federal Register, Vol. 43, No. 91 - Wednesday, May 10, 1978.

[4] U.S. Department of Energy, "Engineering Analysis Covering Energy Efficiency Standards for Consumer Products," Technical Support Document No. 5, DOE/CS-0166, June 1980.

[5] Sparrow, E.M., and R.D. Cess, Radiation Heat Transfer, McGraw Hill Book Company, 1978.

[6] Incropera, Frank P., and David P. DeWitt, Fundamentals of Heat Transfer, John Wiley and Sons, Inc., 1981.

[7] Holman, J.P., Heat Transfer, McGraw Hill Book Company, 1976.

[8] Rebrov, "Heat Transfer with Free Motion About a Horizontal Cylinder in Air," Journal of Engineering Physics, Inzh.-Fiz.zh. 4(9), 32-39, 1961.

[9] Martin, William T., "Thermal Performance and Control of an Energy Efficiency Domestic Electric Oven," M.S. Thesis, School of Mechanical Engineering, Purdue University, August 1981.

[10] Martin, Wm., T., "Thermal Model and Calibration of the Cake-Pan Radiometer," Heat Transfer Laboratory Report 072578 to Whirlpool Corporation, School of Mechanical Engineering, July 1978.

[11] Kline, S.J., and F.A. McClintock, "Describing Uncertainties in Single Sample Experiments," Mechanical Engineering, January 1953.

APPENDICES

APPENDIX A

MODEL I: IRRADIANCE DISTRIBUTION

A.1 Analysis Technique

Analytical Model I (Program COIL) is used to determine the irradiance distribution over the baking plane (or product surface) as a function of the heating element configuration. The analysis technique is to subdivide both the heating element and baking plane into arbitrarily small, rectangular-shaped areas which are assumed differential in size. View factors are found from each differential heating element area to each differential baking plane area. A simple summation process then determines the view factor from the entire heating element to each differential baking plane area. With these values, the irradiance distribution over the baking plane can be determined in non-dimensional form. If absolute irradiance values are preferred, assuming an isothermal heating element of temperature T_c and emissivity ε_c, an indication of the irradiance levels at the baking plane can be obtained through the use of Equation A-1.

$$G_{bp} = A_c \varepsilon_c \sigma T_c^4 \, F_{A_c - A_{bp}} \qquad \text{(A-1)}$$

where G_{bp} is the irradiance level at a differential baking plane area, A_c is the surface area of a differential heating element area, ε_c is the emissivity of the heating element, T_c is the temperature of the heating

element, A_{bp} is the surface area of the differential baking plane area, and $F_{A_c-A_{bp}}$ is the view factor from A_c to A_{bp}.

A.2 Input to Program COIL

Table A-1 lists the user specified input parameters for Program COIL. Definitions for each input variable can be found at the head of the program listing in Appendix E. When specifying coordinate values, (X,Y,Z), the origin is taken to be the lower-back, left-hand corner of the oven cavity.

CARD 1 specifies the user options, as described in complete detail in the Main Program Variable List for Program COIL, found in Appendix E.

CARD 2 gives the oven cavity size.

CARD 3 specifies the pan location, size, and depth. It also defines BPASL which is the length of a side for a differential rectangular baking plane area. Circular pans are approximated as shown in Figure A-1.

CARD 4 defines the specular reflectivity for each of the cavity walls.

CARD 5 lists the absorptivities of the product bottom and product top.

CARD 6 gives the upper and lower heating element temperatures. This card is necessary only when IOUT = 2.

CARD 7 defines the number of finite linear sections which approximate the heating element. Also defined are the Z locations of the

TABLE A-1. Input Variables for Program COIL

CARD NO.	VARIABLES	INPUT FORMAT
1.	IOPT,IPAN,ICONT,IOUT	(I2,3(1X,I1))
2.	DEPTH,WIDTH,HEIGHT	(3(F9.6,1X))
If IPAN=1		
3.	PANX,PANY,PANR,PAND,BPASL	(5(F9.6,1X))
If IPAN=2		
3.	PANX,PANY,PANL,PANW,PAND,BPASL	(6(F9.6,1X))
If IPAN=3		
3.	BPASL	(F9.6)
4.	RFB,RFT,RF1,RF2,RF3,RF4	(6(F9.6,1X))
5.	ABPBOT,ABPTOP	(2(F9.6,1X))
6.	IF(IOUT=3) CTUPR,CTLOWR	(2(F9.6,1X))
7.	NSECS,BPZ,CZ,CASL,W,CEMIS	(I3,5(1X,F9.6))
8.	CX(I),CY(I) I = 1,NENPS	(2(F9.6,1X))
If IOPT=4,9,10,14,19,20		
	CZ	(F9.6)

ORNL-DWG. 81-23736

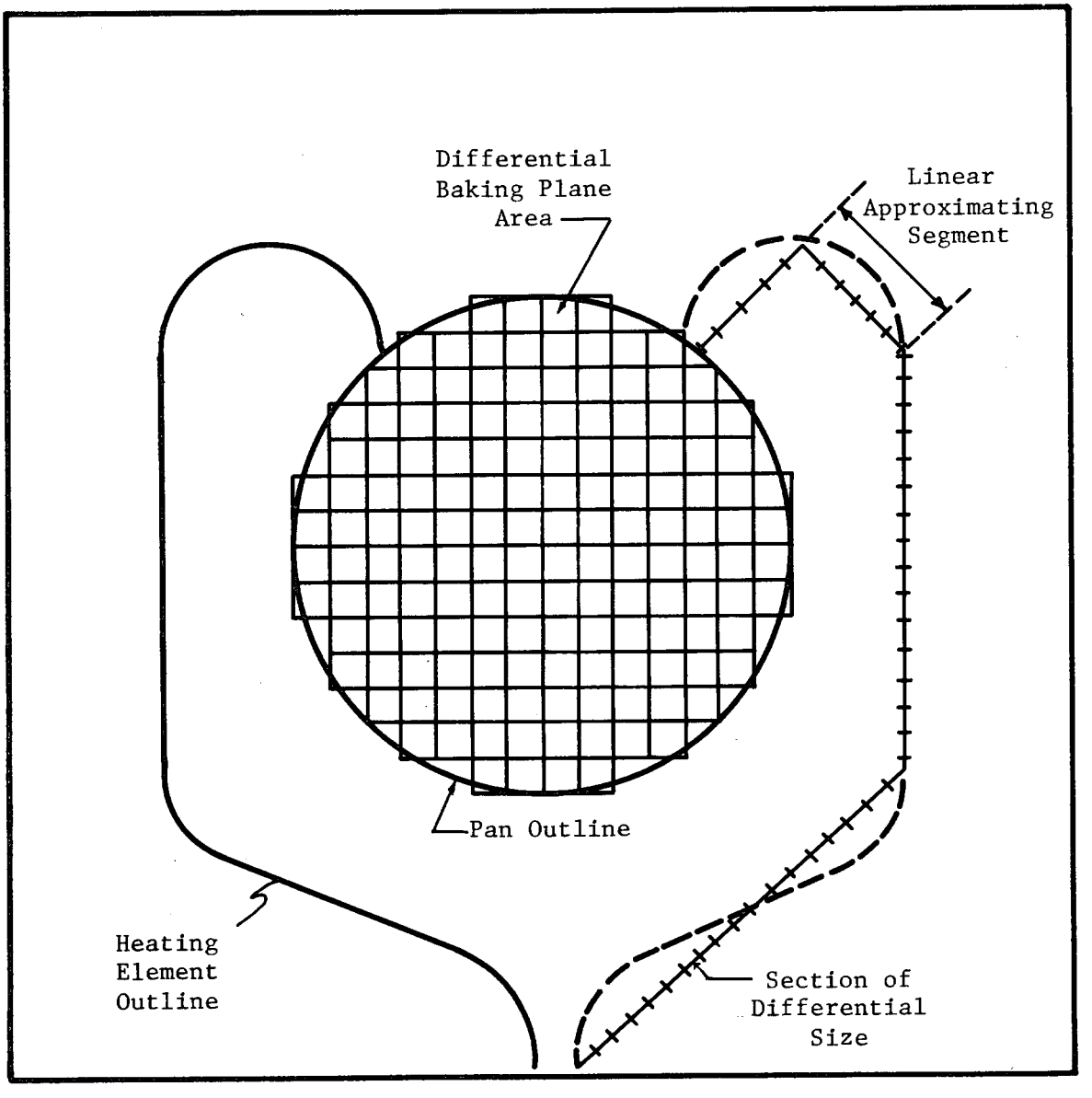

Figure A-1 Division of the Product Utensil and Heating Element into Differential Areas

baking plane (or product utensil) and the heating element, the side length of a differential area on the heating element, the heating element width (or diameter), and the heating element emissivity.

CARDS 8 and on specify the X and Y coordinates of the endpoints of the linear sections which approximate the heating element, the analysis further subdivides these approximating lengths into differential rectangular areas of length CASL and width W. An example of an approximated heating element is shown in Figure A-1.

THE FINAL INPUT CARD gives the Z location of the upper heating element if IOPT = 4, 9, or 10. If IOPT = 14, 19, or 20, CZ is the Z location of the lower heating element.

A.3 Program COIL, Logic Flow

Program COIL is divided into a main program and several supporting subroutines. Each subroutine handles a specific path for thermal radiation emitted from the heating element and intercepted at the baking plane (or surface of the product utensil). The subroutines are as follows:

1. DIRECT calculates the view factors for direct radiant transfer from the lower/upper heating element to the lower/upper pan surface.

2. REFA calculates the view factors for radiation emitted by the lower/upper heating element and intercepted at the lower/upper pan surface through a single specular reflection off the lower/upper cavity wall.

3. REFB calculates the view factors for a single specular reflection from the lower/upper heating element off the four oven side walls to the lower/upper pan surface.

4. REFC calculates the view factor for a single specular reflection from the upper/lower heating element off the lower/upper cavity wall to the lower/upper pan surface. This subroutine accounts for shading effects caused by the pan.

A.4 Specific Programming Methods

Many of the programming methods are explained in comment cards within the program (Appendix E), but two techniques which are used deserve a more detailed treatment.

A.4.1 Determining the Radiant Exchange View Factor Values and the Cosβ Term at the Heating Element

The general relation for calculating the view factor values from each heating element differential area to each differential baking plane area is of the form [6]

$$F_{c-bp} = \frac{1}{A_c}\iint \cos\beta_c \cos\beta_{bp} \frac{dA_c\, dA_{bp}}{\pi l^2} \qquad \text{(A-2)}$$

where A_c is the surface area of the differential heating element area, A_{bp} is the surface area of the differential baking plane area, l is the distance separating the differential areas A_c and A_{bp}, β_c is the angle between the normal to surface A_c and the line joining A_c and A_{bp}, and β_{bp} is the angle between the normal to surface A_{bp} and the line joining A_c and A_{bp}.

Approximating the cylindrical heating element area with a horizontal, rectangular element of the same length and width, and assuming the Cosβ factors do not vary over the small areas of either the heating element or baking plane, Equation A-2 can be integrated to obtain

$$F_{c-bp} = \frac{1}{A_c}\left[\text{Cos}\beta_c \text{Cos}\beta_{bp} \frac{A_{r,c} A_{bp}}{\pi l^2}\right] \qquad \text{(A-3)}$$

where $A_{r,c}$ is the surface area of the rectangular approximation to the cylindrical heating element area.

Since A_c equals πDL and $A_{r,c}$ equals DL, where D and L are the diameter and length of the rectangular approximation to the differential heating element area, respectively, substituting into Equation A-3 yields

$$F_{c-bp} = \text{Cos}\beta_c \ \text{Cos}\beta_{bp} \ A_{bp}/(\pi l)^2 \qquad \text{(A-4)}$$

For Equation A-4 to be a good approximation of the view factor from the differential heating element area to the differential baking plane area, the Cosβ factor at the heating element, represented by the rectangular approximation, must be a close estimate of the Cosβ factor for the actual, differential, cylindrical area. This is accomplished by rotating the rectangular, approximating area about the axis of the original cylindrical heating element area until its Cosβ factor has been minimized.

Figure A-2 depicts an arbitrary differential cylindrical heating element area and an arbitrary location of a differential rectangular baking plane area. The X,Y,Z coordinates of the center of each differen-

ORNL-DWG. 81-23737

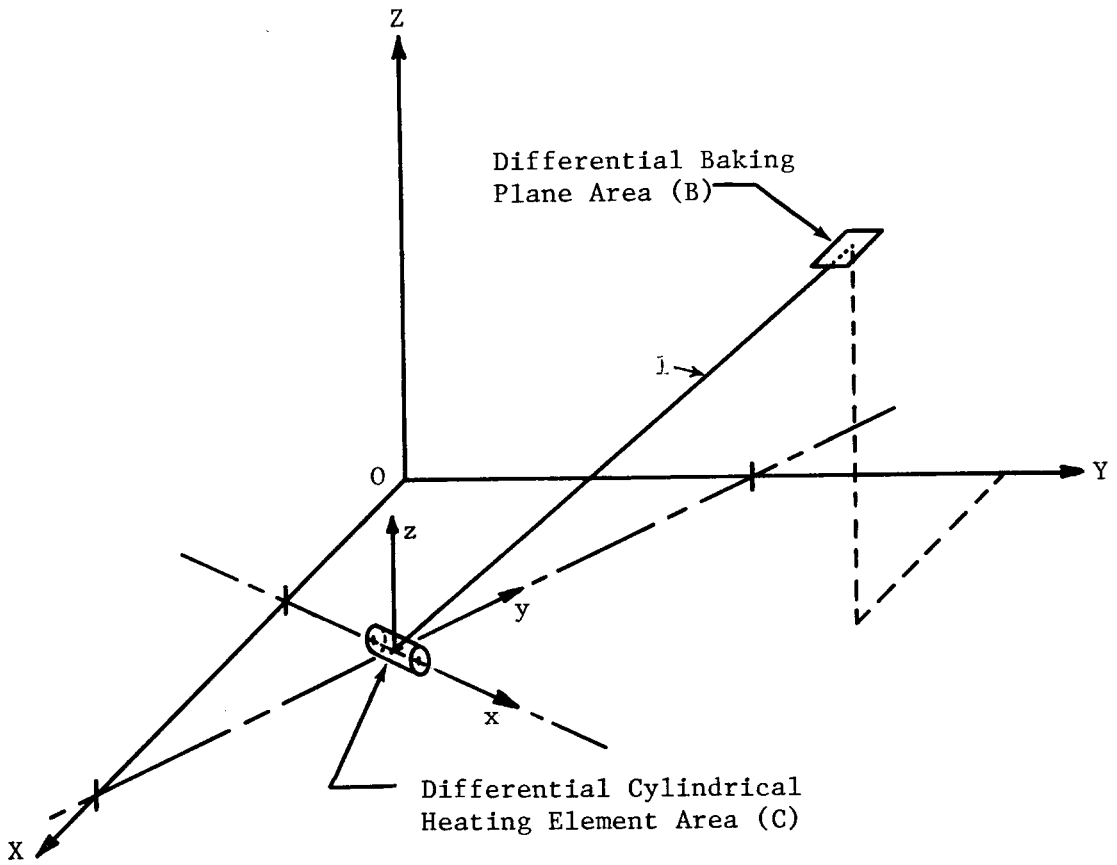

Figure A-2 Oven Coordinate System Showing Coordinates for Differential Areas on the Heating Element and at the Baking Plane

tial area are also indicated. Note that the X,Y,Z axis has been shifted such that the center of the cylindrical heating element area is in the X,Y plane. A minor coordinate axis labeled x,y,z has been established such that x lies along the heating element axis and z is parallel to Z. (The actual positive x and y directions are arbitrary.)

From Figure A-3 it is seen that the Cosβ factor at a differential rectangular area which approximates the cylindrical heating element will be minimized when the normal to its surface lies along line CA. When this alignment occurs, the Cosβ factor at the heating element (Cosβ_c) becomes

$$\mathrm{Cos}\beta_C = \frac{CA}{l} \qquad \text{(A-5)}$$

where l is the length of the line connecting the center of the heating element area (C) and the center of the baking plane area (B).

Defining y_c as the y coordinate of the point B, and performing an axis transformation from X,Y,Z to x,y,z generates a value for y_c as

$$y_c = -(X_{bp}-X_c)\mathrm{Sin}\alpha + (Y_{bp}-Y_c)\mathrm{Cos}\alpha \qquad \text{(A-6)}$$

where Sinα and Cosα are the direction cosines along the x-axis in the X,Y plane. Interpreting from Figure A-3, and applying the Pythagorean Theorem,

$$CA = \left[y_c^2 + (X_{bp} - X_c)^2\right]^{1/2} \qquad \text{(A-7)}$$

Substituting Equation A-7 into Equation A-5 gives

$$\mathrm{Cos}\beta_c = \left[y_c^2 + (X_{bp} - X_c)^2\right]^{1/2} /l \qquad \text{(A-8)}$$

ORNL-DWG. 81-23738

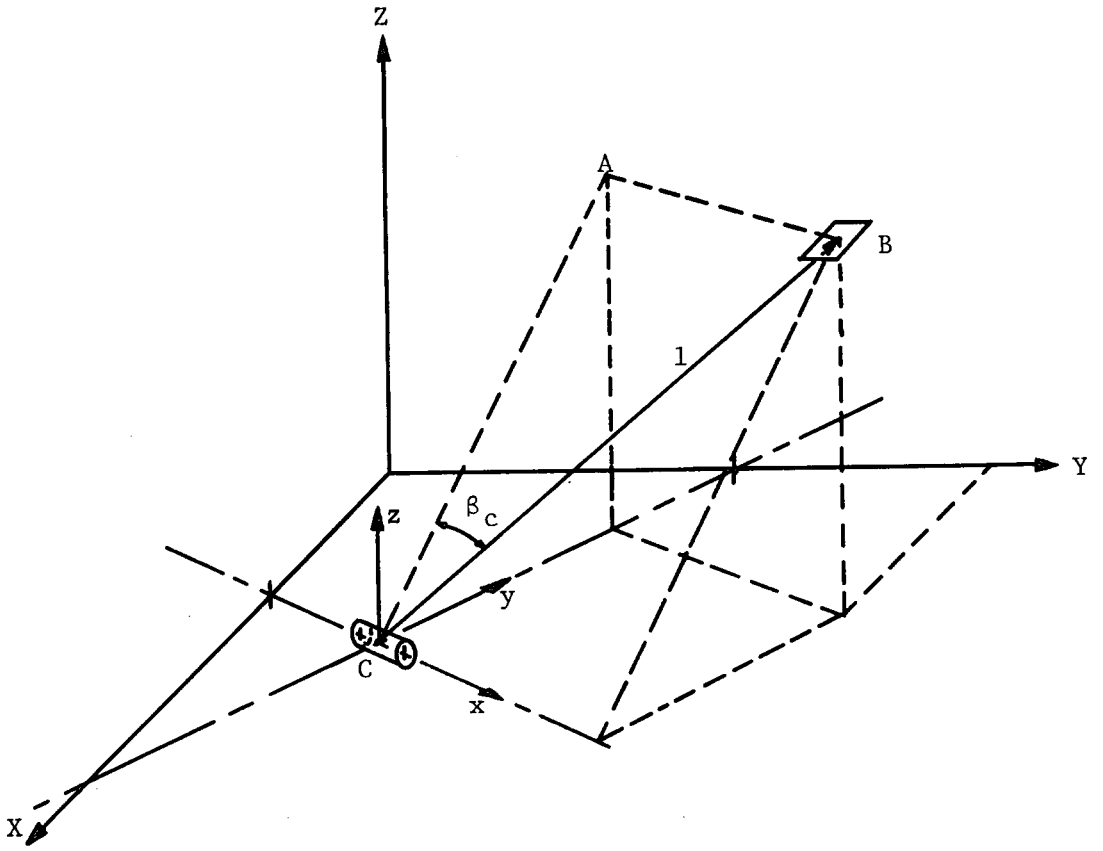

Figure A-3 Determination of β_c, the Angle Between the Normal to the Heating Element Differential Area and the Line Connecting the Two Differential Areas

Defining Fortran variables as shown in Table A-2, and substituting into Equations A-6 and A-7 results in

```
YC= -(BPX-X)*DCYS+(BPY-Y)*DCXS                    (A-9)
CCB = SQRT(YC**2+(BPX-X)**2)/R                    (A-10)
```

These two equations appear exactly as shown in subroutine DIRECT of Program COIL.

A.4.2 Accounting for a Single Specular Reflection at the Cavity Wall

The method of handling single specular reflections will be demonstrated for thermal radiation emitted from the lower heating element which is reflected off the lower cavity wall and intercepts the lower surface of a product utensil. Figure A-4 depicts this process where distances and coordinates are defined in terms of their Fortran variables, identified as follows:

θ_1 and θ_2 = Angles of incidence and reflection

DCRP = Distance from the heating element area to the reflection point.

DBPRP = Distance from the baking plane area element to the reflection point.

RX,RY = X and Y coordinates at the reflection point.

X,Y,CZ = X,Y and Z coordinates at the center of the heating element area.

BPX,BPY,BPZ = X,Y and Z coordinates at the center of the baking plane area element.

$$DXY = DCRP + DBPRP = \left[(BPX-X)^2+(BPY-Y)^2\right]^{1/2}$$

TABLE A-2. Definition of Fortran Variables used for Determining Cos at the Heating Element

FORTRAN VARIABLES	ALGEBRAIC EQUIVALENT
YC	y_c
DCXS	Cos
DCYS	Sin
BPX	X_{bp}
BPY	Y_{bp}
X	X_c
Y	Y_c
CCB	Cos_c
R	1

ORNL-DWG. 81-23739

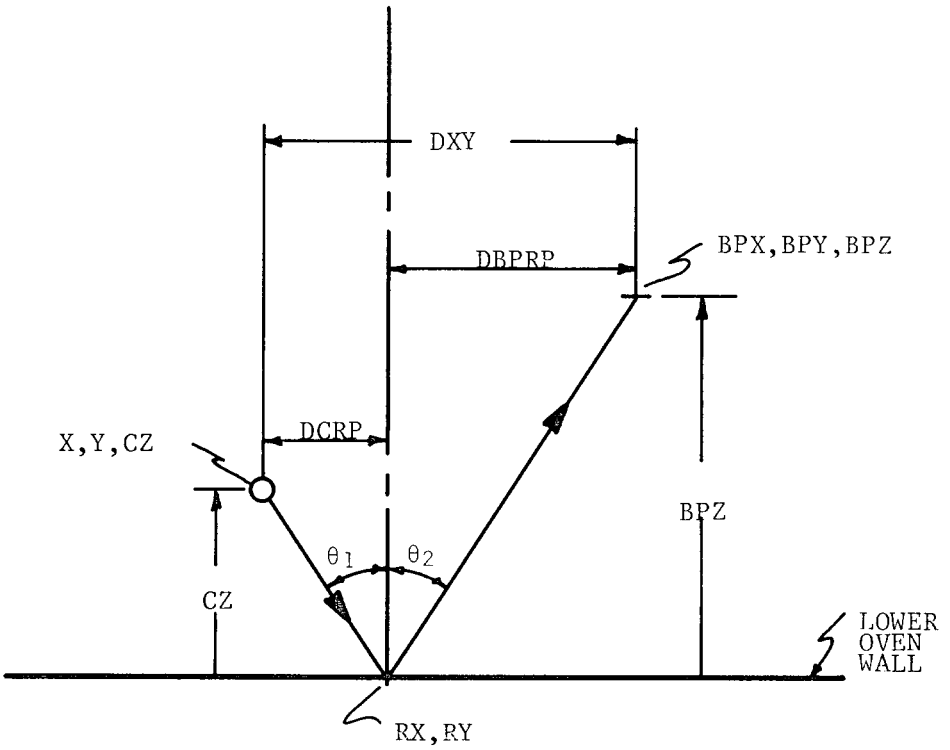

Figure A-4 Thermal Radiation Emitted from the Lower Heating Element, Reflecting off the Lower Oven Wall, and Intercepting a Baking Plane Differential Area.

Since at the reflection point, (RX,RY), the angle of incidence must equal the angle of reflection, then θ_1 must equal θ_2, and since DBPRP=DXY-DCRP, by using similar triangles,

$$\frac{DCRP}{CZ} = \frac{DXY-DCRP}{BPZ} \tag{A-11}$$

Solving for DCRP gives

$$DCRP = \frac{DXY*CZ}{CZ+BPZ} \tag{A-12}$$

Defining the X and Y direction cosines from the heating element area to the baking plane area as DCX and DCY,

$$DCX = (BPX-X)/DXY \tag{A-13}$$

$$DCY = (BPY-Y)/DXY \tag{A-14}$$

With Equations A-13 and A-14 it is possible to solve for the X and Y coordinates of the reflection point

$$RX = X+DCX*DCRP \tag{A-15}$$

$$RY = Y+DCY*DCRP \tag{A-16}$$

Knowing the coordinates of the reflection point (in this case, RZ=0), the view factor from the heating element area to the baking plane area is calculated as demonstrated in Section A.4.1. The Cosβ factors at the heating element area and the baking plane area are determined with reference to the reflection point.

Equations A-12 through A-16 appear exactly as shown in subroutine REFA of Program COIL.

APPENDIX B

MODEL II: TRANSIENT THERMAL ANALYSIS

Model II is composed of two separate Fortran programs. The first of these programs, OVENRAD, solves for the view factor matrix for determining the radiant exchange between surfaces within the oven cavity. The second program, AGTAP (Abbreviated General Thermal Analysis Program), defines the oven as a number of nodal points and calculates the temperature of each nodal point as a function of time.

B.1 Program OVENRAD

Program OVENRAD considers the geometrical arrangement of diffuse-gray surfaces within the oven cavity and calculates the view factor matrix for radiant exchange between these surfaces. Since the view factor matrix is only a function of the geometry of the surfaces, it remains unchanged throughout the transient analysis.

B.1.1 Analysis Techniques for Program OVENRAD

Program OVENRAD considers each surface within the oven cavity to be a diffuse-gray radiator. Each finite surface is subdivided into smaller differential areas before the view factor calculations are made. The heating elements and product are handled in the same manner as indicated in Appendix A for Program COIL. Finite surfaces used to define the walls are subdivided into differential areas and a simple summation is

then used to find the view factors for the finite surfaces.

The program also identifies existing symmetrical relations which will lessen the number of computer calculations required. By accounting for symmetry, the length of run time (and therefore the cost of the run) can be substantially reduced. It is suggested that a symmetrical location of the product and the heating elements be used whenever possible in order to realize these savings.

The program is capable of handling any arbitrary heating element shape and location, any product size and location, and any cavity size. The limiting factors being that the heating elements be of conventional Calrod design, the product be either in a rectangular or round pan, and the oven cavity be of the conventional 6 sided, cubical enclosure.

B.1.2 Input to Program OVENRAD

The input parameters of Table B-1 must be specified when using Program OVENRAD. In addition to this input (which is very nearly identical to that used in Program COIL), the user may vary the sizes of the differential areas which approximate the heating elements, the product, and the finite wall sections, and may also specify the number of finite sections used to represent each of the cavity walls. These options are obtained through the following variables (the coordinate system is given in Figure A-2):

N = Number of sections along a pan side

CASL = Differential heating element area side length

NX = Finite wall subsections along X-axis

NY = Finite wall subsections along Y-axis

TABLE B-1. Input Variables for Program OVENRAD

CARD NO.	VARIABLES	INPUT FORMAT
1	ALPHA NUMERIC STATEMENT	(7A10)
2	DEPTH,WIDTH,HEIGHT	(6F10.4)
3	IPAN	(I3)
IF IPAN=1		
4	PANX,PANY,PANZ,PANHZ	(6F10.4)
IF IPAN=2		
4	PANX,PANY,PANZ,PANLX,PANLY,PANHZ	(6F10.4)
5	ICOIL	(I3)
6	CZL,CZU,DL,DU	(6F10.4)
7	NENPS	(I3)
8 THRU N	CX(I),CY(I), I=1,NENPS	(6F10.4)
IF ICOIL=2	UPPER COIL DATA	
N+1	NENPS	(I3)
N+2	CX(I),CY(I), I=1,NENPS	(6F10.4)

NZ = Finite wall subsections along Z-axis

NSUBD = SQRT (Number of differential area subdivisions in each finite wall subsection.)

These 6 control variables appear as the first 6 executable statements in Program OVENRAD. They are also closely related to the sizes of the arrays dimensioned just prior to their definitions. When altering these variables it is essential that the following minimum array dimensions be maintained.

BPX(N),BPY(N)

CX(NENPS),CY(NENPS),S(NENPS-1)

WALLX(NX*NSUBD),WALLY(NY*NSUBD),WALLZ(NZ*NSUBD)

F(D,D) where D=5+2*(NX*NZ+NY*NZ+NX*NY)

If these minimum dimension sizes are not maintained, Program OVENRAD may still run, but will produce erroneous results.

B.1.3 Program OVENRAD, Logic Flow

Program OVENRAD consists of a main program and 9 subroutines. Each subroutine controls the calculation of a specific type of view factor, while the main program directs the calling order of the subroutines. A list of the subroutines and a short description of their assigned tasks are given below.

1. PROGRAM MAIN handles input, output, subroutine calls, and minor calculations.

2. ELTOPN generates view factors from the heating elements to the pan (product). Called from MAIN.

3. ELTWLS generates view factors from the heating elements to the walls. Called from MAIN.

4. WLTWLS generates view factors from finite wall sections to other finite wall sections. Called from MAIN.

5. EXCHNG calculates the view factor between two distinct but arbitrary wall elements i and j. Called from WLTWLS.

6. SHADOW determines if the radiant exchange path between two distinct area elements i and j is obstructed by the pan (product). Called from EXCHNG.

7. WLSTPN generates the view factors from the cavity walls to the pan (product). Called from MAIN.

8. SURFACE calculates the view factor value from a distinct wall element to the upper and lower surfaces of the pan (product). Called from WLSTPN.

9. SIDES calculates the view factor values from a distinct area element on the walls or on a heating element to the sides of the pan. Called from both ELTOPN and WLSTPN.

10. SURFICB solves for the Cosβ factor at surface i needed for calculating the view factors to the pan sides. Called from SIDES.

B.1.4 OVENRAD Output to AGTAP

In order to couple the solely geometrical calculations performed in OVENRAD with the time dependent analysis of AGTAP, use has been made of user accessible, semi-permanent storage space. Output results from OVENRAD which are required as input to AGTAP are stored here, then, whenever AGTAP is used, it recalls this information from storage. The data passed between OVENRAD and AGTAP consists of the heating element diameters, the number of finite surfaces involved in radiant exchange with the heating elements, the surface area of each of these surfaces, and the view factor matrix. Note that the input data stored by OVENRAD may be used for more than one running of AGTAP.

B.2 Program AGTAP

Program AGTAP is used for determining the transient thermal behavior of the oven. AGTAP is able to analyze the thermal radiation exchange between the interior cavity surfaces, to specify dependent versus independent properties through a tabular input procedure, to format additional output information, and to calculate the temperature versus time at each user specified nodal point.

B.2.1 Analysis Techniques for Program AGTAP

At each time increment in the transient thermal analysis, AGTAP completes three tasks. It determines the thermal radiation exchange between surfaces within the oven cavity, it analyzes the convective activity at the upper and lower heating elements [8], and it performs an iterative procedure employing a lumped heat capacitance analysis to determine the nodal temperatures.

B.2.2 Input to Program AGTAP

As has been previously mentioned, input to AGTAP comes from both semi-permanent storage space and from the user. The information from storage and the first portion of the user input pertain to the thermal radiation exchange analysis. The remaining user input is required by AGTAP in order to conduct the convection analysis and the lumped heat capacitance analysis which predicts the nodal temperatures.

B.2.2.1 Input for the Thermal Radiation Exchange Analysis

Since the data in semi-permanent storage is read in automatically at each running of AGTAP, the user need only be sure that AGTAP is reading the correct data file. Additional information required for the radiation exchange analysis is provided on the first 5 cards of the input deck, as shown in Table B-2. The input variables of Table B-2 are defined as follows;

IP = 0 If there is no pan.

IP = 1 If there is a pan.

IAIR1= Node number of air node involved in convective heat exchange with the lower heating element.

IAIR2= Node number of air node involved in convective heat exchange with the upper heating element.

ICONV1= The conduction/convection link between the lower heating element and IAIR1.

ICONV2= The conduction/convection link between the upper heating element and IAIR2.

TABLE B-2. AGTAP Input for the Radiation Exchange Analysis

CARD	VARIABLES	FORMAT
1	IP,IAIR1,IAIR2,ICONV1,ICON	(5I5)
2	PL,PU	(8F10.4)
3	E(1),E(2),E(3),E(4),E(5),E(6)	(8F10.4)
4	K,L,M	(3I5)
5	NR,NC	(3I5)

TABLE B-3. AGTAP Input for the Transient Thermal Analysis

CARD	VARIABLES	FORMAT
6	IC1,IC2,ROW,CP	(2I5,2F10.4)
7	K1(N),K2(N),XK1(N),XK2(N)	(2I5,2F10.4)
	Where N=1 up to 50	

PL,PU = Input power to the lower,upper heating elements.

E(1) = Lower heating element emissivity.

E(2) = Upper heating element emissivity.

E(3) = Lower pan surface emissivity.

E(4) = Upper pan surface emissivity.

E(5) = Pan sides emissivity.

E(6) = Wall material emissivity.

K,L,M = Rows (and columns) in view factor array which are all zeros.

NR,NC = Number of nonzero rows and columns in the view factor matrix. NR will always equal NC.

AGTAP use the above input to calculate the coefficient matrix for the radiation exchange analysis. This matrix is obtained before the data for the transient thermal analysis is read in.

B.2.2.2 Input for the Transient Thermal Analysis

When initially received, AGTAP required a specific input format and order. The above radiation analysis input is a completely new addition to these input requirements. The following general information input is also new to these input requirements. This general form allows for changing certain material properties with a single line of input. The initial method would have demanded the change of many additional, even hundreds, of lines of input. The input format for the general specification of nodal properties is shown in Table B-3.

In Table B-3, ROW and CP are the density and specific heat of nodal points IC1, through IC2. If this card is blank, or a zero value of IC1 is specified, then this option is ignored by the computer.

Conduction links K1(N) through K2(N) are multiplied by the factors XK1(N) and WALLT(N). This allows for thermal conductivities and the insulation thickness to be specified as general input. Note that the value of N can range from 1 up to 50. A blank card, or zero value of K1(N), indicates the termination of this specialized input form. If the first card is blank, or K1(1) is zero, this option is ignored by the computer.

The remaining input cards, as shown in Table B-4, contain the original input as required for running AGTAP. Defining some of these variables: If KILL is 0, the input data is listed with the program output. KOUT specifies the output interval, in terms of time steps, where TIME, DTIME, FTIME define the initial, delta, and final time for the test, respectively. KODE is the job control card. (If KODE = 11100, the job is terminated.)

Note that there will be no radiation couplings defined for the interior cavity nodes since Program OVENRAD and subroutine CLC1 are employed for these calculations. Radiation couplings are defined, however, for exchange between the exterior oven cover and the surrounding ambient. Also note that the tabular input is useful in specifying the temperature dependent properties of many of the nodal elements. For more information on the above input, see the AGTAP description package.[1]

[1] Program AGTAP, when received from our sponsors, was accompanied with a short description packet describing its operation and input.

TABLE B-4. Primary Input for Program AGTAP

INPUT	FORMAT
10 TITLE CARDS	(7A10)
KILL,KOUT	(5X,2I5)
TIME,DTIME,FTIME	(5X,3E10.0)
TEMPERATURES OF ITERATED NODES	
N,T(N),II,JJ	(5X,I5,E10.0,2I5)
11100	(I5)
TEMPERATURES OF BOUNDARY NODES	
N,T(N),II,JJ	(5X,I5,E10.0,2I5)
11100	(I5)
CAPACITANCES OF ITERATED NODE	
N,CAP(N),II,JJ	(5X,I5,E10.0,2I5)
11100	(I5)
CONDUCTANCE LINKS	
N,I,J,COND(N),II,JJ	(5X,3I5,E10.0,2I5)
11100	(I5)
RADIATION COUPLINGS	
N,I,J,RAD(N),II,JJ	(5X,3I5,E10.0,2I5)
11100	(I5)
HEAT SOURCES	
N,I,Q(N)	(5X,2I5,E10.0)
11100	(I5)
TABLES	
L1,L2,TITLE	(5X,2I5,16A4,A1)
DATA	(7E10.0)
11100	(I5)
CONTROL CARD	
KODE	(I5)

B.2.3 Program AGTAP Logic Flow

Information concerning the basic subroutines in AGTAP, their specific tasks, and their source of call is supplied in the AGTAP description package. As a general program, AGTAP allows for additional user manipulation in order to solve more complex problems or situations. For the oven analysis, the necessary manipulations were as follows;

1. In Main Program AGTAP, input data is read from PFILES in order to perform the radiation analysis. Additional general input is also read prior to the 10 TITLE CARDS, which are the first part of the primary input.

2. In Subroutine RITE, the general input is combined with the specific input required by AGTAP to produce the correct thermal mass and conduction link values.

3. In Subroutine CLC1, called at the start of every iteration, the thermal mass of the air nodes is determined from the tabular input, the convective phenomena at the heating elements is examined, and the thermal radiation exchange within the oven cavity is analyzed. If it is desired to include additional analysis concerning the convective phenomena, it would be placed in this subroutine.

4. In Subroutine CLC2, called just prior to the incrementing of time, the temperature dependent properties of the oven nodes are handled. Use is made of the table inputs which are allowed by AGTAP to accomplish this. Also, the block temperature is examined to check if it has reached 130°C above its

initial temperature. If so, the oven thermal efficiency is calculated and printed.

5. In Subroutine CLC3, called immediately after temperature printout, the calculated convective and radiative heat exchange values for nodes within the oven cavity are included with the nodal temperature printout.

APPENDIX C

HEAT FLUX MEASUREMENTS

In order to experimentally characterize the heating environment within an oven, a heat flux gage was developed to provide measurements of the irradiance, G (W/m^2), and the convection heat flux, q" (W/m^2). Operation principles of the gage are explained, calibration of the gage is described, and the calibration results are compared with those supplied by the manufacturer.[1]

C.1 Principles of Operation of the Heat Flux Gage

The theory of operation of a single Gardon Heat Flux sensor follows from Figure C-1, showing a cross-sectional view of the sensing element and depicting the heat flow through the sensing element. In this figure,

q'' = Net heat flux to the sensing element

r_o = Radius of the sensing element

t = Thickness of the sensing element

T_1 = Temperature at $r = 0$ on the sensing element

T_2 = Temperature at $r = r_o$ on the sensing element

e = Gage output (mV)

1 The sensors were supplied by Thermogage Inc., Frostburg, Maryland.

ORNL-DWG. 81-23740

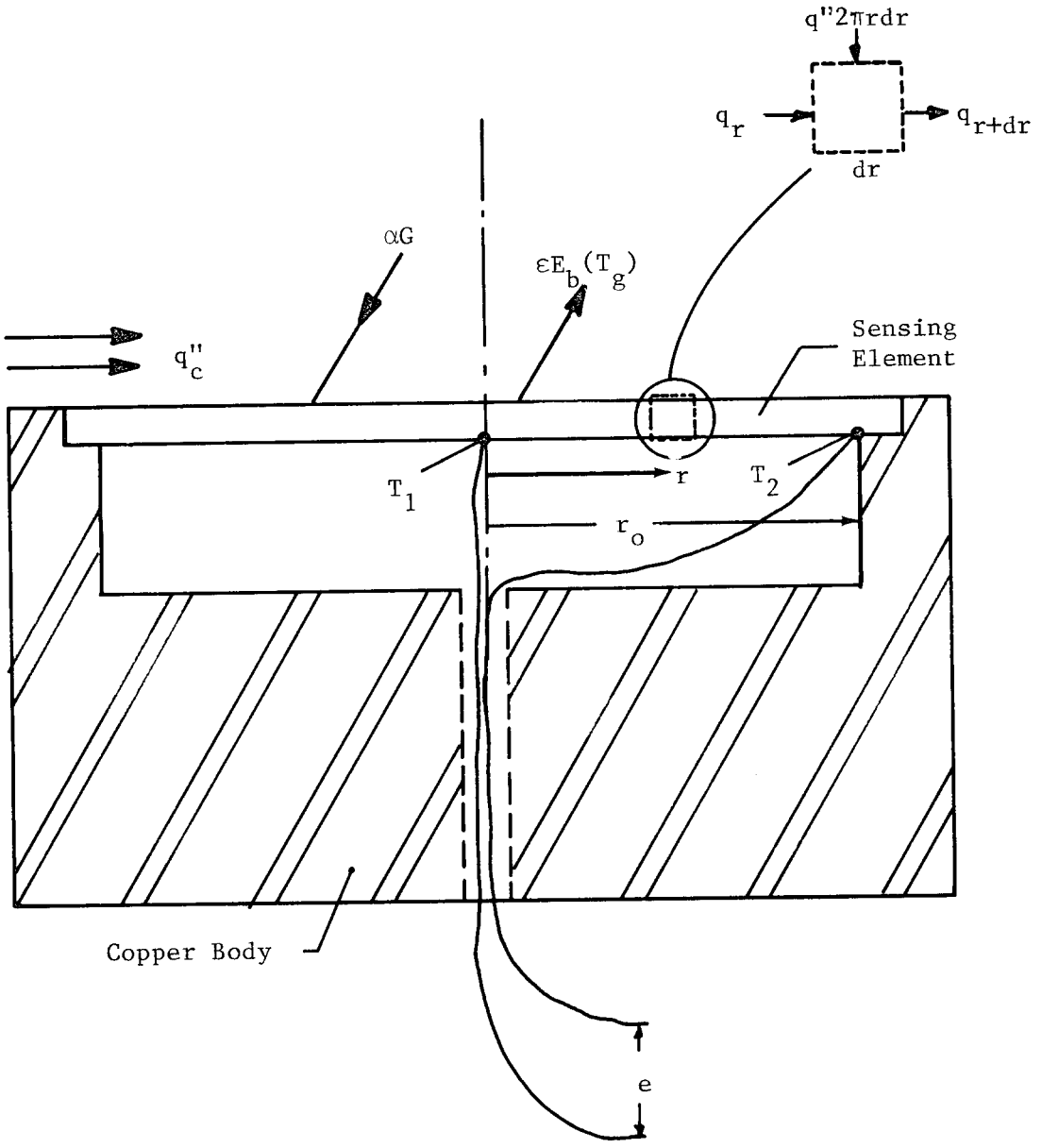

Figure C-1 Cross-Sectional View of the Sensing Element Depicting the Heat Flow Through the Sensing Element and the Net Heat Flux to the Sensing Element

From an energy balance on the elemental control volume of Figure C-1, it can be shown that the temperature distribution across the sensor surface can be expressed as [10]

$$T(r) - T_2 = \frac{q''}{4kt}\left[r_o^2 - r^2\right] \tag{C-1}$$

which, for $r = 0$, $T(0) = T_1$, gives

$$q'' = \frac{4kt}{r_o^2}\left[T_1 - T_2\right] \tag{C-2}$$

Through the Seebeck effect, $T_1 - T_2$ is proportional to the gage output, e. Therefore,

$$q'' \sim e$$

Defining the proportionality constant as 1/R, where R (mV/(W/m^2)) is the responsivity of the gage, gives

$$e = Rq'' \tag{C-3}$$

In a closer examination of q", the net heat flux to the sensing element, it is seen from Figure C-1 that

$$q'' = \alpha G + q''_c - \varepsilon E_b(T_g)$$

where q''_c is the convected heat flux to the sensing element, αG is the absorbed irradiation at the sensing element, and $\varepsilon E_b(T_g)$ is the emissive power of the sensing element. Since $\varepsilon E_b(T_g) = \varepsilon\sigma T_g^4$, where ε and T_g are the emissivity and temperature of the sensing element, the heat flux to the sensing element becomes

$$q'' = \alpha G + q''_c - \varepsilon\sigma T_g^4 \tag{C-4}$$

Writing Equation C-4 for the black (b) and reflective (r) sensors produces the two equations

$$q''_b = \alpha_b G_b + q''_{c,b} - \varepsilon_b \sigma T^4_{g,b} \qquad \text{(C-5a)}$$

$$q''_r = \alpha_r G_r + q''_{c,r} - \varepsilon_r \sigma T^4_{g,r} \qquad \text{(C-5b)}$$

When Equations C-5 are substituted into Equation C-3, the following measurement equations are obtained for the sensors,

$$e_b = R_b(\alpha_b G_b + q''_{c,b} - \varepsilon_b \sigma T^4_{g,b}) \qquad \text{(C-6a)}$$

$$e_r = R_r(\alpha_r G_r + q''_{c,r} - \varepsilon_r \sigma T^4_{g,r}) \qquad \text{(C-6b)}$$

In Equations C-6, e_b and e_r are the sensor signal outputs from the two units, R_b and R_r are the sensor responsivities obtained through a primary calibration (See section C.2.) The emissivity, ε, for each gage is specified by the manufacturer, or can be measured on separate samples of identical finish.[2] The absorptivity, α, is assumed equal to the emissivity, since the incident and emitted thermal radiation have nearly the same spectral distribution.

Equation C-6 can be simplified by recognizing that the sensing elements are in close proximity and of similar surface roughness such that the irradiances (G_b and G_r) and the convective heat fluxes (q''_b and q''_r) are identical for both sensors. Also, $T_{g,b}$ is assumed equal to $T_{g,r}$, and these temperatures are replaced by the average temperature of the

2 See Appendix D for these emissivity measurements

sensors, T_g. Using these simplifications, Equations C-6 can be rewritten as

$$e_b = R_b(\varepsilon_b G + q''_c - \varepsilon_b \sigma T_g^4) \tag{C-7a}$$

$$e_r = R_r(\varepsilon_r G + q''_c - \varepsilon_r \sigma T_g^4) \tag{C-7b}$$

which are a pair of simultaneous equations that can be solved for the incident irradiation, G, and the convective heat flux, q''_c, at the gage surface. If desired, the heat transfer coefficient, h, can be obtained through the relation

$$h = q''_c/(T_\infty - T_g) \tag{C-8}$$

where T_∞ is the ambient air temperature.

Strictly speaking, T_g should represent the area average of the temperature across the gage, which can be expressed as

$$T_{ave} = \frac{1}{A_g} \int T(r)dA \tag{C-9}$$

Recognizing that $A_g = \pi R^2$ and $dA = 2\pi r dr$, and that the temperature distribution across the sensing disk is given by Equation C-1, the integral of Equation C-9 can be evaluated to obtain

$$T_{ave} = \frac{q''R^2}{8kt} + T_2$$

By substituting from Equation C-2 for q", assumed to be uniform over the sensor surface, the average sensor temperature reduces to the form

$$T_g = T_{ave} = \frac{1}{2}(T_1 + T_2) \tag{C-10}$$

In other words, the gage temperature T_g is simply the average between the rim and center temperatures of the sensor. However, when calculations of the irradiance are made using the measured base plate temperature for T_g, as opposed to the more complex method of using the area averaged temperature, an error of less than 3% is incurred[9]. For the convective heat flux, the error is on the order of 1%. Since these errors are acceptably small, it is sufficient to use the monitored base plate temperature for T_g.

C.2 Calibration of the Heat Flux Gage

In all, three separate heat flux sensors, presumed to have the same responsivity, were purchased for the manufacturer. Two of the three sensors, identified as Gage Nos. 2003 and 2004, are identical with their sensing surfaces being highly absorbing, (ε = 0.95). The third unit, Gage No. 2002, is mounted on the same water cooled plate as Gage No. 2003, but has a highly reflective surface, (ε = 0.16). (This is the heat flux gage shown in Figure 2.5)

Primary calibration tests were performed by placing each sensor at a known distance from a laboratory-type blackbody radiator. By measuring the signal output as a function of the calculated irradiance level, the sensor responsivity could be directly determined. To check the repeatability of the sensors, and of the calibration results, several independent tests were conducted under nearly identical conditions.

When a gage is placedin front of the blackbody furnace opening, as shown in Figure C-2, the irradiance, G, on the gage is

$$G = q_{fg}/A_g$$

ORNL-DWG. 81-23741

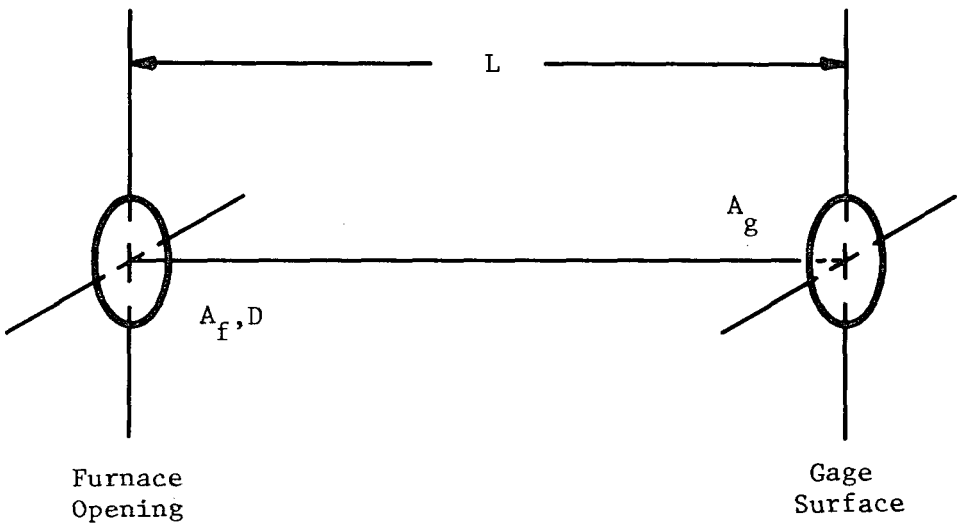

Figure C-2 Placement of the Gage in Front of a Blackbody Furnace for Calibration

where q_{fg} is the radiant heat flux from the furnace intercepting the gage surface and A_g is the surface area of the gage. Assuming diffuse emission from the furnace aperture,

$$q_{fg} = \frac{E_b(T_f)}{\pi} A_f \Omega_{f-g}$$

where $E_b(T_f)$ is the blackbody emission from the furnace at temperature T_f and Ω_{f-g} is the solid angle subtended by A_g from the furnace opening. If A_f and A_g are small in comparison to their separation distance, L, then

$$\Omega_{f-g} = A_g/L^2$$

and

$$q_{fg} = \frac{\sigma T_f^4}{\pi} A_f \frac{A_g}{L^2}$$

Therefore, since $A_f = \pi D^2/4$, the irradiance on the gage becomes

$$G = \frac{\sigma T_f^4}{4L^2} D^2 \qquad \text{(C-11)}$$

where D is the diameter of the furnace opening.

During calibration, a gage is first allowed to come to equilibrium with the surroundings, for the conditions of the furnace <u>off</u>, Equations C-7 become

$$e_{off} = R\left[\alpha G_{off} + h_{off}(T_a - T_{g,off}) + \varepsilon\sigma(T_a^4 - T_{g,off}^4)\right] \qquad \text{(C-12)}$$

where T_a is the temperature of the ambient air. Here, however, G_{off} is equal to zero, so that

$$e_{off} = R\left[h_{off}(T_a - T_{g,off}) + \varepsilon\sigma(T_a^4 - T_{g,off}^4)\right] \qquad \text{(C-13)}$$

Since the view factor from the furnace to the gage is on the order of 10^{-3}, when the furnace is turned on the change in the background radiation exchange will be negligible. Hence, the measurement equation for when the furnace is <u>on</u> becomes,

$$e_{on} = R\left[\alpha G_{on} + h_{on}(T_a - T_{g,on}) + \varepsilon\sigma(T_a^4 - T_{g,on}^4)\right] \qquad \text{(C-14)}$$

When the assumption is made that T_g and h remain constant, Equations C-13 and C-14 can be combined and rearranged to give the responsivity of the sensor as

$$R = \frac{e_{on} - e_{off}}{\alpha G_{on}} \qquad \text{(C-15)}$$

Each Gardon sensor was positioned relative to the blackbody source where nominal irradiance levels of 1000, 2000, and 3000 W/m^2 were experienced. Signal outputs from each unit were recorded and are shown in Table C-1. For the purpose of comparison, the averaged output from the two similar units, Gage Nos. 2003 and 2004, is shown in the last column of the table.

From the information in Table C-1, the responsivity of each sensor can be determined for each irradiance level. This observed responsivity can be compared with the value specified by the manufacturer, namely 0.0160 $mV/(W/m^2)$. The difference between these two values is presented in Table C-2. Note that for each gage, the deviations show no consistent trend with increasing irradiance levels. This could be due to a nonlinear behavior of the gages or to an experimental error associated with determining the irradiance value. Based upon the construction features of the gages, a linear response is to be expected. Thus, the

Table C-1 Gage Response to Incident Heat Flux

Irradiance* Level G (W/m^2)	Gage 2002 Output e (mV)	Gage 2003 Output e (mV)	Gage 2004 Output e (mV)	Average of Gage 2003 and 2004 e (mV)
1000	8.49	14.28	15.06	14.67
2000	18.37	31.03	32.47	31.75
3000	30.33	51.33	53.47	52.4

Table C-2 Comparison of the Heat Flux Gages with Manufacturer's Specification

Irradiance* Level G (W/m^2)	Deviation from Manufacturer's Specification (%)†		
	2002	2003	2004
1000	-46.7	-10.4	5.5
2000	-41.5	-1.2	3.4
3000	-36.2	8.0	12.5

Table C-3 Intercomparison of Gage Responsivities

Irradiance* Level G (W/m^2)	Gage 200 and 2004 % Diff
1000	-43.62
2000	-43.42
3000	-43.28

*Nominal values are used for these comparisons.

†The manufacturer's specification assumes gage responsivity is linear with a value 0.0160 mV/(W/m^2)

deviations are most likely caused by uncertainties in the irradiance levels as determined from the blackbody furnace. Considering the possible errors, the most accurate calibration test is that conducted at the nominal irradiance level of 1000 W/m^2. With this in mind the responsivity of Gage Nos. 2003 and 2004 are,

$$R_{2003} = 0.0142 \text{ mV}/(W/m^2)$$
$$R_{2004} = 0.0158 \text{ mV}/(W/m^2)$$

The responses for the combination of sensor units which comprise the heat flux gage are compared in Table C-3. Note that the response for Gage No. 2002 is consistently lower than Gage No. 2004 by approximately 43%. Using this information, the value for the responsivity of Gage No. 2002, R_r, is calculated as follows.

From Table C-3, $e_r = (1.0 - 0.4344)e_b$. Applying Equation C-3, and substituting for e_r, gives

$$e_b = R_b(q'') \tag{C-16}$$
$$0.5656e_b = R_r(q'') \tag{C-17}$$

Dividing Equation C-17 by Equation C-16 gives

$$0.5656 = R_r/R_b$$

and using $R_b = R_{2004}$ results in

$$R_r = 0.008914 \text{ mV}/(W/m^2) \tag{C-18}$$

Therefore, for the reflective and black sensors which combine to form the water-cooled heat flux gage of Figure 2.5, the responsivity of the reflective sensor, Gage No. 2002, has been calculated to be 43% less

than the responsivity of the black sensor, Gage No. 2004.

C.3 Uncertainty Analysis in Determining the Sensitivity of the Heat Flux Gage

The uncertainty [11] in determining the sensitivity of Gage No. 2004 (the black sensor which is combined with Gage No. 2002 in the construction of the heat flux gage) places a bound on the experimental error when heat flux measurements are taken. From Equation C-10 for the irradiation, G, and Equation C-15 for the sensitivity, S, (the reciprocal of the responsivity), the sensitivity of Gage No. 2004, S_{2004}, can be expressed as

$$S_{2004} = \frac{\alpha_b \sigma T_f^4}{4 \Delta e_b L^2} D^2 \qquad \text{(C-19)}$$

where $e_{on} - e_{off}$ has been replaced by Δe_b. Assuming σ and D are exact values, the uncertainty in determining S_{2004} becomes,

$$\omega_S = \left[\left[\frac{\partial S}{\partial T_f} \omega_f \right]^2 + \left[\frac{\partial S}{\partial L} \omega_L \right]^2 + \left[\frac{\partial S}{\partial \alpha} \omega_\alpha \right]^2 + \left[\frac{\partial S}{\partial \Delta e_b} \omega_{e_b} \right]^2 \right]^{1/2} \qquad \text{(C-20)}$$

where ω_S = uncertainty in determinimg S_{2004}

ω_f = uncertainty in measuring T_f = ± 5 K

ω_L = uncertainty in measuring L = ± 0.4 cm

ω_α = uncertainty in specifying α = ± 0.03

ω_e = uncertainty in determining e_b = ± 1 mV

Calculating the partial derivatives, substituting into Equation C-16, and dividing by S results in

$$\frac{\omega_S}{S} = \left[\left[\frac{4\omega_f}{T_f}\right]^2 + \left[\frac{-2\omega_L}{L}\right]^2 + \left[\frac{\omega_\alpha}{\alpha}\right]^2 + \left[\frac{-\omega_e}{\Delta e_b}\right]^2\right]^{1/2} \qquad \text{(C-21)}$$

Consider the calibration case when the distance from the front panel of the furnace to the gage is 12 cm (the distance from the front panel to the aperture of the furnace is 3.5 cm), and the conditions of T_f equal to 1275°K, L equal to 15.5 cm, α equal to 0.95, and Δe_b equal to 15.06 mV. From these parameter values, and Equations (C-10) and (C-19), then,

$$G = 1006 \text{ W/m}^2$$

$$S_{2004} = 63.45 \text{ (W/m}^2\text{)/mV}$$

Solving for ω_S from (C-21), the sensitivity of Gage 2004, and the uncertainty in this value are expressed as,

$$S_{2004} = 63.45 \pm 5.06 \text{ (W/m}^2\text{)/mV} \qquad \text{(C-22)}$$

Thus, there is a possible error of 7.9% in the sensitivity or responsivity value obtained from the calibration procedure.

APPENDIX D

EMISSIVITY MEASUREMENTS FOR VARIOUS OVEN MATERIALS

Measurements of normal total emissivity were made through a direct comparison method in which the normal emissive power of a sample is compared to that of a blackbody at the same temperature. Comparisons were made using a Wahl, Model HSA-8E, radiometer having a spectral band pass in the 1-15 micrometer range. At a temperature of 150°C, this range encompasses 76% of the sample emission, the remaining 14% being beyond this range. For the oven materials examined, this does not present a problem since their emissivities are expected to be spectrally independent at longer wavelengths.

The experimental apparatus consists of an eight sided aluminum block with four imbedded heaters. A blackbody cavity has been drilled into one of the eight sides and samples can be mounted on the remaining seven. The block size is approximately 15 cm. high by 12 cm. diameter and the sample sizes are approximately 2.5 cm in diameter. Prior to conducting measurements, power is supplied to the four heaters, raising the block temperature to approximately 150°C. Due to the high conductivity of the block, the temperature of the samples mounted on the block are assumed to be the same as the temperature of the blackbody cavity.

Once the block has reached 150°C, measurements are taken using the radiometer.

The output level from the radiometer depends on the intensity of the incoming irradiation, and is available in two forms. Needle deflection on a calibrated scale indicating the irradiation source temperature, and a 0-1 Voltage output providing a hard copy recording of the output level. The radiometer is calibrated to indicate the temperature of an irradiation source, assuming such source is an ideal blackbody. For non-ideal sources of emissivity less than 1.0, the radiometer is equipped with an emissivity control dial which, when set to the non-ideal source emissivity, enables the correct indication of the source temperature.

Experimental measurements of sample emissivities are accomplished by reversing the role of the emissivity dial. First, the radiometer output jack is connected to a strip chart recorder, then measurements taken from the blackbody cavity. Next, the radiometer is aimed at one of the samples (whose temperature is the same as that of the blackbody). The emissivity control dial is then adjusted until the output produced by the sample is identical to the output produced by the blackbody. The sample emissivity is then read directly from the dial.

This method of dialing in the emissivity of the sample is limited by the range of the emissivity dial, which is 1.00 - 0.20. For surfaces of emissivity less than 0.20, an extrapolation technique is used. Readings at various settings of the emissivity dial are taken and a plot is made of the surface emissivity versus radiometer output (Volts). This

plot is then extrapolated to the output voltage level which was produced by the blackbody cavity. The value of the sample emissivity is then read directly from the graph.

Results from the emissivity measurements are given in Table D-1. Note that the emissivity values obtained from the extrapolation technique are given larger error bounds due to the greater inaccuracies of this method.

TABLE D-1. Normal Total Emissivity Values for Various Oven Materials

Aluminum Wall Samples	Emissivity
Highly Polished	0.03 $^{+0.04}_{-0.01}$
Hand Polished	0.11 ±0.03
Sand Blasted	0.32 ±0.02
Exterior Oven Cover	0.91 ±0.01
Utensil (Pan) Samples	
Conventional Metallic Cake Pan	0.10 ±0.03
Black Anodized Aluminum Pan	0.87 ±0.01
DuPont Silverstone	0.80 ±0.03
G&S Metal Products	
Baker-eze Cookie Sheet	0.55 ±0.03
Black Beauty Cookie Sheet	0.88 ±0.03
Heat Flux Gage Sensor Surface	
Reflective Sensor Surface	0.16 ±0.03
Black Sensor Surface	0.95 ±0.03

APPENDIX E

PROGRAM LISTINGS

PROGRAM COIL

```
C
C
C*******************MAIN PROGRAM COIL VARIABLE LIST*********************
C**                                                                   **
C**                                                                   **
C** ABPBOT=ABSORPTIVITY OF THE PRODUCT BOTTOM                          **
C** ABPTOP=ABSORPTIVITY OF THE PRODUCT TOP                             **
C** BPAREA=SIZE OF AN AREA ELEMENT IN THE BAKING PLANE                 **
C** BPASL=THE LENGTH OF A SIDE FOR THE SQUARE AREA ELEMENTS WHICH      **
C**     COMPRISE THE BAKING PLANE                                     **
C** BPX=X COORDINATES OF AREA ELEMENTS IN THE BAKING PLANE             **
C** BPY=Y COORDINATES OF AREA ELEMENTS IN THE BAKING PLANE             **
C** BPZ=Z COORDINATE OF THE BAKING PLANE                               **
C** CASL=LENGTH OF A RECTANGULAT AREA ELEMENT ON THE HEATING COIL.     **
C**        CASL IS MEASURED PARALLEL TO THE COIL AXIS.                **
C** CEMIS=EMISSIVITY OF THE HEATING ELEMENT                            **
C** CTUPR=UPPER COIL TEMPERATURE (DEGREES C)                           **
C** CTLOWR=LOWER COIL TEMPERATURE (DEGREES C)                          **
C** CX=X COORDINATES OF AREA SEGMENTS ON THE HEATING COIL              **
C** CY=Y COORDINATES OF AREA SEGMENTS ON THE HEATING COIL              **
C** CZ=Z COORDINATE OF THE HEATING COIL                                **
C** DEPTH=X DIMENSION OF THE OVEN CAVITY                               **
C** HEIGHT=Z DIMENSION OF OVEN CAVITY                                  **
C** ICONT=CONTOUR PLOTTING OPTION                                      **
C**      ICONT=1   NO CONTOUR PLOT                                    **
C**      ICONT=2   CONTOUR PLOT REQUESTED                             **
C** IOPT=OPTION CODE TO SPECIFY THE MODES OF RADIATION WHICH ARE       **
C**     OF INTEREST.  ALSO INDICATES WHETHER RADIATION INCIDENT        **
C**     ON THE TOP OF THE PAN OR ON THE BOTTOM OF THE PAN IS TO        **
C**     BE CONSIDERRED.                                                **
C**      IOPT=1    DIRECT RADIATION FROM THE LOWER ELEMENT TO          **
C**        THE LOWER BAKING SURFACE                                   **
C**      IOPT=2    REFLECTED RADIATION FROM THE LOWER ELEMENT OFF THE **
C**        OVEN BOTTOM TO THE LOWER BAKING SURFACE                    **
C**      IOPT=3    REFLECTED RADIATION FROM THE LOWER ELEMENT OFF THE **
C**        OVEN WALLS TO THE LOWER BAKING SURFACE                     **
C**      IOPT=4    REFLECTED RADIATION FROM THE UPPER ELEMENT OFF     **
C**        THE OVEN BOTTOM TO THE LOWER BAKING SURFACE.               **
C**      IOPT=7    INDICATES 1,2,AND 3 PLUS THEIR COMBINED TOTAL      **
C**      IOPT=8    THE COMBINED TOTAL FROM 1,2,AND 3                  **
C**      IOPT=9    INDICATES 1,2,3,AND 4 PLUS THEIR COMBINED TOTAL    **
C**      IOPT=10   THE COMBINED TOTAL FROM 1,2,3,AND 4                **
C**      IOPT=11   DIRECT RADIATION FROM THE UPPER ELEMENT            **
C**        TO THE UPPER BAKING SURFACE                                **
C**      IOPT=12   REFLECTED RADIATION FROM THE UPPER ELEMENT OFF THE **
C**        OVEN TOP TO THE UPPER BAKING SURFACE                       **
C**      IOPT=13   REFLECTED RADIATION FROM THE UPPER ELEMENT OFF THE **
C**        OVEN WALLS TO THE UPPER BAKING SURFACE                     **
C**      IOPT=14   REFLECTED RADIATION FROM THE LOWER ELEMENT         **
C**        OFF THE OVEN TOP TO THE UPPER BAKING SURFACE.              **
C**      IOPT=17   INDICATES 11,12,AND 13 PLUS THEIR COMBINED TOTAL   **
C**      IOPT=18   THE COMBINED TOTAL FROM 11,12,AND 13               **
C**      IOPT=19   INDICATES 11,12,13,14 AND THEIR COMBINED TOTAL     **
C**      IOPT=20   THE COMBINED TOTAL FROM 11,12,13,AND 14            **
C** IOUT=PROVIDES CONTROL OVER THE AMOUNT OF OUTPUT DESIRED            **
C**      IOUT=1    TOTAL VF (TVF) PLUS THE ARRAY (VF) ARE PRINTED     **
C**      IOUT=2    TOTAL VF (TVF) ONLY IS PRINTED                     **
C**      IOUT=3    TOTAL IRRADIANCE PLUS THE ARRAY ARE PRINTED (W/M2) **
C**      IOUT=4    TOTAL IRRADIANCE ONLY IS PRINTED (W/M2)            **
C** IPAN=INDICATES THE TYPE OF PAN GEOMETRY                            **
C**      IPAN=1    THE PAN IS ROUND                                   **
C**      IPAN=2    THE PAN IS RECTANGULAR                             **
C**      IPAN=3    THE IRRADIANCE DISTRUBUTION OVER THE ENTIRE        **
C**        BAKING PLANE IS CONSIDERED.                                **
C** LVFPRE=LOWER COIL VIEW FACTOR PREFIX.  SEE VFPRE                   **
C** MXMIN=INTEGER INDICES WHICH CORRESPOND TO                          **
C** MXMAX=THE MINIMUM AND MAXIMUM X AND Y VALUES                       **
C** NYMIN=OF A SPECIFIC SECTION IN THE BAKING PLANE                    **
C** NYMAX=(THIS SECTION CONTAINS THE PAN)                              **
C** NENPS=NUMBER OF ENDPOINTS FOR THE LINEAR SECTIONS WHICH            **
```

```
C**         APPROXIMATE THE HEATING COIL                                **
C** PAND=DEPTH OF THE PAN                                               **
C** PANL=LENGTH OF THE PAN ALONG THE X-DIRECTION                        **
C** PANR=RADIUS OF THE PAN                                              **
C** PANW=WIDTH OF THE PAN ALONG THE Y-DIRECTION                         **
C** PANX=X COORDINATE FOR THE CENTER OF THE PAN IN THE BAKING PLANE     **
C** PANY=Y COORDINATE FOR THE CENTER OF THE PAN IN THE BAKING PLANE     **
C** RFB=REFLECTIVITY OF OVEN BOTTOM                                     **
C** RFT=REFLECTIVITY OF OVEN TOP                                        **
C** RF1=REFLECTIVITY OF WALL1                                           **
C** RF2=REFLECTIVITY OF WALL2                                           **
C** RF3=REFLECTIVITY OF WALL3                                           **
C** RF4=REFLECTIVITY OF WALL4                                           **
C** S=STORES THE INDIVIDUAL LENGTHS OF THE LINEAR SECTIONS WHICH        **
C**     APPROXIMATE THE HEATING COIL                                    **
C** SIGMA=STEFAN-BOLTZMANN CONSTANT                                     **
C** STOT=TOTAL LENGTH OF THE HEATING ELEMENT                            **
C** TOT=THE OVERALL TOTAL VIEW FACTOR FOR ALL MODES OF                  **
C**         RADIATION CONSIDERED (AS BY IOPT)                           **
C** TVF=TOTAL VIEW FACTOR TO THE PAN CONSIDERING ALL MODES              **
C**     OF INCIDENT RADIATION                                           **
C** UVFPRE=UPPER COIL VIEW FACTOR PREFIX.  SEE VFPRE.                   **
C** VF=STORES THE VIEW FACTOR ASSOCIATED WITH EACH AREA ELEMENT         **
C**     IN THE BAKING PLANE FOR A SPECIFIC MODE OF INCIDENT RADIATION **
C** VFPRE=VIEW FACTOR PREFIX, IS THE NUMBER MULTIPLIED BY THE VIEW      **
C**     FACTOR TO OBTAIN IRRADIANCE (W/M2)                              **
C** VFTOT=STORES THE TOTOAL (ACCUMULATED) VIEW FACTOR ASSOCIATED        **
C**     WITH EACH AREA ELEMENT IN THE BAKING PLANE FOR ALL MODES        **
C**     OF INCIDENT RADIATION                                           **
C** W=DIAMETER OF THE HEATING ELEMENT                                   **
C** WIDTH=Y DIMENSION OF OVEN CAVITY                                    **
C**                                                                     **
C**                                                                     **
C***********************************************************************
C
C
      PROGRAM BAKE(INPUT,OUTPUT,PLOT,TAPE3,TAPE5=INPUT,TAPE6=OUTPUT)
      DIMENSION BPX(100),BPY(100),VF(100,100),VFTOT(100,100)
      DIMENSION S(30),CX(30),CY(30)
C
C ********************************************************************
C **                                                                 **
C ** THE FOLLOWING STATEMENTS DEAL WITH THE COUNTOUR                 **
C**     PLOTTING ROUTINE                                            **
C **                                                                 **
C  ******************************************************************
C
      REAL CVAL(11)
      INTEGER WORK(4600),CLAB(11)
      COMMON/INFO/XLEN,YLEN,NX,NY,NCH
      COMMON/FRAME/XMAX,YMAX,XMIN,YMIN,NXG,NYG,HTNBR
      COMMON/NDEV/IDEV
      DATA CLAB/1HA,1HB,1HC,1HD,1HE,1HF,1HG,1HH,1HI,1HJ,1HK/
C
C  ******************************************************************
C **                                                                 **
C **  THE COMMON BLOCKS ARE DEFINED AS FOLLOWS                       **
C **     BPPAN-CONSISTS OF THOSE VARIABLES WHICH ARE RELATED TO      **
C **   THE BAKING PLANE PLUS THOSE WHICH DEFINE THE PAN LOCATION     **
C **   AND PAN SIZE                                                  **
C **     LIMIT-CONSISTS SOLEY OF INTEGER VARIABLES.  IPAN IS         **
C **   AS DESCRIBED IN THE VARIABLE LIST.  THE MIN. AND MAX.         **
C **   VARIABLES REPRESENT A SECTION OF THE BAKING PLANE OVER        **
C **   WHICH ITERATIONS WILL BE PERFORMED.                           **
C **     VWFCT-CONSISTS OF VIEW FACTOR VARIABLES WHICH ARE           **
C **   COMMON TO VARIOUS SUBROUTINES.                                **
C **     REFL-CONSISTS OF THE REFLECTIVE VALUES FOR THE OVEN WALLS   **
C **   AND PRODUCT                                                   **
C **                                                                 **
C  ******************************************************************
```

```
C
      COMMON/BPPAN/BPX,BPY,PANX,PANY,PANR,BPAREA,PANL,PANW,PAND
      COMMON/LIMIT/IPAN,MXMIN,MXMAX,NYMIN,NYMAX,IOPT,IOUT
      COMMON/VWFCT/VFTOT,VFPRE
      COMMON/OVEN/DEPTH,WIDTH,HEIGHT
      COMMON/REFL/RFB,RFT,RF1,RF2,RF3,RF4,ABPTOP,ABPBOT
      IDEV=2
      VFTOTX=-10.0
      VFTOTN=10.0
      SIGMA=5.669E-08
      PI=3.141592654
      LC=1
C
C  ******************************************************************
C **                                                                **
C **  READ IN (AND WRITE OUT) THE OVEN AND PAN PARAMETERS           **
C **                                                                **
C  ******************************************************************
C
      READ(5,10)IOPT,IPAN,ICONT,IOUT
      READ(5,20)DEPTH,WIDTH,HEIGHT
      WRITE(6,30)IOPT,IPAN,ICONT,IOUT
      WRITE(6,40)DEPTH,WIDTH,HEIGHT
      IF(IPAN.EQ.2)GO TO 50
      IF(IPAN.EQ.3)GO TO 60
        READ(5,70)PANX,PANY,PANR,PAND,BPASL
        WRITE(6,80)PANR,PAND,PANX,PANY
      GO TO 90
   50 READ(5,100)PANX,PANY,PANL,PANW,PAND,BPASL
      WRITE(6,110)PANL,PANW,PAND,PANX,PANY
      GO TO 90
   60 READ(5,120)BPASL
      PAND=0.0
      WRITE(6,130)
C
C  ******************************************************************
C **                                                                **
C **  CALCULATE THE PERTINENT DATA FOR THE BAKING PLANE.  SECTION   **
C **  THE BAKING PLANE INTO SQUARE AREA ELEMENTS OF SIZE BPAREA.    **
C **  ASSIGN AN X AND Y COORDINATE TO THE GEOMETRICAL CENTER OF     **
C **  EACH AREA ELEMENT AND DETERMINE WHICH OF THESE BEST           **
C **  APPROXIMATE THE PAN, ITS SHAPE AND LOCATION.  CAREFULLY       **
C **  ACCOUNT FOR INTEGER TRUNCATION WHEN NEEDED.                   **
C **                                                                **
C  ******************************************************************
C
   90 BPAREA=BPASL**2
      ID=IFIX(DEPTH/BPASL)+1
      IW=IFIX(WIDTH/BPASL)+1
      BPX(1)=BPASL/2.0
      BPY(1)=BPASL/2.0
      DO 140 J=1,ID
        BPX(J)=BPX(1)+BPASL*FLOAT(J-1)
  140 CONTINUE
      DO 150 K=1,IW
        BPY(K)=BPY(1)+BPASL*FLOAT(K-1)
  150 CONTINUE
      IF(IPAN.EQ.2)GO TO 160
      IF(IPAN.EQ.3)GO TO 170
        MXMIN=IFIX((PANX-PANR)/BPASL)
        MXMAX=IFIX((PANX+PANR)/BPASL)+1
        NYMIN=IFIX((PANY-PANR)/BPASL)
        NYMAX=IFIX((PANY+PANR)/BPASL)+1
      GO TO 180
  160   MXMIN=IFIX((PANX-PANL/2.0)/BPASL)
        MXMAX=IFIX((PANX+PANL/2.0)/BPASL)+1
        NYMIN=IFIX((PANY-PANW/2.0)/BPASL)
        NYMAX=IFIX((PANY+PANW/2.0)/BPASL)+1
      GO TO 180
  170 MXMIN=1
```

```
      MXMAX=IFIX(DEPTH/BPASL)
      NYMIN=1
      NYMAX=IFIX(WIDTH/BPASL)
      IF(LC.EQ.2)GO TO 241
      LC=2
C
C  ******************************************************************
C **                                                                **
C **  READ IN THE Z LOCATION FOR THE COIL AND FOR THE BAKING PLANE.  **
C **  READ IN OVEN AND WALL REFLECTIVITIES                          **
C **  READ IN THE PRODUCT ABSORPTIVITIES                            **
C **  READ IN UPPER AND LOWER ELEMENT TEMPERATURES                  **
C **  ALSO, READ IN THE LENGTH OF AN AREA ELEMENT ON THE COIL,      **
C **  THE NUMBER OF LINEAR SECTIONS USED TO APPROXIMATE THE         **
C **  COIL, AND THE X AND Y COORDINATES FOR THE ENDPOINTS OF EACH   **
C **  SECTION.                                                      **
C **                                                                **
C  ******************************************************************
C
  180 READ(5,190)RFB,RFT,RF1,RF2,RF3,RF4
      READ(5,200)ABPBOT,ABPTOP
      IF(IOUT.LT.3)GO TO 183
      READ(5,200)CTUPR,CTLOWR
  183 READ(5,210)NSECS,BPZ,CZ,CASL,W,CEMIS
      NENPS=NSECS+1
      DO 220 I=1,NENPS
        READ(5,230)CX(I),CY(I)
  220 CONTINUE
C
C  ******************************************************************
C **                                                                **
C **  DETERMINE THE LENGTH OF EACH SECTION USED IN                  **
C **  APPROXIMATING THE HEATING COIL.                               **
C **                                                                **
C  ******************************************************************
C
      STOT=0.0
      DO 240 J=1,NSECS
        S(J)=((CX(J)-CX(J+1))**2+(CY(J)-CY(J+1))**2)**0.5
        STOT=STOT+S(J)
  240 CONTINUE
  241 WRITE(6,250)BPZ,BPASL,CZ,NSECS,CASL,W,CX(1),CY(1)
      DO 260 J=1,NSECS
        WRITE(6,270)CX(J+1),CY(J+1),S(J)
  260 CONTINUE
      WRITE(6,280)STOT
      WRITE(6,290)RFB,RFT,RF1,RF2,RF3,RF4
      WRITE(6,300)ABPTOP,ABPBOT
      IF(IOUT.LT.3)GO TO 263
      WRITE(6,310)CTUPR,CTLOWR
  263 WRITE(6,320)CEMIS
C
C  ******************************************************************
C **                                                                **
C ** SET THE VFTOT ARRAY TO THE MAX. VALUE USED IN THE CONTOUR      **
C **     PLOTTING ROUTINE.                                          **
C **                                                                **
C  ******************************************************************
C
      DO 330 M=1,100
        DO 340 N=1,100
          VFTOT(M,N)=10.0
  340   CONTINUE
  330 CONTINUE
      DO 350 M=MXMIN,MXMAX
        DO 360 N=NYMIN,NYMAX
          VFTOT(M,N)=0.0
  360   CONTINUE
  350 CONTINUE
      LVFPRE=(PI*W*STOT/BPAREA)*CEMIS*SIGMA*(CTLOWR+273.15)**4
```

```
      UVFPRE=(PI*W*STOT/BPAREA)*CEMIS*SIGMA*(CTUPR+273.15)**4
C
C  ****************************************************************
C **                                                              **
C **  AS SPECIFIED BY THE OPTION CODE, THE PROGRAM BEGINS CALLING  **
C **  SUBROUTINES WHICH ACCOUNT FOR THE SEPARATE MODES RADIANT     **
C **  TRANSFER.                                                   **
C **                                                              **
C  ****************************************************************
C
      IF(IOPT.GT.10)GO TO 2000
C
C  ****************************************************************
C **                                                              **
C ** OPTIONS CONSIDERING THE LOWER BAKING SURFACE                  **
C **                                                              **
C  ****************************************************************
C
      VFPRE=LVFPRE
      IF(IOPT.GT.1)GO TO 1010
        CALL DIRECT(NENPS,BPZ,CZ,S,CASL,CX,CY,TVF,VF)
        WRITE(6,1020)
        CALL PRINT(TVF,VF)
      GO TO 999
 1010 IF(IOPT.GT.2)GO TO 1030
        CALL REFA(NENPS,BPZ,CZ,S,CASL,CX,CY,TVF,VF)
        WRITE(6,1040)
        CALL PRINT(TVF,VF)
      GO TO 999
 1030 IF(IOPT.GT.3)GO TO 1050
        CALL REFB(NENPS,BPZ,CZ,S,CASL,CX,CY,TVF,VF)
        WRITE(6,1060)
        CALL PRINT(TVF,VF)
      GO TO 999
 1050 IF(IOPT.GT.4)GO TO 1070
C
C  ****************************************************************
C **                                                              **
C ** ASSUME TOP AND BOTTOM COILS ARE IDENTICAL.  READ IN THE       **
C ** Z-LOCATION OF THE LOWER COIL.                                 **
C **                                                              **
C  ****************************************************************
C
        READ(5,1080)CZ
      VFPRE=LVFPRE
        CALL REFC(NENPS,BPZ,CZ,S,CASL,CX,CY,TVF,VF)
        WRITE(6,1090)CZ
        CALL PRINT(TVF,VF)
      GO TO 999
 1070 IF(IOPT.GT.7) GO TO 1100
        CALL DIRECT(NENPS,BPZ,CZ,S,CASL,CX,CY,TVF,VF)
        TOT=TVF
        WRITE(6,1020)
        CALL PRINT(TVF,VF)
        CALL REFA(NENPS,BPZ,CZ,S,CASL,CX,CY,TVF,VF)
        TOT=TOT+TVF
        WRITE(6,1040)
        CALL PRINT(TVF,VF)
        CALL REFB(NENPS,BPZ,CZ,S,CASL,CX,CY,TVF,VF)
        TOT=TOT+TVF
        WRITE(6,1060)
        CALL PRINT(TVF,VF)
        WRITE(6,1120)
        CALL PRINT(TOT,VFTOT)
      GO TO 999
 1100 IF(IOPT.GT.8)GO TO 1110
        CALL DIRECT(NENPS,BPZ,CZ,S,CASL,CX,CY,TVF,VF)
        TOT=TVF
        CALL REFA(NENPS,BPZ,CZ,S,CASL,CX,CY,TVF,VF)
        TOT=TOT+TVF
```

```
        CALL REFB(NENPS,BPZ,CZ,S,CASL,CX,CY,TVF,VF)
        TOT=TOT+TVF
        WRITE(6,1120)
        CALL PRINT(TOT,VFTOT)
      GO TO 999
 1110 IF(IOPT.GT.9)GO TO 1130
        CALL DIRECT(NENPS,BPZ,CZ,S,CASL,CX,CY,TVF,VF)
        TOT=TVF
        WRITE(6,1020)
        CALL PRINT(TVF,VF)
        CALL REFA(NENPS,BPZ,CZ,S,CASL,CX,CY,TVF,VF)
        TOT=TOT+TVF
        WRITE(6,1040)
        CALL PRINT(TVF,VF)
        CALL REFB(NENPS,BPZ,CZ,S,CASL,CX,CY,TVF,VF)
        TOT=TOT+TVF
        WRITE(6,1060)
        CALL PRINT(TVF,VF)
        READ(5,1080)CZ
        VFPRE=UVFPRE
        CALL REFC(NENPS,BPZ,CZ,S,CASL,CX,CY,TVF,VF)
        TOT=TOT+TVF
        WRITE(6,1090)CZ
        CALL PRINT(TVF,VF)
        WRITE(6,1120)
        CALL PRINT(TOT,VFTOT)
      GO TO 999
 1130 IF(IOPT.GT.10)GO TO 999
        CALL DIRECT(NENPS,BPZ,CZ,S,CASL,CX,CY,TVF,VF)
        TOT=TVF
        CALL REFA(NENPS,BPZ,CZ,S,CASL,CX,CY,TVF,VF)
        TOT=TOT+TVF
        CALL REFB(NENPS,BPZ,CZ,S,CASL,CX,CY,TVF,VF)
        TOT=TOT+TVF
        READ(5,1080)CZ
        VFPRE=UVFPRE
        CALL REFC(NENPS,BPZ,CZ,S,CASL,CX,CY,TVF,VF)
        TOT=TOT+TVF
        WRITE(6,1120)
        CALL PRINT(TOT,VFTOT)
      GO TO 999
C
C  ******************************************************************
C **                                                                **
C ** OPTIONS CONSIDERING THE UPPER BAKING SURFACE                   **
C **                                                                **
C  ******************************************************************
C
 2000 VFPRE=UVFPRE
      IF(IOPT.GT.11)GO TO 2010
        CALL DIRECT(NENPS,BPZ,CZ,S,CASL,CX,CY,TVF,VF)
        WRITE(6,2020)
        CALL PRINT(TVF,VF)
      GO TO 999
 2010 IF(IOPT.GT.12)GO TO 2030
        CALL REFA(NENPS,BPZ,CZ,S,CASL,CX,CY,TVF,VF)
        WRITE(6,2040)
        CALL PRINT(TVF,VF)
      GO TO 999
 2030 IF(IOPT.GT.13)GO TO 2050
        CALL REFB(NENPS,BPZ,CZ,S,CASL,CX,CY,TVF,VF)
        WRITE(6,2060)
        CALL PRINT(TVF,VF)
      GO TO 999
 2050 IF(IOPT.GT.14)GO TO 2070
C
C  ******************************************************************
C **                                                                **
C ** ASSUME TOP AND BOTTOM COILS ARE IDENTICAL.  READ IN THE        **
C ** Z-LOCATION OF THE UPPER COIL.                                  **
```

```
C **                                                                  **
C  ***********************************************************************
C
      READ(5,1080)CZ
      VFPRE=LVFPRE
      CALL REFC(NENPS,BPZ,CZ,S,CASL,CX,CY,TVF,VF)
      WRITE(6,2080)CZ
      CALL PRINT(TVF,VF)
    GO TO 999
 2070 IF(IOPT.GT.17)GO TO 2090
      CALL DIRECT(NENPS,BPZ,CZ,S,CASL,CX,CY,TVF,VF)
      TOT=TVF
      WRITE(6,2020)
      CALL PRINT(TVF,VF)
      CALL REFA(NENPS,BPZ,CZ,S,CASL,CX,CY,TVF,VF)
      TOT=TOT+TVF
      WRITE(6,2040)
      CALL PRINT(TVF,VF)
      CALL REFB(NENPS,BPZ,CZ,S,CASL,CX,CY,TVF,VF)
      TOT=TOT+TVF
      WRITE(6,2060)
      CALL PRINT(TVF,VF)
      WRITE(6,1120)
      CALL PRINT(TOT,VFTOT)
    GO TO 999
 2090 IF(IOPT.GT.18)GO TO 2100
      CALL DIRECT(NENPS,BPZ,CZ,S,CASL,CX,CY,TVF,VF)
      TOT=TVF
      CALL REFA(NENPS,BPZ,CZ,S,CASL,CX,CY,TVF,VF)
      TOT=TOT+TVF
      CALL REFB(NENPS,BPZ,CZ,S,CASL,CX,CY,TVF,VF)
      TOT=TOT+TVF
      WRITE(6,1120)
      CALL PRINT(TOT,VFTOT)
    GO TO 999
 2100 IF (IOPT.GT.19)GO TO 2110
      CALL DIRECT(NENPS,BPZ,CZ,S,CASL,CX,CY,TVF,VF)
      TOT=TVF
      WRITE(6,2020)
      CALL PRINT(TVF,VF)
      CALL REFA(NENPS,BPZ,CZ,S,CASL,CX,CY,TVF,VF)
      TOT=TOT+TVF
      WRITE(6,2040)
      CALL PRINT(TVF,VF)
      CALL REFB(NENPS,BPZ,CZ,S,CASL,CX,CY,TVF,VF)
      TOT=TOT+TVF
      WRITE(6,2060)
      CALL PRINT(TVF,VF)
      READ(5,1080)CZ
      VFPRE=LVFPRE
      CALL REFC(NENPS,BPZ,CZ,S,CASL,CX,CY,TVF,VF)
      TOT=TOT+TVF
      WRITE(6,2080)CZ
      CALL PRINT(TVF,VF)
      WRITE(6,1120)
      CALL PRINT(TOT,VFTOT)
    GO TO 999
 2110 IF(IOPT.GT.20)GO TO 999
      CALL DIRECT(NENPS,BPZ,CZ,S,CASL,CX,CY,TVF,VF)
      TOT=TVF
      CALL REFA(NENPS,BPZ,CZ,S,CASL,CX,CY,TVF,VF)
      TOT=TOT+TVF
      CALL REFB(NENPS,BPZ,CZ,S,CASL,CX,CY,TVF,VF)
      TOT=TOT+TVF
      READ(5,1080)CZ
      VFPRE=LVFPRE
      CALL REFC(NENPS,BPZ,CZ,S,CASL,CX,CY,TVF,VF)
      TOT=TOT+TVF
      WRITE(6,1120)
      CALL PRINT(TOT,VFTOT)
```

```
C
  999 CONTINUE
      IF(ICONT.EQ.1)GO TO 9999
C
C  ******************************************************************
C **                                                                **
C ** THE FOLLOWING STATEMENTS EMPLOY THE USE OF THE LIBRARY         **
C **     SUBROUTINE CONTOUR, WHICH CREATES A CONTOUR POLT OF THE    **
C **     IRRADIANCE DISTRIBUTION.                                   **
C ** FIRST THE CONTOUR PLOTTING INTERVAL IS FOUND AND THEN THE      **
C **     VALUE OF EACH CONTOUR LINE IS DETERMINED.  THE INPUT       **
C **     CALLING INFORMATION IS LISTED AND THE SUBROUTINE           **
C **     CONTOUR IS THEN CALLED.                                    **
C **                                                                **
C ** VFINT=CONTOUR PLOTTING INTERVALS BETWEEN FVTOT MINIMUM         **
C **     AND VFTOT MAXIMUM.                                         **
C ** CVAL=VALUE OF CONTOUR LEVELS.                                  **
C ** XMM=MAX./MIN. RADIATION LEVELS.                                **
C **                                                                **
C  ******************************************************************
C
      DO 3000 M=MXMIN,MXMAX
        DO 3010 N=NYMIN,NYMAX
          IF(VFTOT(M,N).GT.0.0)GO TO 3020
          VFTOT(M,N)=10.0
          GO TO 3010
 3020     IF(VFTOT(M,N).GT.VFTOTX)VFTOTX=VFTOT(M,N)
          IF(VFTOT(M,N).LT.VFTOTN)VFTOTN=VFTOT(M,N)
 3010   CONTINUE
 3000 CONTINUE
      WRITE(6,3030)VFTOTN,VFTOTX
      VFINT=(VFTOTX-VFTOTN)/10.0
      CVAL(1)=VFTOTN+VFINT/5.0
      DO 3050 I=2,10
        CVAL(I)=VFTOTN+FLOAT(I-1)*VFINT
 3050 CONTINUE
      CVAL(11)=VFTOTX-VFINT/5.0
      XMM=VFTOTX/VFTOTN
      WRITE(6,3060)CVAL(1),CVAL(2),CVAL(3),CVAL(4),CVAL(5),CVAL(6)
     $,CVAL(7),CVAL(8),CVAL(9),CVAL(10),CVAL(11),XMM
      NX=100
      NY=100
      NF=11
      XMAX=17.0
      YMAX=23.0
      XMIN=0.0
      YMIN=0.0
      YLEN=3.8*100.*BPASL/YMAX
      XLEN=3.5*100.*BPASL/XMAX
      NXG=IFIX(DEPTH*2.54/2.0)
      NYG=IFIX(WIDTH*2.54/2.0)
      HTNBR=0.1
      NCH=-1
      NCODE=0
      NDIM=(NX*NY*NF)/24
      CALL PLOTS
      CALL CONTOUR(VFTOT,NX,NY,CVAL,NF,10.0,WORK,NDIM,CLAB,NCODE)
      CALL PLOT(0.0,0.0,999)
C
C  ******************************************************************
C **                                                                **
C ** ALL FORMAT STATEMENTS ARE GIVEN BELOW                          **
C **                                                                **
C  ******************************************************************
C
   10 FORMAT(I2,1X,I1,1X,I1,1X,I1)
   20 FORMAT(3(F9.6,1X))
   30 FORMAT(1H1,////,20X,≠IOPT =    ≠,I2,15X,≠IPAN =    ≠,I2,
     $15X,≠ICONT =    ≠,I2,15X,≠IOUT =    ≠,I2)
   40 FORMAT(1X,///,10X,≠THE OVEN CAVITY HAS DIMENSIONS:   DEPTH=≠,F9.6,
```

```
   $≠   WIDTH=≠,F9.6,≠   HEIGHT=≠,F9.6)
 70   FORMAT(5(F9.6,1X))
 80   FORMAT(/,10X,≠A ROUND PAN OF RADIUS   R=≠,F9.6,
   $≠   AND DEPTH   D=≠,F9.6,
   $//,10X,≠IS LOCATED IN THE BAKING PLANE SUCH THAT ITS CENTER ≠,
   $≠HAS X,Y COORDINATES   X=≠,F9.6,≠   Y=≠,F9.6)
100 FORMAT(6(F9.6,1X))
110 FORMAT(/,10X,≠A RECTANGULAR PAN OF LENGTH   L=≠,F9.6,
   $≠   WIDTH   W=≠,F9.6,≠   AND DEPTH   D=≠,F9.6,
   $//,10X,≠IS LOCATED IN THE BAKING PLANE SUCH THAT ITS CENTER ≠,
   $≠HAS X,Y COORDINATES   X=≠,F9.6,≠   Y=≠,F9.6)
120 FORMAT(F9.6)
130 FORMAT(/,10X,≠THE IRRADIANCE DISTRIBUTION IS DETERMINED≠,
   $≠ OVER THE ENTIRE BAKING PLANE.≠)
190 FORMAT(6(F9.6))
200 FORMAT(F9.6,1X,F9.6)
210 FORMAT(I3,1X,5(F9.6,1X))
230 FORMAT(F9.6,1X,F9.6)
250 FORMAT(/,10X,≠THE BAKING PLANE HAS Z-COORDINATE   Z=≠,F9.6,
   $≠   AND IS DIVIDED INTO SQUARE AREA ELEMENTS OF SIDE LENGTH   L=≠,
   $F9.6,
   $//,10X,≠THE HEATING COIL HAS Z-COORDINATE   Z=≠,F9.6,
   $≠   AND IS APPROXIMATED BY   ≠,I3,≠   LINEAR SEGMENTS.≠,
   $//,10X,≠THE RECTANGULAR AREA ELEMENTS OF THE HEATING COIL HAVE≠,
   $≠ SIDE LENGTHS   L=≠,F9.6,≠   AND WIDTH   W=   ≠,F9.6,
   $//,10X,≠THE LINEAR COIL SECTIONS HAVE ENDPOINTS AND LENGTHS,≠,
   $//,14X,≠X≠,14X,≠Y≠,11X,≠LENGTH≠,/,10X,F9.6,5X,F9.6)
270 FORMAT(10X,F9.6,5X,F9.6,5X,F9.6)
280 FORMAT(1X,16X,≠TOTAL LENGTH  =  ≠,F9.5)
290 FORMAT(////,10X,≠THE REFLECTIVITIES OF THE OVEN WALLS ARE;≠,
   $//,15X,≠BOTTOM =  ≠,F9.6,/,15X,≠TOP    =  ≠,F9.6,/,
   $15X,≠WALL1  =  ≠,F9.6,/,15X,≠WALL2  =  ≠,F9.6,/,
   $15X,≠WALL3  =  ≠,F9.6,/,15X,≠WALL4  =  ≠,F9.6)
300 FORMAT(1H1,/////,10X,≠THE PRODUCT ABSORPTIVITIES ARE;≠,
   $//,15X,≠PRODUCT TOP    =   ≠,F9.6,
   $/,15X,≠PRODUCT BOTTOM =   ≠,F9.6)
310 FORMAT(////,10X,≠THE ELEMENT TEMPERATURES ARE;≠,
   $//,15X,≠UPPER ELEMENT =   ≠,F9.3,
   $/,15X,≠LOWER ELEMENT =   ≠,F9.3)
320 FORMAT(////,10X,≠THE ELEMENT EMISSIVITY =  ≠,F6.3)
1020 FORMAT(1H1,//,35X,≠DIRECT RADIATION FROM THE LOWER ELEMENT TO≠,
   $  ≠ THE LOWER BAKING SURFACE≠)
1040 FORMAT(1H1,//,28X,≠REFLECTED RADIATION FROM THE LOWER ELEMENT≠,
   $  ≠ OFF THE OVEN BOTTOM TO THE LOWER BAKING SURFACE≠)
1060 FORMAT(1H1,//,28X,≠REFLECTED RADIATION FROM THE LOWER≠,
   $  ≠ ELEMENT OFF THE OVEN WALLS TO THE LOWER BAKING SURFACE≠)
1080 FORMAT(F9.6)
1090 FORMAT(1H1,//,8X,≠REFLECTED RADIATION FROM THE UPPER ELEMENT≠,
   $  ≠ OFF THE OVEN BOTTOM TO THE LOWER BAKING SURFACE.≠,/,46X,
   $  ≠THE UPPER ELEMENT IS LOCATED AT   Z=≠,F9.6)
1120 FORMAT(1H1,//,50X,≠TOTAL VIEW FCTOR FOR ALL MODES CONSIDERED≠)
2020 FORMAT(1H1,//,35X,≠DIRECT RADIATION FROM THE UPPER ELEMENT TO≠,
   $  ≠ THE UPPER BAKING SURFACE≠)
2040 FORMAT(1H1,//,29X,≠REFLECTED RADIATION FROM THE UPPER ELEMENT≠,
   $  ≠ OFF THE OVEN TOP TO THE UPPER BAKING SURFACE≠)
2060   FORMAT(1H1,//,28X,≠REFLECTED RADIATION FROM THE UPPER ELEMENT≠,
   $  ≠ OFF THE OVEN WALLS TO THE UPPER BAKING SURFACE≠)
2080 FORMAT(1H1,//,28X,≠REFLECTED RADIATION FROM THE LOWER ELEMENT≠,
   $  ≠ OFF THE OVEN TOP TO THE UPPER BAKING SURFACE≠,/,48X,
   $  ≠THE LOWER ELEMENT IS LOCATED AT   Z=≠,F9.6)
3030 FORMAT(1H1,///,20X,≠THE MAXIMUM AND MINIMUM VIEW FACTOR VALUES≠,
   $≠, AND THE CONTOUR VALUEW ARE GIVEN BELOW≠,//,10X,
   $≠THE MINIMUM VIEW FACTOR VALUE =   ≠,E8.2,//,10X,
   $≠THE MAXIMUN VIEW FACTOR VALUE =   ≠,E8.2)
3060 FORMAT(//,10X,≠A =   ≠,E8.2,/,10X,≠B =   ≠,E8.2,
   $/,10X,≠C =   ≠,E8.2,/,10X,≠D =   ≠,E8.2,/,10X,≠E =   ≠,E8.2,
   $/,10X,≠F =   ≠,E8.2,/,10X,≠G =   ≠,E8.2,/,10X,≠H =   ≠,E8.2,
   $/,10X,≠I =   ≠,E8.2,/,10X,≠J =   ≠,E8.2,/,10X,≠K =   ≠,E8.2,
   $////,10X,≠(VIEW FACTOR MAX.)/(VIEW FACTOR MIN.) =   ≠,F9.6)
9999 STOP
```

```
      END
C
C
C*****************SUBROUTINE DIRECT VARIABLE LIST*********************
C**                                                                 **
C**                                                                 **
C** ABP=ABSORPTIVITY OF THE PRODUCT SURFACE                          **
C** BPCB=COSINE FACTOR AT THE AREA ELEMENT IN THE BAKING PLANE       **
C** CCB=COSINE FACTOR AT THE AREA ELEMENT ON THE COIL                **
C** D=DISTANCE PASSED ON HEATING COIL APPROXIMATING SECTION          **
C** DCXS=DIRECTION COSINE IN THE X DIRECTION FOR LINEAR COIL SECTION S**
C** DCYS=DIRECTION COSINE IN THE Y DIRECTION FOR LINEAR COIL SECTION S**
C** DHOLD=HOLDS THE INCREMENTAL VIEW FACTOR BETWEEN AN AREA ELEMENT  **
C**     ON THE COIL AND AN AREA ELEMENT IN THE BAKING PLANE          **
C** DIST=ABSOLUTE DISTANCE BETWEEN AN AREA ELEMENT IN THE BAKING     **
C**     PLANE AND THE GEOMETRICAL CENTER OF THE PAN (ROUND PAN)      **
C** DISTX=X DISTANCE OF AN AREA ELEMENT IN THE BAKING PLANE FROM THE **
C**     GEOMETRICAL CENTER OF THE PAN (RECTANGULAR PAN)              **
C** DISTY=Y DISTANCE OF AN AREA ELEMENT IN THE BAKING PLANE FROM THE **
C**     GEOMETRICAL CENTER OF THE PAN (RECTANGULAR PAN)              **
C** LC=LOOP COUNTER; DETERMINES THE TOTAL NUMBER OF BAKING           **
C**     PLANE AREA ELEMENTS INVOLVED                                 **
C** M=LOOP COUNTER;  INDEXES THE X LOCATION IN THE BAKING PLANE      **
C** N=LOOP COUNTER;  INDEXES THE Y LOCATION IN THE BAKING PLANE      **
C** NC=TOTAL NUMVER OF DIFFERENTIAL AREA ELEMENTS USED TO            **
C**     APPROXIMATE THE HEATING COIL                                 **
C** NEND=INDEX FOR THE ENDPOINT OF CURRENT INTEREST.                 **
C** R=SEPARATION DISTANCE BETWEEN AREA ELEMENTS                      **
C** TEMP=TEMPORARILY STORES THE VIEW FACTOR FROM A SPECIFIC AREA     **
C**     ELEMENT TO A SPECIFIC AREA ELEMENT IN THE BAKING PLANE       **
C** X=X COORDINATE FOR THE CENTER OF AN AREA ELEMENT ON THE COIL     **
C** Y=Y COORDINATE FOR THE CENTER OF AN AREA ELEMENT ON THE COIL     **
C** YC=Y-VALUE FOR THE AXIS TRANSFORMATION OF THE PROJECTION         **
C**     OF THE BAKING PLANE ELEMENT IN THE XY PLANE.                 **
C**                                                                 **
C**                                                                 **
C*********************************************************************
C
C
      SUBROUTINE DIRECT(NENPS,BPZ,CZ,S,CASL,CX,CY,TVF,VF)
      DIMENSION BPX(100),BPY(100),VF(100,100),VFTOT(100,100)
      DIMENSION S(30),CX(30),CY(30)
      COMMON/BPPAN/BPX,BPY,PANX,PANY,PANR,BPAREA,PANL,PANW,PAND
      COMMON/LIMIT/IPAN,MXMIN,MXMAX,NYMIN,NYMAX,IOPT,IOUT
      COMMON/VWFCT/VFTOT,VFPRE
      COMMON/REFL/RFB,RFT,RF1,RF2,RF3,RF4,ABPTOP,ABPBOT
      ABP=ABPBOT
      IF(IOPT.LE.10)GO TO 3
        BPZ=BPZ+PAND
        ABP=ABPTOP
    3 CONTINUE
C
C  ******************************************************************
C **                                                                **
C **  SET INITIAL VALUES FOR THE NECESSARY VARIABLES                **
C **                                                                **
C  ******************************************************************
      NEND=1
      TVF=0.0
      NC=0
      TEMP=0.0
      PI=3.141592654
C
C  ******************************************************************
C **                                                                **
C ** SET THE VIEW FACTOR ARRAY TO ZERO                              **
C **                                                                **
C  ******************************************************************
C
      DO 10 M=MXMIN,MXMAX
```

```
      DO 20 N=NYMIN,NYMAX
        VF(M,N)=0.0
   20 CONTINUE
   10 CONTINUE
C
C  ******************************************************************
C **                                                                **
C **  SET THE FIRST INCREMENTAL LENGTH TRAVERSED ALONG THE HEATING  **
C **  COIL AS THE DISTANCE FORM THE FIRST ENDPOINT TO THE CENTER    **
C **  OF THE FIRST AREA ELEMENT.  DETERMINE THE DIRECTION           **
C **  COSINES FOR THE LINEAR SECTION OF THE HEATING COIL BEING      **
C **  TRAVERSED.  FIND THE X AND Y COORDINATES FOR THE CENTER OF THE **
C **  AREA ELEMENT OF CURRENT INTEREST.                             **
C **                                                                **
C  ******************************************************************
C
      D=CASL/2.0
   30 DCXS=(CX(NEND+1)-CX(NEND))/S(NEND)
      DCYS=(CY(NEND+1)-CY(NEND))/S(NEND)
   40 X=CX(NEND)+D*DCXS
      Y=CY(NEND)+D*DCYS
      IF(X.LE.0.0)GO TO 90
      IF(Y.LE.0.0)GO TO 90
      LC=0
C
C  ******************************************************************
C **                                                                **
C **  THE FOLLOWING DO LOOPS CONSIDER EACH INDIVIDUAL AREA ELEMENT  **
C **  OF THE BAKING PLANE (WITHIN THE SECTION SET OFF BY MXMIN,     **
C **  MXMAX,AND NYMIN,NYMAX)  AND FINDS THE INCREMENTAL VIEW        **
C **  FACTOR TO EACH OF THESE AREA ELEMENTS DUE TO A SINGLE AREA    **
C **  ELEMENT OF THE HEATING COIL.                                  **
C **                                                                **
C  ******************************************************************
C
      DO 50 M=MXMIN,MXMAX
        DO 60 N=NYMIN,NYMAX
C
C  ******************************************************************
C **                                                                **
C **  DETERMINE IF A CERTAIN AREA ELEMENT OF THE BAKING PLANE IS    **
C ** ACTUALLY WITHIN THE CONFINES OF THE PAN.                       **
C **                                                                **
C  ******************************************************************
C
          IF(IPAN.EQ.1)GO TO 70
          IF(IPAN.EQ.3)GO TO 80
            DISTX=ABS(BPX(M)-PANX)
            DISTY=ABS(BPY(N)-PANY)
            IF(DISTX.GT.(PANL/2.0))GO TO 60
            IF(DISTY.GT.(PANW/2.0))GO TO 60
          GO TO 80
   70     DIST=((BPX(M)-PANX)**2+(BPY(N)-PANY)**2)**0.5
          IF((DIST-PANR).GT.0.0)GO TO 60
C
C  ******************************************************************
C **                                                                **
C **  DETERMINE THE INCREMENTAL VIEW FACTOR FROM THE COIL AREA      **
C **  ELEMENT LOCATED AT X,Y TO THE BAKING PLANE AREA ELEMENT BPX,BPY.**
C **                                                                **
C  ******************************************************************
C
   80   R=((BPX(M)-X)**2+(BPY(N)-Y)**2+(BPZ-CZ)**2)**0.5
        BPCB=ABS(BPZ-CZ)/R
        YC=(X-BPX(M))*DCYS+(BPY(N)-Y)*DCXS
        CCB=(((BPZ-CZ)**2+YC**2)**0.5)/R
        DHOLD=ABP*BPCB*CCB*BPAREA/((PI*R)**2)
        VF(M,N)=VF(M,N)+DHOLD
        TEMP=TEMP+DHOLD
        LC=LC+1
```

```
   60   CONTINUE
   50 CONTINUE
      TVF=TVF+TEMP
C
C  ***********************************************************************
C **                                                                     **
C **  PREPARE FOR EXAMINATION OF THE NEXT DIFFERENTIAL AREA              **
C **  ELEMENT OF THE HEATING COIL.  SET TEMP BACK TO ZERO, COUNT THE     **
C **  NUMBER OF COIL AREA ELEMENTS (NC), INCREMENT THE DISTANCE D        **
C **  TO THE NEXT AREA ELEMENT OF THE HEATING COIL.                      **
C **                                                                     **
C  ***********************************************************************
C
      TEMP=0.0
      NC=NC+1
      D=D+CASL
      IF(D.LE.S(NEND))GO TO 40
        D=D-S(NEND)
        NEND=NEND+1
C
C  ***********************************************************************
C **                                                                     **
C **  DETERMINE IF THE CURRENT LINEAR APPROXIMATING SECTION HAS          **
C **  BEEN COMPLETELY TRAVERSED AND IF THE NEXT SECTION NEEDS TO BE      **
C **  CONSIDERED OR IF THE ALL THE SECTIONS HAVE BEEN COMPLETED.         **
C **                                                                     **
C  ***********************************************************************
C
        IF(NEND.EQ.NENPS)GO TO 90
      GO TO 30
C
C  ***********************************************************************
C **                                                                     **
C **  CONVERT THE VIEW FACTOR VALUES (VF AND TVF) INTO VALUES            **
C **  REPRESENTATIVE OF THE TOTAL COIL BY DIVIDING BY THE NUMBER OF      **
C **  COIL AREA ELEMENTS (NC).                                           **
C **                                                                     **
C  ***********************************************************************
C
   90 DO 100 M=MXMIN,MXMAX
        DO 110 N=NYMIN,NYMAX
          IF(IOUT.GT.2)GO TO 120
          VF(M,N)=VF(M,N)/FLOAT(NC)
          VFTOT(M,N)=VFTOT(M,N)+VF(M,N)
          GO TO 110
  120     VF(M,N)=VFPRE*VF(M,N)/FLOAT(NC)
          VFTOT(M,N)=VFTOT(M,N)+VF(M,N)
  110   CONTINUE
  100 CONTINUE
      TVF=TVF/FLOAT(NC)
      IF(IOUT.GT.2)TVF=VFPRE/FLOAT(LC)*TVF
      RETURN
      END
C
C
C*******************SUBROUTINE REFA VARIABLE LIST*********************
C**                                                                   **
C**                                                                   **
C** DCRP=DISTANCE BETWEEN THE CENTER OF THE COIL AREA ELEMENT AND     **
C**     THE REFLECTION POINT WHEN BOTH ARE PROJECTED ONTO THE         **
C**     SAME X,Y PLANE                                                **
C** DCX=X-DIRECTION COSINE OF THE LINE SEGMENT DCRP                   **
C** DCY=Y-DIRECTION COSINE OF THE LINE SEGMENT DCRP                   **
C** DREFBP=ABSOLUTE DISTANCE BETWEEN THE REFLECTION POINT AND THE     **
C**     CENTER OF THE BAKING PLANE AREA ELEMENT                       **
C** DREFC=ABSOLUTE DISTANCE BETWEEN THE REFLECTION POINT AND          **
C**     THE CENTER OF THE COIL AREA ELEMENT                           **
C** DREFL=TOTAL DISTANCE SEPARATING THE TWO AREA ELEMENTS (TAKING     **
C**     INTO ACCOUNT THE REFLECTED PATH)                              **
C** DXY=DISTANCE BETWEEN THE CENTERS OF THE TWO AREA ELEMENTS WHEN    **
```

```
C**     THEY ARE PROJECTED ONTO THE SAME X,Y PLANE                      **
C** RCCB=REFLECTED COIL COSINE FACTOR                                   **
C** RBPCB=REFLECTED BAKING PLANE COSINE FACTOR                          **
C** RHOLD=HOLDS THE INCREMENTAL VIEW FACTOR FOR SINGLE                  **
C**     REFLECTED RADIATION                                             **
C** RX=REFLECTION POINT X COORDINATE                                    **
C** RY=REFLECTION POINT Y COORDINATE                                    **
C** RYC=REFLECTION Y-VALUE FOR THE AXIS TRANSFORMATION                  **
C**                                                                     **
C**                                                                     **
C***********************************************************************
C
C
      SUBROUTINE REFA(NENPS,BPZ,CZ,S,CASL,CX,CY,TVF,VF)
      DIMENSION BPX(100),BPY(100),VF(100,100),VFTOT(100,100)
      DIMENSION S(30),CX(30),CY(30)
      COMMON/BPPAN/BPX,BPY,PANX,PANY,PANR,BPAREA,PANL,PANW,PAND
      COMMON/LIMIT/IPAN,MXMIN,MXMAX,NYMIN,NYMAX,IOPT,IOUT
      COMMON/VWFCT/VFTOT,VFPRE
      COMMON/OVEN/DEPTH,WIDTH,HEIGHT
      COMMON/REFL/RFB,RFT,RF1,RF2,RF3,RF4,ABPTOP,ABPBOT
      RF=RFB
      ABP=ABPBOT
      IF(IOPT.LE.10)GO TO 3
        CZ=HEIGHT-CZ
        BPZ=HEIGHT-BPZ-PAND
        RF=RFT
        ABP=ABPTOP
    3 CONTINUE
      NEND=1
      TVF=0.0
      NC=0
      TEMP=0.0
      PI=3.141592654
C
C  ******************************************************************
C **                                                                 **
C ** SET THE VIEW FACTOR ARRAY TO ZERO                               **
C **                                                                 **
C  ******************************************************************
C
      DO 10 M=MXMIN,MXMAX
        DO 20 N=NYMIN,NYMAX
          VF(M,N)=0.0
   20   CONTINUE
   10 CONTINUE
C
C  ******************************************************************
C **                                                                 **
C **  SET THE FIRST INCREMENTAL LENGTH TRAVERSED ALONG THE HEATING   **
C **  COIL AS THE DISTANCE FORM THE FIRST ENDPOINT TO THE CENTER     **
C **  OF THE FIRST AREA ELEMENT.  DETERMINE THE DIRECTION            **
C **  COSINES FOR THE LINEAR SECTION OF THE HEATING COIL BEING       **
C **  TRAVERSED.  FIND THE X AND Y COORDINATES FOR THE CENTER OF THE **
C **  AREA ELEMENT OF CURRENT INTEREST.                              **
C **                                                                 **
C  ******************************************************************
C
      D=CASL/2.0
   30 DCXS=(CX(NEND+1)-CX(NEND))/S(NEND)
      DCYS=(CY(NEND+1)-CY(NEND))/S(NEND)
   40 X=CX(NEND)+D*DCXS
      Y=CY(NEND)+D*DCYS
      IF(X.LE.0.0)GO TO 90
      IF(Y.LE.0.0)GO TO 90
      LC=0
C
C  ******************************************************************
C **                                                                 **
C **  THE FOLLOWING DO LOOPS CONSIDER EACH INDIVIDUAL AREA ELEMENT   **
```

```
C **  OF THE BAKING PLANE (WITHIN THE SECTION SET OFF BY MXMIN,        **
C **  MXMAX,AND NYMIN,NYMAX)  AND FINDS THE INCREMENTAL VIEW           **
C **  FACTOR TO EACH OF THESE AREA ELEMENTS DUE TO A SINGLE AREA       **
C **  ELEMENT OF THE HEATING COIL.                                     **
C **                                                                   **
C  ***********************************************************************
C
      DO 50 M=MXMIN,MXMAX
        DO 60 N=NYMIN,NYMAX
C
C  ***********************************************************************
C **                                                                   **
C **  DETERMINE IF A CERTAIN AREA ELEMENT OF THE BAKING PLANE IS       **
C ** ACTUALLY WITHIN THE CONFINES OF THE PAN.                          **
C **                                                                   **
C  ***********************************************************************
C
          IF(IPAN.EQ.1)GO TO 70
          IF(IPAN.EQ.3)GO TO 80
            DISTX=ABS(BPX(M)-PANX)
            DISTY=ABS(BPY(N)-PANY)
            IF(DISTX.GT.(PANL/2.0))GO TO 60
            IF(DISTY.GT.(PANW/2.0))GO TO 60
          GO TO 80
   70     DIST=((BPX(M)-PANX)**2+(BPY(N)-PANY)**2)**0.5
          IF((DIST-PANR).GT.0.0)GO TO 60
C
C  ***********************************************************************
C **                                                                   **
C **  DETERMINE THE INCREMENTAL VIEW FACTOR FROM THE COIL AREA         **
C **  ELEMENT LOCATED AT X,Y TO THE BAKING PLANE AREA ELEMENT BPX,BPY.**
C **                                                                   **
C  ***********************************************************************
C
   80   DXY=((BPX(M)-X)**2+(BPY(N)-Y)**2)**0.5
        DCRP=CZ*DXY/(CZ+BPZ)
        IF(DXY.LT.0.000001)GO TO 83
        DCX=(BPX(M)-X)/DXY
        DCY=(BPY(N)-Y)/DXY
        RX=X+DCX*DCRP
        RY=Y+DCY*DCRP
        GO TO 85
   83   RX=X
        RY=Y
   85   DREFC=((X-RX)**2+(Y-RY)**2+CZ**2)**0.5
        DREFBP=((RX-BPX(M))**2+(RY-BPY(N))**2+BPZ**2)**0.5
        DREFL=DREFC+DREFBP
        RBPCB=BPZ/DREFBP
        RYC=(X-RX)*DCYS+(RY-Y)*DCXS
        RCCB=((CZ**2+RYC**2)**0.5)/DREFC
        RHOLD=RF*ABP*RBPCB*RCCB*BPAREA/((PI*DREFL)**2)
        VF(M,N)=VF(M,N)+RHOLD
        TEMP=TEMP+RHOLD
        LC=LC+1
   60   CONTINUE
   50 CONTINUE
      TVF=TVF+TEMP
C
C  ***********************************************************************
C **                                                                   **
C **  PREPARE FOR EXAMINATION OF THE NEXT DIFFERENTIAL AREA            **
C **  ELEMENT OF THE HEATING COIL.  SET TEMP BACK TO ZERO, COUNT THE   **
C **  NUMBER OF COIL AREA ELEMENTS (NC), INCREMENT THE DISTANCE D      **
C **  TO THE NEXT AREA ELEMENT OF THE HEATING COIL.                    **
C **                                                                   **
C  ***********************************************************************
C
      TEMP=0.0
      NC=NC+1
      D=D+CASL
```

```
C
C  ******************************************************************
C **                                                                **
C **  DETERMINE IF THE CURRENT LINEAR APPROXIMATING SECTION HAS     **
C **  BEEN COMPLETELY TRAVERSED AND IF THE NEXT SECTION NEEDS TO BE **
C **  CONSIDERED OR IF THE ALL THE SECTIONS HAVE BEEN COMPLETED.    **
C **                                                                **
C  ******************************************************************
C
      IF(D.LE.S(NEND))GO TO 40
        D=D-S(NEND)
        NEND=NEND+1
        IF(NEND.EQ.NENPS)GO TO 90
      GO TO 30
C
C  ******************************************************************
C **                                                                **
C **  CONVERT THE VIEW FACTOR VALUES (VF AND TVF) INTO VALUES       **
C **  REPRESENTATIVE OF THE TOTAL COIL BY DIVIDING BY THE NUMBER OF **
C **  COIL AREA ELEMENTS (NC).                                      **
C **                                                                **
C  ******************************************************************
C
   90 DO 100 M=MXMIN,MXMAX
        DO 110 N=NYMIN,NYMAX
          IF(IOUT.GT.2)GO TO 120
          VF(M,N)=VF(M,N)/FLOAT(NC)
          VFTOT(M,N)=VFTOT(M,N)+VF(M,N)
          GO TO 110
  120     VF(M,N)=VFPRE*VF(M,N)/FLOAT(NC)
          VFTOT(M,N)=VFTOT(M,N)+VF(M,N)
  110   CONTINUE
  100 CONTINUE
      TVF=TVF/FLOAT(NC)
      IF(IOUT.GT.2)TVF=VFPRE/FLOAT(LC)*TVF
      RETURN
      END
C
C
      SUBROUTINE REFB(NENPS,BPZ,CZ,S,CASL,CX,CY,TVF,VF)
      DIMENSION BPX(100),BPY(100),VF(100,100),VFTOT(100,100)
      DIMENSION S(30),CX(30),CY(30)
      COMMON/BPPAN/BPX,BPY,PANX,PANY,PANR,BPAREA,PANL,PANW,PAND
      COMMON/LIMIT/IPAN,MXMIN,MXMAX,NYMIN,NYMAX,IOPT,IOUT
      COMMON/VWFCT/VFTOT,VFPRE
      COMMON/OVEN/DEPTH,WIDTH,HEIGHT
      COMMON/REFL/RFB,RFT,RF1,RF2,RF3,RF4,ABPTOP,ABPBOT
      IF(IOPT.LE.10)GO TO 3
      BPZ=BPZ+PAND
      ABP=ABPTOP
    3 CONTINUE
      NEND=1
      TVF=0.0
      NC=0
      TEMP1=0.0
      TEMP2=0.0
      TEMP3=0.0
      TEMP4=0.0
      PI=3.141592654
C
C  ******************************************************************
C **                                                                **
C ** SET THE VIEW FACTOR ARRAY TO ZERO                              **
C **                                                                **
C  ******************************************************************
C
      DO 10 M=MXMIN,MXMAX
        DO 20 N=NYMIN,NYMAX
          VF(M,N)=0.0
   20   CONTINUE
```

```
   10 CONTINUE
C
C  ******************************************************************
C **                                                                **
C **  SET THE FIRST INCREMENTAL LENGTH TRAVERSED ALONG THE HEATING  **
C **  COIL AS THE DISTANCE FORM THE FIRST ENDPOINT TO THE CENTER    **
C **  OF THE FIRST AREA ELEMENT.  DETERMINE THE DIRECTION           **
C **  COSINES FOR THE LINEAR SECTION OF THE HEATING COIL BEING      **
C **  TRAVERSED.  FIND THE X AND Y COORDINATES FOR THE CENTER OF THE **
C **  AREA ELEMENT OF CURRENT INTEREST.                             **
C **                                                                **
C  ******************************************************************
C
      D=CASL/2.0
   30 DCXS=(CX(NEND+1)-CX(NEND))/S(NEND)
      DCYS=(CY(NEND+1)-CY(NEND))/S(NEND)
   40 X=CX(NEND)+D*DCXS
      Y=CY(NEND)+D*DCYS
      IF(X.LE.0.0)GO TO 90
      IF(Y.LE.0.0)GO TO 90
      LC=0
C
C  ******************************************************************
C **                                                                **
C **  THE FOLLOWING DO LOOPS CONSIDER EACH INDIVIDUAL AREA ELEMENT  **
C **  OF THE BAKING PLANE (WITHIN THE SECTION SET OFF BY MXMIN,     **
C **  MXMAX,AND NYMIN,NYMAX)  AND FINDS THE INCREMENTAL VIEW        **
C **  FACTOR TO EACH OF THESE AREA ELEMENTS DUE TO A SINGLE AREA    **
C **  ELEMENT OF THE HEATING COIL.                                  **
C **                                                                **
C  ******************************************************************
C
      DO 50 M=MXMIN,MXMAX
        DO 60 N=NYMIN,NYMAX
C
C  ******************************************************************
C **                                                                **
C **  DETERMINE IF A CERTAIN AREA ELEMENT OF THE BAKING PLANE IS    **
C ** ACTUALLY WITHIN THE CONFINES OF THE PAN.                       **
C **                                                                **
C  ******************************************************************
C
          IF(IPAN.EQ.1)GO TO 70
          IF(IPAN.EQ.3)GO TO 80
            DISTX=ABS(BPX(M)-PANX)
            DISTY=ABS(BPY(N)-PANY)
            IF(DISTX.GT.(PANL/2.0))GO TO 60
            IF(DISTY.GT.(PANW/2.0))GO TO 60
          GO TO 80
   70     DIST=((BPX(M)-PANX)**2+(BPY(N)-PANY)**2)**0.5
          IF((DIST-PANR).GT.0.0)GO TO 60
C
C  ******************************************************************
C **                                                                **
C **  DETERMINE THE INCREMENTAL VIEW FACTOR FROM THE COIL AREA      **
C **  ELEMENT LOCATED AT X,Y TO THE BAKING PLANE AREA ELEMENT BPX,BPY.**
C **                                                                **
C  ******************************************************************
C
C
C     CALCULATIONS FOR WALL 1
C
   80   DXZ1=((BPX(M)-X)**2+(BPZ-CZ)**2)**0.5
        DCRP1=Y*DXZ1/(Y+BPY(N))
        IF(DXZ1.LT.0.000001)GO TO 83
        DCX1=(BPX(M)-X)/DXZ1
        DCZ1=(BPZ-CZ)/DXZ1
        RX1=X+DCX1*DCRP1
        RZ1=CZ+DCZ1*DCRP1
        GO TO 85
```

```
83    RX1=X
      RZ1=CZ
85    PATHA1=((X-RX1)**2+Y**2+(CZ-RZ1)**2)**0.5
      PATHB1=((RX1-BPX(M))**2+BPY(N)**2+(RZ1-BPZ)**2)**0.5
      DREFL1=PATHA1+PATHB1
      RBPCB1=ABS(BPZ-RZ1)/PATHB1
      RYC1=(X-RX1)*DCYS+(-Y)*DCXS
      RCCB1=(((CZ-RZ1)**2+RYC1**2)**0.5)/PATHA1
      RHOLD1=RF1*ABP*RBPCB1*RCCB1*BPAREA/((PI*DREFL1)**2)
      VF(M,N)=VF(M,N)+RHOLD1
      TEMP1=TEMP1+RHOLD1
C     CALCULATIONS FOR WALL 2
      DYZ2=((BPY(N)-Y)**2+(BPZ-CZ)**2)**0.5
      IF(DYZ2.LT.0.000001)GO TO 82
      DCRP2=X*DYZ2/(X+BPX(M))
      DCY2=(BPY(N)-Y)/DYZ2
      DCZ2=(BPZ-CZ)/DYZ2
      RY2=Y+DCY2*DCRP2
      RZ2=CZ+DCZ2*DCRP2
      GO TO 84
82    RY2=Y
      RZ2=CZ
84    PATHA2=((Y-RY2)**2+X**2+(CZ-RZ2)**2)**0.5
      PATHB2=((RY2-BPY(N))**2+BPX(M)**2+(RZ2-BPZ)**2)**0.5
      DREFL2=PATHA2+PATHB2
      RBPCB2=ABS(BPZ-RZ2)/PATHB2
      RYC2=(X)*DCYS+(RY2-Y)*DCXS
      RCCB2=(((CZ-RZ2)**2+RYC2**2)**0.5)/PATHA2
      RHOLD2=RF2*ABP*RBPCB2*RCCB2*BPAREA/((PI*DREFL2)**2)
      VF(M,N)=VF(M,N)+RHOLD2
      TEMP2=TEMP2+RHOLD2
C     CALCULATIONS FOR WALL 3
      IF(DXZ1.LT.0.000001)GO TO 86
      DXZ3=DXZ1
      DCRP3=(WIDTH-Y)*DXZ3/(2.*WIDTH-Y-BPY(N))
      DCX3=DCX1
      DCZ3=DCZ1
      RX3=X+DCX3*DCRP3
      RZ3=CZ+DCZ3*DCRP3
      GO TO 88
86    RX3=X
      RZ3=CZ
88    PATHA3=((X-RX3)**2+(WIDTH-Y)**2+(CZ-RZ3)**2)**0.5
      PATHB3=((RX3-BPX(M))**2+(WIDTH-BPY(N))**2+(RZ3-BPZ)**2)**0.5
      DREFL3=PATHA3+PATHB3
      RBPCB3=ABS(BPZ-RZ3)/PATHB3
      RYC3=(X-RX3)*DCYS+(WIDTH-Y)*DCXS
      RCCB3=(((CZ-RZ3)**2+RYC3**2)**0.5)/PATHA3
      RHOLD3=RF3*ABP*RBPCB3*RCCB3*BPAREA/((PI*DREFL3)**2)
      VF(M,N)=VF(M,N)+RHOLD3
C     CALCULATIONS FOR WALL 4
      IF(DYZ2.LT.0.000001)GO TO 87
      DYZ4=DYZ2
      DCRP4=(DEPTH-X)*DYZ4/(2.0*DEPTH-X-BPX(M))
      DCY4=DCY2
      DCZ4=DCZ2
      RY4=Y+DCY4*DCRP4
      RZ4=CZ+DCZ4*DCRP4
      GO TO 89
87    RY4=Y
      RZ4=CZ
89    PATHA4=((DEPTH-X)**2+(Y-RY4)**2+(CZ-RZ4)**2)**0.5
      PATHB4=((DEPTH-BPX(M))**2+(RY4-BPY(N))**2+(RZ4-BPZ)**2)**0.5
      DREFL4=PATHA4+PATHB4
      RBPCB4=ABS(BPZ-RZ4)/PATHB4
      RYC4=(X-DEPTH)*DCYS+(RY4-Y)*DCXS
      RCCB4=(((CZ-RZ4)**2+RYC4**2)**0.5)/PATHA4
      RHOLD4=RF4*ABP*RBPCB4*RCCB4*BPAREA/((PI*DREFL4)**2)
      VF(M,N)=VF(M,N)+RHOLD4
      TEMP4=TEMP4+RHOLD4
```

```
        LC=LC+1
   60   CONTINUE
   50 CONTINUE
C
C  ******************************************************************
C **                                                                **
C **  DETERMINE THE PERCENT OF COIL SURFACE AREA INVOLVED IN        **
C **  RADIANT TRANSFER.  INCREMENT THE TOTAL VIEW FACTOR BY THE     **
C **  CORRECTED FRACTION OF TEMP.                                   **
C **                                                                **
C  ******************************************************************
C
      TVF=TVF+TEMP1+TEMP2+TEMP3+TEMP4
C
C  ******************************************************************
C **                                                                **
C **  PREPARE FOR EXAMINATION OF THE NEXT DIFFERENTIAL AREA         **
C **  ELEMENT OF THE HEATING COIL.  SET TEMP BACK TO ZERO, COUNT THE **
C **  NUMBER OF COIL AREA ELEMENTS (NC), INCREMENT THE DISTANCE D   **
C **  TO THE NEXT AREA ELEMENT OF THE HEATING COIL.                 **
C **                                                                **
C  ******************************************************************
C
      TEMP1=0.0
      TEMP2=0.0
      TEMP3=0.0
      TEMP4=0.0
      NC=NC+1
      D=D+CASL
C
C  ******************************************************************
C **                                                                **
C **  DETERMINE IF THE CURRENT LINEAR APPROXIMATING SECTION HAS     **
C **  BEEN COMPLETELY TRAVERSED AND IF THE NEXT SECTION NEEDS TO BE **
C **  CONSIDERED OR IF THE ALL THE SECTIONS HAVE BEEN COMPLETED.    **
C **                                                                **
C  ******************************************************************
C
      IF(D.LE.S(NEND))GO TO 40
        D=D-S(NEND)
        NEND=NEND+1
        IF(NEND.EQ.NENPS)GO TO 90
      GO TO 30
C
C  ******************************************************************
C **                                                                **
C **  CONVERT THE VIEW FACTOR VALUES (VF AND TVF) INTO VALUES       **
C **  REPRESENTATIVE OF THE TOTAL COIL BY DIVIDING BY THE NUMBER OF **
C **  COIL AREA ELEMENTS (NC).                                      **
C **                                                                **
C  ******************************************************************
C
   90 DO 100 M=MXMIN,MXMAX
        DO 110 N=NYMIN,NYMAX
          IF(IOUT.GT.2)GO TO 120
          VF(M,N)=VF(M,N)/FLOAT(NC)
          VFTOT(M,N)=VFTOT(M,N)+VF(M,N)
          GO TO 110
  120     VF(M,N)=VFPRE*VF(M,N)/FLOAT(NC)
          VFTOT(M,N)=VFTOT(M,N)+VF(M,N)
  110   CONTINUE
  100 CONTINUE
      TVF=TVF/FLOAT(NC)
      IF(IOUT.GT.2)TVF=VFPRE/FLOAT(LC)*TVF
      RETURN
      END
C
C
C*******************SUBROUTINE REFC VARIABLE LIST*********************
C**                                                                **
```

```
C**                                                                    **
C** DCBP=DISTANCE FROM THE COIL TO THE X,Y PROJECTION OF THE            **
C**      RADIATION CONE IN THE BAKING PLANE.                           **
C** XBP=X POSITION WHERE RADIATION CONE CROSSED THE BAKING PLANE       **
C** YBP=Y POSITION WHERE RADIATION CONE CROSSED THE BAKING PLANE       **
C**                                                                    **
C**                                                                    **
C**********************************************************************
C
C
      SUBROUTINE REFC(NENPS,BPZ,CZ,S,CASL,CX,CY,TVF,VF)
      DIMENSION BPX(100),BPY(100),VF(100,100),VFTOT(100,100)
      DIMENSION S(30),CX(30),CY(30)
      COMMON/BPPAN/BPX,BPY,PANX,PANY,PANR,BPAREA,PANL,PANW,PAND
      COMMON/LIMIT/IPAN,MXMIN,MXMAX,NYMIN,NYMAX,IOPT,IOUT
      COMMON/VWFCT/VFTOT,VFPRE
      COMMON/OVEN/DEPTH,WIDTH,HEIGHT
      COMMON/REFL/RFB,RFT,RF1,RF2,RF3,RF4,ABPTOP,ABPBOT
      RF=RFB
      ABP=ABPBOT
      IF(IOPT.LE.10)GO TO 3
        CZ=HEIGHT-CZ
        BPZ=HEIGHT-BPZ-PAND
        RF=RFT
        ABP=ABPTOP
    3 CONTINUE
      NEND=1
      TVF=0.0
      NC=0
      TEMP=0.0
      PI=3.141592654
C
C  ******************************************************************
C **                                                                 **
C ** SET THE VIEW FACTOR ARRAY TO ZERO                               **
C **                                                                 **
C  ******************************************************************
C
      DO 10 M=MXMIN,MXMAX
        DO 20 N=NYMIN,NYMAX
          VF(M,N)=0.0
   20   CONTINUE
   10 CONTINUE
C
C  ******************************************************************
C **                                                                 **
C **  SET THE FIRST INCREMENTAL LENGTH TRAVERSED ALONG THE HEATING   **
C **  COIL AS THE DISTANCE FORM THE FIRST ENDPOINT TO THE CENTER     **
C **  OF THE FIRST AREA ELEMENT.  DETERMINE THE DIRECTION            **
C **  COSINES FOR THE LINEAR SECTION OF THE HEATING COIL BEING       **
C **  TRAVERSED.  FIND THE X AND Y COORDINATES FOR THE CENTER OF THE **
C **  AREA ELEMENT OF CURRENT INTEREST.                              **
C **                                                                 **
C  ******************************************************************
C
      D=CASL/2.0
   30 DCXS=(CX(NEND+1)-CX(NEND))/S(NEND)
      DCYS=(CY(NEND+1)-CY(NEND))/S(NEND)
   40 X=CX(NEND)+D*DCXS
      Y=CY(NEND)+D*DCYS
      IF(X.LE.0.0)GO TO 90
      IF(Y.LE.0.0)GO TO 90
      LC=0
C
C  ******************************************************************
C **                                                                 **
C **  THE FOLLOWING DO LOOPS CONSIDER EACH INDIVIDUAL AREA ELEMENT   **
C **  OF THE BAKING PLANE (WITHIN THE SECTION SET OFF BY MXMIN,      **
C **  MXMAX,AND NYMIN,NYMAX)  AND FINDS THE INCREMENTAL VIEW         **
C **  FACTOR TO EACH OF THESE AREA ELEMENTS DUE TO A SINGLE AREA     **
```

```
C **  ELEMENT OF THE HEATING COIL.                                    **
C **                                                                  **
C  ******************************************************************
C
      DO 50 M=MXMIN,MXMAX
        DO 60 N=NYMIN,NYMAX
C
C  ******************************************************************
C **                                                                  **
C **  DETERMINE IF A CERTAIN AREA ELEMENT OF THE BAKING PLANE IS      **
C ** ACTUALLY WITHIN THE CONFINES OF THE PAN.                         **
C **                                                                  **
C  ******************************************************************
C
          IF(IPAN.EQ.1)GO TO 70
          IF(IPAN.EQ.3)GO TO 80
            DISTX=ABS(BPX(M)-PANX)
            DISTY=ABS(BPY(N)-PANY)
            IF(DISTX.GT.(PANL/2.0))GO TO 60
            IF(DISTY.GT.(PANW/2.0))GO TO 60
          GO TO 80
   70     DIST=((BPX(M)-PANX)**2+(BPY(N)-PANY)**2)**0.5
          IF((DIST-PANR).GT.0.0)GO TO 60
C
C  ******************************************************************
C **                                                                  **
C **  DETERMINE THE INCREMENTAL VIEW FACTOR FROM THE COIL AREA        **
C **  ELEMENT LOCATED AT X,Y TO THE BAKING PLANE AREA ELEMENT BPX,BPY.**
C **                                                                  **
C  ******************************************************************
C
   80   DXY=((BPX(M)-X)**2+(BPY(N)-Y)**2)**0.5
        DCRP=CZ*DXY/(CZ+BPZ)
        IF(DXY.LT.0.000001)GO TO 60
        DCX=(BPX(M)-X)/DXY
        DCY=(BPY(N)-Y)/DXY
C
C  ******************************************************************
C **                                                                  **
C ** DETERMINE IF THIS REFLECTION IS ACTUALLY BLOCKED BY THE          **
C ** EXISTENCE OF THE PAN. (IF THE X,Y LOCATION WHERE THE RADIATION   **
C ** CONE INTERSECTS THE BAKING PLANE IS WITHIN THE CONFINES          **
C ** OF THE PAN.)                                                     **
C **                                                                  **
C  ******************************************************************
C
        DCBP=DCRP*(CZ-BPZ)/CZ
        XBP=X+DCX*DCBP
        YBP=Y+DCY*DCBP
        IF(IPAN.EQ.3)GO TO 83
        IF(IPAN.EQ.1)GO TO 86
          DISTX=ABS(XBP-PANX)
          DISTY=ABS(YBP-PANY)
          IF(DISTX.LE.(PANL/2.0))GO TO 60
          IF(DISTY.LE.(PANW/2.0)) GO TO 60
          GO TO 83
   86   DIST=((XBP-PANX)**2+(YBP-PANY)**2)**0.5
        IF(DIST.LE.PANR)GO TO 60
   83 CONTINUE
C
        RX=X+DCX*DCRP
        RY=Y+DCY*DCRP
        DREFC=((X-RX)**2+(Y-RY)**2+CZ**2)**0.5
        DREFBP=((RX-BPX(M))**2+(RY-BPY(N))**2+BPZ**2)**0.5
        DREFL=DREFC+DREFBP
        RBPCB=BPZ/DREFBP
        RYC=(X-RX)*DCYS+(RY-Y)*DCXS
        RCCB=((CZ**2+RYC**2)**0.5)/DREFC
        RHOLD=RF*ABP*RBPCB*RCCB*BPAREA/((PI*DREFL)**2)
        VF(M,N)=VF(M,N)+RHOLD
```

```
        TEMP=TEMP+RHOLD
        LC=LC+1
   60   CONTINUE
   50 CONTINUE
C
C  ****************************************************************
C **                                                              **
C **  DETERMINE THE PERCENT OF COIL SURFACE AREA INVOLVED IN      **
C **  RADIANT TRANSFER.  INCREMENT THE TOTAL VIEW FACTOR BY THE   **
C **  CORRECTED FRACTION OF TEMP.                                 **
C **                                                              **
C  ****************************************************************
C
      TVF=TVF+TEMP
C
C  ****************************************************************
C **                                                              **
C **  PREPARE FOR EXAMINATION OF THE NEXT DIFFERENTIAL AREA       **
C **  ELEMENT OF THE HEATING COIL.  SET TEMP BACK TO ZERO, COUNT THE **
C **  NUMBER OF COIL AREA ELEMENTS (NC), INCREMENT THE DISTANCE D **
C **  TO THE NEXT AREA ELEMENT OF THE HEATING COIL.               **
C **                                                              **
C  ****************************************************************
C
      TEMP=0.0
      NC=NC+1
      D=D+CASL
C
C  ****************************************************************
C **                                                              **
C **  DETERMINE IF THE CURRENT LINEAR APPROXIMATING SECTION HAS   **
C **  BEEN COMPLETELY TRAVERSED AND IF THE NEXT SECTION NEEDS TO BE **
C **  CONSIDERED OR IF THE ALL THE SECTIONS HAVE BEEN COMPLETED.  **
C **                                                              **
C  ****************************************************************
C
      IF(D.LE.S(NEND))GO TO 40
        D=D-S(NEND)
        NEND=NEND+1
        IF(NEND.EQ.NENPS)GO TO 90
      GO TO 30
C
C  ****************************************************************
C **                                                              **
C **  CONVERT THE VIEW FACTOR VALUES (VF AND TVF) INTO VALUES     **
C **  REPRESENTATIVE OF THE TOTAL COIL BY DIVIDING BY THE NUMBER OF **
C **  COIL AREA ELEMENTS (NC).                                    **
C **                                                              **
C  ****************************************************************
C
   90 DO 100 M=MXMIN,MXMAX
        DO 110 N=NYMIN,NYMAX
          IF(IOUT.GT.2)GO TO 120
          VF(M,N)=VF(M,N)/FLOAT(NC)
          VFTOT(M,N)=VFTOT(M,N)+VF(M,N)
  120     VF(M,N)=VFPRE*VF(M,N)/FLOAT(NC)
          VFTOT(M,N)=VFTOT(M,N)+VF(M,N)
  110   CONTINUE
  100 CONTINUE
      TVF=TVF/FLOAT(NC)
      IF(IOUT.GT.2)TVF=VFPRE/FLOAT(LC)*TVF
      RETURN
      END
C
C
C
C
      SUBROUTINE PRINT(TVF,VF)
      DIMENSION VF(100,100)
      COMMON/LIMIT/IPAN,MXMIN,MXMAX,NYMIN,NYMAX,IOPT,IOUT
```

```
      IF(IOUT.LT.3)WRITE(6,10)TVF
   10 FORMAT(/,1X,50X,≠THE VIEW FACTOR FOR THIS CASE=≠,F9.7,//)
      IF(IOUT.GT.2)WRITE(6,40)TVF
   40 FORMAT(/,1X,47X,≠THE IRRADIANCE FOR THIS CASE  (W/M2)=≠,F9.2,//)
      IF(IOUT.EQ.2)GO TO 999
      IF(IOUT.EQ.4)GO TO 999
      DO 20 J=MXMIN,MXMAX
        WRITE(6,30)(VF(J,I),I=NYMIN,NYMAX)
   30   FORMAT(/,1X,15(E8.2,1X))
   20 CONTINUE
  999 RETURN
      END
```

TZ20918. 20 FT. ID10 ENAD.

PROGRAM OVENRAD

```
      PROGRAM MAIN(INPUT,OUTPUT,NDATA2,TAPE1=NDATA2,TAPE5=INPUT,
     $ TAPE6=OUTPUT)
C
C     THIS PROGRAM CALCULATES THE VIEW FACTOR ARRAY FOR ALL
C  SURFACES IN THE OVEN CAVITY.  VIEW FACTOR VALUES ARE STORED
C  IN THE TWO DIMENSIONAL ARRAY  F(I,J).
C
C
C     INPUT TO THE PROGRAM CONSISTS OF,
C
C   CARD              DESCRIPTION                          FORMAT
C    1      ALPHA NUMERIC STATEMENT                        (7A10)
C    2      DEPTH WIDTH HEIGHT                             (6F10.4)
C    3      IPAN                                           (I3,I3)
C              IPAN=1  PAN IS ROUND
C              IPAN=2  PAN IS RECTANGULAR
C    4      IF IPAN=1  PANX,PANY,PANZ,PANR,PANHZ           (6F10.4)
C    4      IF IPAN=2  PANX,PANY,PANZ,PANLX,PANLY,PANHZ(6F10.4)
C    5      ICOIL                                          (I3,I3)
C              ICOIL=1  UPPER AND LOWER COILS ARE IDENTICAL
C              ICOIL=2  UPPER AND LOWER COILS ARE NOT IDENTICAL
C    6      CZL,CZU,DL,DU                                  (6F10.4)
C         DATA FOR THE LOWER HEATING COIL
C    7      NENPS                                          (I3,I3)
C    8      CX(1),CY(1))                                   (6F10.4)
C    9      CX(2),CY(2)                                    (6F10.4)
C           CX(NENPS),CY(NENPS)                            (6F10.4)
C         IF ICOIL = 2
C         DATA FOR THE UPPER HEATING COIL
C           NENPS                                          (I3,I3)
C           CX(1),CY)1)                                    (6F10.4)
C           CX(2),CY(2)                                    (6F10.4)
C           CX(NENPS),CY(NENPS)                            (6F10.4)
C
C
C     PROGRAM VARIABLES WHICH CAN BE CHANGED BY THE USER ARE,
C
C        N    =  NUMBER OF SECTIONS ALONG A PAN SIDE
C        CASL =  COIL AREA SIDE LENGTH
C        NX   =  NUMBER OF WALL SECTIONS ALONG X-AXIS
C        NY   =  NUMBER OF WALL SECTIONS ALONG Y-AXIS
C        NZ   =  NUMBER OF WALL SECTIONS ALONG Z-AXIS
C        NSUBD=  SQRT(NUMBER OF SUBDIVISIONS IN EACH WALL SECTION)
C
C     PROGRAM VARIABLES ARE DIRECTLY RELATED TO ARRAY SIZES.
C  ARRAYS MUST BE DIMENSIONED AT LEAST AS LARGE AS SHOWN BELOW.
C
C        BPX(N),BPY(N)
C        CX(NENPS),CY(NENPS),S(NENPS-1)
C        WALLX(NX*NSUBD),WALLY(NY*NSUBD),WALLZ(NZ*NSUBD)
C             LET D=2*(NX*NZ+NY*NZ+NX*NY)
C        THEN  F(5+D,5+D)
C
C
C     SURFACES WITHIN THE OVEN CAVITY ARE IDENTIFIED AS:
C
C        SURFACE 1 =  LOWER HEATING COIL
C        SURFACE 2 =  UPPER HEATING COIL
C        SURFACE 3 =  LOWER PAN SURFACE
C        SURFACE 4 =  UPPER PAN SURFACE
C        SURFACE 5 =  PAN SIDES
C        SURFACE 6 =  LEFT SIDE WALL
C        SURFACE 7 =  DOOR
C        SURFACE 8 =  RIGHT SIDE WALL
C        SURFACE 9 =  BACK WALL
C        SURFACE 10=  TOP WALL
C        SURFACE 11=  BOTTOM WALL
C
C
C
```

```
      DIMENSION BPX(20),BPY(20)
      DIMENSION CX(30),CY(30),S(30)
      DIMENSION F(100,100)
      DIMENSION WALLX(30),WALLY(30),WALLZ(30)
      COMMON/AREAS/CAREA1,CAREA2,AP,APAN,ASIDE
      COMMON/CAVITY/DEPTH,WIDTH,HEIGHT
      COMMON/COIL/CASL,NENPS
      COMMON/OPT/IPAN,ICOIL,ISYMX,ISYMY,ISYMZ,ISYM
      COMMON/PANELS/COSPI4,XP1,YP1,XP2,YP2,XP3,YP3,XP4,YP4,
     $              XP5,YP5,XP6,YP6,XP7,YP7,XP8,YP8,XPB,XPF,
     $              YPL,YPR,PANLX2,ZP
      COMMON/SUBRTN/LCNX,LCNY,LCNZ,WALLA6,WALLA7,WALLA10,PI
      COMMON/WALLS/NX,NY,NZ,N,NSUBD,NXNY,NXNZ,NYNZ
      N=8
      CASL=1.0
      NX=2
      NY=2
      NZ=2
      NSUBD=5
      NDIM=100
      PI=3.141592654
      DO 60 I=1,NDIM
        DO 61 J=1,NDIM
          F(I,J)=0.0
   61   CONTINUE
   60 CONTINUE
C
C  READ THE INPUT DATA.
C
      READ(5,1)IH1,IH2,IH3,IH4,IH5,IH6,IH7
      READ(5,2)DEPTH,WIDTH,HEIGHT
      WRITE(6,4)IH1,IH2,IH3,IH4,IH5,IH6,IH7
      WRITE(6,5)DEPTH,WIDTH,HEIGHT
      READ(5,3)IPAN
      IF(IPAN.EQ.2)GO TO 100
        READ(5,2)PANX,PANY,PANZ,PANR,PANHZ
        PANLX=PANR
        PANLY=PANR
        COSPI4=COS(PI/4.)
        TEMP=PANLX*COSPI4
        XP1=PANX-PANLX
        YP1=PANY
        XP2=PANX-TEMP
        YP2=PANY-TEMP
        XP3=PANX
        YP3=PANY-PANLX
        XP4=PANX+TEMP
        YP4=PANY-TEMP
        XP5=PANX+PANLX
        YP5=PANY
        XP6=PANX+TEMP
        YP6=PANY+TEMP
        XP7=PANX
        YP7=PANY+PANLX
        XP8=PANX-TEMP
        YP8=PANY+TEMP
        AP=PANLX*PANHZ*PI/4.0
        PANLX2=PANLX**2
        ASIDE=AP*8.0
        APAN=PI*PANR**2
      GO TO 200
  100   READ(5,2)PANX,PANY,PANZ,PANLX,PANLY,PANHZ
        XPB=PANX-PANLX/2.0
        XPF=PANX+PANLX/2.0
        YPL=PANY-PANLY/2.0
        YPR=PANY+PANLY/2.0
        ASIDE=2.*(PANLX+PANLY)*PANHZ
        APAN=PANLX*PANLY
  200 ZP=PANZ+PANHZ/2.0
      ISYMX=0
```

```
      ISYMY=0
      ISYMZ=0
      ISYM =0
      IF(ABS(DEPTH/2.0-PANX).LE.(DEPTH/1000.0))ISYMX=1
      IF(ABS(WIDTH/2.0-PANY).LE.(WIDTH/1000.0))ISYMY=1
      IF(ABS((HEIGHT-PANHZ)/2.0-PANZ).LE.(HEIGHT/1000.0))ISYMZ=1
      IF(ISYMX.EQ.0)GO TO 250
      IF(ISYMZ.EQ.0)GO TO 250
      IF(ISYMY.EQ.0)GO TO 250
      ISYM=1
C
C  DETERMINE IF THE UPPER AND LOWER HEATING COILS HAVE
C  IDENTICAL CONFIGURATIONS.  READ COIL DATA.
C
  250 IF(IPAN.EQ.1)WRITE(6,6)ISYM,ISYMX,ISYMY,ISYMZ,PANX,PANY
     $                       ,PANZ,PANR,PANHZ,ASIDE,APAN
      IF(IPAN.EQ.2)WRITE(6,7)ISYM,ISYMX,ISYMY,ISYMZ,PANX,PANY,
     $                       PANZ,PANLX,PANLY,PANHZ,ASIDE,APAN
      READ(5,3)ICOIL
      READ(5,2)CZL,CZU,DL,DU
      READ(5,3)NENPS
      READ(5,2)CX(1),CY(1)
      IF(ICOIL.EQ.2)GO TO 300
C
C  ICOIL=1, UPPER AND LOWER COILS ARE IDENTICAL
C
        WRITE(6,8)ICOIL
        WRITE(6,15)CZL,CZU,DL,DU
        WRITE(6,9)NENPS,CX(1),CY(1)
        STOT=0.0
        DO 400 LC=2,NENPS
          LC1=LC-1
          READ(5,2)CX(LC),CY(LC)
          S(LC1)=SQRT((CX(LC1)-CX(LC))**2+(CY(LC1)-CY(LC))**2)
          STOT=STOT+S(LC1)
          WRITE(6,11)CX(LC),CY(LC),S(LC1)
  400   CONTINUE
        CAREA1=PI*DL*STOT
        CAREA2=CAREA1
        WRITE(6,12)STOT
        WRITE(6,16)CAREA1
C
C  CALL SUBROUTINES TO CALCULATE VIEW FACTORS
C
C  F LOWER COIL TO LOWER PAN SURFACE AND SIDES
C  F LOWER COIL TO WALLS
C
        CALL ELTOPN(CX,CY,CZL,S,PANX,PANY,PANZ,PANLX,PANLY,
     $              PANHZ,N,BPX,BPY,1,3,NDIM,F)
        CALL ELTWLS(CX,CY,CZL,S,PANX,PANY,PANZ,PANLX,PANLY,
     $              PANHZ,WALLX,WALLY,WALLZ,1,NDIM,F)
        IF(ISYM.EQ.1)GO TO 500
C
C  F UPPER COIL TO WALLS
C  F UPPER COIL TO UPPER PAN SURFACE AND SIDES
C
        CALL ELTWLS(CX,CY,CZU,S,PANX,PANY,PANZ,PANLX,PANLY,
     $              PANHZ,WALLX,WALLY,WALLZ,2,NDIM,F)
        IF(ISYMZ.EQ.1)GO TO 500
        CALL ELTOPN(CX,CY,CZU,S,PANX,PANY,PANZ,PANLX,PANLY,
     $              PANHZ,N,BPX,BPY,2,4,NDIM,F)
      GO TO 500
C
C  ICOIL=2, UPPER AND LOWER COILS HAVE DIFFERENT CONFIGURATIONS
C  OR LOCATIONS WITH RESPECT TO THE TOP OR BOTTOM WALL
C
  300   WRITE(6,13)ICOIL
        WRITE(6,15)CZL,CZU,DL,DU
        WRITE(6,9)NENPS,CX(1),CY(1)
        STOT=0.0
```

```
C
C  READ LOWER COIL DATA
C
        DO 600 LC=2,NENPS
          LC1=LC-1
          READ(5,2)CX(LC),CY(LC)
          S(LC1)=SQRT((CX(LC1)-CX(LC))**2+(CY(LC1)-CY(LC))**2)
          STOT=STOT+S(LC1)
          WRITE(6,11)CX(LC),CY(LC),S(LC1)
  600   CONTINUE
        CAREA1=PI*DL*STOT
        WRITE(6,12)STOT
        WRITE(6,16)CAREA1
C
C  F LOWER COIL TO LOWER PAN SURFACE
C  F LOWER COIL TO WALLS
C
        CALL ELTOPN(CX,CY,CZL,S,PANX,PANY,PANZ,PANLX,PANLY,
     $              PANHZ,N,BPX,BPY,1,3,NDIM,F)
        CALL ELTWLS(CX,CY,CZL,S,PANX,PANY,PANZ,PANLX,PANLY,
     $              PANHZ,WALLX,WALLY,WALLZ,1,NDIM,F)
C
C  READ UPPER COIL DATA
C
        READ(5,3)NENPS
        READ(5,2)CX(1),CY(1)
        WRITE(6,14)
        WRITE(6,9)NENPS,CX(1),CY(1)
        STOT=0.0
        DO 700 LC=2,NENPS
          LC1=LC-1
          READ(5,2)CX(LC),CY(LC)
          S(LC1)=SQRT((CX(LC1)-CX(LC))**2+(CY(LC1)-CY(LC))**2)
          STOT=STOT+S(LC1)
          WRITE(6,11)CX(LC),CY(LC),S(LC1)
  700 CONTINUE
        CAREA2=PI*DU*STOT
        WRITE(6,12)STOT
        WRITE(6,16)CAREA2
C
C  F UPPER COIL TO UPPER PAN SURFACE
C  F UPPER COIL TO WALLS
C
        CALL ELTOPN(CX,CY,CZU,S,PANX,PANY,PANZ,PANLX,PANLY,
     $              PANHZ,N,BPX,BPY,2,4,NDIM,F)
        CALL ELTWLS(CX,CY,CZU,S,PANX,PANY,PANZ,PANLX,PANLY,
     $              PANHZ,WALLX,WALLY,WALLZ,2,NDIM,F)
  500 CONTINUE
C
C  WALL TO WALL   RADIANT EXCHANGE
C  WALLS TO PAN RADIANT EXCHANGE.
C
       CALL WLTWLS(PANX,PANY,PANZ,PANLX,PANLY,PANHZ,
     $             WALLX,WALLY,WALLZ,NDIM,F)
       CALL WLSTPN(PANX,PANY,PANZ,PANLX,PANLY,PANHZ,
     $             BPX,BPY,WALLX,WALLY,WALLZ,NDIM,F)
C
C  WRITE OUT THE VIEW FACTOR ARRAY
C
C
C  WRITE DATA INTO PFILES
C
       NDIM=5+2*(NX*NZ+NY*NZ+NX*NY)
       WRITE(1,21)NDIM,NSUBD,NXNY,NXNZ,NYNZ
       DL=DL/100.
       DU=DU/100.
       CAREA1=CAREA1/10000.
       CAREA2=CAREA2/10000.
       APAN=APAN/10000.
       ASIDE=ASIDE/10000.
```

```
      WALLA6=WALLA6/10000.
      WALLA7=WALLA7/10000.
      WALLA10=WALLA10/10000.
      WRITE(1,20)DL,DU,CAREA1,CAREA2,APAN,ASIDE,WALLA6
     $,WALLA7,WALLA10
      DO 52 I=1,NDIM
        DO 53 J=1,NDIM
          WRITE(1,20)F(I,J)
   53 CONTINUE
   52 CONTINUE
      WRITE(6,19)
      DO 54 LC1=1,NDIM
      SF=0.0
      DO 154 I=1,NDIM
        SF=SF+F(LC1,I)
  154 CONTINUE
        WRITE(6,18)(F(LC1,LC2),LC2=1,NDIM),SF
   54 CONTINUE
C
C  WRITE OUT THE VIEW FACTOR MATRIX
C
C
C     FORMAT STATEMENTS
C
    1 FORMAT(7A10)
    2 FORMAT(6F10.4)
    3 FORMAT(I3,I3)
    4 FORMAT(1H1,///,5X,7A10)
    5 FORMAT(///,10X,≠OVEN INPUT DATA≠,
     $       //,5X,≠DIMENSIONS OF THE OVEN CAVITY≠,
     $      /,5X,≠DEPTH=≠,F10.4,≠  WIDTH=≠,F10.4,≠  HEIGHT=≠,F10.4)
    6 FORMAT(5X,≠THE PAN IS ROUND    ISYM =≠,I3,
     $       /,25X,≠ISYMX=≠,I3,/,25X,≠ISYMY=≠,I3,/,25X,≠ISYMZ=≠,I3,
     $       /,5X,≠THE COORDINATES FOR THE CENTER OF THE PAN ≠,
     $       ≠BOTTOM ARE≠,
     $       /,5X,≠X=≠,F10.4,≠  Y=≠,F10.4,≠  Z=≠,F10.4,
     $       /,5X,≠THE PAN RADIUS=≠,F10.4,
     $       /,5X,≠THE PAN DEPTH=≠,F10.4,
     $       /,5X,≠AREA OF THE PAN SIDES =≠,F10.4,
     $       /,5X,≠AREA OF THE PAN SURFACE =≠,F10.4)
    7 FORMAT(5X,≠THE PAN IS RECTANGULAR    ISYM =≠,I3,
     $       /,31X,≠ISYMX=≠,I3,/,31X,≠ISYMY=≠,I3,/,31X,≠ISYMZ=≠,I3,
     $       /,5X,≠THE COORDINATES FOR THE CENTER OF THE ≠,
     $       ≠PAN BOTTOM ARE≠,
     $       /,5X,≠X=≠,F10.4,≠  Y=≠,F10.4,≠  Z=≠,F10.4,
     $       /,5X,≠THE LENGTH OF THE PAN IN THE ≠,
     $       ≠X-DIRECTION=≠,F10.4,
     $       /,5X,≠THE LENGTH OF THE PAN IN THE Y-DIRECTION=≠,F10.4,
     $       /,5X,≠THE PAN DEPTH=≠,F10.4,
     $       /,5X,≠AREA OF THE PAN SIDES =≠,F10.4,
     $       /,5X,≠AREA OF THE PAN SURFACE =≠,F10.4)
    8 FORMAT(//,10X,≠INFORMATION FOR THE HEATING ELEMENTS   ICOIL=≠,I3,/
     $       /,5X,≠UPPER AND LOWER ELEMENTS HAVE IDENTICAL≠,
     $       ≠ CONFIGURATIONS≠)
    9 FORMAT(5X,≠THERE ARE ≠,I2,≠ ENDPOINTS WHICH HAVE X AND Y ≠,
     $       ≠COORDINATES≠,/,5X,≠AS SHOWN BELOW≠,
     $       /,15X,≠X≠,15X,≠Y≠,12X,≠LENGTH≠,
     $       /,11X,F10.4,5X,F10.4)
   11 FORMAT(11X,F10.4,5X,F10.4,5X,F10.4)
   12 FORMAT(5X,≠TOTAL HEATING ELEMENT LENGTH=≠,F10.4)
   13 FORMAT(//,10X,≠INFORMATION FOR THE HEATING ELEMENTS   ICOIL=≠,I3,
     $       //,5X,≠LOWER ELEMEMT≠)
   14 FORMAT(/,5X,≠UPPER ELEMENT≠)
   15 FORMAT(10X,≠CZL=≠,F10.4,5X,≠CZU=≠,F10.4,
     $        /,10X,≠LOWER HEATING ELEMENT DIAMETER=≠,F10.4,
     $        /,10X,≠UPPER HEATING ELEMENT DIAMETER=≠,F10.4)
   16 FORMAT(5X,≠HEATING ELEMENT SURFACE AREA=≠,F10.4)
   18 FORMAT(1X,12E10.3)
   19 FORMAT(////)
   20 FORMAT(1X,10E12.5)
```

```
   21 FORMAT(5I5)
      STOP
      END
C
C
C
C
      SUBROUTINE ELTOPN(CX,CY,CZ,S,PANX,PANY,PANZ,PANLX,PANLY,
     $                  PANHZ,N,BPX,BPY,I,J,NDIM,F)
C
C  THIS ROUTINE CALCULATES THE SHAPE FACTOR FOR RADIANT
C  EXCHANGE FROM THE HEATING ELEMENT TO THE PAN SURFACE AND
C  TO THE PAN SIDES.
C
      COMMON/AREAS/CAREA1,CAREA2,AP,APAN,ASIDE
      COMMON/COIL/CASL,NENPS
      COMMON/DC/DCXS,DCYS
      COMMON/OPT/IPAN,ICOIL,ISYMX,ISYMY,ISYMZ,ISYM
      DIMENSION CX(1),CY(1),S(1)
      DIMENSION BPX(1),BPY(1)
      DIMENSION F(NDIM,NDIM)
      IF(PANLX.LT.0.0001)GO TO 9999
      CAREA=CAREA1
      IF(I.EQ.2)CAREA=CAREA2
      NY=N
      INT=NY
      INT=INT/2
      INT=INT*2
      IF(NY.NE.INT)GO TO 5
      IF(ISYMY.EQ.1)NY=NY/2
    5 XN=FLOAT(N)
      ZCHK=PANZ-CZ
      IF(I.EQ.2)ZCHK=-ZCHK
      IF(ZCHK.GT.0)GO TO 7
        ITEMP=J
        IF(ITEMP.EQ.3)J=4
        IF(ITEMP.EQ.4)J=3
    7 PI=3.141592654
C
C  THE PAN SURFACE IS SUBDIVIDED INTO RECTANGULAR SHAPED
C  DIFFERENTIAL AREA ELEMENTS WHICH HAVE DIMENSIONS
C  BPSLX AND BPSLY.
C
      BPSLX=PANLX/XN
      BPSLY=PANLY/XN
      BPX(1)=PANX-PANLX/2.0+BPSLX/2.0
      BPY(1)=PANY-PANLY/2.0+BPSLY/2.0
      IF(IPAN.EQ.2)GO TO 9
        BPSLX=BPSLX*2.0
        BPSLY=BPSLY*2.0
        BPX(1)=PANX-PANLX+BPSLX/2.0
        BPY(1)=PANY-PANLY+BPSLY/2.0
    9 DO 10 LC=2,N
      BPX(LC)=BPX(1)+BPSLX*FLOAT(LC-1)
      BPY(LC)=BPY(1)+BPSLY*FLOAT(LC-1)
   10 CONTINUE
      BPAREA=BPSLX*BPSLY
      BPZ=PANZ
      IF(J.EQ.4)BPZ=PANZ+PANHZ
      NEND=1
      VF1=0.0
C
C  VARIABLES NC,D,DCXS,DCYS,X AND Y ALL DEAL WITH
C  SPECIFYING A DIFFERENTIAL AREA ELEMENT ON THE
C  HEATING COIL.
C
      NC=0
      D=CASL/2.0
      TEMPZ=BPZ-CZ
   20 DCXS=(CX(NEND+1)-CX(NEND))/S(NEND)
```

```
      DCYS=(CY(NEND+1)-CY(NEND))/S(NEND)
   30 X=CX(NEND)+D*DCXS
      Y=CY(NEND)+D*DCYS
C
C  DO LOOPS 40 AND 50 COVER THE SURFACE OF THE PAN.
C  THE VIEW FACTOR TO THE PAN SIDES IS CALCULATED IN
C  SUBROUTINE SIDES.
C
      NBP=0
      DO 40 LCX=1,N
        TEMPX=BPX(LCX)-X
        DO 50 LCY=1,NY
        TEMPY=BPY(LCY)-Y
        IF(IPAN.EQ.2)GO TO 60
        DIST=SQRT((BPX(LCX)-PANX)**2+(BPY(LCY)-PANY)**2)
        IF((DIST-PANLX).GT.0.0)GO TO 50
   60   R=SQRT(TEMPX**2+TEMPY**2+TEMPZ**2)
        BPCB=ABS(TEMPZ)/R
        YC=(-TEMPX)*DCYS+TEMPY*DCXS
        CCB=SQRT(TEMPZ**2+YC**2)/R
        VF1=VF1+BPCB*CCB*BPAREA/((PI*R)**2)
        NBP=NBP+1
   50   CONTINUE
   40 CONTINUE
        IF(PANHZ.LT.0.0001)GO TO 55
        CALL SIDES(I,1,X,Y,CZ,BPX,BPY,PANX,PANY,
     $            PANLX,PANHZ,BPSLX,BPSLY,NDIM,F)
C
C  THE POSITION ON THE HEATING COIL IS INCREMENTED AND
C  THE VIEW FACTOR FOR THE NEW DIFFERENTIAL AREA ELEMENT ON
C  THE COIL TO THE PAN SURFACE AND SIDES IS CALCULATED.
C
   55 NC=NC+1
      D=D+CASL
      IF(D.LE.S(NEND))GO TO 30
        D=D-S(NEND)
        NEND=NEND+1
      IF(NEND.EQ.NENPS)GO TO 99
      GO TO 20
   99 VF1=VF1/FLOAT(NC)
      VF2=F(I,5)/FLOAT(NC)
      APAN=BPAREA*FLOAT(NBP)
C
C  CHECK FOR SYMMETRICAL RELATIONS
C
      IF(ISYMY.EQ.0)GO TO 999
      IF(INT.NE.N)GO TO 999
      VF1=VF1*2.0
      VF2=VF2*2.0
      APAN=APAN*2.0
  999 WRITE(6,1)APAN
      F(I,J)=VF1
      F(I,5)=VF2
C
C  APPLY RECIPROCITY.
C
      F(J,I)=CAREA/APAN*F(I,J)
      IF(PANHZ.LT.0.0001)GO TO 9998
      F(5,I)=CAREA/ASIDE*F(I,5)
C
C  CHECK FOR SYMMETRY BETWEEN UPPER AND LOWER COILS
C
 9998 IF(ISYMZ.NE.1)GO TO 9999
      IF(ICOIL.EQ.2)GO TO 9999
        F(2,4)=F(1,3)
        F(2,5)=F(1,5)
        F(4,2)=F(3,1)
        F(5,2)=F(5,1)
 9999 RETURN
    1 FORMAT(//,1X,≠APPROXIMATED PAN SURFACE AREA≠,F10.4)
```

```
      END
C
C
C
C
      SUBROUTINE ELTWLS(CX,CY,CZ,S,PANX,PANY,PANZ,PANLX,PANLY,
     $                  PANHZ,WALLX,WALLY,WALLZ,IC,NDIM,F)
C
C     THIS ROUTINE CALCULATES THE RADIANT EXCHANGE FACTORS
C  FROM THE HEATING COIL TO THE WALL SECTIONS.  WHERE
C  POSSIBLE, SYMMETRY IS USED TO DECREASE THE AMOUNT OF
C  CALCULATIONS REQUIRED.
C
      DIMENSION CX(1),CY(1),S(1)
      DIMENSION F(NDIM,NDIM)
      DIMENSION WALLX(1),WALLY(1),WALLZ(1)
      COMMON/AREAS/CAREA1,CAREA2,AP,APAN,ASIDE
      COMMON/CAVITY/DEPTH,WIDTH,HEIGHT
      COMMON/COIL/CASL,NENPS
      COMMON/OPT/IPAN,ICOIL,ISYMX,ISYMY,ISYMZ,ISYM
      COMMON/SUBRTN/LCNX,LCNY,LCNZ,WALLA6,WALLA7,WALLA10,PI
      COMMON/WALLS/NX,NY,NZ,N,NSUBD,NXNY,NXNZ,NYNZ
      PI=3.141592654
      LCNX=NX*NSUBD
      LCNY=NY*NSUBD
      LCNZ=NZ*NSUBD
      DX=DEPTH/FLOAT(LCNX)
      DY=WIDTH/FLOAT(LCNY)
      DZ=HEIGHT/FLOAT(LCNZ)
      CAREA=CAREA1
      IF(IC.EQ.2)CAREA=CAREA2
      IF(IC.EQ.2)PANZ=PANZ+PANHZ
C
C  THE DIFFERENTIAL AREA ELEMENTS WHICH MAKE UP THE SEPARATE
C  WALL SUBSECTIONS CAN BE DEFINED BY THE X,Y, AND Z COORDINATES
C  OF ARRAYS WALLX,WALLY, AND WALLZ RESPECTIVELY.
C
      WALLX(1)=DX/2.0
      WALLY(1)=DY/2.0
      WALLZ(1)=DZ/2.0
C
      DO 10 LC=2,LCNX
        WALLX(LC)=WALLX(1)+DX*FLOAT(LC-1)
   10 CONTINUE
C
      DO 20 LC=2,LCNY
        WALLY(LC)=WALLY(1)+DY*FLOAT(LC-1)
   20 CONTINUE
      YSTORE=(NY+1)/2*NSUBD
      IF(ISYMY.EQ.1)LCNY=YSTORE
C
      DO 30 LC=2,LCNZ
        WALLZ(LC)=WALLZ(1)+DZ*FLOAT(LC-1)
   30 CONTINUE
C
C  SURFACE 6 =  LEFT WALL
C  SURFACE 7 =  DOOR
C  SURFACE 8 =  RIGHT WALL
C  SURFACE 9 =  BACK WALL
C  SURFACE 10=  TOP WALL
C  SURFACE 11=  BOTTOM WALL
C
      WALLA6=DX*DZ
      WALLA7=DY*DZ
      WALLA10=DX*DY
C
C  VARIABLES NC,D,DCXS,DCYS,X, ANC Y DEAL WITH SPECIFYING A
C  DIFFERENTIAL AREA ELEMENT ON THE HEATING COIL.
C
      NEND=1
```

```
      NC=0
      D=CASL/2.0
      TEMPZ1=PANZ-CZ
      PLX2=PANLX/2.0
      PLY2=PANLY/2.0
      NXNZ=NX*NZ
      NXNZ2=NXNZ*2
      NYNZ=NY*NZ
      NYNZ2=NYNZ*2
      NXNY=NX*NY
   40 DCXS=(CX(NEND+1)-CX(NEND))/S(NEND)
      DCYS=(CY(NEND+1)-CY(NEND))/S(NEND)
   50 X=CX(NEND)+D*DCXS
      Y=CY(NEND)+D*DCYS
C
C  ALL 6 WALLS ARE EXAMINED.  IF SYMMETRY EXIST ONLY HALF
C  THE OVEN MUST BE ANALYZED.  (ISYMY=1)
C
      I8=0
      I9=0
      I11=0
C
C  SURFACE 6  LEFT SIDE WALL
C
      LCVF=6
      TEMPY=-Y
  110 LCHK2=1
      DO 60 LCZ=1,LCNZ
        LCHK1=0
        LCHK3=1
        ITEMP=NSUBD*LCHK2
        IF(LCZ.GT.ITEMP)LCVF=LCVF+NX
        IF(LCZ.GT.ITEMP)LCHK2=LCHK2+1
        TEMPZ=WALLZ(LCZ)-CZ
      DO 70 LCX=1,LCNX
        ITEMP=NSUBD*LCHK3
        IF(LCX.GT.ITEMP)LCHK1=LCHK1+1
        IF(LCX.GT.ITEMP)LCHK3=LCHK3+1
        TEMPX=WALLX(LCX)-X
        R1=SQRT(TEMPX**2+TEMPY**2+TEMPZ**2)
        DCXR1=TEMPX/R1
        DCYR1=TEMPY/R1
        DCZR1=TEMPZ/R1
        IF((DCZR1*TEMPZ1).LT.0.0)GO TO 90
        IF(ABS(DCZR1).LT.0.00001)GO TO 90
        RBP=TEMPZ1/DCZR1
        XBP=RBP*DCXR1+X
        YBP=RBP*DCYR1+Y
C
C  CHECK IF THIS EXCHANGE PATH IS BLOCKED BY THE PAN.
C
      IF(IPAN.EQ.2)GO TO 80
      DIST=SQRT((XBP-PANX)**2+(YBP-PANY)**2)
      IF(DIST.LE.PANLX)GO TO 70
      GO TO 90
   80 IF(ABS(XBP-PANX).GT.PLX2)GO TO 90
      IF(ABS(YBP-PANY).GT.PLY2)GO TO 90
      GO TO 70
   90   WCB=ABS(TEMPY)/R1
        YC=(-TEMPX)*DCYS+TEMPY*DCXS
        CCB=SQRT(TEMPZ**2+YC**2)/R1
        F(IC,LCVF+LCHK1)=F(IC,LCVF+LCHK1)+WCB*CCB*WALLA6/
     $  ((PI*R1)**2)
   70 CONTINUE
   60 CONTINUE
C
C  SURFACE 8  RIGHT SIDE WALL
C
      IF(ISYMY.EQ.1)GO TO 100
      IF(I8.NE.0)GO TO 100
```

```
      I8=1
      LCVF=6+NXNZ+NYNZ
      TEMPY=DEPTH-Y
      GO TO 110
  100 CONTINUE
C
C  SURFACE 7  DOOR
C
      LCVF=6+NXNY
      TEMPX=DEPTH-X
  170 LCHK2=1
      DO 120 LCZ=1,LCNZ
        LCHK1=0
        LCHK3=1
        ITEMP=NSUBD*LCHK2
        IF(LCZ.GT.ITEMP)LCVF=LCVF+NY
        IF(LCZ.GT.ITEMP)LCHK2=LCHK2+1
        TEMPZ=WALLZ(LCZ)-CZ
      DO 130 LCY=1,LCNY
        ITEMP=NSUBD*LCHK3
        IF(LCY.GT.ITEMP)LCHK1=LCHK1+1
        IF(LCY.GT.ITEMP)LCHK3=LCHK3+1
        TEMPY=WALLY(LCY)-Y
        R1=SQRT(TEMPX**2+TEMPY**2+TEMPZ**2)
        DCXR1=TEMPX/R1
        DCYR1=TEMPY/R1
        DCZR1=TEMPZ/R1
        IF((DCZR1*TEMPZ1).LT.0.0)GO TO 150
        IF(ABS(DCZR1).LT.0.00001)GO TO 150
        RBP=TEMPZ1/DCZR1
        XBP=RBP*DCXR1+X
        YBP=RBP*DCYR1+Y
      IF(IPAN.EQ.2)GO TO 140
      DIST=SQRT((XBP-PANX)**2+(YBP-PANY)**2)
      IF(DIST.LE.PANLX)GO TO 130
      GO TO 150
  140 IF(ABS(XBP-PANX).GT.PLX2)GO TO 150
      IF(ABS(YBP-PANY).GT.PLY2)GO TO 150
      GO TO 130
  150   WCB=ABS(TEMPX)/R1
        YC=(-TEMPX)*DCYS+TEMPY*DCXS
        CCB=SQRT(TEMPZ**2+YC**2)/R1
        F(IC,LCVF+LCHK1)=F(IC,LCVF+LCHK1)+WCB*CCB*WALLA7/
     $  ((PI*R1)**2)
  130 CONTINUE
  120 CONTINUE
C
C  SURFACE 9  BACK WALL
C
      IF(I9.NE.0)GO TO 160
      I9=1
      LCVF=6+NXNZ2+NYNZ
      TEMPX=-X
      GO TO 170
  160 CONTINUE
C
C  SURFACE 10 TOP WALL
C
      LCVF=6+NXNZ2+NYNZ2
      TEMPZ=HEIGHT-CZ
  230 LCHK2=1
      DO 180 LCY=1,LCNY
        LCHK1=0
        LCHK3=1
        ITEMP=NSUBD*LCHK2
        IF(LCY.GT.ITEMP)LCVF=LCVF+NX
        IF(LCY.GT.ITEMP)LCHK2=LCHK2+1
        TEMPY=WALLY(LCY)-Y
      DO 190 LCX=1,LCNX
        ITEMP=NSUBD*LCHK3
```

```
        IF(LCX.GT.ITEMP)LCHK1=LCHK1+1
        IF(LCX.GT.ITEMP)LCHK3=LCHK3+1
        TEMPX=WALLX(LCX)-X
        R1=SQRT(TEMPX**2+TEMPY**2+TEMPZ**2)
        DCXR1=TEMPX/R1
        DCYR1=TEMPY/R1
        DCZR1=TEMPZ/R1
        IF((DCZR1*TEMPZ1).LT.0.0)GO TO 200
        IF(ABS(DCZR1).LT.0.00001)GO TO 200
        RBP=TEMPZ1/DCZR1
        XBP=RBP*DCXR1+X
        YBP=RBP*DCYR1+Y
      IF(IPAN.EQ.2) GO TO 210
      DIST=SQRT((XBP-PANX)**2+(YBP-PANY)**2)
      IF(DIST.LE.PANLX)GO TO 190
      GO TO 200
  210 IF(ABS(XBP-PANX).GT.PLX2)GO TO 200
      IF(ABS(YBP-PANY).GT.PLY2)GO TO 200
      GO TO 190
  200   WCB=ABS(TEMPZ)/R1
        YC=(-TEMPX)*DCYS+TEMPY*DCXS
        CCB=SQRT(TEMPZ**2+YC**2)/R1
        F(IC,LCVF+LCHK1)=F(IC,LCVF+LCHK1)+WCB*CCB*WALLA10/
     $  ((PI*R1)**2)
  190 CONTINUE
  180 CONTINUE
C
C  SURFACE 11  BOTTOM WALL
C
      IF(I11.NE.0)GO TO 220
      I11=1
      LCVF=6+NXNZ2+NYNZ2+NXNY
      TEMPZ=-CZ
      GO TO 230
C
C  THE POSITION ON THE HEATING COIL IS INCREMENTED AND THE
C  VIEW FACTORS FOR THIS NEW AREA ELEMENT ON THE HEATING COIL
C  TO ALL THE WALL SECTIONS ARE CALCULATED.
C
  220 NC=NC+1
      D=D+CASL
      IF(D.LE.S(NEND))GO TO 50
        D=D-S(NEND)
        NEND=NEND+1
      IF(NEND.EQ.NENPS)GO TO 999
      GO TO 40
C
C  DETERMINE THE FINAL VIEW FACTOR VALUES
C
  999 IF(ISYMY.EQ.0)GO TO 240
C
C  USE SYMMETRY TO FILL IN VIEW VACTOR ARRAY.
C
C  ACCOUNT FOR RECIPROCITY
C
C   CALCULATIONS FOR WALL6 AND WALL8
C
      LCVF8=5+NXNZ+NYNZ
      NSUBD2=NSUBD**2
      WALLA=WALLA6*NSUBD2
      DO 250 LC=1,NXNZ
        LCVF6=5+LC
        F(IC,LCVF6)=F(IC,LCVF6)/FLOAT(NC)
        F(IC,LCVF8+LC)=F(IC,LCVF6)
      F(LCVF6,IC)=CAREA/WALLA*F(IC,LCVF6)
      F(LCVF8+LC,IC)=F(LCVF6,IC)
  250 CONTINUE
C
C  CALCULATIONS FOR WALL7 AND WALL9
C
```

```
      LCYF=(NY+1)/2
      LCVF7=5+NXNZ
      LCVF9=5+NXNZ2+NYNZ
      WALLA=WALLA7*NSUBD2
      DO 260 LCZ=1,NZ
        LCVF1=LCVF7+(LCZ-1)*NY
        LCVF3=LCVF9+(LCZ-1)*NY
        DO 270 LCY=1,LCYF
          LCVF2=LCVF1+LCY
          F(IC,LCVF2)=F(IC,LCVF2)/FLOAT(NC)
          F(IC,LCVF1+NY+1-LCY)=F(IC,LCVF2)
      F(LCVF2,IC)=CAREA/WALLA*F(IC,LCVF2)
      F(LCVF1+NY+1-LCY,IC)=F(LCVF2,IC)
          LCVF4=LCVF3+LCY
          F(IC,LCVF4)=F(IC,LCVF4)/FLOAT(NC)
          F(IC,LCVF3+NY+1-LCY)=F(IC,LCVF4)
      F(LCVF4,IC)=CAREA/WALLA*F(IC,LCVF4)
      F(LCVF3+NY+1-LCY,IC)=F(LCVF4,IC)
  270   CONTINUE
  260 CONTINUE
C
C  CALCULATIONS FOR WALL10 AND WALL11
C
      LCVF10=5+NXNZ2+NYNZ2
      LCVF11=LCVF10+NXNY
      WALLA=WALLA10*NSUBD2
      DO 280 LCY=1,LCYF
        LCVF1=LCVF10+(LCY-1)*NX
        LCVF3=LCVF11+(LCY-1)*NX
        DO 290 LCX=1,NX
          LCVF2=LCVF1+LCX
          F(IC,LCVF2)=F(IC,LCVF2)/FLOAT(NC)
          F(IC,LCVF10+NXNY-NX*LCY+LCX)=F(IC,LCVF2)
      F(LCVF2,IC)=CAREA/WALLA*F(IC,LCVF2)
      F(LCVF10+NXNY-NX*LCY+LCX,IC)=F(LCVF2,IC)
          LCVF4=LCVF3+LCX
          F(IC,LCVF4)=F(IC,LCVF4)/FLOAT(NC)
          F(IC,LCVF11+NXNY-NX*LCY+LCX)=F(IC,LCVF4)
      F(LCVF4,IC)=CAREA/WALLA*F(IC,LCVF4)
      F(LCVF11+NXNY-NX*LCY+LCX,IC)=F(LCVF4,IC)
  290   CONTINUE
  280 CONTINUE
      IF(ISYM.EQ.0)GO TO 9999
C
C  TOTAL SYMMETRY; RELATE VIEW FACTORS ASSOCIATED WITH THE
C  LOWER COIL TO VIEW FACTORS ASSOCIATED WITH THE UPPER COIL
C
      DO 320 LC1=1,NZ
        DO 330 LC2=1,NX
C       WALL6;
        LCVF1=5+(LC1-1)*NX+LC2
        LCVF2=5+NXNZ-NX*LC1+LC2
        F(2,LCVF2)=F(1,LCVF1)
      F(LCVF2,2)=F(LCVF1,1)
C       WALL7;
        LCVF3=5+NXNZ+(LC1-1)*NY+LC2
        LCVF4=5+NXNZ+NYNZ-NY*LC1+LC2
        F(2,LCVF4)=F(1,LCVF3)
      F(LCVF4,2)=F(LCVF3,1)
C       WALL8;
        LCVF1=LCVF1+NXNZ+NYNZ
        LCVF2=LCVF2+NYNZ+NXNZ
        F(2,LCVF2)=F(1,LCVF1)
      F(LCVF2,2)=F(LCVF1,1)
C       WALL9;
        LCVF3=LCVF3+NYNZ+NXNZ
        LCVF4=LCVF4+NXNZ+NYNZ
        F(2,LCVF4)=F(1,LCVF3)
      F(LCVF4,2)=F(LCVF3,1)
  330   CONTINUE
```

```
  320 CONTINUE
C  WALL10 AND WALL11
      DO 340 LC1=1,NY
        DO 350 LC2=1,NX
        LCVF2=5+NXNZ+NYNZ+NXNZ+NYNZ
        LCVF1=LCVF2+(LC1-1)*NY+LC2
        LCVF2=LCVF1+NXNY
        F(2,LCVF2)=F(1,LCVF1)
        F(2,LCVF1)=F(1,LCVF2)
      F(LCVF2,2)=F(LCVF1,1)
      F(LCVF1,2)=F(LCVF2,1)
  350   CONTINUE
  340 CONTINUE
      GO TO 9999
C
C  ISYMY=0   NO SYMMETRICAL RELATIONSHIP CAN BE ASSUMED
C
C  CALCULATIONS FOR WALL6 AND WALL8
C
  240 LCVF=5+NXNZ+NYNZ
      WALLA=WALLA6*NSUBD2
      DO 300 LC=1,NXNZ
        LCVF6=5+LC
        LCVF8=LCVF+LC
        F(IC,LCVF6)=F(IC,LCVF6)/FLOAT(NC)
        F(IC,LCVF8)=F(IC,LCVF8)/FLOAT(NC)
      F(LCVF6,IC)=CAREA/WALLA*F(IC,LCVF6)
      F(LCVF8,IC)=CAREA/WALLA*F(IC,LCVF8)
  300 CONTINUE
C
C  CALCULATIONS FOR WALL7 AND WALL9
C
      LCVF1=5+NXNZ
      LCVF2=5+NXNZ2+NYNZ
      WALLA=WALLA7*NSUBD2
      DO 310 LC=1,NYNZ
        LCVF7=LCVF1+LC
        LCVF9=LCVF2+LC
        F(IC,LCVF7)=F(IC,LCVF7)/FLOAT(NC)
        F(IC,LCVF9)=F(IC,LCVF9)/FLOAT(NC)
      F(LCVF7,IC)=CAREA/WALLA*F(IC,LCVF7)
      F(LCVF9,IC)=CAREA/WALLA*F(IC,LCVF9)
  310 CONTINUE
C
C  CALCULATIONS FOR WALL10 AND WALL11
C
      LCVF1=5+NXNZ2+NYNZ2
      LCVF2=LCVF1+NXNY
      WALLA=WALLA10*NSUBD2
      DO 360 LC=1,NXNY
        LCVF10=LCVF1+LC
        LCVF11=LCVF2+LC
        F(IC,LCVF10)=F(IC,LCVF10)/FLOAT(NC)
        F(IC,LCVF11)=F(IC,LCVF11)/FLOAT(NC)
      F(LCVF10,IC)=CAREA/WALLA*F(IC,LCVF10)
      F(LCVF11,IC)=CAREA/WALLA*F(IC,LCVF11)
  360 CONTINUE
 9999 RETURN
      END
C
C
C
C
      SUBROUTINE WLTWLS(PANX,PANY,PANZ,PANLX,PANLY,PANHZ,
     $                  WALLX,WALLY,WALLZ,NDIM,F)
C
C     THIS ROUTINE CALCULATES THE RADIANT EXCHANGE FACTORS
C  BETWEEN THE WALL SUBSECTIONS.
C
      DIMENSION F(NDIM,NDIM)
```

```
      DIMENSION WALLX(1),WALLY(1),WALLZ(1)
      COMMON/BLOCK/A1,A2,B1,B2,C1,C2,XC,YC,PANR,IPAN1
      COMMON/CAVITY/DEPTH,WIDTH,HEIGHT
      COMMON/OPT/IPAN,ICOIL,ISYMX,ISYMY,ISYMZ,ISYM
      COMMON/SUBRTN/LCNX,LCNY,LCNZ,WALLA6,WALLA7,WALLA10,PI
      COMMON/WALLS/NX,NY,NZ,N,NSUBD,NXNY,NXNZ,NYNZ
C
C     IT IS ASSUMED THAT NO SURFACE CAN SEE ITSELF, OR ANY
C  OTHER SURFACES WHICH ARE ON THE SAME WALL.
C
C     VARIABLES A1,A2,B1,B2,C1,C2,XC,YC,R ARE
C  PASSED TO SUBROUTINE SHADOW.
C
      A1=PANX-PANLX/2.0
      A2=PANX+PANLX/2.0
      B1=PANY-PANLY/2.0
      B2=PANY+PANLY/2.0
      C1=PANZ
      C2=PANZ+PANHZ
      XC=PANX
      YC=PANY
      PANR=PANLX
      IPAN1=IPAN
      I1=0
      I2=0
      I3=0
      LCNY=NY*NSUBD
C
C     BY EMPLOYING RECIPROCITY, ONLY HALF THE OVEN CAVITY
C  MUSY BE ANALYZED
C
      LCVF6=6
      LCHK26=1
      DO 10 LCZ6=1,LCNZ
        LCHK16=0
        LCHK36=1
        ITEMP=NSUBD*LCHK26
        IF(LCZ6.LE.ITEMP)GO TO 20
          LCVF6=LCVF6+NX
          LCHK26=LCHK26+1
   20 DO 30 LCX6=1,LCNX
        ITEMP=NSUBD*LCHK36
        IF(LCX6.LE.ITEMP)GO TO 40
          LCHK16=LCHK16+1
          LCHK36=LCHK36+1
   40   TEMPX7=DEPTH-WALLX(LCX6)
        TEMPX9=-WALLX(LCX6)
        I6=LCVF6+LCHK16
        I8=I6+NXNZ+NYNZ
C
      LCVF7=6+NXNZ
      LCVF8=LCVF7+NYNZ
C
      LCHK27=1
      DO 50 LCZ7=1,LCNZ
        LCHK17=0
        LCHK18=0
        LCHK37=1
        LCHK38=1
        ITEMP=NSUBD*LCHK27
        IF(LCZ7.LE.ITEMP)GO TO 60
          LCVF7=LCVF7+NY
          LCVF8=LCVF8+NX
          LCHK27=LCHK27+1
   60   TEMPZ=WALLZ(LCZ7)-WALLZ(LCZ6)
      DO 70 LCY7=1,LCNY
        ITEMP=NSUBD*LCHK37
        IF(LCY7.LE.ITEMP)GO TO 80
          LCHK17=LCHK17+1
          LCHK37=LCHK37+1
```

```
   80   TEMPY=WALLY(LCY7)
        TEMPY7=TEMPY-WIDTH
        J7=LCVF7+LCHK17
        J9=J7+NYNZ+NXNZ
C
C  IF ISYMX=1       WALL6-WALL9=WALL6-WALL7
C                   WALL8-WALL9=WALL8-WALL7
C                   WALL9-WALL10=WALL7-WALL10
C                   WALL9-WALL11=WALL7-WALL11
C  IF ISYMY=1       WALL8-WALL7=WALL6-WALL7
C                   WALL8-WALL9=WALL6-WALL9
C                   WALL8-WALL10=WALL6-WALL10
C                   WALL8-WALL11=WALL6-WALL11
C  IF ISYMZ=1       WALL6-WALL11=WALL6-WALL10
C                   WALL8-WALL11=WALL8-WALL10
C                   WALL7-WALL11=WALL7-WALL10
C                   WALL9-WALL11=WALL9-WALL10
C
C  IF ISYM=1        ALL THE ABOVE
C
C
C  WALL6-WALL7
C
      CALL EXCHNG(TEMPX7,TEMPY,TEMPZ,WALLA7,WALLX(LCX6),DEPTH,
     $            0.0,WALLY(LCY7),WALLZ(LCZ6),WALLZ(LCZ7),
     $            I6,J7,TEMPY,TEMPX7,NDIM,F)
      IF(ISYM.EQ.1)GO TO 90
C
C  WALL8-WALL7
C
      IF(ISYMY.EQ.1)GO TO 100
      CALL EXCHNG(TEMPX7,TEMPY7,TEMPZ,WALLA7,WALLX(LCX6),DEPTH,
     $            WIDTH,WALLY(LCY7),WALLZ(LCZ6),WALLZ(LCZ7),
     $            I8,J7,-TEMPY7,TEMPX7,NDIM,F)
C
C  WALL6-WALL9
C
  100 IF(ISYMX.EQ.1)GO TO 95
      CALL EXCHNG(TEMPX9,TEMPY,TEMPZ,WALLA7,WALLX(LCX6),0.0,
     $            0.0,WALLY(LCY7),WALLZ(LCZ6),WALLZ(LCZ7),
     $            I6,J9,TEMPY,-TEMPX9,NDIM,F)
C
C  WALL8-WALL9
C
   95 IF(ISYMY.EQ.1)GO TO 90
      CALL EXCHNG(TEMPX9,TEMPY7,TEMPZ,WALLA7,WALLX(LCX6),0.0,
     $            WIDTH,WALLY(LCY7),WALLZ(LCZ6),WALLZ(LCZ7),
     $            I8,J9,-TEMPY7,-TEMPX9,NDIM,F)
C
C     IF THIS IS THE FIRST TIME THROUGH THE COMBINATION OF DO
C  LOOPS 50 AND 70 (I1=0) THEN CALCULATE WALL7-WALL9.
C
   90 IF(I1.NE.0)GO TO 110
      LCHK29=1
      LCVF92=6+NXNZ+NYNZ+NXNZ
      DO 120 LCZ9=1,LCNZ
        LCHK19=0
        LCHK39=1
        ITEMP=NSUBD*LCHK29
        IF(LCZ9.LE.ITEMP)GO TO 130
          LCVF92=LCVF92+NY
          LCHK29=LCHK29+1
  130   TEMPZ9=WALLZ(LCZ9)-WALLZ(LCZ7)
      DO 140 LCY9=1,LCNY
        ITEMP=NSUBD*LCHK39
        IF (LCY9.LE.ITEMP)GO TO 150
          LCHK19=LCHK19+1
          LCHK39=LCHK39+1
  150   TEMPY9=WALLY(LCY9)-WALLY(LCY7)
        J92=LCVF92+LCHK19
```

```
C
C  WALL7-WALL9
C
      CALL EXCHNG(-DEPTH,TEMPY9,TEMPZ9,WALLA7,DEPTH,0.0,
     $            WALLY(LCY7),WALLY(LCY9),WALLZ(LCZ7),WALLZ(LCZ9),
     $            J7,J92,DEPTH,DEPTH,NDIM,F)
  140 CONTINUE
  120 CONTINUE
C
C
  110 LCHK2T=1
      LCVFT=6+NXNZ+NYNZ+NXNZ+NYNZ
      LCVFB=LCVFT+NXNY
      TMPZT6=HEIGHT-WALLZ(LCZ6)
      TMPZB6=-WALLZ(LCZ6)
      TMPZT7=HEIGHT-WALLZ(LCZ7)
      TMPZB7=-WALLZ(LCZ7)
      DO 160 LCY10=1,LCNY
        LCHK1T=0
        LCHK3T=1
        ITEMP=NSUBD*LCHK2T
        IF(LCY10.LE.ITEMP)GO TO 170
          LCVFT=LCVFT+NX
          LCVFB=LCVFB+NX
          LCHK2T=LCHK2T+1
  170   TMPYT6=WALLY(LCY10)
        TMPYT7=WALLY(LCY10)-WALLY(LCY7)
        TMPYT8=WALLY(LCY10)-WIDTH
      DO 180 LCX10=1,LCNX
        ITEMP=NSUBD*LCHK3T
        IF(LCX10.LE.ITEMP)GO TO 190
          LCHK1T=LCHK1T+1
          LCHK3T=LCHK3T+1
  190   TMPXT6=WALLX(LCX10)-WALLX(LCX6)
        TMPXT7=WALLX(LCX10)-DEPTH
        TMPXT9=WALLX(LCX10)
        J10=LCVFT+LCHK1T
        J11=LCVFB+LCHK1T
C
C  IF WALL6,8 - WALL10,11 HAVE ALREADY BEEN CALCULATED FOR
C  THE CURRENT LCZ6 AND LCX6 (I3 .NE. 0) THEN SKIP THIS SECTION.
C
      IF(I3.NE.0)GO TO 200
C
C  WALL6-WALL10
C
      CALL EXCHNG(TMPXT6,TMPYT6,TMPZT6,WALLA10,WALLX(LCX6),WALLX(LCX10),
     $            0.0,WALLY (LCY10),WALLZ(LCZ6),HEIGHT,
     $            I6,J10,TMPYT6,TMPZT6,NDIM,F)
      IF(ISYM.EQ.1)GO TO 200
C
C  WALL8-WALL10
C
      IF(ISYMY.EQ.1)GO TO 210
      CALL EXCHNG(TMPXT6,TMPYT8,TMPZT6,WALLA10,WALLX(LCX6),WALLX(LCX10),
     $            WIDTH,WALLY(LCY10),WALLZ(LCZ6),HEIGHT,
     $            I8,J10,-TMPYT8,TMPZT6,NDIM,F)
C
C  WALL6-WALL11
C
  210 IF(ISYMZ.EQ.1)GO TO 200
      CALL EXCHNG(TMPXT6,TMPYT6,TMPZB6,WALLA10,WALLX(LCX6),WALLX(LCX10),
     $            0.0,WALLY (LCY10),WALLZ (LCZ6),0.0,
     $            I6,J11,TMPYT6,-TMPZB6,NDIM,F)
C
C  WALL8-WALL11
C
      IF(ISYMY.EQ.1)GO TO 200
      CALL EXCHNG(TMPXT6,TMPYT8,TMPZB6,WALLA10,WALLX(LCX6),WALLX(LCX10),
     $            WIDTH,WALLY(LCY10),WALLZ(LCZ6),0.0,
```

```
     $            I8,J11,-TMPYT8,-TMPZB6,NDIM,F)
C
C     IF THIS IS THE FIRST TIME THROUGH THE CONBINATION OF DO
C  LOOPS 50 AND 70,  (I1=0), THEN CALCULATE WALL7,9-WALL10,11.
C
  200 IF(I1.NE.0)GO TO 180
C
C  WALL7-WALL10
C
      CALL EXCHNG(TMPXT7,TMPYT7,TMPZT7,WALLA10,DEPTH,WALLX(LCX10),
     $            WALLY(LCY7),WALLY(LCY10),WALLZ(LCZ7),HEIGHT,
     $            J7,J10,-TMPXT7,TMPZT7,NDIM,F)
      IF(ISYM.EQ.1)GO TO 220
C
C  WALL9-WALL10
C
      IF(ISYMX.EQ.1)GO TO 230
      CALL EXCHNG(TMPXT9,TMPYT7,TMPZT7,WALLA10,0.0,WALLX(LCX10),
     $            WALLY(LCY7),WALLY(LCY10),WALLZ(LCZ7),HEIGHT,
     $            J9,J10,TMPXT9,TMPZT7,NDIM,F)
C
C  WALL7-WALL11
C
  230 IF(ISYMZ.EQ.1)GO TO 220
      CALL EXCHNG (TMPXT7,TMPYT7,TMPZB7,WALLA10,DEPTH,WALLX(LCX10),
     $            WALLY(LCY7),WALLY(LCY10),WALLZ(LCZ7),0.0,
     $            J7,J11,-TMPXT7,-TMPZB7,NDIM,F)
C
C  WALL9-WALL11
C
      IF(ISYMX.EQ.1)GO TO 220
      CALL EXCHNG(TMPXT9,TMPYT7,TMPZB7,WALLA10,0.0,WALLX(LCX10),
     $            WALLY(LCY7),WALLY(LCY10),WALLZ(LCZ7),0.0,
     $            J9,J11,TMPXT9,-TMPZB7,NDIM,F)
C
C     IF THIS IS THE FIRST TIME THROUGH THE DO LOOP COMBINATIONS
C  OF 160 AND 180, (I2=0), THEN CALCULATE WALL10-WALL11.
C
  220 IF(I2.NE.0)GO TO 180
      LCHK2B=1
      LCVF11=6+NXNZ+NYNZ+NXNZ+NYNZ+NXNY
      DO 240 LCY11=1,LCNY
        LCHK1B=0
        LCHK3B=1
        ITEMP=NSUBD*LCHK2B
        IF(LCY11.LE.ITEMP)GO TO 250
          LCVF11=LCVF11+NX
          LCHK2B=LCHK2B+1
  250   TMPY11=WALLY(LCY11)-WALLY (LCY10)
      DO 260 LCX11=1,LCNX
        ITEMP=NSUBD*LCHK3B
        IF(LCX11.LE.ITEMP)GO TO 270
          LCHK1B=LCHK1B+1
          LCHK3B=LCHK3B+1
  270   TMPX11=WALLX(LCX11)-WALLX(LCX10)
        J112=LCVF11+LCHK1B
C
C  WALL10-WALL11
C
      CALL EXCHNG(TMPX11,TMPY11,-HEIGHT,WALLA10,WALLX(LCX10),
     $            WALLX(LCX11),WALLY(LCY10),WALLY(LCY11),HEIGHT,0.0,
     $            J10,J112,HEIGHT,HEIGHT,NDIM,F)
  260 CONTINUE
  240 CONTINUE
  180 CONTINUE
  160 CONTINUE
      I2=1
      I3=1
   70 CONTINUE
C
```

```
C  WALL6-WALL8
C
      DO 280 LCX8=1,LCNX
        ITEMP=NSUBD*LCHK38
        IF(LCX8.LE.ITEMP)GO TO 290
          LCHK18=LCHK18+1
          LCHK38=LCHK38+1
  290   TMPX8=WALLX(LCX8)-WALLX(LCX6)
        J8=LCVF8+LCHK18
      CALL EXCHNG(TMPX8,WIDTH,TEMPZ,WALLA6,WALLX(LCX6),WALLX(LCX8),
     $            0.0,WIDTH,WALLZ(LCZ6),WALLZ(LCZ7),
     $            I6,J8,WIDTH,WIDTH,NDIM,F)
  280 CONTINUE
   50 CONTINUE
      I1=1
      I3=0
   30 CONTINUE
   10 CONTINUE
C
C     DEPENDING ON THE TYPE OF SYMMETRY WHICH EXISTS,
C  FILL IN THE VIEW FACTOR ARRAY.
C
      IF(ISYMX.NE.0)GO TO 300
      IF(ISYMY.NE.0)GO TO 300
      IF(ISYMZ.NE.0)GO TO 300
      GO TO 410
C
C  IF ISYMX=1       WALL6-WALL9=WALL6-WALL7
C                   WALL8-WALL9=WALL8-WALL7
C                   WALL9-WALL10=WALL7-WALL10
C                   WALL9-WALL11=WALL7-WALL11
C  IF ISYMY=1       WALL8-WALL7=WALL6-WALL7
C                   WALL8-WALL9=WALL6-WALL9
C                   WALL8-WALL10=WALL6-WALL10
C                   WALL8-WALL11=WALL6-WALL11
C  IF ISYMZ=1       WALL6-WALL11=WALL6-WALL10
C                   WALL8-WALL11=WALL8-WALL10
C                   WALL7-WALL11=WALL7-WALL10
C                   WALL9-WALL11=WALL9-WALL10
C
C
C   COVER WALL6
C
  300 LA6=5+NXNZ
      LA7=LA6+NYNZ
      LA8=LA7+NXNZ
      LA9=LA8+NYNZ
      LA10=LA9+NXNY
      LA11=LA10+NXNY
      DO 310 I6=6,LA6
        DO 320 J6=LA6+1,LA11
C
C  EXAMINE WALL6-WALL7
C
      IF(J6.GT.LA7)GO TO 330
        J7=J6
C  WALL8-WALL7
        IF(ISYMY.EQ.0)GO TO 340
        I8=I6+NXNZ+NYNZ
        N7=J6-LA6
        IROW=(N7-1)/NY
        NROW=N7-IROW*NY
        J72=(LA6+1)+(IROW+1)*NY-NROW
          F(I8,J72)=F(I6,J7)
C  WALL6-WALL9
  340   IF(ISYMX.EQ.0)GO TO 320
        J9=J7+NYNZ+NXNZ
        N6=I6-5
        IROW=(N6-1)/NX
        NROW=N6-IROW*NX
```

```
        I62=6+(IROW+1)*NX-NROW
          F(I62,J9)=F(I6,J7)
        GO TO 320
C
C  SKIP WALL6-WALL8
C
  330 IF(J6.LE.LA8)GO TO 320
C
C  EXAMINE WALL6-WALL9
C
      IF(J6.GT.LA9)GO TO 350
        IF(ISYMY.EQ.0)GO TO 320
C  WALL8-WALL9
        J9=J6
        I8=I6+NXNZ+NYNZ
        N9=J6-LA8
        IROW=(N9-1)/NY
        NROW=N9-IROW*NY
        J92=(LA8+1)+(IROW+1)*NY-NROW
          F(I8,J92)=F(I6,J9)
      GO TO 320
C
C  EXAMINE WALL6-WALL10
C
  350 IF(J6.GT.LA10)GO TO 320
        IF(ISYMZ.EQ.0)GO TO 365
C  WALL6-WALL11
        J10=J6
        J11=J6+NXNY
        N6=I6-5
        IROW=(N6-1)/NX
        NROW=N6-IROW*NX
        I62=LA6-(IROW+1)*NX+NROW
          F(I62,J11)=F(I6,J10)
C  WALL8-WALL10
  365   IF(ISYMY.EQ.0)GO TO 320
        J10=J6
        I8=I6+NXNZ+NYNZ
        N10=J6-LA9
        IROW=(N10-1)/NX
        NROW=N10-IROW*NX
        J102=LA10-(IROW+1)*NX+NROW
          F(I8,J102)=F(I6,J10)
C
  320   CONTINUE
  310 CONTINUE
C  EXAMINE WALL6-WALL11
C
      IF(ISYMY.EQ.0)GO TO 345
C  WALL8-WALL11
      DO 355 I6=6,LA6
        DO 360 J11=LA10+1,LA11
        I8=I6+NXNZ+NYNZ
        N11=J11-LA10
        IROW=(N11-1)/NX
        NROW=N11-IROW*NX
        J112=LA11-(IROW+1)*NX+NROW
          F(I8,J112)=F(I6,J11)
  360   CONTINUE
  355 CONTINUE
C
C  IF ISYMX=1 COVER WALL8-WALL7
C
  345 IF(ISYMX.NE.1)GO TO 370
C  WALL8-WALL9
      DO 375 I8=LA7+1,LA8
        DO 380 J7=LA6+1,LA7
          J9=J7+NYNZ+NXNZ
          N8=I8-LA7
          IROW=(N8-1)/NX
```

```
          NROW=N8-IROW*NX
          I82=(LA7+1)+(IROW+1)*NX-NROW
            F(I82,J9)=F(I8,J7)
  380   CONTINUE
  375 CONTINUE
C
C  COVER WALL7
C
  370 DO 385 I7=LA6+1,LA7
        DO 390 J7=LA9+1,LA11
        IF(J7.GT.LA10)GO TO 395
        IF(ISYMZ.EQ.0)GO TO 400
C  WALL7-WALL11
          J10=J7
          J11=J7+NXNY
          N7=I7-LA6
          IROW=(N7-1)/NY
          NROW=N7-IROW*NY
          I72=LA7-(IROW+1)*NY+NROW
            F(I72,J11)=F(I7,J10)
C  WALL9-WALL10
  400 IF(ISYMX.EQ.0)GO TO 390
        J10=J7
        I9=I7+NYNZ+NXNZ
        N10=J7-LA9
        IROW=(N10-1)/NX
        NROW=N10-IROW*NX
        J102=(LA9+1)+(IROW+1)*NX-NROW
          F(I9,J102)=F(I7,J10)
        GO TO 390
C  WALL9-WALL11
  395 IF(ISYMX.EQ.0)GO TO 390
        J11=J7
        I9=I7+NYNZ+NXNZ
        N11=J7-LA10
        IROW=(N11-1)/NX
        NROW=N11-IROW*NX
        J112=(LA10+1)+(IROW+1)*NX-NROW
          F(I9,J112)=F(I7,J11)
  390  CONTINUE
  385 CONTINUE
C
C  IF ISYMZ=1 COVER WALL9-WALL10
C                AND WALL8-WALL10
C
      IF(ISYMZ.NE.1)GO TO 410
C  WALL9-WALL11
      DO 405 I9=LA8+1,LA9
        DO 406 J10=LA9+1,LA10
          J11=J10+NXNY
          N9=I9-LA8
          IROW=(N9-1)/NY
          NROW=N9-IROW*NY
          I92=LA9-(IROW+1)*NY+NROW
            F(I92,J11)=F(I9,J10)
  406   CONTINUE
  405 CONTINUE
C  WALL8-WALL11
      DO 407 I8=LA7+1,LA8
        DO 408 J10=LA9+1,LA10
          J11=J10+NXNY
          N8=I8-LA7
          IROW=(N8-1)/NX
          NROW=N8-IROW*NX
          I82=LA8-(IROW+1)*NX+NROW
            F(I82,J11)=F(I8,J10)
  408   CONTINUE
  407 CONTINUE
C
C     APPLY THE PRINCIPAL OF RECIPROCITY TO COMPLETE THE
```

```
C  VIEW FACTOR ARRAY FOR THE WALLS.
C
C  ACTUALLY, A1=WALL1*NSUBD2 AND A2=WALLA2*NSUBD2.  BUT, WHEN
C  THE RATIO A1/A2 IS TAKEN, NSUBD2 CANCELS OUT.  THUS, NSUBD2
C  IS NOT INCLUDED IN THE AREA CALCULATIONS.
C
  410 LC=LA6+1
      SUBD2=FLOAT(NSUBD**2)
      IFLAG1=0
      IFLAG2=0
      IFLAG3=0
      DO 420 LC1=6,LA10
      IF(LC1.GT.LA6)LC=LA7+1
      IF(LC1.GT.LA7)LC=LA8+1
      IF(LC1.GT.LA8)LC=LA9+1
      IF(LC1.GT.LA9)LC=LA10+1
        IF(LC1.GT.LA6)GO TO 430
          A1=WALLA6
        GO TO 470
  430   IF(LC1.GT.LA7)GO TO 440
          A1=WALLA7
        IFLAG1=1
          GO TO 470
  440   IF(LC1.GT.LA8)GO TO 450
          A1=WALLA6
          GO TO 470
  450   IF(LC1.GT.LA9)GO TO 460
          A1=WALLA7
          GO TO 470
  460   A1=WALLA10
  470 DO 480 LC2=LC,LA11
        IF(LC2.GT.LA7)GO TO 490
          A2=WALLA7
          GO TO 520
  490   IF(LC2.GT.LA8)GO TO 500
          A2=WALLA6
        IFLAG2=1
          GO TO 520
  500   IF(LC2.GT.LA9)GO TO 510
          A2=WALLA7
          GO TO 520
  510   A2=WALLA10
  520 I=LC1
      J=LC2
      IF(IFLAG1.EQ.0)GO TO 530
      IF(IFLAG2.EQ.0)GO TO 530
      IFLAG3=1
      I=LC2
      J=LC1
      TEMP=A1
      A1=A2
      A2=TEMP
  530 F(I,J)=F(I,J)/SUBD2
      F(J,I)=A1/A2*F(I,J)
      IF(IFLAG3.NE.0)A1=A2
      IFLAG2=0
      IFLAG3=0
  480 CONTINUE
      IFLAG1=0
  420 CONTINUE
      RETURN
      END
C
C
C
C
      SUBROUTINE EXCHNG(TX,TY,TZ,A,X1,X2,Y1,Y2,Z1,Z2,I,J,
     $                  WCBT1,WCBT2,NDIM,F)
C
C     THIS ROUTINE CALCULATES THE RADIANT EXCHANGE BETWEEN
```

```
C  TWO WALL ELEMENTS, I AND J.
C
      DIMENSION F(NDIM,NDIM)
      PI=3.141592654
      D=SQRT(TX**2+TY**2)
      XM=TX/D
      XL=TY/D
      CALL SHADOW(X1,X2,Y1,Y2,Z1,Z2,XM,XL,IFLAG)
      IF(IFLAG.EQ.1)GO TO 10
        R=SQRT(TX**2+TY**2+TZ**2)
C
C  ERROR CONTROL
C
      Y=(R**2)/A
      Y=-5.084722E-01 + 2.540100E-02*Y - 3.686233E-04*Y**2
     $  +1.574209E-06*Y**3
      IF((R**2/A).GT.100.0)Y=0.0
        WCB1=WCBT1/R
        WCB2=WCBT2/R
        F(I,J)=F(I,J)+WCB1*WCB2*A/(PI*R**2)/(1.0-Y)
   10 RETURN
      END
C
C
C
C
C
C
      SUBROUTINE SHADOW(X1,X2,Y1,Y2,Z1,Z2,XM,XL,IFLAG)
C
C     THIS ROUTINE DETERMINES IF THE RADIANT EXCHANGE PATH BETWEEN
C  DIFFERENTIAL WALL SECTIONS IS BLOCKED BY THE PAN.
C
      COMMON/BLOCK/A1,A2,B1,B2,C1,C2,XC,YC,R,IPAN
      IFLAG=0
      IA=0
      IB=0
      IC=0
      A=A1
      B=B1
      C=C1
C
C     THIS FIRST PART DETERMINES IF THE EXCHANGE PATH STRIKES
C  THE UPPER OR LOWER SURFACE OF THE PAN.
C
      IF(ABS(Z2-Z1).LT.0.0001)GO TO 4
    5 X3=(X2-X1)/(Z2-Z1)*(C-Z1)+X1
      IF(X3.LT.A1)GO TO 2
      IF(X3.GT.A2)GO TO 2
      Y3=(Y2-Y1)/(Z2-Z1)*(C-Z1)+Y1
      IF(Y3.LT.B1)GO TO 2
      IF(Y3.GT.B2)GO TO 2
      IF(IPAN.EQ.1)GO TO 3
        IFLAG=1
        RETURN
    2 IF(IC.NE.0)GO TO 4
        IC=1
        C=C2
      GO TO 5
    3 D=SQRT((X3-XC)**2+(Y3-YC)**2)
      IF(D.GT.R)GO TO 2
        IFLAG=1
        RETURN
C
```

PROGRAM AGTAP

```
      PROGRAM AGTAP(INPUT,OUTPUT,NDATA2,
     $              TAPE1=NDATA2,TAPE5=INPUT,TAPE6=OUTPUT)
      DIMENSION E(6),E1(6),E2(100)
      COMMON STG(5000),NPOS(50),L1(50),L2(50),NLAST(50),FCT(50)
      COMMON KILL, NTABS
      COMMON BUFF(100),T(1000),CAP(1000),COND(2000),RAD(3000),Q(100),
     1    NCOND(2,2000),NRAD(2,3000),NIN(1000),NBN(250),KEY(5),NQ(100),
     2    KAY(4),FLUX(1000)
      COMMON TIME,DTIME,FTIME,DUM,SIGMA,KNIN,KNBN,N4,N5,KODE,KNQ,
     1    KOUT,KOUNT,NOSRT
      COMMON F(100,100)
      COMMON/COIL/DL,DU,CAREA1,CAREA2,PL,PU,VENT,QCONVL,QCONVU,QT,QB,QS
      COMMON/NRIP/NR,IP,TSS,TEMPK
      COMMON/TT04/T4(100),IAIR1,IAIR2,ICONV1,ICONV2
      COMMON/PRPTS/IC1,IC2,ROW,CP,K(100),XK(50),WALLT(50)
      TEMPK=.043
      TSS=0.0
      READ(1,21)NDIM,NSUBD,NXNY,NXNZ,NYNZ
      READ(1,22)DL,DU,CAREA1,CAREA2,APAN,ASIDE,
     $WALLA6,WALLA7,WALLA10
      DO 20 I=1,NDIM
        DO 30 J=1,NDIM
          READ(1,22)F(I,J)
   30 CONTINUE
   20 CONTINUE
      READ(5,21)IP,IAIR1,IAIR2,ICONV1,ICONV2
      READ(5,23)PL,PU,VENT
      READ(5,23)E(1),E(2),E(3),E(4),E(5),E(6)
      WRITE(6,17)E(1),E(2),E(3),E(4),E(5),E(6)
      IF(IP.EQ.1)WRITE(6,15)
      IF(IP.EQ.0)WRITE(6,14)
      WRITE(6,16)IAIR1,IAIR2,ICONV1,ICONV2
      WRITE(6,24)PL,PU,VENT
C
C  MANIPULATE EMISSIVITY VALUES INTO EASILY USED FORMS.
C
      DO 50 I=1,6
        E1(I)=-(1.0-E(I))/E(I)
   50 CONTINUE
      DO 800 I=1,NDIM
        DO 900 J=1,NDIM
          IF(I.GT.5)GO TO 850
            F(I,J)=E1(I)*F(I,J)
            IF(I.EQ.J)F(I,J)=1.0/E(I)
          GO TO 900
  850       F(I,J)=E1(6)*F(I,J)
            IF(I.EQ.J)F(I,J)=1.0/E(6)
  900   CONTINUE
  800 CONTINUE
C
C  CALL SUBROUTINE COEF
C
      SIGMA=5.669E-08
      E2(1)=E(1)/(1.0-E(1))*SIGMA*CAREA1
      E2(2)=E(2)/(1.0-E(2))*SIGMA*CAREA2
      E2(3)=E(3)/(1.0-E(3))*SIGMA*APAN
      E2(4)=E(4)/(1.0-E(4))*SIGMA*APAN
      E2(5)=E(5)/(1.0-E(5))*SIGMA*ASIDE
      ETEMP=E(6)/(1.0-E(6))*SIGMA
      LA6=5+NXNZ
      LA7=LA6+NYNZ
      LA8=LA7+NXNZ
      LA9=LA8+NYNZ
      LA10=LA9+NXNY
      LA11=LA10+NXNY
      SUBD2=FLOAT(NSUBD**2)
      DO 950 LC=6,LA11
        IF(LC.GT.LA6)GO TO 960
          E2(LC)=ETEMP*WALLA6*SUBD2
        GO TO 950
```

```
960 IF(LC.GT.LA7)GO TO 970
        E2(LC)=ETEMP*WALLA7*SUBD2
      GO TO 950
970 IF(LC.GT.LA8)GO TO 980
        E2(LC)=ETEMP*WALLA6*SUBD2
      GO TO 950
980 IF(LC.GT.LA9)GO TO 990
        E2(LC)=ETEMP*WALLA7*SUBD2
      GO TO 950
990 E2(LC)=ETEMP*WALLA10*SUBD2
950 CONTINUE
    CALL COEF(NDIM,E2)
    WRITE(6,19)
    DO 57 LC1=1,NR
      WRITE(6,18)(F(LC1,LC2),LC2=1,NR)
 57 CONTINUE
    WRITE(6,19)
    READ(5,25)IC1,IC2,ROW,CP
    WRITE(6,26)IC1,IC2,ROW,CP
    WRITE(6,19)
    J=1
    NLOOP=1
    DO 100 I=1,50
      IF(NLOOP.EQ.0)GO TO 100
      READ(5,25)K(J),K(J+1),XK(I),WALLT(I)
      WRITE(6,26)K(J),K(J+1),XK(I),WALLT(I)
      IF(K(J).LT.1)NLOOP=0
      J=J+2
100 CONTINUE
 5  CALL INITL
 3  CALL XREDE
    IF(KODE-1001)7,8,7
 7  CALL YREDE
    IF(KODE-1001)9,8,9
 9  IF(KILL)1,2,1
 2  CALL RITE
 1  CALL XTABS
    IF(KODE-1001)10,8,10
 10 CALL RCMIN
    CALL TEMP
    READ(5,1901,END=1011)KODE
    IF(KODE-12300)6,5,6
 6  IF(KODE-11100)3,4,3
1011 WRITE(6,1902)
 4  STOP
 8  CALL XERR
    CALL RITE
    GO TO 5
 14 FORMAT(1H1,///,5X,≠THERE IS NO PAN≠)
 15 FORMAT(1H1,///,5X,≠THERE IS A PRODUCT IN THE OVEN CAVITY≠)
 16 FORMAT(//,10X,≠FOR THE CAVITY AIR≠,/,
   $        /,5X,≠LOWER CAVITY AIR NODE NUMBER =≠,I5,
   $        /,5X,≠UPPER CAVITY AIR NODE NUMBER =≠,I5,
   $        /,5X,≠LOWER ELEMENT TO LOWER AIR CONVECTION LINK =≠,I5,
   $        /,5X,≠UPPER ELEMENT TO UPPER AIR CONVECTION LINK =≠,I5)
 17 FORMAT(10X,≠SURFACE EMISSIVITIES≠,//,5X,
   $        ≠LOWER HEATING ELEMENT EMISSIVITY =≠,F10.4,
   $        /,5X,≠UPPER HEATING ELEMENT EMISSIVITY =≠,F10.4,
   $        /,5X,≠LOWER PRODUCT EMISSIVITY         =≠,F10.4,
   $        /,5X,≠UPPER PRODUCT EMISSIVITY         =≠,F10.4,
   $        /,5X,≠PRODUCT SIDES EMISSIVITY         =≠,F10.4,
   $        /,5X,≠WALL SURFACES - EMISSIVITY       =≠,F10.4)
 18 FORMAT(1X,12E10.3)
 19 FORMAT(////)
 21 FORMAT(5I5)
 22 FORMAT(1X,10E12.5)
 23 FORMAT(8F10.4)
 24 FORMAT(///5X,≠FOR THE HEATING ELEMENTS≠,/
   $        /,15X,≠POWER LOWER=≠,F10.5,
   $        /,15X,≠POWER UPPER=≠,F10.5,
```

```
     $////,5X,≠OVEN VENT RATE = ≠,F5.3,≠ PERCENT PER MINUTE≠)
   25 FORMAT(2I5,2F10.4)
   26 FORMAT(5X,I5,2X,I5,2X,E10.4,2X,E10.4)
 1901 FORMAT(I5)
 1902 FORMAT(≠END OF DATA ENCOUNTERED-EXECUTION TERMINATED≠)
      END
C
C
C
C
      SUBROUTINE COEF(NDIM,E2)
      DIMENSION E2(100)
      COMMON STG(5000),NPOS(50),L1(50),L2(50),NLAST(50),FCT(50)
      COMMON KILL, NTABS
      COMMON BUFF(100),T(1000),CAP(1000),COND(2000),RAD(3000),Q(100),
     1    NCOND(2,2000),NRAD(2,3000),NIN(1000),NBN(250),KEY(5),NQ(100),
     2    KAY(4),FLUX(1000)
      COMMON TIME,DTIME,FTIME,DUM,SIGMA,KNIN,KNBN,N4,N5,KODE,KNQ,
     1    KOUT,KOUNT,NOSRT
      COMMON F(100,100)
      COMMON/COIL/DL,DU,CAREA1,CAREA2,PL,PU,VENT,QCONVL,QCONVU,QT,QB,QS
      COMMON/NRIP/NR,IP,TSS,TEMPK
      COMMON/TT04/T4(100),IAIR1,IAIR2,ICONV1,ICONV2
C     THIS SUBROUTINE MANIPULATES THE VIEW FACTOR ARRAY SO AS
C  TO REMOVE ANY ZERO COLUMNS (IF NECESSARY).  A ZERO COLUMN
C  WILL APPEAR IF THE ASSOCIATED SURFACE DOES NOT EXIST OR IS
C  TOTALLY BLOCKED (AS BY THE PAN).  THE VIEW FACTOR ARRAY
C  IS THEN INVERTED.
C
C     NOTE:  REMOVING A ZERO COLUMN IS THE SAME AS REMOVING
C  A SURFACE.  SURFACE RENUMBERING MUST BE ACCOUNTED FOR IN
C  FURTHER ANALYSIS (AS WHEN USING AGTAP)
C
C     IF NO ZERO COLUMNS APPEAR IN THE VIEW FACTOR ARRAY
C  THE USER NEED NOT DO ANYTHING.  IF A ZERO COLUMN DOES EXIST,
C  IT IS UP TO THE USER TO REMOVE IT BY SPECIFYING WHICH
C  COLUMNS ARE ZERO.
C
C  K=1ST ZERO COLUMN
C  L=2ND ZERO COLUMN
C  M=3RD ZERO COLUMN
C
      READ(5,2)K,L,M
      IF(K.EQ.0)GO TO 10
      DO 20 I=1,NDIM
        I1=I
        IF(I.GE.K)I1=I+1
        IF(L.EQ.0)GO TO 25
        IF(I1.GE.L)I1=I+2
        IF(M.EQ.0)GO TO 25
        IF(I1.GE.M)I1=I+3
        IF(I1.GT.NDIM)GO TO 20
   25   E2(I)=E2(I1)
        DO 30 J=1,NDIM
          F(I,J)=F(I1,J)
   30   CONTINUE
   20 CONTINUE
      DO 40 I=1,NDIM
        DO 50 J=1,NDIM
        J1=J
        IF(J.GE.K)J1=J+1
        IF(L.EQ.0)GO TO 45
        IF(J1.GE.L)J1=J+2
        IF(M.EQ.0)GO TO 45
        IF(J1.GE.M)J1=J+3
   45   F(I,J)=F(I,J1)
   50   CONTINUE
   40 CONTINUE
C
C     THE USER MUST ALSO SPECIFY NR AND NC
```

```
C
C  NR=NUMBER OF ROWS IN MANIPULATED VIEW FACTOR MATRIX
C  NC=NUMBER OF COLUMNS IN MANIPULATED VIEW FACTOR MATRIX
C
C     NR AND NC PERTAIN TO THE REDUCED MATRIX (AFTER ZERO
C  COLUMNS HAVE BEEN REMOVED)
C
   10 READ(5,2)NR,NC
C
C   INVERT THE VIEW FACTOR MATRIX
C
      CALL GINV2(F,100,NR,NC,KZ)
      IF(KZ.EQ.0)WRITE(6,1)
C
C  OBTAIN THE COEFFICIENT MATRIX FOR DETERMINING THE HEAT
C  FLUX LEVELS AT EACH SURFACE AS A FUNCTION OF ALL
C  SURFACE TEMPERATURES.
C
      DO  90 I=1,NR
        DO 100 J=1,NC
          IF(I.NE.J)F(I,J)= F(I,J)*E2(I)
          IF(I.EQ.J)F(I,J)=-(1.0-F(I,J))*E2(I)
  100   CONTINUE
   90 CONTINUE
    1 FORMAT(///,1X,≠THE VIEW FACTOR MATRIX IS SINGULAR≠)
    2 FORMAT(3I5)
      RETURN
      END
C
C
C
C
      SUBROUTINE XTABS
      DIMENSION ALPH(17)
      COMMON STG(5000),NPOS(50),L1(50),L2(50),NLAST(50),FCT(50)
      COMMON KILL,NTABS
      K2=0
      NKEY=NTABS
    4 NTABS=NTABS+1
      READ(5,901,END=11,ERR=12)KODE,LL1,LL2,(ALPH(II),II=1,17)
      IF(KODE-11100)1,2,1
    1 IF(NKEY)10,101,90
   90 NTABS=1
      NKEY=0
  101 L1(NTABS)=LL1
      L2(NTABS)=LL2
      IF(KILL)7,8,7
    8 WRITE(6,903)NTABS,L1(NTABS),L2(NTABS),(ALPH(II),II=1,17)
    7 NPOS(NTABS)=K2+1
      K3=L2(NTABS)+1
      DO 3 J=1,K3
      K1=K2+1
      K2=K2+L1(NTABS)
      READ(5,902,END=11,ERR=12)(STG(I),I=K1,K2)
      IF(KILL)3,9,3
    9 WRITE(6,904)(STG(I),I=K1,K2)
    3 CONTINUE
      GO TO 4
    2 IF(NKEY)10,6,10
    6 DO 5 I=1,NTABS
    5 NLAST(I)=NPOS(I)
   10 RETURN
   11 WRITE(6,905)
      CALL RITE
      STOP
   12 KODE=1001
      RETURN
  901 FORMAT(3I5,16A4,A1)
  902 FORMAT(7E10.0)
  903 FORMAT(///3I5,16A4,A1)
```

```
  904 FORMAT(7X,8F8.3)
  905 FORMAT(≠4 END OF DATA ENCOUNTERED IN SUBROUTINE XTABS - EXECUTION
     1 TERMINATED ABNORMALLY≠/≠4≠)
      END
C
C
C
C
      SUBROUTINE XINTP(NTAB,X)
      COMMON STG(5000),NPOS(50),L1(50),L2(50),NLAST(50),FCT(50)
      COMMON KILL, NTABS
      COMMON BUFF(100),T(1000),CAP(1000),COND(2000),RAD(3000),Q(100),
     1    NCOND(2,2000),NRAD(2,3000),NIN(1000),NBN(250),KEY(5),NQ(100),
     2    KAY(4),FLUX(1000)
      COMMON TIME,DTIME,FTIME,DUM,SIGMA,KNIN,KNBN,N4,N5,KODE,KNQ,
     1    KOUT,KOUNT,NOSRT
      I=NPOS(NTAB)
      IF(X-STG(I))3,6,2
    2 I=I+L1(NTAB)-1
      IF(X-STG(I))4,6,3
    4 I=NLAST(NTAB)
      IF(X-STG(I))5,6,7
    7 I=I+1
      IF(X-STG(I))8,6,7
    5 I=I-1
      IF(X-STG(I))5,6,9
    8 I=I-1
    9 RATIO=(X-STG(I))/(STG(I+1)-STG(I))
   11 K=L2(NTAB)
      DO 10 J=1,K
      I=I+L1(NTAB)
   10 FCT(J)=RATIO*STG(I+1)+(1.-RATIO)*STG(I)
      RETURN
    6 RATIO=0.
      GO TO 11
    3 WRITE(6,901)NTAB,X
      KODE=-3
      CALL XERR
      RETURN
  901 FORMAT(≠4 INDEPENDENT VARIABLE IS OFF TABLE IN SUBROUTINE XINTP≠//
     1 ≠   TABLE NUMBER≠,I5,≠   VALUE OF IND VAR =≠,E20.8)
      END
      FUNCTION MAX(I,J)
      IF(I-J)1,2,2
    1 MAX=J
      RETURN
    2 MAX=I
      RETURN
      END
C
C
C
C
      SUBROUTINE INITL
      COMMON STG(5000),NPOS(50),L1(50),L2(50),NLAST(50),FCT(50)
      COMMON KILL, NTABS
      COMMON BUFF(100),T(1000),CAP(1000),COND(2000),RAD(3000),Q(100),
     1    NCOND(2,2000),NRAD(2,3000),NIN(1000),NBN(250),KEY(5),NQ(100),
     2    KAY(4),FLUX(1000)
      COMMON TIME,DTIME,FTIME,DUM,SIGMA,KNIN,KNBN,N4,N5,KODE,KNQ,
     1    KOUT,KOUNT,NOSRT
      KNIN=0
      KNBN=0
      NTABS=0
      N4=0
      N5=0
      KNQ=0
      KODE=0
      KILL=0
      DO 1 I=1,1000
```

```
      T(I)=0.
      CAP(I)=0.0
      NIN(I)=0
    1 FLUX(I)=0.
      DO 2 I=1,2000
      COND(I)=0.
      RAD(I)=0.
      NCOND(1,I)=0
      NCOND(2,I)=0
      NRAD(1,I)=0
    2 NRAD(2,I)=0
      DO 3 I=1,100
      Q(I)=0.
    3 NQ(I)=0
      DO 4 I=1,250
    4 NBN(I)=0
      RETURN
      END
C
C
C
C
      SUBROUTINE XREDE
      COMMON STG(5000),NPOS(50),L1(50),L2(50),NLAST(50),FCT(50)
      COMMON KILL, NTABS
      COMMON BUFF(100),T(1000),CAP(1000),COND(2000),RAD(3000),Q(100),
     1    NCOND(2,2000),NRAD(2,3000),NIN(1000),NBN(250),KEY(5),NQ(100),
     2    KAY(4),FLUX(1000)
      COMMON TIME,DTIME,FTIME,DUM,SIGMA,KNIN,KNBN,N4,N5,KODE,KNQ,
     1    KOUT,KOUNT,NOSRT
      WRITE(6,901)
      WRITE(6,902)
      DO 200 I=1,10
        READ(5,50)IH1,IH2,IH3,IH4,IH5,IH6,IH7
        WRITE(6,903)IH1,IH2,IH3,IH4,IH5,IH6,IH7
  200 CONTINUE
    2 READ(5,904,END=33,ERR=34)KODE,KILL,KOUT,NOSRT
      IF(KODE-22200)3,2,3
    3 READ(5,905,END=33,ERR=34)KODE,TIME,DTIME,FTIME
      IF(KODE-22200)4,3,4
    4 IF(KNIN)30,5,30
C   READ IN INITIAL TEMPERATURES OF ITERATED NODES
    5 READ(5,906,END=33,ERR=34)KODE,N,DUM,II,JJ
      IF(KODE-22200)6,5,6
    6 IF(KODE-11100)7,10,7
    7 IF(II)8,9,8
    9 T(N)=DUM
      KNIN=KNIN+1
      NIN(KNIN)=N
      GO TO 5
    8 IF(II-N)5,11,11
   11 T(N)=DUM
      KNIN=KNIN+1
      NIN(KNIN)=N
      N=N+JJ
      GO TO 8
C   READ IN INITIAL TEMPERATURES OF BOUNDARY NODES
   10 READ(5,906,END=33,ERR=34)KODE,N,DUM,II,JJ
      IF(KODE-22200)12,10,12
   12 IF(KODE-11100)19,13,19
   19 IF(II)14,15,14
   15 T(N)=DUM
      KNBN=KNBN+1
      NBN(KNBN)=N
      GO TO 10
   14 IF(II-N)10,16,16
   16 T(N)=DUM
      KNBN=KNBN+1
      NBN(KNBN)=N
      N=N+JJ
```

```
      GO TO 14
C  READ IN REPLACEMENT TEMPERATURES
   30 READ(5,906,END=33,ERR=34)KODE,N,DUM,II,JJ
      IF(KODE-22200)17,30,17
   17 IF(KODE-11100)18,13,18
   18 IF(II)42,20,42
   20 T(N)=DUM
      GO TO 30
   42 IF(II-N)30,41,41
   41 T(N)=DUM
      N=N+JJ
      GO TO 42
C  READ IN THERMAL CAPICITANCES
   13 READ(5,906,END=33,ERR=34)KODE,N,DUM,II,JJ
      IF(KODE-22200)21,13,21
   21 IF(KODE-11100)22,23,22
   22 IF(II)24,25,24
   25 CAP(N)=DUM
      GO TO 13
   24 IF(II-N)13,26,26
   26 CAP(N)=DUM
      N=N+JJ
      GO TO 24
C  READ IN CONDUCTANCES
   23 READ(5,907,END=33,ERR=34)KODE,N,I,J,DUM,II,JJ
      IF(KODE-22200)27,23,27
   27 IF(KODE-11100)28,29,28
   28 IF(II)43,31,43
   31 N4=MAX(N,N4)
      NCOND(1,N)=I
      NCOND(2,N)=J
      COND(N)=DUM
      GO TO 23
   43 IF(II-N)23,32,32
   32 N4=MAX(N,N4)
      NCOND(1,N)=I
      NCOND(2,N)=J
      COND(N)=DUM
      I=I+JJ
      J=J+JJ
      N=N+JJ
      GO TO 43
   33 WRITE(6,908)
      CALL RITE
      STOP
   34 KODE=1001
   29 RETURN
   50 FORMAT(7A10)
  901 FORMAT(1H1)
  902 FORMAT(////)
  903 FORMAT(5X,7A10)
  904 FORMAT(4I5)
  905 FORMAT(I5,3E10.0)
  906 FORMAT(2I5,E10.0,2I5)
  907 FORMAT(4I5,E10.0,2I5)
  908 FORMAT(≠4 END OF DATA ENCOUNTERED IN SUBROUTINE XREDE - EXECUTION
     1 TERMINATED ABNORMALLY≠/≠4≠)
      END
C
C
C
C
      SUBROUTINE YREDE
      COMMON STG(5000),NPOS(50),L1(50),L2(50),NLAST(50),FCT(50)
      COMMON KILL, NTABS
      COMMON BUFF(100),T(1000),CAP(1000),COND(2000),RAD(3000),Q(100),
     1    NCOND(2,2000),NRAD(2,3000),NIN(1000),NBN(250),KEY(5),NQ(100),
     2    KAY(4),FLUX(1000)
      COMMON TIME,DTIME,FTIME,DUM,SIGMA,KNIN,KNBN,N4,N5,KODE,KNQ,
     1    KOUT,KOUNT,NOSRT
```

```
C  READ IN RADIATION LINKS
      SIGMA=5.669E-8
   29 READ(5,907,END=41,ERR=42)KODE,N,I,J,DUM,II,JJ
      IF(KODE-22200)33,29,33
   33 IF(KODE-11100)34,35,34
   34 IF(II)36,37,36
   37 N5=MAX(N,N5)
      NRAD(1,N)=I
      NRAD(2,N)=J
      RAD(N)=DUM*SIGMA
      GO TO 29
   36 IF(II-I)29,44,44
   44 N5=MAX(N,N5)
      NRAD(1,N)=I
      NRAD(2,N)=J
      RAD(N)=DUM*SIGMA
      I=I+JJ
      N=N+JJ
      GO TO 36
C  READ IN HEAT SOURCES
   35 READ(5,908,END=41,ERR=42)KODE,N,I,DUM
      IF(KODE-22200)38,35,38
   38 IF(KODE-11100)39,40,39
   39 KNQ=MAX(N,KNQ)
      NQ(N)=I
      Q(N)=DUM
      GO TO 35
   40 WRITE(6,909)
      IF(NOSRT)47,45,47
   47 K=1
  100 L=K
      K=K+1
      IF(K-KNIN)110,110,170
  110 DO 140 I=1,L
      IF(NIN(K)-NIN(I))150,140,140
  140 CONTINUE
      GO TO 100
  150 IX=NIN(K)
      J=K
      DO 160 M=I,L
      NIN(J)=NIN(J-1)
  160 J=J-1
      NIN(I)=IX
      GO TO 100
  170 IF(KNBN)45,45,46
   46 K=1
  101 L=K
      K=K+1
      IF(K-KNBN)111,111,45
  111 DO 141 I=1,L
      IF(NBN(K)-NBN(I))151,141,141
  141 CONTINUE
      GO TO 101
  151 IX=NBN(K)
      J=K
      DO 161 M=I,L
      NBN(J)=NBN(J-1)
  161 J=J-1
      NBN(I)=IX
      GO TO 101
   41 WRITE(6,910)
      CALL RITE
      STOP
   42 KODE=1001
   45 RETURN
  907 FORMAT(4I5,E10.0,2I5)
  908 FORMAT(3I5,E10.0)
  909 FORMAT(1H1)
  910 FORMAT(≠4 END OF DATA ENCOUNTERED IN SUBROUTINE YREDE - EXECUTION
     1 TERMINATED ABNORMALLY≠/≠4≠)
```

```
      END
C
C
C
C
      SUBROUTINE RITE
      COMMON STG(5000),NPOS(50),L1(50),L2(50),NLAST(50),FCT(50)
      COMMON KILL, NTABS
      COMMON BUFF(100),T(1000),CAP(1000),COND(2000),RAD(3000),Q(100),
     1    NCOND(2,2000),NRAD(2,3000),NIN(1000),NBN(250),KEY(5),NQ(100),
     2    KAY(4),FLUX(1000)
      COMMON TIME,DTIME,FTIME,DUM,SIGMA,KNIN,KNBN,N4,N5,KODE,KNQ,
     1    KOUT,KOUNT,NOSRT
      COMMON F(100,100)
      COMMON/COIL/DL,DU,CAREA1,CAREA2,PL,PU,VENT,QCONVL,QCONVU,QT,QB,QS
      COMMON/NRIP/NR,IP,TSS,TEMPK
      COMMON/TTO4/T4(100),IAIR1,IAIR2,ICONV1,ICONV2
      COMMON/PRPTS/IC1,IC2,ROW,CP,K(100),XK(50),WALLT(50)
      DIMENSION KN(5)
      IF(IC1.LT.1)GO TO 150
      DO 100 I=IC1,IC2
        CAP(I)=CAP(I)*ROW*CP
  100 CONTINUE
  150 J=1
      DO 200 I=1,50
        IF(K(J).LT.1)GO TO 200
          DO 300 I2=K(J),K(J+1)
            COND(I2)=COND(I2)*XK(I)*WALLT(I)
  300     CONTINUE
        J=J+2
  200 CONTINUE
      SIGMA=5.669E-8
      WRITE(6,901)KNIN,TIME,KNBN,DTIME,N4,FTIME,N5,KNQ,KOUT,NOSRT
      WRITE(6,902)
      N=0
      KODE=1
    1 I=0
    4 N=N+1
      I=I+1
      KEY(I)=NIN(N)
      J=KEY(I)
      BUFF(I)=T(J)
      J=KEY(I)
      BUFF(I)=T(J)
      IF(N-KNIN)2,3,96
    2 IF(I-5)4,3,96
    3 WRITE(6,903)(KEY(J),BUFF(J),J=1,I)
      IF(N-KNIN)1,5,96
    5 WRITE(6,904)
      N=0
      KODE=2
      IF(KNBN)96,10,6
    6 I=0
    7 N=N+1
      I=I+1
      KEY(I)=NBN(N)
      J=KEY(I)
      BUFF(I)=T(J)
      IF(N-KNBN)8,9,96
    8 IF(I-5)7,9,96
    9 WRITE(6,903)(KEY(J),BUFF(J),J=1,I)
      IF(N-KNBN)6,10,96
   10 WRITE(6,905)
      N=0
      KODE=3
   11 I=0
   12 N=N+1
      I=I+1
      KEY(I)=NIN(N)
      J=KEY(I)
```

```
      BUFF(I)=CAP(J)
      IF(N-KNIN)13,14,96
   13 IF(I-4)12,14,96
   14 WRITE(6,911)(KEY(J),BUFF(J),J=1,I)
      IF(N-KNIN)11,15,96
   15 WRITE(6,906)
      N=0
      KODE=4
      IF(N4)96,20,16
   16 I=0
   17 N=N+1
      I=I+1
      KN(I)=N
      KEY(I)=NCOND(1,N)
      KAY(I)=NCOND(2,N)
      BUFF(I)=COND(N)
      IF(N-N4)18,19,96
   18 IF(I-3)17,19,96
   19 WRITE(6,907)(KN(J),KEY(J),KAY(J),BUFF(J),J=1,I)
      IF(N-N4)16,20,96
   20 WRITE(6,908)
      N=0
      KODE=5
      IF(N5)96,25,21
   21 I=0
   22 N=N+1
      I=I+1
      KN(I)=N
      KEY(I)=NRAD(1,N)
      KAY(I)=NRAD(2,N)
      BUFF(I)=RAD(N)/SIGMA
      IF(N-N5)23,24,96
   23 IF(I-4)22,24,96
   24 WRITE(6,913)(KN(J),KEY(J),KAY(J),BUFF(J),J=1,I)
      IF(N-N5)21,25,96
   25 WRITE(6,909)
      N=0
      KODE=6
      IF(KNQ)96,30,26
   26 I=0
   27 N=N+1
      I=I+1
      KN(I)=N
      KEY(I)=NQ(N)
      BUFF(I)=Q(N)
      IF(N-KNQ)28,29,96
   28 IF(I-4)27,29,96
   29 WRITE(6,910)(KN(J),KEY(J),BUFF(J),J=1,I)
      IF(N-KNQ)26,30,96
   30 RETURN
   96 WRITE(6,912)KODE,I,N,J
      STOP
  901 FORMAT(≠ NUMBER OF ITERATED NODES    =≠,I6,20X,≠   TIME  =≠,E10.4/
     1       ≠ NUMBER OF BOUNDARY NODES    =≠,I6,20X,≠  DTIME =≠,E10.4/
     2       ≠ NUMBER OF CONDUCTION LINKS =≠,I6,20X,≠  FTIME =≠,E10.4/
     3       ≠ NUMBER OF RADIATION LINKS  =≠,I6/
     4       ≠ NUMBER OF HEAT SOURCE SINKS=≠,I6/
     5       ≠ OUTPUT INTERVAL COUNT      =≠,I6/
     6       ≠ NODE SORT SUPPRESS CODE    =≠,I6)
  902 FORMAT(39H0INITIAL TEMPERATURES OF ITERATED NODES)
  903 FORMAT(1X,5(4H  T(,I3,3H) =,E10.4))
  904 FORMAT(39H0INITIAL TEMPERATURES OF BOUNDARY NODES)
  905 FORMAT(47H0INITIAL THERMAL CAPACITANCES OF ITERATED NODES)
  906 FORMAT(21H0INITIAL CONDUCTANCES)
  907 FORMAT(1X,3(≠   COND(≠,I4,≠)(≠,I3,≠-≠,I3,≠) =≠,E10.4,3X))
  908 FORMAT(24H0INITIAL RADIATION LINKS)
  909 FORMAT(20H0INITIAL HEAT FLUXES)
  910 FORMAT(1X,4(≠   Q(≠,I5,≠)(≠,I5,≠) =≠,E10.4,2X))
  911 FORMAT(1X,4(4HCAP(,I3,3H) =,E10.4,4X))
  912 FORMAT(29H1ERROR IN RITE - EXIT FROM 96,4I8)
```

```
913 FORMAT(1X,4(≠ RAD(≠,I4,≠)(≠,I3,≠-≠,I3,≠)=≠,E12.6,2X))
    END
    SUBROUTINE TEMP
    COMMON STG(5000),NPOS(50),L1(50),L2(50),NLAST(50),FCT(50)
    COMMON KILL, NTABS
    COMMON BUFF(100),T(1000),CAP(1000),COND(2000),RAD(3000),Q(100),
   1     NCOND(2,2000),NRAD(2,3000),NIN(1000),NBN(250),KEY(5),NQ(100),
   2     KAY(4),FLUX(1000)
    COMMON TIME,DTIME,FTIME,DUM,SIGMA,KNIN,KNBN,N4,N5,KODE,KNQ,
   1     KOUT,KOUNT,NOSRT
    COMMON/NRIP/NR,IP,TSS,TEMPK
    GO TO 8
 1  CONTINUE
    KODE=1
    CALL CLC1
    DO 2 I=1,KNIN
    N=NIN(I)
 2  FLUX(N)=0.
    IF(N4)96,22,23
 23 DO 3 N=1,N4
    I=NCOND(1,N)
    J=NCOND(2,N)
    QUE=COND(N)*(T(I)-T(J))
    FLUX(I)=FLUX(I)-QUE
 3  FLUX(J)=FLUX(J)+QUE
 22 IF(N5)96,25,24
 24 DO 4 N=1,N5
    I=NRAD(1,N)
    J=NRAD(2,N)
    QUE=RAD(N)*((T(I))**4-(T(J))**4)
    FLUX(I)=FLUX(I)-QUE
 4  FLUX(J)=FLUX(J)+QUE
 25 IF(KNQ)96,26,27
 27 DO 5 N=1,KNQ
    I=NQ(N)
 5  FLUX(I)=FLUX(I)+Q(N)
 26 DO 6 N=1,KNIN
    I=NIN(N)
    T(I)=T(I)+FLUX(I)*DTIME/CAP(I)
 6  CONTINUE
    CALL CLC2
    TIME=TIME+DTIME
    KOUNT=KOUNT+1
    IF(TIME-FTIME)7,8,8
 7  IF(KOUNT-KOUT)1,8,8
 8  WRITE(6,905)
    WRITE(6,901)TIME
    KOUNT=0
    N=0
 10 I=0
    KODE=2
 11 N=N+1
    I=I+1
    KEY(I)=NIN(N)
    J=KEY(I)
    BUFF(I)=T(J)-273.15
    IF(N-KNIN)12,13,96
 12 IF(I-5)11,13,96
 13 WRITE(6,902)(KEY(J),BUFF(J),J=1,I)
    IF(N-KNIN)10,15,96
 15 N=0
    IF(KNBN)96,20,16
 16 I=0
    KODE=3
 17 N=N+1
    I=I+1
    KEY(I)=NBN(N)
    J=KEY(I)
    BUFF(I)=T(J)-273.15
    IF(N-KNBN)18,19,96
```

```
   18 IF(I-5)17,19,96
   19 WRITE(6,902)(KEY(J),BUFF(J),J=1,I)
      IF(N-KNBN)16,20,96
   20 WRITE(6,910)
  910 FORMAT(1X)
      CALL CLC3
      IF(TIME-FTIME)1,21,21
   96 WRITE(6,903)KODE,I,N,J
   21 RETURN
  901 FORMAT(4X,≠ * TIME=≠,E10.4,≠  *≠)
  902 FORMAT(1X,5(4H  T(,I3,3H) =,E10.4))
  903 FORMAT(15H0 ERROR IN TEMP,4I8)
  905 FORMAT(1X,≠ ***********************************************************
     1*************************************************************
     2*≠)
      END
C
C
C
C
      SUBROUTINE SYSRXT(I,J,A)
      COMMON STG(5000),NPOS(50),L1(50),L2(50),NLAST(50),FCT(50)
      COMMON KILL, NTABS
      COMMON BUFF(100),T(1000),CAP(1000),COND(2000),RAD(3000),Q(100),
     1    NCOND(2,2000),NRAD(2,3000),NIN(1000),NBN(250),KEY(5),NQ(100),
     2    KAY(4),FLUX(1000)
      COMMON TIME,DTIME,FTIME,DUM,SIGMA,KNIN,KNBN,N4,N5,KODE,KNQ,
     1    KOUT,KOUNT,NOSRT
      DIMENSION A(3)
      WRITE(6,901)I,(A(K),K=1,3)
      WRITE(6,902)
      CALL RITE
      KODE=-3
      CALL XERR
      J=0
      RETURN
  901 FORMAT(35H1SUBROUTINE SYSRXT HAS BEEN ENTERED///
     1  13H FAULT CODE =,I3///26H FAULT OCCURED IN ROUTINE,2X,3A4)
  902 FORMAT(1H4)
      END
C
C
C
C
      SUBROUTINE RCMIN
C  CALCULATES STABILITY CRITERION FOR AGTAP
      COMMON STG(5000),NPOS(50),L1(50),L2(50),NLAST(50),FCT(50)
      COMMON KILL, NTABS
      COMMON BUFF(100),T(1000),CAP(1000),COND(2000),RAD(3000),Q(100),
     1    NCOND(2,2000),NRAD(2,3000),NIN(1000),NBN(250),KEY(5),NQ(100),
     2    KAY(4),FLUX(1000)
      COMMON TIME,DTIME,FTIME,DUM,SIGMA,KNIN,KNBN,N4,N5,KODE,KNQ,
     1    KOUT,KOUNT,NOSRT
      X1=1.E38
      WRITE(6,907)
      WRITE(6,908)
      WRITE(6,901)
      WRITE(6,906)
      DO 3 L=1,KNIN
      SUMK=0.
      I=NIN(L)
      IF(N4)11,12,11
   11 CONTINUE
      DO 4 J=1,N4
      K=NCOND(1,J)
      IF(I-K)5,6,5
    5 K=NCOND(2,J)
      IF(I-K)4,6,4
    6 SUMK=SUMK+COND(J)
    4 CONTINUE
```

```
   12 IF(N5)13,14,13
   13 CONTINUE
      DO 7 J=1,N5
      K=NRAD(1,J)
      IF(I-K)8,9,8
    8 K=NRAD(2,J)
      IF(I-K)7,9,7
    9 M=NRAD(1,J)
      N=NRAD(2,J)
      SUMK=SUMK+RAD(J)*((T(M))**2+(T(N))**2)*(T(M)+T(N))
    7 CONTINUE
   14 IF(SUMK)1,2,1
    1 TCRIT=CAP(I)/SUMK
      IF(X1-TCRIT)3,10,10
   10 II=I
      X2=SUMK
      X1=TCRIT
      GO TO 3
    2 WRITE(6,905)I
    3 CONTINUE
      WRITE(6,904)II
      WRITE(6,903)II,X2,X1
      RETURN
  901 FORMAT(//4X,≠ NODE≠,3X,≠ SUMK≠,3X,≠ T CRIT≠)
  903 FORMAT(I10,1X,F10.4,1X,F10.4)
  904 FORMAT(5HONODEI5,22H HAS THE MINIMUM TCRIT)
  905 FORMAT(I10,36X,≠WARNING SUMK FOR THIS NODE IS ZERO≠)
  906 FORMAT(6X,≠ ----≠,3X,≠ ----≠,5X,≠------≠)
  907 FORMAT(/5X,≠ STABILITY DATA≠)
  908 FORMAT(5X,≠ --------------≠)
      END
C
C
C
C
      SUBROUTINE XERR
C SEARCHES FOR NEW SUBJOB IF ERROR IN DATA INPUT IS ENCOUNTERED
C  OR IF CERTAIN PROGRAM FAULTS OCCUR
      COMMON STG(5000),NPOS(50),L1(50),L2(50),NLAST(50),FCT(50)
      COMMON KILL, NTABS
      COMMON BUFF(100),T(1000),CAP(1000),COND(2000),RAD(3000),Q(100),
     1    NCOND(2,2000),NRAD(2,3000),NIN(1000),NBN(250),KEY(5),NQ(100),
     2    KAY(4),FLUX(1000)
      COMMON TIME,DTIME,FTIME,DUM,SIGMA,KNIN,KNBN,N4,N5,KODE,KNQ,
     1    KOUT,KOUNT,NOSRT
      DIMENSION A(20)
      IF(KODE.EQ.-3)GO TO 7
      WRITE(6,901)
    6 DO 1 I=1,20
      READ(5,902,END=2,ERR=3)KODE,(A(J),J=1,19)
      WRITE(6,903)I,KODE,(A(J),J=1,19)
      IF(KODE-12300)1,4,1
    1 CONTINUE
    5 READ(5,904,END=2,ERR=3)KODE
      IF(KODE-12300)5,4,5
    2 WRITE(6,905)
      STOP
    4 RETURN
    3 WRITE(6,906)
      GO TO 6
    7 WRITE(6,907)
      CALL RITE
      TIME=FTIME
      GO TO 6
  901 FORMAT(≠1 ILLEGAL CHARACTER ENCOUNTERED DURING DATA INPUT OPERATIO
     1N - SEARCH INITIATED FOR NEXT SUBJOB≠//≠  THE NEXT 20 OR REMAINING
     2 CARDS IN THIS SUBJOB ARE;≠///)
  902 FORMAT(I5,18A4,A3)
  903 FORMAT(I5,≠ ***≠,18A4,A3,≠***≠)
  904 FORMAT(I5)
```

```
  905 FORMAT(≠4 END OF DATA ENCOUNTERED IN SUBROUTINE XERR  -  SEARCH FO
     1R NEW SUBJOB REINITIATED≠/≠4≠)
  906 FORMAT(≠4 END OF DATA ENCOUNTERED IN SUBROUTINE XERR - SEARCH FOR
     1NEW SUBJOB REINITIATED≠/≠4≠)
  907 FORMAT(≠ CONTROL HAS BEEN TRANSFERRED TO SUBROUTINE XERR AFTER A P
     1ROGRAM FAULT OR TABLE ERROR≠//
     2≠ SEARCH FOR START OF NEXT SUBJOB WILL BE MADE AND TIME SET EQUAL
     3TO FTIME TO TERMINATE THIS SUBJOB≠/≠4≠)
      END
C
C
C
C
      SUBROUTINE CLC1
C  THIS SUBROUTINE IS CALLED AT THE START OF EVERY ITERATION
      COMMON STG(5000),NPOS(50),L1(50),L2(50),NLAST(50),FCT(50)
      COMMON KILL, NTABS
      COMMON BUFF(100),T(1000),CAP(1000),COND(2000),RAD(3000),Q(100),
     1    NCOND(2,2000),NRAD(2,3000),NIN(1000),NBN(250),KEY(5),NQ(100),
     2    KAY(4),FLUX(1000)
      COMMON TIME,DTIME,FTIME,DUM,SIGMA,KNIN,KNBN,N4,N5,KODE,KNQ,
     1    KOUT,KOUNT,NOSRT
      COMMON F(100,100)
      COMMON/COIL/DL,DU,CAREA1,CAREA2,PL,PU,VENT,QCONVL,QCONVU,QT,QB,QS
      COMMON/NRIP/NR,IP,TSS,TEMPK
      COMMON/TTO4/T4(100),IAIR1,IAIR2,ICONV1,ICONV2
C
C  USE TABULATED VALUES OF AIR MC TO SPECIFY VENT LOSS
C
      X=T(IAIR1)
      CALL XINTP(1,X)
      CP1=FCT(1)
      X=T(IAIR2)
      CALL XINTP(1,X)
      CP2=FCT(1)
      X=T(162)
      CALL XINTP(1,X)
      CAMB=FCT(1)
      Q(NR+1)=VENT*DTIME/60.*(T(162)*CAMB-T(IAIR1)*CP1)
      Q(NR+2)=VENT*DTIME/60.*(T(162)*CAMB-T(IAIR2)*CP2)
C*********************************************************
C
C     THIS ROUTINE CALCULATES THE TRANSIENT EFFECTS ON THE
C  HEATING COIL.  INPUT TO THIS SUBROUTINE CONSISTS OF
C  CURRENT COIL AND AMBIENT AIR TEMPERATURES, AND THE NET
C  RADIATIVE HEAT FLUX TO THE COIL, PLUS THE GENERAL THERMO-
C  PHYSICAL HEATING COIL PROPERTIES.
C     THE ANALYSIS USES THE REBROV EQUATION TO DETERMINE THE
C  CONVECTIVE HEAT FLUX FROM THE HEATING COIL.  (REFERENCE
C  IS MADE TO STEVE KUHLMAN, LABORATORY NOTEBOOK 1)
C     OUTPUT FROM THIS ROUTINE IS THE NEW SURFACE TEMPERATURE
C  OF THE HEATING COIL.
C
      IC=1
        CASURF=CAREA1
        TS=T(1)
        D=DL
        TA=T(IAIR1)
      GO TO 20
   10 CASURF=CAREA2
      TS=T(2)
      D=DU
      TA=T(IAIR2)
C
C  FROM THE REBROV EQUATION
C
C  XNU=(0.98-0.01(LOG(RA))**2)(RA)**K
C
C        WHERE     K=0.14+0.15(LOG(RA))
C                  NU=H*D/COND
```

```
C                    RA=GR*PR
C
   20 G=9.81
      TF=1.0/2.0*(TA+TS)
      BETA=1.0/TF
      ALPHA=(0.1823E-06)*TF-33.7E-06
      V=(0.12E-06)*TF-22.07E-06
      XKOND=(70.6E-06)*TF+5312.E-06
      RA=(G*BETA*(TS-TA)*D**3)/(V*ALPHA)
      XK=0.14+0.015*ALOG10(RA)
      XNU=((0.98-0.01*(ALOG10(RA))**2)*RA**XK)
      H=XNU*XKOND/D
      QCONV=CASURF*H*(TS-TA)
      IF(IC.EQ.2)GO TO 30
        QCONVL=QCONV
        COND(ICONV1)=H*CAREA1
        IC=2
        GO TO 10
   30   QCONVU=QCONV
        COND(ICONV2)=H*CAREA2
C*********************************************************
C
C     THIS ROUTINE DETERMINES THE HEAT FLUX AT EACH
C  SURFACE WITHIN THE OVEN CAVITY.
C
      DO 100 I=1,NR
        Q(I)=0.0
        T4(I)=T(I)**4
  100 CONTINUE
      IF(IP.EQ.0)GO TO 250
        DO 150 I=1,NR-3
          J=NR+1-I
          T4(J)=T4(J-2)
  150   CONTINUE
        T4(4)=T4(3)
        T4(5)=T4(3)
  250 DO 200 I=1,NR
        DO 300 J=1,NR
          Q(I)=Q(I)+F(I,J)*T4(J)
  300   CONTINUE
  200 CONTINUE
      IF(IP.EQ.0)GO TO 400
C
C  IP=1.  THERE IS A PAN IN THE OVEN.  NODE 3 IS THE PAN.
C  Q(3), THE TOTAL HEAT FLUX TO THE PAN = Q(3)+Q(4)+Q(5).
C  THAT IS, THE HEAT FLUX TO THE BOTTOM PLUS THE HEAT
C  FLUX TO THE TOP PLUS THE HEAT FLUX TO THE SIDES OF THE PAN.
C
      QT=Q(4)
      QB=Q(3)
      QS=Q(5)
      Q(3)=Q(3)+Q(4)+Q(5)
      DO 500 I=4,NR-2
        Q(I)=Q(I+2)
  500 CONTINUE
      Q(NR-1)=0.0
      Q(NR)=0.0
C
C  ACCOUNT FOR POWER INPUT TO THE HEATING ELEMENTS AS A HEAT SOURCE.
C
  400 Q(1)=Q(1)+PL
      Q(2)=Q(2)+PU
      RETURN
      END
C
C
C
C
      SUBROUTINE CLC2
C  THIS SUBROUTINE IS CALLED AT THE END OF EVERY
```

```
C  ITERATION BEFORE TIME IS INCREMENTED
      COMMON STG(5000),NPOS(50),L1(50),L2(50),NLAST(50),FCT(50)
      COMMON KILL, NTABS
      COMMON BUFF(100),T(1000),CAP(1000),COND(2000),RAD(3000),Q(100),
     1    NCOND(2,2000),NRAD(2,3000),NIN(1000),NBN(250),KEY(5),NQ(100),
     2    KAY(4),FLUX(1000)
      COMMON TIME,DTIME,FTIME,DUM,SIGMA,KNIN,KNBN,N4,N5,KODE,KNQ,
     1    KOUT,KOUNT,NOSRT
      COMMON F(100,100)
      COMMON/COIL/DL,DU,CAREA1,CAREA2,PL,PU,VENT,QCONVL,QCONVU,QT,QB,QS
      COMMON/NRIP/NR,IP,TSS,TEMPK
      COMMON/TT04/T4(100),IAIR1,IAIR2,ICONV1,ICONV2
C
C  DETERMINE THE THERMAL MASS OF THE AIR NODE
C
      CAP(IAIR1)=0.0
      CAP(IAIR2)=0.0
      DO 5 I=1,3
        X=T(IAIR1)
        CALL XINTP(I,X)
        CAP(IAIR1)=CAP(IAIR1)+FCT(1)
        X=T(IAIR2)
        CALL XINTP(I,X)
        CAP(IAIR2)=CAP(IAIR2)+FCT(1)
    5 CONTINUE
C
C  CALCULATE THE THERMAL MASS OF THE BLOCK
C
      X=T(3)
      CALL XINTP(4,X)
      CAP(3)=FCT(1)
C
C  CALCULATE THE THERMAL CONDUCTIVITY OF THE INSULATION
C
      AVE=0.0
      DO 100 IINS=28,57
        AVE=AVE+T(IINS)
  100 CONTINUE
      X=AVE/30.
      CALL XINTP(5,X)
      XKINS=FCT(1)
      DO 200 I=77,200
        COND(I)=COND(I)*XKINS/TEMPK
  200 CONTINUE
      DO 300 I=490,513
        COND(I)=COND(I)*XKINS/TEMPK
  300 CONTINUE
      TEMPK=XKINS
      DELTA=T(3)-T(162)
      IF(DELTA.LT.130)GO TO 999
C     DELTA1=ABS(TSS-T(3))
C     IF(DELTA1.GT.0.0001)GO TO 998
        ETA=3736.8*DELTA/((PL+PU)*TIME)*100.0
        WRITE(6,10)ETA
   10   FORMAT(////,5X,≠EFFICIENCY FACTOR = ≠,F10.4)
        WRITE(6,20)TIME
   20   FORMAT(/,5X,≠TIME = ≠,F10.4)
        TIME = FTIME
C 998 TSS=T(3)
  999 RETURN
      END
C
C
C
C
      SUBROUTINE CLC3
C  THIS SUBROUTINE IS CALLED IMMEDIATELY AFTER TEMPERATURE PRINTOUT
      COMMON STG(5000),NPOS(50),L1(50),L2(50),NLAST(50),FCT(50)
      COMMON KILL, NTABS
      COMMON BUFF(100),T(1000),CAP(1000),COND(2000),RAD(3000),Q(100),
```

```
 1     NCOND(2,2000),NRAD(2,3000),N9N(1000),NBN(250),KEY(5),NQ(100),
 2     KAY(4),FLUX(1000)
  COMMON TIME,DTIME,FTIME,DUM,SIGMA,KNIN,KNBN,N4,N5,KODE,KNQ,
 1     KOUT,KOUNT,NOSRT
  COMMON F(100,100)
  COMMON/COIL/DL,DU,CAREA1,CAREA2,PL,PU,VENT,QCONVL,QCONVU,QT,QB,QS
  COMMON/NRIP/NR,IP,TSS,TEMPK
  WRITE(6,1)QCONVL,QCONVU,QT,QB,QS
  WRITE(6,2)(N,Q(N),N=1,NR+2)
1 FORMAT(5X,≠QCONVL=≠,F10.4,5X,≠QCONVU=≠,F10.4,
 $5X,≠QT=≠,F10.4,5X,≠QB=≠,F10.4,5X,≠QS=≠,F10.4)
2 FORMAT(5X,5(≠Q(≠,I3,≠)=≠,F10.2,1X))
  RETURN
  END
```

APPENDIX F

NODAL PLACEMENT AND SAMPLE CALCULATIONS

The purpose of this appendix is to describe the location of individual nodal elements defining the oven structure. A photograph of the experimental apparatus with the data acquisition system is shown in the photograph of Figure F-1. An expanded schematic of the outer covers and support structure is given in Figure F-2.

F.2 Placement of Nodal Elements

The nodal elements used by Program AGTAP to define the oven structure are listed in Table F-1. The locations for interior cavity wall nodes, insulation nodes, and exterior oven cover nodes are depicted in Figures F-3, F-4, and F-5, respectively.

F.2 Thermal Mass and Resistance Calculations

The thermal capacitance of a node is defined as the mass of the node times its specific heat. Conductive couplings (linking two nodes) are defined as the product of the thermal conductivity and the cross-sectional area between two nodes. Convective couplings are defined as the product of the convective heat transfer coefficient and the surface area involved in convective heat transfer. Radiative coupling from node i to node j is determined from the surface area of node i times the total exchange factor from node i to node j. Note that radiative cou-

ORNL-Photo 7957-81

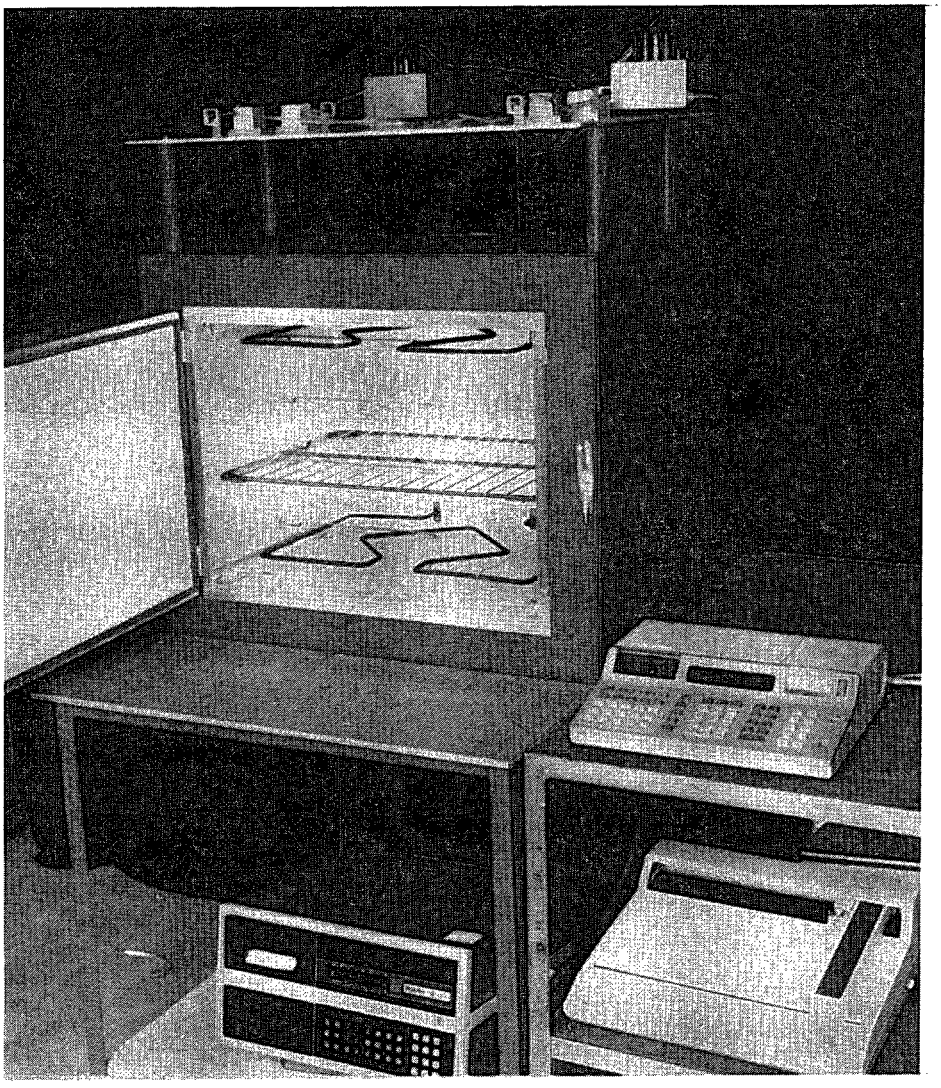

Figure F-1 Photograph of the Experimental Apparatus, Bi-Radiant Oven IV-B

TABLE F-1. Nodal Element Definitions

NODAL ELEMENT	DEFINITION
1	Lower heating element
2	Upper heating element
3	DOE test block
4-27	Inner cavity walls
28-71	Cavity insulation
72-159	Exterior oven cover
160	Cavity air, lower half
161	Cavity air, upper half
162	Ambient surroundings

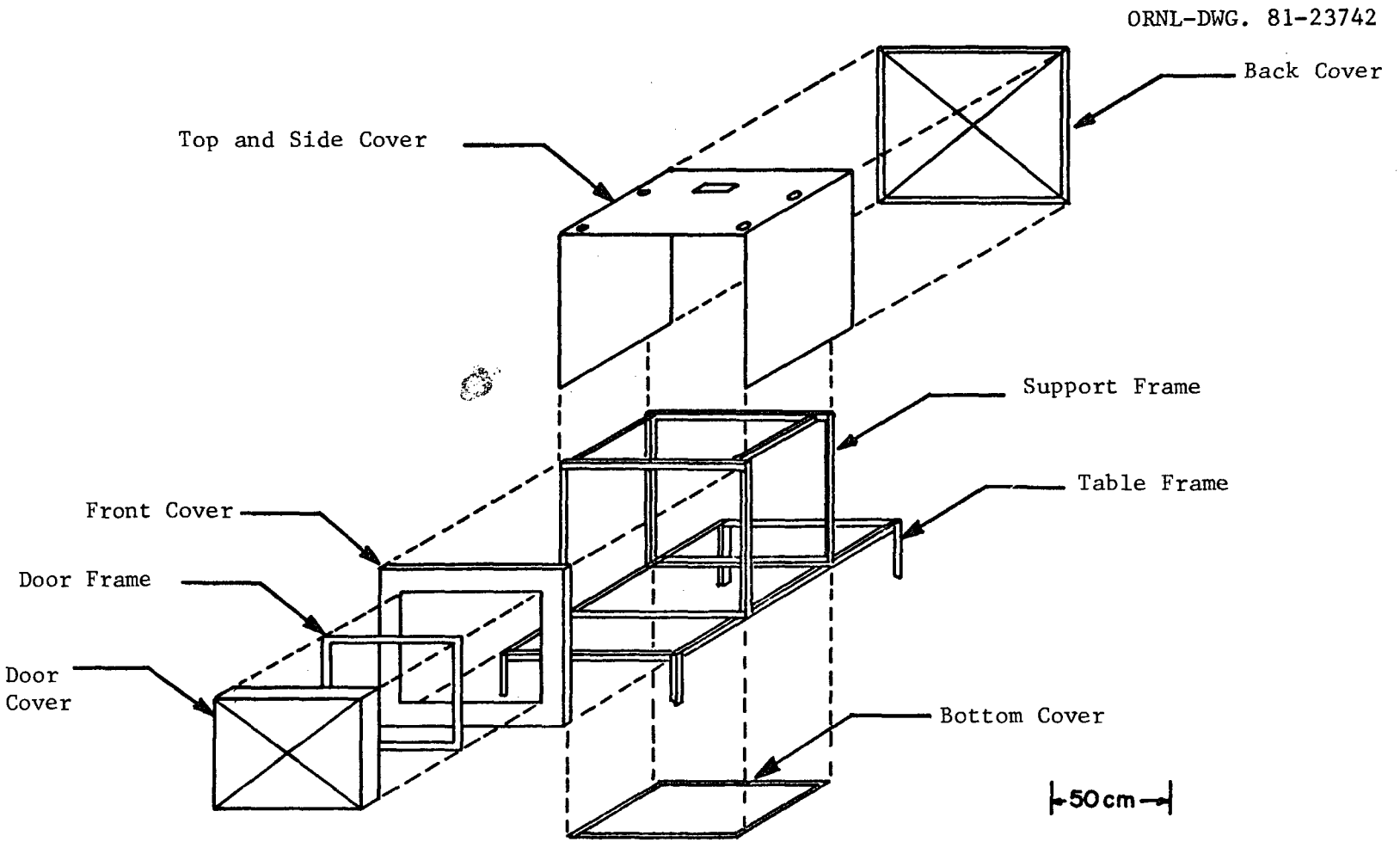

Figure F-2 Expanded Schematic of the Outer Covers and Support Structure

ORNL-DWG. 81-23743

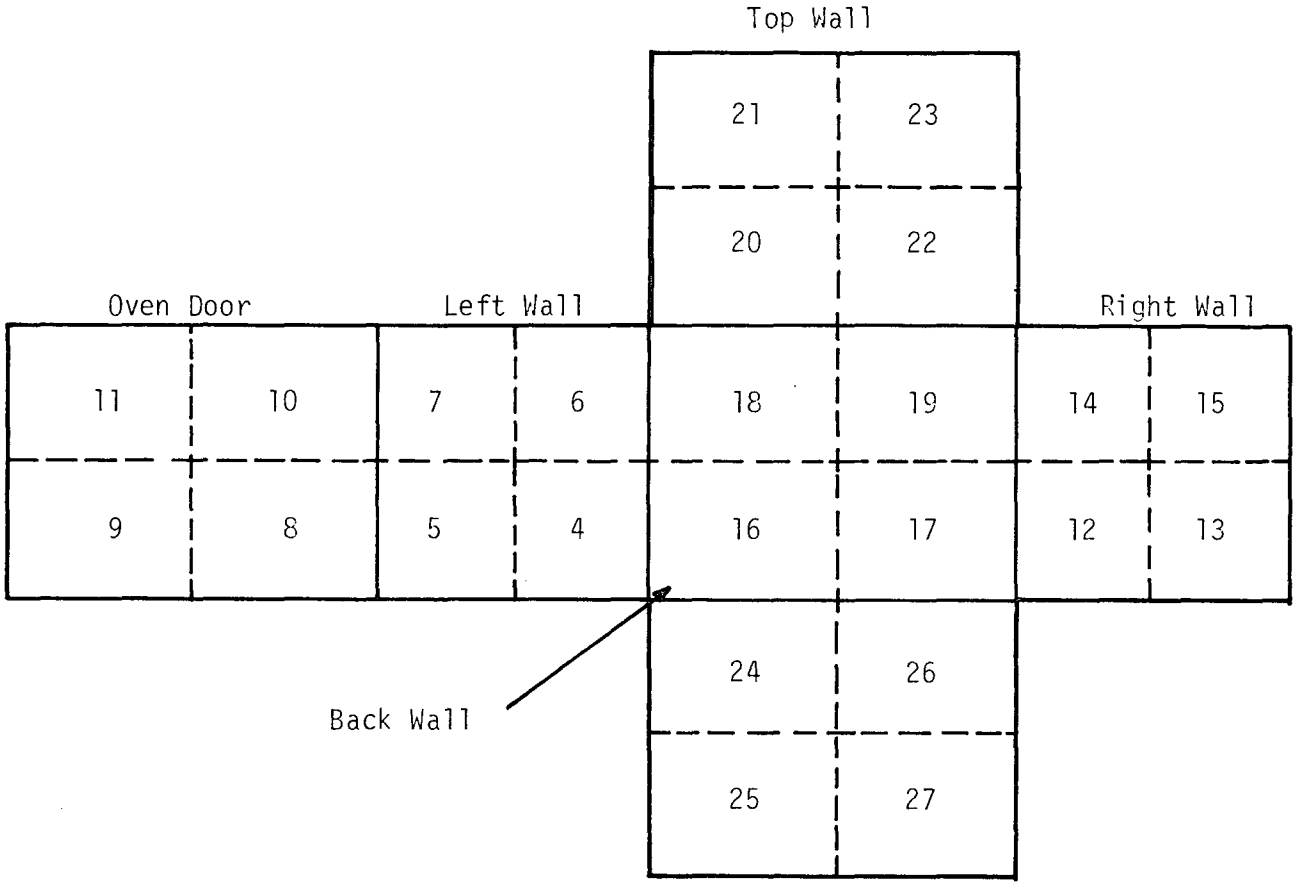

Figure F-3 Location of Inner Cavity Wall Nodal Elements

ORNL-DWG. 81-23744

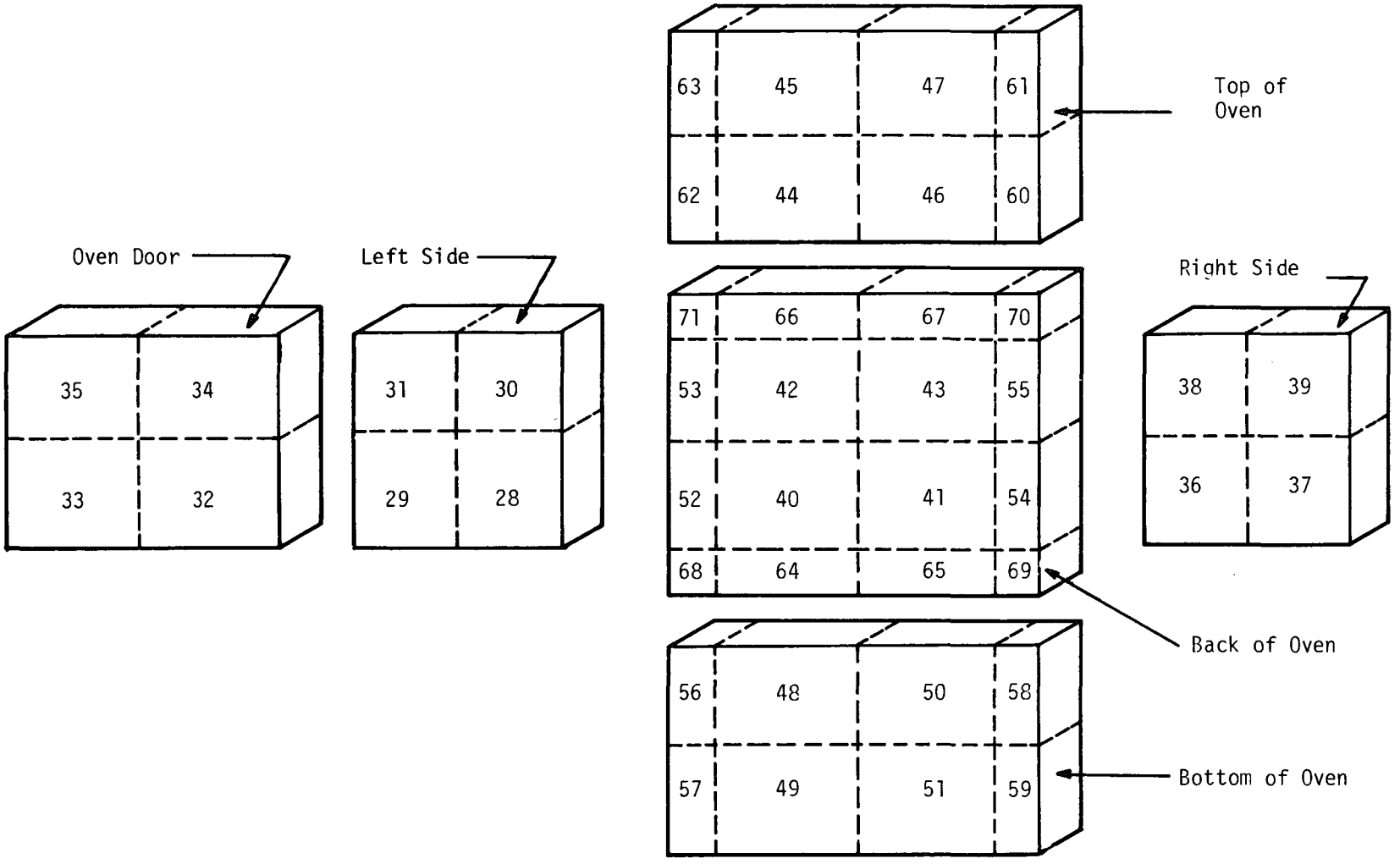

Figure F-4 Location of Insulation Nodal Elements

ORNL-DWG. 81-23745

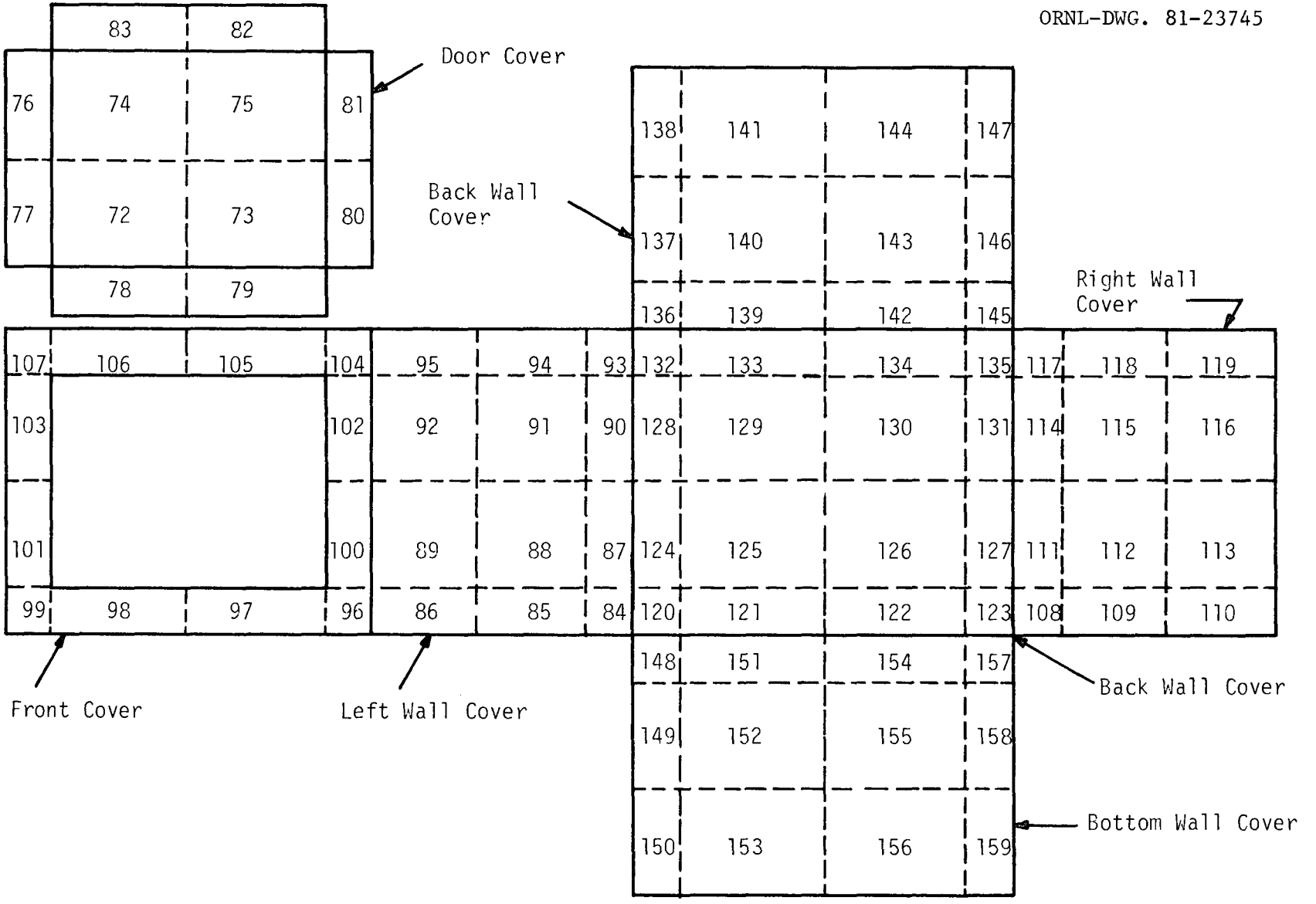

Figure F-5 Location of Exterior Oven Cover Nodal Elements

plings are defined only for radiative exchange from the outer oven cover to the ambient surroundings.

The thermal capacitance for an interior cavity wall node (for example, node 4) is calculated as follows: The walls are made of 2024-T3 aluminum alloy, having a density of 2767 kg/m^3, a specific heat of 921.0 J/kg-K , and a thermal conductivity of 188.9 W/m-K. The wall thickness is 0.63 mm and by employing the information from Table 2.1 the volume of the wall material, not including oven door, is found to be

$$V(\text{walls}) = 7.1734 \times 10^{-4}\ m^3$$

Thus, the total thermal mass of the oven walls is

$$mc_p(\text{walls}) = 1828.1\ J/K$$

Included with the thermal mass of the wall nodal elements are the thermal masses of the four corner members, the front flange, the back flange, and the 16 flange mounts; or 507.6 J/K, 398.5 J/K, 355.5 J/K, and 788.2 J/K, respectively. Thus, the lumped total thermal mass for the cavity walls (not including the oven door) becomes

$$mc_p(\text{walls}) = 3877.9\ J/K$$

This total thermal mass is distributed among the 24 interior cavity wall nodal elements depending on their percent of the total cavity wall volume. For nodal element 4, this becomes

$$mc_p(\text{node 4}) = mc_p(\text{walls})\ \frac{V_{\text{node 4}}}{V_{\text{walls}}}$$

Substituting numerical values into this equation the thermal capacitance

of node 4, CAP(4)--see Table F-3,

$$mc_p(\text{node } 4) = 160 \text{ J/K}$$

The conductive coupling between interior wall nodal elements 4 and 24, is COND (4)(4-24)--see Table F-4, is determined by

$$K_{4-24} = \frac{kA_c}{l_{ij}} = \frac{[188.9\text{W/m-K}] \times [0.00063 \times 0.218\text{m}^2]}{[0.108 + 0.145]\text{m}} = 0.102 \text{ W/K}$$

where l_{ij} is the distance separating the centers of the two nodes.

The convective coupling between interior wall nodal element 4 and the cavity air nodal element 160, COND (373)(4-160)--see Table F-4, is found from

$$K_{4-160} = hA = [5 \text{ W/m}^2\text{-K}] \times [0.215 \times 0.215\text{m}^2] = 0.233 \text{ W/K}$$

The value of the heat transfer coefficient for all surfaces (block, interior and exterior) was assumed to be $5\text{W/m}^2\text{-K}$, a value which is consistent with appropriate convection correlations and heat flux gage measurements. A sensitivity analysis showed that for values in the range 4 to 6 $\text{W/m}^2\text{K}$ the efficiency changed by 0.5% units.

Finally, a radiative coupling between exterior cover node 88 and the ambient surroundings (room external to oven) node 162 is given by

$$R_{88-162} = A_{88} \quad 88-162$$

where F is the total exchange factor between nodes 88 and 162. For two gray surfaces exchanging radiation only with each other, F can be written as

$$F_{1-2} = \left[\frac{1-\varepsilon_1}{A_1\varepsilon_1} + \frac{1}{A_1F_{1-2}} + \frac{1-\varepsilon_2}{A_2\varepsilon_2}\right]^{-1}$$

For a small body A_1 completely enclosed by a larger area A_2, $F_{1-2}=1$ and $A_2 >> A_1$, then F_{1-2} becomes

$$F_{1-2} = \left[\frac{1-\varepsilon_1}{\varepsilon_1} + 1\right]^{-1} = \varepsilon_1$$

Therefore, the radiation link between nodes 88 and 162, RAD (65)(88-162)--see Table F-5, is

$$R_{88-162} = A_{88}\varepsilon_{88} = [0.125 \times 0.215m^2] \times 0.91 = 0.0424m^2$$

Note that radiation coupling terms are expressed in units of area (m^2) for the program while the other coupling terms have conductance units (W/K).

F.3 Data Listing for the Nodal Elements

The nodal element input data to Program AGTAP are listed on the following tables which are generated as an output listing by the program. Table F-2 provides summary details of the nodal system and the initial temperature (K) of the nodes. The thermal capacitances CAP (Node), [J/K], of the 161 nodes are listed in Table F-3. The conductive and convective coupling terms, referred to as K_{m-n} above, are listed in Table F-4 expressed as COND (p)(m-n), [W/K], where p varies from 1 to 541, the total number of terms used in the analysis. The radiative coupling terms, referred to as R_{m-n} above, are listed in Table F-5 expressed as RAD(p)(m-n), [m^2], where the maximum value of p is 88. Initial heat fluxes can be prescribed, which for the present analysis

are assumed to be zero as shown on the table. Table F-6 lists the relevant temperature dependent thermal properties where the temperature units are kelvins and the units of the thermal mass and thermal conductivity are [J/K] and [W/m-K], respectively.

Table F-2 Nodal System Initial Temperatures - Program AGTAP

```
NUMBER OF ITERATED NODES    =   161                    TIME  =          0
NUMBER OF BOUNDARY NODES    =     1                   DTIME =5.0000E+00
NUMBER OF CONDUCTION LINKS  =   541                   FTIME =1.0000E+05
NUMBER OF RADIATION LINKS   =    88
NUMBER OF HEAT SOURCE SINKS=     31
OUTPUT INTERVAL COUNT       =   360
NODE SORT SUPPRESS CODE     =     0
INITIAL TEMPERATURES OF ITERATED NODES
  T(  1) =2.9700E+02  T(  2) =2.9700E+02  T(  3) =2.9645E+02  T(  4) =2.9645E+02  T(  5) =2.9645E+02
  T(  6) =2.9645E+02  T(  7) =2.9645E+02  T(  8) =2.9645E+02  T(  9) =2.9645E+02  T( 10) =2.9645E+02
  T( 11) =2.9645E+02  T( 12) =2.9645E+02  T( 13) =2.9645E+02  T( 14) =2.9645E+02  T( 15) =2.9645E+02
  T( 16) =2.9645E+02  T( 17) =2.9645E+02  T( 18) =2.9645E+02  T( 19) =2.9645E+02  T( 20) =2.9645E+02
  T( 21) =2.9645E+02  T( 22) =2.9645E+02  T( 23) =2.9645E+02  T( 24) =2.9645E+02  T( 25) =2.9645E+02
  T( 26) =2.9645E+02  T( 27) =2.9645E+02  T( 28) =2.9645E+02  T( 29) =2.9645E+02  T( 30) =2.9645E+02
  T( 31) =2.9645E+02  T( 32) =2.9645E+02  T( 33) =2.9645E+02  T( 34) =2.9645E+02  T( 35) =2.9645E+02
  T( 36) =2.9645E+02  T( 37) =2.9645E+02  T( 38) =2.9645E+02  T( 39) =2.9645E+02  T( 40) =2.9645E+02
  T( 41) =2.9645E+02  T( 42) =2.9645E+02  T( 43) =2.9645E+02  T( 44) =2.9645E+02  T( 45) =2.9645E+02
  T( 46) =2.9645E+02  T( 47) =2.9645E+02  T( 48) =2.9645E+02  T( 49) =2.9645E+02  T( 50) =2.9645E+02
  T( 51) =2.9645E+02  T( 52) =2.9645E+02  T( 53) =2.9645E+02  T( 54) =2.9645E+02  T( 55) =2.9645E+02
  T( 56) =2.9645E+02  T( 57) =2.9645E+02  T( 58) =2.9645E+02  T( 59) =2.9645E+02  T( 60) =2.9645E+02
  T( 61) =2.9645E+02  T( 62) =2.9645E+02  T( 63) =2.9645E+02  T( 64) =2.9645E+02  T( 65) =2.9645E+02
  T( 66) =2.9645E+02  T( 67) =2.9645E+02  T( 68) =2.9645E+02  T( 69) =2.9645E+02  T( 70) =2.9645E+02
  T( 71) =2.9645E+02  T( 72) =2.9645E+02  T( 73) =2.9645E+02  T( 74) =2.9645E+02  T( 75) =2.9645E+02
  T( 76) =2.9645E+02  T( 77) =2.9645E+02  T( 78) =2.9645E+02  T( 79) =2.9645E+02  T( 80) =2.9645E+02
  T( 81) =2.9645E+02  T( 82) =2.9645E+02  T( 83) =2.9645E+02  T( 84) =2.9645E+02  T( 85) =2.9645E+02
  T( 86) =2.9645E+02  T( 87) =2.9645E+02  T( 88) =2.9645E+02  T( 89) =2.9645E+02  T( 90) =2.9645E+02
  T( 91) =2.9645E+02  T( 92) =2.9645E+02  T( 93) =2.9645E+02  T( 94) =2.9645E+02  T( 95) =2.9645E+02
  T( 96) =2.9645E+02  T( 97) =2.9645E+02  T( 98) =2.9645E+02  T( 99) =2.9645E+02  T(100) =2.9645E+02
  T(101) =2.9645E+02  T(102) =2.9645E+02  T(103) =2.9645E+02  T(104) =2.9645E+02  T(105) =2.9645E+02
  T(106) =2.9645E+02  T(107) =2.9645E+02  T(108) =2.9645E+02  T(109) =2.9645E+02  T(110) =2.9645E+02
  T(111) =2.9645E+02  T(112) =2.9645E+02  T(113) =2.9645E+02  T(114) =2.9645E+02  T(115) =2.9645E+02
  T(116) =2.9645E+02  T(117) =2.9645E+02  T(118) =2.9645E+02  T(119) =2.9645E+02  T(120) =2.9645E+02
  T(121) =2.9645E+02  T(122) =2.9645E+02  T(123) =2.9645E+02  T(124) =2.9645E+02  T(125) =2.9645E+02
  T(126) =2.9645E+02  T(127) =2.9645E+02  T(128) =2.9645E+02  T(129) =2.9645E+02  T(130) =2.9645E+02
  T(131) =2.9645E+02  T(132) =2.9645E+02  T(133) =2.9645E+02  T(134) =2.9645E+02  T(135) =2.9645E+02
  T(136) =2.9645E+02  T(137) =2.9645E+02  T(138) =2.9645E+02  T(139) =2.9645E+02  T(140) =2.9645E+02
  T(141) =2.9645E+02  T(142) =2.9645E+02  T(143) =2.9645E+02  T(144) =2.9645E+02  T(145) =2.9645E+02
  T(146) =2.9645E+02  T(147) =2.9645E+02  T(148) =2.9645E+02  T(149) =2.9645E+02  T(150) =2.9645E+02
  T(151) =2.9645E+02  T(152) =2.9645E+02  T(153) =2.9645E+02  T(154) =2.9645E+02  T(155) =2.9645E+02
  T(156) =2.9645E+02  T(157) =2.9645E+02  T(158) =2.9645E+02  T(159) =2.9645E+02  T(160) =2.9645E+02
  T(161) =2.9645E+02  T(
INITIAL TEMPERATURES OF BOUNDARY NODES
  T(162) =2.9645E+02  T(
```

Table F-3 Nodal System Thermal Capacitances - Program AGTAP Input

INITIAL THERMAL CAPACITANCES OF ITERATED NODES

CAP(1) =1.6400E+02	CAP(2) =1.6400E+02	CAP(3) =3.7368E+03	CAP(4) =1.6001E+02
CAP(5) =1.6001E+02	CAP(6) =1.6001E+02	CAP(7) =1.6001E+02	CAP(8) =2.9766E+02
CAP(9) =2.9766E+02	CAP(10) =2.9766E+02	CAP(11) =2.9766E+02	CAP(12) =1.6001E+02
CAP(13) =1.6001E+02	CAP(14) =1.6001E+02	CAP(15) =1.6001E+02	CAP(16) =2.1649E+02
CAP(17) =2.1649E+02	CAP(18) =2.1649E+02	CAP(19) =2.1649E+02	CAP(20) =2.1649E+02
CAP(21) =2.1649E+02	CAP(22) =2.1649E+02	CAP(23) =2.1649E+02	CAP(24) =2.1649E+02
CAP(25) =2.1649E+02	CAP(26) =2.1649E+02	CAP(27) =2.1649E+02	CAP(28) =4.7453E+01
CAP(29) =4.7453E+01	CAP(30) =4.7453E+01	CAP(31) =4.7453E+01	CAP(32) =6.4202E+01
CAP(33) =6.4202E+01	CAP(34) =6.4202E+01	CAP(35) =6.4202E+01	CAP(36) =4.7453E+01
CAP(37) =4.7453E+01	CAP(38) =4.7453E+01	CAP(39) =4.7453E+01	CAP(40) =6.4202E+01
CAP(41) =6.4202E+01	CAP(42) =6.4202E+01	CAP(43) =6.4202E+01	CAP(44) =6.4202E+01
CAP(45) =6.4202E+01	CAP(46) =6.4202E+01	CAP(47) =6.4202E+01	CAP(48) =6.4202E+01
CAP(49) =6.4202E+01	CAP(50) =6.4202E+01	CAP(51) =6.4202E+01	CAP(52) =2.2331E+01
CAP(53) =2.2331E+01	CAP(54) =2.2331E+01	CAP(55) =2.2331E+01	CAP(56) =2.2331E+01
CAP(57) =2.2331E+01	CAP(58) =2.2331E+01	CAP(59) =2.2331E+01	CAP(60) =2.2331E+01
CAP(61) =2.2331E+01	CAP(62) =2.2331E+01	CAP(63) =2.2331E+01	CAP(64) =3.0213E+01
CAP(65) =3.0213E+01	CAP(66) =3.0213E+01	CAP(67) =3.0213E+01	CAP(68) =1.0509E+01
CAP(69) =1.0509E+01	CAP(70) =1.0509E+01	CAP(71) =1.0509E+01	CAP(72) =2.6147E+02
CAP(73) =2.6147E+02	CAP(74) =2.6147E+02	CAP(75) =2.6147E+02	CAP(76) =9.0945E+01
CAP(77) =9.0945E+01	CAP(78) =1.2304E+02	CAP(79) =1.2304E+02	CAP(80) =9.0945E+01
CAP(81) =9.0945E+01	CAP(82) =1.2304E+02	CAP(83) =1.2304E+02	CAP(84) =4.2112E+01
CAP(85) =8.9488E+01	CAP(86) =8.9488E+01	CAP(87) =8.9488E+01	CAP(88) =1.9016E+02
CAP(89) =1.9016E+02	CAP(90) =8.9488E+01	CAP(91) =1.9016E+02	CAP(92) =1.9016E+02
CAP(93) =4.2112E+01	CAP(94) =8.9488E+01	CAP(95) =8.9488E+01	CAP(96) =4.2112E+01
CAP(97) =1.2107E+02	CAP(98) =1.2107E+02	CAP(99) =4.2112E+01	CAP(100) =8.9488E+01
CAP(101) =8.9488E+01	CAP(102) =8.9488E+01	CAP(103) =8.9488E+01	CAP(104) =4.2112E+01
CAP(105) =1.2107E+02	CAP(106) =1.2107E+02	CAP(107) =4.2112E+01	CAP(108) =4.2112E+01
CAP(109) =8.9488E+01	CAP(110) =8.9488E+01	CAP(111) =8.9488E+01	CAP(112) =1.9016E+02
CAP(113) =1.9016E+02	CAP(114) =8.9488E+01	CAP(115) =1.9016E+02	CAP(116) =1.9016E+02
CAP(117) =4.2112E+01	CAP(118) =8.9488E+01	CAP(119) =8.9488E+01	CAP(120) =4.2112E+01
CAP(121) =1.2107E+02	CAP(122) =1.2107E+02	CAP(123) =4.2112E+01	CAP(124) =8.9488E+01
CAP(125) =2.5728E+02	CAP(126) =2.5728E+02	CAP(127) =8.9488E+01	CAP(128) =8.9488E+01
CAP(129) =2.5728E+02	CAP(130) =2.5728E+02	CAP(131) =8.9488E+01	CAP(132) =4.2112E+01
CAP(133) =1.2107E+02	CAP(134) =1.2107E+02	CAP(135) =4.2112E+01	CAP(136) =4.2112E+01
CAP(137) =8.9488E+01	CAP(138) =8.9488E+01	CAP(139) =1.2107E+02	CAP(140) =2.5728E+02
CAP(141) =2.5728E+02	CAP(142) =1.2107E+02	CAP(143) =2.5728E+02	CAP(144) =2.5728E+02
CAP(145) =4.2112E+01	CAP(146) =8.9488E+01	CAP(147) =8.9488E+01	CAP(148) =4.2112E+01
CAP(149) =8.9488E+01	CAP(150) =8.9488E+01	CAP(151) =1.2107E+02	CAP(152) =2.5728E+02
CAP(153) =2.5728E+02	CAP(154) =1.2107E+02	CAP(155) =2.5728E+02	CAP(156) =2.5728E+02
CAP(157) =4.2112E+01	CAP(158) =8.9488E+01	CAP(159) =8.9488E+01	CAP(160) =3.2800E+02
CAP(161) =3.2800E+02	CAP(		

Table F-4 Nodal System Conductance Terms - Program AGTAP

INITIAL CONDUCTANCES

COND(1)(4- 5) =1.1995E-01	COND(2)(4- 6) =1.1995E-01	COND(3)(4- 16) =1.0196E-01
COND(4)(4- 24) =1.0196E-01	COND(5)(5- 7) =1.1995E-01	COND(6)(5- 8) =1.0196E-01
COND(7)(5- 25) =1.0196E-01	COND(8)(6- 7) =1.1995E-01	COND(9)(6- 18) =1.0196E-01
COND(10)(6- 20) =1.0196E-01	COND(11)(7- 10) =1.0196E-01	COND(12)(7- 21) =1.0196E-01
COND(13)(8- 9) =8.8660E-02	COND(14)(8- 10) =1.6229E-01	COND(15)(8- 25) =1.6229E-01
COND(16)(9- 11) =1.6229E-01	COND(17)(9- 13) =1.0196E-01	COND(18)(9- 27) =1.6229E-01
COND(19)(10- 11) =8.8660E-02	COND(20)(10- 21) =1.6229E-01	COND(21)(11- 15) =1.0196E-01
COND(22)(11- 23) =1.6229E-01	COND(23)(12- 13) =1.1995E-01	COND(24)(12- 14) =1.1995E-01
COND(25)(12- 17) =1.0196E-01	COND(26)(12- 26) =1.0196E-01	COND(27)(13- 15) =1.1995E-01
COND(28)(13- 27) =1.0196E-01	COND(29)(14- 15) =1.1995E-01	COND(30)(14- 19) =1.0196E-01
COND(31)(14- 22) =1.0196E-01	COND(32)(15- 23) =1.0196E-01	COND(33)(16- 17) =8.8660E-02
COND(34)(16- 18) =1.6229E-01	COND(35)(16- 24) =1.6229E-01	COND(36)(17- 19) =1.6229E-01
COND(37)(17- 26) =1.6229E-01	COND(38)(18- 19) =8.8660E-02	COND(39)(18- 20) =1.6229E-01
COND(40)(19- 22) =1.6229E-01	COND(41)(20- 21) =1.6229E-01	COND(42)(20- 22) =8.8660E-02
COND(43)(21- 23) =8.8660E-02	COND(44)(22- 23) =1.6229E-01	COND(45)(28- 29) =4.3688E-03
COND(46)(28- 30) =4.3688E-03	COND(47)(29- 31) =4.3688E-03	COND(48)(30- 31) =4.3688E-03
COND(49)(32- 33) =3.2291E-03	COND(50)(32- 34) =5.9107E-03	COND(51)(33- 35) =5.9107E-03
COND(52)(34- 35) =3.2291E-03	COND(53)(36- 37) =4.3688E-03	COND(54)(36- 38) =4.3688E-03
COND(55)(37- 39) =4.3688E-03	COND(56)(38- 39) =4.3688E-03	COND(57)(40- 41) =3.2291E-03
COND(58)(40- 42) =5.9107E-03	COND(59)(41- 43) =5.9107E-03	COND(60)(42- 43) =3.2291E-03
COND(61)(44- 45) =5.9107E-03	COND(62)(44- 46) =3.2291E-03	COND(63)(45- 47) =3.2291E-03
COND(64)(46- 47) =5.9107E-03	COND(65)(48- 49) =5.9107E-03	COND(66)(48- 50) =3.2291E-03
COND(67)(49- 51) =3.2291E-03	COND(68)(50- 51) =5.9107E-03	COND(69)(52- 53) =2.0559E-03
COND(70)(54- 55) =2.0559E-03	COND(71)(56- 57) =2.0559E-03	COND(72)(58- 59) =2.0559E-03
COND(73)(60- 61) =2.0559E-03	COND(74)(62- 63) =2.0559E-03	COND(75)(64- 65) =1.5196E-03
COND(76)(66- 67) =1.5196E-03	COND(77)(28- 52) =5.9416E-03	COND(78)(28- 56) =5.9416E-03
COND(79)(29- 57) =5.9416E-03	COND(80)(30- 53) =5.9416E-03	COND(81)(30- 62) =5.9416E-03
COND(82)(31- 63) =5.9416E-03	COND(83)(36- 54) =5.9416E-03	COND(84)(36- 58) =5.9416E-03
COND(85)(37- 59) =5.9416E-03	COND(86)(38- 55) =5.9416E-03	COND(87)(38- 60) =5.9416E-03
COND(88)(39- 61) =5.9416E-03	COND(89)(40- 64) =8.0386E-03	COND(90)(41- 65) =8.0386E-03
COND(91)(42- 66) =8.0386E-03	COND(92)(43- 67) =8.0386E-03	COND(93)(44- 68) =8.0386E-03
COND(94)(46- 67) =8.0386E-03	COND(95)(48- 64) =8.0386E-03	COND(96)(50- 65) =8.0386E-03
COND(97)(40- 52) =4.7916E-03	COND(98)(41- 54) =4.7916E-03	COND(99)(42- 53) =4.7916E-03
COND(100)(43- 55) =4.7916E-03	COND(101)(44- 62) =4.7916E-03	COND(102)(45- 63) =4.7916E-03
COND(103)(46- 60) =4.7916E-03	COND(104)(47- 61) =4.7916E-03	COND(105)(48- 56) =4.7916E-03
COND(106)(49- 57) =4.7916E-03	COND(107)(50- 58) =4.7916E-03	COND(108)(51- 59) =4.7916E-03
COND(109)(52- 68) =2.7960E-03	COND(110)(53- 71) =2.7960E-03	COND(111)(54- 69) =2.7960E-03
COND(112)(55- 70) =2.7960E-03	COND(113)(56- 68) =2.7960E-03	COND(114)(58- 69) =2.7960E-03
COND(115)(60- 70) =2.7960E-03	COND(116)(62- 71) =2.7960E-03	COND(117)(64- 68) =2.2549E-03
COND(118)(65- 69) =2.2549E-03	COND(119)(66- 71) =2.2549E-03	COND(120)(67- 70) =2.2549E-03
COND(121)(28- 88) =3.9456E-02	COND(122)(29- 89) =3.9456E-02	COND(123)(30- 91) =3.9456E-02
COND(124)(31- 92) =3.9456E-02	COND(125)(32- 72) =5.3381E-02	COND(126)(33- 73) =5.3381E-02
COND(127)(34- 74) =5.3381E-02	COND(128)(35- 75) =5.3381E-02	COND(129)(36-112) =3.9456E-02
COND(130)(37-113) =3.9456E-02	COND(131)(38-115) =3.9456E-02	COND(132)(39-116) =3.9456E-02

Table F-4 Nodal System Conductance Terms - Program AGTAP (Continued)

```
COND( 133)( 40-125) =5.3381E-02
COND( 136)( 43-130) =5.3381E-02
COND( 139)( 46-143) =5.3381E-02
COND( 142)( 49-153) =5.3381E-02
COND( 145)( 52- 84) =1.8567E-02
COND( 148)( 53-128) =1.8567E-02
COND( 151)( 55-115) =1.8567E-02
COND( 154)( 56-149) =1.8567E-02
COND( 157)( 58-109) =1.8567E-02
COND( 160)( 59-159) =1.8567E-02
COND( 163)( 61-119) =1.8567E-02
COND( 166)( 62-137) =1.8567E-02
COND( 169)( 64-121) =2.5121E-02
COND( 172)( 65-154) =2.5121E-02
COND( 175)( 67-134) =2.5121E-02
COND( 178)( 68-120) =8.7376E-03
COND( 181)( 69-123) =8.7376E-03
COND( 184)( 70-135) =8.7376E-03
COND( 187)( 71-132) =8.7376E-03
COND( 190)( 31-102) =8.7376E-03
COND( 193)( 45-105) =1.1821E-02
COND( 196)( 51- 93) =1.1821E-02
COND( 199)( 61-107) =4.7916E-05
COND( 202)( 72- 74) =2.3547E-01
COND( 205)( 88- 89) =1.7404E-01
COND( 208)( 91- 92) =1.7404E-01
COND( 211)(113-116) =1.7404E-01
COND( 214)(125-129) =2.3547E-01
COND( 217)(140-141) =2.3547E-01
COND( 220)(143-144) =2.3547E-01
COND( 223)(153-156) =1.2864E-01
COND( 226)( 73- 79) =3.2024E-01
COND( 229)( 88- 85) =2.3670E-01
COND( 232)( 88-100) =2.3670E-01
COND( 235)( 92- 95) =2.3670E-01
COND( 238)(112-111) =2.3670E-01
COND( 241)(115-114) =2.3670E-01
COND( 244)(116-103) =2.3670E-01
COND( 247)(129-133) =3.2024E-01
COND( 250)(141-105) =3.2024E-01
COND( 253)(152-151) =3.2024E-01
COND( 256)(156- 98) =3.2024E-01
COND( 259)( 74- 76) =1.9088E-01
COND( 262)(126-127) =1.9088E-01
COND( 265)(140-137) =1.9088E-01
COND( 268)(144-147) =1.9088E-01
COND( 271)(155-158) =1.9088E-01
```

```
COND( 134)( 41-126) =5.3381E-02
COND( 137)( 44-140) =5.3381E-02
COND( 140)( 47-144) =5.3381E-02
COND( 143)( 50-155) =5.3381E-02
COND( 146)( 52-124) =1.8567E-02
COND( 149)( 54-111) =1.8567E-02
COND( 152)( 55-131) =1.8567E-02
COND( 155)( 57- 86) =1.8567E-02
COND( 158)( 58-158) =1.8567E-02
COND( 161)( 60-118) =1.8567E-02
COND( 164)( 61-147) =1.8567E-02
COND( 167)( 63- 95) =1.8567E-02
COND( 170)( 64-151) =2.5121E-02
COND( 173)( 66-133) =2.5121E-02
COND( 176)( 67-142) =2.5121E-02
COND( 179)( 68-148) =8.7376E-03
COND( 182)( 69-157) =8.7376E-03
COND( 185)( 70-145) =8.7376E-03
COND( 188)( 71-136) =8.7376E-03
COND( 191)( 37-101) =8.7376E-03
COND( 194)( 47-106) =1.1821E-02
COND( 197)( 57- 96) =4.7916E-05
COND( 200)( 63-104) =4.7916E-05
COND( 203)( 73- 75) =2.3547E-01
COND( 206)( 88- 91) =1.7404E-01
COND( 209)(112-113) =1.7404E-01
COND( 212)(115-116) =1.7404E-01
COND( 215)(126-130) =1.2864E-01
COND( 218)(140-143) =1.2864E-01
COND( 221)(152-153) =1.2864E-01
COND( 224)(155-156) =2.3547E-01
COND( 227)( 74- 83) =3.2024E-01
COND( 230)( 88- 87) =2.3670E-01
COND( 233)( 91- 90) =2.3670E-01
COND( 236)( 92-102) =2.3670E-01
COND( 239)(113-110) =2.3670E-01
COND( 242)(115-118) =2.3670E-01
COND( 245)(125-121) =3.2024E-01
COND( 248)(130-134) =3.2024E-01
COND( 251)(143-142) =3.2024E-01
COND( 254)(153- 97) =3.2024E-01
COND( 257)( 72- 77) =1.9088E-01
COND( 260)( 75- 81) =1.9088E-01
COND( 263)(129-128) =1.9088E-01
COND( 266)(141-133) =1.9088E-01
COND( 269)(152-149) =1.9088E-01
COND( 272)(156-159) =1.9088E-01
```

```
COND( 135)( 42-129) =5.3381E-02
COND( 138)( 45-141) =5.3381E-02
COND( 141)( 48-152) =5.3381E-02
COND( 144)( 51-156) =5.3381E-02
COND( 147)( 53- 90) =1.8567E-02
COND( 150)( 54-127) =1.8567E-02
COND( 153)( 56- 85) =1.8567E-02
COND( 156)( 57-150) =1.8567E-02
COND( 159)( 59-110) =1.8567E-02
COND( 162)( 60-149) =1.8567E-02
COND( 165)( 62- 94) =1.8567E-02
COND( 168)( 63-138) =1.8567E-02
COND( 171)( 65-122) =2.5121E-02
COND( 174)( 66-139) =2.5121E-02
COND( 177)( 68- 84) =8.7376E-03
COND( 180)( 69-108) =8.7376E-03
COND( 183)( 70-117) =8.7376E-03
COND( 186)( 71- 93) =8.7376E-03
COND( 189)( 29-100) =8.7376E-03
COND( 192)( 39-103) =8.7376E-03
COND( 195)( 48- 97) =1.1821E-02
COND( 198)( 59- 99) =4.7916E-05
COND( 201)( 72- 73) =1.2864E-01
COND( 204)( 74- 75) =1.2864E-01
COND( 207)( 89- 92) =1.7404E-01
COND( 210)(112-115) =1.7404E-01
COND( 213)(125-126) =1.2864E-01
COND( 216)(129-130) =2.3547E-01
COND( 219)(141-144) =1.2864E-01
COND( 222)(152-155) =1.2864E-01
COND( 225)( 72- 78) =3.2024E-01
COND( 228)( 75- 82) =3.2024E-01
COND( 231)( 89- 86) =2.3670E-01
COND( 234)( 91- 94) =2.3670E-01
COND( 237)(112-109) =2.3670E-01
COND( 240)(113-101) =2.3670E-01
COND( 243)(116-119) =2.3670E-01
COND( 246)(126-122) =3.2024E-01
COND( 249)(140-139) =3.2024E-01
COND( 252)(144-106) =3.2024E-01
COND( 255)(155-154) =3.2024E-01
COND( 258)( 73- 80) =1.9088E-01
COND( 261)(125-124) =1.9088E-01
COND( 264)(130-131) =1.9088E-01
COND( 267)(143-146) =1.9088E-01
COND( 270)(153-150) =1.9088E-01
COND( 273)( 76- 77) =3.8177E-03
```

Table F-4 Nodal System Conductance Terms - Program AGTAP (Continued)

```
COND( 274)( 76- 83) =4.4914E-03   COND( 275)( 77- 78) =4.4914E-03   COND( 276)( 78- 79) =5.1651E-03
COND( 277)( 79- 80) =4.4914E-03   COND( 278)( 80- 81) =3.8177E-03   COND( 279)( 81- 82) =4.4914E-03
COND( 280)( 82- 83) =5.1651E-03   COND( 281)( 85- 86) =3.8177E-03   COND( 282)( 87- 90) =3.8177E-03
COND( 283)( 94- 95) =3.8177E-03   COND( 284)( 97- 98) =5.1651E-03   COND( 285)(100-102) =3.8177E-03
COND( 286)(101-103) =3.8177E-03   COND( 287)(105-106) =5.1651E-03   COND( 288)(109-110) =3.8177E-03
COND( 289)(111-114) =3.8177E-03   COND( 290)(118-119) =3.8177E-03   COND( 291)(121-122) =5.1651E-03
COND( 292)(124-128) =3.8177E-03   COND( 293)(127-131) =3.8177E-03   COND( 294)(133-134) =5.1651E-03
COND( 295)(137-138) =3.8177E-03   COND( 296)(139-142) =5.1651E-03   COND( 297)(146-147) =3.8177E-03
COND( 298)(149-150) =3.8177E-03   COND( 299)(151-154) =5.1651E-03   COND( 300)(158-159) =5.1651E-03
COND( 301)( 84- 85) =1.1139E+00   COND( 302)( 84- 87) =1.1139E+00   COND( 303)( 86- 96) =1.1139E+00
COND( 304)( 93- 90) =1.1139E+00   COND( 305)( 93- 94) =1.1139E+00   COND( 306)( 95-104) =1.1139E+00
COND( 307)(100- 96) =1.1139E+00   COND( 308)(101- 99) =1.1139E+00   COND( 309)(102-104) =1.1139E+00
COND( 310)(103-107) =1.1139E+00   COND( 311)(108-109) =1.1139E+00   COND( 312)(108-111) =1.1139E+00
COND( 313)(110- 99) =1.1139E+00   COND( 314)(117-114) =1.1139E+00   COND( 315)(117-118) =1.1139E+00
COND( 316)(119-107) =1.1139E+00   COND( 317)(120-124) =1.1139E+00   COND( 318)(123-127) =1.1139E+00
COND( 319)(132-128) =1.1139E+00   COND( 320)(135-131) =1.1139E+00   COND( 321)(136-137) =1.1139E+00
COND( 322)(138-104) =1.1139E+00   COND( 323)(145-146) =1.1139E+00   COND( 324)(147-107) =1.1139E+00
COND( 325)(148-149) =1.1139E+00   COND( 326)(150- 96) =1.1139E+00   COND( 327)(157-158) =1.1139E+00
COND( 328)(159- 99) =1.1139E+00   COND( 329)( 96- 97) =8.9827E-01   COND( 330)( 99- 98) =8.9827E-01
COND( 331)(104-105) =8.9827E-01   COND( 332)(107-106) =8.9827E-01   COND( 333)(120-121) =8.9827E-01
COND( 334)(123-122) =8.9827E-01   COND( 335)(132-133) =8.9827E-01   COND( 336)(135-134) =8.9827E-01
COND( 337)(138-139) =8.9827E-01   COND( 338)(145-142) =8.9827E-01   COND( 339)(148-151) =8.9827E-01
COND( 340)(157-154) =8.9827E-01   COND( 341)( 85-149) =3.6934E-01   COND( 342)( 86-150) =3.6934E-01
COND( 343)( 87-124) =3.6934E-01   COND( 344)( 90-128) =3.6934E-01   COND( 345)( 94-137) =3.6934E-01
COND( 346)( 95-138) =3.6934E-01   COND( 347)(109-158) =3.6934E-01   COND( 348)(110-159) =3.6934E-01
COND( 349)(111-127) =3.6934E-01   COND( 350)(114-131) =3.6934E-01   COND( 351)(118-146) =3.6934E-01
COND( 352)(119-147) =3.6934E-01   COND( 353)(121-151) =5.0037E-01   COND( 354)(122-154) =5.0037E-01
COND( 355)(133-139) =5.0037E-01   COND( 356)(134-142) =5.0037E-01   COND( 357)( 84-120) =1.7404E-01
COND( 358)( 84-148) =1.7404E-01   COND( 359)( 93-132) =1.7404E-01   COND( 360)( 93-136) =1.7404E-01
COND( 361)(108-123) =1.7404E-01   COND( 362)(108-157) =1.7404E-01   COND( 363)(117-135) =1.7404E-01
COND( 364)(117-145) =1.7404E-01   COND( 365)(120-148) =1.7404E-01   COND( 366)(123-157) =1.7404E-01
COND( 367)(132-136) =1.7404E-01   COND( 368)(135-145) =1.7404E-01   COND( 369)(  1-160) =1.0000E+00
COND( 370)(  2-161) =1.0000E+00   COND( 371)(  3-160) =1.5146E-01   COND( 372)(  3-161) =1.5146E-01
COND( 373)(  4-160) =2.3306E-01   COND( 374)(  5-160) =2.3306E-01   COND( 375)(  6-161) =2.3306E-01
COND( 376)(  7-161) =2.3306E-01   COND( 377)(  8-160) =3.1532E-01   COND( 378)(  9-160) =3.1532E-01
COND( 379)( 10-161) =3.1532E-01   COND( 380)( 11-161) =3.1532E-01   COND( 381)( 12-160) =2.3306E-01
COND( 382)( 13-160) =2.3306E-01   COND( 383)( 14-161) =2.3306E-01   COND( 384)( 15-161) =2.3306E-01
COND( 385)( 16-160) =3.1532E-01   COND( 386)( 17-160) =3.1532E-01   COND( 387)( 18-161) =3.1532E-01
COND( 388)( 19-161) =3.1532E-01   COND( 389)( 20-161) =3.1532E-01   COND( 390)( 21-161) =3.1532E-01
COND( 391)( 22-161) =3.1532E-01   COND( 392)( 23-161) =3.1532E-01   COND( 393)( 24-160) =3.1532E-01
COND( 394)( 25-160) =3.1532E-01   COND( 395)( 26-160) =3.1532E-01   COND( 396)( 27-160) =3.1532E-01
COND( 397)( 72-162) =3.7839E-01   COND( 398)( 73-162) =3.7839E-01   COND( 399)( 74-162) =3.7839E-01
COND( 400)( 75-162) =3.7839E-01   COND( 401)( 88-162) =2.7968E-01   COND( 402)( 89-162) =2.7968E-01
COND( 403)( 91-162) =2.7968E-01   COND( 404)( 92-162) =2.7968E-01   COND( 405)(112-162) =2.7968E-01
COND( 406)(113-162) =2.7968E-01   COND( 407)(115-162) =2.7968E-01   COND( 408)(116-162) =2.7968E-01
COND( 409)(125-162) =3.7839E-01   COND( 410)(126-162) =3.7839E-01   COND( 411)(129-162) =3.7839E-01
COND( 412)(130-162) =3.7839E-01   COND( 413)(140-162) =3.7839E-01   COND( 414)(141-162) =3.7839E-01
```

Table F-4 Nodal System Conductance Terms - Program AGTAP (Continued)

```
COND( 415)(143-162) =3.7839E-01
COND( 416)(144-162) =3.7839E-01
COND( 417)(152-162) =3.7839E-01
COND( 418)(153-162) =3.7839E-01
COND( 419)(155-162) =3.7839E-01
COND( 420)(156-162) =3.7839E-01
COND( 421)( 76-162) =1.3161E-01
COND( 422)( 77-162) =1.3161E-01
COND( 423)( 78-162) =1.7806E-01
COND( 424)( 79-162) =1.7806E-01
COND( 425)( 80-162) =1.3161E-01
COND( 426)( 81-162) =1.3161E-01
COND( 427)( 82-162) =1.7806E-01
COND( 428)( 83-162) =1.7806E-01
COND( 429)( 85-162) =1.3161E-01
COND( 430)( 86-162) =1.3161E-01
COND( 431)( 87-162) =1.3161E-01
COND( 432)( 90-162) =1.3161E-01
COND( 433)( 94-162) =1.3161E-01
COND( 434)( 95-162) =1.3161E-01
COND( 435)( 95-162) =1.3161E-01
COND( 436)( 97-162) =1.7806E-01
COND( 437)(100-162) =1.7806E-01
COND( 438)(101-162) =1.3161E-01
COND( 439)(102-162) =1.3161E-01
COND( 440)(103-162) =1.3161E-01
COND( 441)(105-162) =1.7806E-01
COND( 442)(106-162) =1.7806E-01
COND( 443)(109-162) =1.3161E-01
COND( 444)(110-162) =1.3161E-01
COND( 445)(111-162) =1.3161E-01
COND( 446)(114-162) =1.3161E-01
COND( 447)(118-162) =1.3161E-01
COND( 448)(119-162) =1.3161E-01
COND( 449)(121-162) =1.7806E-01
COND( 450)(122-162) =1.7806E-01
COND( 451)(124-162) =1.3161E-01
COND( 452)(127-162) =1.3161E-01
COND( 453)(128-162) =1.3161E-01
COND( 454)(131-162) =1.3161E-01
COND( 455)(133-162) =1.7806E-01
COND( 456)(134-162) =1.7806E-01
COND( 457)(137-162) =1.3161E-01
COND( 458)(138-162) =1.3161E-01
COND( 459)(139-162) =1.7806E-01
COND( 460)(142-162) =1.7806E-01
COND( 461)(146-162) =1.3161E-01
COND( 462)(147-162) =1.3161E-01
COND( 463)(149-162) =1.3161E-01
COND( 464)(150-162) =1.3161E-01
COND( 465)(151-162) =1.7806E-01
COND( 466)(154-162) =1.7806E-01
COND( 467)(158-162) =1.3161E-01
COND( 468)(159-162) =1.3161E-01
COND( 469)( 84-162) =6.1935E-02
COND( 470)( 93-162) =6.1935E-02
COND( 471)( 96-162) =6.1935E-02
COND( 472)( 99-162) =6.1935E-02
COND( 473)(104-162) =6.1935E-02
COND( 474)(107-162) =6.1935E-02
COND( 475)(108-162) =6.1935E-02
COND( 476)(117-162) =6.1935E-02
COND( 477)(120-162) =6.1935E-02
COND( 478)(123-162) =6.1935E-02
COND( 479)(132-162) =6.1935E-02
COND( 480)(135-162) =6.1935E-02
COND( 481)(136-162) =6.1935E-02
COND( 482)(145-162) =6.1935E-02
COND( 483)(148-162) =6.1935E-02
COND( 484)(157-162) =6.1935E-02
COND( 485)(160-161) =1.0000E+00
COND( 486)( 24- 25) =1.6229E-01
COND( 487)( 24- 23) =8.8860E-02
COND( 488)( 25- 27) =8.8860E-02
COND( 489)( 26- 27) =1.6229E-01
COND( 490)(  4- 28) =3.9456E-02
COND( 491)(  5- 29) =3.9456E-02
COND( 492)(  6- 30) =3.9456E-02
COND( 493)(  7- 31) =3.9456E-02
COND( 494)(  8- 32) =5.3381E-02
COND( 495)(  9- 33) =5.3381E-02
COND( 496)( 10- 34) =5.3381E-02
COND( 497)( 11- 35) =5.3381E-02
COND( 498)( 12- 39) =3.9456E-02
COND( 499)( 13- 37) =3.9456E-02
COND( 500)( 14- 38) =3.9456E-02
COND( 501)( 15- 39) =3.9456E-02
COND( 502)( 16- 40) =5.3381E-02
COND( 503)( 17- 41) =5.3381E-02
COND( 504)( 18- 42) =5.3381E-02
COND( 505)( 19- 43) =5.3381E-02
COND( 506)( 20- 44) =5.3381E-02
COND( 507)( 21- 45) =5.3381E-02
COND( 508)( 22- 46) =5.3381E-02
COND( 509)( 23- 47) =5.3381E-02
COND( 510)( 24- 48) =5.3381E-02
COND( 511)( 25- 49) =5.3381E-02
COND( 512)( 26- 50) =5.3381E-02
COND( 513)( 27- 51) =5.3381E-02
COND( 514)(  4- 88) =9.6774E-02
COND( 515)(  5- 89) =9.6774E-02
COND( 516)(  6- 91) =9.6774E-02
COND( 517)(  7- 92) =9.6774E-02
COND( 518)( 12-112) =9.6774E-02
COND( 519)( 13-113) =9.6774E-02
COND( 520)( 14-115) =9.6774E-02
COND( 521)( 15-116) =9.6774E-02
COND( 522)( 16-125) =9.6774E-02
COND( 523)( 17-126) =9.6774E-02
COND( 524)( 18-129) =9.6774E-02
COND( 525)( 19-130) =9.6774E-02
COND( 526)( 20-140) =9.6774E-02
COND( 527)( 21-141) =9.6774E-02
COND( 528)( 22-143) =9.6774E-02
COND( 529)( 23-144) =9.6774E-02
COND( 530)( 24-152) =9.6774E-02
COND( 531)( 25-153) =9.6774E-02
COND( 532)( 26-155) =9.6774E-02
COND( 533)( 27-156) =9.6774E-02
COND( 534)(  8- 78) =2.1855E-01
COND( 535)(  9- 79) =2.1855E-01
COND( 536)( 10- 83) =2.1855E-01
COND( 537)( 11- 82) =2.1855E-01
COND( 538)(  8- 77) =1.3027E-01
COND( 539)(  9- 80) =1.3027E-01
COND( 540)( 10- 76) =1.3027E-01
COND( 541)( 11- 81) =1.3027E-01
COND(
```

Table F-5 Nodal System Radiative Links - Program AGTAP Input

```
INITIAL RADIATION LINKS
 RAD(   1)( 76-162)=1.996100E-02   RAD(   2)( 77-162)=1.996100E-02   RAD(   3)( 80-162)=1.996100E-02   RAD(   4)( 81-162)=1.996100E-
 RAD(   5)( 85-162)=1.996100E-02   RAD(   6)( 86-162)=1.996100E-02   RAD(   7)( 87-162)=1.996100E-02   RAD(   8)( 90-162)=1.996100E-
 RAD(   9)( 94-162)=1.996100E-02   RAD(  10)( 95-162)=1.996100E-02   RAD(  11)(100-162)=1.996100E-02   RAD(  12)(101-162)=1.996100E-
 RAD(  13)(102-162)=1.996100E-02   RAD(  14)(103-162)=1.996100E-02   RAD(  15)(109-162)=1.996100E-02   RAD(  16)(110-162)=1.996100E-
 RAD(  17)(111-162)=1.996100E-02   RAD(  18)(114-162)=1.996100E-02   RAD(  19)(116-162)=1.996100E-02   RAD(  20)(119-162)=1.996100E-
 RAD(  21)(120-162)=1.996100E-02   RAD(  22)(127-162)=1.996100E-02   RAD(  23)(128-162)=1.996100E-02   RAD(  24)(131-162)=1.996100E-
 RAD(  25)(137-162)=1.996100E-02   RAD(  26)(138-162)=1.996100E-02   RAD(  27)(146-162)=1.996100E-02   RAD(  28)(147-162)=1.996100E-
 RAD(  29)(149-162)=1.996100E-02   RAD(  30)(150-162)=1.996100E-02   RAD(  31)(158-162)=1.996100E-02   RAD(  32)(159-162)=1.996100E-
 RAD(  33)( 78-162)=2.700600E-02   RAD(  34)( 79-162)=2.700600E-02   RAD(  35)( 82-162)=2.700600E-02   RAD(  36)( 83-162)=2.700600E-
 RAD(  37)( 97-162)=2.700600E-02   RAD(  38)( 98-162)=2.700600E-02   RAD(  39)(105-162)=2.700600E-02   RAD(  40)(106-162)=2.700600E-
 RAD(  41)(121-162)=2.700600E-02   RAD(  42)(122-162)=2.700600E-02   RAD(  43)(133-162)=2.700600E-02   RAD(  44)(134-162)=2.700600E-
 RAD(  45)(139-162)=2.700600E-02   RAD(  46)(140-162)=2.700600E-02   RAD(  47)(151-162)=2.700600E-02   RAD(  48)(154-162)=2.700600E-
 RAD(  49)( 84-162)=9.333000E-03   RAD(  50)( 93-162)=9.333000E-03   RAD(  51)( 96-162)=9.333000E-03   RAD(  52)( 99-162)=9.333000E-
 RAD(  53)(104-162)=9.333000E-03   RAD(  54)(107-162)=9.333000E-03   RAD(  55)(108-162)=9.333000E-03   RAD(  56)(117-162)=9.333000E-
 RAD(  57)(128-162)=9.333000E-03   RAD(  58)(133-162)=9.333000E-03   RAD(  59)(132-162)=9.333000E-03   RAD(  60)(135-162)=9.333000E-
 RAD(  61)(138-162)=9.333000E-03   RAD(  62)(145-162)=9.333000E-03   RAD(  63)(148-162)=9.333000E-03   RAD(  64)(157-162)=9.333000E-
 RAD(  65)( 88-162)=4.241800E-02   RAD(  66)( 89-162)=4.241800E-02   RAD(  67)( 91-162)=4.241800E-02   RAD(  68)( 92-162)=4.241800E-
 RAD(  69)(112-162)=4.241800E-02   RAD(  70)(113-162)=4.241800E-02   RAD(  71)(115-162)=4.241800E-02   RAD(  72)(119-162)=4.241800E-
 RAD(  73)( 72-162)=5.738900E-02   RAD(  74)( 73-162)=5.738900E-02   RAD(  75)( 74-162)=5.738900E-02   RAD(  76)( 75-162)=5.738900E-
 RAD(  77)(125-162)=5.738900E-02   RAD(  78)(126-162)=5.738900E-02   RAD(  79)(129-162)=5.738900E-02   RAD(  80)(130-162)=5.738900E-
 RAD(  81)(140-162)=5.738900E-02   RAD(  82)(141-162)=5.738900E-02   RAD(  83)(143-162)=5.738900E-02   RAD(  84)(144-162)=5.738900E-
 RAD(  85)(152-162)=5.738900E-02   RAD(  86)(153-162)=5.738900E-02   RAD(  87)(155-162)=5.738900E-02   RAD(  88)(156-162)=5.738900E-
INITIAL HEAT FLOWS
  Q(   1)(   1) =        0   Q(   2)(   2) =        0   Q(   3)(   3) =        0   Q(   4)(   4) =        0
  Q(   5)(   5) =        0   Q(   6)(   6) =        0   Q(   7)(   7) =        0   Q(   8)(   8) =        0
  Q(   9)(   9) =        0   Q(  10)(  10) =        0   Q(  11)(  11) =        0   Q(  12)(  12) =        0
  Q(  13)(  13) =        0   Q(  14)(  14) =        0   Q(  15)(  15) =        0   Q(  16)(  16) =        0
  Q(  17)(  17) =        0   Q(  18)(  18) =        0   Q(  19)(  19) =        0   Q(  20)(  20) =        0
  Q(  21)(  21) =        0   Q(  22)(  22) =        0   Q(  23)(  23) =        0   Q(  24)(  24) =        0

  Q(  25)(  25) =        0   Q(  26)(  26) =        0   Q(  27)(  27) =        0   Q(  28)(  28) =        0
  Q(  29)(  29) =        0   Q(  30)( 100) =        0   Q(  31)( 161) =        0   Q(
```

Table F-6 Temperature Dependent Thermal Properties - Program AGTAP Input

```
1    9    1 THERMAL MASS FOR THE AIR NODES
    250.000 300.000 350.000 400.000 450.000 500.000 550.000 600.000
    650.000
     78.000  65.000  56.000  49.000  44.000  40.000  37.000  34.000
     32.000


2    5    1 THERMAL MASS OF THE RACK (PLAIN CARBON STEEL)
    200.000 300.000 400.000 600.000 800.000
    212.000 242.000 271.000 311.000 381.000


3    5    1 THERMAL MASS OF THE AIR TEMP. PROBES (CARTRIDGE BRASS)
    200.000 300.000 400.000 600.000 800.000
     19.000  20.000  20.000  22.000  24.000


4    5    1 THERMAL MASS FOR THE BLOCK
    200.000 273.000 400.000 600.000 800.000
   3523.0403736.4404108.9204434.8404873.280


5    6    1 THERMAL CONDUCTIVITY FOR THE INSULATION
    270.000 285.000 300.000 310.000 365.000 400.000
       .039    .042    .046    .049    .069    .082
```

BI-RADIANT OVEN

A LOW-ENERGY OVEN SYSTEM

Part 2 — Thermal Performance and Control

BI-RADIANT OVEN

A

LOW ENERGY OVEN SYSTEM

VOLUME III — APPLICATION AND TRANSFER
OF THE TECHNOLOGY

PART 2 - THERMAL PERFORMANCE AND CONTROL

William T. Martin
Dr. D. P. DeWitt

Heat Transfer Laboratory
School of Mechanical Engineering
PURDUE UNIVERSITY
W. Lafayette, Indiana 47907

June 15, 1981

Prepared under Subcontract 86X-0082C for the

OAK RIDGE NATIONAL LABORATORY
Oak Ridge, Tennessee 37830

Operated by

UNION CARBIDE CORPORATION
for the
U.S. DEPARTMENT OF ENERGY
Contract No. W-7405-eng-26

TABLE OF CONTENTS

	Page
LIST OF TABLES	2-v
LIST OF FIGURES	2-vii
NOMENCLATURE	2-xi
ABSTRACT	2-xv
CHAPTER 1 - INTRODUCTION	2-1
CHAPTER 2 - EXPERIMENTAL APPARATUS	2-7
2.1 Experimental Bi-Radiant Oven	2-9
2.2 Instrumentation	2-12
2.2.1 Temperature Measurement	2-12
2.2.2 Mass Loss, Electrical Power, and Heat Flux Measurements	2-17
2.3 Data Acquisition System	2-19
CHAPTER 3 - THERMAL PERFORMANCE OF THE BI-RADIANT OVEN	2-20
3.1 Single-Layer Yellow Cake Measurements	2-20
3.2 Efficiency Measurements	2-37
3.3 Heat Loss Analysis	2-42
3.4 Discussion of Results	2-45
CHAPTER 4 - CONTROL SYSTEM	2-49
4.1 System Variables	2-49
4.2 Methodology	2-51
4.3 Digital Control Algorithm	2-55
4.4 Heat Flux Predictor Algorithm	2-56
4.4.1 Analytical Development	2-56
4.4.2 Experimental Validation	2-58
4.5 Performance Evaluation	2-67
CHAPTER 5 - SUMMARY AND CONCLUSIONS	2-88
LIST OF REFERENCES	2-95

APPENDICES

Appendix A - Instrumentation Details..... 2-99

Appendix B - Cake Formulation..... 2-117

Appendix C - Calculations for Heat Loss Analysis... 2-118

Appendix D - Proportional-Integral Digital Control Algorithm..... 2-125

Appendix E - Derivation of the Heat Flux Predictor Algorithm..... 2-129

LIST OF TABLES

Table		Page
3.1	Overall Cavity Thermal Efficiency, Bi-Radiant Ovens IV-A and IV-B.....	2-38
3.2	Summary of Heat Loss Analysis, Bi-Radiant Oven IV-A, Efficiency Test 940 W.....	2-43
3.3	Summary of Heat Loss Analysis, Bi-Radiant Oven IV-B, Efficiency Test 956 W.....	2-44
4.1	View Factor Matrix for Validation Experiments with the Heat Flux Gage.....	2-60
4.2	Total Exchange Factor Matrix for Validation Experiments with the Heat Flux Gage.....	2-61
4.3	Coefficients of the Heat Flux Predictor Algorithm for Validation Experiments with the Heat Flux Gage.....	2-63
4.4	Coefficients of the Heat Flux Predictor Algorithm for Controller Performance Evaluation.	2-69
Appendix Tables		
A.1	Product Weighing System Calibration Data.....	2-107
A.2	Variation in the Bridge Output Due to Load (500 g) Location on the Oven Rack.....	2-109
C.1	Thermal Mass of Oven Components.....	2-120
C.2	Correlation of the Heat Loss to the Surroundings.	2-122
D.1	Coefficients of the PI Digital Control Algorithm.	2-128

LIST OF FIGURES

Figure		Page
2.1	Photograph of the Experimental Apparatus.....	2-8
2.2	Expanded Schematic of the Outer Covers and Support Structure of Bi-Radiant Oven IV.....	2-10
2.3	Details of the Air Temperature Probe.....	2-13
2.4	Placement of the Heating Element Thermocouples..	2-15
2.5	Photograph Showing the Placement of the Cake Temperature Probes.....	2-16
3.1	Input Power, Single-Layer Yellow Cake, Bi-Radiant Oven IV-A.....	2-22
3.2	Element Temperature Response, Single-Layer Yellow Cake, Bi-Radiant Oven IV-A.....	2-23
3.3	Centerline Air Temperature Response, Single-Layer Yellow Cake, Bi-Radiant Oven IV-A.....	2-25
3.4	Air Temperature Response Adjacent to Side Wall, Single-Layer Yellow Cake, Bi-Radiant Oven IV-A..	2-26
3.5	Average Wall Temperatures, Single-Layer Yellow Cake, Bi-Radiant Oven IV-A.....	2-27
3.6	Cake Temperature Response, Single-Layer Yellow Cake, Bi-Radiant Oven IV-A.....	2-28
3.7	Cake Mass Loss, Single-Layer Yellow Cake, Bi-Radiant Oven IV-A.....	2-29
3.8	Element Temperature Response, Single-Layer Yellow Cake, Bi-Radiant Oven IV-B.....	2-31
3.9	Centerline Air Temperature Response, Single-Layer Yellow Cake, Bi-Radiant Oven IV-B.....	2-32
3.10	Air Temperature Response Adjacent to Side Wall, Single-Layer Yellow Cake, Bi-Radiant Oven IV-B..	2-33

3.11 Average Wall Temperatures, Single-Layer Yellow Cake, Bi-Radiant Oven IV-B..... 2-34

3.12 Cake Temperature Response, Single-Layer Yellow Cake, Bi-Radiant Oven IV-B..... 2-35

3.13 Cake Mass Loss, Single-Layer Yellow Cake, Bi-Radiant Oven IV-B..... 2-36

3.14 Cavity Thermal Efficiency by Rate Method, Bi-Radiant Oven IV-A, 940 W Input Power..... 2-40

3.15 Cavity Thermal Efficiency by Rate Method, Bi-Radiant Oven IV-B, 956 W Input Power..... 2-41

4.1 Schematic of the Digital Control System for the Bi-Radiant Oven..... 2-54

4.2 Node Designation for Radiative Enclosure Analysis Used in the Heat Flux Predictor Algorithm..... 2-57

4.3 Comparison of Predicted and Measured Net Radiative Heat Flux, Gage Viewing Up..... 2-65

4.4 Comparison of Predicted and Measured Net Radiative Heat Flux, Gage Viewing Down..... 2-66

4.5 Controller Response - DOE Test Block..... 2-72

4.6 Controlled Input Power - DOE Test Block..... 2-73

4.7 Net Heat Flux Predictions Based on Block Temperature Data..... 2-74

4.8 Net Heat Flux Predictions for Constant Input Power - DOE Test Block..... 2-76

4.9 Controller Response - Repetitive Cakes..... 2-78

4.10 Controlled Input Power - Repetitive Cakes..... 2-79

4.11 Element Temperature Response - Repetitive Cakes. 2-81

4.12 Cake Temperature Response - Repetitive Cakes.... 2-83

4.13 Terms of the Heat Flux Predictor for the Lower Product Surface - Repetitive Cakes..... 2-84

Appendix Figure

A.1 Wall Thermocouple Locations, Bi-Radiant Oven IV-A 2-100

A.2 Wall Thermocouple Locations, Bi-Radiant Oven IV-B 2-101

A.3 Element Thermocouple Locations, Bi-Radiant Oven IV-A..... 2-102

A.4 Element Thermocouple Locations, Bi-Radiant Oven IV-B..... 2-102

A.5 Air Thermocouple Locations, Bi-Radiant Ovens IV-A and IV-B..... 2-103

A.6 Schematic of the Cantilever Beam Load Cell..... 2-104

A.7 Null Bridge Circuit Diagram..... 2-105

A.8 Product Weighing System Calibration..... 2-108

A.9 Convection Heat Transfer Coefficient on the Lower Surface of the Heated Heat Flux Gage in a Quiescent Medium..... 2-112

A.10 Convection Heat Transfer Coefficient on the Upper Surface of the Heated Heat Flux Gage in a Quiescent Medium..... 2-113

NOMENCLATURE

A	area, m^2
a,b,c,d	coefficients of algorithms and correlations
c	feedback signal or control variable
c_p	specific heat at constant pressure, J/kg-K
E	electrical energy, total stored energy, J
e	electrical signal, mV, specific stored energy, J/kg, error signal in the control system
F	view factor
$\hat{F}$	total exchange factor
G	irradiation, W/m^2
h	convection heat transfer coefficient, W/m^2-K
K_c	coupling coefficient
K_I	integral coefficient, m^2/s
K_P	proportional coefficient, m^2
L^*	characteristic length based on A/P, m
m	mass, kg, manipulated variable in the control system corresponding to the input power to the heating elements, W
N	number of surfaces in the radiative enclosure analysis of the heat flux predictor algorithm
P	perimeter, m, electrical power, W

Pr	Prandtl number
p	pressure, atm
Q	heat interaction, total heat transfer, J
q	heat transfer rate, W
R	electrical resistance, Ω, gas constant, atm-m^3/kg-K
Ra	Rayleigh number
r	controller reference signal or set point corresponding to the desired product net heat flux, W/m^2
Sc	Schmidt number
T	temperature, K
t	elapsed baking time, min
U	total internal energy, J
u	specific internal energy, J/kg
V	volume, m^3
v	specific volume, m^3/kg
W	work interaction, J

Greek Letters

α	absorptivity
Δ	prefix denoting a finite change in a variable
δ_{ij}	Kronecker Delta function, see Equation (E.6)
ε	emissivity
ρ	reflectivity, mass density, kg/m^3
σ	Stefan-Boltzmann constant, 5.669×10^{-8} W/m^2-K^4

Subscripts

A	oven air

B	blackened sensor on the heat flux gage
f	final value
in	input quantity
i	arbitrary flow interaction at the boundary of an open thermodynamic system, arbitrary surface, initial value
j	arbitrary surface
k	arbitrary surface value at the kth time interval
net	net value
p	product
rad	radiative quantity
w	product weighing system
1,2,...	node designation, see Figure 4.2

Superscripts

"	per unit area
-	average value

ABSTRACT

The major function of any oven system is to provide the necessary environment to satisfactorily bake or roast food products. This investigation has been restricted to an experimental electric oven, intended solely for domestic applications, with greatly improved efficiency over currently available conventional ovens. The experimental oven, referred to as the Bi-Radiant Oven, attempts to radiatively decouple the cavity walls from the heating elements and improve the radiative coupling of the product with the heating elements by using highly reflective walls and absorptive utensils. These modifications cause the heating elements to become a major radiant heat source and necessitates their continuous operation. The overall goal of this work has been to establish the principles of the Bi-Radiant Oven, primarily through experimental observations on a working model.

The thermal performance of the Bi-Radiant Oven under real baking conditions was reported in terms of the temperature response of the major oven components as well as the temperature response and mass loss of the test product, a single-layer yellow cake. An energy audit was also performed to characterize the heat losses and efficiency of the

Bi-Radiant Oven. Efficiencies of 22% and 18% were measured for the full sized prototype oven with conventional calrod type heating elements using wall materials with emissivities of 0.03 and 0.31, respectively.

The unconventional aspects of the Bi-Radiant Oven required special consideration of a control method for providing proper power levels to the upper and lower heating elements to accommodate various products, initial and oven operating conditions, and disturbances such as opening of the door. A digital control system was proposed using the net heat fluxes at the upper and lower product surfaces as control variables. This control system was implemented into the data acquisition system using a special heat flux predictor algorithm which was based on element, wall, air, and product temperatures and was tested under various oven conditions. These tests demonstrated the ability of the Bi-Radiant Oven to satisfactorily perform under practical conditions.

CHAPTER 1 - INTRODUCTION

The major function of any oven system is to provide the necessary environment to satisfy the thermal requirements of food products. This is achieved in conventional ovens by cyclically inputting power so as to maintain a single set point temperature. Many food products (breads, cakes, pastries, etc.) have significant mass loss (in the form of water vapor and carbon dioxide) and the oven environment must also satisfy these mass transfer requirements to insure product quality. In general, any change in the oven environment affects both the heat and mass transfer processes. The baking process, in general, is a thermochemical reaction with phase change and two phase (liquid and vapor) internal mass transfer. Thus, even holding other (external) mass transfer boundary conditions constant, the overall mass transfer process is strongly coupled to the heat transfer process.

An ideal method for determining an appropriate baking environment would include four steps. The first step would be to model the baking process in a general way so that reaction rates, temperature distribution, vapor generation and transfer, solid phase changes, etc. within the product can all be predicted from a knowledge of the external heat and mass transfer boundary conditions. The second step would be to identify some performance index which would quantify the desirable

product characteristics such as texture,color,moisture content, density, etc. The next step would be to optimize this index with respect to the appropriate basic heat and mass transfer parameters. The final step would be to physically construct an oven and utensil system which would cause the optimal value of these parameters to occur. There are many constraints that could be imposed in this optimization process. One of the most important constraints would be the selection of the appropriate basic heat and mass transfer parameters. The least restrictive (and the most difficult) approach would be to allow these parameters to be local quantities which vary with time. In conventional oven systems, thermal energy is absorbed at the surface of the product, by conduction from the utensil and by direct convection and radiation from the oven environment, and is subsequently transferred into the product by diffusion. Thus, in conventional oven systems the local net heat flux (including emission) at the product surface would be the basic heat transfer parameter. This idealized method for determining an appropriate baking environment has not been employed because the present knowledge of the baking process is insufficient. Even if a sufficiently detailed model were available, there would be difficulty in identifying a suitable performance index.

A more practical technique to provide a suitable baking environment is to vary the major oven parameters (heating element configuration, input electrical power levels, materials, coatings, utensil, vent size and location, etc.) on existing conventional oven systems. This parametric approach has been quite successful in yielding satisfactory baking performance for a wide variety of foods.

With the present trend of energy conservation, manufacturers are now attempting to maintain these same satisfactory baking results, but with greater thermal efficiency. Oven thermal efficiency represents the ratio of the energy absorbed by a food product to the energy consumed by the oven. In order to quantify the energy absorbed by a food product, the Department of Energy (DOE) has established procedures for determining the thermal efficiency of all conventional ovens based upon the temperature rise of a standard anodized aluminum test block [8]. A model of the conventional, domestic, electric oven relating oven efficiency (based on the DOE test block) to various oven parameters including cavity dimensions, insulation properties, heating element area, vent flow rate, window area, and rack height was developed by Erickson [7]. A 13.6% baseline efficiency was reported and is in general agreement with values observed in many ovens. Erickson concludes that if all the recommended energy related improvements are implemented on oven designs, then the oven efficiency would increase to nearly 17%. These recommended improvements would in no way alter the basic operating principle of the conventional oven.

Based upon pending DOE legislative standards for 1986 [5], the baseline oven specified by Erickson [7] would be required to have a cavity thermal efficiency of approximately 15.3%.[1] Although Erickson's results indicate that these standards can be obtained, other oven concepts which have improved thermal efficiency are also being considered.

---

1 This value was based upon a specified baseline oven volume of 3.62 ft^3 and includes the energy usage of a clock as specified by DOE test procedures [8] with an assumed continuous clock consumption of 2.0 W.

The present study deals with one such oven concept, which utilizes several major modifications to conventional oven systems and yields thermal efficiencies greater than 20% in full-sized enclosures. These modifications alter the basic operating principle of the conventional oven and yield greatly improved thermal efficiency, while maintaining the conventional method of surface heating. The rational of these modifications can be more easily understood by recognizing some of the weaknesses of conventional oven systems. Power is cyclically supplied to the upper and lower heating elements at a fixed ratio, with the greatest percentage (from approximately 80 to 100%) of the total power being consumed by the lower element. The walls are highly absorptive of the radiation emitted by the elements and provide the major source of radiation for the product during element off periods. Many products must be baked in highly reflective utensils to protect the lower product surface from the high incident radiant fluxes that occur during on periods. Thus, direct radiative coupling of the product and the lower element is frequently avoided. Simply increasing the upper-to-lower input power ratio so that more absorptive utensils could be used, would cause the lower surface of products that are normally baked in absorptive utensils to be under cooked.

To more effectively utilize radiant heat transfer, three major modifications were proposed and are as follows: (1) both the upper and lower heating elements are powered continuously and independently at relatively low power levels rather than cyclically with a fixed power ratio at high power levels, (2) the cavity walls are highly reflective to the radiation emitted by the heating elements, and (3) the baking

utensil is highly absorptive to the radiation emitted by the heating elements and walls.

These modifications attempt to radiatively decouple the cavity walls from the heating elements and improve the radiative coupling of the heating elements and the product. These modifications tend to cause the heating elements to become the primary radiation source (rather than the walls as in conventional ovens) and necessitates their continuous operation. The use of two heat sources providing improved radiant heat transfer to the product has led to the naming of this new oven concept as a Bi-Radiant Oven [18].

Two major advantages of this oven system can easily be recognized. First, since the oven walls are highly reflective, their overall temperature should be lower and thereby reduce both conduction and storage losses. Secondly, preheating of the oven enclosure, which is frequently necessary in conventional ovens to provide balanced heating, is not necessary since the elements are the primary heating source.

The goal of this work is to substantiate the concepts of the Bi-Radiant Oven principle by careful measurements on a working model. This goal implies not only an analysis of the energy utilization, but also identifying the manner in which energy should be delivered to the product. With this goal in mind, the following objectives were identified:

1. Construct an experimental Bi-Radiant Oven to serve as an engineering prototype for generating a data base,

2. Characterize the thermal performance of the prototype oven under

real and standard conditions, using detailed measurements of the prototype oven,

3. Develop a control method for controlling the proper power levels to the upper and lower heating elements so as to accommodate various products.

These objectives provided the framework upon which this report was organized. A separate chapter was devoted for each objective. The fifth and final chapter contains a summary and concluding remarks.

CHAPTER 2 - EXPERIMENTAL APPARATUS

The experimental apparatus consisted of prototype Bi-Radiant Oven IV,[2] its associated instrumentation and a data (acquisition, storage, retrieval, and reduction) system. The purpose of this apparatus was to provide a data base upon which to evaluate the performance of the Bi-Radiant Oven principle. The flexibility of the experimental apparatus to accommodate a wide variety of tests was of concern in its design. An overall view of the experimental apparatus is shown in the photograph of Figure 2.1. The oven door is open to show inner cavity details. Conventional heating elements were located near the upper and lower walls. A single rack was suspended by four cables which passed through the upper wall and attached to a weight monitoring system which was used to continuously measure the mass loss of products during baking. Shielded air temperature probes were located at the oven centerline and near the left side wall at four elevations. All sensors were monitored by a 64-channel data logger which was interfaced to a desk top calculator with magnetic tape and graphics capability.

---

2 A numbering scheme was adopted to distinguish this particular oven configuration from previous prototype ovens, see Scheitlin [19], Table 2.1.

ORNL-Photo 7957-81

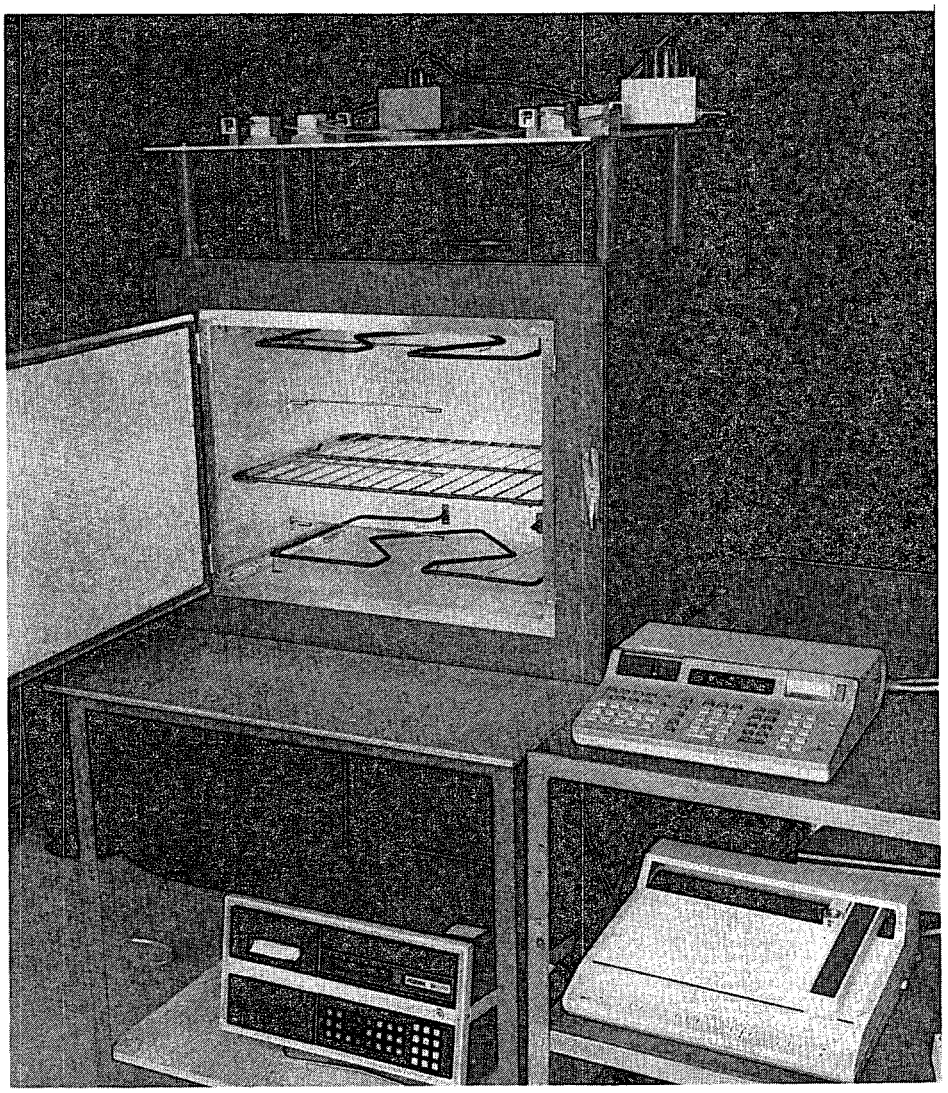

Figure 2.1 Photograph of the Experimental Apparatus.

2.1 Experimental Bi-Radiant Oven

In order to make a valid efficiency comparison of the Bi-Radiant Oven with full-sized conventional ovens, the inner cavity dimensions (width, height, depth) were selected to be 58.4 cm by 43.2 cm by 43.8 cm (23 in by 17 in by 17.25 in). The inner cavity was designed to allow replacement of the cavity walls. Two sets of walls were considered. The first set was constructed from 0.635 mm (0.025 in) thick 6061-T4 aluminum sheet and was mechanically polished to produce a near specular surface. The normal total emissivity of this material was measured[3] to be 0.032 near 150°C with an uncertainty of +0.04, -0.01 [19]. The second set of walls was constructed from 0.635 mm (0.025 in) thick 2024-T3 aluminum sheet and was sandblasted[4] to produce a diffuse surface. Preliminary tests indicated a normal total emissivity of 0.35 near 150°C. Later measurements of two wall specimens gave values of 0.30 and 0.32 with an uncertainty of ±0.02 on both values [19]. Other than the surface preparation and the aluminum alloy, both sets of walls were identical. As a matter of distinction, the oven will be referred to as Bi-Radiant Oven IV-A when the specular walls (ε = 0.032) are installed and as Bi-Radiant Oven IV-B when the diffuse walls (ε = 0.31) are installed.

Figure 2.2 gives an exploded view of the oven covers and support frames. All oven cover panels, except the door cover, were constructed from 1.02 mm (0.040 in) thick aluminum sheet with an as-received, brown

3 The procedure for measuring the normal total emissivity is given by Scheitlin [19]; degradation of the surface with $\varepsilon > 0.07$ was suspected.

4 Sandblasted with Glas-Shot, glass bead abrasive, grade MS-H, manufactured by Ferro Corp., Jackson, MS.

ORNL-DWG. 81-23746

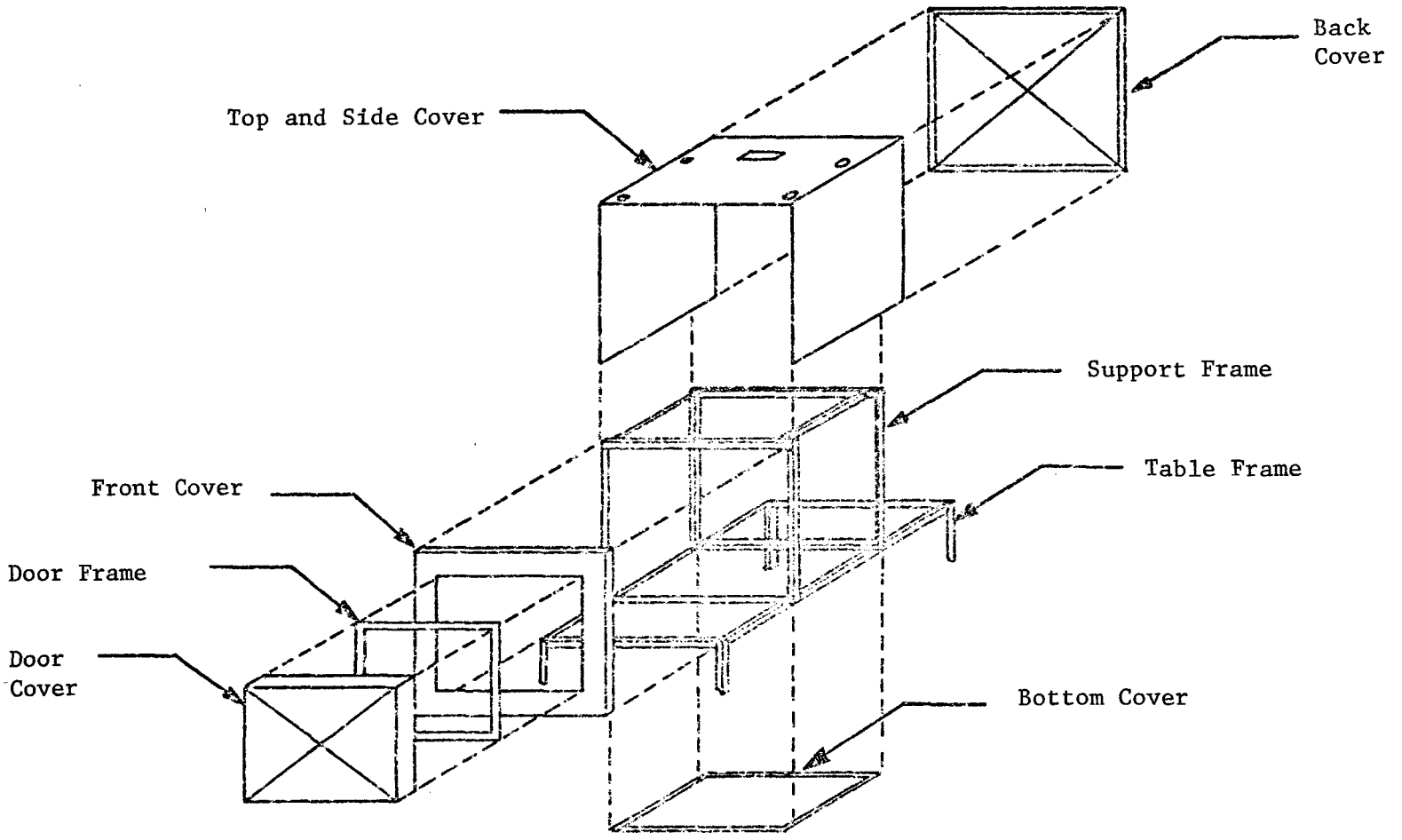

Figure 2.2 Expanded Schematic of the Outer Covers and Support Structure of Bi-Radiant Oven IV.

baked enamel surface. The door cover was constructed from 1.59 mm (0.0625 in) thick aluminum sheet and was brush painted on the outside surface with primer paint.

A full door seal was selected to reduce leakage. The oven door seal was made from a conventional silicone rubber oven door seal[5] and was attached to the aluminum door frame using clear Silicone Glue & Seal (General Electric, Waterford, NY). The door was hinged on the left as a matter of convenience. A brass cam and wiper device was used for a door latch. The space between the cavity walls and the oven cover, including the door, was filled with 10 cm (4 in) of typical, high temperature, fiberglass, oven insulation. The heating elements (Teledyne Stillman, Cookeville, TN) were conventional calrod type, with a diameter of 6.58 mm (0.259 in) and an overall length of 244 cm (96 in). The design process for selecting the heating element shape, as shown in Figure A.3 of Appendix A, is described by Scheitlin [19] and was based upon predictions of the irradiance distribution over a baking plane. Electrical power to the upper and lower heating elements was supplied by 115 V, 7.5 A Powerstats (Superior Electric Co., Bristol, CT). For several high power tests a 240 V, 28 A Powerstat was used for the upper heating element. The oven rack, 56.0 cm by 40.2 cm (22.1 in by 15.8 in), was modified from a conventional domestic oven rack[6] to accommodate the suspension cables and product weighing system and had a mass of 1.112 kg (2.45 lb_m). The thermal mass of the inner-cavity, including the rack, heating elements, and door frame was estimated to be 5.20 kJ/K. This value was

5 Kenmore Model 911.9257611, part no. 296102.

6 Kenmore Model 911.9257611, part no. 305408.

calculated by knowing the dimensions and material properties of each component.

2.2 Instrumentation

The experimental apparatus was instrumented for the measurement of temperatures within the enclosure and product, power consumption of the heating elements, and the continuous measurement of product mass loss during baking. A special water-cooled heat flux gage was also used to measure radiative heat fluxes within the enclosure.

2.2.1 Temperature Measurement

Wall, air, cover, product, and test block[7] temperatures were measured using (30 gauge, glass wrap) copper-constantan thermocouples. Wall thermocouples were attached to the outer surface of the cavity wall using Scotch-Weld Structural Adhesive 1838 B/A (3M Company, Springfield, MO). Figure 2.3 shows details of a chrome-plated air temperature probe fabricated from brass tube and rod stock. The cover thermocouples were attached to the inside surface of the oven cover using a conventional two part epoxy. The location of each wall, element, air, and cover thermocouple is given in Appendix A. The test block temperature was measured by a single thermocouple placed in a 1.27 cm (0.50 in) deep hole of diameter 2.13 mm (0.084 in) located at the center of the upper surface. Thermalcote thermal joint compound (Thermalloy, Inc., Dallas, TX) was used to fill the space around the thermocouple.

7 DOE specified standard test block (8.5 lb anodized 6061 aluminum, 6.25 in. diameter, and 2.8 in. high) used for measuring oven thermal efficiency [8].

ORNL-DWG. 81-23747

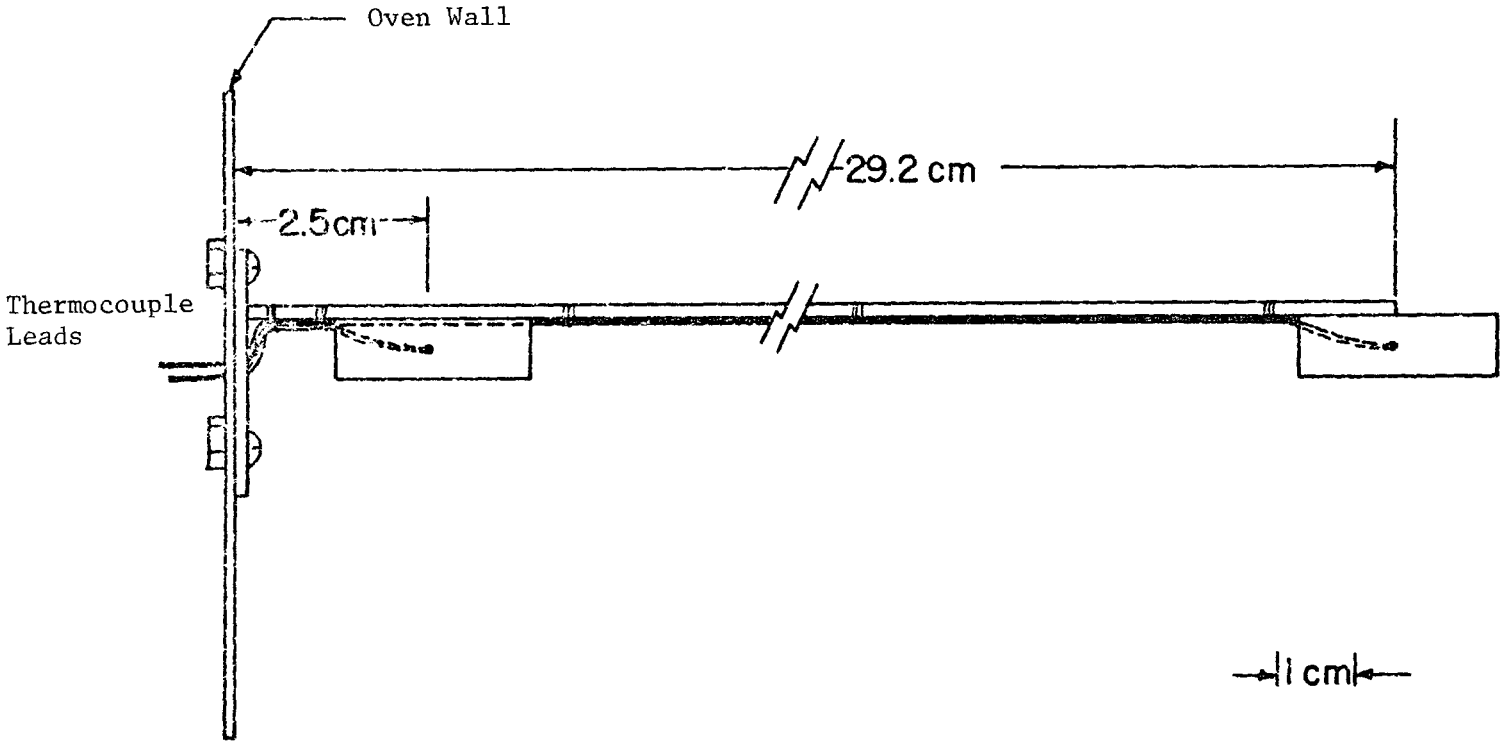

Figure 2.3 Details of the Air Temperature Probe.

Heating element surface temperatures were measured using (30 gauge glass wrap) chromel-alumel thermocouples. The two thermocouple leads were separately welded to the heating element sheath as shown in Figure 2.4. This arrangement, referred to as tempering, was used to reduce conduction errors. The Inconel stainless steel sheath serves as an intermediate metal in the thermocouple circuit.

Oven manufacturers generally approve of the single-layer cake as a good product to test the overall baking performance of conventional domestic oven systems [3]. For this reason the single-layer yellow cake was selected as the test product in this study. To characterize the temperature distribution within the cake, three temperature probes were constructed as shown in the photograph of Figure 2.5. The selection of this horizontal configuration was based on a previous study [17] which indicated that relatively small radial and angular temperature gradients exist in the cake during the baking process. Copper-constantan thermocouples (Teflon coated, 0.005 in diameter wire) were located at the tip of each horizontal, slender, stainless steel, guide tube (0.050 in o.d. and 0.004 in wall thickness). The thermocouples were in direct contact with the cake batter, except for a thin layer of a cyanoacrylate adhesive used to seal the tip of the probe. The probes were located near the pan centerline at 5, 15, and 30 mm (0.20, 0.59, and 1.18 in) from the pan bottom. Each probe had a 30° angular offset to avoid plume effects that may occur from adjacent probes as the batter rises. The supporting post was made of 3.18 mm (0.125 in) diameter Bakelite rod with an NF 2-56 thread tapped in the lower end for fastening to the pan bottom. Copper-constantan thermocouple leads (30 gauge, glass wrap)

ORNL-DWG. 81-23748

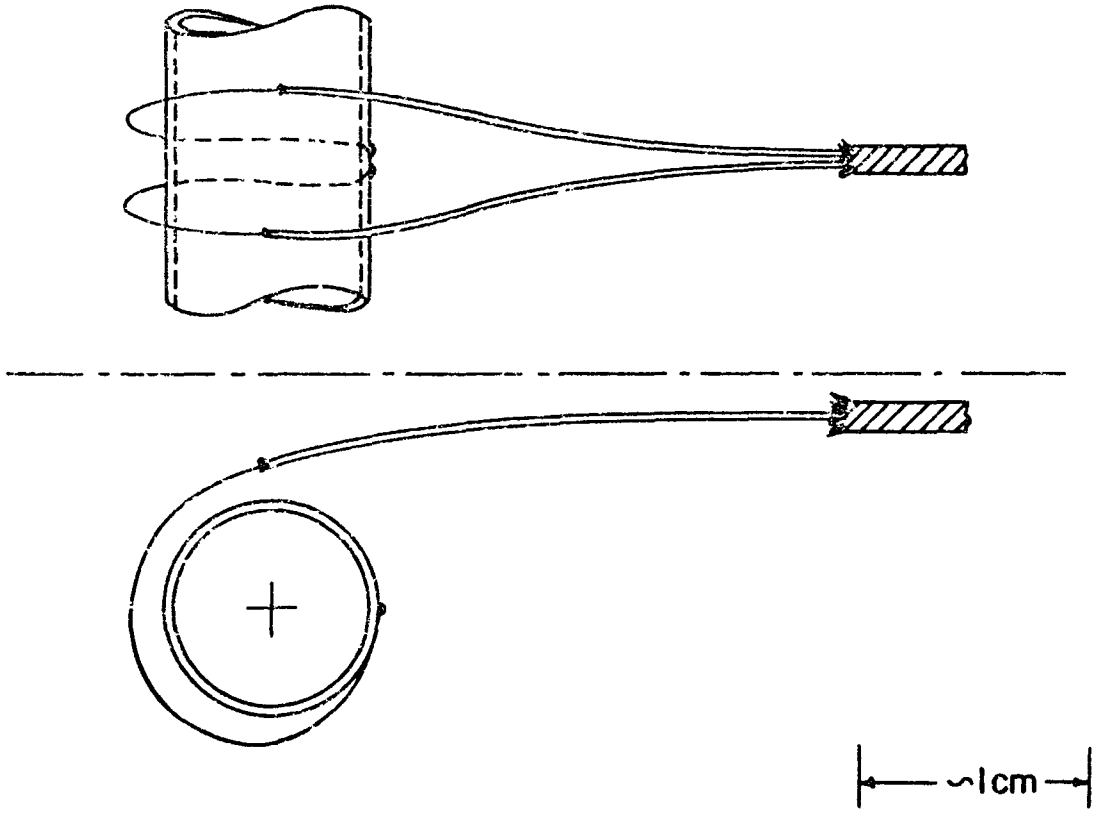

Figure 2.4 Placement of the Heating Element Thermocouples.

ORNL-Photo 8878-81

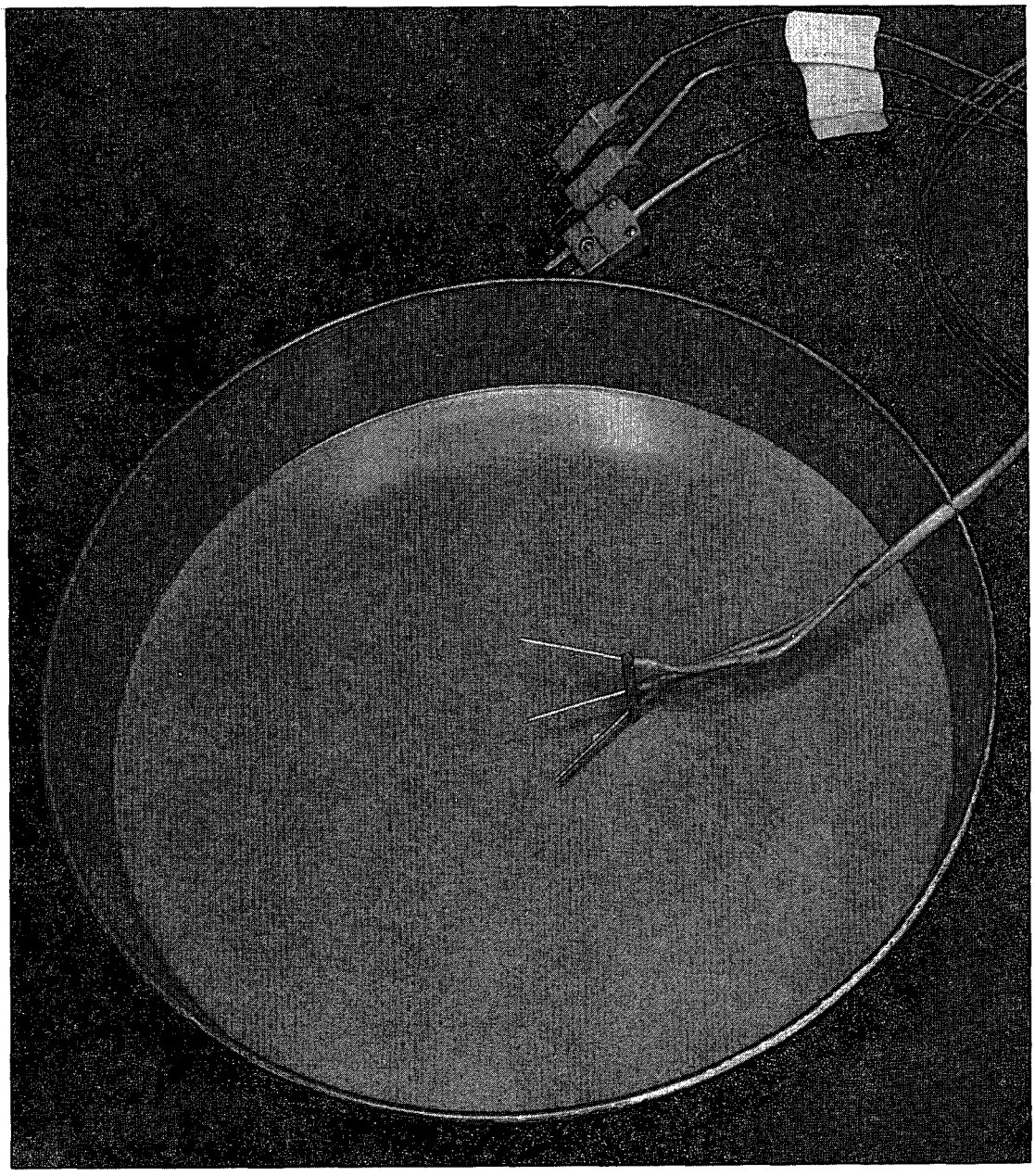

Figure 2.5 Photograph Showing Placement of the Cake Temperature Probes.

were welded to each thermocouple and exit the cake pan as shown in Figure 2.5. These thermocouple leads were routed horizontally through the oven enclosure so as to provide minimal interference with the product weighing system and were exited between the front flange and the door seal.

2.2.2 Mass Loss, Electrical Power, and Heat Flux Measurements

The product mass loss was measured during the baking process by four cantilever beam type load cells attached to the four oven rack suspension cables. Dual strain gages (Micro-Measurements, Romulus, MI, gage type EA-13-125PC-120-LE) were attached (using a cyanoacrylate adhesive) to the upper and lower surfaces of each cantilever beam to provide good temperature and expansion compensation. The cantilever beams (aluminum alloy 2024-T3) were 1.59 mm (0.0625 in) thick, 1.27 cm (0.50 in) wide, and extended 8.89 cm (3.50 in) from the line of action to the supporting clamp. The strain gages were located 5.72 cm (2.25 in) from the line of action. The four load cells were mounted on a 6.35 mm (0.25 in) thick base plate which was elevated approximately 18 cm (7 in) above the oven cover as shown in Figure 2.1. It was necessary to elevate the product weighing system to reduce the thermal effect of the oven enclosure. Each of the four load cells were connected to a single bridge circuit so as to provide a single output. The bridge was zeroed with the rack in place thus, the output of the bridge circuit indicated the total weight of the product and utensil. Because the load cells were constructed to be as identical as possible, the variation of the product weighing system output with the position of a load on the rack was within ±2.5% of the center position value. With proper electrical

shielding a resolution of ±1 g was obtained. Very small offset errors (±0.5 g) were possible because of coarse and fine zeroing potentiometers used in the bridge circuit. Based upon a 2 kg (4.41 lb) full scale range (including the rack and hardware), the accuracy of the product weighing system, for loads placed near the center of the rack, was within ±0.1%. Details of the bridge circuit and calibration of the product weighing system are given in Appendix A.

The electrical power consumed by each heating element was measured by two AC watt transducers (American Aerospace Controls, Inc., Farmingdale, NY, model 415A-10-115). Manufacturer's specifications and independent calibration indicate that these transducers have an accuracy of better than ±2% of the full-scale rated input of 1 kW. For high power tests, a 10 kW full-scale transducer (model 415A-50-230) was used, again with a specified full-scale accuracy of ±2%.

The construction and calibration of the water-cooled heat flux gage are discussed in great detail by Scheitlin [19]. This gage utilizes two Gardon foil-type, radial-flow, net heat flux sensors mounted on the same side of the water-cooled base plate. One of the sensors had a high emissivity (approximately 0.95) and the other had a low emissivity (approximately 0.16). The convective and the total, incident, radiative heat fluxes (irradiation) at the gage surface were determined by simultaneously solving the governing equations for the two net heat flux sensors. During oven tests with the gage oriented horizontally with sensors facing downward, the convective heat flux indicated by the gage was in substantial disagreement with standard horizontal flat plate correlations. These results, along with results of the gage in a quiescent

medium, are discussed in section 3 of Appendix A. It appears that these discrepancies are caused by differences in flow patterns that exist for the lower face of the cooled gage (or the upper face when it was heated in the quiescent medium) and the experimental test cells used to generate the standard correlations.

2.3 Data Acquisition System

The data acquisition system consisted of three major components; an Esterline Angus PD2064 data logger, Hewlett-Packard 9815S desk top calculator, and Hewlett-Packard 7225A/17600A graphics plotter. The major features of the data logger included 64 analog input channels, printed paper tape output, programmable features such as automatic data scanning and channel selection, direct temperature readout for thermocouple types T, K, and E, and a one-way digital output port which provided for data flow to the calculator. The major features of the desk top calculator included a 3800 program step memory, any part of which could be allocated for temporary data storage, permanent program/data storage and retrieval via magnetic cassette tape, thermal paper tape printer, and dual input/output ports which provided the capability to display results on the plotter while an experiment was in progress. The calculator/plotter combination had the capability to draw and label axes, plot a single on-center symbol (+), plot straight lines, and digitize graphical data.

CHAPTER 3 - THERMAL PERFORMANCE OF THE BI-RADIANT OVEN

The major reason for characterizing the thermal performance of the Bi-Radiant Oven was to gain a better understanding of the heat and mass transfer processes occurring in the oven and of the overall energy utilization (efficiency and loss mechanisms) of the oven. Typical temperature responses of the major oven components are presented as well as cavity thermal efficiency and an overall energy audit to characterize the loss mechanisms. These results are presented for both sets of oven walls to show the effect of wall surface preparation on the performance of the Bi-Radiant Oven. A single-layer yellow cake was used to demonstrate actual baking conditions while the DOE test block was used to quantify the energy absorbed by a typical product. Sections 3.1 through 3.3 are devoted solely for the presentation of the experimental results. The discussion of these results are combined into Section 3.4 to allow for general comments and easy comparison of the results of Ovens IV-A and IV-B.

3.1 Single-Layer Yellow Cake Measurements

Single-layer yellow cakes, prepared according to the formula given in Appendix B, were baked in Ovens IV-A and IV-B. The baking utensil was a 22.9 cm (9 in.) diameter, anodized, aluminum cake pan with a normal total emissivity of 0.87 near 150°C [19]. The pan was placed near

the center of the rack which was elevated 18.5 cm (7.3 in.) from the lower wall. Initially the oven was at room temperature and isothermal (i.e., not preheated). Electrical power to the elements was switched on at time zero and data was recorded every 30 seconds. Baking was terminated when all three cake thermocouples reached or exceeded 93.0°C. Suitable power settings for Bi-Radiant Oven IV-A were obtained from results of an earlier study [6]. The power settings for Oven IV-B were obtained from a series of experiments where the power levels were adjusted until the cake response was similar to that produced by Oven IV-A.

The input power to the upper and lower elements over the duration of the baking test is given by Figure 3.1 for Oven IV-A. The slight decrease in the input power to the upper element near the beginning of the test is due to the change in the resistance of the element because of its temperature rise. Other variations are probably caused by fluctuations in the line voltage. The average power to the upper and lower elements were 809 W and 46.4 W, respectively, giving an upper-to-lower ratio of 17.4. For the remaining tests, only the average power will be reported.

The temperature response of the heating elements is given in Figure 3.2 for Oven IV-A. These curves represent the average of four thermocouples for each element. This and all the remaining temperature results were plotted using piecewise linear segments between data points. The largest temperature difference observed among the four thermocouples for the upper and lower elements was 23.8 and 4.6°C, respectively.

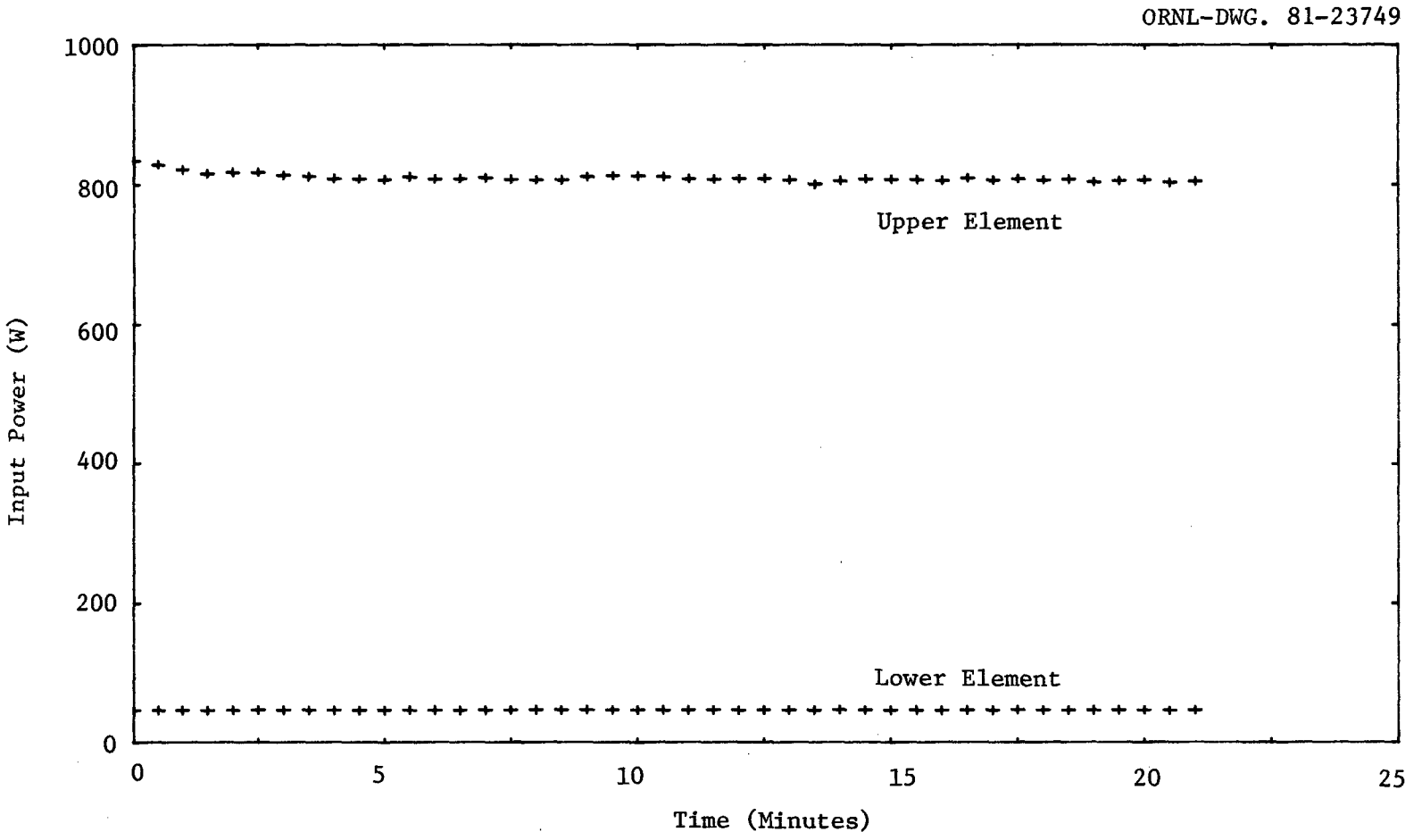

Figure 3.1 Input Power, Single-Layer Yellow Cake, Bi-Radiant Oven IV-A.

ORNL-DWG. 81-23750

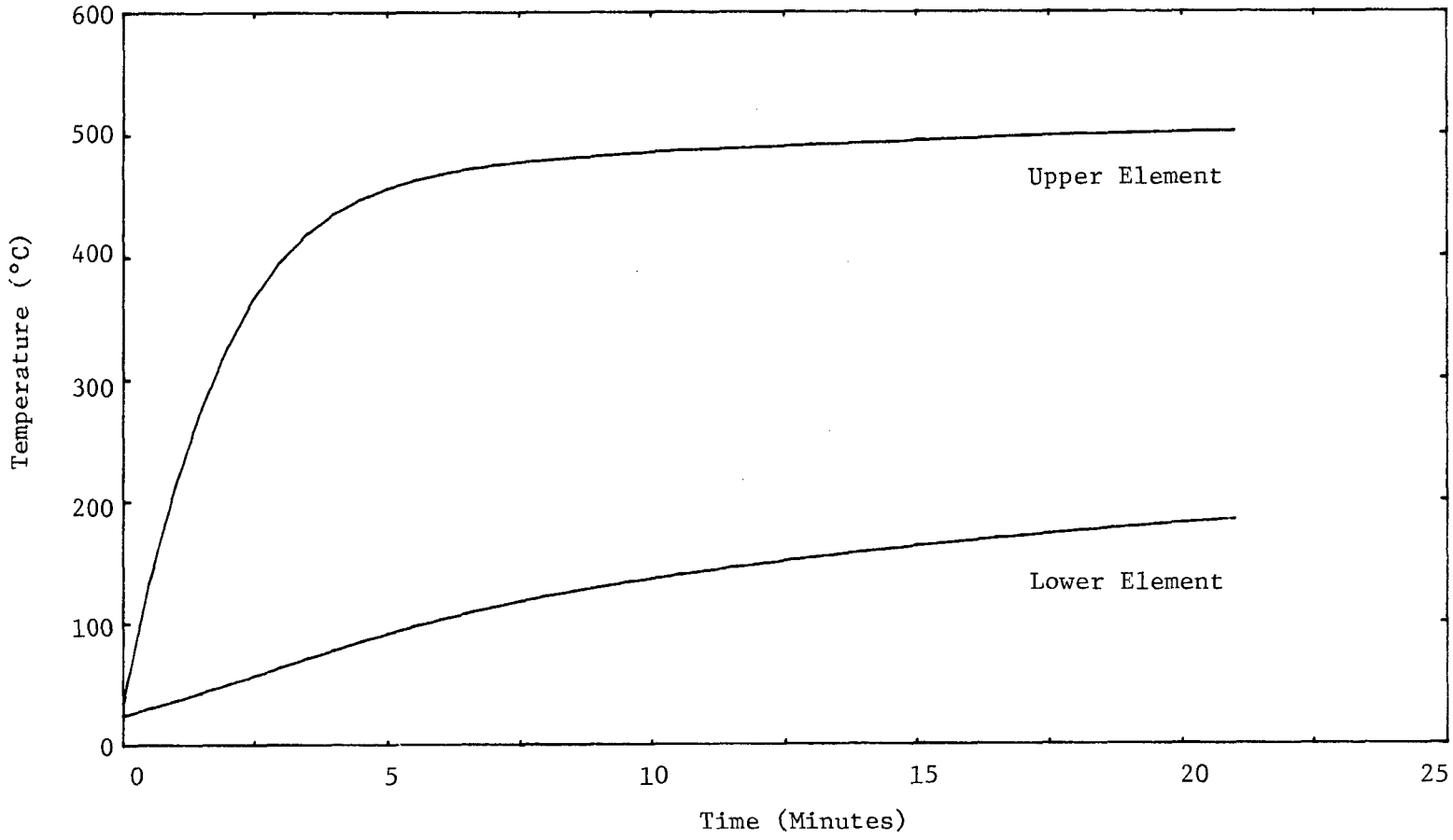

Figure 3.2 Element Temperature Response, Single-Layer Yellow Cake, Bi-Radiant Oven IV-A.

Figure 3.3 gives air temperature results for Oven IV-A from the four centerline probes which were located 5.4, 16, 27, and 38 cm from the lower oven wall. Additional results for Oven IV-A from the four probes located 2.54 cm from the left side wall and at the same above elevations are presented in Figure 3.4.

Average wall temperatures are presented in Figure 3.5. The top and bottom results are averages of four thermocouples on each wall while the door and back results are averages of six thermocouples on each wall. The side wall curve is an average of the nine thermocouples on the right side wall. The side wall has essentially the same response as the back wall. A comparison of the center side wall thermocouples indicates that the left side was slightly warmer than the right side. A maximum difference of 5.5^{o}C was observed at the end point. The maximum temperature difference among the four thermocouples on the top and bottom walls was observed to be 12.0 and 3.2^{o}C, respectively, both of which occurred at the end point. The maximum vertical temperature gradients in each of the back, door, and right side walls also occurred at the end point. An area averaged vertical temperature gradient of 1.77^{o}C/cm was observed for the back, door, and side walls at the end point. This value was calculated assuming that the left side wall experienced the same temperature gradient as the right side wall.

Temperature and mass loss results for the cake are presented in Figures 3.6 and 3.7, respectively. The initial batter level (approximately 18 mm) covered the first two thermocouples and the 30 mm thermocouple was exposed to the air until the batter rose above that level. Figure 3.7 shows the output of the product weighing system indicating

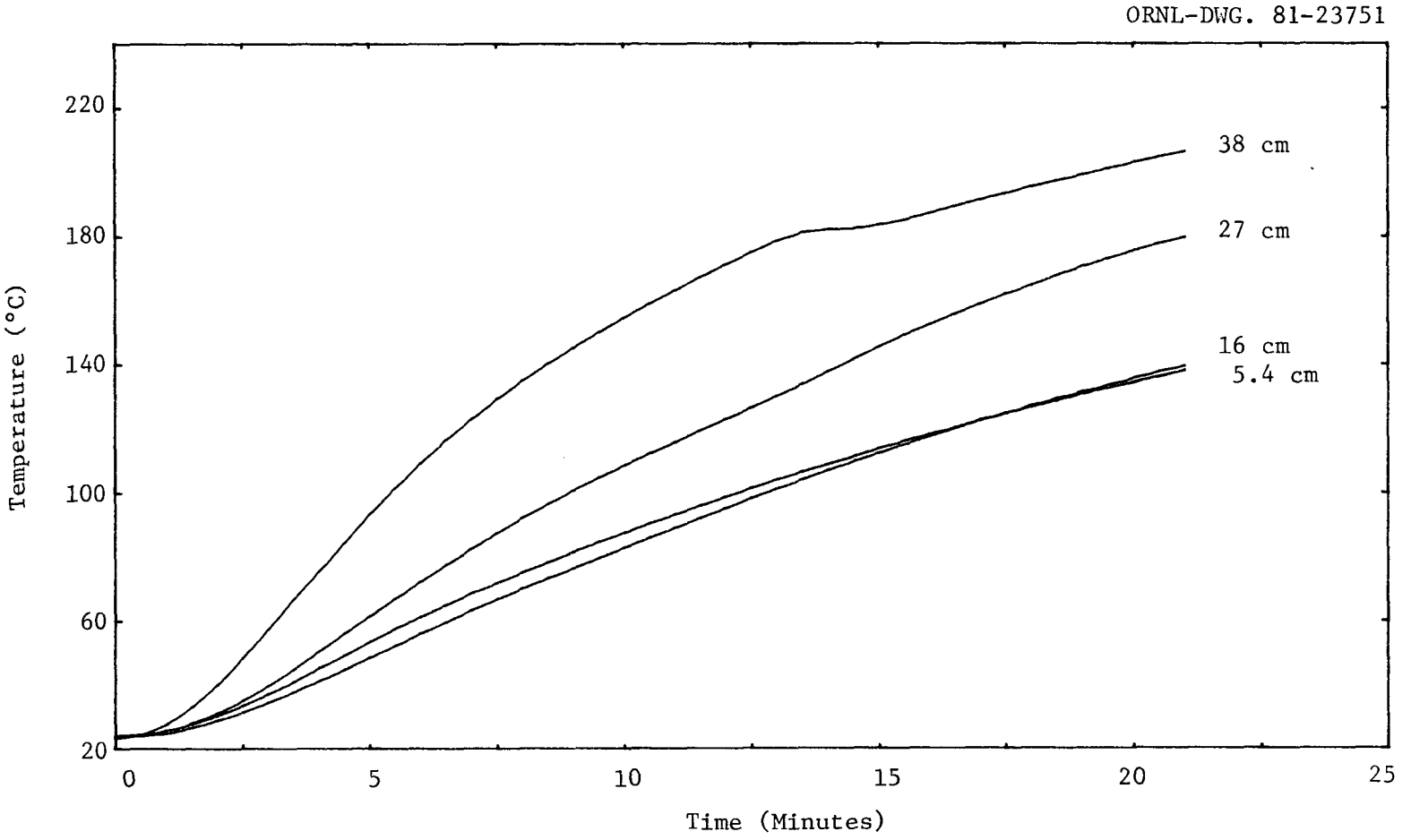

Figure 3.3 Centerline Air Temperature Response, Single-Layer Yellow Cake, Bi-Radiant Oven IV-A.

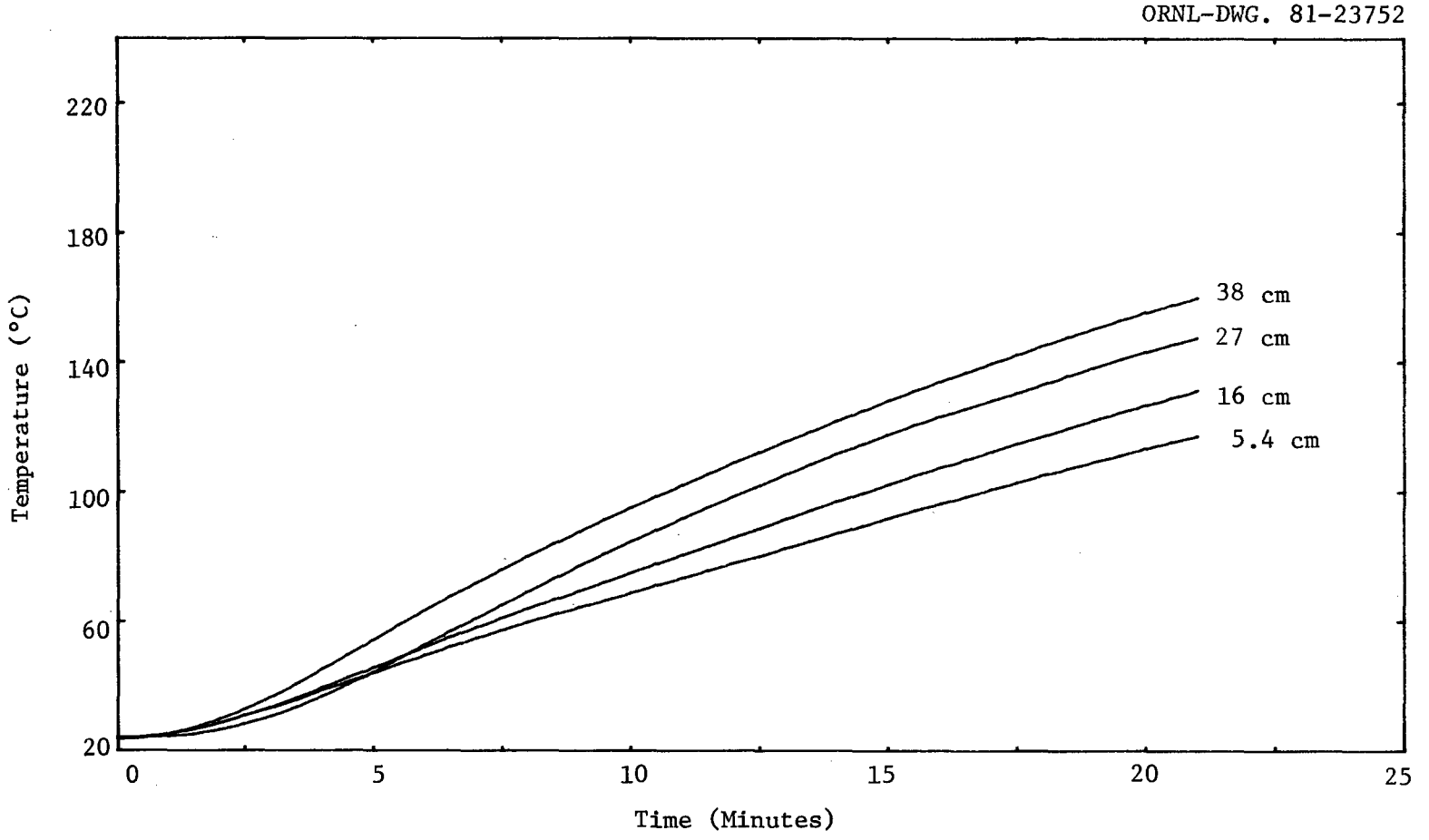

Figure 3.4 Air Temperature Response Adjacent to Side Wall, Single-Layer Yellow Cake, Bi-Radiant Oven IV-A.

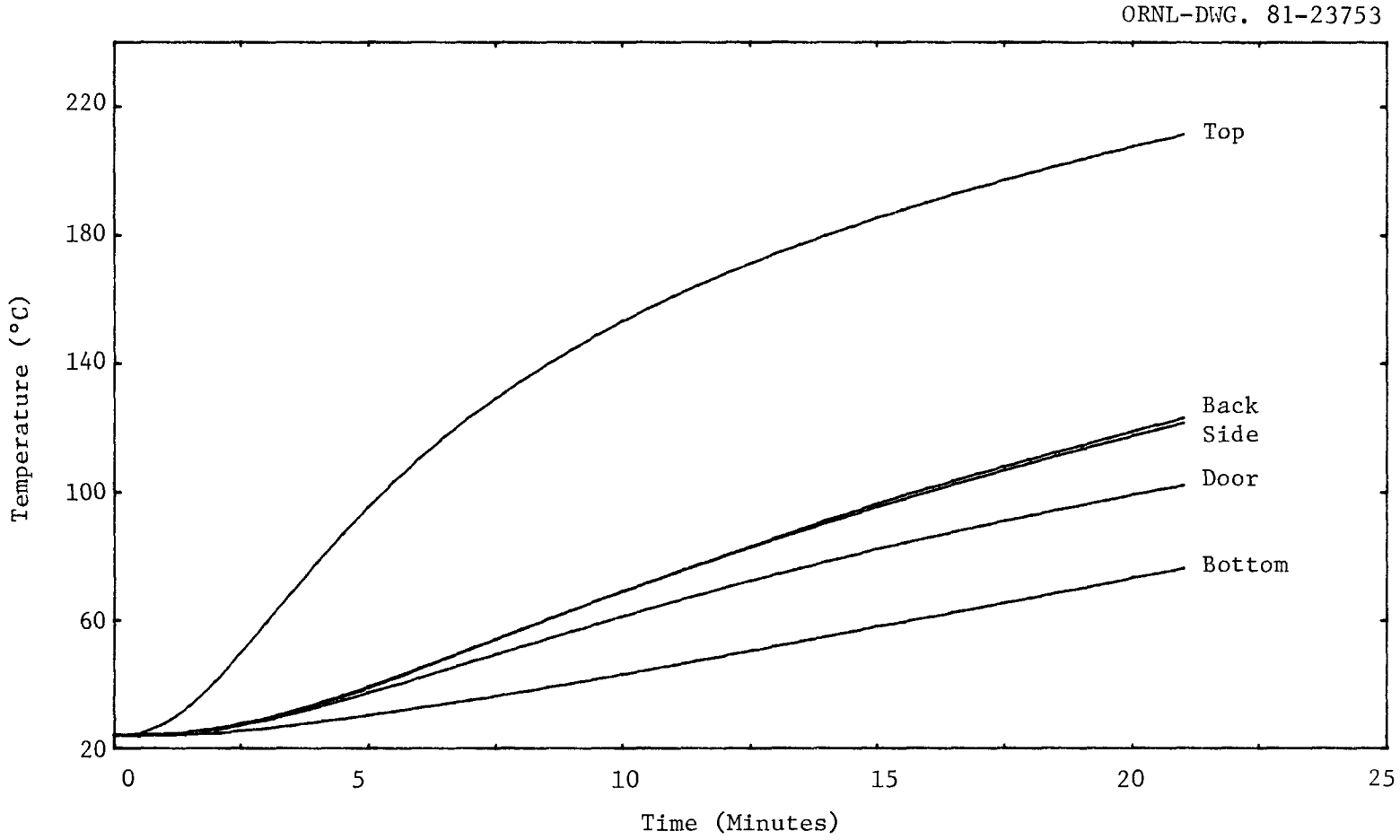

Figure 3.5 Average Wall Temperatures, Single-Layer Yellow Cake, Bi-Radiant Oven IV-A.

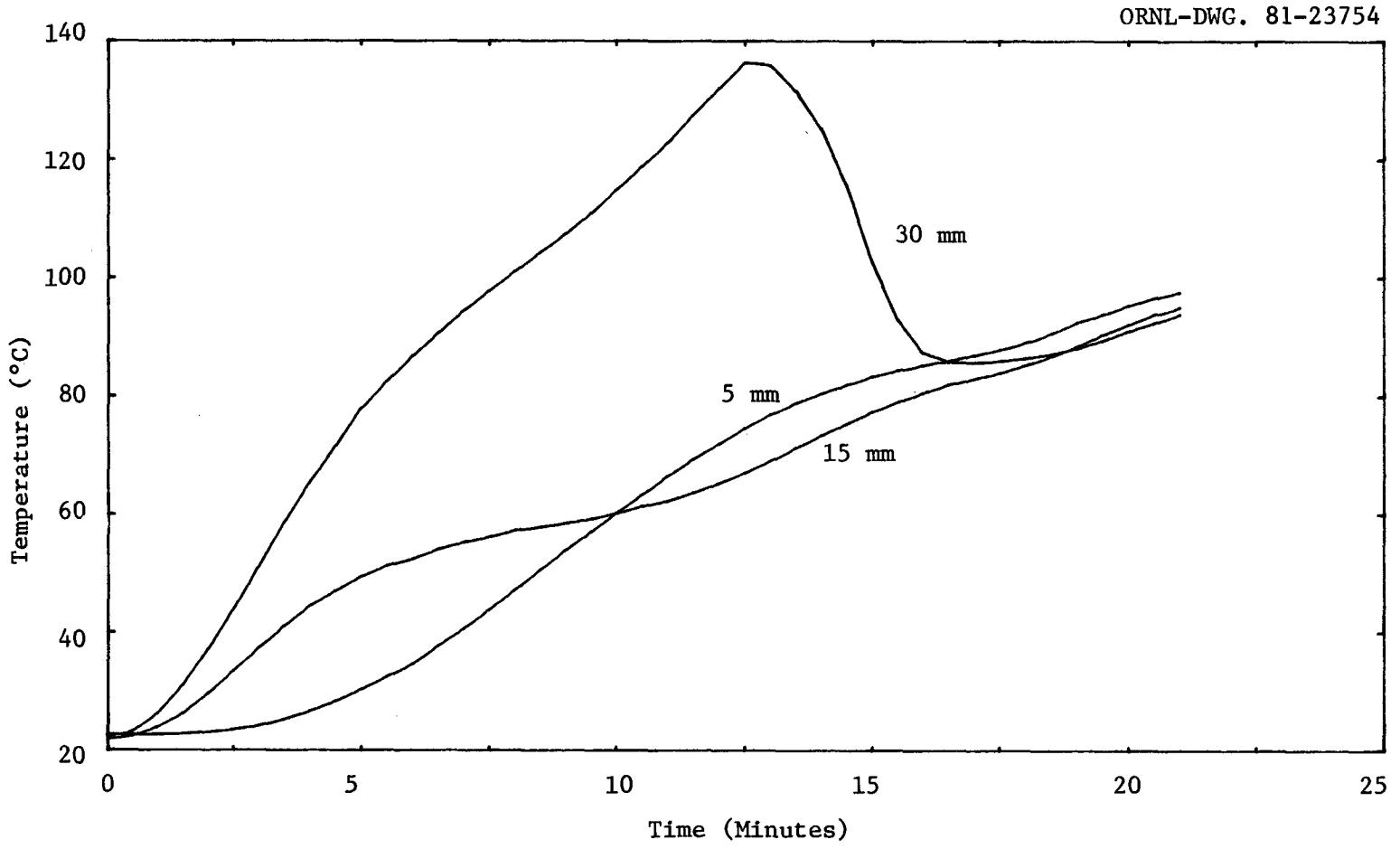

Figure 3.6 Cake Temperature Response, Single-Layer Yellow Cake, Bi-Radiant Oven IV-A.

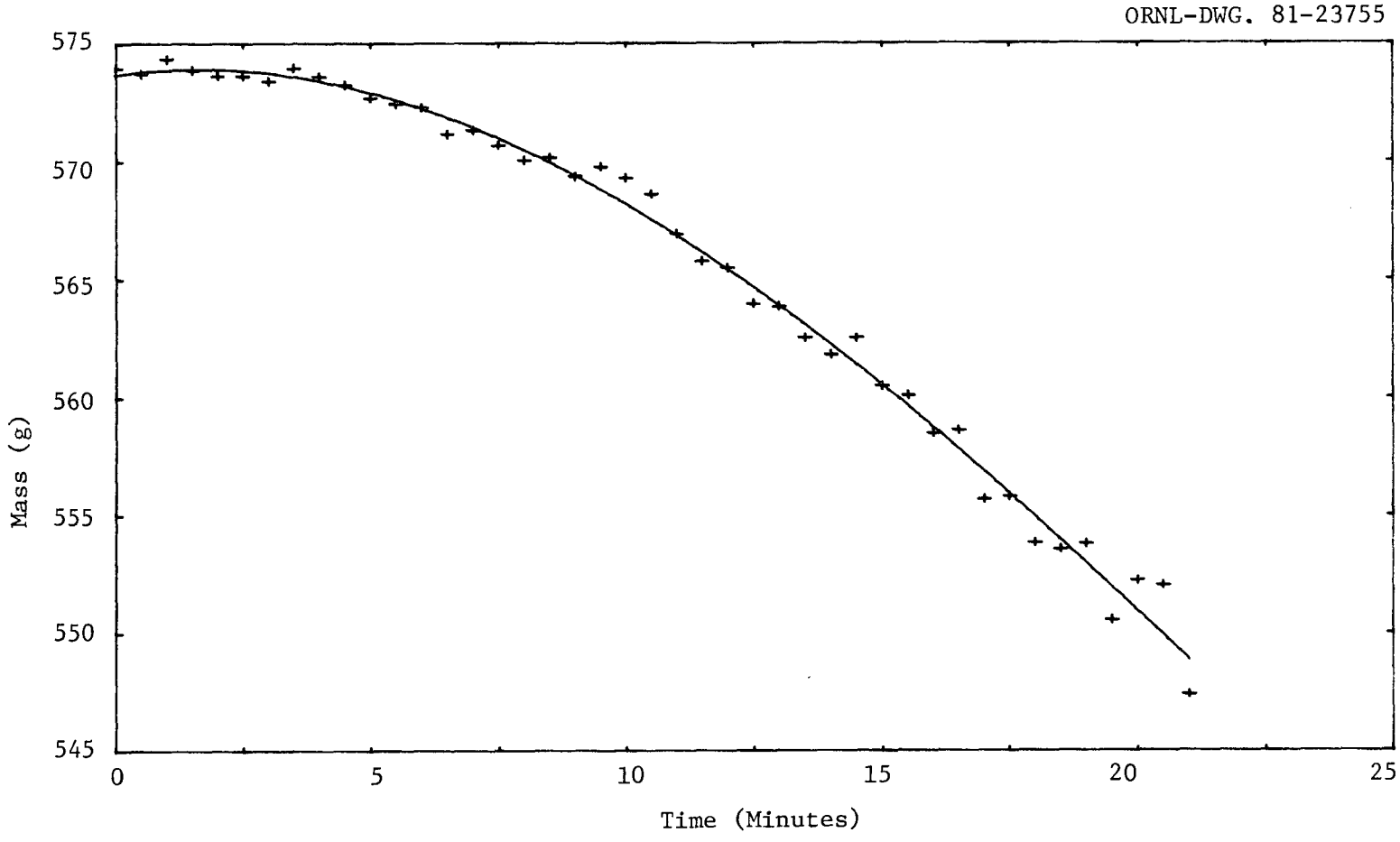

Figure 3.7 Cake Mass Loss, Single-Layer Yellow Cake, Bi-Radiant Oven IV-A.

the total mass of the cake and utensil. The curve is a least squares cubic fit of the data, and indicates a total mass loss of 24.8 g.

Single-layer yellow cake results for Oven IV-B are presented in Figures 3.8 through 3.13. As mentioned earlier, the power levels were adjusted until the cake temperature response was similar to Oven IV-A. Average power levels of 876 W and 221 W to the upper and lower elements, respectively, (giving an upper to lower ratio of 3.96) were used in this test.

In Oven IV-B, each element was characterized by two thermocouples, and the results of Figure 3.8 represent the average of these two thermocouples. The largest temperature difference between the two thermocouples on the upper and lower elements was 5.0 and 2.8°C, respectively.

Air temperature results of Figures 3.9 and 3.10 were obtained in the same locations as for Oven IV-A.

Figure 3.11 presents average wall temperatures for Oven IV-B. Only four thermocouples were used to characterize each wall (except the left side wall) in Oven IV-B, instead of four, six, or even nine as in Oven IV-A. The maximum temperature difference among the four thermocouples on the top and bottom walls was observed to be 16.9 and 8.4°C, respectively, only the latter of which occurred at the end point. The maximum difference on the top wall occurred after 8.5 minutes. The maximum vertical temperature gradients in each of the back, door, and right side walls occurred at or within 30 seconds of the end point. An area averaged vertical temperature gradient of 1.46°C/cm was observed for the back, door, and side walls at the end point. Again, this value was

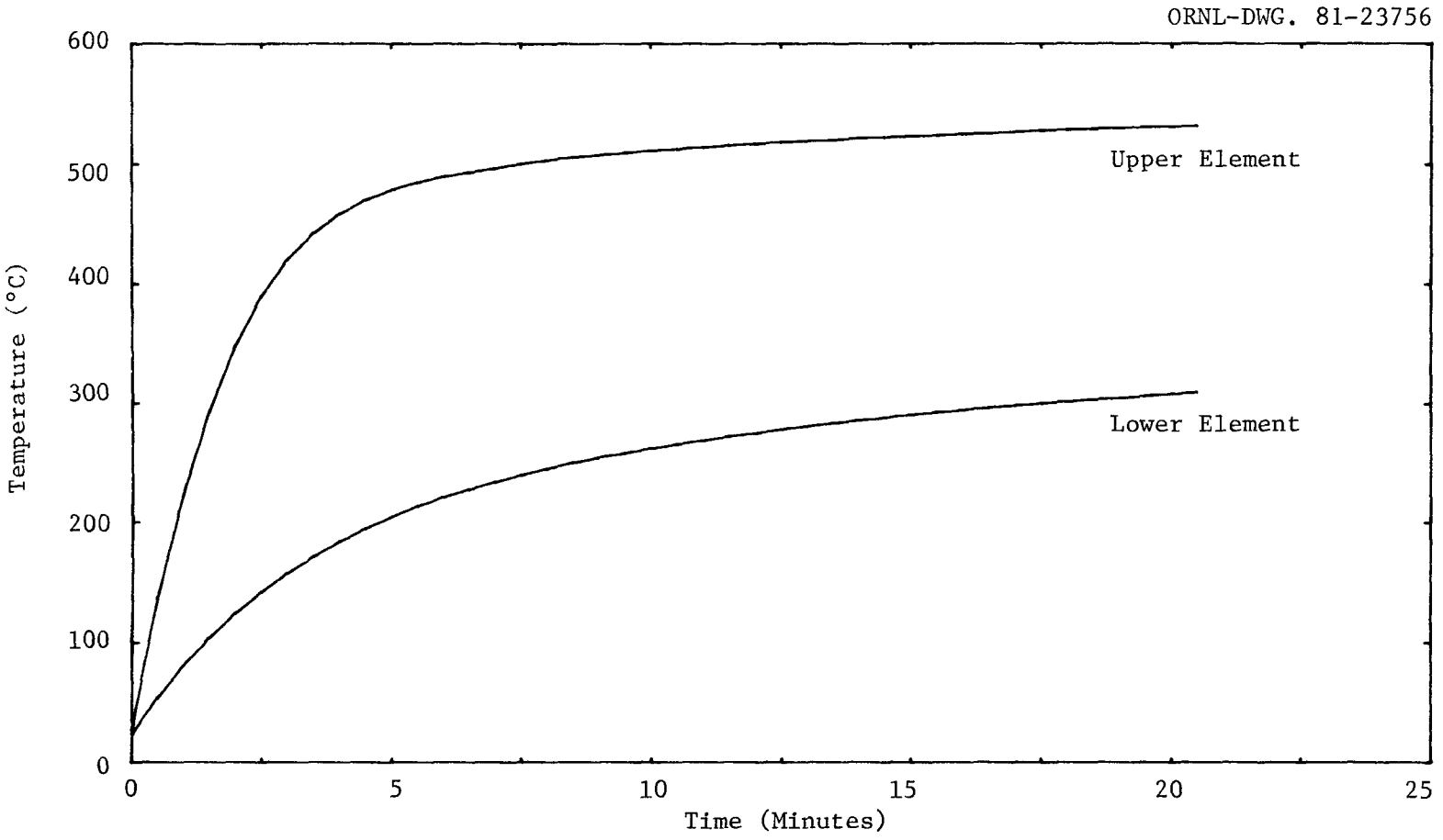

Figure 3.8 Element Temperature Response, Single-Layer Yellow Cake, Bi-Radiant Oven IV-B.

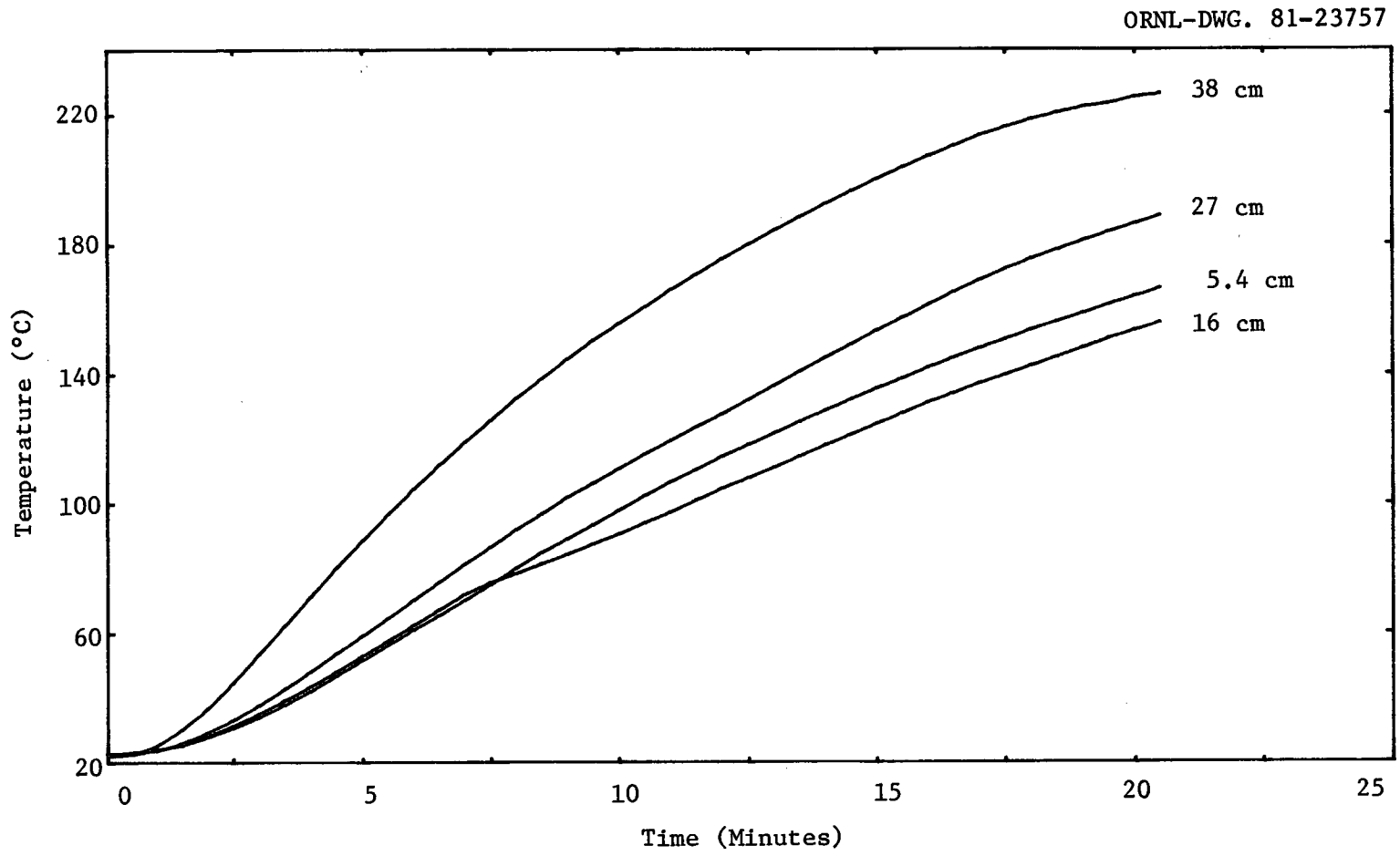

Figure 3.9 Centerline Air Temperature Response, Single-Layer Yellow Cake, Bi-Radiant Oven IV-B.

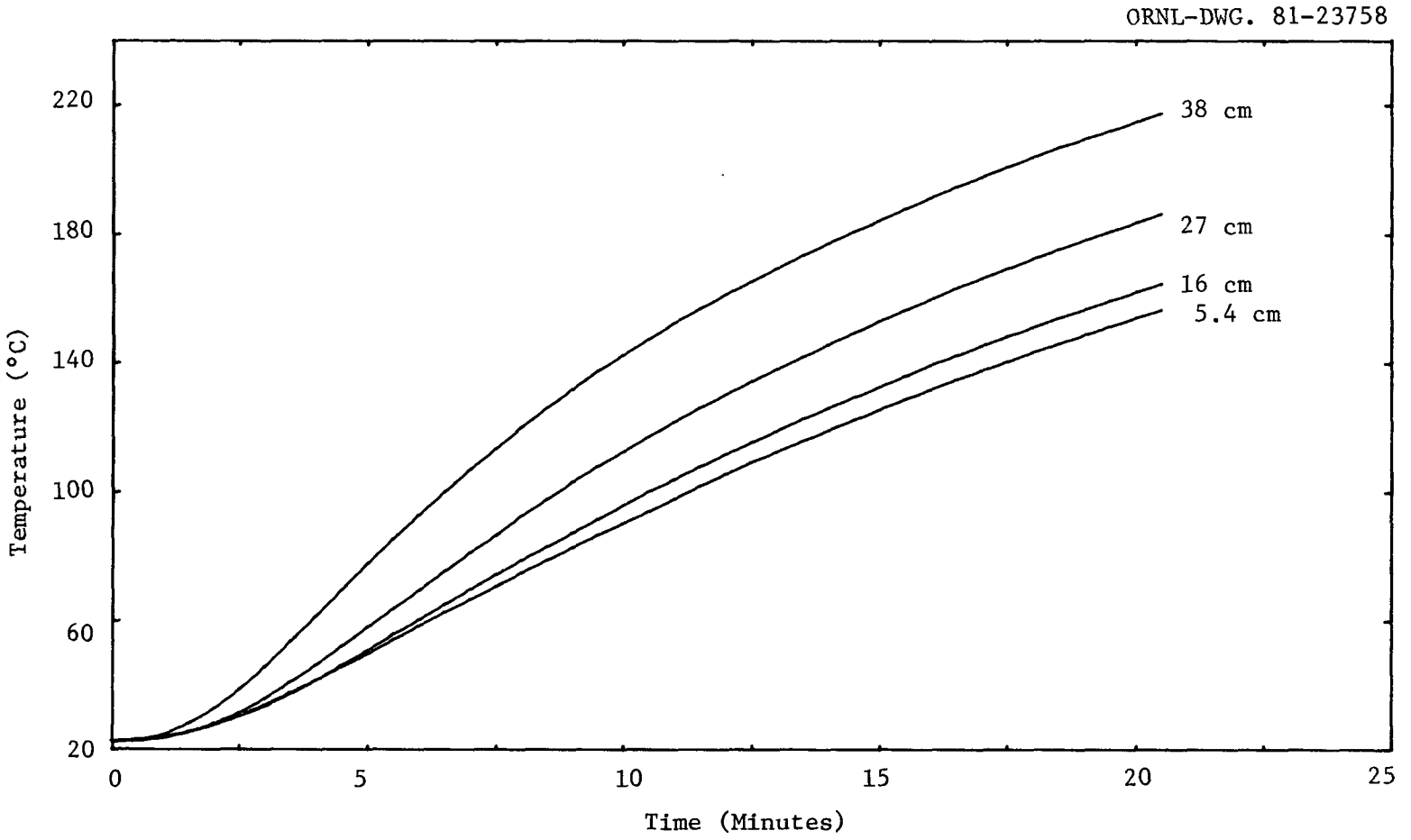

Figure 3.10 Air Temperature Response Adjacent to Side Wall, Single-Layer Yellow Cake, Bi-Radiant Oven IV-B.

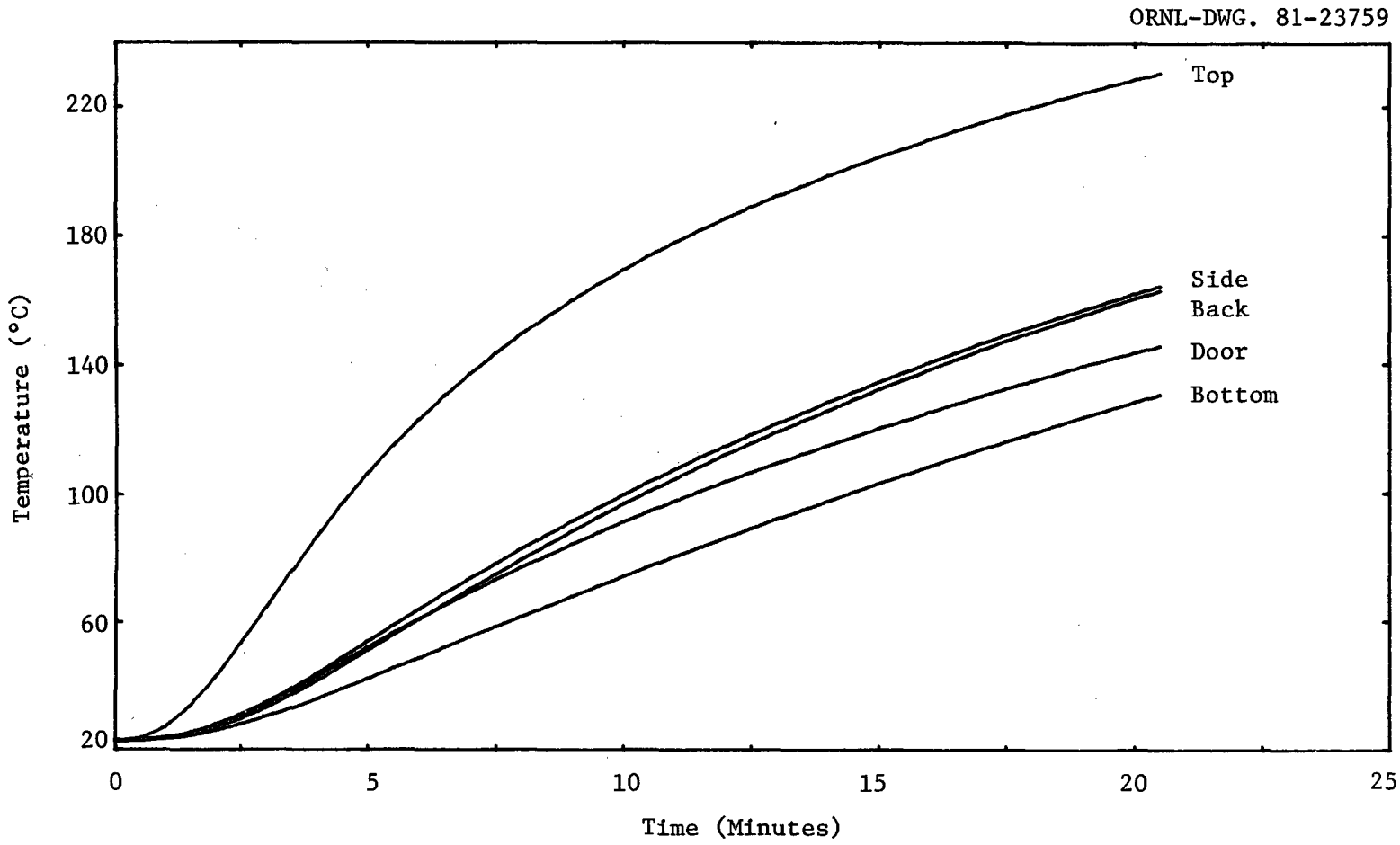

Figure 3.11 Average Wall Temperatures, Single-Layer Yellow Cake, Bi-Radiant Oven IV-B.

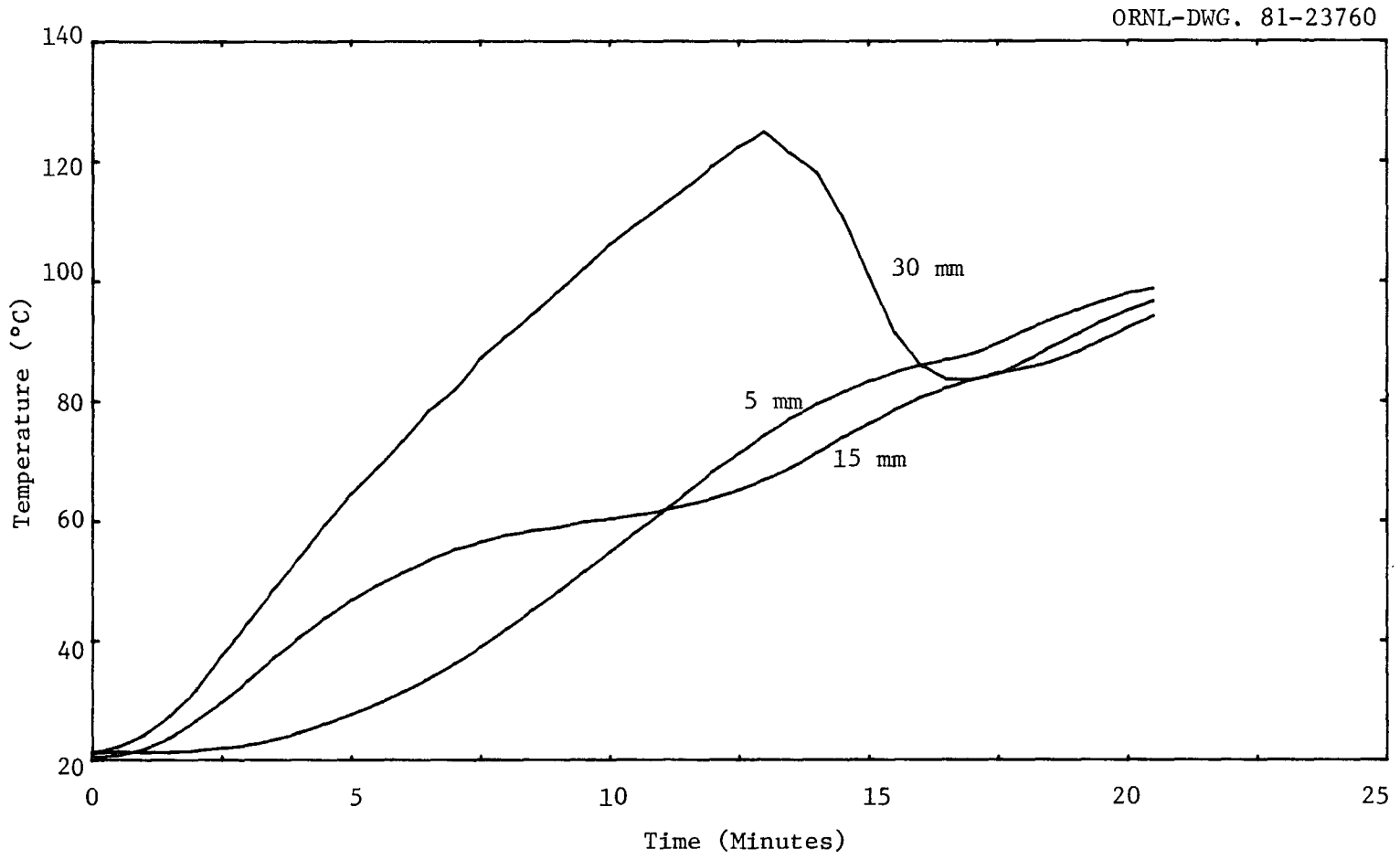

Figure 3.12 Cake Temperature Response, Single-Layer Yellow Cake, Bi-Radiant Oven IV-B.

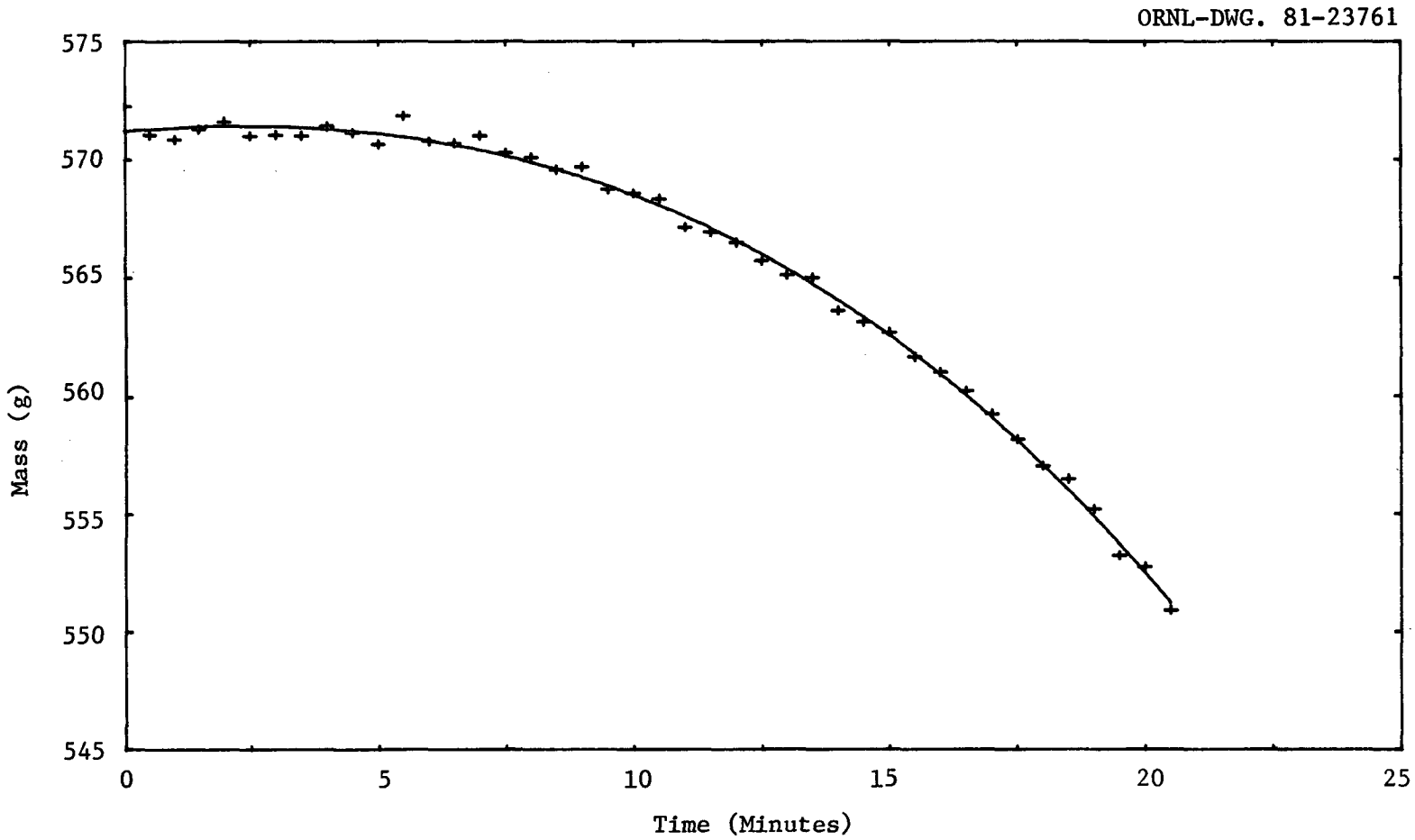

Figure 3.13 Cake Mass Loss, Single-Layer Yellow Cake, Bi-Radiant Oven IV-B.

calculated assuming that the left side wall experienced the same temperature gradient as the right side wall, as was done for Oven IV-A.

Cake temperature and mass loss results for Oven IV-B are presented in Figures 3.12 and 3.13 and were obtained in the same manner as Figures 3.6 and 3.7 for Oven IV-A.

3.2 Efficiency Measurements

The problem of measuring the cavity thermal efficiency for conventional ovens involves three major considerations: first, quantifying the energy absorbed by a food product; second, identifying a "typical" product (mass, shape, absorptivity, initial and final temperature, etc.); and third, identifying "typical oven operating conditions (thermostat setting, preheat conditions, venting conditions, etc.). DOE, in conjunction with the National Bureau of Standards (NBS), have addressed the problem for conventional ovens and have established a standard test block (described in section 2.2.1) to have an initial temperature within $\pm 2.2°C$ of ambient room air temperature and a final temperature rise of 130°C [8]. The oven thermostat was to be adjusted so that the average internal air temperature in an empty oven would be 180.5°C above ambient. This test further specified that the oven was not to be preheated.

This test is directly applicable to the Bi-Radiant oven except for thermostatic operation, therefore, oven efficiency was measured at various power settings. Table 3.1 gives results of these efficiency measurements for Ovens IV-A and IV-B. These values represent the ratio of the energy absorbed by the block to the energy consumed by the

Table 3.1 Overall Cavity Thermal Efficiency, Bi-Radiant Ovens IV-A and IV-B.

Oven	Input Power (W)			Block Temperature Rise (°C)	Test Duration (Minutes)	Efficiency (Percent)
	Upper Element	Lower Element	Total			
IV-A	413	413	826	130.7	54.0	18.24+
IV-A	449	448	897	131.0	49.0	18.55+
IV-A	325	325	650	130.2	59.0	21.15
IV-A	470	470	940	131.4	39.0	22.32
IV-A	1090	0	1090	131.5	33.5	22.42
IV-A	0	2333	2333	134.2	15.5	23.12
IV-B	478	478	956	130.7	47.5	17.92

+No insulation.

elements. The energy absorbed by the block is simply the product of its specific heat, mass, and temperature rise. The energy consumed by the elements was obtained by numerical integration of the input power data using Simpson's rules [10]. The input power was approximately constant as it was for the single-layer cake results. The second, third, and fourth columns of Table 3.1 give the input power conditions which vary from full power at the upper element, to even power, to full power at the lower element. The fifth and sixth columns list the measured block temperature rise and the time to achieve that temperature rise, respectively. Note that the first two lines of Table 3.1 give results for Oven IV-A without the fiberglass insulation.

An alternative method of evaluating the efficiency was based upon the ratio of the rate of energy absorbed by the block to the input power. This rate method allows the calculation of the efficiency at any point in time. Results from each oven are plotted in Figures 3.14 and 3.15 using this method. The rate of energy absorbed by the block was obtained by numerical differentiation of the block temperature data with respect to time using a fourth-order Stirling central difference polynomial [10]. The large variation in the data is due to a loss of accuracy in the numerical differentiation process. Lower efficiencies were expected early in the test when the elements were heating up. Under these conditions, the efficiency remained fairly constant after 15 minutes. The overall efficiency value, as discussed earlier, represents the time average of the instantaneous efficiency.

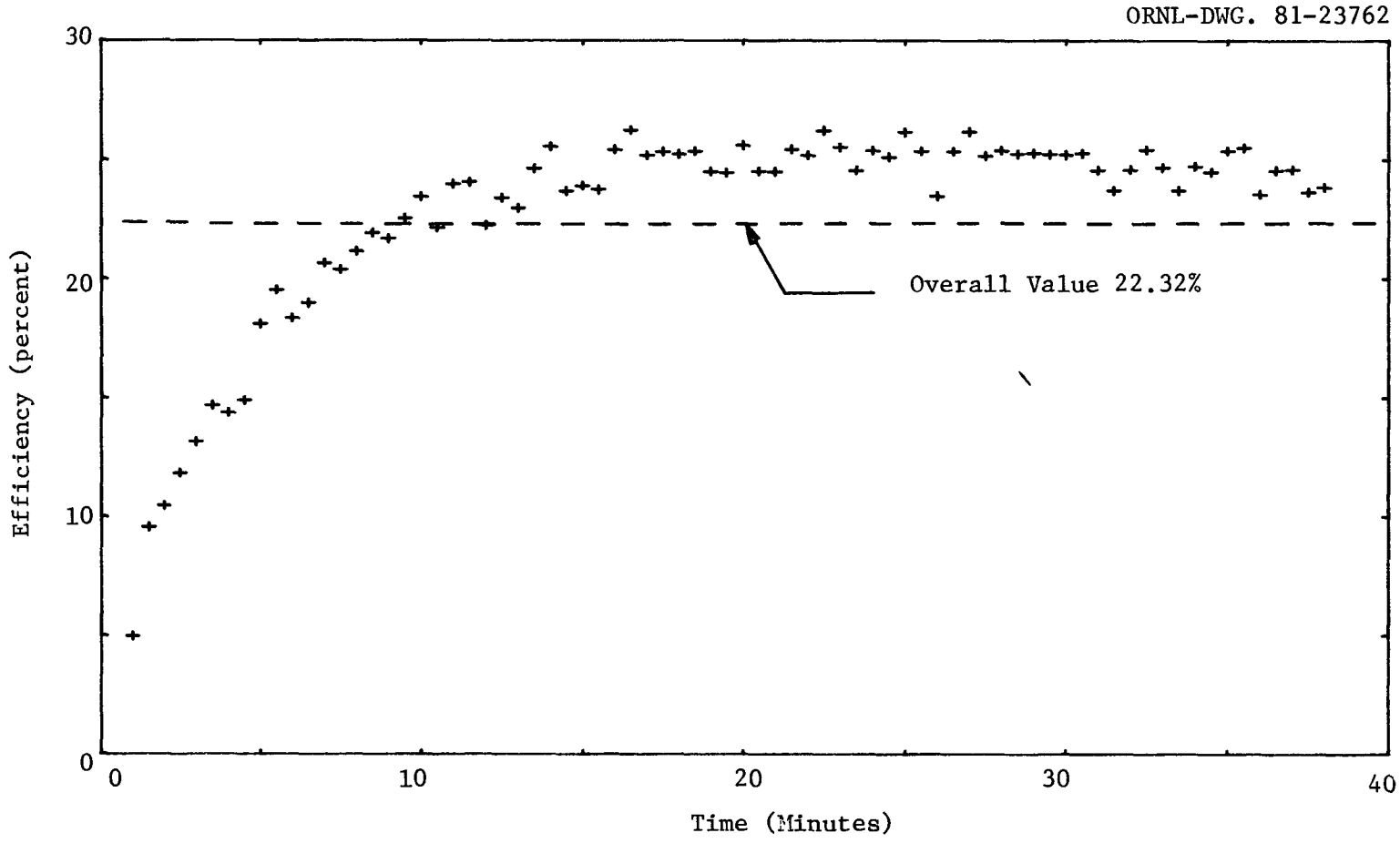

Figure 3.14 Cavity Thermal Efficiency by Rate Method, Bi-Radiant Oven IV-A, 940 W Input Power.

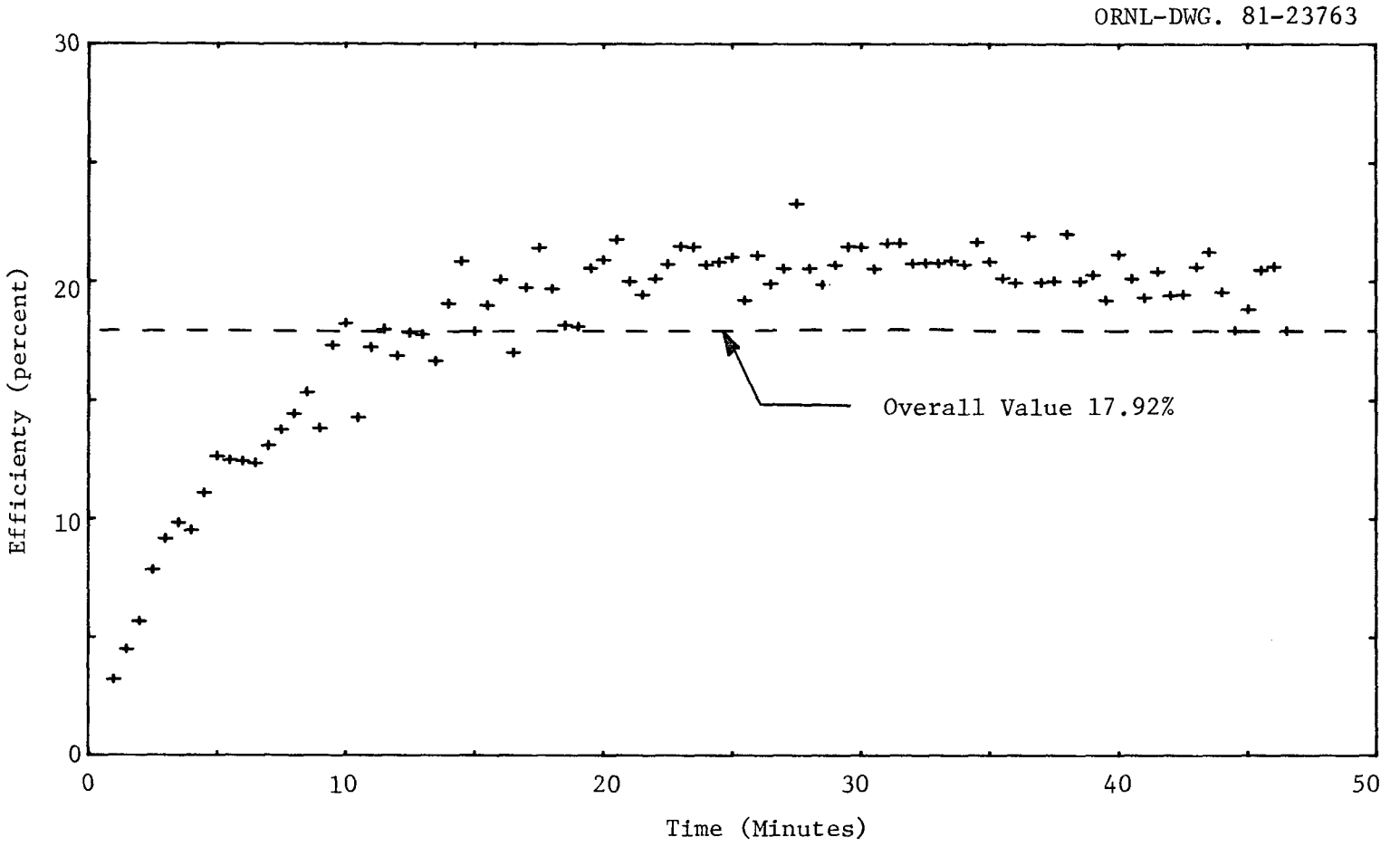

Figure 3.15 Cavity Thermal Efficiency by Rate Method, Bi-Radiant Oven IV-B, 956 W Input Power.

3.3 Heat Loss Analysis

The 940 W and 956 W efficiency tests for Ovens IV-A and IV-B, respectively, Table 3.1, were selected for an energy audit. The energy audit included both a rate method and an overall method as was done for the efficiency analysis. Stored energy in the oven components was estimated from temperature measurement. Heat lost to the environment was determined by correlating the steady-state losses of Oven IV-B at several operating points with the overall temperature difference between the outside covers and the room air. The heat absorbed by the air in the cavity was analyzed by treating the enclosure as a constant pressure, open system. The details of the heat loss calculations are presented in Appendix C.

Table 3.2 and 3.3 summarize the results of the heat loss and efficiency analysis for Ovens IV-A and IV-B, respectively. Results from the rate or power analysis are presented at three times - one near the beginning, middle, and end of the test. Heat losses were determined for eight components. Six of these represent storage losses in each of the major oven components. Results tabulated for the block correspond to oven efficiency. Results tabulated for air losses are the energy to raise its temperature. Loss to the surroundings represents heat lost to the environment from the outer oven structure. The values of the last row give an indication of how accurately the analysis accounted for all the input power/energy. The same numerical differentiation technique used to determine oven efficiency was used to determine the rate of energy absorbed by various oven components. This technique causes a loss of accuracy and reduces

Table 3.2 Summary of Heat Loss Analysis, Bi-Radiant Oven IV-A, Efficiency Test 940 W.

	q/P_{in} (Percent)			Q/E_{in} (Percent)
Component \ Elapsed Time (Min)	2.0	20.0	38.0	Overall
Block	10.45	25.59	23.85	22.32
Inner Cavity	33.70	27.89	15.55	30.49
Insulation	8.58	7.99	4.67	8.40
Rack (Single)	8.25	3.82	2.23	4.98
Cover & Support Frames	0.0	8.30	6.75	5.93
Elements	38.80	1.18	0.59	6.32
Air	1.93	0.62	0.33	0.95
Surroundings	0.91	10.63	27.91	12.08
Totals	102.62	86.02	81.88	91.47

Table 3.3 Summary of Heat Loss Analysis, Bi-Radiant Oven IV-B, Efficiency Test 956 W.

	q/P_{in} (Percent)			Q/E_{in} (Percent)
Component \ Elapsed Time (Min)	2.0	24.0	46.5	Overall
Block	5.69	20.67	17.90	17.92
Inner Cavity	45.34	24.29	9.33	29.99
Insulation	11.62	7.60	3.27	8.39
Rack (Single)	6.82	3.28	1.48	4.12
Cover & Support Frames	0.0	11.89	4.85	6.89
Elements	38.72	0.80	0.23	5.18
Air	1.62	0.53	0.22	0.86
Surroundings	0.90	15.25	47.10	18.54
Totals	110.71	84.31	84.38	91.89

the confidence with which the rate analysis can account for all the input power. Figures 3.14 and 3.15 show approximately a 20% variation in the predicted efficiency which gives an indication of the accuracy of the rate analysis.

3.4 Discussion of Results

The temperature responses illustrated previously result from a constant input power condition. The dominant characteristic of the temperature response of a conventional oven is cyclic behavior about an operating point [11] due to thermostatic control. Harris [11] reports an average thermostat bulb temperature of 189.5°C with a temperature swing of 17°C for a thermostat setting of 177°C (350°F)[8] which is also typical of average wall and air temperatures. In the Bi-Radiant Oven only the upper wall and the adjacent air reached such high temperatures (Figures 3.3, 3.5, 3.9 and 3.11). Large vertical temperature gradients in the Bi-Radiant Oven (Figures 3.3 through 3.5 and 3.9 through 3.11) are caused by the higher input power to the upper element and by stagnation of air against the upper wall.

The cake temperature response (Figures 3.6 and 3.12) shows a reversal of the cake's vertical temperature gradient and is in agreement with Marston [17]. The early positive gradient was expected because of the higher heat rates to the upper surface. The reversal of this temperature gradient appears to be caused by the evaporative cooling occurring near the upper surface. The slow temperature rise of the 15 mm probe after approximately five minutes is likely caused by the rise, of cooler

8 In an empty Whirlpool continuous clean range model RFE 3360 W.

batter to that level. Insufficient data exists to confirm these explanations. These measurements were not taken to enhance the understanding of the baking process, but to provide a quantitative measure for doneness and an intercomparison between various oven operating conditions. For further information concerning the baking process, see Marston [17].

Results from the single-layer cake tests, efficiency tests, and heat loss analyses can be used for comparing the thermal performance of Ovens IV-A and IV-B. For the cake results, the input power levels to the two ovens were changed so as to obtain similar baking performance. A comparison of cake temperatures and mass loss for Ovens IV-A and IV-B (Figures 3.6, 3.7, 3.12 and 3.13) shows that the product responses were similar but not identical. For the efficiency and heat loss comparisons, the input power levels to the two ovens were comparable.

Single-layer cake results (Figures 3.3 through 3.5 and 3.9 through 3.11) show that Oven IV-B reached higher overall air and wall temperatures but was more nearly isothermal than Oven IV-A. The smaller vertical gradients in Oven IV-B were due to the higher input power level to the lower element. As indicated by the higher air temperatures, the convective heat transfer to the walls was positive in both ovens except at the top wall. Comparing the average top wall temperature and the centerline air temperature (at the 38 cm height) responses (Figures 3.3, 3.5, 3.9, and 3.11) shows that the top wall in Oven IV-A had minimal convective heat transfer with the oven air, while the convective heat transfer to the top wall in Oven IV-B was negative.

Efficiency results (Table 3.1) show that the measured cavity

efficiency was relatively insensitive to the power level and power ratio, but as expected, the efficiency was very sensitive to wall surface preparation. Oven IV-B had approximately a 29% lower reflectivity and a 20% lower efficiency than Oven IV-A.

Comparison of the heat loss analyses for Ovens IV-A and IV-B (Tables 3.2 and 3.3, respectively) shows a much faster temperature response of the inner cavity for Oven IV-B even though the final temperature rise was comparable to oven IV-A. The effect of the early wall temperature response can be seen in the greater loss to the surroundings and larger storage losses in the cover and support frames for Oven IV-B. The higher wall emissivity in Oven IV-B improves the radiative coupling between the heating elements and the cavity walls causing element temperatures and storage losses to decrease (assuming identical input power). The heat loss analyses systematically underpredicted the total input power/energy. A possible explanation for this error is that the energy stored in the product weighing system and base plate, located above the oven enclosure, was not included in the audit. No temperature data was taken for the product weighing system and thus its stored energy was neglected in the heat loss analysis.

It should be pointed out that although there was no vent in Bi-Radiant Oven IV, flow out of the oven did occur due to the expansion of the air as its temperature increased, and due to water vapor given off by the cake. The 20 g of water vapor typically lost by a single-layer cake would have a partial pressure of 0.93 atm at 140°C if it were contained in the cavity volume. Some dropwise condensation occurred on the lower corners of the door wall in Oven IV-A, but no condensation was

observed on the sandblasted walls of Oven IV-B. Assuming a homogeneous gas mixture and taking a dew point temperature of 70°C,[9] then the partial pressure of the water vapor in the oven cavity would be 0.31 atm. Thus the total mass of water vapor in the oven enclosure, assuming an average mixture temperature of 140°C, would be 6.9 g. The remaining water vapor must have been lost due to condensation and flow out of the cavity.

For measuring the efficiency of conventional ovens, the DOE test procedures identify an absorptive test block (product) with no preheating. These test procedures are typical of the actual operating conditions of the Bi-Radiant Oven; but are favorably biased toward conventional ovens which typically use reflective utensils in a preheated cavity. In addition, an unrepresentatively higher radiative component exists during the cold start-up transient in conventional ovens which improves the heat transfer to the absorptive test block and biases the efficiency results further. Thus, the efficiency values obtained using the DOE test procedures tend to understate the actual energy consumption of conventional ovens, but should be representative of the actual energy consumption of Bi-Radiant Ovens.

9 Estimate of the final door temperature where condensation occurred in Oven IV-A, Figure 3.5.

CHAPTER 4 - CONTROL SYSTEM

Up to this point, all of the experimental results were obtained under constant input power conditions with the initial temperature of the oven enclosure very near room temperature. These operating conditions yielded satisfactory results under laboratory conditions, but are unreasonable under domestic use, where various initial oven conditions and disturbances (such as opening of the door and placing additional food products in the oven) can be expected. A suitable control system for the Bi-Radiant Oven must handle transient thermal conditions which would occur from a cold start-up, as well as, extended operation for repetitive baking.

4.1 System Variables

The purpose of any control system is to provide the necessary inputs to a system so as to achieve and maintain desired outputs. The electrical power to the upper and lower heating elements are the inputs to the Bi-Radiant Oven and serve as the input or manipulated variables in the control system. The output of the oven on the other hand is not as easily identified. Generally speaking, product quality is the desired output, but it is unsuited as a control variable. By removing the product and the internal baking process from the control loop, the inputs to the product serve as the output of the controlled system. The inputs

to the product are not well defined either. As discussed earlier, these inputs relate to some basic heat and mass transfer parameters. Because of the strong coupling of the overall mass transfer process to the heat transfer process, it seems appropriate to concentrate on the basic heat transfer parameters.

In conventional ovens (and in many other thermal processes as well) a single temperature sensor is used to characterize the overall heat transfer rate to the product. This approach works well when the oven (or furnace) is operated under steady conditions. Then the only variation in the heat transfer rate is due to any cyclical heat source and to the temperature rise of the product. The variation of the upper to lower heat rate is accomplished by selection of utensil. This method is unsuitable for the Bi-Radiant Oven for two reasons. First, one of the more desirable energy saving features of the Bi-Radiant Oven is that the entire oven enclosure does not need to be preheated. This necessitates operation of the oven under transient thermal conditions and a separate temperature sensor is needed to characterize each major heat source (elements, walls, and air). Second, major restrictions are placed on the selection of proper utensils to be used in the Bi-Radiant Oven, thus the variation of the upper to lower heat rate must be accomplished by properly controlling the input power levels to both the upper and lower heating elements.

One possible control scenario for the Bi-Radiant Oven would be to use several temperature sensors to characterize the overall heat rate to the product to control the total input power and then to specify the ratio of the upper to lower input power to allow for different upper and

lower product heat rates. There are two disadvantages to this approach. First, no real savings in terms of hardware is expected (since the same multiple temperature sensors can be used to characterize the heat rate to the upper and lower product surfaces as discussed later) while the basic heat transfer parameters are obscured from the user. The second disadvantage is that a specified input power ratio would not be expected to maintain the same upper to lower product net heat flux ratio under various operating conditions.

For surface heating, the local net heat flux at the product surface completely describes the thermal input to the product. In order to provide desirable product characteristics (crust formation, browning, moisture content, etc.) a uniform net heat flux distribution over the upper and lower product surfaces was assumed to be desirable. Recognizing that the energy requirements of many products will be different on the upper and the lower surfaces (due to moisture loss), the net heat fluxes at the upper and lower product surface were selected as the desired output of the controlled oven system. In using this approach, the thermal requirements of the product side surfaces are assumed to be adequately satisfied by the combined effects of the upper and lower baking environments. The selection of the net heat fluxes at the upper and lower product surfaces as control variables not only gives the user two degrees of freedom, but also provides control of basic heat transfer quantities.

4.2 Methodology

Having identified appropriate input (manipulated) and output (control) variables a suitable control system must be selected. Two major

categories of control systems exist, open and closed loop control systems. In closed loop control systems, the input variable is modified by the actual output to achieve the desired output. In open loop control systems, the input variable is programmed a priori to achieve the desired output. In order for an open loop control system to handle both transient thermal conditions and extended operation of the Bi-Radiant Oven, details of the oven and product initial conditions and transient behavior must be known. A substantial effort would be required to calculate the appropriate value of the manipulated variables as a function of time. Also, any unexpected disturbance (such as opening of the door) would cause the control variable to deviate from its desired level. These disadvantages prohibit the use of an open loop control system on the Bi-Radiant Oven.

In order to close the control loop, the control variables must either be measured or predicted from measurable quantities. The inconvenience, expense, and need of individual calibration of reliable and repeatable heat flux sensors, prohibits the direct measurement of heat flux under practical operating conditions. A suitable heat flux predictor algorithm, based on temperature data, was developed and is presented in Section 4.4.

Direct digital control using a microprocessor provides a convenient means to implement such an algorithm. Once the control variable is generated by the heat flux predictor algorithm, additional calculations must be performed to ascertain the proper control action on the manipulated variables. These additional calculations are referred to as a

digital control algorithm when implemented into a microprocessor. The digital control algorithm is discussed further in Section 4.3 and Appendix D. Direct digital control and the associated algorithms are quite common in process control applications [14, 1]. The introduction of microprocessors made stand-alone, direct, digital control economically feasible [1].

An overall schematic of the control system is given in Figure 4.1. The reference signals are the desired net heat fluxes at the upper and lower product surfaces. These parameters can vary in time and are either supplied by the user or generated by some internal device or auxiliary algorithm. The reference signals are compared to the inferred control variables (feedback signals) which were generated by the heat flux predictor algorithm. Based upon both error signals, the control algorithm specifies appropriate changes to the manipulated (or input) variables which are the input power to the upper and lower elements, and the actuators act on the power supplies to achieve these changes. The product is considered as part of the controlled system because it is the interaction of the oven and product which generates the output (net heat fluxes). Should the selection of various products have a major effect on the overall response of the oven, the coefficients in either or both of the control and heat flux predictor algorithms can be modified to obtain satisfactory control performance. A limited number of temperature sensors provide information to the heat flux predictor algorithm about the temperature response of the major heat sources (elements, walls, and air).

ORNL-DWG. 81-23764

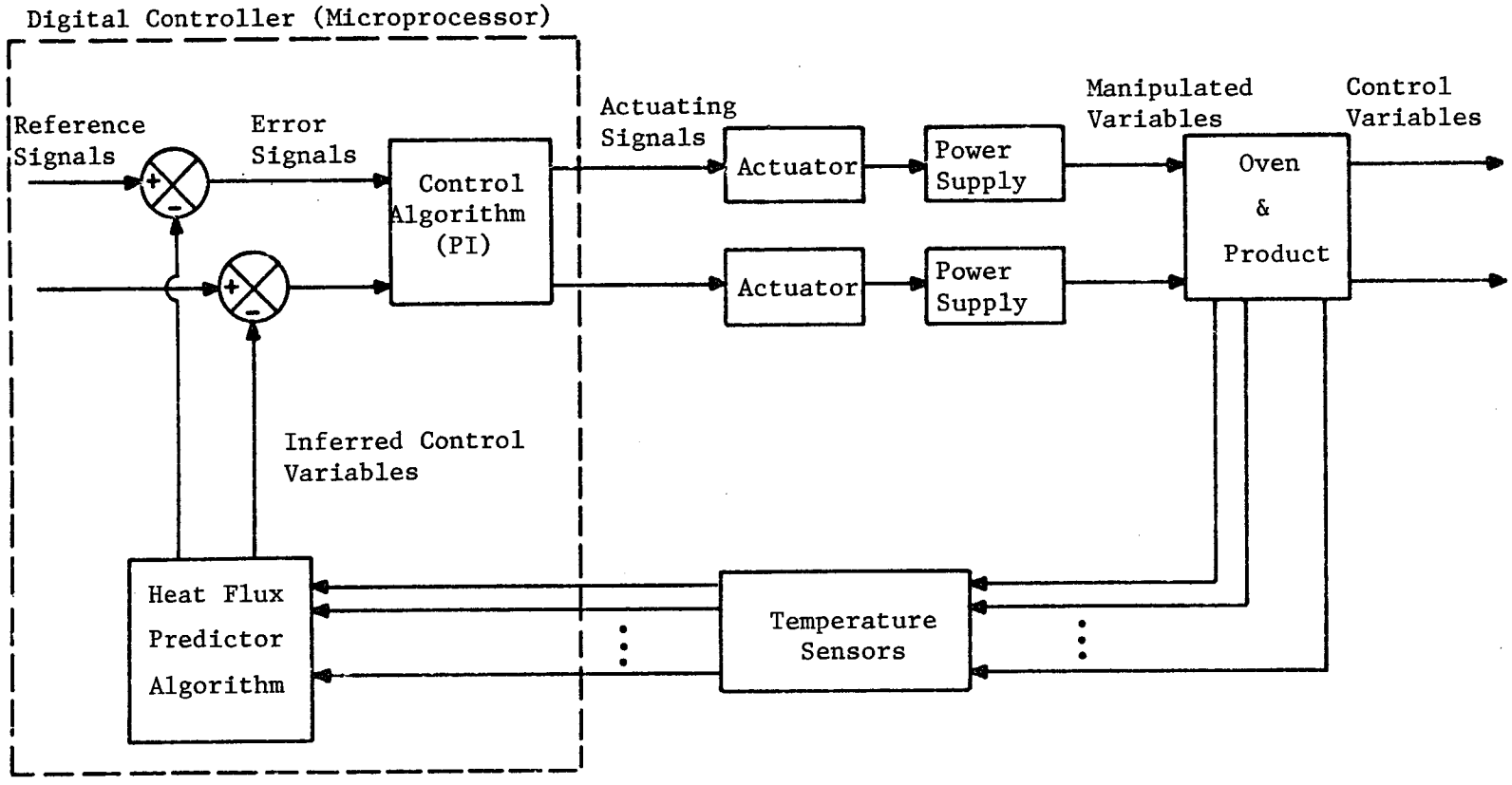

Figure 4.1 Schematic of the Digital Control System for the Bi-Radiant Oven.

4.3 Digital Control Algorithm

Many digital control algorithms have been developed. The most common algorithms are a discretized version of the classical proportional-integral-derivative (PID) analog controller [1]. The purpose of this study was to demonstrate the ability of a microprocessor based controller, using the heat flux predictor algorithm, to properly control the input power levels to the Bi-Radiant Oven. For this reason a proportional-integral (PI) digital control algorithm was selected for its simplicity and ease of operation. No attempt was made to optimize this algorithm. The details of the control algorithm are given in Appendix D. Derivative control was not implemented because of errors that occur in the numerical differentiation process.

This control algorithm operates in a velocity mode where an incremental change in the manipulated variable is calculated for every time step. It also operates under the PI control mode over all error bands (rather than branched PI modes where integral control may be disabled outside a certain error band, as was done by Jacobs and Donaghey [14]). An additional feature was added to the control algorithm which set the incremental change in either manipulated variable to zero whenever its magnitude fell below a certain value. This is similar to deadbanding used in process control [4], where the error signal is "deadened" rather than the manipulated variable. The purpose of this feature is simply to avoid over-control and control response to noise. Each heating element not only affects the net heat flux at the adjacent product surface but also the opposite surface through reflections. For this reason, the PI digital control algorithm was modified to couple the response of both

control variables, rather than operate as dual independent control loops.

4.4 Heat Flux Predictor Algorithm

The purpose of the heat flux predictor algorithm is to predict the net heat flux at the upper and lower surfaces of a food product from temperature data. Since it is to be incorporated into a microprocessor based digital controller with very limited memory and computational capabilities, it must be a simple algorithm. Iterative calculations, transcendental equations, etc. are therefore undesirable. Compromises between accuracy and computation speed must be carefully considered.

4.4.1 Analytical Development

The analytical development of the heat flux predictor algorithm was considered in two parts - the net radiative and the convective heat fluxes. The net radiative heat flux was treated using a simplified enclosure analysis with six nodes as shown in Figure 4.2. The usual assumptions of gray, diffuse, isothermal surfaces with uniform irradiation give conditions under which this analysis is exact. The convective heat flux was treated using simplified standard horizontal flat plate correlations for air.

A detailed derivation of the heat flux predictor algorithm is presented in Appendix E and has the final form (equations E.28 and E.29)

$$q''_{net,3} = a_3T_1^4 + b_3T_2^4 + c_3T_6^4 + d_3T_p^4 + h_3(T_A - T_p) \qquad (4.1)$$

ORNL-DWG. 81-23765

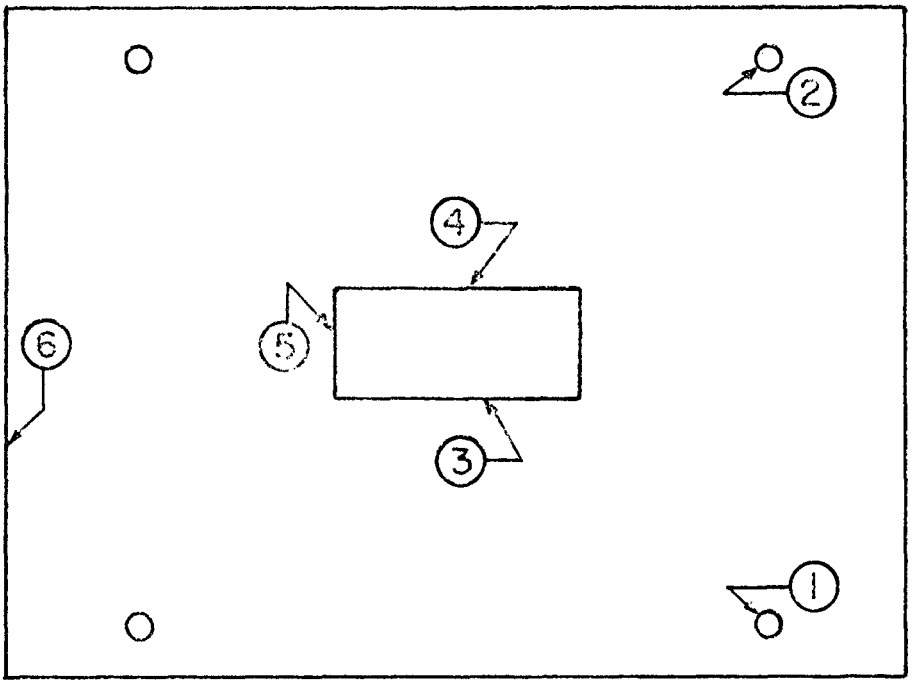

1, Lower Element

2, Upper Element

3, Lower Product Surface

4, Upper Product Surface

5, Side Product Surface

6, Cavity Walls

Figure 4.2 Node Designation for Radiative Enclosure Analysis Used in the Heat Flux Predictor Algorithm.

$$q''_{net,4} = a_4T_1^4 + b_4T_2^4 + c_4T_6^4 + d_4T_p^4 + h_4(T_A - T_p) \tag{4.2}$$

where T_A is a characteristic air temperature, T_p is a characteristic product temperature, the subscripts 1, 2, 3, 4 and 6 represent values associated with the lower element, upper element, lower product surface, upper product surface and walls, respectively; h_3 and h_4 are the convection coefficients for the lower and upper product surfaces, respectively; and are given by equations E.26 and E.27. The coefficients a, b, c, and d are constants which resulted from the radiative enclosure analysis and depend on surface properties and geometry (equations E.15 through E.22). Physically, the terms in equations 4.1 and 4.2 can be considered as contributions to the net heat flux due to emission from the lower element, upper element, walls, and product and due to convection.

4.4.2 Experimental Validation

The net heat flux predictor algorithm must predict the heat flux trends under all oven operating conditions with reasonable accuracy. To verify the accuracy of the predictor algorithm, the water-cooled heat flux gage was placed in the oven during a cold start-up transient and the output from the gage was compared to predictions based upon the heat flux algorithm.

Two tests were performed with the gage oriented horizontally, one with the sensors viewing up and the the other with the sensors viewing down. For both of these tests the center of the heat flux gage was

located 25.4 cm (10.0 in) from the back wall, 39.4 cm (15.5 in) from the left side wall, and 22.7 cm (8.9 in) from the bottom wall. The thickness of the gage was neglected, thereby reducing the number of surfaces in the enclosure to five (delete the fifth node of Figure 4.2). The gage was placed to the right of center to avoid shadowing by the air temperature probes. Table 4.1 gives the view factor matrix for this configuration. The view factors from each element to itself and to each other were assumed to be zero. The view factors from each element to the facing gage surface were calculated by the method given by Scheitlin [19]. The remaining non-zero view factors were calculated using view factor algebra.

Before calculating the total exchange factors, which are needed to evaluate the coefficients of the heat flux predictor algorithm, surface properties must be identified. The validation experiments were implemented in Oven IV-B. The emissivity of the wall material was reported in section 2.1. Two values (from two samples) were given, 0.30 and 0.32 both with an uncertainty of ±0.02. An average value of 0.31 with an uncertainty of ±0.03 was taken in this test. The total emissivity of a typical section of element material was measured[10] to be 0.91 near 600 ^{o}C. The emissivity of the chrome plated baseplate of the heat flux gage was estimated to be 0.12. Using these values, the total exchange factors were calculated by matrix inversion according to equation E.5 and are given in Table 4.2.

10 The measurements were made on the multiproperty apparatus located in the Thermophysical Properties Research Laboratory, School of Mechanical Engineering.

Table 4.1 View Factor Matrix for Validation Experiments with the Heat Flux Gage.

i \ j	1	2	3	4	6
1	0.0+	0.0+	0.003462†	0.0	0.996538
2	0.0+	0.0+	0.0	0.003916†	0.996084
3	0.04343	0.0	0.0	0.0	0.95657
4	0.0	0.04912	0.0	0.0	0.95088
6	0.03261	0.03260	0.002496	0.002481	0.929810

+Assumed zero.

†Calculated by Program OVENRAD; see Schietlin [19] or Section 2.2, Part 1, this report.

Table 4.2 Total Exchange Factor Matrix for Validation Experiments with the Heat Flux Gage.

i \ j	1	2	3	4	6
1	6.431×10^{-2}	6.417×10^{-2}	8.379×10^{-3}	4.890×10^{-3}	2.844
2	6.417×10^{-2}	6.434×10^{-2}	4.917×10^{-3}	8.806×10^{-3}	2.843
3	1.051×10^{-1}	6.167×10^{-2}	4.739×10^{-3}	4.700×10^{-3}	2.733
4	6.134×10^{-2}	1.105×10^{-1}	4.700×10^{-3}	4.692×10^{-3}	2.718
6	9.306×10^{-2}	9.305×10^{-2}	7.130×10^{-3}	7.091×10^{-3}	2.674

In completing the calculation of the heat flux predictor coefficients (equations E.15 through E.22) it should be recognized that the absorptivity (or emissivity) of the heat flux sensor should be used for the values of α_3, ε_3, α_4, and ε_4 rather than the emissivity of the chrome plated base plate which was used in the calculation of the total exchange factors. The reason for the distinction is that in the latter case the interaction of the gage as a whole is being treated, while in the former case, the net heat flux at a specific location (the heat flux sensor) is being predicted. This simply assumes that the presence of the sensors on the base plate has no effect on the irradiation. In fact, because of its size, the entire gage has very little effect on the irradiation.

Specifications for the heat flux gage are given by Scheitlin [19]. The emissivity of the black sensor was reported to be 0.95 with an estimated uncertainty of ±0.03. His calibration indicates a sensitivity of 63.45 ± 5.06 W/m^2-mV for the black sensor. The same calibration also indicates that the polished sensor was 1.768 times as sensitive as the black sensor. Using a baseline sensor emissivity of 0.95 and the total exchange factors of Table 4.2, the coefficients of the heat flux predictor algorithm were calculated as given in Table 4.3.

For comparison purposes, only the radiative component of the net heat flux at the surface of the blackened sensor was considered. The total net heat flux was not compared because of the possible addition or cancellation of errors due to the empirical treatment of convection in the heat flux predictor algorithm. The gage temperature was measured by a single (30 gauge, glass wrap) copper-constantan thermocouple placed in

Table 4.3 Coefficients of the Heat Flux Predictor Algorithm for Validation Experiments with the Heat Flux Gage.

Coefficient	Value $(W/m^2\text{-}K^4)\times10^{-9}$
a_3	5.1509
b_3	3.0223
c_3	45.621
d_3	-53.794
a_4	3.0063
b_4	5.4134
c_4	45.375
d_4	-53.795

a hole drilled into the water cooled base plate. Element temperatures were taken to be the average of the two element thermocouples. An area weighted average of the 20 wall thermocouples was used to characterize the wall temperatures.

Figure 4.3 shows the response of the net radiative heat flux on the black sensor as measured by the heat flux gage and as predicted by the heat flux predictor algorithm. These results were obtained under constant input power conditions (1040 W upper and 64 W lower element) with the gage facing directly up. The shaded region above and below the measured results represents the uncertainty in the gage results based on the specified uncertainty in the emissivity and sensitivity of both sensors.[11] The gage uncertainty reduces to ±8.8% of reading. The shaded region above and below the predicted results represents the uncertainty in the predictor algorithm based on the uncertainty of the emissivity of the walls and the blackened sensor and remains less than ±8% of reading after one minute. Figure 4.4 gives similar results for the gage facing directly down. The shaded region through the measured results again represents the ±8.8% uncertainty in the gage results based on the uncertainty in the emissivity and sensitivity of both sensors, but was generated about a least squares cubic fit of the measured data rather than the actual data. The uncertainty of the predicted results in this case was less than ±14% after one minute. For this test, the input power was again constant with 1025 W to the upper element and 64 W to the lower element. Clearly, the indicated uncertainty band does not account for the large variation in the measured result, which appears to be caused

11 Uncertainties were propagated using the single sample uncertainty method [15].

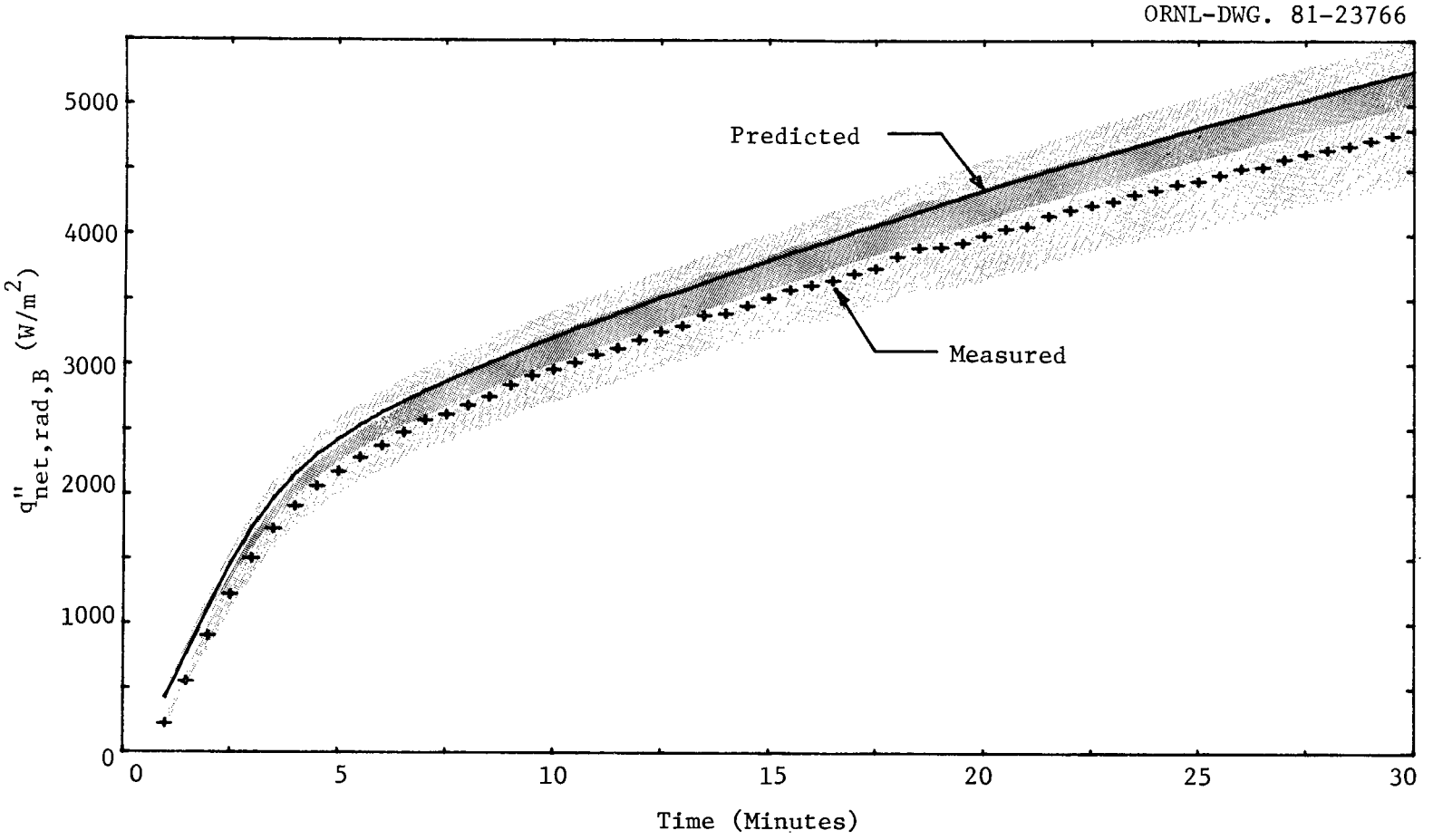

Figure 4.3 Comparison of Predicted and Measured Net Radiative Heat Flux, Gage Viewing Up.

ORNL-DWG. 81-23767

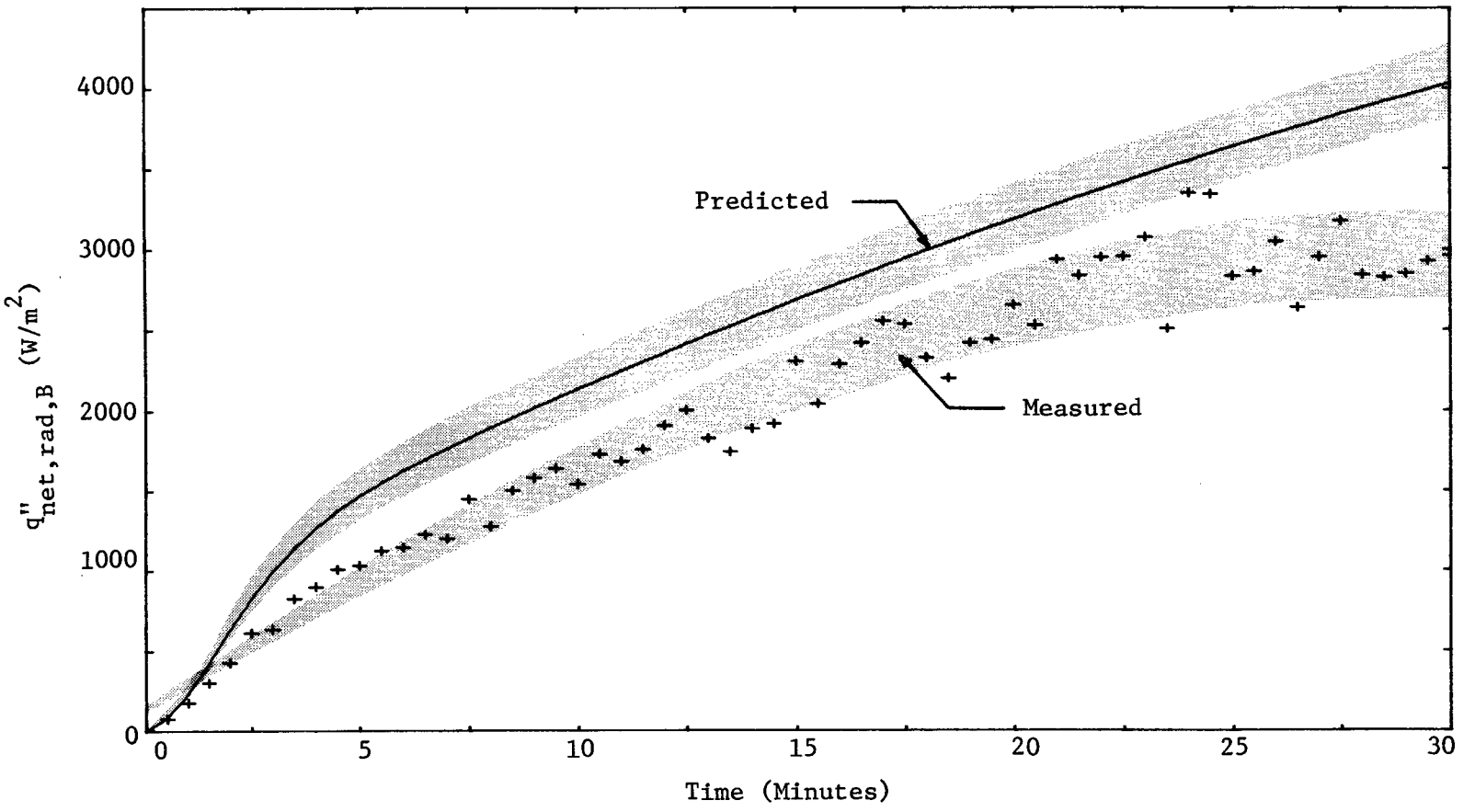

Figure 4.4 Comparison of Predicted and Measured Net Radiative Heat Flux, Gage Viewing Down.

by local variations in the convective heat flux on the lower gage surface as discussed in Appendix A. In both tests the heat flux gage was supported by the oven rack from its back side to avoid any possible interference from the rack on the heat flux sensors.

The agreement between the predicted and measured results of Figure 4.3 is very good, better than 9%. The erratic convection phenomenon on the lower surface, which apparently caused the larger variation in the measured results, may also be responsible for the larger disagreement between the predicted and measured results of Figure 4.4. The ability of the heat flux predictor algorithm to accurately predict the cold start-up transient is a good indication that the algorithm accurately accounts for all the important radiative heat transfer mechanisms and can thus be expected to perform satisfactorily under all oven operating conditions.

4.5 Performance Evaluation

In order to evaluate the performance of the control system in conjunction with the Bi-Radiant Oven, the control algorithm and the heat flux predictor algorithm were implemented into the software of the data acquisition system. The calculator served as the Digital Controller of Figure 4.1. The calculator was programmed to print out the input power in terms of the voltage output of the watt transducers. The Powerstats were manually adjusted until the output of the watt transducers matched the print out from the calculator. The data logger and calculator operations were set to minimize the time delay between data scan and print out of the new power settings. This time delay was approximately

7 seconds and the scan interval was 30 seconds. This approach was selected in lieu of a fully automatic system because of its simplicity of implementation, and yet, could still serve to demonstrate the ability of the control system.

Two major tests were run to demonstrate the ability of the control system to handle both thermal transients at cold start-up and extended operation for repetitive baking, as well as, recover from a door opening and prevent overheating when the oven is accidentally left on. Both the DOE test block and a series of single-layer yellow cakes were baked under controlled input power in Oven IV-B. For both of these tests a constant net heat flux was specified for lack of information concerning desirable heat fluxes to food products.

The coefficients of the heat flux predictor algorithm were calculated by the same method used in section 4.4.2, except that the view factors were based on the DOE test block located in the center of the oven cavity. The view factors to each of the three product surfaces (Figure 4.2) were again calculated by the method given by Scheitlin [19]. The product emissivity was also taken to be 0.95 on all three surfaces. The wall emissivity was based on the preliminary value of 0.35 for lack of the more accurate results at the time of the experiment. Again an element emissivity of 0.91 was used. Based on these values the coefficients of the predictor algorithm were calculated as given in Table 4.4. These values, although based on the DOE test block, were also used for the single-layer cake tests since they are intended to represent a typical product geometry.

Table 4.4 Coefficients of the Heat Flux Predictor Algorithm for Controller Performance Evaluation.

Coefficient	Value $(W/m^2\text{-}K^4) \times 10^{-9}$
a_3	5.1734
b_3	2.2643
c_3	42.510
d_3	-49.948
a_4	2.2643
b_4	5.1734
c_4	42.510
d_4	-49.948

As in section 4.4.2 the element temperatures were taken to be the average of the two thermocouples and the wall temperature was taken to be an area average of the 20 wall thermocouples. The air temperature was taken to be the average of the centerline thermocouples at the 27 and 38 cm elevations, thermocouples A4 and A6 of Figure A.5. Since practical operation of the oven will generally prohibit the use of a product temperature sensor, the product temperature, which is needed in the heat flux predictor algorithm, was predicted from an auxiliary algorithm where the user supplies additional input data. This auxiliary algorithm predicts the product temperature at any time in the baking process by assuming a linear temperature response. The product temperature algorithm is given by

$$T_p(t) = \begin{cases} T_i+(T_f-T_i)\frac{t}{t_f}, & t \le t_f \\ T_f, & t > t_f \end{cases} \tag{4.3}$$

where T_i, T_f, and t_f are the estimated initial and final product temperatures and baking time, respectively, and are all supplied by the user a priori, and t is the elapsed time from the start of baking. A maximum product temperature is necessary to prevent a runaway condition which would occur if the controller attempted to provide constant net heat flux to an (imaginary) object whose temperature continued to rise indefinitely, as would occur if the oven was accidentally left on after baking. In addition to the product temperature information, the heat flux predictor algorithm also needs the characteristic length of the product to calculate the convection coefficient on the upper and lower surfaces.

Results from the controlled baking test using the DOE test block are presented in Figures 4.5, 4.6 and 4.7. The oven and block were initially at room temperature. The output of the heat flux predictor algorithm during the test is plotted in Figure 4.5. The user-specified inputs are listed with Figure 4.5, where r_3 and r_4 are the desired net heat fluxes at the lower and upper product surfaces, respectively, and are plotted as dashed lines. Start-up was initiated by the step change in these parameters, which caused the input power to both elements to switch to their full power condition as shown in Figure 4.6. As the net heat flux on the lower surface approached its set point the power to the lower element decreased. The set point value for the lower surface was maintained for the short period until the lower power was switched off. At this point the controller reached a physical constraint in the manipulated variable and the set point could no longer be maintained. This phenomenon demonstrates the limitation of the Bi-Radiant Oven to generate large disparities in the net heat fluxes to the upper and lower surfaces of products. After this point essentially 100% of the input power went to the upper element. The lower element was reactivated only during the recovery periods after the door was opened for 20 seconds at an elapsed time of 45 minutes and at 60 minutes to remove the block from the oven. After the initial transient the net heat flux at the upper surface closely followed its set point and quickly recovered from the door and product removal disturbances. The oven was left on for an hour after the block was removed to demonstrate the overheat and runaway prevention capability of the control system. Note that once the block was removed, less power was needed to maintain the same baking environment.

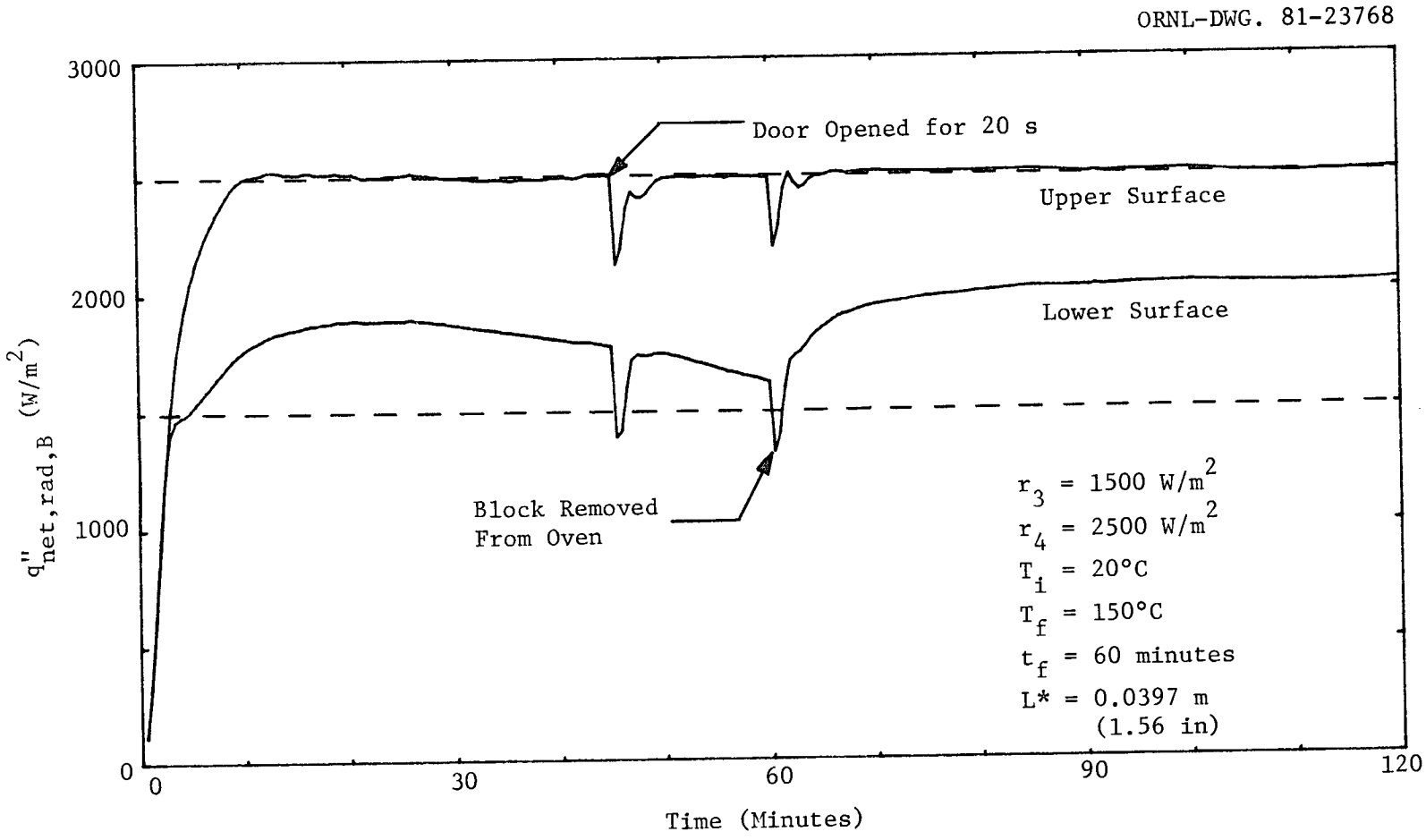

Figure 4.5 Controller Response - DOE Test Block.

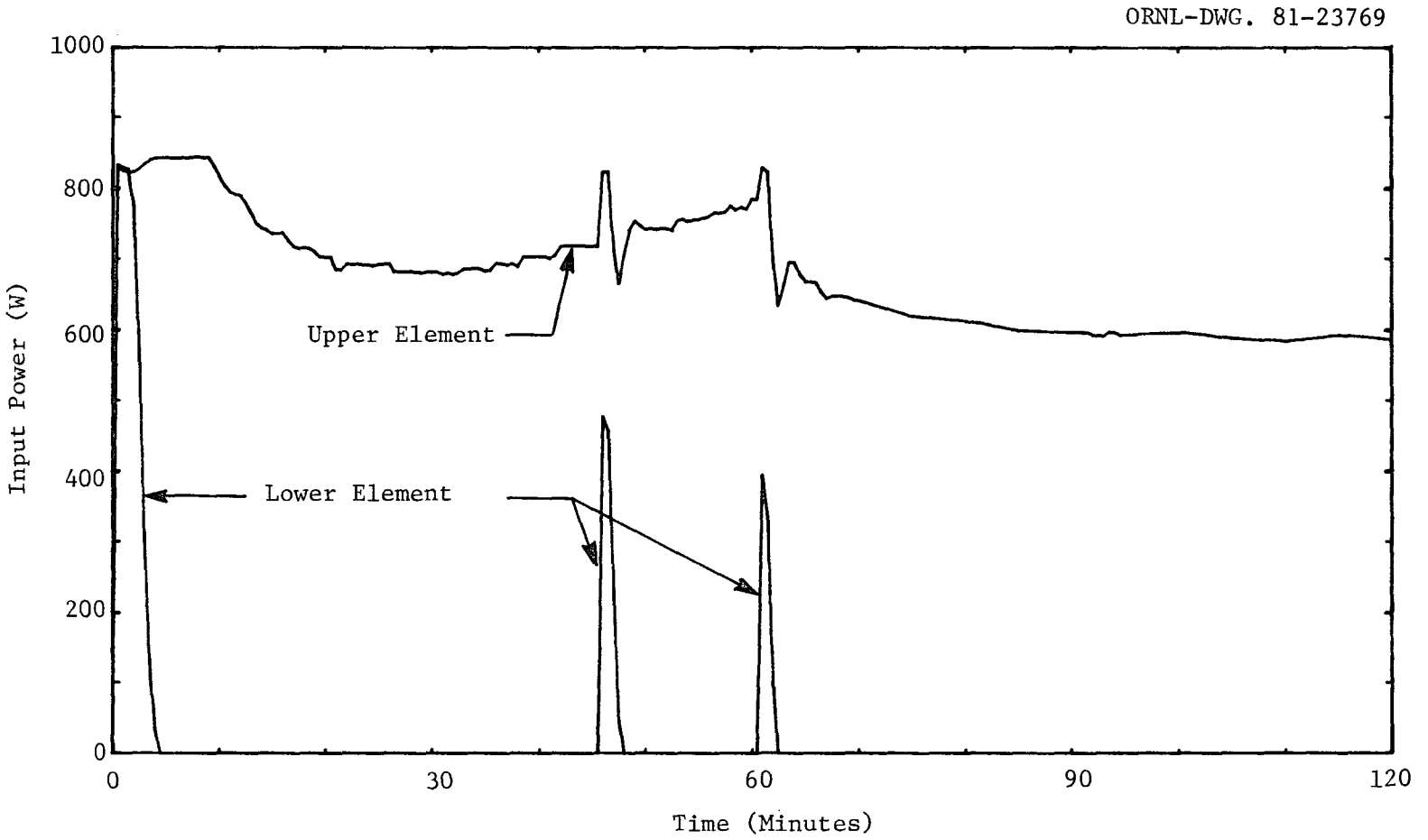

Figure 4.6 Controlled Input Power - DOE Test Block.

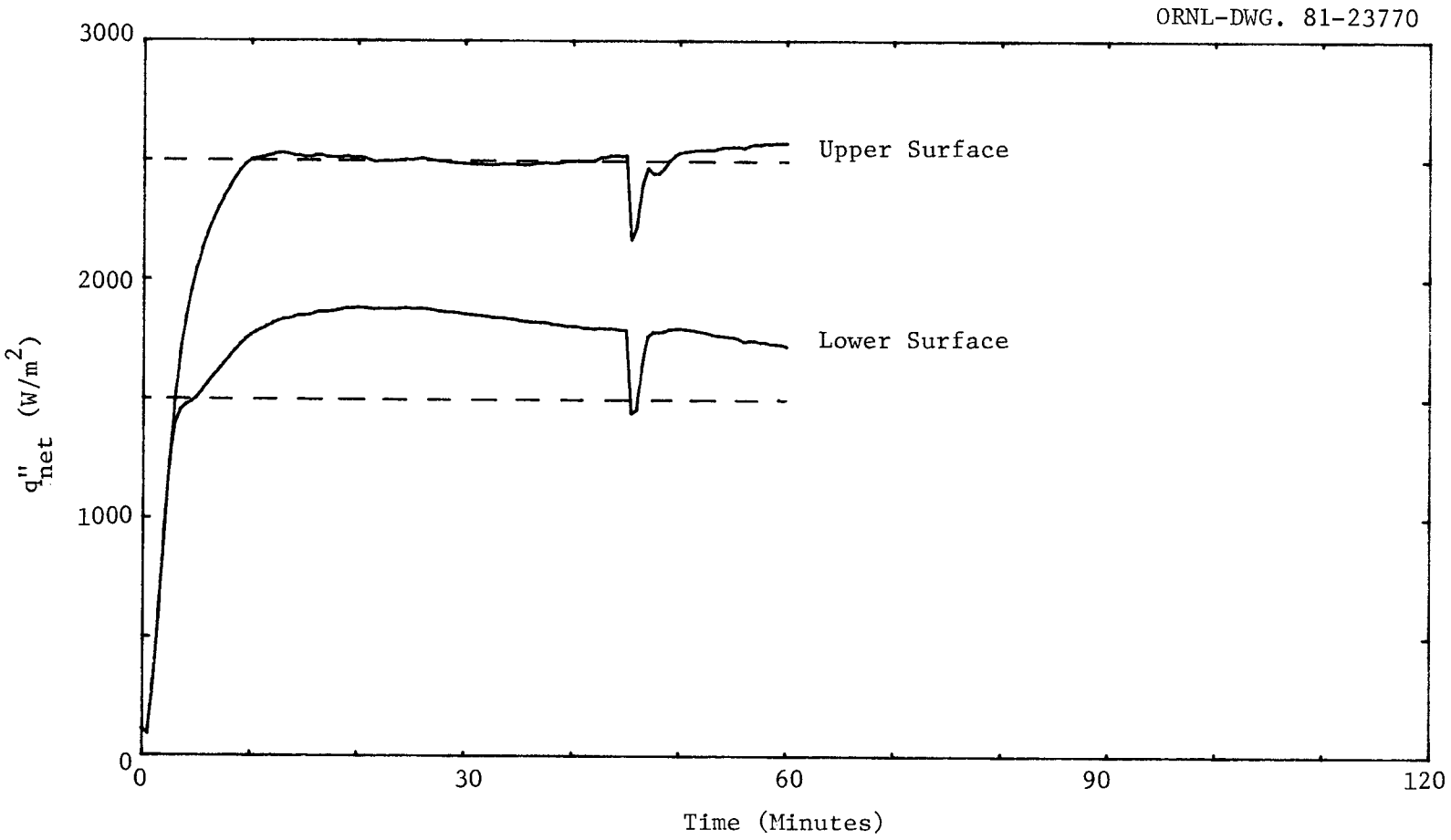

Figure 4.7 Net Heat Flux Predictions Based on Block Temperature Data.

As a matter of comparison, the output of the net heat flux predictor based on the actual block temperature data, rather than the prediction of equation 4.30, is given in Figure 4.7. These curves closely follow those of Figure 4.5 and indicate that, at least for this case, the errors caused by predicting the product temperature were minimal.

To contrast the controlled response, the DOE test block was also baked under constant input power conditions. Figure 4.8 gives the output of the net heat flux predictor for the case of 705 W to the upper element and the lower element off. Again the oven and block were initially at room temperature and the door was opened for 20 seconds at an elapsed time of 45 minutes and again at 60 minutes to remove the block from the oven. Although the net heat flux reached the same levels as the controlled case, the response was significantly slower. Also the recovery from the door disturbance was much poorer. The predicted net heat fluxes rose to much higher levels after the block was removed because the input power was not reduced as it was in the controlled case. The same prediction of block temperature used in the controlled case (Figure 4.5) was also used to plot the lower curve for each surface in Figure 4.8. Because of the slower oven response for the constant input case, the block temperature did not rise as quickly and the predicted block temperature was systematically high, causing the divergence of both sets of curves on Figure 4.8. Thus the control system improves the oven start-up response and recovery from disturbances as well as providing overheat protection when the oven is accidentally left on.

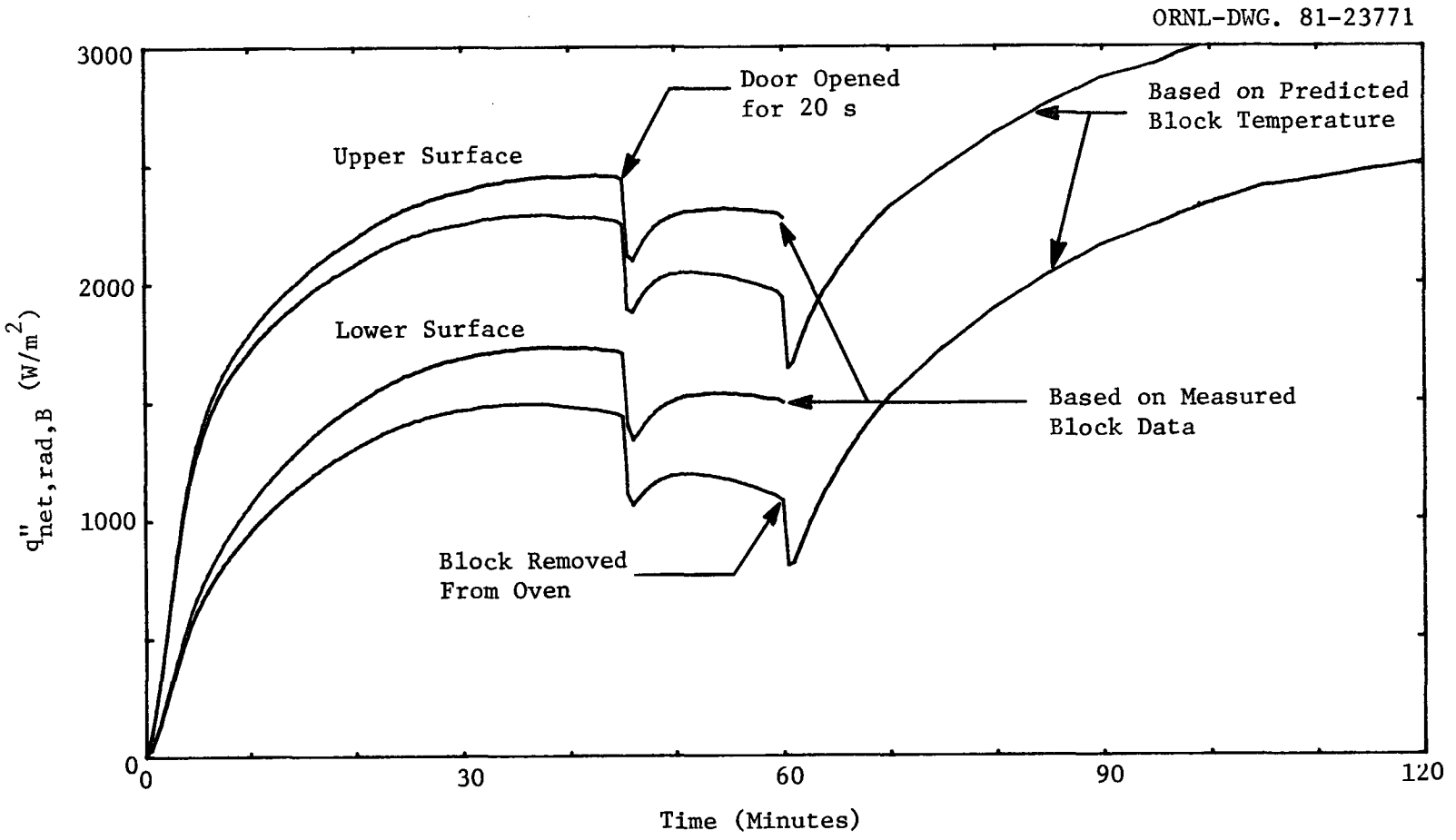

Figure 4.8 Net Heat Flux Predictions for Constant Input Power - DOE Test Block.

As a final test of the control system, a food demonstration was prepared where a series of three single-layer yellow cakes were baked successively. The purpose of this demonstration was not to show that the Bi-Radiant Oven could bake cakes (which has already been established) but to show that the control system could successfully maintain a suitable baking environment for repetitive baking.

The desired net heat fluxes were selected to be 1800 and 2500 W/m^2 on the lower and upper surfaces respectively. These values were based on the constant power results of section 3.1. Data was again scanned every 30 seconds. When a new cake was inserted, the product temperature algorithm was reinitialized to calculate the elapsed time from the next data scan. The baking time of the three successive cakes were 21.7, 18.1, and 20.4 minutes, respectively. These values are based on a minimum done temperature (as measured by the three cake thermocouples) of 93^oC. All three cakes were of satisfactory quality with the second cake having a darker appearance than the other two.

The output of the heat flux predictor algorithm during the repetitive cake tests is plotted in Figure 4.9. Again the user-specified inputs are listed with the figure and the set points are indicated by dashed lines. Each of the three sets of curves correspond to a single cake. The abscissa represents the actual elapsed time from cold start-up. As with the DOE test block, the controller initially switched both elements on at full power as shown in Figure 4.10. The upper element remained at full power for approximately 12 minutes until the net heat flux approached its set point. The apparent disturbance in the net heat fluxes at 20 minutes was caused by the product temperature predictor

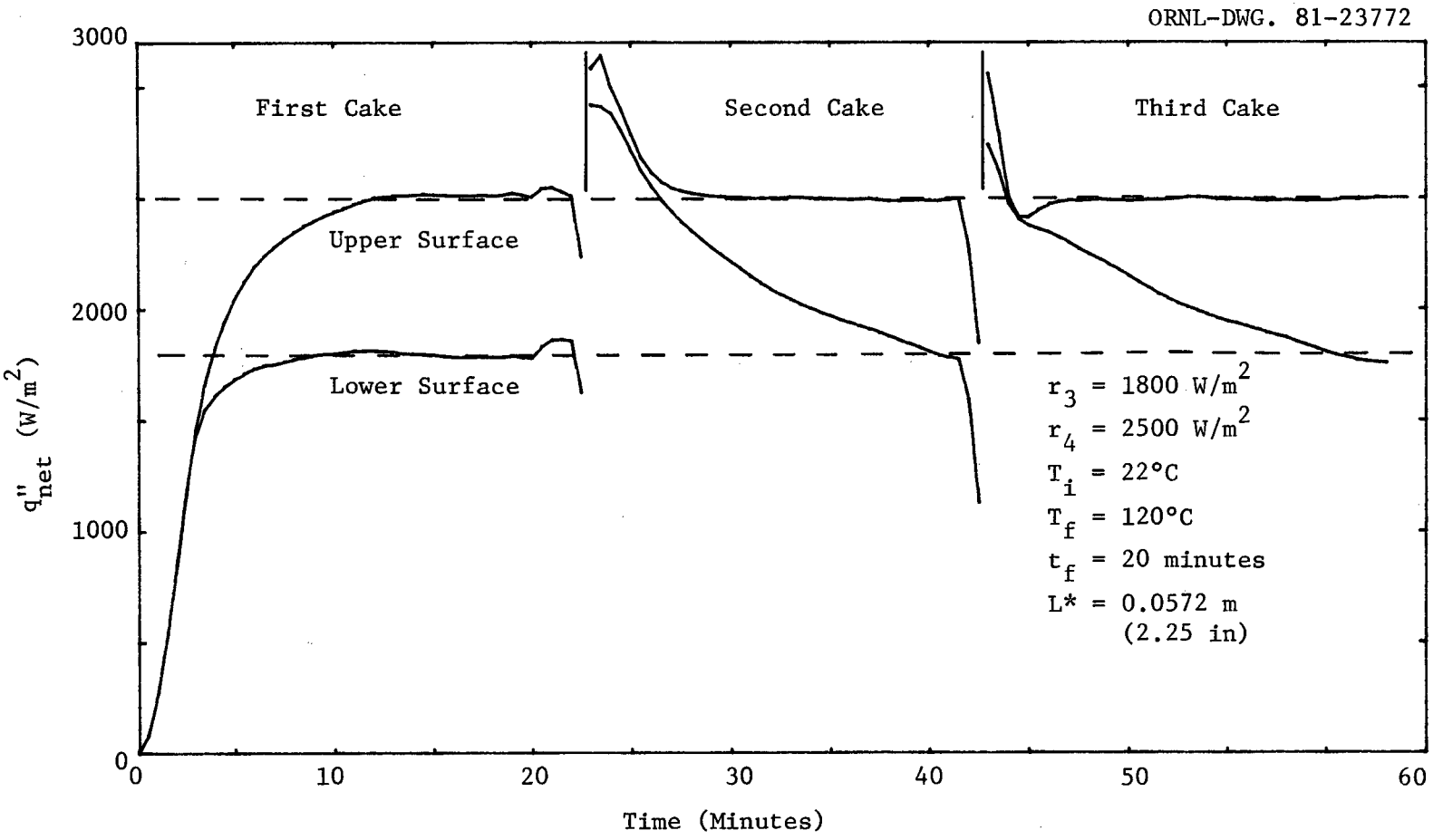

Figure 4.9 Controller Response - Repetitive Cakes.

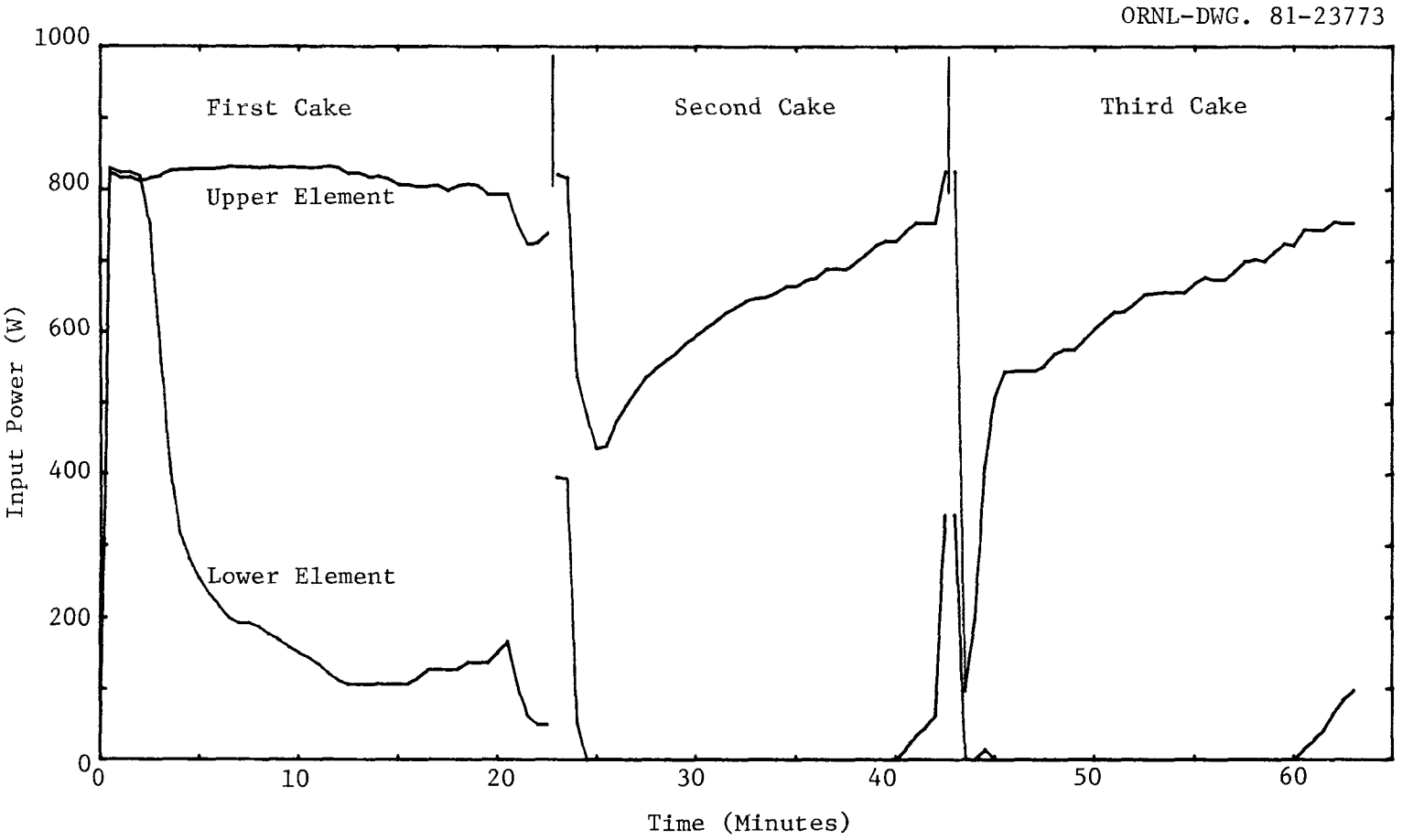

Figure 4.10 Controlled Input Power - Repetitive Cakes.

algorithm reaching its estimated done time, thus causing the predicted product temperature to remain at the final value of 120°C. The decrease in the net heat fluxes at 22 minutes was caused by the opening of the door. When the controller sensed this decrease, the input power to both elements was increased. By the next data scan, the second cake was in place and the net heat fluxes drastically increases because of the lower product temperature. This caused the input power to the lower element to be switched off and the upper element to be greatly reduced. The lower element remained off until late into the baking period when the net heat flux had reached its set point. Again the decrease in the net heat fluxes at 41.5 minutes was caused by the opening of the door. The response of the third cake was similar to the second cake except that the net heat flux at the upper surface recovered faster. This faster recovery was caused by a greater reduction in the input power to the upper element as shown in Figure 4.10. The greater reduction in the input power occurred because of the lower net heat fluxes at the end of the second cake, causing the controller to sense a much faster increase in the (apparent) net heat flux and thus take more drastic control action. This effect can be clearly seen by noting the effect of a sudden decrease in the error signal on the controller algorithm given by equations D.5 and D.6.

Comparing the element temperature response of Figure 4.11 with the input power of Figure 4.10 shows that relatively large fluctuations in the input power were needed to overcome the thermal mass of the elements. The element temperature response during the first cake run can be compared to the constant input power case of Figure 3.8. The upper

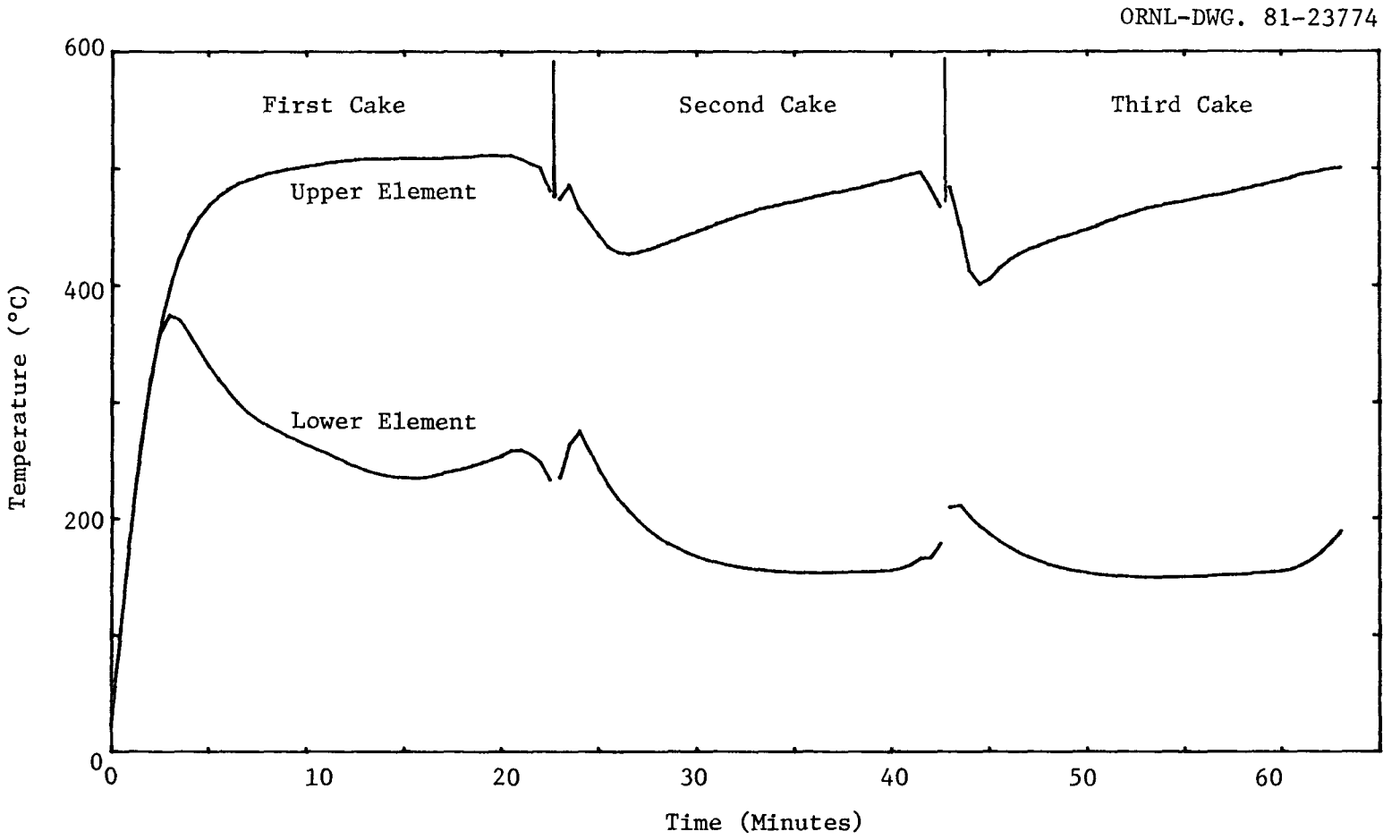

Figure 4.11 Element Temperature Response - Repetitive Cakes.

element response was similar in both cases but the lower element response was much faster under controlled input. The cake temperature response of all three cakes is given in Figure 4.12. The response of the first cake was very similar to the constant input power case of Figure 3.12. The second and third cakes have similar responses which were much faster early in the baking periods due to the higher net heat fluxes as seen in Figure 4.9. The higher initial temperature of the third cake was probably due to a longer interval between the time the cake was inserted and the initial data scan.

Each term in the heat flux predictor algorithm for the lower product surface is plotted separately in Figure 4.13. The results have been presented this way to recognize the effect of each heat source on the net heat flux. The five curves on Figure 4.13 are labeled by their corresponding term in the heat flux predictor algorithm of equation 4.1 in section 4.4.1. The first three terms in the predictor algorithm, $a_3T_1^4$, $b_3T_2^4$, and $c_3T_6^4$, represent the contributions to the absorbed irradiation from the lower element, upper element, and oven walls respectively. The fourth term, $d_3T_p^4$, is largely the product emission, since the total exchange factors in equation E.24 are much less than unity. The last term, $h_3(T_A - T_p)$, accounts for convection. The discontinuity of the emission and convection terms at 20 minutes was caused by the product temperature predictor algorithm reaching its final value. The response of emission was identical for each successive cake since the same product temperature predictor was used. The contribution to the absorbed irradiation by the upper element was significantly greater than the lower element except during the initial oven transient. This effect

ORNL-DWG. 81-23775

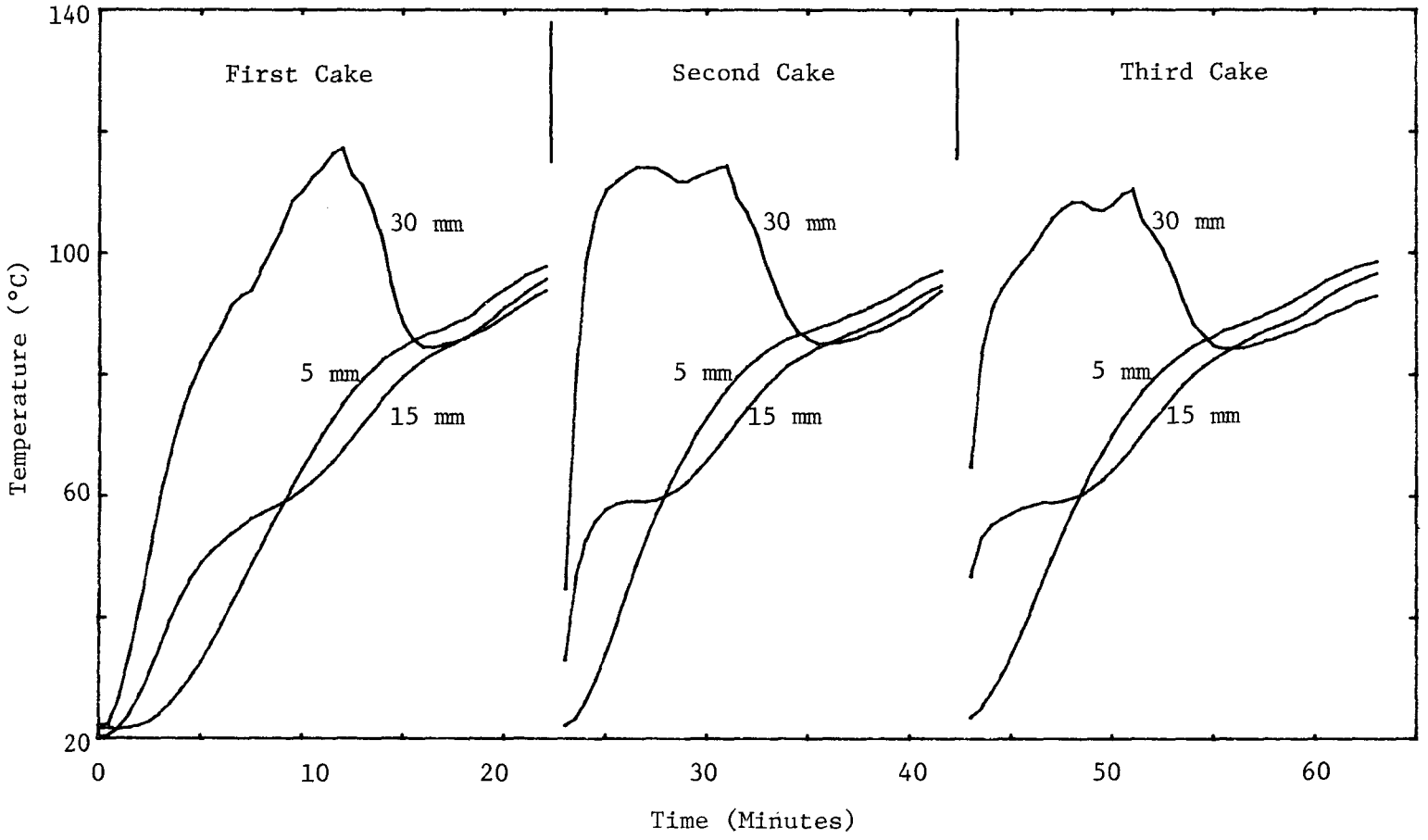

Figure 4.12 Cake Temperature Response - Repetitive Cakes.

ORNL-DWG. 81-23776

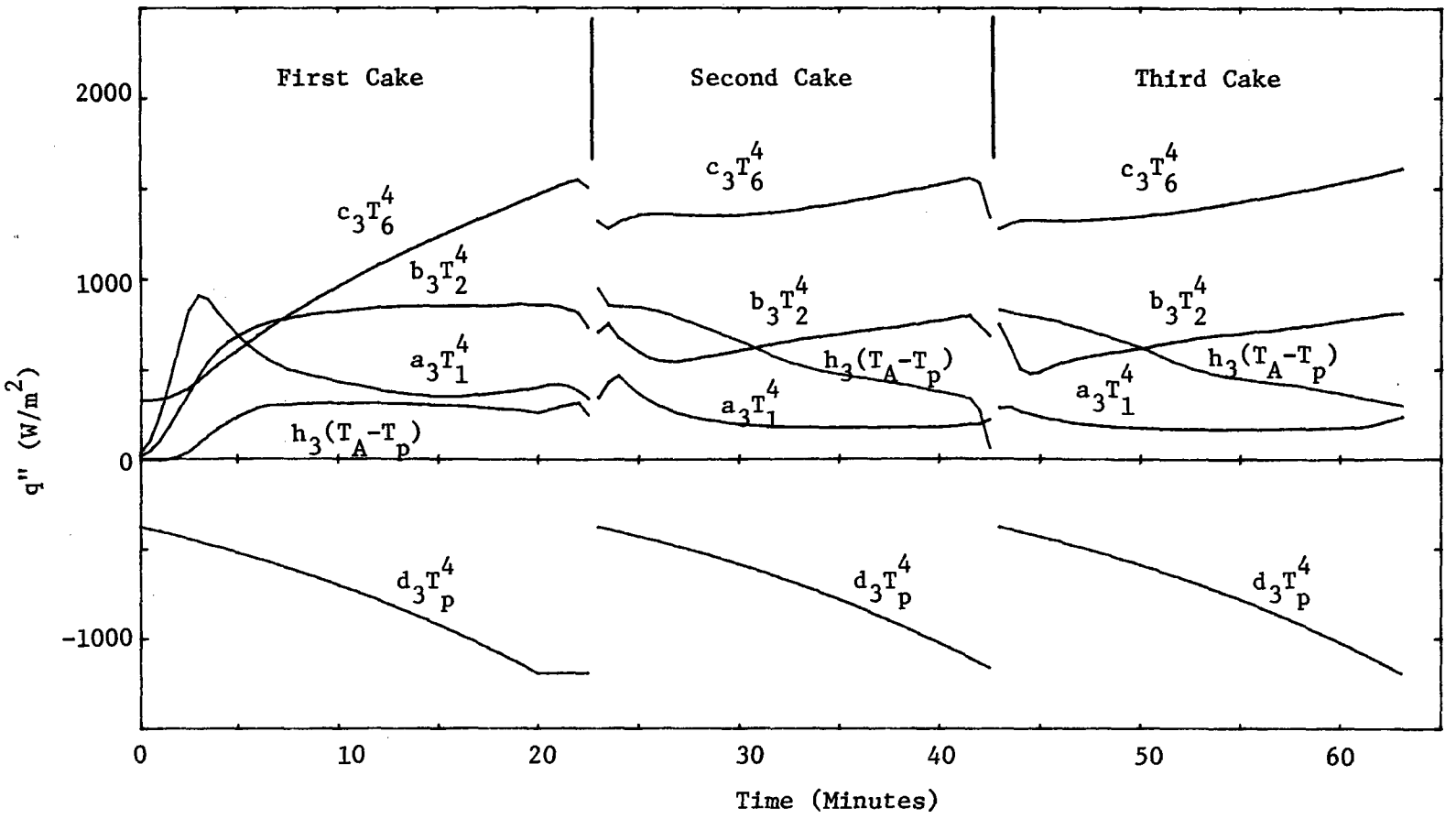

Figure 4.13 Terms of the Heat Flux Predictor for the Lower Product Surface - Repetitive Cakes.

demonstrates the importance of reflective coupling within the Bi-Radiant Oven. After seven minutes the walls were the single largest contributor to the net heat flux at the lower surface. Recall that these results were obtained in Oven IV-B with a wall emissivity of 0.31. The contribution from the walls is expected to diminish as the wall emissivity is decreased. As expected, convection made little contribution during the initial oven transient, but made a significant contribution thereafter, especially at the beginning of a new baking period where the product temperature was relatively low.

After the initial oven transient, constant net heat flux was maintained by the offsetting effects of increased product emission and increased wall temperature. When a new cake was inserted, the lower product temperature caused emission to decrease and convection to increase resulting in a much greater net heat flux as shown in Figure 4.9.

On the upper surface, the contributions to the net heat flux due to the walls and product emission were the same as the lower surface, since c_4 and d_4 were equal to c_3 and d_3 respectively. The contribution from the upper element to the absorbed irradiation on the upper surface was over twice as large as it was for the lower surface, making the upper element the single largest contributor to the net heat flux at the upper surface. Similarly the contribution from the lower element was less than half as large as it was for the lower surface. A comparison of equations E.26 and E.27 shows that the convection coefficient on the upper surface was also less than half as large as it was on the lower surface.

The accuracy of these heat flux predictions should be considered in view of the approximations made concerning product temperature, convection, and radiative properties. Although an accuracy of ±15% in the heat flux predictions may be optimistic, the control system performed quite well under practical operating conditions of the Bi-Radiant Oven.

To assure the accuracy of the heat flux predictor algorithm, multiple temperature sensors were used for each of the elements, air, and walls. Functionally, the minimum number of temperature sensors required for the heat flux predictor is four; one for each of the upper and lower elements, oven air, and cavity walls, with the product temperature being estimated a priori. These sensors would have to be judiciously located to assure that their output was representative of the average value.

In its present form, the control system is somewhat awkward for the user because of the required input data concerning the product temperature response and characteristic length. This difficulty could easily be eliminated by assuming some typical characteristic length and product temperature response and applying them to all products. Then the user would only be required to reset the controller for successive products. An even simpler solution would be to assume a constant product temperature. These approximations would further degrade the accuracy of the heat flux predictor algorithm, but considering the ability of food products to tolerate variations in the net heat flux (such as occurs in conventional ovens due to element cycling), satisfactory baking performance could still be expected. The ability of the control system to respond to cold start-up and disturbances and to prevent overheat would not be affected by these approximations.

The use of a higher maximum input power would be desirable since it would decrease the response time of the oven, but it could also affect the stability of the control system by causing greater overshoot and a longer settling time. By modifying the control algorithm parameters and possibly using a more sophisticated algorithm, these problems should be manageable.

CHAPTER 5 - SUMMARY AND CONCLUSIONS

This study has been largely an experimental investigation of the principles of the Bi-Radiant Oven using a special, full-sized, prototype oven instrumented to measure the temperature of each of the major oven components (elements, walls, air, and covers) the power consumption of each element, and the mass loss of products during the baking process. Experimental observations using two wall materials with emissivities of 0.03 and 0.31 (referred to as Oven IV-A and IV-B, respectively) have provided an understanding of the thermal behavior of the oven in terms of temperature responses, thermal efficiency, and heat loss. Efficiencies of 22 and 18 percent were observed in Ovens IV-A and IV-B, respectively, using conventional calrod type heating elements and were shown to be fairly insensitive to the input power levels. A strong thermal gradient exists in the oven cavity due to higher input power at the upper element and due to stratification of the oven air. Single-layer yellow cakes baked satisfactorily in both ovens without venting, and in a shorter period of time than conventional ovens. Results using the single-layer cake indicate that the Oven IV-B had higher overall cavity temperatures but was more isothermal than Oven IV-A. The convective heat transfer to the walls was positive in both ovens except near the top wall.

The unconventional aspects of the Bi-Radiant Oven prompted special consideration of a new control method for providing proper power levels to the upper and lower heating elements so as to accommodate various products and oven operating conditions. Based on the thermal performance results, a control method was identified in general terms where the net heat fluxes at the upper and lower product surfaces were used as the control variables. Because of the difficulties of measuring heat flux, a digital control system was proposed to accommodate a heat flux predictor algorithm which was based on element, wall, air, and product temperatures. The radiative component of the predictor was based on a simple enclosure analysis and was in good agreement with experimental measurements. The convective component was evaluated using standard flat plate correlations. The digital control system was implemented into the data acquisition system and tested under various oven conditions. These tests showed that the control system provided faster response, more constant heat flux, and better overheat protection than constant input power. The control system also performed well for repetitive baking.

In designing a Bi-Radiant Oven for greater efficiency, the following guidelines should be considered:

1. Reduce the thermal mass of all oven components, especially those comprising the inner cavity, to reduce storage losses.

2. Keep the oven enclosure as small as possible to reduce both conduction and storage losses.

3. The wall emissivity should be kept to a minimum to reduce the radiative coupling of the heat source and the walls.

4. Maintain only enough venting to satisfy food requirements. Although an automatic vent controller may not be economically feasible, a two position vent may be acceptable, where the vent could be closed for food products that do not need it.

5. The design of the heating elements is important for obtaining both good performance and high efficiency. The configuration of the element is important for the uniformity of irradiation over the baking plane [19]. The efficiency of the Bi-Radiant Oven should improve if the heating elements were more effective radiators. Reducing the percentage of total heat dissipation by the convective mode reduces the indirect coupling of the heating elements with both the product and the oven walls. The improvement in efficiency is expected since more of the convective heat dissipated from the elements is lost to the walls and due to leakage than is gained by the product. High element temperatures are needed to increase the percentage of the total heat dissipation by emission. To achieve higher element temperatures without increasing the input power levels or changing the overall element length and configuration, the element diameter must be reduced. If possible, filament type of heating elements should be used in the Bi-Radiant Oven. The analytical results of Scheitlin [19] are in agreement with this prediction. To maintain the radiative effectiveness of the filament type of heating elements, it may be desirable to have auxiliary elements that only switch on during cold start-up and recovery

from a door opening. With the filament type of heating elements it may also be possible to neglect their response time and thereby eliminate element temperature sensors by relating the filament temperature to the input power. Filament type of heating elements would also have the additional benefit of a low thermal mass, thereby reducing their storage losses.

6. The use of recirculation or forced air flow would decrease the stratification effect as well as increase both the convective heat transfer to the product and mass transfer from the product. But it would also increase losses by improving the convective coupling of the heat source and the walls. Thus, it is not likely that recirculation would improve the efficiency of the Bi-Radiant Oven.

7. The use of focusing reflectors behind the heating elements would tend to cause the radiation field to become much less isotropic. Conceptually, the product makes no distinction between diffuse and collimated irradiation, but only the uniformity of the irradiation would seem to be important. The main advantage of a focusing system would be to reduce the average number of wall reflections before the emitted radiation from the elements reached the product and thus would further decouple the walls from the heat source. A focusing system would also tend to decouple the upper heating element from the lower product surface, and vice versa, allowing a greater disparity in the heat fluxes at the upper and lower product surfaces. Although any type of focusing system will greatly complicate a complete radiation analysis, the potential saving warrants further investigation.

The optimization of the oven insulating system has not been treated in this study. Although additional insulation will reduce the steady state losses, it will also increase storage losses because of the additional thermal mass. Thus, any optimization process should include transient effects. It is likely that conduction losses through the cavity support structure and door may overtake conduction losses through the insulation well before the optimal insulation thickness is reached.

Because of the strong contribution to the product's net heat flux from the heating elements, a single rack design is strongly recommended. The position of the rack can be adjustable to accommodate large products, but the overall shape of the Bi-Radiant cavity should be shorter than full-sized conventional ovens.

The overall goal of this work has been to substantiate the concepts of the Bi-Radiant principle. This was accomplished not only by experimental observation of its thermal performance, but also by developing the Bi-Radiant Oven to a level suited for domestic application through development of the proper control technology. This work provides a strong technical framework for development of the Bi-Radiant Oven into a marketable appliance.

LIST OF REFERENCES

LIST OF REFERENCES

[1] Auslander, David M., Takahashi, Yasundo, and Tomizuka, Masayoshi, "Direct Digital Process Control: Practice and Algorithms for Microprocessor Application," Proc. IEEE, v66, n2, Feb., 1978, pp 199-208.

[2] Beckman, W. A., "Solution of Heat Transfer Problems on a Digital Computer," Solar Energy, v13, n3, 1971, pp 293-300.

[3] Connelly, S. M., "Irradiation Heat Flux Gauge: A Predictor of Oven Irradiation Levels," M.S. Thesis, School of Consumer and Family Sciences, Purdue University, May 1980.

[4] Crutchley, Wayne, "Microcomputer Control Course - Part 3. The Quest for Control-Interfaces and Algorithms. How a Microcomputer Becomes a Control System," Instruments & Control Systems, v52, n3, March 1979, pp 49-51.

[5] Department of Energy, "Energy Conservation Program for Consumer Products," Federal Register, v45, n127, p 43998, Monday, June 30, 1980.

[6] DeWitt, D. P., and Peart, M. V., "Bi-Radiant Oven A Low-Energy Oven System, Volume 1 - Development and Assessment," Oak Ridge National Laboratory, ORNL/Sub-80/0082/1, Dist: Category UC-95d, U.S. Department of Energy, Office of Buildings and Community Systems, April 1980.

[7] Erickson, Robert C., "Energy Efficiency Program for Kitchen Ranges & Ovens," Science Applications, Inc., LaJolla, CA, Report to the Department of Energy under contract no: CR-04-60727-00, Nov., 1977.

[8] Federal Energy Administration, "Energy Conservation Program for Appliances," Federal Register, v43, n91, pp 20118-20128, Wednesday, May 10, 1978.

[9] Fujii, T., and Imura, H., "Natural-Convection Heat Transfer from a Plate with Arbitrary Inclination," Int. J. Heat Mass Transfer, v15, 1972, pp 755-767.

[10] Gerald, C. F., Applied Numerical Analysis, 2nd ed., Addison-Wesley, Reading, MA, 1978.

[11] Harris, G. D., "Instrumentation and Procedures for Evaluation of Domestic Oven Thermal Performance," Heat Transfer Laboratory Report 072778 to Whirlpool Corporation, School of Mechanical Engineering, Purdue University, July 1978.

[12] Holman, J. P., Heat Transfer, 4th ed., McGraw-Hill, New York, 1976, p253.

[13] Incropera, F. P., and DeWitt, D. P., Fundamentals of Heat Transfer, John Wiley & Sons, New York, 1981.

[14] Jacobs, D. and Donaghey, L. F., "Microcomputer Implementation of Direct Digital Control Algorithms for Thermal Process Control Applications," ASME paper no. 77-WA/Aut-4, 1977.

[15] Kline, S. J., and McClintock, F. A., "Describing Uncertainties in Single Sample Experiments," Mechanical Engineering, V 75, n 1, Jan. 1953, pp 3-8.

[16] Lloyd, J. R., and Moran, W. R., "Natural Convection Adjacent to Horizontal Surface of Various Planforms," ASME paper no. 74-WA/HT-66, 1974.

[17] Marston, C. K., "Simultaneous Heat and Mass Transfer within a Product During the Baking Process," M.S. Thesis, School of Mechanical Engineering, Purdue University, August 1980.

[18] Peart, M. Virginia, DeWitt, David P., and Kern, Susan T., "Energy-Efficient Bi-Radiant Oven," U.S. Patent 4,164,643, August 14, 1979.

[19] Scheitlin, Gordon G., "Enclosure Analysis for Determining Cavity Efficiency of an Energy-Efficient Electric Oven," M.S. Thesis, School of Mechanical Engineering, Purdue University, August 1981.

[20] Singh, S. N., Birkebak, R. C., and Drake, R. M., "Laminar Free Convection Heat Transfer from Downward-Facing Horizontal Surfaces of Finite Dimensions," Prog. Heat Mass Transfer, v2, p 87-98, 1969.

[21] Vaccari, J. A., (editor), "1978 Materials Selector," Materials Engineering, v86, n6, Nov. 1977.

APPENDICES

APPENDIX A - INSTRUMENTATION DETAILS

A.1 Thermocouple Locations

Figures A.1 and A.2 give the locations of the wall thermocouples for Ovens IV-A and IV-B, respectively. Similarly, Figures A.3 and A.4 give the locations of the element thermocouples for both ovens. Note that fewer thermocouples were used to instrument Oven IV-B. Figure A.5 gives the locations of the air thermocouples. Five cover thermocouples were located near the center of each of the back, top, bottom, right side, and door cover panels. The same air and cover thermocouple locations were used for both oven configurations.

A.2 Product Weighing System and Calibration

Figure A.6 is a schematic of a cantilever beam load cell which comprises the product weighing system. The cap screw provides both point contact and leveling capability. Figure A.7 is the null bridge circuit diagram including the ±15 V regulated power supply (Polytron Devices Inc., Paterson, NJ, model P34-1AS).

The product weighing system was calibrated by placing weights (Central Scientific Co., Chicago, IL) near the center of the oven rack. The bridge was zeroed with the rack in place. The system was allowed to stabilize for 20 seconds. The bridge output was then scanned every 2.0 seconds for 1.0 minute for each data point. The mean bridge output and

ORNL-DWG. 81-23777

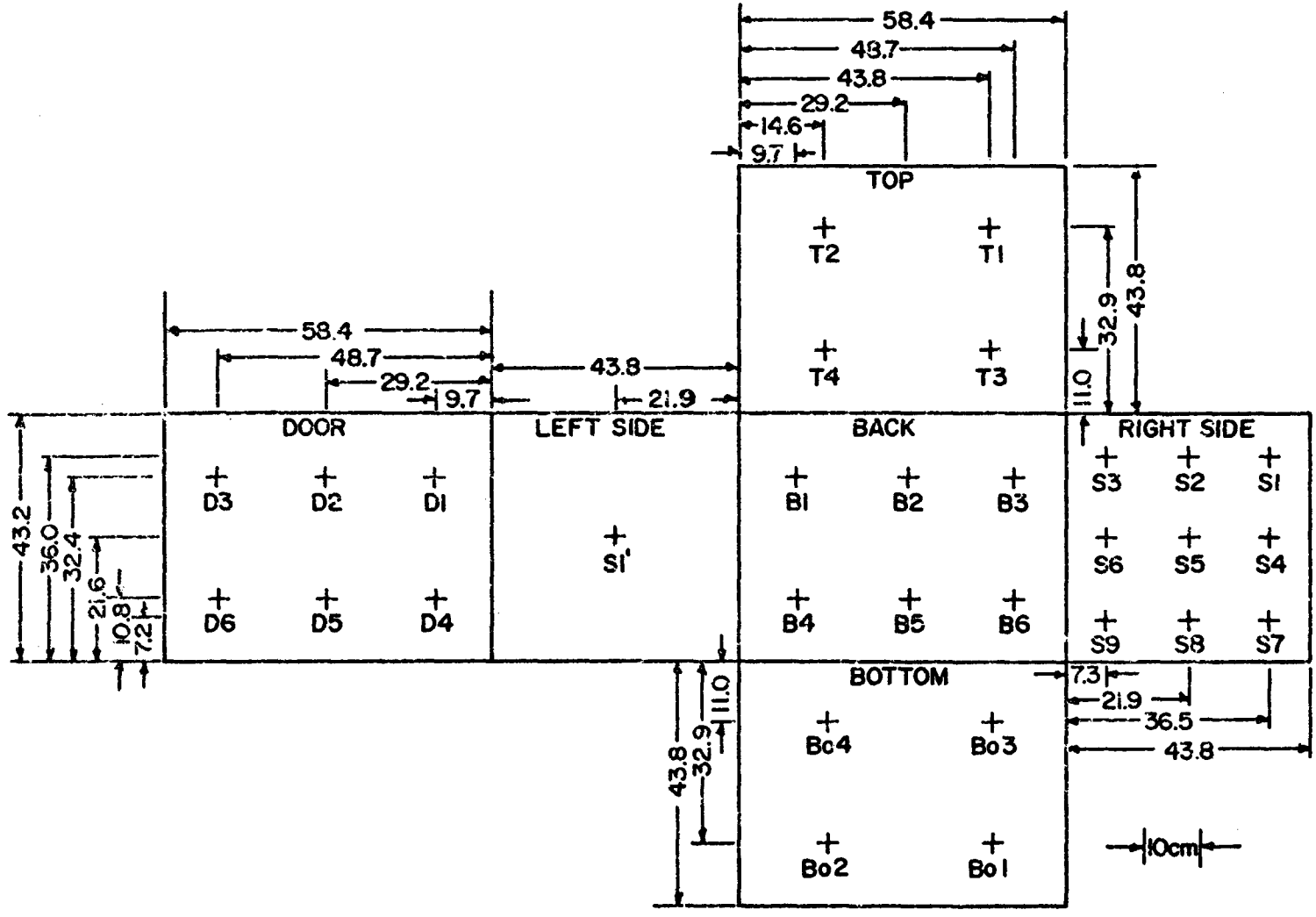

Figure A.1 Wall Thermocouple Locations, Bi-Radiant Oven IV-A.

ORNL-DWG. 81-23778

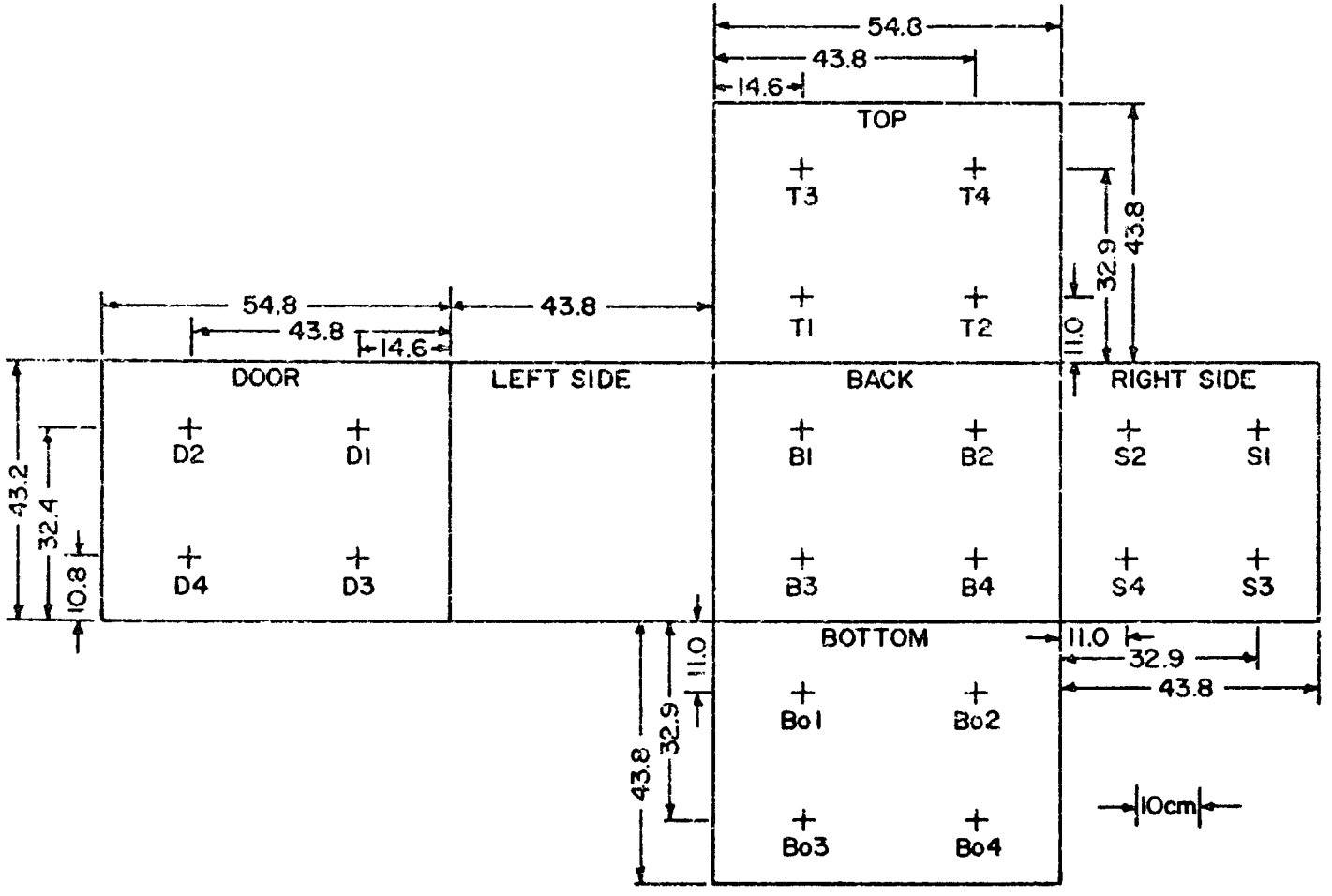

Figure A.2 Wall Thermocouple Locations, Bi-Radiant Oven IV-B.

ORNL-DWG. 81-23779

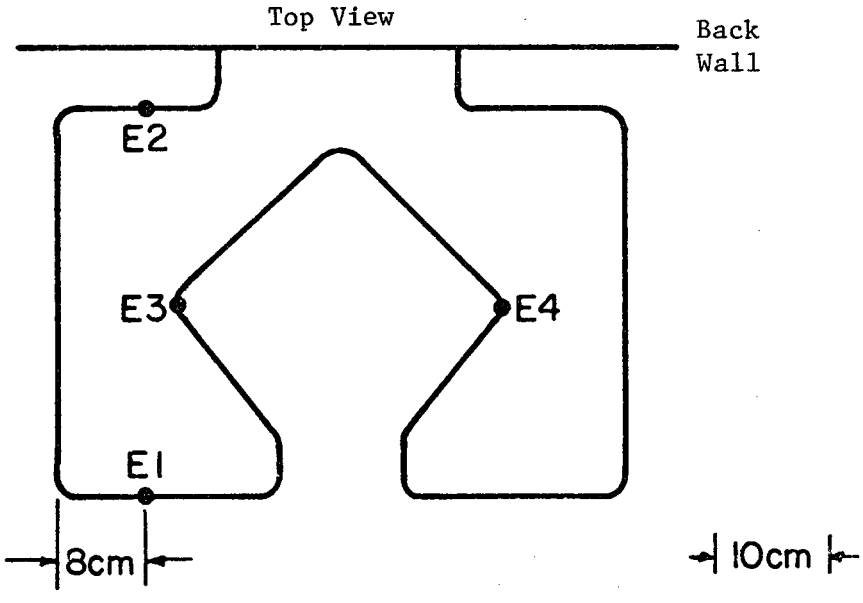

Figure A.3 Element Thermocouple Locations, Bi-Radiant Oven IV-A.

ORNL-DWG. 81-23780

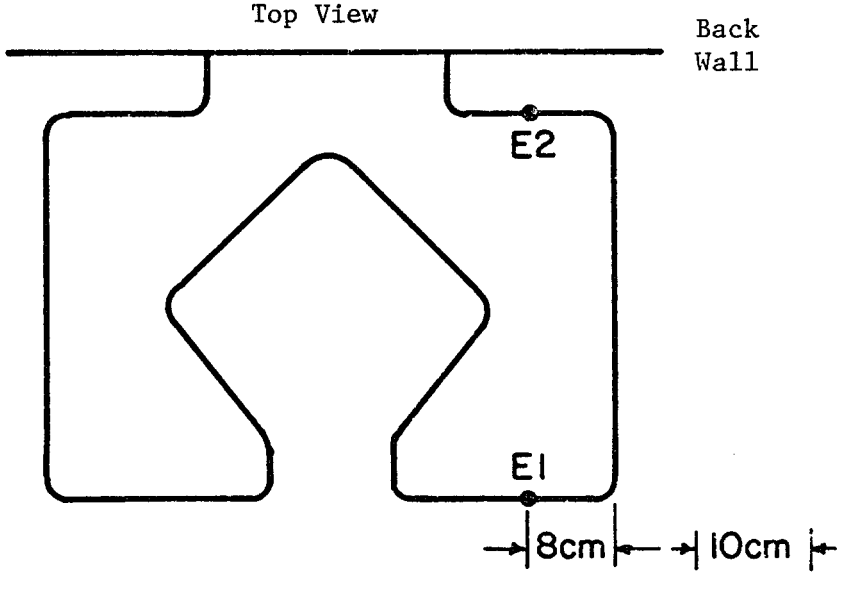

Figure A.4 Element Thermocouple Locations, Bi-Radiant Oven IV-B.

ORNL-DWG. 81-23781

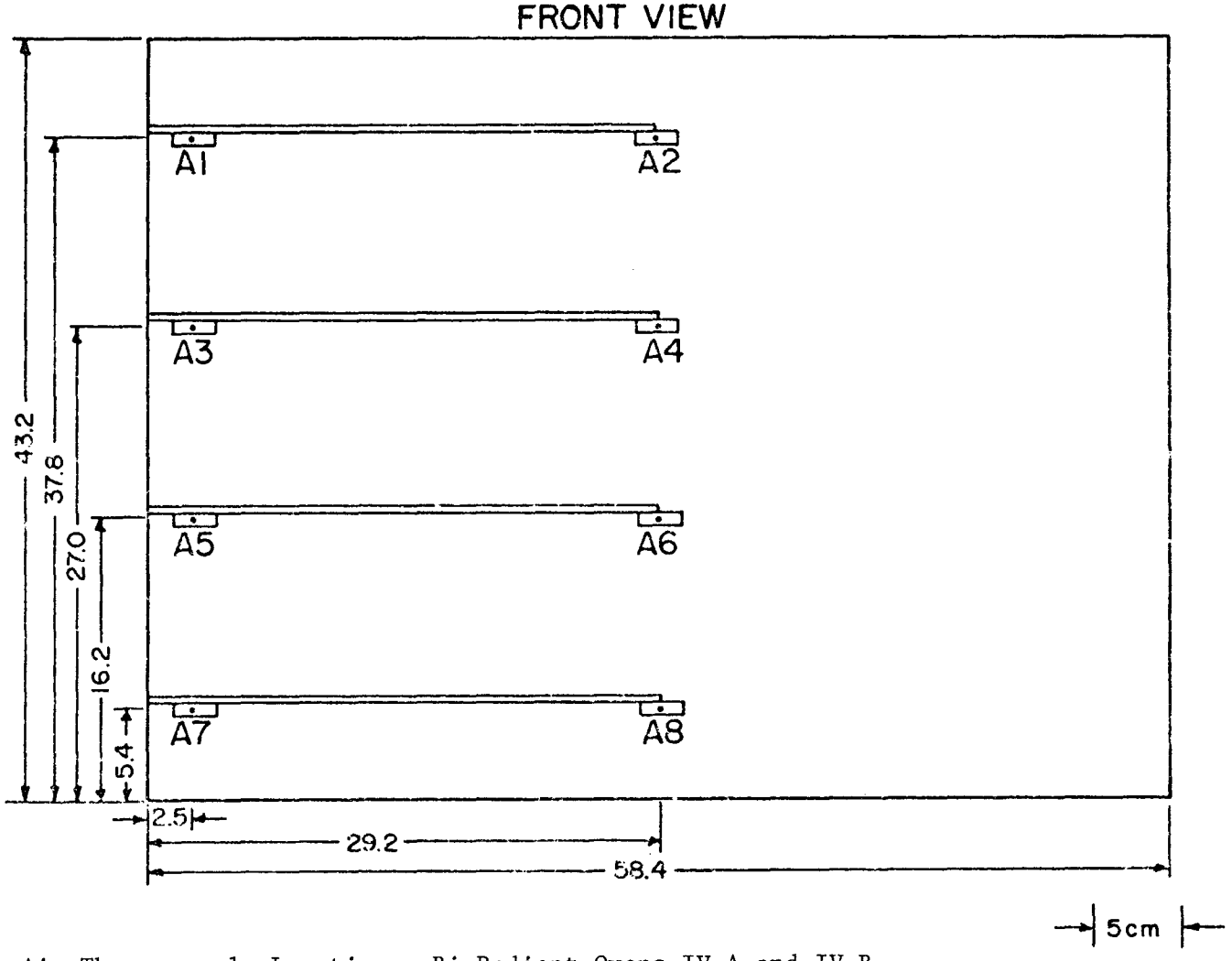

Figure A.5 Air Thermocouple Locations, Bi-Radiant Ovens IV-A and IV-B.

ORNL-DWG. 81-23782

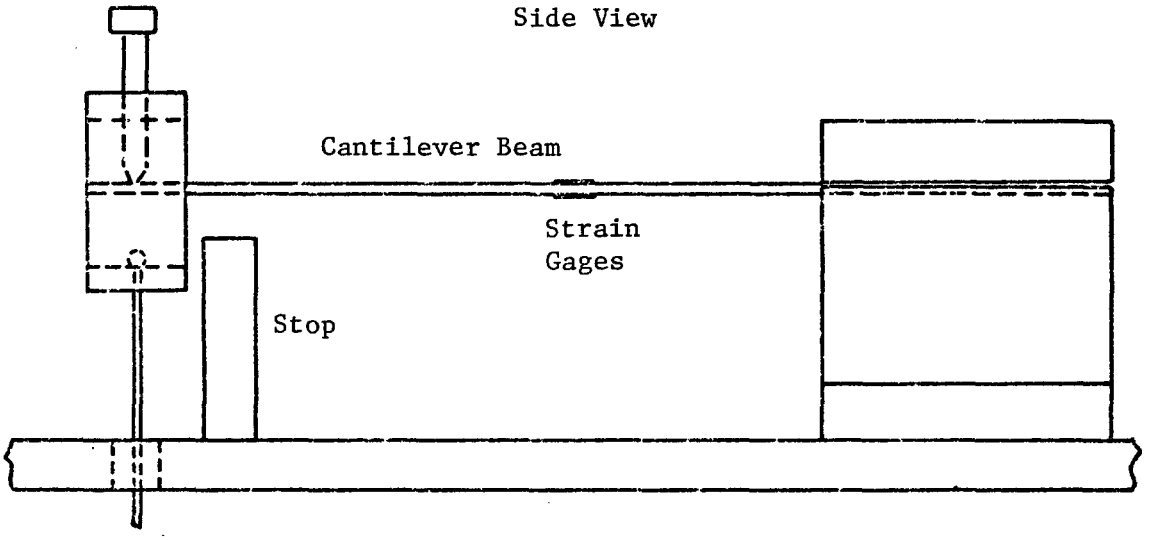

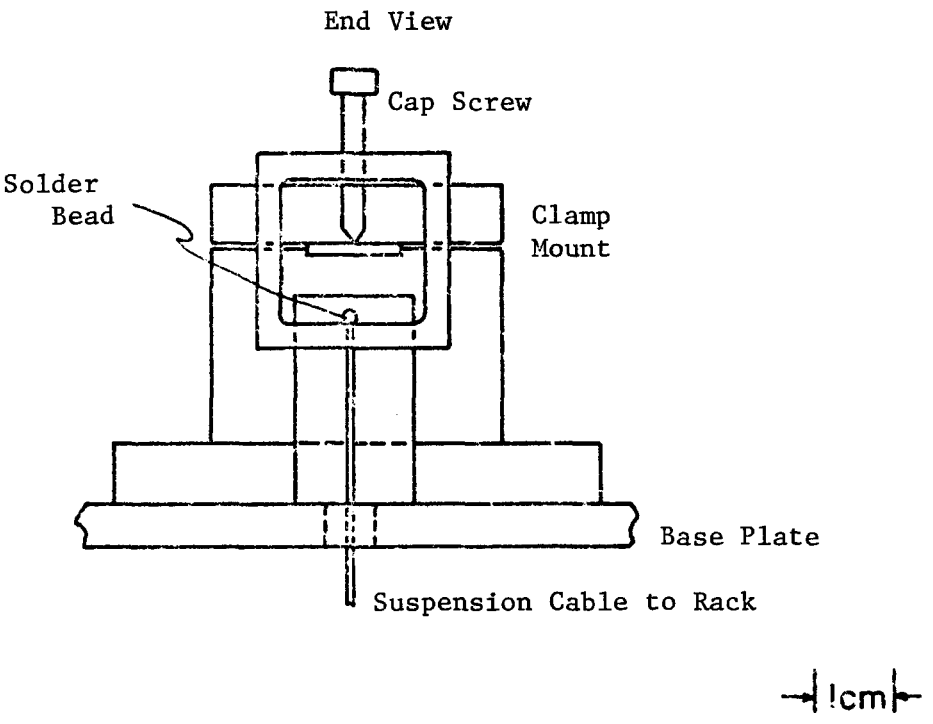

Figure A.6 Schematic of the Cantilever Beam Load Cell.

ORNL-DWG. 81-23783

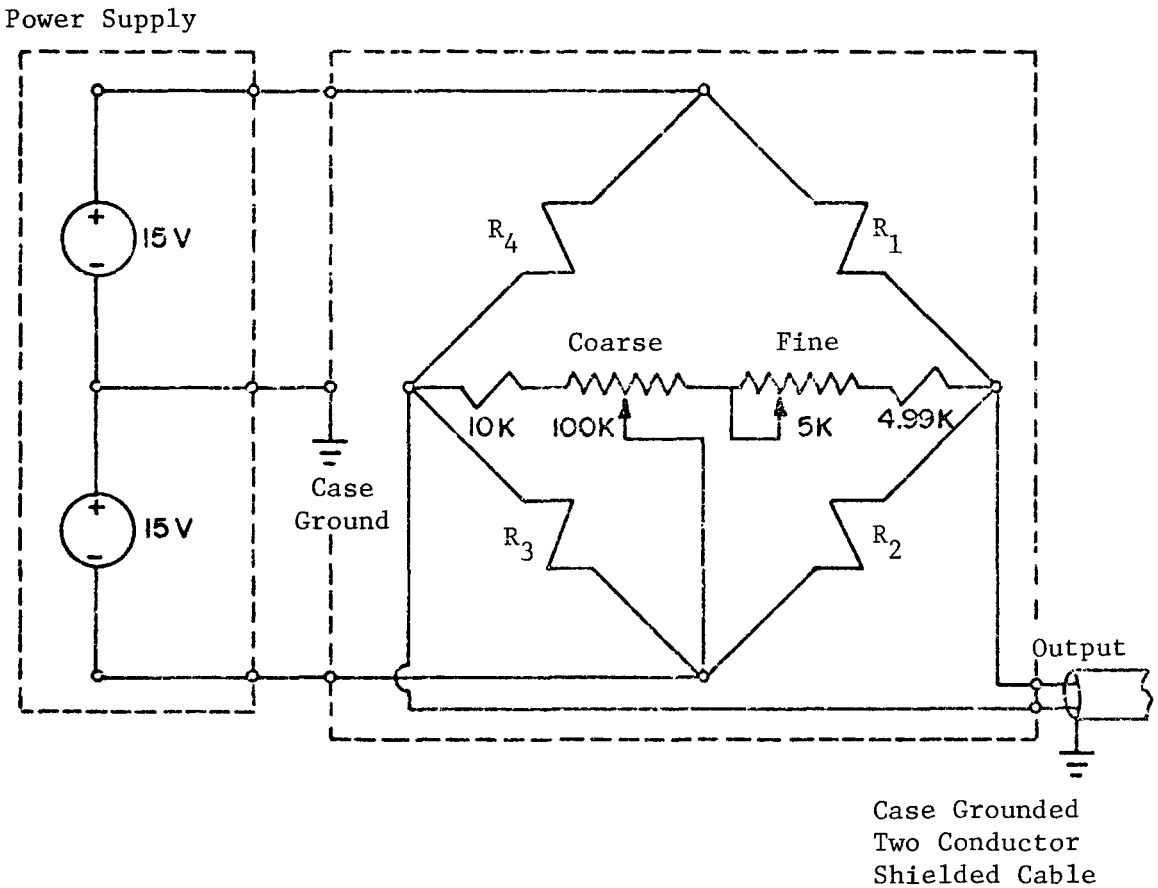

R_1, Series combination of the lower (compressive) inside gage from each of the four load cells.

R_2, Series combination of the upper (tensile) inside gage from each of the four load cells.

R_3, Series combination of the lower (compressive) outside gage from each of the four load cells.

R_4, Series combination of the upper (tensile) outside gage from each of the four load cells.

Figure A.7 Null Bridge Circuit Diagram.

standard deviation for each data point is given in Table A.1. These results are also plotted in Figure A.8 along with a least squares linear fit with a correlation coefficient greater than 0.999. The resolution of the weighing system is limited by the noise level on the output. Assuming a three standard deviation resolution and taking the worst case value of 8.41μV from Table A.1,the resolution of the product weighing system is 1.01 g.

To observe the effect of load location on the oven rack on the product weighing system output, a 500 g weight was placed on the oven rack at five locations - center and near each of the four corners. The results of this experiment are given in Table A.2 and indicate a total variation of less than ± 2.5% from the center position value.

A.3 Convective Heat Transfer Considerations of the Heat Flux Gage

The performance of the heat flux gage became suspect when convection results from oven experiments were in disagreement with standard correlations. The results from section 4.4.2 for the gage in Oven IV-B indicated large variations (>300 W/m^2) in the convective heat flux to the lower gage surface, while the variations on the upper surface were much smaller (<50 W/m^2). These values yield heat transfer coefficients of approximately 4.5 W/m^2-K on the upper surface and from 1.0 to 4.0 W/m^2-K on the lower surface. Values of 5.5 and 14 W/m^2-K were predicted* for the upper and lower surfaces, respectively, using correlations from Fujii and Imura [9] and from Lloyd and Moran [16],

* The predictions are based on a Ra of 8.82×10^3 which was calculated from experimental data at 20 minutes into the test with the gage viewing up, using a characteristic length equal to the gage area divided by its perimeter.

Table A.1 Product Weighing System Calibration Data.

Mass (g)	Mean Bridge Output (mv)	Standard Deviation (μV)
0	0.00013	6.01
20	0.49765	6.83
40	0.99271	7.30
50	1.25958	6.88
75	1.87958	6.24
100	2.50903	7.12
150	3.75006	6.45
200	5.00958	5.68
250	6.24900	6.18
300	7.51794	3.09
350	8.75787	5.66
400	10.03194	6.61
450	11.26532	6.00
500	12.49971	5.45
550	13.74839	8.41
600	15.00306	5.76
650	16.23371	4.38
700	17.47881	4.21
750	18.73935	4.28
800	19.97132	4.17
850	21.24487	6.34
900	22.48910	5.08
950	23.74042	4.84
1000	25.00290	5.08

ORNL-DWG. 81-23784

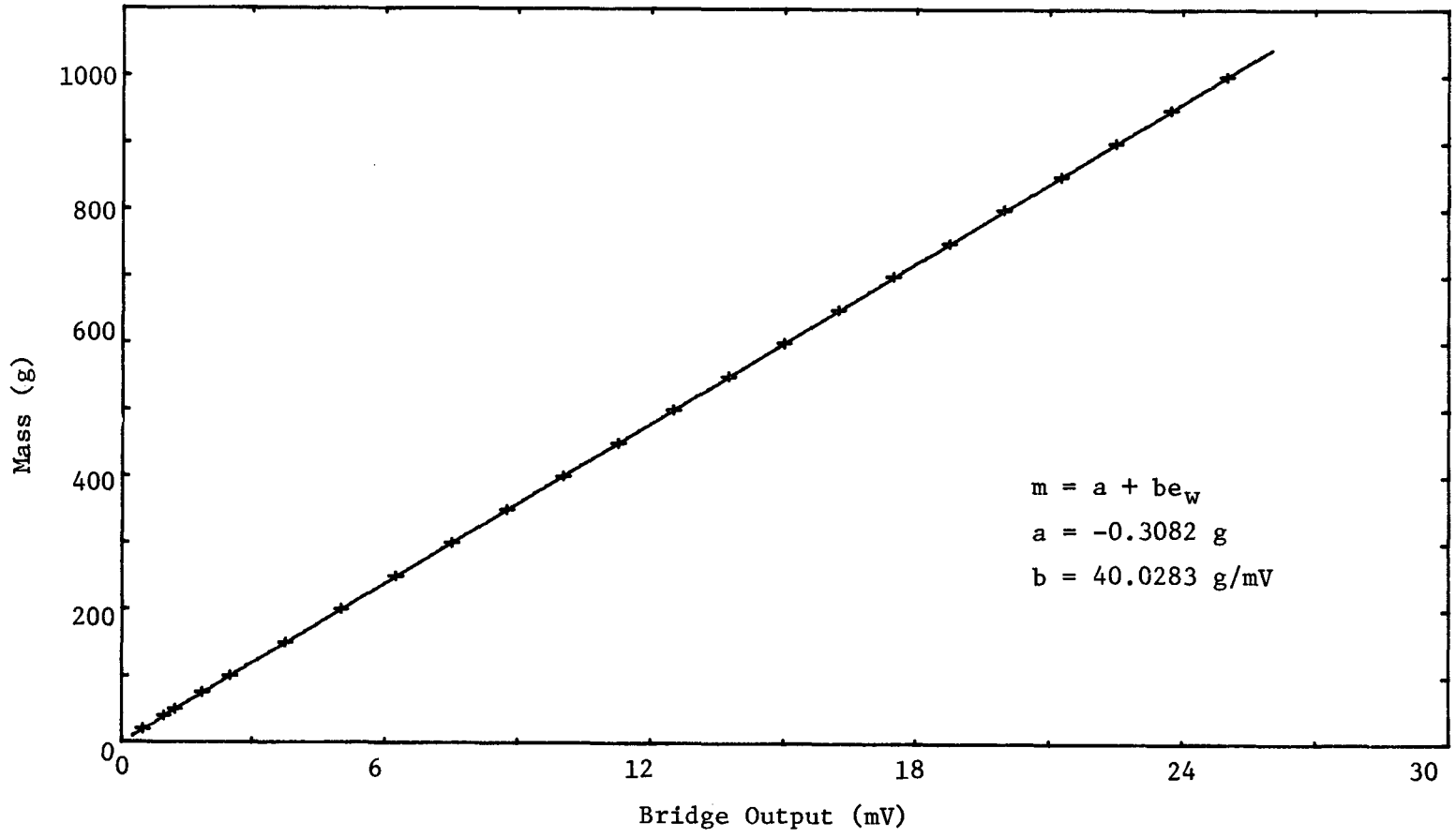

Figure A.8 Product Weighing System Calibration.

Table A.2 Variation in the Bridge Output Due to Load (500 g) Location on the Oven Rack.

Load Location	Bridge Output (mV)	Deviation from Center Value (%)
Center	12.517	---
Left Front Corner	12.828	2.5
Left Rear Corner	12.503	-0.11
Right Rear Corner	12.262	-2.0
Right Front Corner	12.443	-0.59

respectively. Singh et al. [20] performed an analytical study using boundary layer approximations to predict the overall and local Nu on the lower surface of finite horizontal heated surfaces. Their analysis gives an overall coefficient of 9.0 W/m^2-K and a local coefficient corresponding to the sensor locations of 6.1 W/m^2-K . The Ra used in the predictions was slightly below the specified experimental ranges of both Lloyd and Moran [16] and Fujii and Imura [9]. Since the gage is an unshrouded object, the results of Fujii and Imura, who used a heated plate shrouded by vertical walls, are not directly applicable to the gage but are included for comparison. In view of the approximations in their analysis and the uncertainties in the gage, the agreement between Singh et al. (6.1 W/m^2-K) and the gage (4.5 W/m^2-K) is just fair.

Singh et al. [20] also give a description of the flow phenomenon adjacent to finite-sized horizontal surfaces, where boundary layer flow toward the edges of the surface develops on the stagnant face (lower surface of heated plates and the upper surface of cooled plates). For the upper surface of a horizontal heated plate (or the lower surface of a cooled plate), there appears to be no orderly flow. The gage algorithm for determining the convective and radiative heat fluxes assumes that both sensors are exposed to identical convective boundary conditions [19]. Thus, the large variations in the gage results which occur when it was facing down, can be attributed to local variations and instabilities in the flow pattern. This also explains the large variation in the measured data of Figure 4.4 for the net radiative heat transfer to the blackened sensor. In addition to the variation of the data on the lower gage face, the magnitude of the experimental and

predicted results of Lloyd & Moran [9] are in considerable disagreement (14 vs 1.0 to 4.0 W/m^2-K). There are several factors which could contribute to this discrepancy: gage errors, gage geometry, enclosure effects, boundary layer interaction on the lower surface from the upper surface, low Ra, or the very high Sc (analogous to very high Pr) used by Lloyd & Moran [9].

In an effort to isolate possible enclosure effects, the gage was placed horizontally in a large ($2.65m^3$), isothermal enclosure at room temperature to simulate a quiescent medium. Hot water was circulated through the gage causing the gage temperature to rise to approximately 54 ^oC. The air temperature was measured with a single unshielded (30 gauge, glass wrap) copper-constantan thermocouple. The system was allowed to stabilize for 10 minutes and data was recorded every 3 seconds for approximately 20 minutes using the data acquisition system of section 2.3. This data was reduced to the convection coefficient using the gage algorithm and sensor emissivities given by Scheitlin [19] and is plotted in Figures A.9 and A.10 for the lower and upper surfaces, respectively. Keep in mind that the corresponding roles of the lower and upper surface are reversed in this case since the gage was heated rather than being cooled as it was in the oven. These results indicate a convection coefficient from 5 to 6 W/m^2-K on the lower surface and from 3.5 to 5.5 W/m^2-K on the upper surface. On the upper surface there appears to be two distinct values (approximately 4 and 5 W/m^2-K) about which the convection coefficient stabilizes, but oscillates between, with a period on the order of 13 minutes.

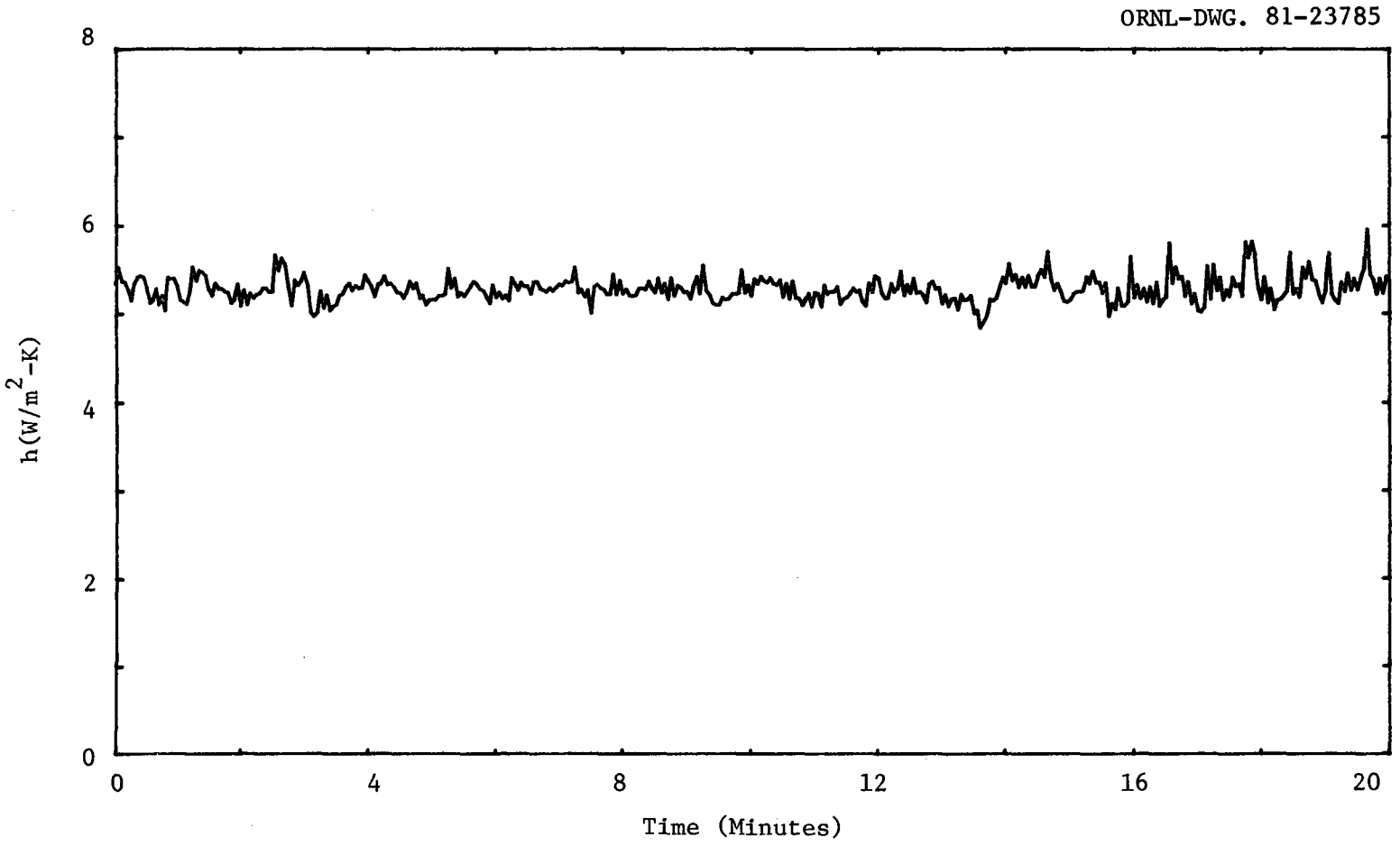

Figure A.9 Convection Heat Transfer Coefficient on the Lower Surface of the Heated Heat Flux Gage in a Quiescent Medium.

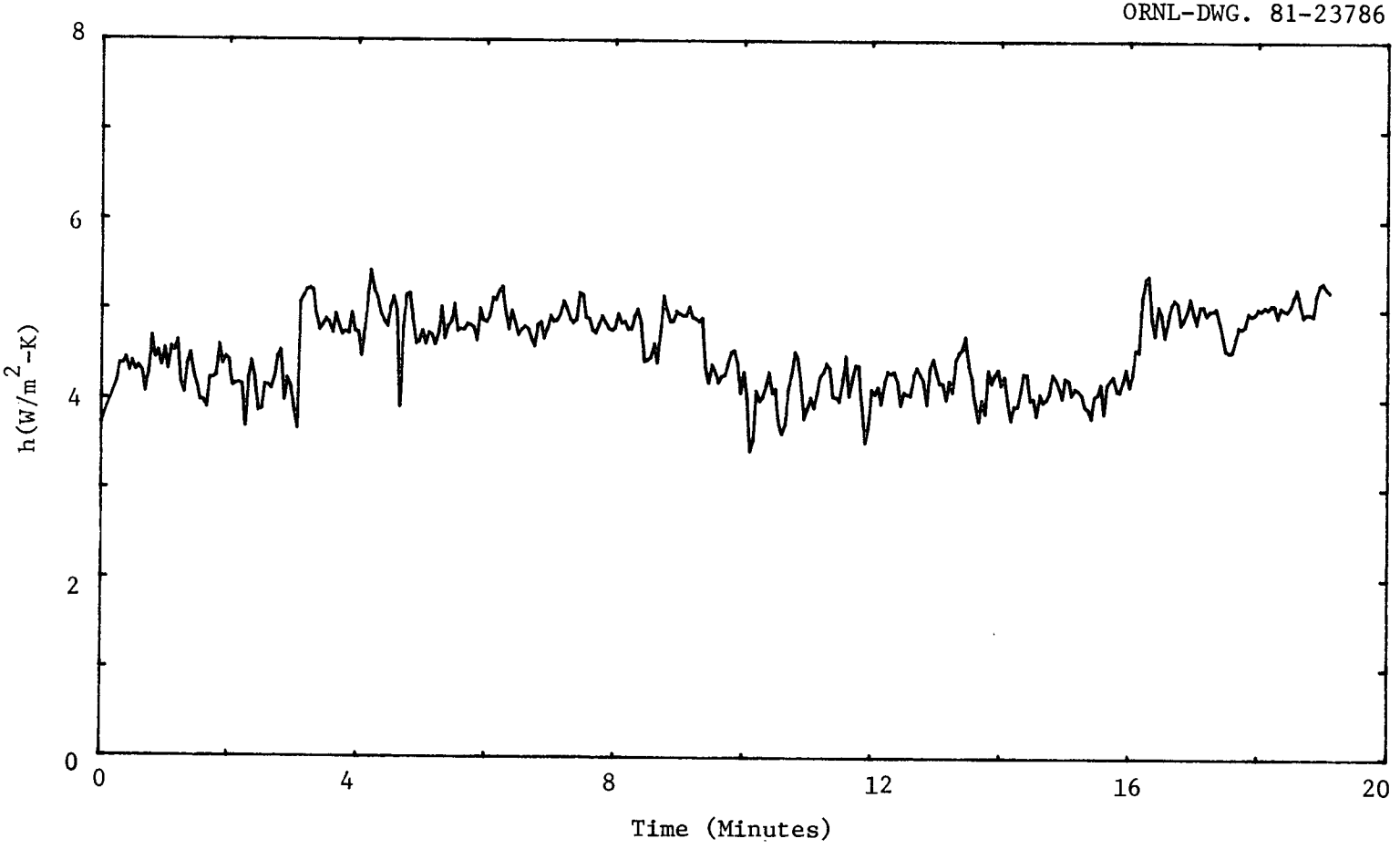

Figure A.10 Convection Heat Transfer Coefficient on the Upper Surface of the Heated Heat Flux Gage in a Quiescent Medium.

For these conditions the Ra was 8.84×10^3, again based on a characteristic length of gage area divided by its perimeter. The Lloyd and Moran correlation [16], which corresponds to an unshrouded surface, yields a coefficient of 9.4 W/m^2-K for the upper surface. Fujii and Imura [9] also give a correlation for the upper surface of a heated plate which yields a coefficient of 5.9 W/m^2-K; on the lower surface, their correlation gives a coefficient of 3.7 W/m^2-K. The correlations of Singh et al. [20] give an overall coefficient of 6.0 W/m^2-K and a local coefficient corresponding to the sensor locations of 4.1 W/m^2-K for the lower gage surface. The quiescent medium experiment yields improved agreement between experimental results and the correlation of Singh et al.

The heat flux gage is an unshrouded surface; as such, it is possible that flow patterns on the upper and lower surface will interact. The overall tendency would be for the boundary layer flow from the lower face of a heated plate to rise and interact with the flow patterns on the upper surface due to bouyancy effects and vice versa for a cooled plate. With this in mind, the results from the lower face of the heated heat flux gage should be closely represented by the unshrouded results of Singh et al.[20]. Reasonable agreement between the experimental gage results and Singh et al., both in the oven and in a quiescent medium, seem to confirm this conclusion. The results from the gage and Lloyd & Moran [16] are again in significant disagreement. A possible explanation of this disagreement may be the flow interactions mentioned above.

From these results it appears that the heat flux gage provides reasonable coefficients on its stagnant face, but the results from the opposite face are systematically lower than those predicted by published correlations. The lack of any well behaved boundary layer flow on the opposite face causes large variations in the gage output, and the enclosure tends to enhance these variations but does not alter the overall trend where the heat transfer coefficient is greater on the stagnant face. This trend seems to indicate that flow interactions from the stagnant face are interfering with the flow patterns on the opposite face so as to reduce the overall heat transfer coefficient on the opposite face. The effect of the oven enclosure also seems to reduce the overall heat transfer coefficient compared to the quiescent medium. The correlations of Fujii & Imura [9] indicate that shrouded plates have lower coefficients on both faces. The effect of other factors such as the high Sc (~2200) used by Lloyd & Moran [16] (which corresponds to very high Pr in heat transfer) and the very low Ra observed in these experiments cannot easily be ascertained.

APPENDIX B - CAKE FORMULATION

Ingredients

260g Duncan Hines Deluxe II Yellow Cake Mix

140g Water

50g Whole Egg

Add all ingredients and mix for one minute at low speed with a hand mixer (Oster, model 348). Scrape the sides of the mixing bowl with a rubber spatula. Mix for one more minute, again at low speed. Use 400g of batter for a 9 inch single-layer cake. Use the batter within 30 minutes of preparation.

APPENDIX C - CALCULATIONS FOR HEAT LOSS ANALYSIS

The energy audit of section 3.3 accounts for the change in the internal energy of the oven components, heat loss to the environment, and the energy absorbed by the air. The change (or rate of change) in the internal energy of the oven can be calculated from the thermal mass of each oven component and its temperature rise (or rate of temperature rise). Table C.1 gives the thermal mass of the major oven components listed in Tables 3.2 and 3.3. The inner cavity consists of the aluminum walls, flanges, and door frame, as well as the steel corner members and the brass air temperature probes. The cover and support frames consist of all the aluminum covers and supporting structure including a 43 cm (17 in) segment of the steel supporting table. The values tabulated for the elements represent a single element. Both elements have the same values.

The temperature rise of the rack and air temperature probes were taken to be the same as the air. The temperature rise of the remainder of the inner cavity was taken to be the same as the oven walls. The temperature rise of the outer support structure was taken to be the same as the cover. The temperature rise of the insulation was taken to be the average of the oven walls and cover. Equations C.1 and C.2 give the expressions for the average wall and cover temperatures used in the heat loss analysis.

Table C.1 Thermal Mass of Oven Components.

Oven Component	Material	ρ (kg/m^3)	c_p (J/kg-K)	Reference Property Data	Volume (m^3)	Mass (kg)	Thermal Mass (J/K)
Block	Aluminum (6061)	--	963.1	[8]	--	3.88	3737
Inner Cavity	Aluminum (6061) Brass (70% Cu) Steel (C1030)	2712 8524 7832	962.9 376.7 439.5	[21] [21] [21]	1.46×10^{-3} 1.20×10^{-5} 1.47×10^{-4}		4359
Insulation	Glass Fiber	16	835.	[13]	0.168		2239
Rack	Steel (C1030)	--	439.5	[21]	--	1.11	489
Cover & Support Frame	Aluminum (6061) Steel (C1030)	2712 7832	962.9 439.5	[21] [21]	4.25×10^{-3} 1.64×10^{-5}		11,143
Elements	Ceramic (fireclay) brick) Steel (C1030)	2000 7832	960. 439.5	[12] [21]	5.29×10^{-5} 2.10×10^{-5}		174

$$\overline{T}_{Walls} = \frac{1}{6}[2\overline{T}_{Rt.Side} + \overline{T}_{Door} + \overline{T}_{Top} + \overline{T}_{Bottom} + \overline{T}_{Back}] \qquad (C.1)$$

$$\overline{T}_{Covers} = \frac{1}{6}[4T_{Bottom} + T_{Top} + T_{Door}] \qquad (C.2)$$

The average air temperature was taken as the average of the eight air temperature thermocouples. The rate of temperature rise was obtained by numerical differentiation using a fourth order Stirling central difference polynomial about a base point [10] and is given by

$$\left.\frac{dT}{dt}\right|_t = \frac{1}{12\Delta t}[-T(t+2\Delta t)+8T(t+\Delta t)-8T(t-\Delta t)+T(t-2\Delta t)] \qquad (C.3)$$

where Δt is the time interval between data points.

The heat loss to the environment was characterized by the temperature difference between the covers and room air since this loss mechanism is governed by external temperature conditions. Bi-Radiant Oven IV-B was operated at three steady-state conditions so that the total input power was equal to the losses to the surroundings. The results of these tests along with a zero point were correlated using a quadratic least squares fit and are given in Table C.2 along with the coefficients of the correlation having the form

$$q_{surroundings} = a + b\Delta T + c\Delta T^2 \qquad (C.4)$$

where ΔT is the temperature difference between the covers and the room air. These results were also applied to Oven IV-A since its outer structure was the same as Oven IV-B. To estimate the total energy lost to the environment, the losses to the surroundings were evaluated at each data point and then numerically integrated over time using Simpson's rules [10].

Table C.2 Correlation of the Heat Loss to the Surroundings.

$q_{surroundings}$ (W)	$\bar{T}_{covers} - T_{room\ air}$ (K)	a (W)	b (W/K)	c (W/K^2)
514.6	20.2	-2.37	17.2	0.999
243.6	10.9			
121.6	6.6			
0.0	0.0			

The energy absorbed by the oven air not only raised its temperature but was also used to expand the air against atmospheric pressure. To account for these effects, the oven air was treated as a stationary open thermodynamic system with boundaries coincident with the inner cavity. The first law of thermodynamics gives

$$\delta Q - \delta W + \Sigma(e_i + p_i v_i)\delta m_i = dE \qquad (C.5)$$

where Q is the heat input to the system (and is the desired result), W is the work interactions out of the system (and is zero since the system boundaries are fixed), E is the stored energy of the system, δm_i is the incremental mass flow into the system at some location i on the system boundary, and e, p, and v are the fluid properties specific stored energy, pressure, and specific volume respectively at location i. By taking the system volume as a constant; neglecting kinetic, potential and all other forms of stored energy except internal energy; assuming the air to be an ideal gas with uniform properties at constant pressure (1 atm); and assuming that all flow across the system boundaries is always negative, so that no outside room air enters the system, Equation C.5 reduces to

$$\delta Q = \frac{pVc_p}{R}\frac{dT}{T} \qquad (C.6)$$

Integrating equation C.6 from an initial to a final state, holding c_p constant (since c_p for air does not very greatly over moderate temperature ranges) yields the final result for the energy absorbed by the air.

$$Q_{Air} = \frac{pV\overline{c}_p}{R}\ln\frac{T_f}{T_i} \qquad (C.7)$$

where p is one atmosphere, V is the volume of the inner cavity, R is the gas constant for air, $\overline{c}_p$ is the average specific heat at constant pressure of the air evaluated at the mean temperature between the initial and final temperatures T_i and T_f respectively.

A similar analysis on a rate basis yields

$$q_{Air} = mc_p \frac{dT}{dt} \tag{C.8}$$

or

$$q_{Air} = V\rho c_p \frac{dT}{dt} \tag{C.9}$$

The density and specific heat were evaluated at $\overline{T}_{Air}$ from tabular property data for dry air [13] and $\frac{dT}{dt}$ was evaluated according to equation C.3.

APPENDIX D - PROPORTIONAL-INTEGRAL DIGITAL CONTROL ALGORITHM

The position form of the PI analog controller can be written as

$$m(t) = K_p\ e(t) + K_I \int_0^t e(t)\ dt + m(t=0) \qquad (D.1)$$

where m is the manipulated variable, K_p and K_I are the proportional and integral constants, respectively, t is time, and e is the error signal. The error signal e is given by

$$e = r - c \qquad (D.2)$$

where r is the reference signal or set point and c is the feedback signal or control variable. Discretizing equation D.1 into k time intervals of length Δt yields

$$m_k = K_p\ e_k + K_I\ \Delta t \sum_{n=1}^{k} e_n + m_o \qquad (D.3)$$

Subtracting m_{k-1} from m_k yields the incremental change in the manipulated variable over each time interval

$$\Delta m_k = m_k - m_{k-1} = K_p\ (e_k - e_{k-1}) + K_I\ \Delta t\ e_k \qquad (D.4)$$

Equation D.4 is the discretized version of the velocity form of the PI controller. For this application, the velocity form is preferred because the position form (equation D.3) continues to accumulate the

error signal when the manipulated variable reaches a physical constraint.

Realizing that each element greatly contributes to the heat flux at the opposite product surface by multiple reflections, a coupling term was added to the proportional part of the controller. Thus, the final form of the PI digital control algorithm is given by

$$\Delta m_{1,k} = K_{P,1} \left[e_{1,k} - e_{1,k-1} + K_{c,1} \left(e_{2,k} - e_{2,k-1}\right)\right] + K_{I,1} \Delta t \, e_{1,k} \tag{D.5}$$

$$\Delta m_{2,k} = K_{P,2} \left[e_{2,k} - e_{2,k-1} + K_{c,2} \left(e_{1,k} - e_{1,k-1}\right)\right] + K_{I,2} \Delta t \, e_{2,k} \tag{D.6}$$

where Δm is the incremental change in the manipulated variable (input power), the subscripts 1 and 2 represent values associated with the lower and upper element (or product surface), respectively, and e_1 and e_2 are the error signals,

$$e_1 = r_3 - q''_{net,3} \tag{D.7}$$

$$e_2 = r_4 - q''_{net,4} \tag{D.8}$$

where r_3 and r_4 are the reference signals which are the desired net heat fluxes at the lower and upper product surfaces. Physically the coupling terms provide compensating action whenever the opposite error signal changes. For instance, if the heat flux at the upper product surface increases (for any reason), e_2 will decrease (becoming either less positive or more negative) and the coupling term causes Δm_1, the incremental change in the lower input power, to be less positive or more negative

than if there had been no change in the heat flux at the upper surface.

Deadbands on the manipulated variables were imposed such that whenever the magnitude of Δm, as given by equations D.5 and D.6, fell below a certain value no control action was taken on that manipulated variable. A deadband of ±6.0W was imposed on both manipulated variables throughout this study and is representative of the resolution of the Powerstats.

Table D.1 gives values of the coefficients of the PI digital control algorithm used throughout this study. These values were obtained from a series of trial and error experiments, using the 115 V Powerstats, where each coefficient was varied until satisfactory control performance was achieved. These experiments were performed with a scan rate of two per minute or a time increment of 30 seconds.

Table D.1 Coefficients of the PI Digital Control Algorithm.

Coefficient	$K_{P,1}$ (m^2)	$K_{c,1}$	$K_{I,1}$ (m^2/s)	$K_{P,2}$ (m^2)	$K_{c,2}$	$K_{I,2}$ (m^2/s)
	0.8	0.4	0.01	0.6	0.4	0.01

APPENDIX E - DERIVATION OF THE HEAT FLUX PREDICTOR ALGORITHM

E.1 Net Radiative Heat Flux

The net radiative heat flux at any surface i is given by

$$q''_{net,rad,i} = \alpha_i G_i - \varepsilon_i \sigma T_i^4 \tag{E.1}$$

where α_i, ε_i, and T_i are the absorptivity, emissivity, and temperature of surface i respectively, G_i is the irradiation on surface i, and σ is the Stefan-Boltzmann constant. The absorptivity and emissivity are equal because of the diffuse-gray assumption. For an enclosure with N surfaces, the irradiation on surface i can conveniently be expressed as [2]

$$G_i = \frac{1}{A_i} \sum_{j=1}^{N} \varepsilon_j A_j \hat{F}_{ji} \sigma T_j^4 \tag{E.2}$$

where $\hat{F}_{ji}$ is the total exchange factor and is defined as the ratio of radiant power leaving j and reaching i, directly and by all possible (diffuse) reflections, to the emissive power of j. The total exchange factors can be written in terms of view factors, surface properties, and other total exchange factors as

$$\hat{F}_{ij} = F_{ij} + F_{i1}\rho_1\hat{F}_{1j} + \dots + F_{ii}\rho_i\hat{F}_{ij} + \dots + F_{ij}\rho_j\hat{F}_{jj} + \dots + F_{iN}\rho_N\hat{F}_{Nj} \tag{E.3}$$

$$\text{or} \qquad \hat{F}_{ij} = F_{ij} + \sum_{k=1}^{N} F_{ik}\rho_k\hat{F}_{kj} \tag{E.4}$$

where F_{ij} is the view factor from surface i to j. The first term in equation E.4 represents the energy from i that reached j directly. Each term in the summation of equation E.4 represents the energy from i that is reflected from k and then reaches j directly and by all possible reflections.

Equation E.4 can be written in matrix notation as

$$[\hat{F}_{ij}] = [\delta_{ij} - F_{ij}\rho_j]^{-1}[F_{ij}] \tag{E.5}$$

where δ_{ij} is the Kronecker Delta function and is given by

$$\delta_{ij} = \begin{cases} 0 & i \neq j \\ 1 & i = j \end{cases} \tag{E.6}$$

Equation E.4 represents N^2 equations which can be solved by a variety of other means. Summation and reciprocity also apply to the total exchange factors

$$\sum_{j=1}^{N} \hat{F}_{ij}\alpha_j = 1 \tag{E.7}$$

and

$$A_i\hat{F}_{ij} = A_j\hat{F}_{ji} \tag{E.8}$$

Reciprocity can be shown for the special case of thermodynamic equilibrium and then generalized to any case since the total exchange factors depend only on geometry and surface properties (which are assumed to be independent of temperature and wavelength).

Combining equations E.1, E.2, and E.8 yields

$$q''_{net,rad,i} = \alpha_i \sum_{j=1}^{N} \epsilon_j \hat{F}_{ij}\sigma T_j^{\,4} - \epsilon_i \sigma T_i^{\,4} \tag{E.9}$$

The net radiative heat flux at surfaces 3 and 4 of Figure 4.2 (lower and upper product surfaces respectively) can be expressed as

$$q''_{net,rad,3} = \alpha_3\sigma[\varepsilon_1\hat{F}_{31}T_1^{\,4} + \varepsilon_2\hat{F}_{32}T_2^{\,4} + \varepsilon_3\hat{F}_{33}T_3^{\,4} + \varepsilon_4\hat{F}_{34}T_4^{\,4} + \varepsilon_5\hat{F}_{35}T_5^{\,4} + \varepsilon_6\hat{F}_{36}T_6^{\,4}] - \varepsilon_3\sigma T_3^{\,4} \tag{E.10}$$

$$q''_{net,rad,4} = \alpha_4\sigma[\varepsilon_1\hat{F}_{41}T_1^{\,4} + \varepsilon_2\hat{F}_{42}T_2^{\,4} + \varepsilon_3\hat{F}_{43}T_3^{\,4} + \varepsilon_4\hat{F}_{44}T_4^{\,4} + \varepsilon_5\hat{F}_{45}T_5^{\,4} + \varepsilon_6\hat{F}_{46}T_6^{\,4}] - \varepsilon_4\sigma T_4^{\,4} \tag{E.11}$$

Equations E.10 and E.11 can be simplified by assuming that the product surface temperatures T_3, T_4, and T_5 can be expressed by a single value T_p. Letting

$$T_3 = T_4 = T_5 = T_p \tag{E.12}$$

and collecting terms yields

$$q''_{net,rad,3} = a_3T_1^{\,4} + b_3T_2^{\,4} + c_3T_6^{\,4} + d_3T_p^{\,4} \tag{E.13}$$

$$q''_{net,rad,4} = a_4T_1^{\,4} + b_4T_2^{\,4} + c_4T_6^{\,4} + d_4T_p^{\,4} \tag{E.14}$$

where the coefficients a, b, c, and d are constants and are given by

$$a_3 = \alpha_3\varepsilon_1\hat{F}_{31}\sigma \tag{E.15}$$

$$b_3 = \alpha_3\varepsilon_2\hat{F}_{32}\sigma \tag{E.16}$$

$$c_3 = \alpha_3\varepsilon_6\hat{F}_{36}\sigma \tag{E.17}$$

$$d_3 = (\alpha_3\varepsilon_3\hat{F}_{33} + \alpha_3\varepsilon_4\hat{F}_{34} + \alpha_3\varepsilon_5\hat{F}_{35} - \varepsilon_3)\sigma \tag{E.18}$$

$$a_4 = \alpha_4\varepsilon_1\hat{F}_{41}\sigma \tag{E.19}$$

$$b_4 = \alpha_4\varepsilon_2\hat{F}_{42}\sigma \tag{E.20}$$

$$c_4 = \alpha_4\varepsilon_6\hat{F}_{46}\sigma \tag{E.21}$$

$$d_4 = (\alpha_4\varepsilon_3\hat{F}_{43} + \alpha_4\varepsilon_4\hat{F}_{44} + \alpha_4\varepsilon_5\hat{F}_{45} - \varepsilon_4)\sigma \qquad (E.22)$$

In most cases, the emissivity of the baking utensil will be very high and approximately the same value as the emissivity of food products. Thus, equations E.18 and E.22 can be further simplified by letting

$$\varepsilon_3 = \varepsilon_4 = \varepsilon_5 = \varepsilon_p \qquad (E.23)$$

Combining equation E.23 with equations E.18 and E.22 and setting emissivity and absorptivity equal, yields

$$d_3 = [\varepsilon_p(\hat{F}_{33} + \hat{F}_{34} + \hat{F}_{35}) - 1]\varepsilon_p\sigma \qquad (E.24)$$

$$d_4 = [\varepsilon_p(\hat{F}_{43} + \hat{F}_{44} + \hat{F}_{45}) - 1]\varepsilon_p\sigma \qquad (E.25)$$

E.2 Convective Heat Flux

Convection heat transfer can become an important fraction of the total heat transfer to a product in the Bi-Radiant Oven. Free convection to the heat flux gage, both in the oven cavity and in a quiescent medium, is discussed in section 3 of Appendix A. Because of large variations in the gage output when facing down and because many products have utensils which shroud the upper surface, the gage convection results are not applicable to products in the oven. For lack of any better alternative, standard correlations must be used to predict convection. On the lower surface the laminar correlation of Lloyd & Moran [16] and on the upper surface the correlation of Fujii & Imura [9] were selected to estimate the convection heat flux to a product. The laminar correlation can be used because of the low Ra encountered in the oven as mentioned in Appendix A.

To maintain the simplicity of the overall algorithm, the standard correlations were cast into a simplified form by evaluating air properties at a single film temperature and assuming that they remain constant. Solving the Lloyd & Moran correlation [16] for h and evaluating all air properties at 400K, yields

$$h_3 = 1.287(W/m^{7/4}\text{-}K^{5/4})\left[\frac{T_A - T_p}{L^*}\right]^{1/4} \qquad (E.26)$$

where h_3 is the convection coefficient for the lower product surface, T_A is a characteristic air temperature, T_p is the product temperature, and L^* is the characteristic length of the product based on area divided by perimeter. Fujii & Imura [9] compare their results with infinite strip results from other authors and use the width of the strip as the characteristic length. For an infinite strip, L^* is equal to one half the strip width. Solving the Fujii & Imura correlation for h, evaluating all air properties at a film temperature of 400K, and correcting for the more general characteristic length, L^*, yields

$$h_4 = 0.447(W/m^{8/5}\text{-}K^{6/5})\left[\frac{T_A - T_p}{(L^*)^2}\right]^{1/5} \qquad (F.27)$$

where h_4 is the convection coefficient for the upper product surface.

Adding the convective heat flux to the net radiative heat fluxes at the lower and upper surfaces (equations E.13 and F.14 respectively) yields the final form of the heat flux predictor algorithm

$$q''_{net,3} = a_3T_1^4 + b_3T_2^4 + c_3T_6^4 + d_3T_p^4 + h_3(T_A - T_p) \qquad (F.28)$$

$$q''_{net,4} = a_4T_1^4 + b_4T_2^4 + c_4T_6^4 + d_4T_p^4 + h_4(T_A - T_p) \qquad (E.29)$$

where T_A is a characteristic air temperature, T_p is a characteristic product temperature, the subscripts 1, 2, 3, 4, and 6 represent values associated with the lower element, upper element, lower product surface, upper product surface, and walls respectively, h_3 and h_4 are the convection coefficients for lower and upper product surfaces, respectively and are given by equations E.26 and F.27, and the coefficients a, b, c, and d are given by equations F.15 through E.22. Physically, the terms in equations F.28 and E.29 can be considered as contributions to the net heat flux due to emission from the lower element, upper element, walls, and product and due to convection.

BI-RADIANT OVEN

A LOW-ENERGY OVEN SYSTEM

Part 3 — Food Requirements and Commercialization

BI-RADIANT OVEN

A

LOW ENERGY OVEN SYSTEM

VOLUME III — APPLICATION AND TRANSFER OF THE TECHNOLOGY

PART 3 - FOOD REQUIREMENTS AND COMMERCIALIZATION

Dr. M. V. Peart
Adel Coates

EQUIPMENT LABORATORY
PURDUE UNIVERSITY
W. Lafayette, Indiana 47907

June 15, 1981

Prepared under Subcontract 86X-0082C for the

OAK RIDGE NATIONAL LABORATORY
Oak Ridge, Tennessee 37830

Operated by

UNION CARBIDE CORPORATION
for the
U.S. DEPARTMENT OF ENERGY
Contract No. W-7405-eng-26

CONTENTS

LIST OF TABLES 3-v

LIST OF FIGURES 3-vii

PREFACE 3-ix

ABSTRACT 3-xi

1. INTRODUCTION 3-1
   1.1 Phase 1 3-1
   1.2 Phase 2 3-1

2. BACKGROUND AND PREVIOUS WORK 3-3
   2.1 Heat adsorption by Food in an Oven 3-3
   Regulating Heating Rates for the Upper and Lower Surfaces of Foods in a Conventional Oven 3-4
   Regulating Heating Rates for the Upper and Lower Surfaces of Foods in a Bi-Radiant Oven 3-5
   2.2 Phase 1 Summary 3-6
   Upper and Lower Heat Rates of Foods 3-6
   Energy Balance Analyses 3-7
   Energy Use Comparison 3-8
   Concern in Commercialization 3-9

3. THERMAL IRRADIATION REQUIREMENTS OF FOODS IN A BI-RADIANT OVEN 3-10
   3.1 Description of Ovens and Measuring Devices 3-11
   3.2 Experimental Procedures for Baking Foods 3-13
   Cakes 3-13
   Other Foods 3-16
   3.3 Irradiation Levels for Baking 3-16
   Irradiation Levels for Cake Baking 3-17
   Accomodating All Conventional Oven Thermostat Settings .. 3-23
   Short Baking Time 3-33
   Utensil Size 3-33
   Utensil Emissivity 3-35
   Utensil Mass 3-47
   Tolerance of Cake to Uneven Irradiation 3-52
   Maintaining the Bi-Radiant Oven Interior 3-57
   Summary 3-59

4. COMMERCIALIZATION OF THE BI-RADIANT OVEN 3-61
   4.1 Merits of the Bi-Radiant Oven System 3-61
   Energy Conservation 3-61
   Baking Capability 3-61
   Spatial Requirements 3-62
   Reduced Insulation Costs 3-62
   Controls for the Bi-Radiant Oven 3-62
   4.2 Concerns in the Commercialization of the Bi-Radiant Oven System 3-63
   Oven Lining Material 3-63

Oven Controls..... 3-64
Baking Utensils..... 3-64

5. REFERENCES..... 3-65

6. APPENDICES..... 3-67
6.1 Appendix A..... 3-67
Schematic Diagram of Bi-Radiant Oven Experimental Controls for Use with Bi-Radiant Ovens II and III. Equipment Laboratory..... 3-67
6.2 Appendix B..... 3-69
Construction of the Irradiation Heat Flux Gauge..... 3-69
Calibration of the Irradiation Heat Flux Gauge..... 3-73
6.3 Appendix C..... 3-75
Standard Procedure for Placement of Thermocouples in Pans..... 3-75
6.4 Appendix D..... 3-77
Procedure for Mixing Cakes..... 3-77

LIST OF TABLES

Number		Page
3.1	Description of Experimental Ovens	3-12
3.2	Bi-Radiant Oven Settings Used for Various Conventional Oven Thermostat Settings. Bi-Radiant Oven III	3-25
3.3	Acceptable Baking Using the Prescribed Upper and Lower Element Settings in Bi-Radiant Oven III	3-30
3.4	Unacceptable Baking Using the Prescribed Upper and Lower Element Settings on Bi-Radiant Oven III	3-32
3.5	Upper and Lower (U/L) Wattage Required to Produce Irradiation Levels for Baking at Six Equivalent Thermostat Settings. Baking Utensils of Three Sizes. Bi-Radiant Oven III	3-36
3.6	Voltage Requirements for Upper and Lower (U/L) Elements to Produce irradiation Levels. Baking Utensils of Three Sizes. Bi-Radiant Oven III	3-37
3.7	Characteristics of Cake Pans	3-41
3.8	Effects of Heat Absorption Capacity of Baking Utensils on Yellow Cakes. Bi-Radiant Oven III	3-44
3.9	Effects of Even and Uneven Irradiation Levels on Cake Baking in a Bi-Radiant Oven	3-53
3.10	Effects of Spattering and Tratment of Oven Cavity on Irradiation Levels. Bi-Radiant Oven III	3-58
D.1	Proportions for Yellow Cake Batter	3-77

LIST OF FIGURES

Number		Page
3.1	Gauge Response to Irradiaton to the Upper and Lower Baking Planes at Upper and Lower Element Settings of 526W and 336W Respectively. Bi-Radiant Oven III	3-14
3.2	Comparison of Cake Temperatures at U/L Irradiation Levels of 3370/2410 W/m^2 in Bi-Radiant Oven II and 3530/2020 W/m^2 in Bi-Radiant Oven III. Center Top Thermocouple	3-19
3.3	Comparison of Cake Temperatures at U/L Irradiation Levels of 3370/2410 W/m^2 in Bi-Radiant Oven II and 3530/2020 W/m^2 in Bi-Radiant Oven III. Center Bottom Thermocouple	3-20
3.4	Comparison of Cake Temperatures at U/L Irradiation Levels of 3690/2930 W/m^2 and 3070/2330 W/m^2 in Bi-Radiant Oven III. Center Top Thermocouple	3-21
3.5	Comparison of Cake Temperatures at U/L Irradiation levels of 3690/2930 W/m^2 and 3070/2330 W/m^2 in Bi-Radiant Oven III. Center Bottom Thermocouple	3-22
3.6	Bi-Radiant Oven Upper (U) and Lower (L) Irradiation Levels that Correspond to Conventional Oven Thermostat Settings	3-24
3.7	Variations in Irradiation Level on the Upper Surface of a 24.8 x 35.2 cm Baking Utensil with Variations in the Upper and Lower Element Wattages. Bi-Radiant Oven III	3-27
3.8	Variations in Irradiation Level on the Lower Surface of a 24.8 x 35.2 cm Baking Utensil with Variations in the Upper and Lower Element Wattages. Bi-Radiant Oven III	3-28
3.9	A Comparison of the Effects of Black and Shiny Aluminum Pans on Cake Temperatures Baked at the Same Setting. Center Top Thermocouples. Bi-Radiant Oven III	3-42
3.10	A Comparison of the Effects of Black and Shiny Aluminum Pans on Cake Temperatures Baked at the Same Setting. Center Bottom Thermocouples. Bi-Radiant Oven III	3-43

3.11 A Comparison of the Effect of Black and Shiny Aluminum Pans on Cake Temperature Baked at Adjusted (Optimum) Settings. Center Top Thermocouples. Bi-Radiant Oven III..... 3-45

3.12 A Comparison of the Effects of Black and Shiny Aluminum Pans on Cake Temperatures Baked at Adjusted (Optimum) Settings. Center Bottom Thermcouples. Bi-Radiant Oven III..... 3-46

3.13 A Comparison of the Effects of Black Aluminum, Black Stainless Steel and Heat Resistant Glass Pans on Cake Temperatures Baked at the Same Setting. Center Top Thermocouples. Bi-Radiant Oven III..... 3-48

3.14 A Comparison of the Effects of Black Aluminum, Black Stainless Steel and Heat Resistant Glass Pans on Cakes Temperatures Baked at the Same Setting. Center Bottom Thermocouples. Bi-Radiant Oven III..... 3-49

3.15 A Comparison of the Effects of Black Aluminum and Heat Resistant Glass on Cake Temperatue, Baked at Adjusted (Optimum) Settings. Center Top Thermocouple. Bi-Radiant Oven III..... 3-50

3.16 A Comparison of the Effects of Black Aluminum and Heat Resistant Glass Pans on Cake Temperatures Baked at Adjusted (Optimum) Settings. Center Bottom Thermocouple. Bi-Radiant Oven III..... 3-51

3.17 Temperature Rise of Top-Mid Thermocouple. Even vs. Uneven Irradiation. Bi-Radiant Oven II..... 3-55

3.18 Temperature Rise of Mid-Bottom Thermocouple. Even vs. Uneven Irradiation. Bi-Radiant Oven II..... 3-56

B.1 Interior view of the irradiation heat flux gauge..... 3-70

B.2 Thermocouple arrangement of the irradiation heat flux gauge..... 3-71

B.3 Exterior view of the irradiation heat flux gauge..... 3-72

PREFACE

This section of the report on the application and transfer of the Bi-Radiant Oven Technology was prepared in the Equipment Laboratory in the School of Consumer and Family Sciences at Purdue University. It covers the activities of the Equipment Laboratory through the second phase of the Bi-Radiant Oven project. In addition to Dr. M. Virginia Peart and Adel Coates who designed test methodology and analyzed the data in addition to helping with data collection, several other people have contributed to work that was done in the Equipment laboratory. Dr. Carolyn Garrison of Brigham Young University helped in the design and implementation of various test procedures and instrumentation that were used. Deborah Schulz and Monica Lonergan each served as a technician performing many of the tests.

ABSTRACT

The Bi-Radiant Oven utilizes a new baking and roasting method to conserve a major portion of the energy required for baking in either a conventional or convection oven. In Phase 1 of the Bi-Radiant project, "The Development and Assessment of the Bi-Radiant Oven," work was done to develop a better understanding of the heating requirements of foods. It was found that excellent quality baked foods can be produced by irradiation only, that the upper and lower surfaces of foods require different heat absorption rates, that the ratio of upper-to-lower irradiation for heat absorption rates is different for different foods, and that the ratio of upper-to-lower irradiation rates can be controlled by the operating wattage level of the upper and lower heating elements. Energy balance analyses were also made to assess how the heat that is absorbed during baking is partitioned among the product being baked, moisture losses that occur during baking and the baking utensil.

This report covers Phase 2 of the project in the Equipment Laboratory, "Application and Transfer of the Bi-Radiant Technology." Foods have been categorized into groups that require common sets of upper and lower irradiation rates so that controls can be developed to meet the baking requirements of all foods. Utensil size, capacity for absorbing and holding heat and thermal emissivity each requires special consideration in the setting of the upper and lower element wattages. Guidelines for dealing with these entities are provided.

LOW ENERGY OVEN SYSTEM

Phase 2 - Application and Transfer of the Technology

FOOD REQUIREMENTS AND COMMERCIALIZATION

1. INTRODUCTION

1.1 Phase 1

During Phase 1 of the project, Development and Assessment of the Bi-Radiant Oven, work in the Equipment Laboratory at Purdue University was involved with developing an understanding of oven heating requirements of foods. Studies were directed toward demonstrating that the upper and lower surfaces of foods being baked require different heating rates. Upper and lower baking rates can be too fast, too slow or unbalanced. It was further demonstrated that the required baking rates for a wide variety of foods could be supplied by radiation in a Bi-Radiant Oven. Energy balance analyses were made to assess how the heat that is absorbed during baking is partitioned among the product being baked, moisture losses that occur during baking and the baking utensil.

1.2 Phase 2

During Phase 2 of the project, Application and Transfer of the Bi-Radiant Oven Technology, the research in the Equipment Laboratory has been directed toward categorizing foods into groups that would have common baking rate requirements, so that controls might be

developed to provide radiation levels at the upper and lower surfaces and meet the baking requirements of any food that might be baked. Additionally, various characteristics (size, capacity for absorbing heat, and thermal emissivity) of baking utensils were studied to determine how these might impose special considerations in the design of controls for the Bi-Radiant Oven.

2. BACKGROUND AND PREVIOUS WORK

To better understand how a Bi-Radiant Oven functions, it is important to understand the baking process and how it is accomplished in a conventional electric oven. Then comparisons can be made as to how Bi-Radiant Oven baking is alike or different.

2.1 Heat absorption by Food in an Oven

When a food is baked it absorbs heat on all surfaces. The upper surface of the food, if not covered, is exposed and directly absorbs heat that is radiated and convected to it. The lower surface and sides of the food absorb heat that is first absorbed by the baking utensil and is then conducted through the utensil material to the food where contact is made. Much of the heat absorbed by the exposed surface of a food being baked is utilized to evaporate moisture. When enough moisture has been evaporated so that the concentration of amino acids and reducing sugars is great enough and the temperature is high enough, Maillard browning occurs. When the lower surface of the food gets hot enough it will drive moisture upward, allowing the same conditions for browning to occur there. It is important to regulate the rates at which heat is absorbed by the upper and lower surfaces of a food so that browning of the two surfaces occurs simultaneously with "doneness" at the center of the food. For a rare roast, doneness would be a pink, juicy roast, with a center temperature at about 60°C. For a food product like cake or bread, the heat absorption process must be timed to allow leavening agents to react and produce gas cells as the protein in the food denatures and the starch becomes partially

gelatinized. Unbalanced baking rates, where the rate of heat transfer to either the bottom or top of a food is too great, will produce a baked food that is unevenly done. For meats, portions would be overcooked and tough before other portions are done. Unbalanced baking rates will cause tunnels or cracked tops in many leavened foods.

Regulating Heating Rates for the Upper and Lower Surfaces of Foods in a Conventional Oven

In a conventional gas or electric oven, regulating and balancing heat absorption rates at the upper and lower surfaces of a food require a prescribed thermostat setting and the use of an appropriate baking utensil. The baking utensil is important because it determines the balance between the upper and lower baking rates.

The use of a bright, shiny utensil with a low emissivity (absorptivity) produces a light lower crust and a fine cell structure in cakes, muffins, cookies and similar foods. The use of the same shiny material for a pie pan will result in a soggy lower pie crust. Many casseroles baked in the same shiny material will be too brown on the top surface before the interior reaches the desired bubbly stage. On the other hand, a dark absorbing material will help brown the bottom crust of a fruit pie or will help bring a moist casserole up to temperature before the top becomes overcooked. A cake baked in a pan of the same absorptive material will be overly brown on the bottom and will have tunnels.

Heat transfer within a conventional electric oven to the upper and lower surfaces of a food is quite inflexible. When the oven

thermostat is set at 177°C (350°F), for example, the combinations of radiant and convective heat transfer to these two primary baking surfaces of food in a utensil though different from each other remains pretty much the same no matter what food or utensil is used. Because the heat source, a resistance heater, is in the bottom of an electric oven, the combination of radiant and convective heat transfer will always be greater on the lower surface of the product (and utensil) than it is on the upper surface. Controlling the rate of heat transfer to the upper surface can be accomplished by use of the desired thermostat setting. Total heat transfer to the lower surface of the food can only be controlled by "subtracting" a portion of irradiation heat transfer by using a utensil that has a lower emissivity and will reflect thermal radiation.

Regulating Heating Rates for the Upper and Lower Surfaces of Foods in a Bi-Radiant Oven

The presence of two heating elements that can be controlled independently, as in a Bi-Radiant Oven, allows an oven design that accomodates foods having quite different heating requirements for the upper and lower cooking surfaces. This aspect of the Bi-Radiant Oven is discussed more fully throughout section 3 in this report.

2.2 Phase 1 Summary

Upper and Lower Heat Rates of Foods

During Phase 1 the heating requirements for baking small beef roasts were studied using Bi-Radiant Oven II [1]. Roasts were baked at five rates (NORMAL, SLOW, FAST, TOPFAST and BOTTOMFAST). The irradiation levels on the upper and lower surfaces were measured using an irradiation heat flux gauge [2]. Roasts baked at upper and lower irradiation rates of 3200 and 2500 W/m^2 (Watts per square meter) respectively, considered for this study to be the NORMAL rate, were juicy with pink interiors and even browning on all surfaces. The roasts prepared at the SLOW rate with upper and lower irra ation levels of about 2200 and 2000 W/m^2 had the same desirable characteristics. Balancing the irradiation levels on the upper and lower surfaces between the two sets of irradiation levels can be expected to produce acceptable roasts in a Bi-Radiant Oven. Using a generally FAST rate or unbalanced baking rates with too much irradiation on either the upper or lower surface of the roast produced poor quality roasts with large cooking losses and consumed more electrical energy in doing so.

A study similar to the one on beef roasts was made using yellow cakes in Bi-Radiant Oven III. Descriptions of Bi-Radiant Oven II and III appear in section 3.1 of this report. Bi-Radiant Oven III was used in the Equipment Laboratory for the cake study before it had been equipped with thermocouples for measuring element and wall temperatures. This oven was equipped with a solid shelf that could be used

to compartmentalize the oven. The cake study was performed in a compartmentalized section of Bi-Radiant Oven III.

In this study upper and lower irradiation levels of about 2500 and 2000 W/m^2 produced the most satisfactory cakes. Faster, slower and unbalanced rates all produced cakes of poor quality although they all consumed about the same amount of energy. Comparing data taken during Phase 2 when the full oven cavity was used has led to the belief that, in the compartmented cavity, the percentage of energy contributed by convection heat transfer is greater than when the full cavity is used.

Energy Balance Analyses

The heat absorption requirements of foods were also studied during Phase 1 by performing energy balance analyses. The energy balance can be expressed as

$$Q_t + Q_b = Q_p + Q_u + Q_e + Q_x \tag{3.1}$$

Where Q_t and Q_b are estimates of the radiant energy absorbed by the top and bottom surfaces of a food product as determined by measurements of irradiation incident on each surface, the area and emissivity of each surface as well as the time of exposure during baking. Q_p is the energy stored in the food calculated from the mass of the food, specific heat and temperature rise during baking. Q_u is the energy stored in the baking utensil as calculated by the utensil mass, specific heat and temperature rise. Q_e represents the energy required

to evaporate the moisture lost during the baking process. Q_x is the unaccounted for difference between $Q_t + Q_b$ and $Q_p + Q_u + Q_e$ and might result from a variety of activities and processes that are not fully understood such as the vaporization of some moisture within some foods and surface changes on foods that might alter the emissive characteristics and the capability of that food to absorb thermal radiation.

The energy balances showed that in most cases the temperature rise in the food itself accounted for most of the energy utilized during baking or roasting. Energy required to evaporate moisture from foods often accounted for two-thirds as much energy as for heating foods and was considerably more for meat products. The baking utensils absorbed the least amount of accountable energy use. Metal utensils used about twenty-five percent as much energy as required to heat the food, but glass baking dishes usually consumed fifty percent or more than required to heat the food.

Energy Use Comparison

Energy requirements for baking in Bi-Radiant Oven II were compared to the energy requirements in a conventional electric oven. The Bi-Radiant Oven consistently used less energy. Of the seven foods included in the energy balance studied, savings in energy ranged from fifty-seven to seventy-three percent.

Concerns in Commercialization

Several concerns in commercialization of the Bi-Radiant Oven were addressed in the Phase 1 report. These concerns included:

1. costs of producing a Bi-Radiant Oven,

2. considerations in maintaining energy efficiency of the Bi-Radiant Oven, during use for baking and roasting,

3. convenience and satisfactions of the Bi-Radiant Oven as compared to a conventional electric oven, and

4. suitable utensils for the Bi-Radiant Oven and whether alternative utensils might successfully be used in a Bi-Radiant Oven.

Items 2 and 4 were investigated more fully in Phase 2. Since Items 1 and 3 are producer and consumer related, they were not addressed in this phase of the work.

For more detail about the activities and results of the Oven Heating Requirements of Foods or Concerns in Commercialization during Phase 1, please refer to sections 4.0 and 5.0 of Volume 1 of Bi-Radiant Oven - A Low-Energy Oven System.[1]

3. THERMAL IRRADIATION REQUIREMENTS OF FOODS IN A BI-RADIANT OVEN

Before controls can be developed for a Bi-Radiant Oven, it is necessary to determine what irradiation levels will produce acceptable baked foods of all types. Instrumentation for measuring irradiation was not available in the Equipment Laboratory until shortly before the report for the first phase of the project was written. During the period before instrumentation was available, each food that was tested was prepared first in a conventional oven so that important characteristics of the baked food might be determined as a guide for what would be acceptable as a baked product in the Bi-Radiant Oven.

Determining the optimum setting of controls for the upper and lower elements for various foods frequently required several trials. During this period the importance of characteristics of baking utensils, in addition to their emissivities (or absorptivities), became evident. Heat treated glass, even though it has a high emissivity, required higher element settings than blackened aluminum which was used as a standard. Biscuits and cookies baked on large baking sheets for short periods of time required higher settings to produce acceptable products in the anticipated time.

The primary objective of the Equipment Laboratory during Phase 2 was to categorize foods into several groups that have common baking requirements so that settings could be designated to accomodate all foods that are normally baked. Additionally, the effects of utensil material and size were addressed. Sensitivity of cakes to uneven irradiation levels was studied to help determine what variations in

irradiation level might be tolerated. It is believed that cakes are less tolerant than other foods to variations in radiation to the upper and lower baking surfaces. Designing an oven to accomodate the requirements of cakes would provide acceptable baking for other foods as well. The effects of spattering of foods on irradiation levels was also evaluated.

3.1 Description of Ovens and Measuring Devices

Bi-Radiant Oven III was used for all of the Phase 2 research in the Equipment Laboratory except for a study on the sensitivity of cakes to variations in irradiation. Descriptions of Bi-Radiant Ovens II and III appear in Table 3.1. They are similar but not identical in size and shape. The interior in Bi-Radiant Oven III was slightly more highly polished. The elements of Bi-Radiant Oven III cover a larger area and the elements are located closer to the oven top and bottom surfaces than were the elements in Bi-Radiant Oven II. The distances between the elements and the baking rack were different for each oven as well. There is no reason to believe that either of the oven designs is optimum as to the combination of baking performance and energy conservation. Both, however, do provide irradiation levels that produce acceptable baked foods and both are energy conserving relative to the conventional oven design.

During the first phase, baking was done with a partitioning shelf in Bi-Radiant Oven III [1]. During Phase 2, the full oven cavity was used.

Table 3.1
Description of Experimental Ovens

	Bi-Radiant Oven II	Bi-Radiant Oven III
Interior		
Dimensions		
Width	54.6 cm	58 cm
Height	40.7 cm	42.8 cm
Depth	48.4 cm	42.5 cm
Material	Aluminum Sheeting	Aluminum Sheeting
Finish	"as received"	Mechanically Polished
Thickness	0.8 mm	0.8 mm
Element		
Configuration	2 Loop	3 Loop
Area	19.5 x 18.4 cm	35.3 x 30.3 cm
Diameter	0.6 cm	0.6 cm
Resistance	13 ohms	19 ohms
Distance from Oven Top and Oven Bottom	4.20 cm	2.5 cm
Baking Rack		
Distance from Top Element	23.5 cm	19.5 cm
Distance from Bottom Element	7.5 cm	17.5 cm

The same set of controls was used for each of the two ovens. Auto transformers equipped with volt meters were used to set the elements to the desired setting (Appendix A). Energy use was measured separately for each element by Duncan Electric kilowatt hour meters. Temperatures of foods being baked and of the oven were recorded by an Esterline Angus 24 point recording potentiometer. Irradiation levels incident on the upper and lower baking planes were estimated from measurements made with an Irradiation Heat Flux Gauge [2] for the variety of utensils used for baking (Appendix B). Steady state equilibrium type measurements of irradiation were made in the utensil center with the gauge facing upward at the level of the upper edge of the utensil and facing downward at a distance of about 0.6 cm below the oven rack. Figure 3.1 displays an example of the millivolt output of the irradiation heat flux gauge for upper and lower surface irradiation levels over the initial 15 minute "oven on" period. The irradiation levels used in this report were calculated from an average millivolt output at 10 and 15 minutes.

3.2 Experimental Procedures for Baking Foods

Cakes

Yellow cake is a good product for evaluating irradiation levels in a Bi-Radiant Oven since the baking process must be carefully timed to permit the activity of leavening agents, the denaturation of protein and the gelatinization of starches to occur in the proper sequence. Browning of the upper and lower surfaces of cake occurs during the final period of the baking process. In some tests, cakes

ORNL-DWG. 81-23787

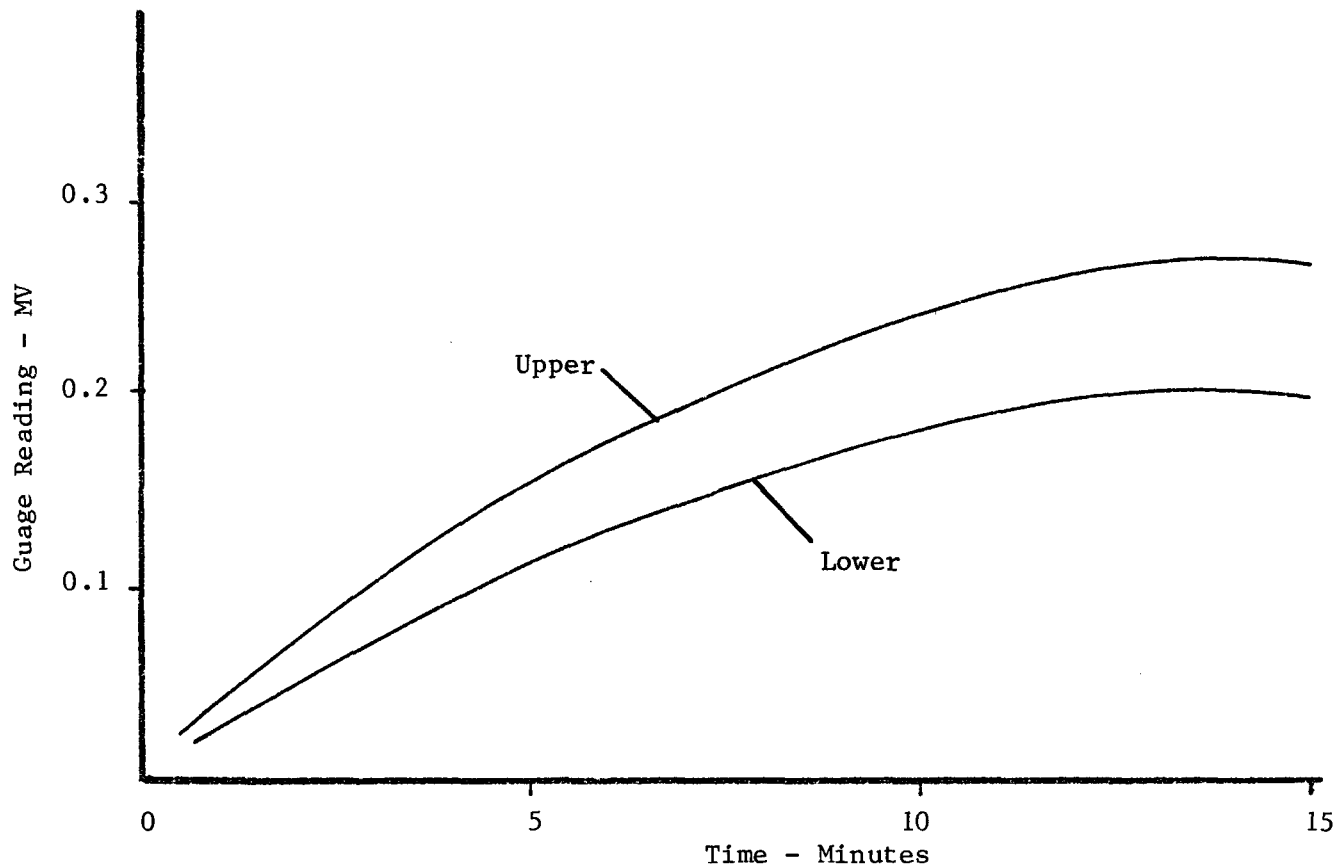

Figure 3.1 Guage Response to Irradiation on the Upper and Lower Baking Planes at Upper and Lower Element Settings of 526W and 336W Respectively. Bi-Radiant Oven III.

were baked in 22.9 cm (9") diameter cake pans. However, when utensil materials and finishes were compared, cake pans of 20.3 cm (8") were used since cake pans of the other materials used were available in only the 20.3 cm size.

In the experiments using cakes, one of the two cake pans used was equipped with nine small gauge (0.075 mm diameter) thermocouples placed in three glass capillary tubes (3 per tube). See Appendix C. This arrangement permitted temperatures to be measured during baking along the bottom of the pan (0.5 cm from the bottom) at the center of the pan and at a mid point about 3.8 cm in from the pan edge, at the edge and at heights of 1.6 and 3.2 cm in each capillary tube. The batter did not cover the center top thermocouple until sometime during the final five to ten minutes of baking.

A yellow cake mix was used for all the cake tests reported (Appendix D). Ingredients were at room temperature when they were mixed and all other procedures were carefully standardized. Batter was weighed into each cake pan. Four hundred grams of batter was used in each 22.8 cm cake pan. The amount of batter used for baking 20.3 cm cakes was varied to provide the same batter depth for each pan to accomodate slightly different sizes and shapes. Temperatures were monitored throughout baking. Cakes were weighed within five minutes of removal from the oven to measure moisture loss during baking. Volume, texture and browning were evaluated. When cakes were baked, three replications were made of each test.

Other Foods

When irradiation levels had been established to simulate conventional oven baking results at common thermostat settings, a variety of foods was baked. Acceptability of Bi-Radiant Oven baked foods other than cakes was determined by comparing results with conventionally baked food. Acceptability of baked products was determined by evaluating a combination of browning of the upper and lower surfaces and thermal setting of ingredients in the center of the food or reaching an acceptable internal serving temperature.

3.3 Irradiation Levels for Baking

Because foods baked during the Phase 1 experiments did not fall into logical groups to be baked with common settings of the elements, various characteristics of foods were studied to determine how each might contribute to baking requirements of any food. The characteristics of the foods that were studied included the mass, specific heat, temperature change to produce a done product, the depth or thickness of the food, moisture content, fat content and density. Various utensil characteristics such as emissivity, mass, specific heat and size were also studied. The important factors appeared to deal primarily with the baking utensil. This is logical since some of the same utensil characteristics affect baking rates in a conventional oven. Looking at baking results, alterations were made in early tests when utensils used had different emissivities or a larger heat capacity. Additionally, the area covered by the utensil contributed to a need to adjust the element settings to produce the best foods. With these

factors in mind foods were categorized into groups that require common thermostat settings for conventional oven baking.

Many groups of foods are quite tolerant of faster and slower baking rates if the rate of heat transfer to the upper surface is properly balanced with the rate to the bottom surface. Many groups of leavened foods and meats, however, are less tolerant than this group. Because of differences in the tolerance to baking rates, it seems important to accept the baking times used by a conventional oven as standards for Bi-Radiant Oven baking. This would allow Bi-Radiant baking rates to correspond to the conventional oven thermostat settings. Once adaptations to accomodate various baking utensil characteristics have been defined, a Bi-Radiant Oven with solid state controls can be designed to provide the appropriate upper and lower irradiation rates to give optimum baking results each time baking is done.

At a later time manufacturers may want to identify for consumers who use their ovens, foods that are tolerant of faster baking rates. Appropriate control settings and shorter baking times could be provided. There would be no problem of overcooking on one baking surface (upper or lower) as might occur when the thermostat setting is advanced in a conventional oven. There was not time to do this in the Equipment Laboratory during Phase 2.

Irradiation Levels for Cake Baking

Many foods including cakes are baked at a 177°C (350°F) thermostat setting. To determine a set of irradiation levels for the upper and lower surfaces of foods to be baked at a Bi-Radiant setting

comparable to a 177°C (350°F) conventional oven thermostat setting, cakes were again baked. When the partitioned form of Bi-Radiant Oven III was used during Phase 1, upper and lower irradiaton levels of 2500 and 2000 W/m^2 produced acceptable yellow cakes. Using the full oven cavity seemed to require higher irradiation levels leading to the belief that in the smaller partitioned cavity more heat transfer by convection occurred during baking. Previously cakes had been baked in Bi-Radiant Oven II at U/L (upper/lower) irradiation levels of 3370/2410 W/m^2. Similar results were obtained in Bi-Radiant Oven III at irradiation levels of 3530/2020 W/m^2. The two sets of irradiation rates baked cakes to a minimum internal temperature of about 88°C in about the same length of time (Figure 3.2). The bottom crusts were very light in color and did not reach 100°C in either case (Figure 3.3).

The ratio of upper to lower irradiation levels was reduced from 1.6 to about 1.3 and cakes were baked at two additional irradiation rates: 3690/2930 W/m^2 and 3070/2330 W/m^2 (Figures 3.4 and 3.5). Again cakes were baked to an internal temperature of about 88°C. Cakes baked at the higher U/L irradiation rates baked in 19.5 minutes and in 26.9 minutes at the lower rates. The temperatures of the center bottom of the cakes were both above 100°C for a long enough period for an acceptable degree of browning to occur.

Since the baking time of cakes baked in Bi-Radiant Oven II at 3070/2330 W/m^2 more closely matched the conventional baking time of 30 minutes, it was selected as the normal setting for foods that are accomodated by a 177°C (350°F) conventional oven thermostat setting.

ORNL-DWG. 81-23788

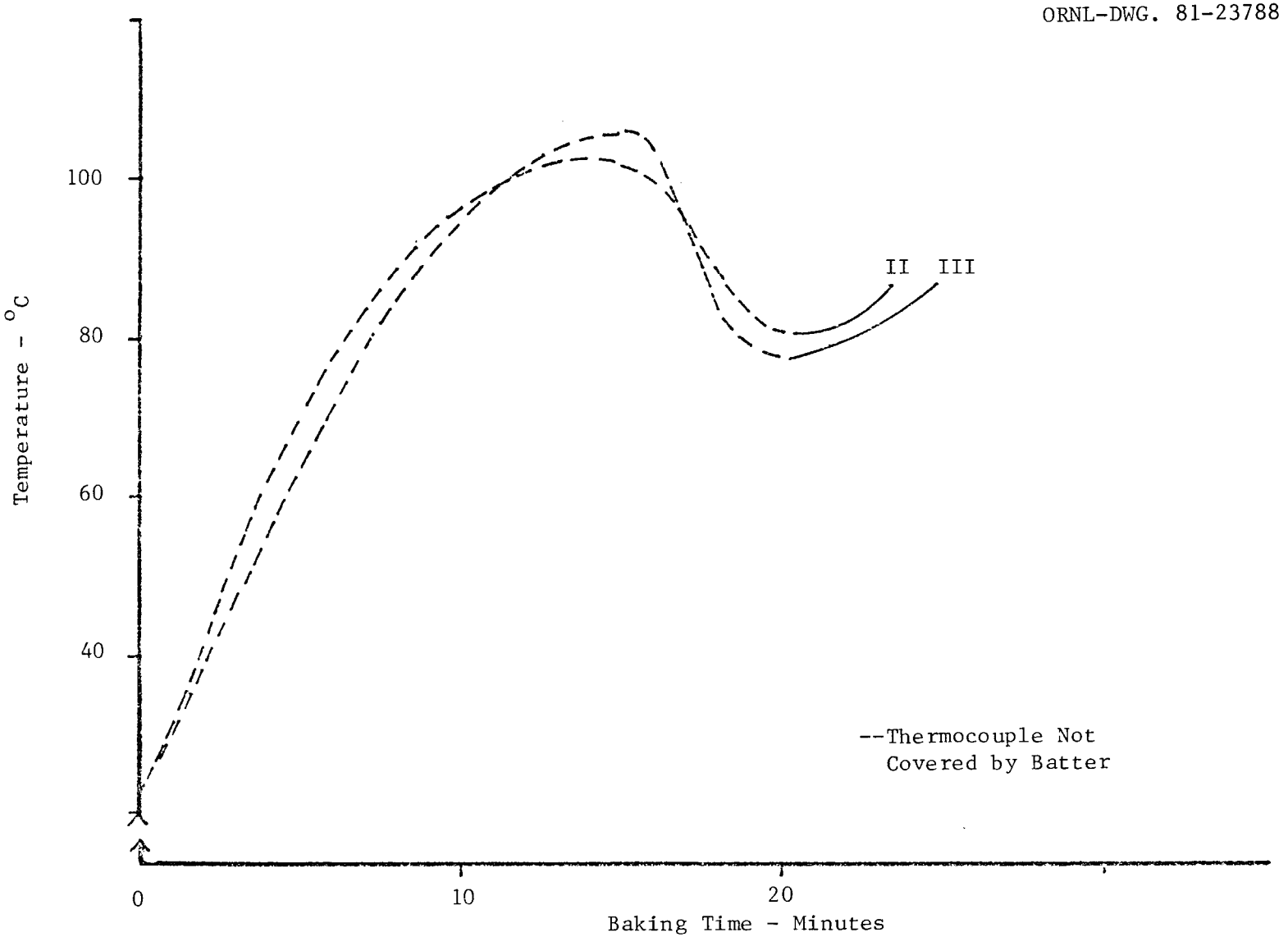

Figure 3.2 Comparison of Cake Temperatures at U/L Irradiation Levels of 3370/2410 W/m^2 in Bi-Radiant Oven II and 3530/2020 W/m^2 in Bi-Radiant Oven III. Center Top Thermocouple.

ORNL-DWG. 81-23789

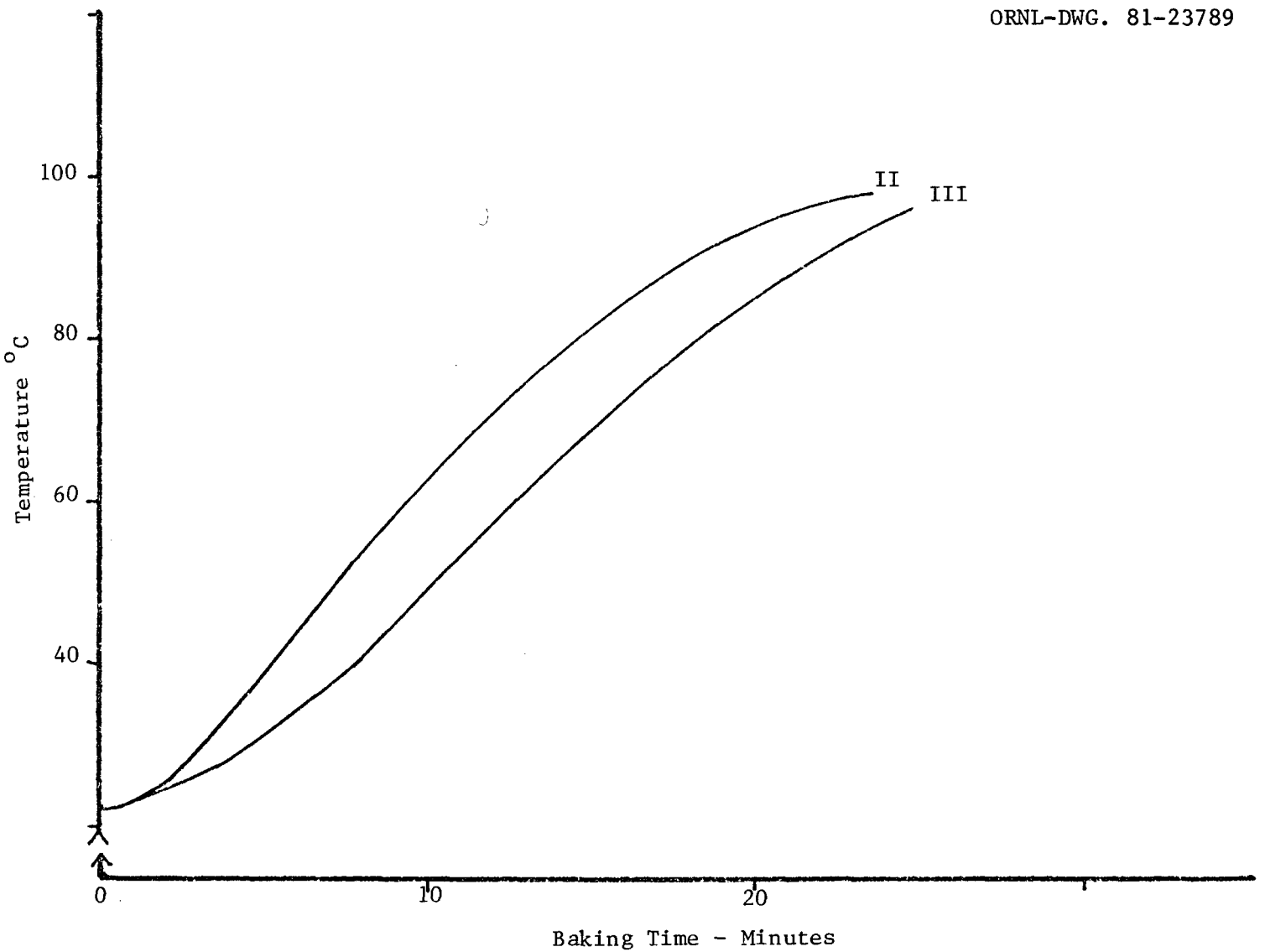

Figure 3.3 Comparison of Cake Temperatures at U/L Irradiation Levels of 3370/2410 W/m^2 in Bi-Radiant Oven II and 3530/2020 W/m^2 in Bi-Radiant Oven III. Center Bottom Thermocouple.

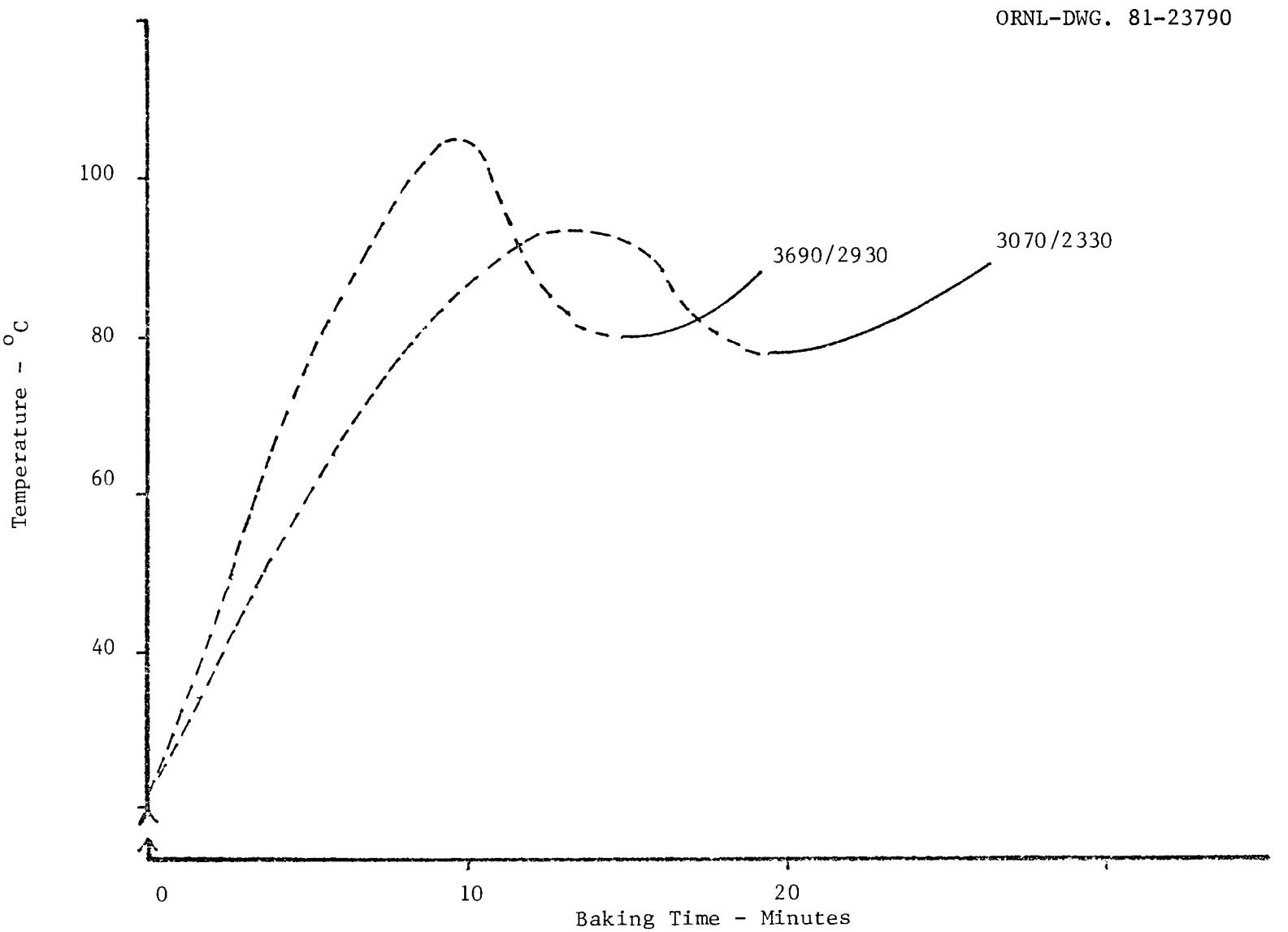

Figure 3.4 Comparison of Cake Temperatures at U/L Irradiation Levels of 3690/2930 W/m^2 and 3070/2330 W/m^2 in Bi-Radiant Oven III. Center Top Thermocouple.

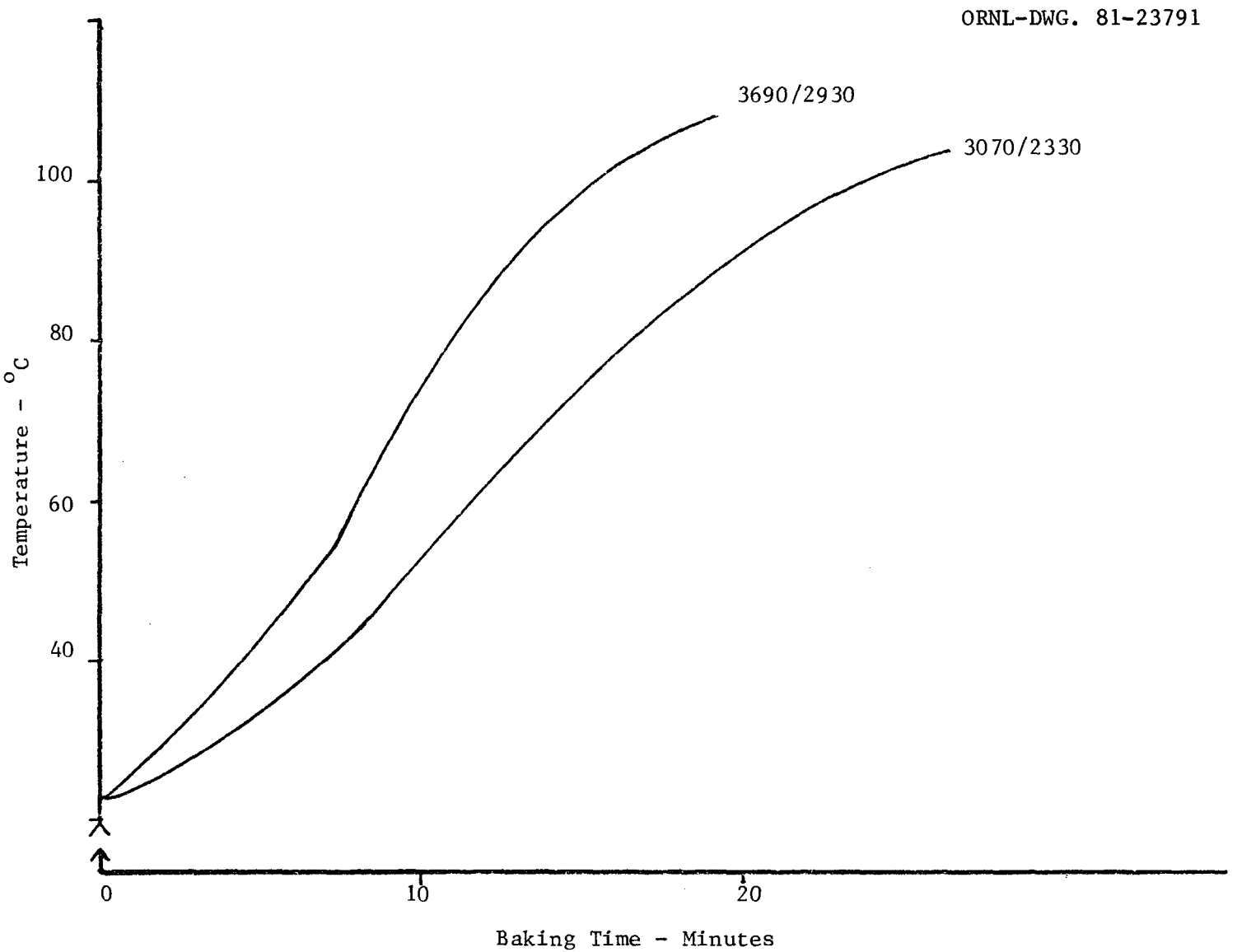

Figure 3.5 Comparison of Cake Temperatures at U/L Irradiation levels of 3690/2930 W/m^2 and 3070/2330 W/m^2 in Bi-Radiant Oven III. Center Bottom Thermocouple.

Accomodating All Conventional Oven Thermostat Settings

The progression of upper and lower irradiation levels to match conventional oven thermostat settings from 163°C (325°F) to 232°C (450°F) are shown in Figure 3.6. Table 3.2 shows the voltages and wattages of the upper and lower (U/L) elements that were required to produce each of the six baking rates. Only two voltage levels were required for the upper element setting, but reflection in the oven from the lower element increased irradiation levels on both the upper and lower baking planes as the voltage on this element was increased from setting to setting.

The relation between the upper and lower irradiation levels and the upper and lower element wattages were determined by use of multiple regression analyses. Irradiation measurements were made at the center of a rectangular utensil (24.8 by 35.2 cm) with the gauge facing upward at the level where the upper surface of a food would be during baking and again as near as possible to the bottom surface of the utensil with the gauge facing downward. Irradiation levels were measured for several combinations of upper and lower voltage settings. The regression analyses showed a high level of significance (0.99) between both element wattages and the resulting upper and lower radiation levels. The two models for estimating irradiation levels in Bi-Radiant Oven III when using a 24.8 by 35.2 cm baking utensil are:

$$UI = 245 + 4.25\ UW + 1.57\ LW \tag{3-2}$$

ORNL-DWG. 81-23792

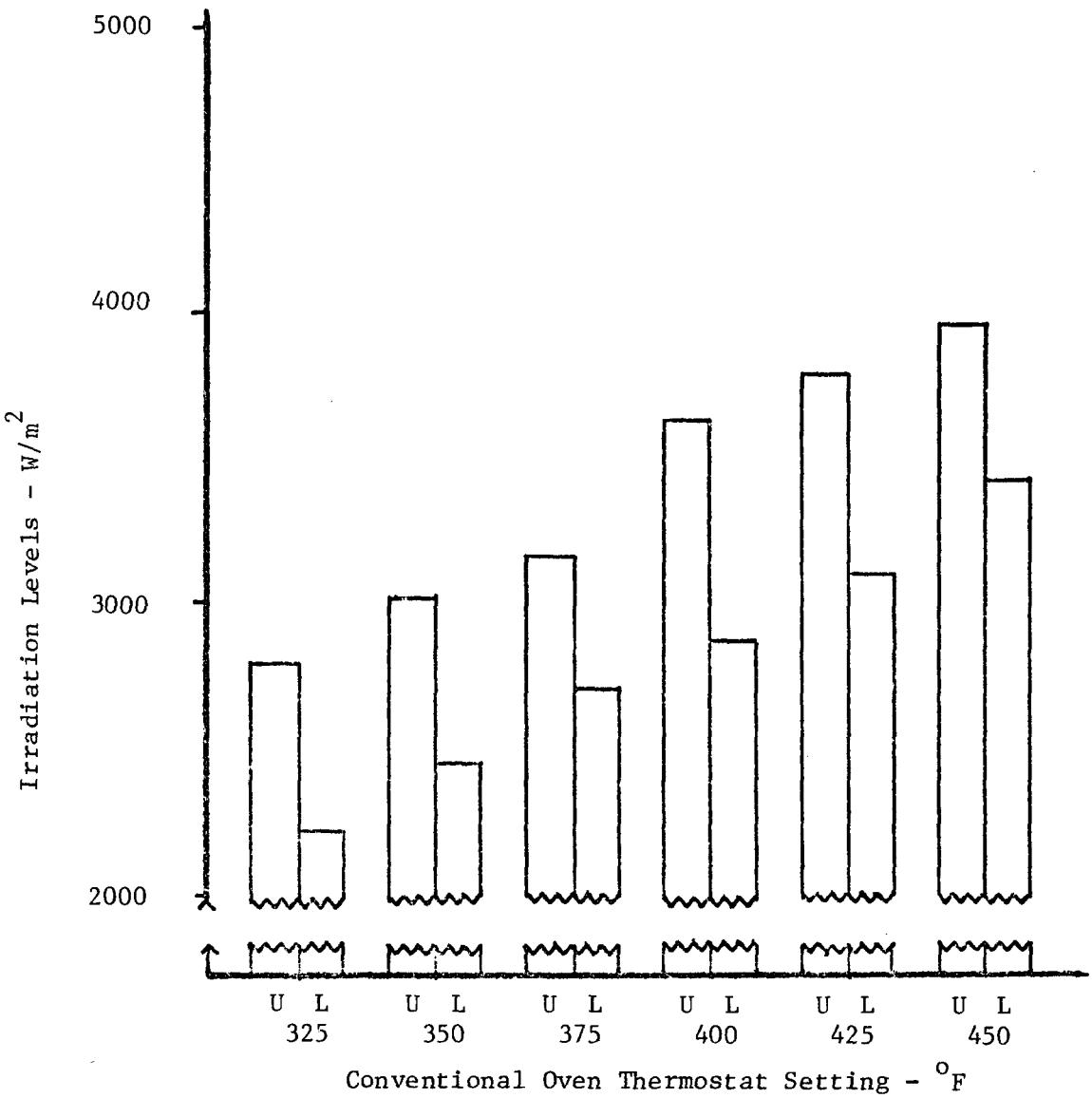

Figure 3.6 Bi-Radiant Oven Upper (U) and Lower (L) Irradiation Levels that Correspond to Conventional Oven Thermostat Settings.

Table 3.2
Bi-Radiant Oven Settings Used for Various Conventional Oven Thermostat Settings. Bi-Radiant Oven III

Conventional Oven Thermostat Setting °C (°F)	Element Voltage V U/L	Element Wattage W U/L	Baking Surface Irradiation* W/m^2 U	L
163 (325)	100/70	526/257	2880	2210
177 (350)	100/80	526/336	3010	2430
191 (375)	100/90	526/426	3150	2680
204 (400)	110/90	636/426	3620	2840
218 (425)	110/100	636/526	3770	3110
232 (450)	110/110	636/636	3950	3420

* As measured using a rectangular baking utensil, 24.8 by 35.2 cm (873 cm^2)

$$LI = 734 + 1.45\ UW + 2.77\ LW \tag{3-3}$$

where UI and LI are the upper and lower irradiation levels in W/m^2 respectively, UW is the wattage in Watts of the upper element, and LW the wattage in Watts of the lower element.

These correlation equations were plotted in Figures 3.7 and 3.8 for various wattages. The relationship between the irradiation and upper element wattages in the range of 400 to 600 W and lower element wattages in the range of 200 to 800 W was a straight line. Figure 3.7 shows the variation in irradiation on the upper surface of a food to be fairly steep by increasing the wattage of the upper element as compared to the increase in irradiation on the lower baking surface (Figure 3.8). The distance between the lower element wattage lines is less on the upper surface showing that increasing the wattage of the lower element increases the irradiation on the lower baking surface more than on the upper surface.

The box made with dashed lines on each figure envelopes the irradiation levels that will accomodate all of the foods that were baked in Bi-Radiant Oven III. Many combinations of upper and lower irradiation levels can be used within the dashed area and beyond within the limits of about 200 W and 800 W for each element.

Equations 3-2 and 3-3 can be solved simultaneously to produce the following equations to estimate the wattage levels required to produce the desired upper and lower irradiation levels:

ORNL-DWG. 81-23793

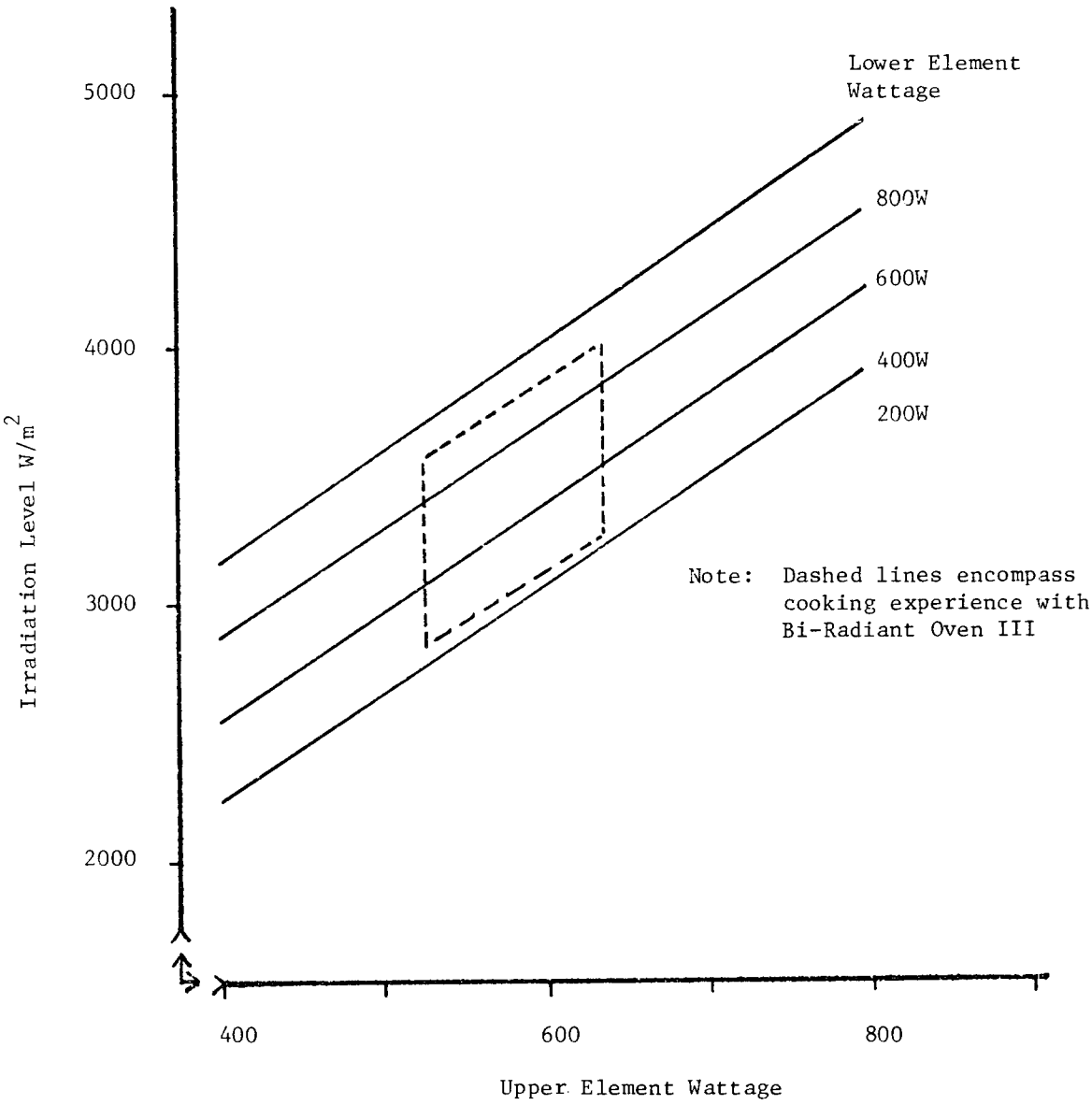

Figure 3.7 Variations in Irradiation Level on the Upper Surface of a 24.8 x 35.2 cm Baking Utensil with Variations in the Upper and Lower Element Wattages. Bi-Radiant Oven III.

ORNL-DWG. 81-23794

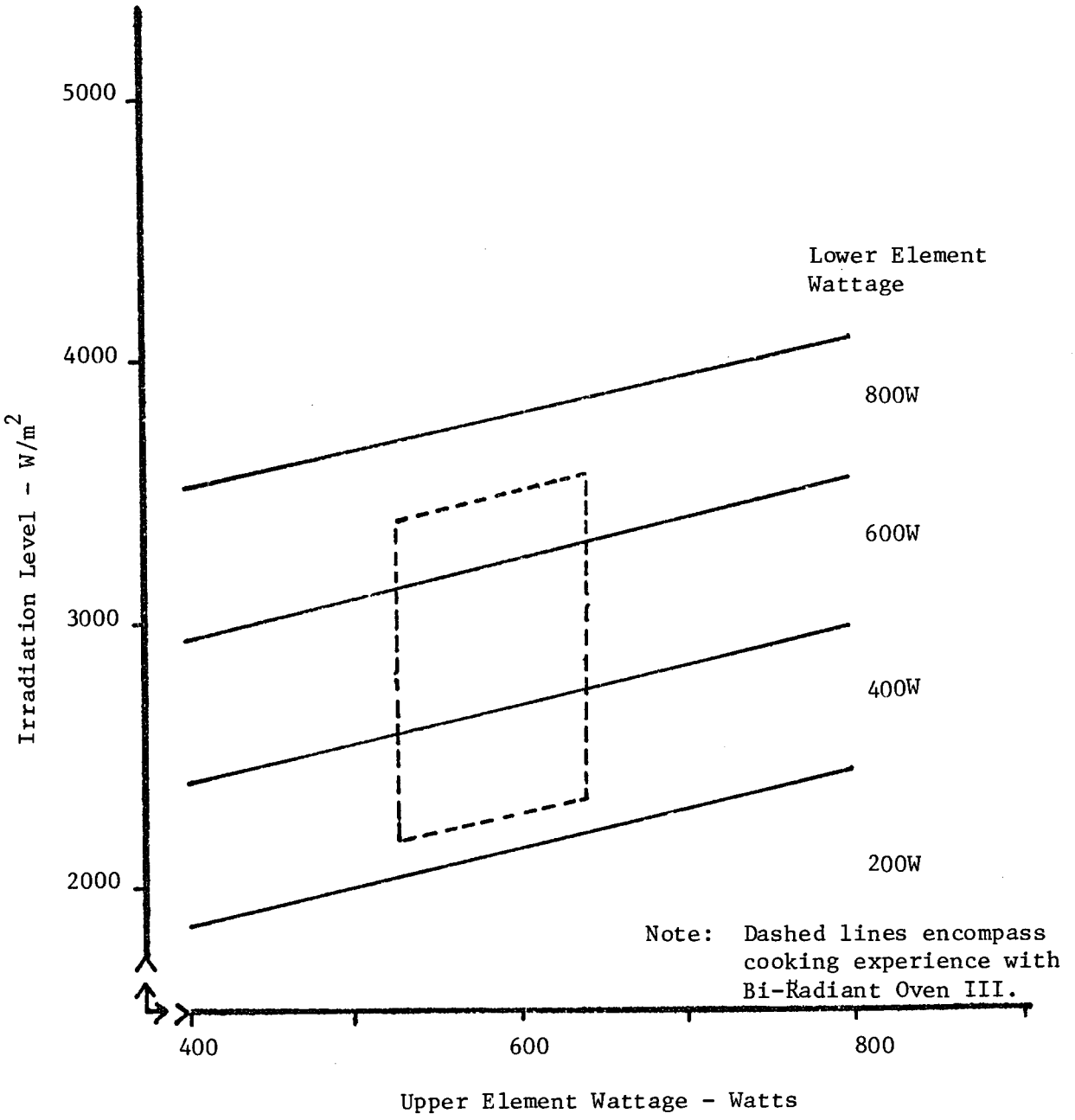

Figure 3.8 Variations in Irradiation Level on the Lower Surface of a 24.8 x 35.2 cm Baking Utensil with Variations in the Upper and Lower Element Wattages. Bi-Radiant Oven III.

$$LW = \frac{2.93\ LI - UI - 1906}{6.55} \tag{3-4}$$

$$UW = \frac{UI - 245 - 1.57\ LW}{6.55} \tag{3-5}$$

Example: to achieve upper and lower irradiation levels of 3500 and 2500 W/m^2 using equations 3-4 and 3-5:

$$LW = \frac{2.93\ (2500) - 3500 - 1906}{6.55} = 293W$$

$$UW = \frac{3500 - 245 - 1.57\ (293)}{4.25} = 658W$$

To demonstrate the adequacy of the upper and lower irradiation levels to accomodate the broad spectrum of foods normally baked in an oven. Each of the settings shown in Table 3.2 was used. Previously all foods that had been tried could be baked successfully in either Bi-Radiant Oven II or III. Now an attempt was being made to categorize foods into logical groups that might each be accomodated in a Bi-Radiant Oven by similar upper and lower element settings. Table 3.3 shows a number of foods that baked well in their prescribed categories. Meats which require a slow oven 163°C (325°F), all baked or roasted well in a time about the equivalent of conventional baking or roasting. For conventional oven roasting the use of a rack is recommended in roasting pans that are very emissive (absorptive). Placing a meat in contact with the bottom of an emissive utensil in a

Table 3.3

Acceptable Baking Using the Prescribed Upper and Lower Element Settings in Bi-Radiant Oven III

Element Setting U/L Volts	Watts	Food	Baking Time hr.	min.
100/70 (325°F)*	526/257	Ham 2.9 kg	2	24
		Turkey 5.2 kg	3	35
		Chicken & Dressing 1.5 kg	1	26
		Rolled Rib Roast 2.4 kg	2	18
100/80 (350°F)	526/336	Lasagna		43
		Fish		31
		Yeast Bread		30
		Brownies		34
100/90 (375°F)	526/426	Angel Food Cake		30
110/90 (400°F)	636/426	Muffins		23
		Cream Puffs		30
		Baked Potatoes		60

*Conventional Oven Thermostat Setting Equivalent

conventional oven results in overcooking and often charring of the lower surface of the meat. The quality of the roast will be poor. In the Bi-Radiant Oven a rack is not used for roasting. Contact of meat and the roasting pan will not result in overcooking since the rate of heat transfer can be controlled at a lower more appropriate irradiation level.

The setting (100/80V) that corresponded to a 177°C (350°F) thermostat setting on a conventional oven produced lasagna, baked fish, a yeast sweet bread and brownies of excellent quality within a normal baking time. This setting, as discussed earlier, bakes cakes well also. Other products that baked well at the anticipated settings and times were angel food cake, muffins, cream puffs and baked potatoes.

The foods in this group bake best in a conventional oven in reflective utensils and in the Bi-Radiant Oven in an absorptive utensil. There seems to be a natural transfer between controlling the baking process if the change from a conventional oven to a Bi-Radiant Oven is accompanied by a change from a reflective to an absorptive baking utensil.

A second group of foods did not bake well at the prescribed settings (Table 3.4). One of four factors seemed to be involved: a short baking time, the utensil size, the utensil emissivity or utensil mass.

Table 3.4

Unacceptable Baking Using the Prescribed Upper and Lower Element Settings in Bi-Radiant Oven III

Element Setting U/L	Food	Result	Solution
100/80 (350°F)*	Meat Loaf	Cooked too fast	Check utensil size
	Macaroni and Cheese	Cooked too slow	Check utensil material
100/90 (375°F)	Yeast Rolls	Cooked too slowly	Check utensil size
	Chocolate Chip Cookies	Cooked too slow	Check utensil size and short time
110/90 (400°F)	Quiche**	Bottom soggy	Check utensil material
110/100 (425°F)	Blueberry Pie**	Bottom soggy	Check utensil material
110/110 (450°F)	Biscuits	Cooked too slow	Check utensil size and short time
	Pizza	Cooked too slowly	Check material and size

*Conventional oven thermostat setting equipment.
**Some shielding of the edge crust with foil is needed to control browning of edge.

Short Baking Time

Biscuits and cookies which bake conventionally in a short time required 5 to 8 minutes longer in Bi-Radiant Oven III. Since the Bi-Radiant Oven isn't preheated, irradiation does not level off until 15 minutes or so (refer to Figure 1 in Section 2). When four batches of cookies were baked consecutively, the first batch took 19.5 minutes. Subsequent batches took about 10 to 12 minutes. Controls being developed by the Heat Transfer Laboratory may be able to deal with this situation. Also heating element types with less mass would respond more quickly when turned on.

Utensil Size

Utensil size influences the distribution of radiation in an oven. The loaf pan (12.7 by 20.3 cm) used for baking meat loaf covered a relatively small area, 257.8 cm^2; the lasagna pan (24.8 by 35.2 cm) covered 873 cm^2 and a cookie sheet (28.4 by 39.4 cm) covered 1120 cm^2.

To study the effects of utensil size on the radiant heat transfer in Bi-Radiant Oven III, irradiation measurements were made on the upper and lower surfaces of utensils of two additional sizes (one larger and one smaller than the 873 cm^2 utensil used for Figures 3.7 and 3.8) at several combinations of upper and lower element wattages. Correlations were derived for the two additional utensil sizes and are shown here with regression models, equations 3-2 and 3-3.

Small Utensil - rectangular, 16.9 by 27.1 cm (458 cm^2)

$$UI = 612 + 3.34\ UW + 1.74\ LW \tag{3-6}$$

$$LI = 639 + 1.42\ UW + 3.20\ LW \tag{3-7}$$

Medium Utensil - rectangular, 24.8 by 35.2 cm (873 cm^2)

$$UI = 245 + 4.25\ UW + 1.57\ LW \tag{3-2}$$

$$LI = 734 + 1.45\ UW + 2.77\ LW \tag{3-3}$$

Large Utensil - rectangular, 28.4 by 39.4 cm (1120 cm^2)

$$UI = 325 + 4.08\ UW + 1.41\ LW \tag{3-8}$$

$$LI = 794 + 1.05\ UW + 2.98\ LW \tag{3-9}$$

Note that the contribution of the upper element to radiation on the lower surface of a product being baked is much less when a large utensil is used. This helps to explain a longer baking period for cookies, biscuits and rolls since all were baked on a large cookie sheet. The contribution of the lower element to irradiation on both the upper and lower surfaces of a food being baked is greater for the

small utensil. The meat loaf pan was smaller than the utensil used in the irradiation estimation model so the increased levels of irradiation help to explain how the meat loaf cooked too quickly.

The wattage levels required to produce the same irradiation levels on the upper and lower food surfaces were calculated for the three utensil sizes (Table 3.5). Using the medium utensil wattages as reference notice that, to achieve the same irradiation levels, a small utensil requires increasing the upper wattage and decreasing the lower wattage. Using a utensil that covers a relatively large area requires an increase in both the upper and lower element wattages.

Voltages (Table 3.6) required to achieve the appropriate irradiation levels were calculated from the wattages in Table 3.5 assuming the elements have a constant resistance. The voltage changes are not large, but then wattage and irradiation levels are related to the square of the voltage.

To summarize, utensil size, by changing view factors, affects reflection of thermal irradiation from the lower element to the upper surface of a food and from the upper element to the lower surface of the utensil the food is being baked in. Thus, utensil size must be taken into account in designing oven controls.

Utensil Emissivity

Many utensil materials that readily absorb thermal radiation are used in conventional ovens for a very good reason. Foods such as filled pies and casseroles bake better when heat is transferred at a

Table 3.5
Upper and Lower (U/L) Wattages Required to Produce Irradiation Levels for Baking at Six Equivalent Thermostat Settings. Baking Utensils of three sizes. Bi-Radiant Oven III

Conventional Oven Thermostat Setting °C (°F)	Prescribed Irradiation W/m^2	Utensil Size		
		Small W	Medium W	Large W
163 (325)	2880/2210	550/247	526/257	526/289
177 (350)	3010/2430	554/314	526/336	533/360
191 (375)	3150/2680	555/392	526/426	540/442
204 (400)	3620/2840	704/376	636/426	650/457
218 (425)	3770/3110	706/460	636/526	656/546
232 (450)	3950/3420	710/555	636/636	665/646

Table 3.6
Voltage Requirements for Upper and Lower (U/L) Elements to Product Irradiation Levels. Baking Utensils of Three Sizes. Bi-Radiant Oven III

Irradiation Levels W/m^2	Utensil Size Small V	Medium V	Large V
2880/2210	102/68	100/70	100/74
3010/2430	102/77	100/80	101/83
3150/2680	103/86	100/90	101/92
3620/2840	110/85	110/90	111/93
3770/3110	116/93	110/100	112/102
3950/3420	114/103	110/110	112/111

faster rate to the utensil bottom. As was discussed earlier in this report, baking utensils with a high emissivity (absorptivity) experience higher radiant to convective heat transfer to the lower surface of a food baked in a conventional oven. This greatly increases the rate at which that food will bake from the lower surface compared to baking in a utensil with a lower emissivity. The emissivity (high or low) of the utensil determines the total heat absorption rate on the bottom surface of a food without changing the heat absorption rate on the upper surface.

When these foods are baked in a Bi-Radiant Oven, the heat transfer to the lower surface will be too slow, even in a utensil with a high emissivity, unless an adjustment is made to compensate for the difference between both radiation and convection which are experienced in a conventional oven and the radiation only that is available in the Bi-Radiant Oven. Foods in Table 3.4 which did not bake well with the elements set as prescribed for their category were macaroni and cheese, quiche and blueberry pie.

Macaroni and cheese was baked in a rectangular utensil in Bi-Radiant Oven III at upper and lower irradiation levles of 3010/2430 W/m^2 which should correspond to a conventional thermostat setting of 177^oC (350^oF). In a conventional oven a 45 minute baking period is required for baking in a glass casserole. In Bi-Radiant Oven III macaroni and cheese was baked for 48.4 minutes. The top was nicely browned, but the cheese was not thoroughly melted. Changing the upper and lower voltage settings from 100/80V to 100/90V produced an acceptible macaroni and cheese product in 35.4 minutes. This meant baking

was faster than conventional oven baking. The estimated new irradiation levels were about 3150/2670 W/m^2. To maintain an upper irradiation level at 3010 W/m^2, which occurs with 100/80V settings, and elevate the lower irradiation level to 2600 W/m^2 from 2430 W/m^2 upper and lower voltages of 97 and 88V would be required in Bi-Radiant Oven III and would keep baking time equal to conventional baking time.

Blueberry pie baked in a black aluminum pie pan for 40.1 minutes in Bi-Radiant Oven III (vs. 35 to 45 minutes at 218°C (425°F) in a conventional oven) had an upper crust that was too dark and a soggy lower crust. Blueberry filling had not reached a bubbly stage. It is estimated that upper and lower surface irradation levels of 3770 and 3100 W/m^2 would require adjustment to 3600 and 3200 W/m^2 to balance browning of the lower crust and heating the pie interior with browning of the upper surface. This would require shifting Bi-Radiant Oven III upper and lower element voltages from 110/100V to about 104/105V.

Quiche was baked in a black pie pan for 33.8 minutes in Bi-Radiant Oven III at irradiation levels of 3150 and 2680 W/m^2 for the upper and lower surfaces of the quiche. These irradiation levels should correspond to a 191°C (375°F) conventional oven thermostat setting. Though the baking time in the Bi-Radiant Oven was shorter than the 35-45 minutes recommended for conventional oven baking, the top was browned nicely but the lower crust was undercooked and the bottom portion of the custard had a very fragile gel. It is estimated that the upper irradiation level should be about 3000 W/m^2 and the lower irradiation level about 2800 W/m^2. This would involve altering voltages to about 94 and 97V for the upper and lower elements.

To summarize, baking foods in a Bi-Radiant Oven which are usually baked in a conventional oven in utensils that readily absorb thermal radiation, requires not only using a utensil that readily absorbs thermal radiation but also changing the balance of upper and lower irradiation levels.

Using a highly reflective pan in a Bi-Radiant Oven for cake baking also requires special consideration. Yellow cake from a commercial mix was baked in both reflective and black cake pans in Bi-Radiant Oven III at upper and lower voltage settings of 100 and 80V. Two layers were baked at once and three replications made with both reflective and black cake pans. See Table 3.7 for descriptions of the pans. Temperatures of the center top and bottom are shown in Figures 3.9 and 3.10. The temperature at the center bottom of the cake leveled off below 100°C (Figure 3.10). The reflective pans took 40 percent longer to bake and produced a poor quality cake, poorly developed and with a very lightly browned lower crust.

Adjusting the voltages of the upper and lower elements from 100/80V to 90/110V reduced the baking time from 37 minutes to 23.1 minutes and produced browning similar to that of the layer baked in the black aluminum cake pans (Table 3.8). Temperatures of the center top and bottom thermocouples are shown in Figures 3.11 and 3.12. By changing the upper and lower voltages from 100/80V to 90/110V, irradiation levels were altered from about 3010/2430 W/m^2 to about 3050/3110 W/m^2. It is likely that increasing the voltage of the lower element this much increased convection heat transfer from the element to the bottom surface of the utensil.

Table 3.7
Characteristics of Cake Pans

Material	Size diam. cm	Size depth cm	Mass, M kg	C_p kJ/kg°K	MC_p* kJ/°K	Emissivity
Aluminum Black	20.3	3.8	0.130	0.921	0.120	0.80
Steel Black	21.7	3.7	0.229	0.502	0.115	0.80
Glass Heat Resistant	21.2	4.9	0.725	0.795	0.576	0.95
Aluminum Reflective	20.6	3.8	0.134	0.921	0.123	0.075 Bottom 0.05 Sides

*Thermal Capacitance - Mass x Specific Heat

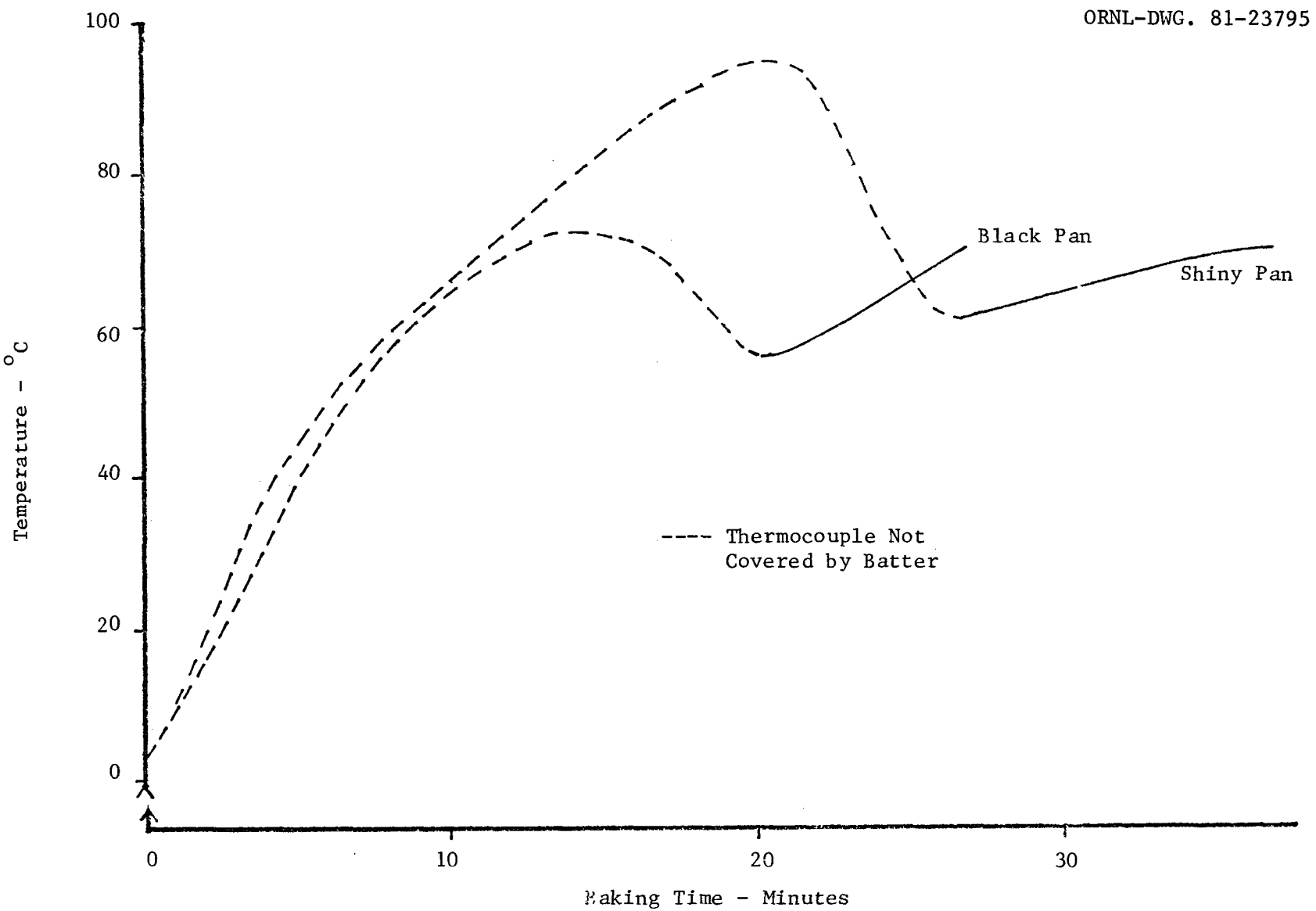

Figure 3.9 A comparison of the Effects of Black and Shiny Aluminum Pans on Cake Temperatures Baked at the Same Setting. Center Top Thermocouples. Bi-Radiant Oven III.

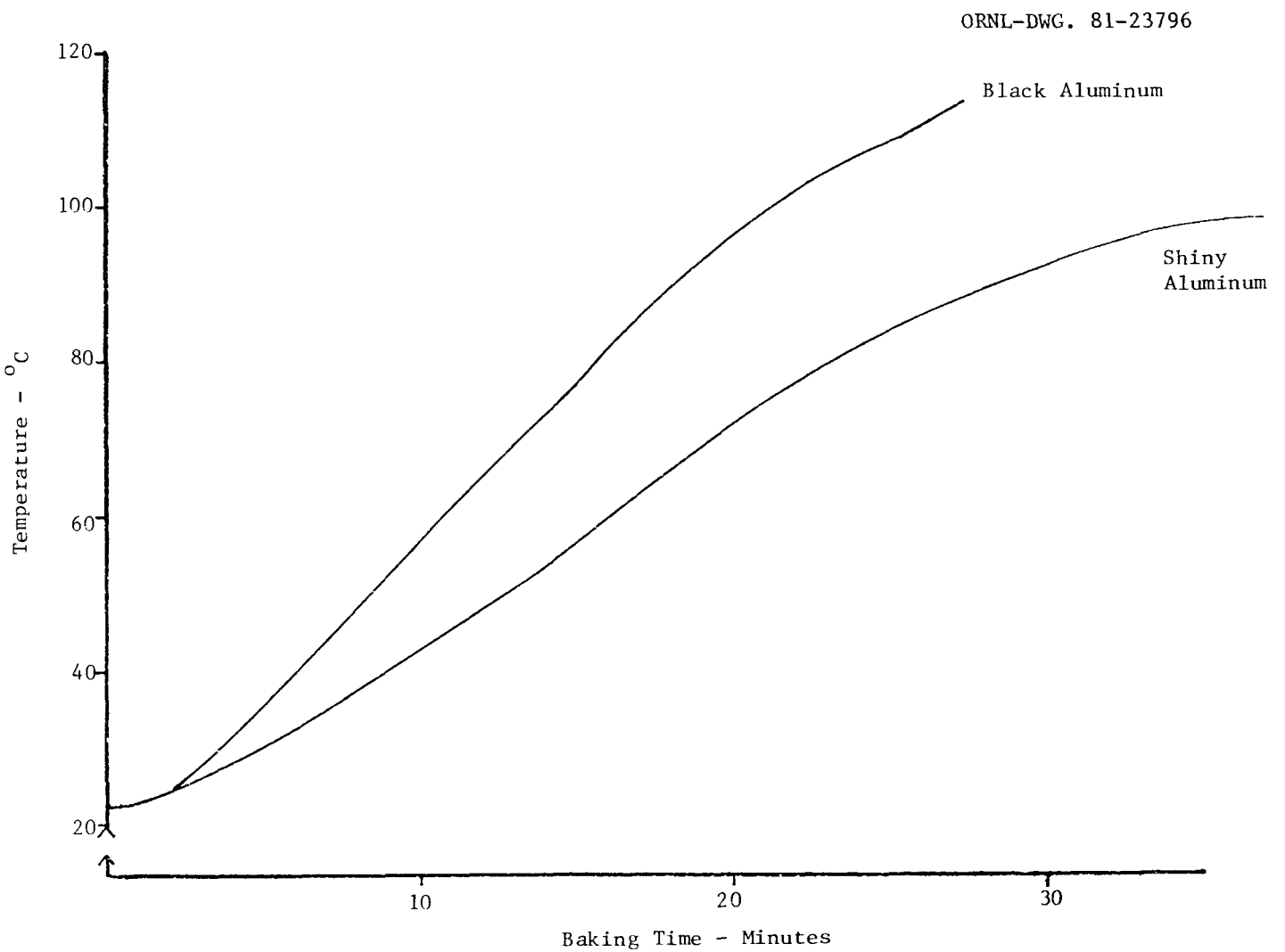

Figure 3.10 A Comparison of the Effects of Black and Shiny Aluminum Pans on Cake Temperatures Baked at the Same Setting. Center Bottom Thermocouples. Bi-Radiant Oven III.

Table 3.8
Effects of Heat Absorption Capacity of Baking Utensil on Yellow Cakes. Bi-Radiant Oven III

Material	Bi-Radiant Setting V	Baking Time min.	Energy Use kWh	Utensil Energy* kJ	Moisture Loss g	Browning** Top	Browning** Bottom
Aluminum, Black	100/80	26.08	0.378	9.6	21.3	4.6	4.2
Steel, Black	100/80	25.21	0.367	10.3	22.3	4.5	4.1
Glass, Heat-Resistant	100/90	30.6	0.486	47.3	27.0	5.8	4.3
Aluminum, Shiny	90/110	23.1	0.440	9.8	19.7	4.7	4.2

*Utensil Energy - $MC_p \Delta T$. T was different for different materials

**Browning Scale 0-9. 3.0 to 6.3 is acceptable

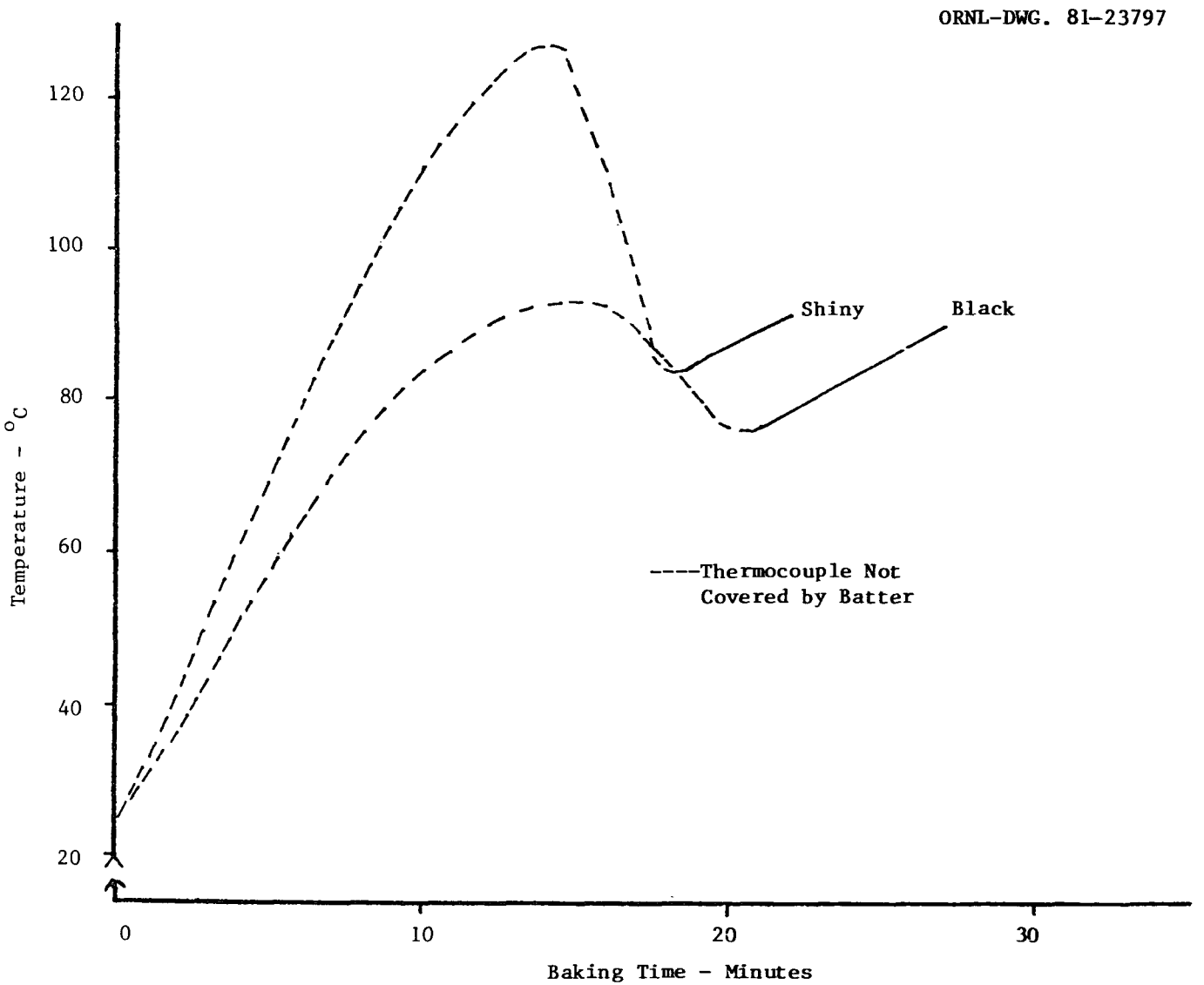

Figure 3.11 A Comparison of the Effect of Black and Shiny Aluminum Pans on Cake Temperature Baked at Adjusted (Optimum) Settings. Center Top Thermocouples. Bi-Radiant Oven III.

ORNL-DWG. 81-23798

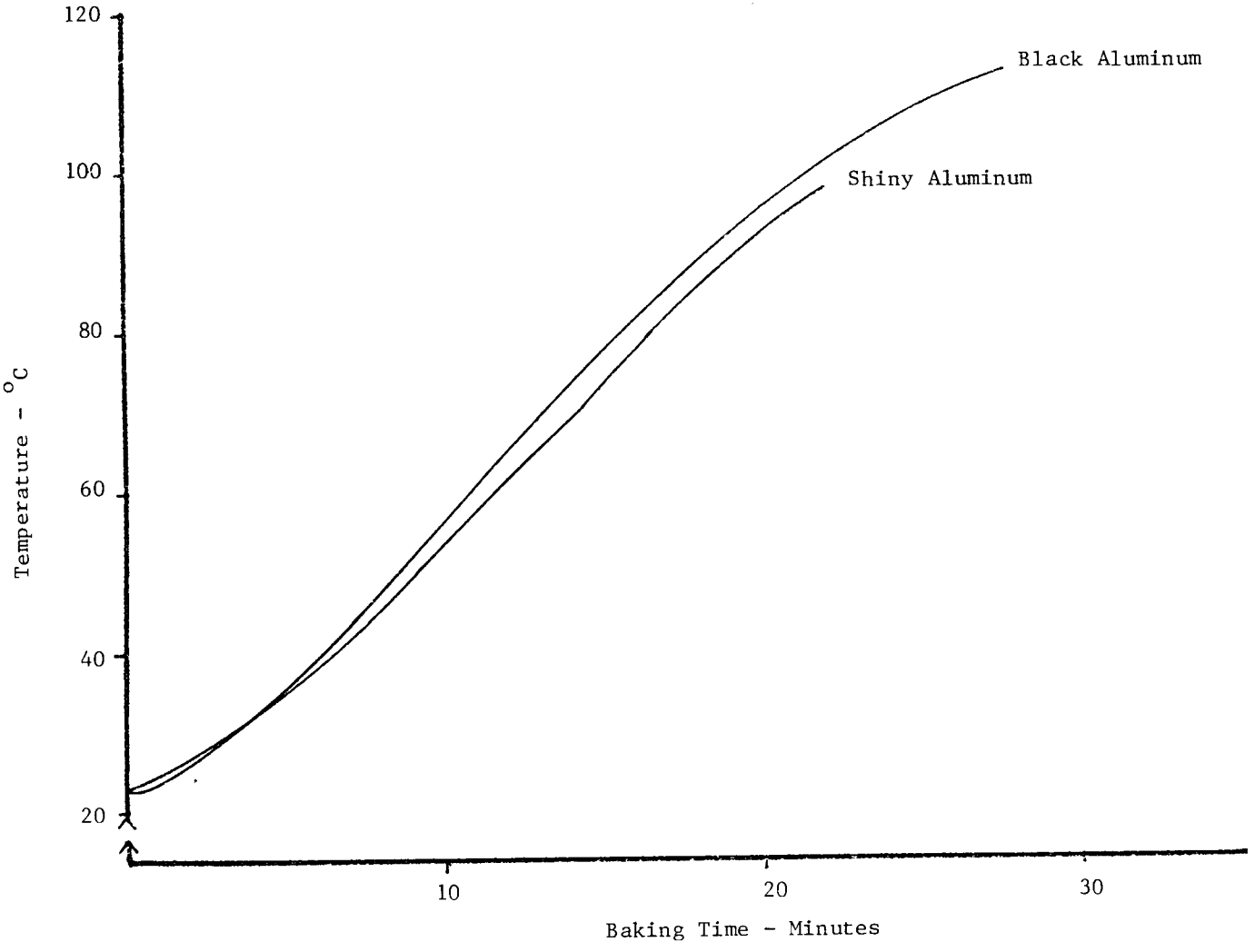

Figure 3.12 A Comparison of the Effects of Black and Shiny Aluminum Pans on Cake Temperatures Baked at Adjusted (Optimum) Settings. Center Bottom Thermocouples. Bi-Radiant Oven III.

To summarize, using a shiny utensil means a major compensation in the upper and lower element wattages.

Utensil Mass

Some materials used for baking, such as heat-resistant glass, glass ceramic and pottery have more mass than aluminum. More energy is required to heat such utensils than would be required for aluminum. Even in a conventional oven a material with a high emissivity (or absorptivity) may require additional irradiation on its lower surface if it has a high mass. To demonstrate this effect two layer cakes were baked in each of two high emissivity materials described in Table 3.7. Cake temperatures were monitored during baking. Figure 3.13 shows that both the black aluminum and black steel baking pans produced "done cakes" (88°C) in about the same time. The cakes baked in the heat-resistant glass took longer. The temperature was higher on the bottom of the cakes in the black steel pan and eventually was higher in the cakes from the heat resistance glass utensil than in the black aluminum (Figure 3.14). From Table 3.7 the mass of the heat resistant glass and its specific heat require almost five times the thermal energy for baking than is required for the aluminum or steel utensil. An adjustment was made in the irradiation levels from 3010/2430 W/m^2 (100/80V) to 3150/2680 W/m^2 (100/90V) for baking in the heat resistant glass utensil. The temperatures of the improved baking results (with a bottom center end temperature greater than 100°C) are shown in Figures 3.15 and 3.16. The layer cakes from this setting were equal in browning and general quality to those baked in the black aluminum utensil at the prescribed settings (Table 3.8).

ORNL-DWG. 81-23799

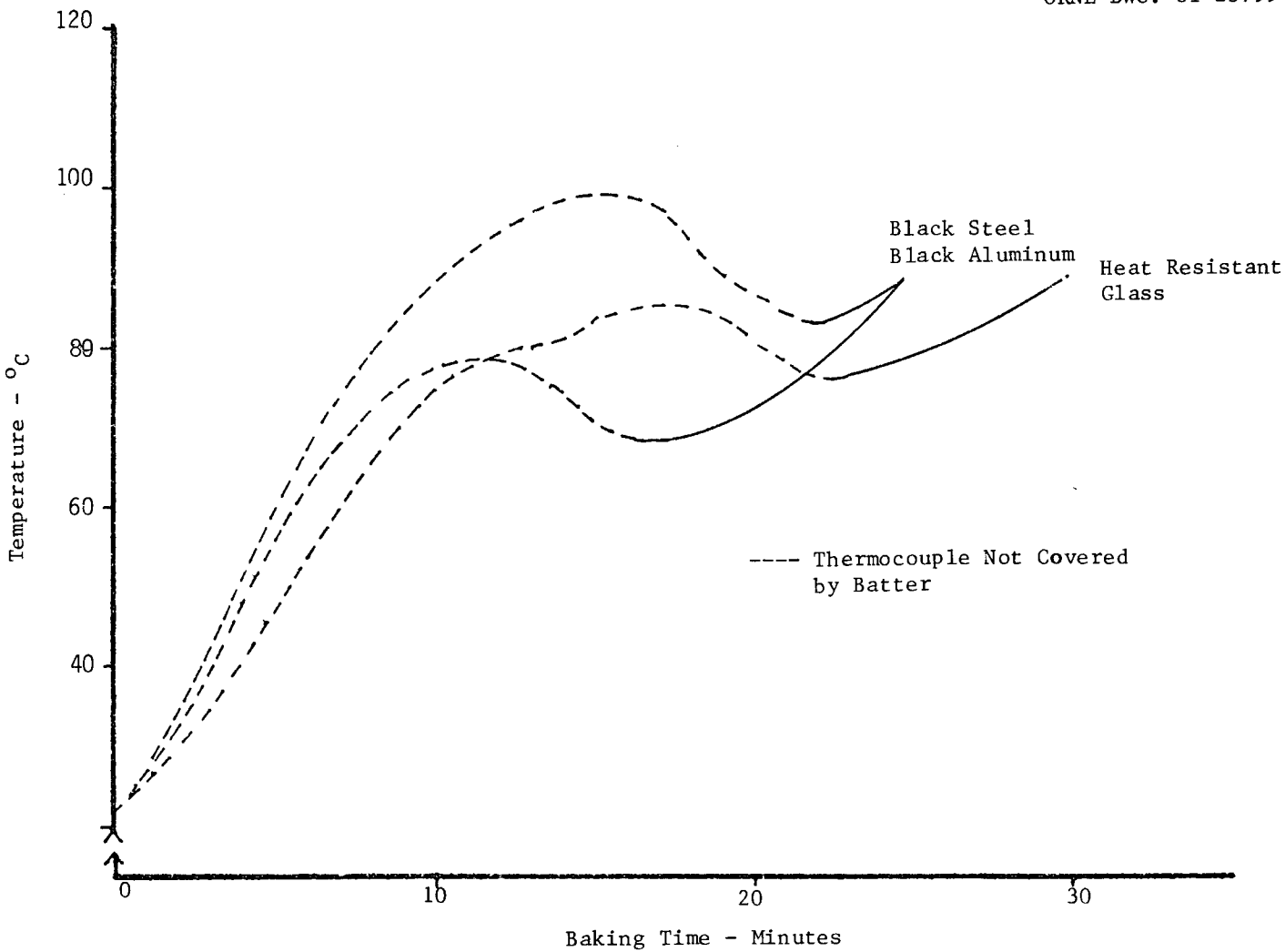

Figure 3.13 A Comparison of the Effects of Black Aluminum, Black Stainless Steel and Heat Resistant Glass Pans on Cake Temperatures Baked at the Same Setting. Center Top Thermocouples. Bi-Radiant Oven III.

ORNL-DWG. 81-23596

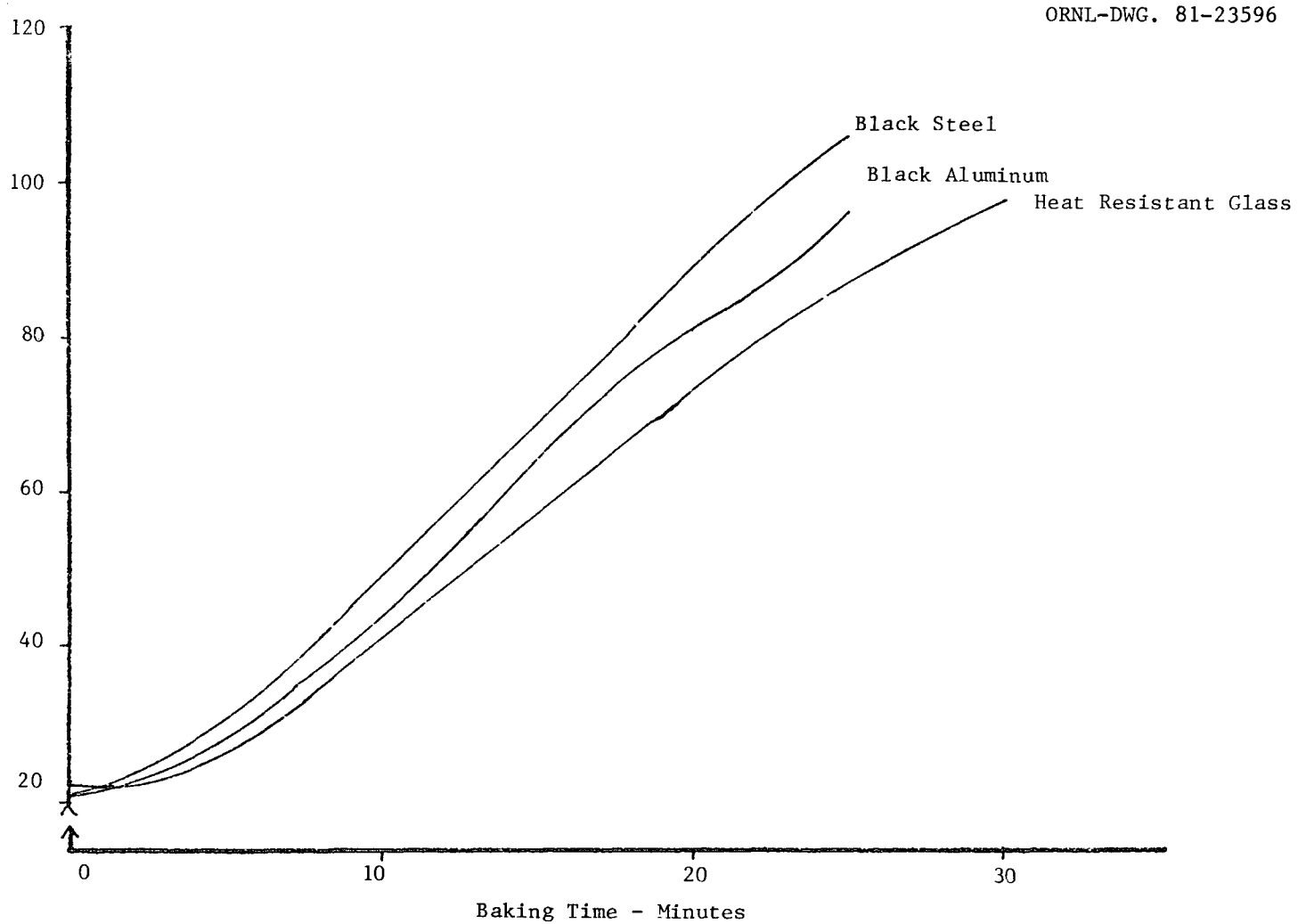

Figure 3.14 A Comparison of the Effects of Black Aluminum, Black Stainless Steel and Heat Resistant Glass Pans on Cakes Temperatures Baked at the Same Setting. Center Bottom Thermocouples. Bi-Radiant Oven III.

ORNL-DWG. 81-23597

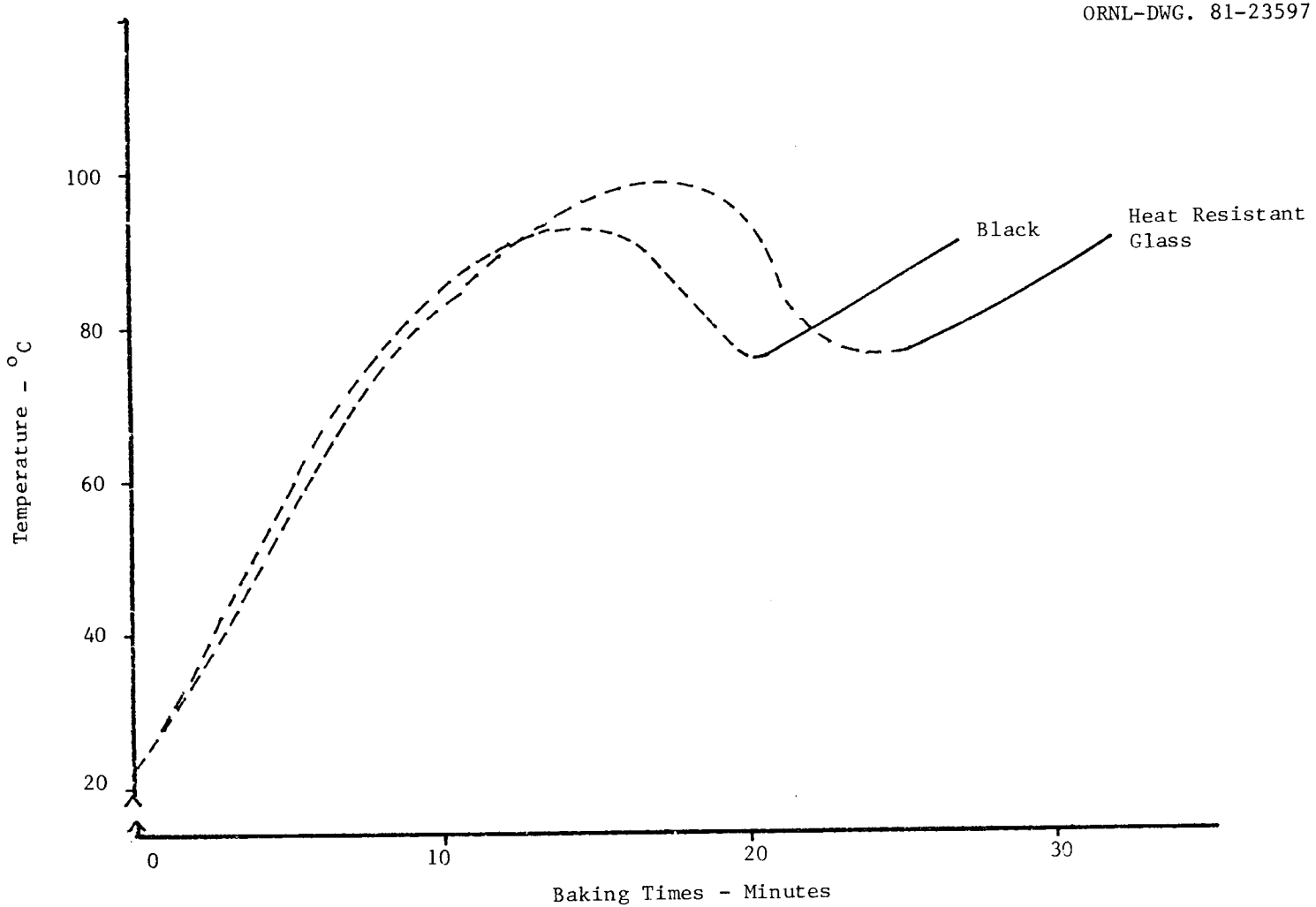

Figure 3.15 A Comparison of the Effects of Black Aluminum and Heat Resistant Glass on Cake Temperature Baked at Adjusted (Optimum) Settings. Center Top Thermo-Couple. Bi-Radiant Oven III.

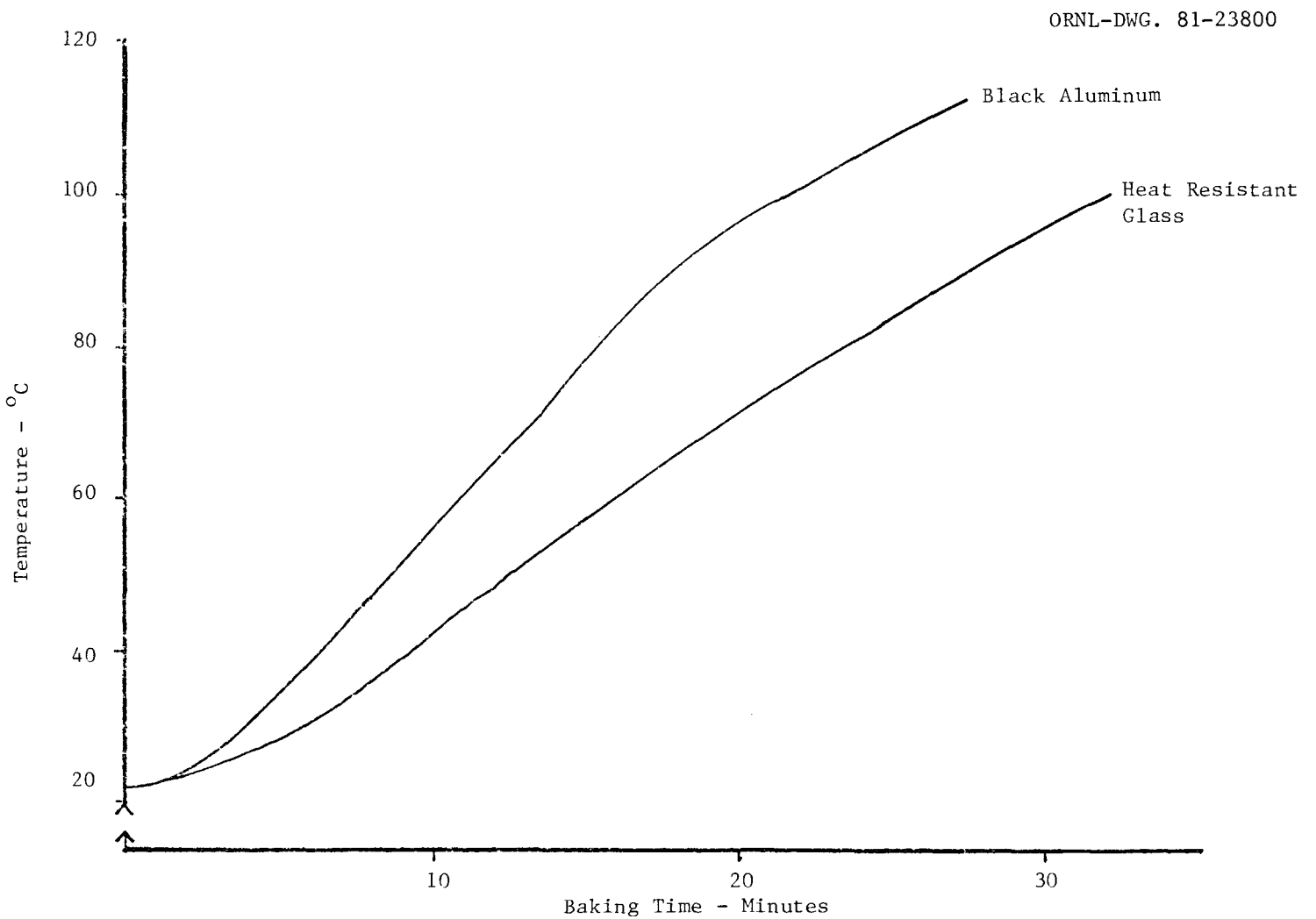

Figure 3.16 A Comparison of the Effects of Black Aluminum and Heat Resistant Glass Pans on Cake Temperatures Baked at Adjusted (Optimum) Settings. Center Bottom Thermocouple. Bi-Radiant Oven III.

The mass of the baking utensil adds to the baking load in either a conventional or Bi-Radiant Oven. Using glass or glass-ceramic utensils, which have high emissivities, in a Bi-Radiant Oven for foods like cake which are normally baked in utensils with a low emissivity in a conventional oven require compensation of upper and lower irradiation levels to accomodate the increased heat absorbed by these materials.

Tolerance of Cake to Uneven Irradiation

In designing a Bi-Radiant Oven, the shape and area coverage of the elements, their placement with respect to the oven interior walls, and the baking rack all contribute to irradiation levels and evenness of irradiation across the upper and lower baking planes. The elements used in Bi-Radiant Ovens II and III are designed so that there is a distance of 7 to 10 cm between loops. Locating the rack near enough to an upper element can produce a difference in browning due to a difference in irradiation across the surface of a cake.

To study the effects of variations in irradiation levels, single cake layers were baked in Bi-Radiant Oven II in a centered position and in two off centered positions - one with the cake baking partially extending to the right of the elements, the second partially extending to the front of the elements. Irradiation levels were measured in the center, back, front, right and left areas of each cake pan position with the cake pan in the oven. Table 3.9 shows the mean irradiation levels for each baking position and the differences between the maximum and minimum irradiation levels. The irradiation in the centered

Table 3.9
Effects of Even and Uneven Irradiation
Levels on Cake Baking in a Bi-Radiant Oven

	Even Baking	Uneven Baking Right*	Front*
Upper Surface Irradiation - W/m^2			
Mean	3340	3100	3210
Diff. between Max. & Min.	450	480	660
Lower Surface Irradiation - W/m^2			
Mean	2890	2830	2620
Diff. between Max. & Min.	310	660	430
Baking Time Minutes	17.5	21.3	20.0
Energy Use - kWh	0.239	0.289	0.271

*Positions in Oven

position showed radiation differences of 450 W/m^2 on the upper surface and 310 W/m^2 on the lower surface. With this amount of variation in irradiation levels cakes were still evenly baked. Irradiation levels of 3340 and 2890 W/m^2 for the upper and lower surfaces produced a done cake in 17.5 minutes. Difference across the upper surface of as much as 450 W/m^2 and 310 W/m^2 on the lower surface did not produce discernable irregularities in baking.

Cakes were baked in the right and front off-centered positions. Replications in the off-centered positions were first made by interrupting baking after 17.5 minutes to observe irregularities in baking. In each case half of the cake appeared normally browned. There was some "done" cake around the edge of the undercooked side that came in from the side about 1.5 cm. Cakes from both positions had a light surface browning on top which covered batter that was almost thermally stable, but gummy. The batter across the cake bottoms was thermally set with stable cell structure. In both cases baking was complete about 0.5 cm up from the bottom at the lowest point.

Cakes were next baked in the off-centered positions until the thermocouples at the top of the mid position had reached a done temperature of 88°C. Temperatures of the batter in the top-mid and bottom mid positions are plotted in Figures 3.17 and 3.18. Thoroughly cooked cakes were produced in the right off-centered position in 21.3 minutes and in the front off-centered position in 20 minutes. Both of these cakes had an uneven hump on the side where the irradiation level was low. Batter on the low irradiation side of the cake became thermally set about a minute later than in the center baked cake. Notice

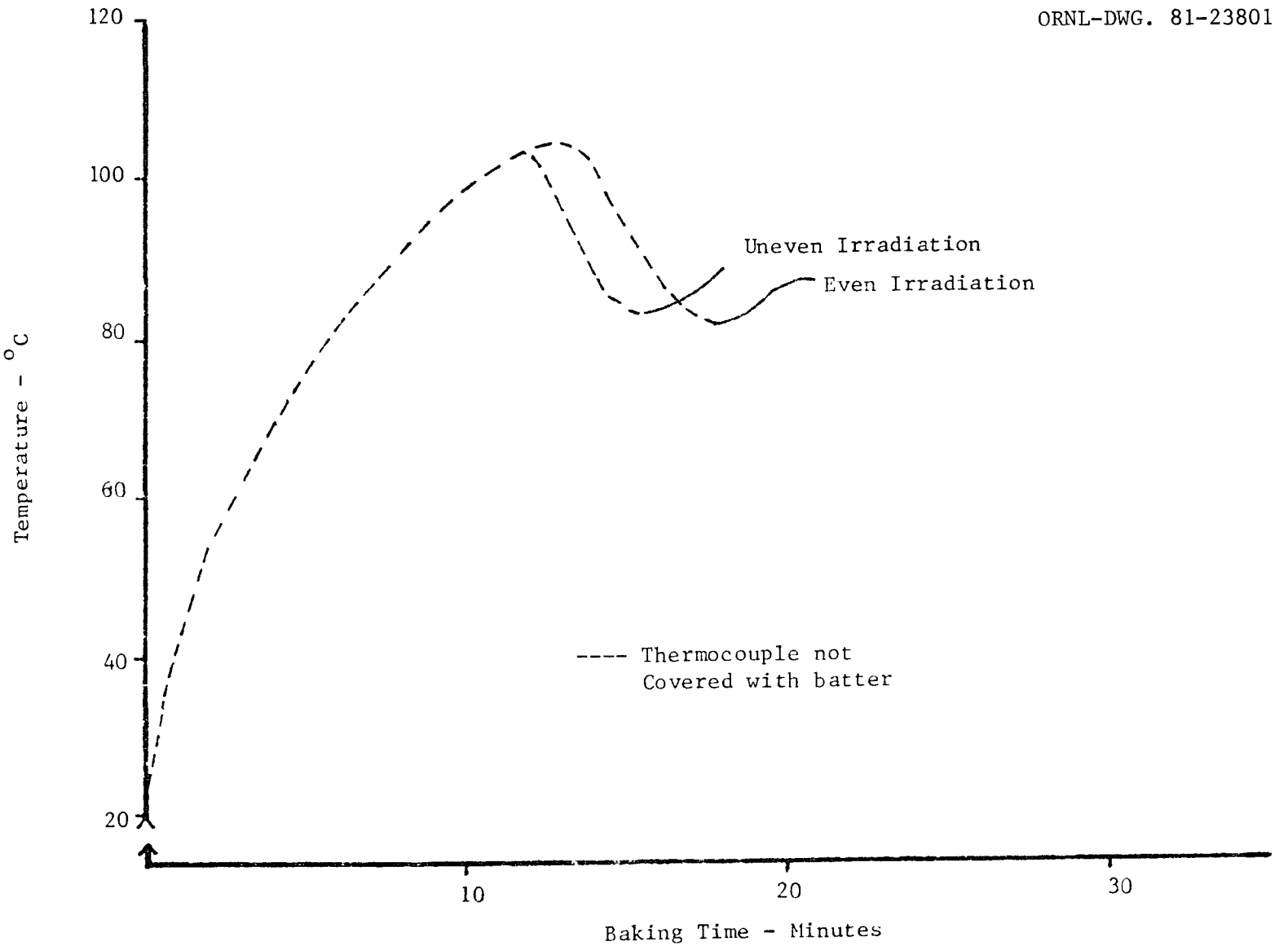

Figure 3.17 Temperature Rise of Top-Mid Thermocouple. Even vs. Uneven Irradiation. Bi-Radiant Oven·II.

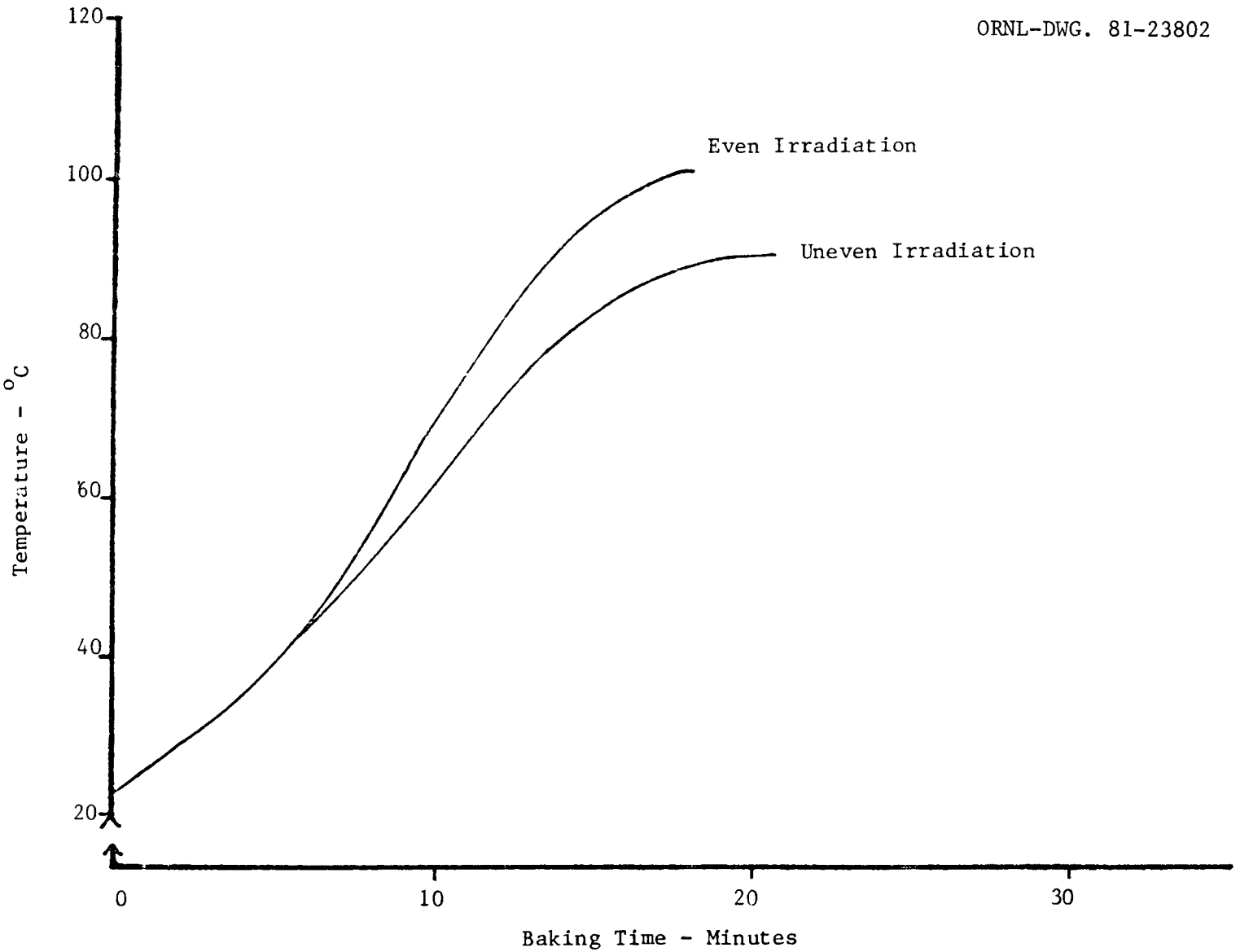

Figure 3.18 Temperature Rise of Mid-Bottom Thermocouple. Even vs. Uneven Irradiation. Bi-Radiant Oven II.

in Figure 3.17, that the batter covered the top-mid thermocouple earlier in the even baked cake. Browning was very light under the area where irradiation was low. Figure 3.18 shows that the temperature in this location never rose above about 86°C. This was too low for browning to occur.

Though exact limits for allowable variations in irradiation have not been set, it appears from these tests that sensitive foods like cakes bake evenly with variations no more than about 450 W/m^2 on one surface if variation is not too high on the other surface. Or if irradiation variation is as high as 660 W/m^2 on either surface and as much as about 450 W/m^2 on the other, irregular baking is sure to occur.

Maintaining the Bi-Radiant Oven Interior

Using normal baking procedures has produced few spatters and spills during Bi-Radiant Oven cooking in the Equipment Laboratory. Only when an incorrect element setting was used for roasting did excessive grease spattering occur. When the oven door was opened after more than two hours of roasting there was grease running down the walls. Grease at the top of the oven had burned on. This is a stubborn problem that did not respond completely to any of a variety of cleaning procedures. A sheet of aluminum foil was trimmed to fit the top of the oven and attached with a silicone sealer. Irradiation levels were measured with spatters burned on the oven and with the foil treatment in place. Table 3.10 shows that the irradiation level on the upper baking surface was reduced about 6 percent and on the

Table 3.10
Effects of Spattering and Treatment of Oven Cavity on Irradiation Levels. Bi-Radiant Oven III

	Irradiation Levels	
	Upper Surface	Lower Surface
Original Condition	2880 W/m^2	2210 W/m^2
After Spattering	2710	2120
Foil Treatment	2880	2200

lower surface about 4 percent due to burned on spatters. The application of foil on the top surface of the oven cavity effectively restored the irradiation levels to that originally existing. Baking subsequent to the spattering-restoration incident proceeded with no change in results from earlier tests.

Summary

Baking in a Bi-Radiant Oven is a function of the irradiation levels on the upper and lower surfaces of the food and baking utensil respectively as compared to the use of thermostat settings in a conventional electric or gas oven. It is, then, important that an oven designer be knowledgeable about the management of Bi-Radiant Oven irradiation. The various factors affecting the production, utilization and maintenance of irradiation in a Bi-Radiant Oven in this project are summarized here.

The heating elements used in Bi-Radiant Ovens II and II were massive enough that they didn't reach an equilibrium temperature for 15 or more minutes. This resulted in longer baking times for foods like cookies or biscuits that usually bake in a fairly short time. Elements with less mass would be more responsive and bake quick-baking foods in less time.

Since large utensils shield irradiation in a Bi-Radiant Oven, user input about whether the utensil used for baking is small, medium or large-sized will assure that irradiation levels can be maintained for optimum baking results. If utensils that have a lower emissivity (or absorptivity) are to be used in the oven, adjustments in

irradiation levels can be made to accomodate this situation and maintain baking quality. Irradiation levels can also be adjusted to accomodate baking utensils with either a low or high mass.

The design of the heating elements and the arrangements of the elements and baking rack in a Bi-Radiant Oven must assure evenness of irradiation over the upper and lower surfaces of foods. If irradiation variation is greater than about 650 W/m^2 on either surface and as great $450W/m^2$ on the other surface, delicate foods such as cake will bake unevenly.

Maintenance of irradiation levels during the useful life of a Bi-Radiant Oven includes maintenance of oven cavity high reflectance (or lower emissivity). The cavity top is most vulnerable to spatter soils, so a replaceable or renewable shield above the upper element would be useful.

The several considerations to provide appropriate irradiation levels that are considered in this report appear complex. They can, however, be dealt with creatively with the design of the Bi-Radiant Oven and its components and the use of solid state controls.

4. COMMERCIALIZATION OF THE BI-RADIANT OVEN

4.1 Merits of the Bi-Radiant Oven System.

Is the Bi-Radiant Oven a product that should be introduced into the market place? This is a question that must be dealt with by manufacturers. The Bi-Radiant Oven has a number of merits that should be carefully weighed.

Energy Conservation

The Bi-Radiant Oven is a baking system that potentially can conserve 50 percent or more of the energy required for baking.

Baking Capability

Energy conservation in an oven has little appeal unless it is accompanied by the ability to produce acceptable quality over the broad array of foods people have enjoyed from their ovens in the past. The Bi-Radiant Oven offers improved convenience along with the capability of producing the brown, crisp, crusty surfaces and moist, tender interiors in meats, casseroles and breads that make baked foods enjoyable. The ability of the oven to provide baking rates at the upper and lower surfaces of foods that will produce the desired combination of surface and interior characteristics that are most desirable for any and all foods is much more flexible than in a conventional oven. A conventional oven cannot be controlled to accomodate changes in baking rates to the lower surfaces of foods that occur when utensils other than the type specifically prescribed for a particular food are used, i.e., reflective pans for cakes and cookies, utensils that

readily absorb thermal radiation for casseroles and filled pies.

Irradiation rates on the upper and lower surfaces of foods can be controlled individually in a Bi-Radiant Oven. The upper and lower irradiation levels can be balanced to compensate for absorptivity, heat holding capacity, and size of the baking utensil. The Bi-Radiant Oven can provide a user with oven baking control that is not available in conventional ovens.

Spatial Requirements

There are no particular limitations on the size or shape that a Bi-Radiant Oven must take. It might fit into the space in a range that otherwise would be occupied by a conventional oven or it might be built-in. It need not look different from any conventional oven.

Reduced Insulation Costs

Since the temperatures of the interior walls in a Bi-Radiant Oven do not rise as much as they might in a conventional oven, less insulation should be required. The highly reflective oven walls stay much cooler, and the air in the oven is much cooler than in a conventional oven.

Controls for the Bi-Radiant Oven

An attraction of the Bi-Radiant Oven should be the control the user has over baking results. Compensations might be made for individual likes and dislikes about foods. Additional browning could be applied to either the upper and lower surface of a food separately or

together. Such control of oven cooking offers a big advantage for a Bi-Radiant Oven over a conventional oven. The use of micro-computers and various solid state devices would allow the user to provide input about any food being cooked and the baking utensil that would provide the characteristics desired in the baked food.

4.2 Concerns in the Commercialization of the Bi-Radiant Oven System

A number of concerns in commercialization of the Bi-Radiant Oven were addressed in Volume I, Development and Assessment of the Bi-Radiant Oven [1]. Some of these can best be dealt with by a manufacturer and the suppliers who provide the materials and components needed in production.

Oven Lining Material

The characteristics of a Bi-Radiant Oven cavity combined with the environment within an oven demand special consideration. A low emissivity (high reflectivity) is an essential property for Bi-Radiant Oven walls to provide the reflection of thermal radiation that contributes both to even baking and energy efficiency.

Baking foods in an oven produces moisture and food substances that potentially may discolor or coat the oven surface. Cleaning is a major problem in ovens. However, using appropriate baking and roasting procedures in a Bi-Radiant Oven produces few problems. The lower surfaces of the oven remain relatively cool and foods that do spill can be easily wiped up and removed. Burning on of food spills has not been a problem in Bi-Radiant Ovens II and III even though many foods

have been cooked over an extended period of time. Even broiling properly controlled would produce fewer problems in a Bi-Radiant Oven than might be encountered in a conventional oven or broiler where the cavity interiors are very emissive (absorptive) and readily absorb thermal radiation. Such walls reach much higher temperatures than Bi-Radiant Oven walls, even when broiling is done.

Maintenance of cavity emissivity may be assisted by either a material that is impervious to the types of spattering that occur with high temperature cooking or the provision of a removable oven cavity top that can be replaced or re-covered with foil.

Oven Controls

The Bi-Radiant Oven should provide convenience and satisfaction in use that match or exceed conventional oven baking. The requirements of foods and guidelines for the required baking levels of various food types have been developed in the Equipment Laboratory. The capability of controlling irradiation levels has been demonstrated in the Heat Transfer Laboratory.

Baking Utensils

A number of baking utensils with highly emissive exteriors are marketed. These utensils are much more suited to use in a Bi-Radiant than a conventional oven. The capability of producing them, and at reasonable costs has been shown. Tests in the Equipment Laboratory have demonstrated the ability of the Bi-Radiant Oven to accomodate a variety of baking utensil materials. The provision of appropriate baking utensils should not be a problem.

5. REFERENCES

1. DeWitt, D.P., Peart, M.V., "Bi-Radiant Oven - A Low - Energy Oven System, Volume I - Development and Assessment," Prepared for Oak Ridge National Laboratory by Purdue Research Foundation, ORNL/Sub-80/0082/1. April 1980.

2. Connelly, S.M., "Irradiation Heat Flux Gauge: A Predictor of Oven Irradiation Levels," M.S. Thesis, School of Consumer and Family Sciences, May 1980.

3. Martin, W.T., "Thermal Model and Calibration of the Cake-Pan Radiometer," Heat Transfer Laboratory Report 072578 to Whirlpool Corporation, School of Mechanical Engineering, Purdue University, July 1978.

6. APPENDICES

6.1 Appendix A

Schematic Diagram of Bi-Radiant Oven Experimental Controls for Use with Bi-Radiant Ovens II and III. Equipment Laboratory.

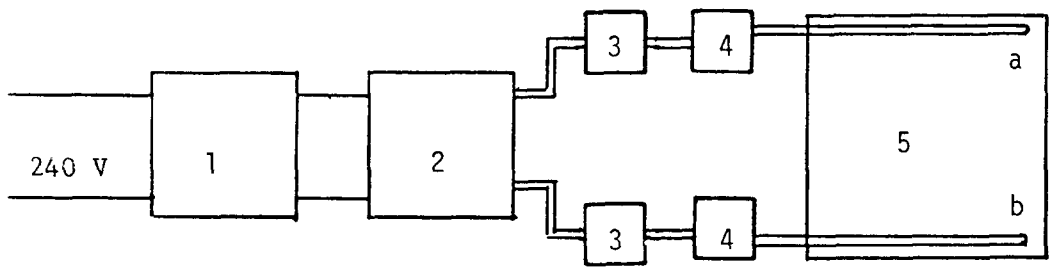

1. Stancor Isolation Transformer 1500VA

2. Superior Instantaneous Electronic Solid State AC Voltage Stabilizer. Input 95-135V Output 110-115V 50/60 Hz 3000 VA. Maximum Output 26.1A.

3. Superior Metered Powerstat Variable Transformer. Input 120V. Output 0-140V. 15A maximum.

4. Duncan Appliance Meters. 120V 60 Hz. 15A maximum.

5. Bi-Radiant Oven
    a. Upper Element
    b. Lower Element

6.2 Appendix B

Construction of the Irradiation Heat Flux Gauge

The irradiation heat flux gauge was constructed from a copper block 5.4 cm x 6.0 cm x 0.6 cm (2-1/8" x 2-3/8" x 1/4"). The two long edges were beveled 45 degrees. Channels were tooled out of the block (Figure B.1) and 0.3 cm (1/8") thick copper plate was soldered over the top. The block was then covered with electrodeposited nickel. Two tubes extending from the channels, were connected to vinyl tubing to allow water to pass through the gauge to maintain it at a constant temperature.

To measure radiant energy, fourteen edgelay thermocouples were connected in series and glued on electrically insulating parchment paper attached to a flat surface of the gauge (Figure B.2). Only one side of the gauge was used in this study, but thermocouple arrays could be placed on both sides. The thermocouples were covered alternately with black, absorptive (ε = 0.95) and shiny, reflective (ε = 0.05) strips (Figure B.3.). The black strips absorb more irradiation than the reflective strips creating a temperature difference which produces an emf which is additive. Lead wires from the thermocouple arrays were taped onto the vinyl water tubing and then wrapped with thin foil strips. This was done to prevent the wires and tubing from becoming too hot and melting in the oven.

ORNL-DWG. 81-23803

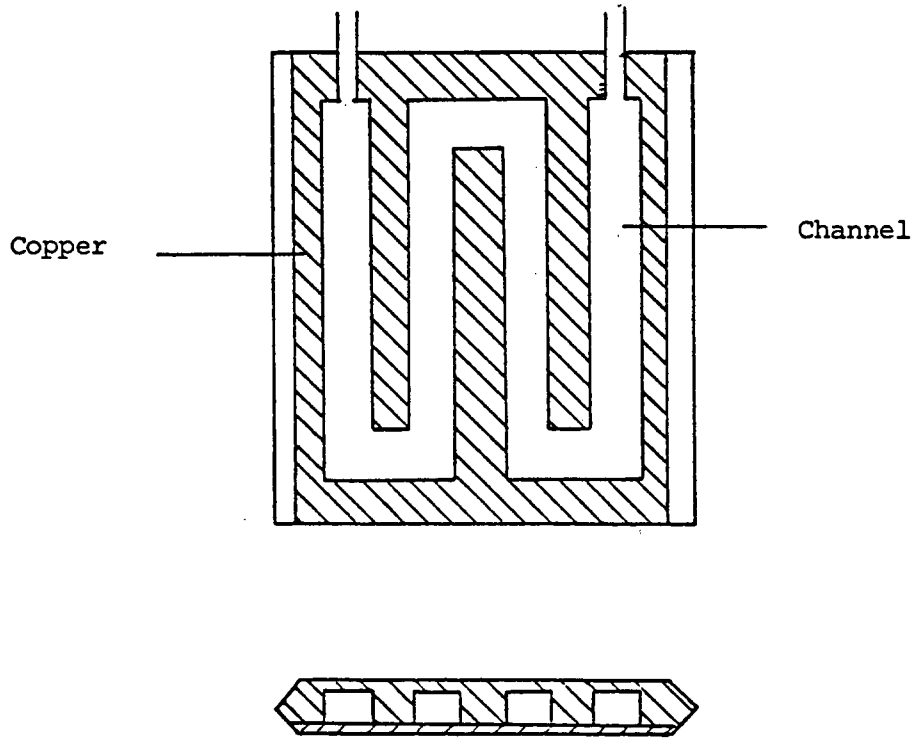

Figure B.1 Interior view of the irradiation heat flux guage.

ORNL-DWG. 81-23804

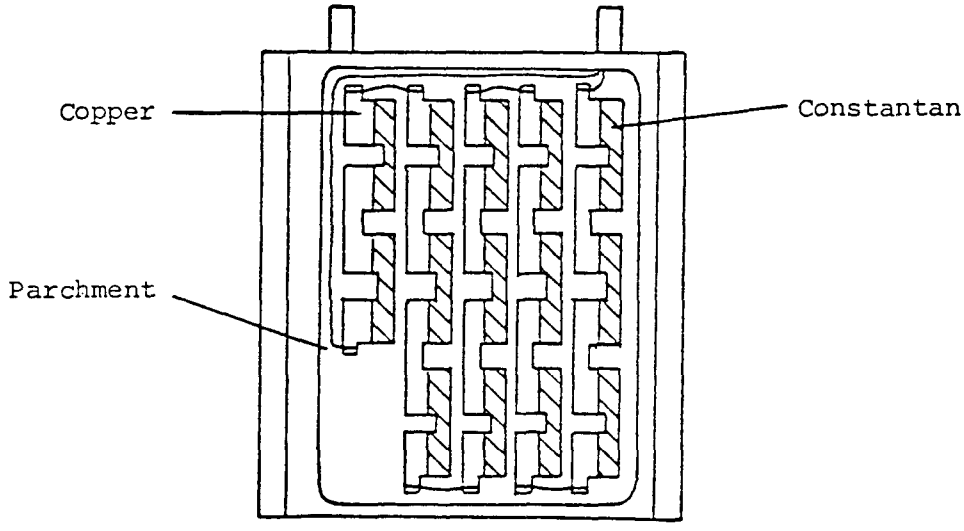

Figure B.2 Thermocouple arrangement of the irradiation heat flux gauge.

ORNL-DWG. 81-23805

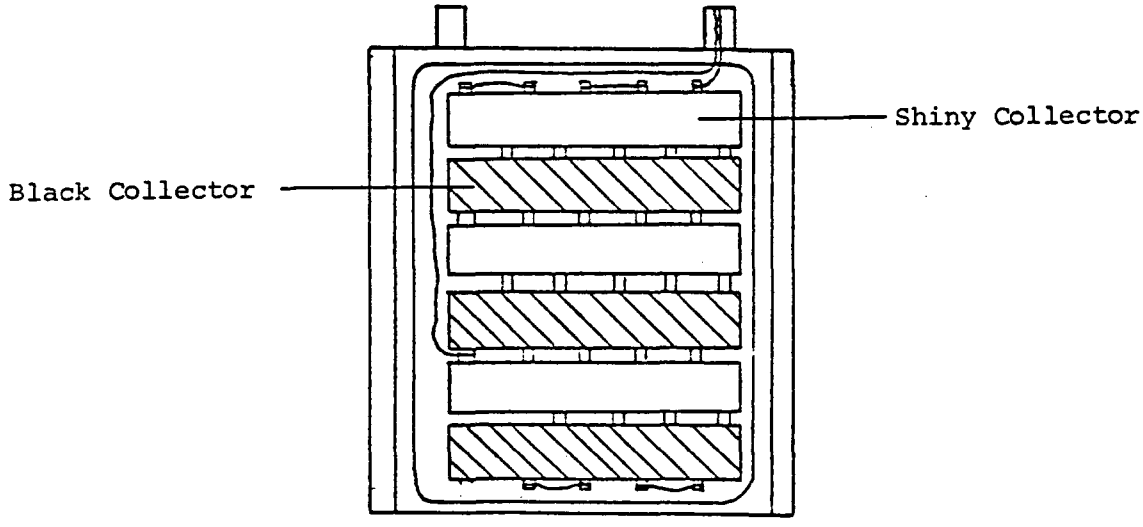

Figure B.3 Exterior view of the irradiation heat flux gauge.

Calibration of the Irradiation Heat Flux Gauge

Calibration of the irradiation heat flux gauge was done under a radiant heat source using a Gardon heat flux gauge as the transfer standard. Voltage on the heater was varied to provide different irradiation levels on the gauges. Millivolt readings from both gauges were recorded for fifteen second intervals. For the Gardon, one millivolt output is equal to 100 W/m^2. From Martin's thermal model [3] it is known that the relationship between the output of the gauges was linear so a least-squares prediction line was obtained from the readings which would have the form

$$G = S_o e + S_i^* \tag{B-1}$$

where G is the irradiation (W/m^2), S_o is the radiant thermopile sensitivity, e is the output of the irradiation heat flux gauge (mv), and S_i is the apparent threshold irradiation (W/m^2).

* S_o = 8133 $W/m^2/mv$
S_i = 1249 W/m^2

6.3 Appendix C

Standard Procedure for Placement of Thermocouples in Pans

For 20.3 cm round cake pans with 9 thermocouples, three holes are drilled in the pans according to specified locations. Three glass capillary tubes (internal diameter 1.6-1.8 x 100 mm) are each cut 3.5 cm long. One end of each is sealed closed by heating it over a gas burner. With the closed end up, the open ends on the capillary tubes are sealed to the 3 holes in the pan with clear Silicone. The pan and capillary tubes are dried overnight.

Small gauge thermocouples (0.075 mm in diameter) are used. Two teflon coated wires - one constantan and one copper - are cut approximately 90 cm long and welded together at one end. Three thermocouples are prepared and are threaded through a piece of shrink tubing so that the thermocouple wires are exposed on both ends and the junctions are 1.6 cm apart. The tubing is then shrunk, using an iron. The three welded ends are placed in a capillary tube and thermocouple plugs are placed on the other ends.

Nine thermocouples are made, three for each capillary tube with thermocouple locations within each capillary tube as follows:

1. One thermocouple is positioned 0.5 cm from the bottom of the pan (inside the capillary tube).

2. One thermocouple is positioned at mid-height of the pan, 1.6 cm from the bottom of the pan (inside the capillary tube).

3. One thermocouple is positioned at the top, 3.2 cm from the bottom of the pan (inside the capillary tube).

The capillary tubes are located in the pans as follows:

1. One capillary tube is centered in pan.

2. One capillary tube is positioned 3.8 cm from edge of pan (midway).

3. One capillary tube is positioned at the edge of the pan - 1.0 cm from edge.

6.4 Appendix D

Procedure for Mixing Cakes

Table D.1
Proportions for Yellow Cake Batter

	20.3 cm (8") Pan		23.8 cm (9") Pan	
	1 layer	2 layers	1 layer	2 layers
Cake Mix	315 gm	430 gm	260 gm	520 gm
Eggs (beaten)	42 gm	83 gm	50 gm	100 gm
Water	115 ml	230 ml	280 ml	

Let eggs and water stand until room temperature is reached.

Beat eggs in a blender on the "blend" speed (Osterizer Classic VIII) for one second.

Combine all ingredients in the metal bowl of the Kitchen Aid Mixer. Mix with the regular beater attachment until moistened. Scrape bowl. Mix two minutes on Speed 2.

Pour into pans that have been greased with approximately 1/2 tablespoon shortening and lightly floured. (330 gm is standard for the 20.3 cm black pan. 400 gm is standard for the 23.8 cm black pan).

Bake until the lowest thermocouple reaches 88°C.

INTERNAL DISTRIBUTION

1. R. S. Carlsmith
2. G. E. Courville
3. G. A. Cristy
4. R. M. Davis
5. W. Fulkerson
6. R. E. Goodson, Consultant
7. D. W. Jared
8. A. F. Johnson
9. S. I. Kaplan
10. M. A. Karnitz
11. M. E. Koons
12. T. R. LaPorte, Consultant
13. A. S. Loebl
14. J. W. Michel
15. R. E. Minturn
16. W. R. Mixon
17. L. I. Moss, Consultant
18. T. W. Reddoch
19. M. W. Rosenthal
20. G. Samuels
21. R. B. Shelton
22. D. B. Trauger
23. T. J. Wilbanks
24. H. E. Zittel
25. A. Zucker
26. Biology Division Library
27-28. Central Research Library
29. Document Reference Section
30-31. Center for Energy and Environmental Information
32. Laboratory Records RC
33-34. Laboratory Records Department
35. ORNL Patent Office

EXTERNAL DISTRIBUTION

36. G. C. Aldous, Director of New Products Development, Still-Man Manufacturing, 1011 Volunteer Drive, Box 789, Cookeville, TN 38501
37. C. A. Allen, Energy Information Administration, EI-60, Federal Building, 1200 Pennsylvania Avenue N.W., Washington DC 20461
38. B. J. Austin, Amana Refrigeration, Inc., Amana, IA 52204
39. E. K. Bastress, Energy Conversion & Utilization Technology Division, CS-142, Forrestal Building, Department of Energy, Washington DC 20585
40. L. Berlik, Modern Maid, Post Office Box 1111, Chattanooga, TN 37401
41. Walter Blanck, Assoc. of Home Appliance Mfgrs., 20 N. Wacker Drive, Chicago, IL 60606
42. C. E. Buerki, Thermador/Waste, Division of Norris Industries, 5119 District Blvd., Los Angeles, CA 90040
43. L. H. Caldwell, Modern Maid, Post Office Box 1111, Chattanooga, TN 37401
44. R. Chisholm, General Electric Company, Major Appliance Business Group, Appliance Park, Louisville, KY 40225
45. P. I. Cohen, General Electric Company, Major Appliance Business Group, Appliance Park, Louisville, KY 40225
46. R. Cooley, King-Seeley Division, 301 W. Ohio, Kendallville, IN 46755
47. J. J. Cuttica, Energy Conversion Equipment Branch, CE-113.2, Department of Energy, 1000 Independence Avenue S.W., Washington DC 20585

48. W. J. Day, Caloric Corporation, Heffner & Washington Streets, Topton, PA 19562
49. Roger Doty, Jenn-Air Corporation, 3035 N. Shadeland Avenue, Indianapolis, IN 46226
50. G. D. Duffy, Air Conditioning News, 700 East Maple, Birmingham, MI 48011
51. Phyllis Eck, Litton Microwave Cooking, 1405 Xenium Lane, N, Minneapolis, MN 55440
52. J. N. Eustis, Department of Energy, Office of Industrial Programs, CE-121.1, 1000 Independence Avenue, S.W., Washington, DC 20585
53. R. J. Fiskum, Energy Conversion Equipment Branch, CE-113.2, Department of Energy, 1000 Independence Avenue S.W., Washington DC 20585
54. Chris Foran, Texas Instruments Incorporated, P.O. Drawer 1255, Erwin Highway, Johnson City, TN 37601
55. D. H. Freund, Roper Appliance, 2207 West Station Street, Kankakee, IL 60901
56. R. C. Gehrke, The Tappan Company, Tappan Park, 222 Chambers Road, Mansfield, OH 44901
57. J. H. Gibbons, Office of Technology Assessment, U.S. Congress, 600 Pennsylvania Avenue S.E., Washington DC 20510
58. E. C. Goeshel, Whirlpool Corporation, Benton Harbor, MI 49022
59. D. E. Grether, Friedrich Air Conditioning & Refrigeration, P.O. Box 1540, San Antonio, TX 78295
60. J. R. Grimes, Chambers Corporation, P.O. Box 927, Oxford, MS 38655
61. G. C. Groff, Research Division, Carrier Corporation, Syracuse, NY 13201
62. R. J. Hemphill, Gas Research Institute, 8600 Bryn Mawr Avenue, Residential & Commercial Util., Chicago, IL 60631
63. Larry Hobart, American Public Power Association, 2000 Virginia Avenue N.W., Washington DC 20037
64. Tina Hobson, Building Equipment Division, CE-113.2, Department of Energy, 1000 Independence Avenue S.W., Washington DC 20585
65. A. Howard, Sharp Electronics Corporation, 10 Keystone Place, Paramus, NJ 07652
66. H. Jaster, General Electric Corporate Research & Development, General Electric Company, P.O. Box 43, Schenectady, NY 13201
67. P. L. Johnson, Oak Ridge Associated Universities, Executive Office, Administration Building, Oak Ridge, TN 37830
68. F. R. Kalhammer, Energy Management and Utilization Division, Electric Power Research Inst., 3412 Hillview Avenue, P.O. Box 10412, Palo Alto, CA 94303
69. R. W. King, Manager, Advanced Engineering, Copeland Corporation, Sydney, OH 45365
70. A. J. Kloska, Sears Laboratories, 925 S. Homan, Chicago, IL 60607
71. D. Kwiatek, Harper-Wyman, 930 N. York Road, Hinsdale, IL 60521
72. Arvo Lannus, Residential & Commercial Applications, Electric Power Research Inst., 3412 Hillview Avenue, P.O. Box 10412, Palo Alto, CA 94303
73. W. E. Lewis, General Electric Company, Major Appliance Business Group, Appliance Park, Louisville, KY 40225
74. D. C. Lim, Energy Conversion Equipment Branch, CE-113.2, Department of Energy, 1000 Independence Avenue S.W., Washington DC 20585

75. H. P. Luckett, Editor in Chief, Popular Science, 380 Madison Avenue, New York, NY 10017
76. Jim McCallum, Executive Editor, Air Cond. & Refrig. Bus., 614 Superior Avenue W., Cleveland, OH 44113
77. J. P. Millhone, Office of Buildings Energy Research & Development, CE-11, Department of Energy, 1000 Independence Avenue S.W., Washington DC 20585
78. Mark Minakuchi, Sharp Electronics Corporation, 10 Keystone Place, Paramus, NJ 07652
79. F. H. Morse, Office of Solar Heat Technologies, CE-31, Department of Energy, 1000 Independence Avenue S.W., Washington DC 20585
80. E. W. Murray, National Sales Manager, Robertshaw Controls Company, 1701 Byrd Avenue, P.O. Box 26544, Richmond, VA 23261
81. Tom Needham, Sears Laboratories, 925 S. Homan, Chicago, IL 60607
82. F. Okada, Litton Microwave Cooking, 1405 Xenium Lane, N., Minneapolis, MN 55440
83. R. L. Perl, The Tappan Company, Tappan Park, 222 Chambers Road, Mansfield, OH 44901
84. T. Ratchford, Committee on Science and Technology, Subcommittee on Energy R & D, House of Representatives, Washington DC 20515
85. Bill Riley, Advance Development, Heil Quaker Corporation, 647 Thompson Lane, P.O. Box 40566, Nashville, TN 37204
86. J. Rizzuto, New York State Energy Research & Development Auth., Agency Building No. 2, Empire State Plaza, Albany, NY 12223
87. F. Ross, Maytag Company, 403 W. 4th Street, North, Newton, IA 50208
88. J. H. Rothenburg, Utilities Systems, Department of Housing & Urban Development, 451 Seventh Street S.W., Washington DC 20410
89. J. D. Ryan, Energy Conversion Equipment Branch, CE-113.2, Department of Energy, 1000 Independence Avenue S.W., Washington DC 20585
90. I. P. Sargunam, Gaffers & Sattler, A Division of, Magic Chef, Inc., 4851 South Alameda Street, Los Angeles, CA 90058
91. L. A. Sarkes, American Gas Association, 1515 Wilson Boulevard, Arlington, VA 22209
92. M. L. Savitz, Deputy Assistant Secretary for Conservation, CE-10, Department of Energy, 1000 Independence Avenue S.W., Washington DC 20585
93. A. Schettle, G. R. Maufacturing Company, 9545 Clyde Park, SW, Grand Rapids, MI 49509
94. W. Schmidt, Jenn-Air Corporation, Heffner & Washington Streets, Topton, PA 19562
95. J. L. Schulze, General Electric Company, Appliance Park, Louisville, KY 40225
96. D. E. Sherpereel, Research and Engineering Center, Whirlpool Corporation, Benton Harbor, MI 49022
97. R. G. Sickert, Long Range Product Research, Whirlpool Corporation, Benton Harbor, MI 49022
98. D. Simon, Jenn-Air Corporation, Heffner & Washington Streets, Topton, PA 19562
99. J. A. Smith, Test and Evaluation Branch, CE-113.2, Department of Energy, 1000 Independence Avenue S.W., Washington DC 20585
100. E. W. Spannhake, White Consolidated Industries, Inc., 11770 Berea Road, Cleveland, OH 44111

101. L. B. Stevens, Jr., Gray & Dudley Company, 2300 Clifton Road, Nashville, TN 37209
102. W. D. Syniuta, Advanced Mechanical Technology, Inc., 141 California Street, Newton, MA 02158
103. J. J. Tacker, Athens Stove Works, P.O. Box 10, Athens, TN 37303
104. W. Teich, Ratheon Company, NPC Foundry Avenue, Waltham, MA 02154
105. C. C. Thiel, Jr., Division of Advanced Technology Applications, National Science Foundation, 1800 G Street N.W., Washington DC 20550
106. W. H. Thielbahr, Energy Conservation Branch, Department of Energy, Idaho Operations Office, 550 Second Street, Idaho Falls, ID 83401
107. H. Tomlin, Caloric Corporation, Heffner & Washington Streets, Topton, PA 19562
108. S. H. Torrey, Roper Appliance, 2207 West Station Street, Kankakee, IL 60901
109. R. D. Triplett, Roper Appliance, 2207 West Station Street, Kankakee, IL 60901
110. M. Valle, Chambers Corporation, P.O. Box 297, Oxford, MS 36855
111. L. Vonasch, General Electric Company, Major Appliance Business Group, Appliance Park, Louisville, KY 40225
112. D. J. Walukas, Foster-Miller Associates, Inc., 795 Oak Ridge Turnpike, Oak Ridge, TN 37830
113. D. Warring, King-Seeley Division, 301 W. Ohio, Kendallville, IN 46755
114. B. J. Weiss, Caloric Corporation, Heffner & Washington Streets, Topton, PA 19562
115. W. S. White, Whirlpool Corporation, Benton Harbor, MI 49022
116. G. R. Wolter, Sunbeam Appliance Company, 201 South York Road, Oak Brook, IL 60521
117. Congressional Information Service, Research Building 83, Kodak Park, Rochester, NY 14050
118. Edison Electric Institute, 8th Floor, 1111 19th Street N.W., Washington, DC 20036
119. Institute for Energy Analysis, ORAU-Library
120. Office of the Assistant Manager for Energy R & D, U.S. Department of Energy, Oak Ridge Operations, Oak Ridge, TN 37830
121. National Energy Information Center, Library, Room 1404, 12th & Pennsylvania Ave. N.W., Washington DC 20461

122-365. Technical Information Center, Department of Energy, P.O. Box 62, Oak Ridge, TN 37830, for Dist. Category UC-95d

366-500. Energy Conservation Distribution, Oak Ridge National Laboratory, Building 9102-2, Rm. 112, Oak Ridge, TN 37830

☆U.S. GOVERNMENT PRINTING OFFICE: 1981-546-067/420